AD-A126 126

AD

AD-E400 962

SPECIAL PUBLICATION ARTSD-SP-81001

COMPUTER CONTROL AND ACTIVATION OF SIX-DEGREE-OF-FREEDOM SIMULATOR

EDWARD G. DAVIES
RICHARD CHOU
JOHN STONE
KACHEUNG TSUI
MAURICE Z. DARWISH
WILLIAM REISENER
FRANKLIN RESEARCH CENTER
TWENTIETH AND PARKWAY
PHILADELPHIA, PA 19103

D. E. FRERICKS
R. J. RADKIEWICZ
PROJECT ENGINEERS
ARRADCOM

JANUARY 1983

US ARMY ARMAMENT RESEARCH AND DEVELOPMENT COMMAND
TECHNICAL SUPPORT DIRECTORATE
DOVER, NEW JERSEY

UNCLASSIFIED

SECURITY CLASSIFICATION OF THIS PAGE *(When Data Entered)*

REPORT DOCUMENTATION PAGE

READ INSTRUCTIONS BEFORE COMPLETING FORM

1. REPORT NUMBER Special Publication ARTSD-SP-81001	2. GOVT ACCESSION NO.	3. RECIPIENT'S CATALOG NUMBER
4. TITLE *(and Subtitle)* COMPUTER CONTROL AND ACTIVATION OF SIX-DEGREE-OF-FREEDOM SIMULATOR		5. TYPE OF REPORT & PERIOD COVERED Final 6. PERFORMING ORG. REPORT NUMBER
7. AUTHOR(s) Edward G. Davies, Richard Chou, John Stone, KaCheung Tsui, Maurice Z. Darwish, William Reisener, Franklin Research Center (cont)		8. CONTRACT OR GRANT NUMBER(s) DAAF03-73-C-0142
9. PERFORMING ORGANIZATION NAME AND ADDRESS Franklin Research Center Twentieth and Parkway Philadelphia, PA 19103		10. PROGRAM ELEMENT, PROJECT, TASK AREA & WORK UNIT NUMBERS AMS Code 3297.06.7313
11. CONTROLLING OFFICE NAME AND ADDRESS ARRADCOM, TSD STINFO Div (DRDAR-TSS) Dover, NJ 07801		12. REPORT DATE January 1983 13. NUMBER OF PAGES 417
14. MONITORING AGENCY NAME & ADDRESS *(if different from Controlling Office)* ARRADCOM, TSD Test and Instrumentation Div (DRDAR-TSE-S) Dover, NJ 07801		15. SECURITY CLASS. *(of this report)* Unclassified 15a. DECLASSIFICATION/DOWNGRADING SCHEDULE

16. DISTRIBUTION STATEMENT *(of this Report)*

Approved for public release; distribution unlimited.

17. DISTRIBUTION STATEMENT *(of the abstract entered in Block 20, if different from Report)*

18. SUPPLEMENTARY NOTES

The mechanical and electrical design drawings for the 6-DOF simulator are on file at the Ware Simulation Center. Other pertinent information can be found under Contract no. DAAF03-73-C-0142.

19. KEY WORDS *(Continue on reverse side if necessary and identify by block number)*

Control system
Hydraulics
Pitch
Simulator
Six-degrees-of-freedom
Spring rate
Vibration
Weapons
Yaw

20. ABSTRACT *(Continue on reverse side if necessary and identify by block number)*

Following the acquisition of a passive multi-degree-of-freedom simulator by the Ware Simulation Section, Rock Island Arsenal, Rock Island, IL, the Franklin Research Center was contracted to design and to make the necessary modifications for conversion from a passive to an activated simulator. This report outlines and details the design philosophy used for providing programmable

(cont)

DD FORM 1 JAN 73 1473 EDITION OF 1 NOV 65 IS OBSOLETE

UNCLASSIFIED

SECURITY CLASSIFICATION OF THIS PAGE *(When Data Entered)*

7. AUTHOR(s) (cont)

D. E. Frericks, R. J. Radkiewicz, Project Engineers, ARRADCOM

20. ABSTRACT (cont)

motions, vibrations, and spring rates required for activating the passive simulator. This report also documents the changes required in the hydraulic power supply, the mechanical changes to the yaw and pitch gimbals, and the electronic changes to the spring rate controller.

CONTENTS

	Page
Introduction	1
Mathematical Model	1
Discussion	1
Computer Requirements	3
Neutral Position	4
Triogonal Actuator Lengths	4
Direction Cosines of Actuators	7
Velocity and Force Transformations	7
Impedance Transformations	11
Actuator Spring Constants	12
Actuator Gravitational Forces	24
Actuator Mass Loads	27
Tail Boom Actuator Force Command	30
Linear Coefficients	30
Linearization of Equations	30
Incremental Gravitational Loading	30
Incremental Changes in Spring Constants	38
Incremental Actuator Extensions	41
Exact Calculations of Pitch Angle Effects	43
Summary of Calculations	48
Mean Values	48
Spring Constants (Off-line)	48
Actuator Forces (On-line)	51
Actuator Extensions (On-line)	52
Effective Mass Loads (Off-line)	52
Pitch Angle Effects (On-line)	52
Spring Constants	52
Effective Mass Load	53
Triogonal Yaw Angle Increment (On-line)	53
Spring Constant Coefficients (Off-line)	53
Actuator Forces (On-line)	53
Actuator Extensions (On-line)	54

Evaluation of Matrices 54

Calculation of Linear Coefficients 54
Off-Line Calculations for Aircraft 59
Off-Line Calculations for Combat Vehicle 61

Table of Symbols 69
System Dynamics 76

Aircraft 76

Aircraft Acceleration 76
Interaction of Systems 80

Combat Vehicle 84

Vehicle Geometry 84
Interaction of Systems 86

Passive System Mathematical Model 89

Purpose 89
Technical Approach 89
Derivation of the Transformation Matix $(B)^T$ 90
Method of Analysis 91
Capabilities of the Computer Program STIFF 2 91

Output Generated 91
Possible Loading Conditions 92
Input Data Required 92
List of Constants Used in STIFF 2 93

Main Hydraulic Power Unit 94

Priority 94
Flow Requirements 94
Component Selection 97
Cooling System 98
Control Center 98

Main Pitch System 100

Main Pitch Actuator 100
System Analysis 101

Main Pitch Actuator 101

Pitch Actuator Control System Circuit Diagram 103

Main Yaw System 103

Main Yaw Actuator 103
System Analysis 105
System Circuit Diagram 106

Triogonal Suspension System 106

6-DOF Suspension 106

6-DOF Springs 107
6-DOF Yaw 108
6-DOF Piping 109
6-DOF Position Indication 110

Study of Spring/Damping Simulator 110
System Analysis 111

Position Servo Analysis 111
Adaptive Control System Block Diagram 113
Adaptive Spring-Rate Control System with Step Force Inputs 115
Effect of Variation in Damping in Hydraulic Actuator 115
Adaptive Spring-Rate Control System-Dynamic Studies 116
Revised Adaptive Spring-Rate Control System Block Diagram 117
System Response Curves Measured from the Computer Simulated Adaptive Control System at Larger Actuator Bypass Opening 118

Tail Rotor Simulator 121

Mechanical Suspension 121
System Analysis 122

Combat Vehicle System 123

Mechanical Suspension 123
System Analysis 125

Vibration Systems 125

Introduction 125
Main Rotor System 126

Design Limitations 126
Design Parameters 127

Tail Rotor System 128
Stability Analyses 128

Main Rotor 130
Tail Rotor 131

Final Designs 132

System and Subsystem Electronic Power Controls 132

System Start Up and Fail-Safe Interlocks 133

Start Up and Fail-Safe System 133
Firing Interlock 133

Electronic Wiring and Packaging 133

Wiring 133
Packaging 134

Conclusions 135

Appendixes

A Computer Control of 6-DOF Simulator and Computer Program 223

B 6-DOF Math Model Actuator Load Mass due to Actuators 263

C Listing of Computer Program STIFF 2 279

D Use of PIPDYNE Computer Program to Verify that $A^T = B^{-1}$ and $B^T = A^{-1}$ 307

E Main Hydraulic Power Unit 317

F Main Pitch System 349

G Determination of Servo Open-Loop Gain Required for Resisting Load Disturbances 359

H Calculation of the Required Open-Loop Gain and Bypass Leakage Coefficient of the Triogonal Actuator Servo System 367

I Main Yaw System 377

J Combat Vehicle System 387

K Tail Rotor Simulator 405

Distribution List 417

TABLES

		Page
1	Actuator variations	137
2	STIFF 2 program input map	137
3	Pump oil flow (gpm) required for various motions	139
4	Accumulators for servo systems	139
5	List of parameter values for calculating the main pitch control system frequency responses	140
6	Servovalve characteristics of main pitch control system	141
7	List of parameter values used for calculating the main yaw control system frequency responses	142
8	Servovalve characteristics of main yaw control system	143
9	Manufacturer's test data	143
10	Recordings on four spring-rates and two damping ratio settings	143
11	Moog servovalve 73-233 manufacturer's data	144
12	Servovalve characteristics for turret control system	144

FIGURES

1	Triogonal system	145
2	Block diagram overall hydraulic system	146
3	Main pitch-actuator feedback control system block diagram	147
4	Transfer characteristics of main pitch-actuator feedback control system	148
5	Main pitch control system AAH payload	149
6	Main pitch control system open loop	150
7	Main pitch control system AH-1G payload	151
8	Main pitch control system closed loop	152

9	Main pitch operating limits	153
10	Main yaw feedback control system block diagram	154
11	Transfer function block diagram of the main yaw feedback control system	155
12	Main yaw control system AAH payload	156
13	Main yaw control system AH-1G payload	157
14	Main yaw control system open loop	158
15	Main yaw control system closed loop	159
16	Main yaw operating limits (AH-1G aircraft)	160
17	6-DOF system spring rate $(\frac{\text{lb}}{\text{in.}})$	161
18	Hydraulic schematic modified 6-DOF suspension (typical)	162
19	Control circuit to verify spring rate and damping control	163
20	Servo system with bypass on actuator open 1 1/2 turns	164
21	Spring and damping test set-up	165
22	Test stand	166
23	Open loop response of actuator	167
24	Theoretical response closed loop	168
25	Servo system with bypass on actuator open 1 1/2 turns; lag network added to forward loop; overdamped system controlled to produce underdamped characteristic	169
26	Servo system with bypass on actuator open 1 1/2 turns; lag network added to forward loop; step change in force and response characteristic	170
27	Servo system with bypass on actuator open 1 1/2 turns; lag network added to forward loop; underdamped system	171
28	Triogonal actuator position servo system block diagram	172
29	Open loop gain constant (45) and the dynamics of the value and actuator	173
30	Calculated frequency response of the triogonal actuator position servo system	174

31 Force sensing schematic block diagram of the adaptive spring-rate control system 175

32 System block diagram of the adaptive spring-rate control system 176

33 Position response of the simulated adaptive spring-rate control system with step force input; K = 200,000 $\frac{lb}{in.}$, $\zeta = 0.3$ 177

34 Position response of the simulated adaptive spring-rate control system with step force input; K = 200,000 $\frac{lb}{in.}$, $\zeta = 1.0$ 178

35 Position response of the simulated adaptive spring-rate control system with step force input; K = 130,000 $\frac{lb}{in.}$, $\zeta = 0.376$ 179

36 Position response of the simulated adaptive spring-rate control system with step force input; K = 130,000 $\frac{lb}{in.}$, $\zeta = 1.24$ 180

37 Position response of the simulated adaptive spring-rate control system with step force input; K = 60,000 $\frac{lb}{in.}$, $\zeta = 0.55$ 181

38 Position response of the simulated adaptive spring-rate control system with step force input; K = 60,000 $\frac{lb}{in.}$, $\zeta = 1.8$ 182

39 Position response of the simulated adaptive spring-rate control system with step force input; K = 1000 $\frac{lb}{in.}$, $\zeta = 0.5$ 183

40 Position response of the simulated adaptive spring-rate control system with step force input; K = 1000 $\frac{lb}{in.}$, $\zeta = 1.0$ 184

41 Theoretical force response of the actuator with 0.5 damping factor 185

42 Theoretical force response of the actuator with 0.7 damping factor 186

43 Theoretical force response of the actuator with 2.1 damping factor 187

44 Effects of actuator damping coefficient on the position response of the simulated adaptive spring-rate control system with a step force input; K = 130,000 $\frac{lb}{in.}$, $\zeta = 0.376$ 188

45 Effects of actuator damping coefficient on the position response of the simulated adaptive spring-rate control system with a step force input; K = 130,000 $\frac{lb}{in.}$, $\zeta = 1.24$ 189

46 Analog computer simulation of the adaptive spring-rate control system with input = 1000 ± 50 $\frac{lb}{in.}$ 190

47 Analog computer simulation of the adaptive spring-rate control system with input = 10,000 ± 500 $\frac{lb}{in.}$ 191

48 Analog computer simulation of the adaptive spring-rate control system with input = 90,000 ± 10,000 $\frac{lb}{in.}$ 192

49 Revised system block diagram of the adaptive spring-rate control system 193

50 Position response of the adaptive spring-rate control system with step force input; K = 300 $\frac{lb}{in.}$, $\zeta = 0.468$ 194

51 Position response of the adaptive spring-rate control system with step force input; K = 300 $\frac{lb}{in.}$, $\zeta = 1.4$ 195

52 Position response of the adaptive spring-rate control system with step force input; K = 1000 $\frac{lb}{in.}$, $\zeta = 0.384$ 196

53 Position response of the adaptive spring-rate control system with step force input; K = 1000 $\frac{lb}{in.}$, $\zeta = 1.0$ 197

54 Position response of the adaptive spring-rate control system with step force input; K = 3000 $\frac{lb}{in.}$, $\zeta - 0.444$ 198

55 Position response of the adaptive spring-rate control system with step force input; K = 3000 $\frac{lb}{in.}$, $\zeta = 1.0$ 199

56 Position response of the adaptive spring-rate control system with step force input; K = 10,000 $\frac{lb}{in.}$, $\zeta = 0.487$ 200

57 Position response of the adaptive spring-rate control system with step force input; K = 10,000 $\frac{lb}{in.}$, $\zeta = 0.81$ 201

58 Position response of the adaptive spring-rate control system with step force input; K = 30,000 $\frac{lb}{in.}$, $\zeta = .468$ 202

59 Physical concept tail-boom control system 203

60 Tail-boom control system block diagram 204

61 Block diagram for position servo tail-boom control 205

62 Block diagram for force servo tail-boom control 206

63 Tail-boom control frequency response of force and position 207

64 Combat vehicle pitch spring rate (in. lb/rad) 208

65 Turret pitch actuator position servo system block diagram 209

66 Turret pitch position control system 210

67 Turret pitch control system open loop 211

68 Turret pitch control system closed loop 212

69 Pitch drive operating limits combat vehicle 213

70 Main yaw drive operating limits combat vehicle 214

71 6-DOF yaw drive operating limits combat vehicle 215

72 Output force limits (main rotor) 216

73 Vibrator-equivalent circuit 217

74 Main rotor system response 218

75 Tail rotor system response 219

76 Vibrator servo system (MR) 220

77 Vibrator servo system (TR) 221

INTRODUCTION

The development phase, as recorded in this report, involved several areas of mutually dependent effort.

1. Calculations were made to determine the various mechanical design parameters and requirements.

2. Considerable effort was made to locate suitable commercial equipment to satisfy the design requirements. Negotiations were carried on with at least three potential suppliers of major components such as hydraulic pumps, motor and controls, servo valves, actuators, etc.

3. Mechanical layouts were made using the selected commercial equipment.

4. Servo analyses were made to verify that selected equipment would perform as required, and that it operated in a stable manner.

5. Hydraulic schematics were developed for the various systems.

6. Standard servo configurations were developed for control of the pitch and yaw circuits including features to insure safe, smooth start-up and fail-safe operation.

7. An extensive study was conducted on the analog and digital computer of the Franklin Institute Research Laboratories to verify the proposed spring rate and damping ratio control system. The design of the actual equipment was then developed.

8. A preliminary design was performed for the three vibration systems. The tail rotor vibrator and the auxiliary device vibrator units have reasonable design parameters. Since the main rotor vibrator unit is considerably more difficult because of the large mass to be moved, a compromise solution is presented.

Each of these phases, including mathematical support, is discussed in this report.

MATHEMATICAL MODEL

Discussion

The purpose of the following derivation is to provide the input data necessary to program the servo systems to:

1. Provide specified spring rates as measured at the platform,

2. Eliminate the effects of gravity, due to the finite spring rate of the triogonal actuators, as a result of variations in the geometry, and

3. Derive the input signals necessary to produce the desired yaw and pitch motion. In addition, a simplified analysis of the system dynamics was presented, to assess the importance of cross-coupling effects among the various servo systems.

The basic analysis has been separated into the following two major sections: (1) Calculation of the mean values, and (2) Calculation of linear derivatives for the combat vehicle. The system dynamics is also presented. A system of linear coefficients was selected to avoid continuous real-time calculation of all the variables, which would require excessive computing time and facilities. By linearizing the solution about the mean values, the time varying components can be derived from the input time functions by means of linear calculations. This greatly reduces the on-line computing facilities required. The mean values and linear derivatives can be computed off-line, and need be modified only if the basic geometry is changed, i.e., location of weapon, type of vehicle, etc.

The analysis was developed in general terms for each of the specified geometries to expand its use. In many cases, many of the parameters will be zero, and the actual calculations can be simplified. The equations were written in terms of state variables to simplify the notation. In most cases, these vectors consist of the six components of velocity or position necessary to specify the state of a particular element in the system--weapon, aircraft, triogonal system, etc. The basic approach was to develop the equations necessary to relate forces and moments in one coordinate system to those in another and to relate the velocities (linear and angular) of one system to another.

The concept of impedance was introduced to describe the relationship between the forces and moments and the resultant velocities. With this method, the weapon impedance can be found in terms of the output impedance of the triogonal actuators. For a desired set of spring constants at the platform, the corresponding spring constants of the actuators are then found.

An important requirement for the system is the elimination of gravitational extensions of the triogonal actuators from their desired neutral position. This is particularly important when the gimbal angles are changed, resulting in a reorientation of the gravity vector for the triogonal system. Before firing, in some cases, it will be necessary to adjust the gimbal angles manually to aim the weapon. For this, a continuous calculation of the gravitational loading must be performed. Since relatively large angular excursions may be required, a linearized approach will not give sufficient accuracy. The fixed coefficients involved in the calculation can be derived prior to the run, once the relationship among vehicle, triogonal system, and gimbal system is established. During a firing run, this same calculation can be used to correct for the time-varying inputs to the gimbal system. In addition, linearized corrections will be made to correct for variations in the triogonal actuator lengths due to yaw variations of the triogonal geometry when used with the combat vehicle.

A description of the vehicle dynamics has also been included, primarily to examine some of the cross-coupling effects. Prior calculations have described the servo systems and the effects of the geometry on them. This has been primarily a description of the output impedance of the support system for the vehicle. To complete the description of the entire system, it is necessary to add

the equations to this, describing those elements external to the support system; i.e., the vehicle dynamics. By combining all these equations, an analytic solution for the system response was obtained. However, this requires the solution of six simultaneous nonlinear differential equations, which would have to be done with the aid of a computer. Even without deriving the overall system response, it is possible to estimate the coupling effects due to the external systems. For this purpose, equations have been derived which describe the servo output quantities (gimbal and triogonal forces and tail boom velocities) in terms of the input quantities (gimbal and triogonal velocities, tail boom forces, and weapon forces). To simplify the results, the mass of the support equipment has been neglected. This will produce an additional inertia load on the servo systems, but because the vehicle mass will be considerably larger, this simplification is justified for estimating purposes.

The cross-coupling terms result from two effects: (1) The inertia terms (acceleration and gyroscopic forces) are due to the mass of the vehicle, and (2) There are direct coupling terms due to the geometry. In this latter class are those between the tail boom and triogonal servos and among individual actuators in the triogonal system. These expressions have been presented in general terms, and the direct coupling terms were evaluated for a particular case. The inertia terms were not evaluated, since this requires a knowledge of the system velocities, which must be obtained from the solution to the system response discussed previously. The inertia effects are most significant for highly underdamped systems, and the energy stored within the system can build up to large values during firing due to inappropriate choices of firing rate and resonant frequencies. Generally, however, it is reasonable to assume the steady state values, due to the direct coupling terms, are representative of the forces and deflections that will be experienced. The passive system mathematical model makes use of the formula derived in the aircraft neutral position and the aircraft linear coefficients as a basis for the development of a computer program for use in operation of the simulator as a passive system. This program accepts as input the desired stiffness in six degrees-of-freedom and prints out corresponding actuator stiffness, accumulator precharge pressure and the top and bottom actuator pressures.

Computer Requirements

Many quantities must be calculated, both in preparing for and during an experimental run. These calculations are usually done off-line before the run on a linearized basis because of the excessive time and the computer facilities required to make continuous real time calculations.

Initially, the mean values of all quantities will be found and stored. Then linear coefficients will be developed to compute real time variations from the means during the run. Since the angular variations will generally be quite small (up to 10 degrees), this method will give reasonable accuracy, and the computational noise generated by this technique will be considerably less than the continuous calculation of total values.

A computer program has been prepared to calculate manual input values of effective mass, spring constant, and actuator lengths for quasi-static operation. In addition, the program can be used in a dynamic situation when the simulator is pitching and yawing. All calculations are based on derivations in the following sections and the computer program is described in detail in appendix A.

Primarily because of the complexity required to make pitch angle corrections to the actuator spring constant, all calculatuions will be performed digitally. The large number of coefficients required to be input to analog circuitry for this calculation would require an excessive number of D/A converters and storage elements. The complete calculation of spring constants, on an analog basis, could be performed, using prewired patch boards, selected for the particular choice of axes for which spring constants are specified. However, the resulting accuracy would be poor, due to the large number of multiplications required.

Neutral Position

Two modes of operation are planned using the aircraft fuselage: (1) A fixed weapon emplacement where the gimbal angles will be fixed to train the weapon on target, and (2) A movable weapon turret with varied gimbal angles with the weapon tracking system used to maintain the weapon on target.

In both cases, it is desired to maintain the triogonal system at or near its neutral position (except for reaction to weapon forces) and to maintain a constant platform impedance. In either case only the mean value calculations are required, since the geometry between the triogonal system and the vehicle is not varied with time.

For the combat vehicle, an additional pitch actuator has been added between the triogonal platform and the vehicle CM. This will supply the necessary dynamic pitch motion, while the triogonal system will supply the yaw motion. The gimbal system will be locked in place at the desired position. The mean triogonal position will again be the neutral position (all actuators equal length). Since, in this case, the geometry between the triogonal system and the vehicle does change with time, both the mean values and the linearized deviations from the mean are required.

Triogonal Actuator Lengths

The mean actuator lengths are determined so that a prescribed linear and angular displacement exists between the gimbal and the aircraft platform mounting plates. This displacement is defined by the vector distance from the origin of the gimbal coordinate system to the origin of the platform coordinate system, as measured in the platform system, and the relative Euler angles required to transform the gimbal system into the platform system. In general, yaw, pitch, and roll will be the rotation order for right-handed systems. The exception is the gimbal system which will operate in the reverse order of pitch and yaw because of

the way it is constructed. The x-axis (roll) is defined in the forward direction, the y-axis (pitch) in the starboard lateral direction, and the z-axis (yaw) in the downward vertical direction.

Displacements defined by the vector are

$$x_1 = \begin{pmatrix} x \\ y \\ z \end{pmatrix} \tag{1}$$

and the Euler angles by

$$x_3 = \begin{pmatrix} \phi \\ \theta \\ \psi \end{pmatrix} \tag{2}$$

The angular velocities of a point from one system to another are given by

$$\dot{x}_2 = \begin{pmatrix} p \\ q \\ r \end{pmatrix} = G'(x_3)\dot{x}_3 \tag{3}$$

where

$$G'(x_3) = \begin{bmatrix} 1 & 0 & -\sin\theta \\ 0 & \cos\phi & \sin\phi\cos\theta \\ 0 & -\sin\phi & \cos\phi\cos\theta \end{bmatrix} \tag{4}$$

for all except the gimbal system. For this

$$G'(x_{3G}) = \begin{bmatrix} \cos\theta_G \cdot \cos\psi_G & \sin\psi_G & 0 \\ -\cos\theta_G \cdot \sin\psi_G & \cos\psi_G & 0 \\ \sin\theta_G & 0 & 1 \end{bmatrix} \tag{5}$$

The displacement of the origins of two systems are defined as measured in the second system, into which the first is transformed. For instance, a point in the gimbal system can be transformed into the platform system through the equation

$$x_{1p} = E(x_{3p})\, x_{1G} - r_p \tag{6}$$

where the angular transformation

$$E(x_3) = E_3(\phi)\, E_2(\theta)\, E_1(\psi) \tag{7}$$

and

$$E_1(\psi) = \begin{bmatrix} \cos\psi & \sin\psi & 0 \\ -\sin\psi & \cos\psi & 0 \\ 0 & 0 & 1 \end{bmatrix} \tag{8}$$

$$E_2(\theta) = \begin{bmatrix} \cos\theta & 0 & -\sin\theta \\ 0 & 1 & 0 \\ \sin\theta & 0 & \cos\theta \end{bmatrix} \tag{9}$$

$$E_3(\phi) = \begin{bmatrix} 1 & 0 & 0 \\ 0 & \cos\phi & \sin\phi \\ 0 & -\sin\phi & \cos\phi \end{bmatrix} \tag{10}$$

The displacement, r_p, is the vector from the origin of the gimbal system to the origin of the platform system and measured there.

The location of the pivot points for the n-th actuator (n=1to6) is given in the gimbal system by

$$b_n = \begin{pmatrix} b_x \\ b_y \\ b_z \end{pmatrix}_n \tag{11}$$

The other end of the n-th actuator is located in the platform system at the point

$$a_n = \begin{pmatrix} a_x \\ a_y \\ a_z \end{pmatrix}_n \tag{12}$$

It then follows that the vector length of the n-th actuator in the platform system is given by

$$\ell_n = r_p + a_n - E(x_{3p})\, b_n \tag{13}$$

If we define

$$c_n = E(x_{3p})\, b_n \tag{14}$$

then

$$\ell_n = r_p + a_n - c_n \tag{15}$$

The scalar length is found by premultiplying this by its transpose

$$(\ell_o)_n = (\ell_{n_t} \cdot \ell_n)^{1/2} \tag{16}$$

These are the desired extended lengths (under gravitational load) for each of the actuators.

Direction Cosines of Actuators

The direction cosines of the actuators in the platform system are given simply by

$$\begin{pmatrix} \alpha \\ \beta \\ \gamma \end{pmatrix}_n = \frac{1}{(\ell_o)_n} \ell_n \tag{17}$$

Velocity and Force Transformations

The scalar actuator velocities are determined from the relative velocity of the platform system to the gimbal system by first finding the vector velocities. For the n-th actuator, the vector velocity, in gimbal coordinate is

$$\dot{\ell}_G = \dot{x}_{1G} + \dot{E}'(x_{3p}) \cdot a_n \tag{18}$$

where

$x_{1G} = E'(x_{3p})\, r_p$ is the location of the origin of the platform system in gimbal coordinates. But

$$\dot{E}'(x_{3p}) = E'(x_{3p})\, W(\dot{x}_{2p}) \tag{19}$$

where

$$W(x_1) = \begin{bmatrix} 0 & -z & y \\ z & 0 & -x \\ -y & x & 0 \end{bmatrix} \tag{20}$$

so that

$$\dot{\ell}_G = \dot{x}_{1G} + E'(x_{3p})\, W(\dot{x}_{2p}) a_n \tag{21}$$

This is also equal to

$$\dot{\ell}_G = \dot{x}_{1G} + E'(x_{3p})\ W(-a)\ \dot{x}_{2p} \tag{22}$$

Relative to the gimbal system, the linear velocity of the platform system in platform coordinates is

$$\dot{x}_{1p} = E(x_{3p})\ \dot{x}_{1G} \tag{23}$$

Then, the actuator velocity in platform coordinates is

$$\dot{\ell}_p = \dot{x}_{1p} - W(a)\ \dot{x}_{2p} \tag{24}$$

The scalar actuator velocity is found by projecting this along the actuator

$$\dot{\ell}_n = \begin{pmatrix} \alpha_n \\ \beta_n \\ \gamma_n \end{pmatrix}_t \cdot \dot{\ell}_p = \left[\begin{pmatrix} \alpha \\ \beta \\ \gamma \end{pmatrix}_t \middle| - \begin{bmatrix} \alpha \\ \beta \\ \gamma \end{bmatrix}_t W(a) \right]_n \begin{pmatrix} \dot{x}_1 \\ \hline \dot{x}_2 \end{pmatrix}_p \tag{25}$$

If we let

$$\begin{pmatrix} \lambda \\ \mu \\ \nu \end{pmatrix} = W(a) \begin{pmatrix} \alpha \\ \beta \\ \gamma \end{pmatrix} \tag{26}$$

This becomes

$$\dot{\ell}_n = \begin{bmatrix} \alpha_n & \beta_n & \gamma_n & \lambda_n & \mu_n & \nu_n \end{bmatrix} \begin{pmatrix} \dot{x}_1 \\ \hline \dot{x}_2 \end{pmatrix}_p \tag{27}$$

The column matrix of scalar actuator velocities is then

$$\dot{\ell} = F' \begin{pmatrix} \dot{x}_1 \\ \hline \dot{x}_2 \end{pmatrix}_p \tag{28}$$

where

$$F' = \begin{bmatrix} \alpha_1 & \beta_1 & \gamma_1 & \lambda_1 & \mu_1 & \nu_1 \\ \alpha_2 & \beta_2 & \gamma_2 & \lambda_2 & \mu_2 & \nu_2 \\ \cdot & & & & & \cdot \\ \cdot & & & & & \cdot \\ \cdot & & & & & \cdot \\ \alpha_6 & \cdot & \cdot & \cdot & \cdot & \nu_6 \end{bmatrix} \tag{29}$$

Since the actuator pivots have no angular restraint, the force exerted on the platform by the actuator is directed along the actuator. If the scalar force in the n-th actuator is f_n, the forces and moments produced by the n-th actuator about the platform system are

$$f_p = \begin{pmatrix} \alpha \\ \beta \\ \gamma \end{pmatrix} f_n \tag{30}$$

$$m_p = W(a)\ f_p = W(a) \begin{pmatrix} \alpha \\ \beta \\ \gamma \end{pmatrix} f_n \tag{31}$$

or

$$\begin{pmatrix} f_p \\ \hline m_p \end{pmatrix}_n = \begin{bmatrix} \begin{pmatrix} \alpha \\ \beta \\ \gamma \end{pmatrix} \\ \hline W(a) \begin{pmatrix} \alpha \\ \beta \\ \gamma \end{pmatrix} \end{bmatrix}_n f_n \tag{32}$$

The sum of the forces and moments of all six actuators is then

$$\begin{pmatrix} f \\ \hline m \end{pmatrix}_p = F_t' \cdot f_\ell \tag{33}$$

where f_ℓ is the column matrix of all actuator scalar forces.

The velocity and force transformations for the rectilinear systems can be derived as follows: A point in the platform system is transformed into the aircraft system by

$$x_{1a} = E\ (x_{3a})\ x_{1p} - r_a \tag{34}$$

The linear velocity of the origin of the aircraft system, if there is no relative motion between the platform and the aircraft systems, is equal to the velocity of the origin of the platform system plus the rotational components of the r_a vector. The velocity of the platform system in aircraft coordinates is

$$(\dot{x}_{1p})_a = E(x_{3a})\, \dot{x}_{1p} \tag{35}$$

while the angular velocity of the platform system in aircraft coordinates is

$$(\dot{x}_{2p})_a = E(x_{3a})\, \dot{x}_{2p} \tag{36}$$

Thus, the linear velocity of the aircraft system is

$$\dot{x}_{1a} = E(x_{3a})\, \dot{x}_{1p} - W(r_a)\, E(x_{3a})\, \dot{x}_{2p} \tag{37}$$

Then, if

$$\begin{pmatrix} \dot{x}_1 \\ \hline \dot{x}_2 \end{pmatrix}_a = H\,(x_{3a}, r_a) \begin{pmatrix} \dot{x}_1 \\ \hline \dot{x}_2 \end{pmatrix}_p \tag{38}$$

The velocity transformation is

$$H\,(x_{3a}, r_a) = \left[\begin{array}{c|c} E\,(x_{3a}) & -W(r_a)\; E(x_{3a}) \\ \hline 0 & E(x_{3a}) \end{array}\right] \tag{39}$$

Forces and moments exerted on the platform system are transformed to the aircraft system by

$$f_a = E(x_{3a})\, f_p \tag{40}$$

$$m_a = E(x_{3a})\, m_p - W(r_a) \cdot E(x_{3a})\, f_p \tag{41}$$

Thus

$$\begin{pmatrix} f \\ \hline m \end{pmatrix}_a = \left[\begin{array}{c|c} E(x_{3a}) & 0 \\ \hline -W(r_a)\; E(x_{3a}) & E\,(x_{3a}) \end{array}\right] \begin{pmatrix} f \\ \hline m \end{pmatrix}_p \tag{42}$$

or

$$\begin{pmatrix} f \\ \hline m \end{pmatrix}_a = H_t{}'(x_{3a}, r_a) \begin{pmatrix} f \\ \hline m \end{pmatrix}_p \tag{43}$$

The force transformation is the inverse transpose of the velocity transformation.

Impedance Transformations

The impedance of a system is defined as the transformation which produces the system velocities in response to impressed forces and moments. Thus, in general

$$\begin{pmatrix} \dot{x}_1 \\ \hline \dot{x}_2 \end{pmatrix} = \mathcal{Z}\begin{pmatrix} f \\ \hline m \end{pmatrix} \tag{44}$$

With this definition, the impedance in the platform coordinate system produced by the triogonal actuator impedances is given by

$$\begin{pmatrix} \dot{x}_{1p} \\ \hline \dot{x}_{2p} \end{pmatrix} = \mathcal{Z}_p \begin{pmatrix} f \\ \hline m \end{pmatrix}_p \tag{45}$$

The impedance matrix describing the actuators is

$$\dot{\ell} = Z_\ell \cdot f_\ell \tag{46}$$

where $\dot{\ell}$ and f_ℓ are the scalar lengths and forces in the actuators. If the impedance is to appear as a spring system

$$\mathcal{Z}_\ell = S \begin{bmatrix} 1/k_1 & 0 & \cdot & \cdot & 0 \\ 0 & 1/k_2 & & & \cdot \\ \cdot\ \cdot & & & & \cdot \\ 0 & 0 & \cdot & \cdot & 1/k_6 \end{bmatrix} = S\, L_\ell \tag{47}$$

then this diagonal matrix uses the diagonal elements as the reciprocals of the spring constants of each actuator. It is also convenient to define a column matrix as

$$\begin{pmatrix} \dfrac{1}{k} \end{pmatrix}_\ell = \begin{bmatrix} 1/k_1 \\ 1/k_2 \\ \vdots \\ 1/k_6 \end{bmatrix} \tag{48}$$

Since

$$\begin{pmatrix} f \\ \hline m \end{pmatrix}_p = F_t' \; f_\ell \tag{49}$$

$$F \begin{pmatrix} \dot{x}_1 \\ \dot{x}_2 \end{pmatrix}_p = \dot{\ell} \tag{50}$$

the platform impedance is given by

$$Z_p = F Z_\ell F_t \tag{51}$$

Similarly the impedance of the aircraft system is

$$Z_a = H\,(x_{3a}, {}^{r}a)\; Z_p\; H_t\,(x_{3a}, {}^{r}a) \tag{52}$$

Actuator Spring Constants

Since the actuator spring constant matrix is diagonal, it is completely determined by specifying six spring constants on the weapons system. These can be the principal (diagonal) constants, or a combination of diagonal and mutual constants. The unspecified elements in the impedance matrix will also be completely determined by the choice of the first six. The only exception to these restrictions is when the diagonal elements are specified, the system in which the specified constants and platform system form a symmetrical geometry, and the triogonal system is in its neutral position. In this case, some of the matrices in the solution become singular, and the solution can only be obtained by specifying a fewer number of spring constants and by imposing arbitrary symmetry conditions on the triogonal system.

The impedance description of the system is preferable to an admittance description for the following reasons: (1) The system disturbance is a force. The response of the system to this force is described by the impedance rather than the admittance, and (2) Since only six of the 36 total elements of the impedance (or admittance) matrix at the weapon system can be specified, it is necessary to accept whatever mutual coupling results from this choice. Under these conditions, the diagonal elements of the impedance matrix cannot be made equal to the reciprocals of the diagonal elements of the admittance matrix, and the motion resulting from a specified input force will not be equal to the desired response, if admittance elements are specified. Instead, this will determine what forces and moments must be applied about all three axes to produce this response along a single axis.

To develop a general solution which can be applied to either the aircraft or combat vehicle configuration, it is assumed that in addition to the gimbal and platform systems described earlier, pitch and vehicle systems will be defined by

$$x_{1H} = E(x_{3H})\, x_{1p} - r_H \tag{53}$$

$$x_{1V} = E(x_{3V})\, x_{1H} - r_V \tag{54}$$

Since the pitch system is restricted to motion about only the pitch axis, it is convenient to orient this system parallel to the platform system in its neutral position. Then

$$E(x_{3H}) = \begin{bmatrix} \cos\theta_H & 0 & -\sin\theta_H \\ 0 & 1 & 0 \\ \sin\theta_H & 0 & \cos\theta_H \end{bmatrix} \tag{55}$$

For the aircraft, the pitch angle, θ_H, is fixed, and the displacement, r_H, is zero. For the combat vehicle, θ_H, varies with time, and the displacement, r_H, as measured in the platform system is constant and contains only a z component.

$$E'(x_{3H})\ r_H = \begin{pmatrix} 0 \\ 0 \\ z_H \end{pmatrix} \tag{56}$$

The vehicle Euler angles, x_{3V}, will normally be zero; that is, the vehicle axes will be parallel to the pitch system axes.

The impedance at the platform,

$$Z_p = F\ Z_\ell\ F_t \tag{57}$$

can be transformed to the pitch system coordinates by

$$Z_H = H(x_{3H}, r_H)\ F\ Z_\ell\ F_t\ H_t\ (x_{3H}, r_H) \tag{58}$$

For the aircraft, the impedance will be defined along the platform axes; for the combat vehicle, it will be defined along the pitch system axes. In either case, it is assumed that only principal elements of the impedance matrix will be specified. If we define

$A = F$ for the aircraft, or

$A = H(x_{3H}, r_H)\ F$

for the combat vehicle, then we can write

$$Z_p = A\ Z_\ell\ A_t \tag{59}$$

for either configuration. Now, since Z_ℓ must be diagonal, it follows that the principal elements of Z_p are given by

$$\left(\frac{1}{k}\right)_p = \begin{bmatrix} a_{11}^2 & a_{12}^2 & \cdots & a_{16}^2 \\ a_{21}^2 & a_{22}^2 & & \vdots \\ \vdots & & & \vdots \\ a_{61}^2 & & \cdots & a_{66}^2 \end{bmatrix} \left(\frac{1}{k}\right)_\ell \tag{60}$$

where

$$\left(\frac{1}{k}\right)_p = \begin{bmatrix} 1/k_x \\ 1/k_y \\ 1/k_z \\ 1/k_\phi \\ 1/k_\theta \\ 1/k_\psi \end{bmatrix} \tag{61}$$

and

$$\left(\frac{1}{k}\right)_\ell = \begin{bmatrix} 1/k_1 \\ 1/k_2 \\ 1/k_3 \\ 1/k_4 \\ 1/k_5 \\ 1/k_6 \end{bmatrix} \tag{62}$$

If we define

$$K = \begin{bmatrix} a_{11}^2 & \cdots & a_{16}^2 \\ \vdots & & \vdots \\ a_{61}^2 & \cdots & a_{66}^2 \end{bmatrix} \tag{63}$$

in which the elements are equal to the square of the corresponding elements of the A matrix

$$k_{mn} = a^2_{mn} \tag{64}$$

then

$$\left(\frac{1}{k}\right)_p = K\left(\frac{1}{k}\right)_\ell \tag{65}$$

The actuator spring constants cannot be found simply by inverting the K matrix due to the symmetry of the triogonal system. As a result, the F matrix has a rank of only three, thereby limiting the number of specified spring constants to three. It is necessary to choose arbitrary relationships among the actuator spring constants to reduce the set of six equations to three, before the resulting matrix can be inverted.

In the neutral position, the triogonal system is symmetrical about three vertical planes, spaced 120° apart in yaw. The definition of the actuator numbering system is shown in figure 1. The platform attachment points are defined for actuator 1, while the gimbal attachment points are defined for actuator 3. If we define the 120° yaw transformation by

$$E = \begin{bmatrix} \cos\psi & \sin\psi & 0 \\ -\sin\psi & \cos\psi & 0 \\ 0 & 0 & 1 \end{bmatrix}_{\psi = 120°} = \begin{bmatrix} -\frac{1}{2} & \frac{1}{2}\sqrt{3} & 0 \\ -\frac{1}{2}\sqrt{3} & -\frac{1}{2} & 0 \\ 0 & 0 & 1 \end{bmatrix} \tag{66}$$

and the x-z plane image transformation by

$$R = \begin{bmatrix} 1 & 0 & 0 \\ 0 & -1 & 0 \\ 0 & 0 & 1 \end{bmatrix} \tag{67}$$

then, because of the symmetry, the following relations are obtained:

$$\left.\begin{aligned} a_4 &= Ra_1 \\ a_2 &= E'a_4 \\ a_5 &= Ra_2 = Ea_1 \\ a_3 &= E'a_1 \\ a_6 &= Ra_3 = Ea_4 \end{aligned}\right\} \tag{68}$$

$$\left.\begin{aligned}
\ell_4 &= R\ell_1 \\
\ell_2 &= E'\ell_4 \\
\ell_5 &= R\ell_2 = E\ell_1 \\
\ell_3 &= E'\ell_1 \\
\ell_6 &= R\ell_3 = E\ell_4
\end{aligned}\right\} \qquad (69)$$

The moment arms appearing in the triogonal transformation are given by

$$\left.\begin{aligned}
W(a_3)\ell_3 &= W(E'a_1)\ell_3 = E'W(a_1)\ell_1 \\
W(a_5)\ell_5 &= W(Ea_1)\ \ell_5 = E\ W(a_1)\ell_1 \\
W(a_2)\ell_2 &= W(E'a_4)\ell_2 = E'W(a_4)\ell_4 \\
W(a_6)\ell_6 &= W(Ea_4)\ \ell_6 = E\ W(a_4)\ell_4 \\
W(a_4)\ell_4 &= W(Ra_1)R\ell_1 = -RW(a_1)\ell_1
\end{aligned}\right\} \qquad (70)$$

Thus

$$\ell_1 = \begin{pmatrix}\alpha\\ \beta\\ \gamma\end{pmatrix}_1 \qquad (71)$$

$$\ell_2 = \begin{pmatrix}\alpha\\ \beta\\ \gamma\end{pmatrix}_2 = E'R\begin{pmatrix}\alpha\\ \beta\\ \gamma\end{pmatrix}_1 = \begin{bmatrix}-\frac{1}{2}\alpha + \frac{1}{2}\sqrt{3}\beta\\ \frac{1}{2}\sqrt{3}\alpha + \frac{1}{2}\beta\\ \gamma\end{bmatrix} \qquad (72)$$

$$\ell_3 = \begin{pmatrix}\alpha\\ \beta\\ \gamma\end{pmatrix}_3 = E'\begin{pmatrix}\alpha\\ \beta\\ \gamma\end{pmatrix}_1 = \begin{bmatrix}-\frac{1}{2}\alpha - \frac{1}{2}\sqrt{3}\beta\\ \frac{1}{2}\sqrt{3}\alpha - \frac{1}{2}\beta\\ \gamma\end{bmatrix} \qquad (73)$$

$$\ell_4 = \begin{pmatrix}\alpha\\ \beta\\ \gamma\end{pmatrix}_4 = R\begin{pmatrix}\alpha\\ \beta\\ \gamma\end{pmatrix}_1 = \begin{pmatrix}\alpha\\ -\beta\\ \gamma\end{pmatrix} \qquad (74)$$

$$\ell_5 = \begin{pmatrix}\alpha\\ \beta\\ \gamma\end{pmatrix}_5 = E\begin{pmatrix}\alpha\\ \beta\\ \gamma\end{pmatrix}_1 = \begin{bmatrix}-\frac{1}{2}\alpha + \frac{1}{2}\sqrt{3}\,\beta\\ -\frac{1}{2}\sqrt{3}\,\alpha - \frac{1}{2}\beta\\ \gamma\end{bmatrix} \tag{75}$$

$$\ell_6 = \begin{pmatrix}\alpha\\ \beta\\ \gamma\end{pmatrix}_6 = ER\begin{pmatrix}\alpha\\ \beta\\ \gamma\end{pmatrix}_1 = \begin{bmatrix}-\frac{1}{2}\alpha - \frac{1}{2}\sqrt{3}\,\beta\\ -\frac{1}{2}\sqrt{3}\,\alpha + \frac{1}{2}\beta\\ \gamma\end{bmatrix} \tag{76}$$

and

$$\begin{pmatrix}\lambda\\ \mu\\ \nu\end{pmatrix}_2 = -E'R\begin{pmatrix}\lambda\\ \mu\\ \nu\end{pmatrix}_1 = \begin{bmatrix}\frac{1}{2}\lambda - \frac{1}{2}\sqrt{3}\,\mu\\ -\frac{1}{2}\sqrt{3}\,\lambda - \frac{1}{2}\mu\\ -\nu\end{bmatrix} \tag{77}$$

$$\begin{pmatrix}\lambda\\ \mu\\ \nu\end{pmatrix}_3 = E'\begin{pmatrix}\lambda\\ \mu\\ \nu\end{pmatrix}_1 = \begin{bmatrix}-\frac{1}{2}\lambda - \frac{1}{2}\sqrt{3}\,\mu\\ \frac{1}{2}\sqrt{3}\,\lambda - \frac{1}{2}\mu\\ \nu\end{bmatrix} \tag{78}$$

$$\begin{pmatrix}\lambda\\ \mu\\ \nu\end{pmatrix}_4 = -R\begin{pmatrix}\lambda\\ \mu\\ \nu\end{pmatrix}_1 = \begin{pmatrix}-\lambda\\ \mu\\ -\nu\end{pmatrix} \tag{79}$$

$$\begin{pmatrix}\lambda\\ \mu\\ \nu\end{pmatrix}_5 = E\begin{pmatrix}\lambda\\ \mu\\ \nu\end{pmatrix}_1 = \begin{bmatrix}-\frac{1}{2}\lambda + \frac{1}{2}\sqrt{3}\,\mu\\ -\frac{1}{2}\sqrt{3}\,\lambda - \frac{1}{2}\mu\\ \nu\end{bmatrix} \tag{80}$$

$$\begin{pmatrix}\lambda\\ \mu\\ \nu\end{pmatrix}_6 = -ER\begin{pmatrix}\lambda\\ \mu\\ \nu\end{pmatrix}_1 = \begin{bmatrix}\frac{1}{2}\lambda + \frac{1}{2}\sqrt{3}\,\mu\\ \frac{1}{2}\sqrt{3}\,\lambda - \frac{1}{2}\mu\\ -\nu\end{bmatrix} \tag{81}$$

Then, the triogonal transformation and its inverse are given by

$$
F' = \left[\begin{array}{cc|c|cc|c}
\alpha & \beta & \gamma & \lambda & \mu & \nu \\
-\frac{1}{2}(\alpha-\sqrt{3}\beta) & \frac{1}{2}(\sqrt{3}\alpha+\beta) & \gamma & \frac{1}{2}(\lambda-\sqrt{3}\mu) & -\frac{1}{2}(\sqrt{3}\lambda+\mu) & -\nu \\
-\frac{1}{2}(\alpha+\sqrt{3}\beta) & \frac{1}{2}(\sqrt{3}\alpha-\beta) & \gamma & -\frac{1}{2}(\lambda+\sqrt{3}\mu) & \frac{1}{2}(\sqrt{3}\lambda-\mu) & \nu \\
\hline
\alpha & -\beta & \gamma & -\lambda & \mu & -\nu \\
-\frac{1}{2}(\alpha-\sqrt{3}\beta) & -\frac{1}{2}(\sqrt{3}\alpha+\beta) & \gamma & -\frac{1}{2}(\lambda-\sqrt{3}\mu) & -\frac{1}{2}(\sqrt{3}\lambda+\mu) & \nu \\
-\frac{1}{2}(\alpha+\sqrt{3}\beta) & -\frac{1}{2}(\sqrt{3}\alpha-\beta) & \gamma & \frac{1}{2}(\lambda+\sqrt{3}\mu) & \frac{1}{2}(\sqrt{3}\lambda-\mu) & -\nu
\end{array}\right] \tag{82}
$$

$$
F = -\frac{1}{6\gamma\nu}\left[\begin{array}{c|c|c|c|c|c}
2\lambda & -(\lambda-\sqrt{3}\mu) & -(\lambda+\sqrt{3}\mu) & 2\lambda & -(\lambda-\sqrt{3}\mu) & -(\lambda+\sqrt{3}\mu) \\
2\mu & (\sqrt{3}\lambda+\mu) & (\sqrt{3}\lambda-\mu) & -2\mu & -(\sqrt{3}\lambda+\mu) & -(\sqrt{3}\lambda-\mu) \\
-\nu & -\nu & -\nu & -\nu & -\nu & -\nu \\
\hline
2\alpha & (\alpha-\sqrt{3}\beta) & -(\alpha+\sqrt{3}\beta) & -2\alpha & -(\alpha-\sqrt{3}\beta) & (\alpha+\sqrt{3}\beta) \\
2\beta & -(\sqrt{3}\alpha+\beta) & (\sqrt{3}\alpha-\beta) & 2\beta & -(\sqrt{3}\alpha+\beta) & (\sqrt{3}\alpha-\beta) \\
-\gamma & \gamma & -\gamma & \gamma & -\gamma & \gamma
\end{array}\right] \tag{83}
$$

If we let

$$
F = \left[\begin{array}{c|c}
F_{11} & F_{12} \\
\hline
F_{21} & F_{22}
\end{array}\right] \tag{84}
$$

it is seen that

$$F_{12} = \begin{bmatrix} 1 & 0 & 0 \\ 0. & -1 & 0 \\ 0 & 0 & 1 \end{bmatrix} F_{11} = RF_{11} \tag{85}$$

$$F_{22} = - \begin{bmatrix} 1 & 0 & 0 \\ 0 & -1 & 0 \\ 0 & 0 & 1 \end{bmatrix} F_{21} = - RF_{21} \tag{86}$$

Since, when specifying the principal elements of the impedance matrix, the spring constant matrix, K, is obtained by squaring the elements of the F matrix, it follows that

$$K = \left[\begin{array}{c|c} K_{11} & K_{11} \\ \hline K_{21} & K_{21} \end{array}\right] \tag{87}$$

Since the last three columns of K are equal to the first three, its rank is three, and only three of the desired spring constants can be specified.

$$\left(\frac{1}{k}\right)_p = K \left(\frac{1}{k}\right)_\ell \tag{88}$$

$$\left[\begin{array}{c} 1/k_x \\ 1/k_y \\ 1/k_z \\ \hline 1/k_\phi \\ 1/k_\theta \\ 1/k_\psi \end{array}\right] = \left[\begin{array}{c} K_{11} \\ \hline K_{21} \end{array}\right] \times \begin{bmatrix} (1/k_1 + 1/k_4) \\ (1/k_2 + 1/k_5) \\ (1/k_3 + 1/k_6) \end{bmatrix} \tag{89}$$

Thus, the sum of the reciprocal spring constants for symmetrical actuators can be found from the three specified spring constants at the platform axes. It would be logical to retain the symmetry about the x-z plane by making $k_1 = k_4$, $k_2 = k_5$, and $k_3 = k_6$, but this is not necessary. By doing this, several of the cross coupling terms can be made zero.

Examination of the six rows of the 6 x 3 matrix shows that the 3 x 3 matrices, K_{11} and K_{21}, are both singular. Thus, the three specified spring constants must be a combination of linear and angular constants. Any three of the six rows can be chosen, which do not result in a singular matrix. The only pairs that cannot be chosen are the z and ψ constants, the x and y constants when combined with either the z or ψ constant, or the ϕ and θ constants when combined with either the z or ψ constant. The possible combinations are listed below.

x, θ, z

ϕ, y, ψ

x, θ, ψ

ϕ, y, z

x, ϕ, z

x, ϕ, ψ

y, θ, z

y, θ, ψ

x, y, ϕ

x, y, θ

x, ϕ, θ

y, ϕ, θ

Of these, it is presumed that one of the desired constants will be k_x. This reduces the list to

x, θ, z

x, θ, ψ

x, ϕ, z

x, ϕ, ψ

x, y, ϕ

x, y, θ

x, ϕ, θ

The first two of these are orthogonal, the others lie in either the x-z or x-y plane. The first two have been evaluated. They are as follows. If we let

$$\begin{bmatrix} 1/k_x \\ 1/k_\theta \\ 1/k_z \end{bmatrix} = K_1 \begin{bmatrix} 1/k_1 + 1/k_4 \\ 1/k_2 + 1/k_5 \\ 1/k_3 + 1/k_6 \end{bmatrix} \tag{90}$$

and

$$\begin{bmatrix} 1/k_x \\ 1/k_\theta \\ 1/k_\psi \end{bmatrix} = K_2 \begin{bmatrix} 1/k_1 + 1/k_4 \\ 1/k_2 + 1/k_5 \\ 1/k_3 + 1/k_6 \end{bmatrix} \tag{91}$$

then

$$K_1 = \frac{1}{36(\gamma\nu)^2} \begin{bmatrix} 4\lambda^2 & (\lambda-\sqrt{3}\mu)^2 & (\lambda+\sqrt{3}\mu)^2 \\ 4\beta^2 & (\sqrt{3}\alpha+\beta)^2 & (\sqrt{3}\alpha-\beta)^2 \\ \nu^2 & \nu^2 & \nu^2 \end{bmatrix} \tag{92}$$

and

$$K_2 = \frac{1}{36(\gamma\nu)^2} \begin{bmatrix} 4\lambda^2 & (\lambda-\sqrt{3}\mu)^2 & (\lambda+(\sqrt{3}\mu)^2 \\ 4\beta^2 & (\sqrt{3}\alpha+\beta)^2 & (\sqrt{3}\alpha-\beta)^2 \\ \gamma^2 & \gamma^2 & \gamma^2 \end{bmatrix} \tag{93}$$

The inverse of K_1 is

$$K_1' = \frac{3\gamma\nu}{(\alpha\mu-\beta\lambda)} \begin{bmatrix} 4\alpha\beta & 4\lambda\mu & \dfrac{4\gamma(3\alpha\mu+\beta\lambda)}{\nu} \\ (\sqrt{3}\alpha+\beta)(\alpha-\sqrt{3}\beta) & (\sqrt{3}\lambda+\mu)(\lambda-\sqrt{3}\mu) & \dfrac{4\gamma[\sqrt{3}(\alpha\lambda-\beta\mu) - 2\beta\lambda]}{\nu} \\ -(\sqrt{3}\alpha-\beta)(\alpha+\sqrt{3}\beta) & -(\sqrt{3}\lambda-\mu)(\lambda+\sqrt{3}\mu) & -\dfrac{4\gamma[\sqrt{3}(\alpha\lambda-\beta\mu) + \beta\lambda]}{\nu} \end{bmatrix} \tag{94}$$

K_2' is identical, except that γ is replaced by ν and ν by γ.

The above relations provide the necessary equations to determine the neutral spring constants when employing the aircraft configuration. For the combat vehicle, the attachment point is further extended along the platform z-axis, and the attachment coordinate system is rotated through a pitch angle, θ_H. The extension along the z-axis does not alter any of the general conclusions that have been made; there is already an extension of 10 inches below the pivot point

plane for the aircraft attachment platform. Thus, neglecting the pitch angle, the rank of the K matrix is still three. Of course, the numerical values are affected by the extension. These can be corrected by assuming a new value of a, the platform pivot location, which will affect the values of λ, μ, and ν, or the F matrix can be premultiplied by the quantity

$$\left[\begin{array}{c|c} 1 & -W(E'_H r_H) \\ \hline 0 & 1 \end{array}\right] \tag{95}$$

$E'r_H$ is the displacement of the pitch system origin from the platform system origin measured in platform coordinates, and is given by

$$E'_H \, r_H = \begin{bmatrix} 0 \\ 0 \\ z_H \end{bmatrix} \tag{96}$$

Thus

$$-W \, (E'_H \, r_H) = z_H \begin{bmatrix} 0 & 1 & 0 \\ -1 & 0 & 0 \\ 0 & 0 & 0 \end{bmatrix} \tag{97}$$

Premultiplying the F matrix by this quantity is equivalent to modifying the pivot location point.

To include the pitch angle, the A matrix is formed by multiplying by the angular conversion matrix.

$$A = \left[\begin{array}{c|c} E_H & 0 \\ \hline 0 & E_H \end{array}\right] \left[\begin{array}{c|c} 1 & -W(E'_H \, r_H) \\ \hline 0 & 1 \end{array}\right] F \tag{98}$$

If we assume that the z extension to the pitch system origin is included in the definition of F, then

$$A = \left[\begin{array}{cc|cc} E_H & F_{11} & E_H & F_{12} \\ \hline E_H & F_{21} & E_H & F_{22} \end{array}\right] \tag{99}$$

Since the relations between F_{11} and F_{12}, and between F_{21} and F_{22} still hold

$$F_{12} = RF_{11} \tag{100}$$

$$F_{22} = - RF_{21} \tag{101}$$

and, since

$$E_H R = RE_H \tag{102}$$

for pitch motion, it follows that

$$A = \left[\begin{array}{c|c} A_{11} & RA_{11} \\ \hline A_{21} & -RA_{21} \end{array}\right] \tag{103}$$

The K matrix is again formed by squaring the elements of the A matrix, so that its rank is still three. The last three columns of the A matrix are the same as the first three, except for sign, which disappears when the elements are squared. Thus, as long as the origin of the attachment system to the vehicle lies on the z-axis of the platform system, and the roll and yaw angles of the attachment system relative to the triogonal system are zero, only three principal elements can be specified.

If we assume that

$$k_1 = k_4 \tag{104}$$

$$k_2 = k_5 \tag{105}$$

and

$$k_3 = k_6 \tag{106}$$

then

$$\begin{bmatrix} 1/k_x \\ 1/k_\theta \\ 1/k_z \end{bmatrix} = 2K_1 \begin{bmatrix} 1/k_1 \\ 1/k_2 \\ 1/k_3 \end{bmatrix} \tag{107}$$

Similar expressions hold for other choices of specified constants. Then

$$\begin{bmatrix} \frac{1}{k_1} \\ \frac{1}{k_2} \\ \frac{1}{k_3} \end{bmatrix} = \begin{bmatrix} \frac{1}{k_4} \\ \frac{1}{k_5} \\ \frac{1}{k_6} \end{bmatrix} = \frac{1}{2} K_1' \begin{bmatrix} 1/k_x \\ 1/k_\theta \\ 1/k_z \end{bmatrix} \tag{108}$$

These equations can now be used to determine the actuator spring constants. It may still be necessary to restrict the choice of specified constants to obtain physically realizable results.

Actuator Gravitational Forces

To find the actuator unextended lengths, it is necessary to subtract from the values found in equations 1-16, the deflection due to supporting the weight of the aircraft The gravitational force is exerted in the earth axes z-direction at the origin of the aircraft coordinates. This must be resolved into the platform system to find the actuator forces.

The vehicle axes are tied to the earth axes through the gimbal coordinate system. The relationship between the earth and the gimbal systems will be defined as

$$x_{1G} = E(x_{3G})\, x_{1E} - r_G \tag{109}$$

Because of the physical construction of the gimbal system, it is appropriate to define the gimbal Euler angles in the reverse order as

$$E(x_{3G}) = E_1\,(\psi_G)\cdot E_2\,(\theta_G) \tag{110}$$

x_{3G} then defines the gimbal angles directly and

$$E(x_{3G}) = \begin{bmatrix} (\cos\psi_G \cdot \cos\theta_G) & \sin\psi_G & (-\cos\psi_G \cdot \sin\theta_G) \\ (-\sin\psi_G \cdot \cos\theta_G) & \cos\theta_G & (\sin\psi_G \cdot \sin\theta_G) \\ \sin\theta_G & 0 & \cos\theta_G \end{bmatrix} \tag{111}$$

The gravitational force in the vehicle system is then equal to

$$g_v = E(x_{3v})\, E(x_{3H})\, E(x_{3p})\, E(x_{3G})\, g_e \tag{112}$$

where

$$g_e = g\begin{pmatrix}0\\0\\1\end{pmatrix} \tag{113}$$

This is transformed into forces and moments about the platform axes equal to

$$g_p = H_t\ (x_{3H}, r_H)\ H_t\ (x_{3v}, r_v)\begin{pmatrix}g_v\\--\\0\end{pmatrix} \tag{114}$$

Finally, resolved along the actuators, the forces in the actuators are

$$f_\ell = mF_t H_t\ (x_{3H}, r_H)\ H_t\ (x_{3v}, r_v)\begin{pmatrix}g_v\\--\\0\end{pmatrix} \tag{115}$$

The actuator extensions are then

$$\Delta\ell = L_\ell\ f_\ell \tag{116}$$

The actuator extensions can also be expressed as

$$\Delta\ell = [f_\ell]\left(\frac{1}{k}\right)_\ell \tag{117}$$

where $[f_\ell]$ is the diagonal matrix formed from the column matrix, f_ℓ.

If we assume

$$E(x_{3v}) = 1 \tag{118}$$

$$E(x_{3p}) = 1 \tag{119}$$

$$E'\ (x_{3H})\ r_H = \begin{bmatrix}0\\0\\z_H\end{bmatrix} \tag{120}$$

$$r_v = \begin{bmatrix}x_v\\y_v\\z_v\end{bmatrix} \tag{121}$$

and making use of the relation

$$E' W(r) E = W(E' r) \qquad (122)$$

the above equations reduce to

$$g_p = \left[\frac{1}{W \left\{ E'_H (r_H + r_v) \right\}} \right] g_G \qquad (123)$$

where

$$g_G = g \begin{bmatrix} -\cos\psi_G \sin\theta_G \\ \sin\psi_G \sin\theta_G \\ \cos\theta_G \end{bmatrix} \qquad (124)$$

If we let

$$r = E'_H (r_H + r_v) \qquad (125)$$

then

$$r = \begin{bmatrix} x_v \cos\theta_H + z_v \sin\theta_H \\ y_v \\ z_H - x_v \sin\theta_H + z_v \cos\theta_H \end{bmatrix} \qquad (126)$$

Thus, it is necessary to resolve the gimbal and pitch angles into sine and cosine components and to perform the indicated multiplications to find the gravitational forces and moments about the platform axes. These can then be summed, using the coefficients given by the elements of the F matrix to find the actuator forces, and then divided by the spring constants to find the actuator extensions.

In the calculation of the displacement, r, an arbitrary value of the pitch angle, θ_H, has been assumed. This calculation can be made in real time to account for the instantaneous pitch angle of the combat vehicle. It still remains to be determined if the instantaneous pitch angle can be used for the calculation of spring constants, since real time matrix inversion may be required. Possibly, for the combat vehicle, spring constants will be calculated for zero pitch angle and variations from these values will be calculated in real time on a linearized basis. To be consistent, the gravitational forces will also be calculated for zero pitch angle, and the variations again calculated on a linearized basis about this point. The displacement then becomes simply

$$r = \begin{bmatrix} x_v \\ y_v \\ z_v + z_H \end{bmatrix} \tag{127}$$

For the aircraft, spring constants are to be specified at the platform system, which does not contain the fixed pitch angle built into the aircraft. In this case, the pitch angle will be included in the calculation of gravitational forces, since it does not vary with time.

Actuator Mass Loads

To improve the performance of the adaptive loops used to program the actuator spring constants, it is desirable to input the effective mass loads on each of the actuators. These loads are found from the linearized equations of the aircraft motion.

Since the x-z plane in the aircraft system will normally be a plane of symmetry, the cross moments of inertia to the y-axis will be zero. The inertia matrix, under these conditions, simplifies to

$$J = \begin{bmatrix} J_{xx} & 0 & J_{xz} \\ 0 & J_{yy} & 0 \\ J_{xz} & 0 & J_{zz} \end{bmatrix} \tag{128}$$

The mass matrix is defined as

$$m = \begin{bmatrix} m & 0 & 0 \\ 0 & m & 0 \\ 0 & 0 & m \end{bmatrix} \tag{129}$$

The moments of inertia should be the effective moments, including the effects of the tail boom simulator and the stability augmentation system if used for the aircraft.

The vehicle motion is defined by summing external forces and moments and equating these to the rates of momentum change by

$$f_v = m \left\{ \ddot{x}_1 + W(\dot{x}_2)\, \dot{x}_1 - E(x_3)\, g_e \right\} \tag{130}$$

$$(m)_v = J\,\ddot{x}_2 + W\,(\dot{x}_2)\,J\,\dot{x}_2 \tag{131}$$

$$\dot{x}_3 = G\,(x_3)\,\dot{x}_2 \tag{132}$$

where the Euler angles and velocities are referenced to the earth system.

By the use of the following transformations,

$$\left(\frac{f}{m}\right)_v = H_t'\,(x_{3v}, r_v)\,H_t'\,(x_{3H}, r_H)\left(\frac{f}{m}\right)_p \tag{133}$$

$$f_\ell = F_t\left(\frac{f}{m}\right)_p \tag{134}$$

$$\left(\frac{\dot{x}_1}{\dot{x}_2}\right)_p = H'(x_{3H}, r_H)\,H'(x_{3v}, r_v)\left(\frac{\dot{x}_1}{\dot{x}_2}\right)_v \tag{135}$$

and

$$\dot{\ell} = F'\left(\frac{\dot{x}_1}{\dot{x}_2}\right)_p \tag{136}$$

the actuator forces are given by

$$\begin{aligned} f_\ell = & \left\{F_t\,H_{H_t}\,H_{v_t}\,m_v\,H_v\,H_H\,F\right\}\ddot{\ell} + \\ & + F_t\,H_{H_t}\,H_{v_t}\,m_v\,\frac{\partial}{\partial t}\left\{H_v\,H_H\,F\right\}\dot{\ell} + \\ & + F_t\,H_{H_t}\,H_{v_t}\left[\begin{array}{c|c} W(\dot{x}_2) & 0 \\ \hline 0 & W(\dot{x}_2)\end{array}\right] m_v\,H_v\,H_H\,F\dot{\ell} \\ & - F_t\,H_{H_t}\,H_{v_t}\left[\begin{array}{c} E(x_3)g_e \\ \hline 0 \end{array}\right] \end{aligned} \tag{137}$$

Thus, the effective mass loads, for small signals, are given by the diagonal elements of

$$m_\ell = F_t \, H_{H_t} \, H_{v_t} \, m_v \, H_v \, H_H \, F \tag{138}$$

where

$$m_v = \left[\begin{array}{c|c} m & 0 \\ \hline 0 & J \end{array}\right] \tag{139}$$

For

$$E(x_{3v}) = 1 \tag{140}$$

and

$$r = E_H' \, (r_H + r_v) = \begin{pmatrix} x \\ 0 \\ z \end{pmatrix} \tag{141}$$

this reduces to

$$\begin{aligned}(m_\ell)_{11} &= \left\{F_{11_t} + F_{21_t} \, W\,(r)\right\} m \left\{F_{11} - W\,(r)\,F_{21}\right\} + \\ &\quad + F_{21_t} \left\{E_H' \, J \, E_H\right\} F_{21}\end{aligned} \tag{142}$$

$$\begin{aligned}(m_\ell)_{12} &= \left\{F_{11_t} + F_{21_t} \, W\,(r)\right\} \dot{m} \, R \left\{F_{11} - W\,(r)\,F_{21}\right\} \\ &\quad - F_{21_t} \left\{E_H' \, JE_H \, R\right\} F_{21}\end{aligned} \tag{143}$$

$$(m_\ell)_{22} = (m_\ell)_{11} \tag{144}$$

$$(m_\ell)_{21} = (m_\ell)_{12} \tag{145}$$

These results are valid if the vehicle center of mass lies in the x-z plane of the triogonal system.

The mass load of the actuator system upon itself must then be added to the mass load of the vehicle. The effective mass of the actuators is derived in appendix B. These values are then used in the computer program to calculate the mass constants for each actuator setting of the simulator.

Tail Boom Actuator Force Command

The tail boom actuator must provide a moment about the aircraft CG equivalent to that normally present due to the tail boom inertia. If the inertia is to be increased by an amount, ΔJ_z, a moment equal to

$$m = \Delta J_z \ddot{\psi} \tag{146}$$

must be applied. The force applied by the tail boom actuator is then

$$f_{TB} = \frac{\Delta J_z}{r_{TB}} \ddot{\psi} \tag{147}$$

where r_{TB} is the moment arm of the actuator.

Linear Coefficients

Linearization of Equations

For the combat vehicle, the relationship between the triogonal system and the vehicle center of mass varies with time due to the yaw angle input to the triogonal system and the pitch angle variations introduced between the platform and vehicle. For this reason, the adaptive servo inputs (spring constant, and unloaded extension) must be varied in real time. This is not necessary for the aircraft. Initially, variations will be investigated on a linearized basis, because of the relatively small angles involved.

Incremental Gravitational Loading

The gravitational vector, at the vehicle center of mass, in vehicle coordinates is

$$g_v = E(x_{3v})\ E(x_{3H})\ E(x_{3p})\ E(x_{3G})\ g_e \tag{148}$$

where

$$g_e = g \begin{pmatrix} 0 \\ 0 \\ 1 \end{pmatrix} \tag{149}$$

The forces provided by the actuators to support the vehicle are then

$$f_\ell = mF_t H_t(x_{3H}) H_t(x_{3v}) \left(\frac{g_v}{0}\right) \tag{150}$$

Since the effects of gimbal angle variations are included in the calculation of g_v, linearization is only required for the triogonal yaw angle, ψ_p, and the pitch angle, θ_H. The time derivative of the actuator forces, neglecting gimbal angle effects, is then

$$\dot{f}_\ell = m\dot{F}_t H_{Ht} H_{vt} \left(\frac{g_v}{0}\right) + mF_t \dot{H}_{Ht} H_{vt} \left(\frac{g_v}{0}\right)$$

$$+ mF_t H_{Ht} H_{vt} \left(\frac{\dot{g}_v}{0}\right) \tag{151}$$

where

$$\dot{g}_v = E_v \dot{E}_H E_p E_G g_e + E_v E_H \dot{E}_p E_G g_e \tag{152}$$

$$\dot{F}_t = \left(\frac{\partial F_t}{\partial \psi_p}\right) \dot{\psi}_p \tag{153}$$

$$\dot{H}_{Ht} = \left(\frac{\partial H_{Ht}}{\partial \theta_H}\right) \dot{\theta}_H = H_{Ht} \left[\begin{array}{c|c} W\begin{pmatrix}0\\1\\0\end{pmatrix} & 0 \\ \hline 0 & W\begin{pmatrix}0\\1\\0\end{pmatrix} \end{array}\right] \dot{\theta}_H \tag{154}$$

$$\dot{E}_H = -W(\dot{x}_{2H}) E_H = -W\begin{pmatrix}0\\1\\0\end{pmatrix} E_H \dot{\theta}_H \tag{155}$$

$$\dot{E}_p = -W(\dot{x}_{2p}) E_p = -W\begin{pmatrix}0\\1\\0\end{pmatrix} E_p \dot{\psi}_p \tag{156}$$

Since the linearization is performed about the neutral position, then

$$E_p = E_H = 1 \tag{157}$$

Also, for convenience, the neutral pitch angle will be chosen so that the pitch system axes are parallel to the vehicle axes. Then

$$E_v = 1 \tag{158}$$

and

$$\dot{g}_v = -W \begin{pmatrix} 0 \\ 1 \\ 0 \end{pmatrix} g_G \dot{\theta}_H - W \begin{pmatrix} 0 \\ 0 \\ 1 \end{pmatrix} g_G \dot{\psi}_P \tag{159}$$

$$\dot{H}_{Ht} = \left[\begin{array}{c|c} 1 & 0 \\ \hline W(r_H) & 1 \end{array} \right] \left[\begin{array}{c|c} W \begin{pmatrix} 0 \\ 1 \\ 0 \end{pmatrix} & 0 \\ \hline 0 & W \begin{pmatrix} 0 \\ 1 \\ 0 \end{pmatrix} \end{array} \right] \dot{\theta}_H \tag{160}$$

The derivative of the forces is then

$$\dot{f}_\ell = m \left(\frac{\partial F_t}{\partial \psi p} \right) \left[\begin{array}{c} 1 \\ \hline W(r_H + r_v) \end{array} \right] g_G \dot{\psi}_p + mF_t \left[\begin{array}{c} 0 \\ \hline W \begin{pmatrix} 3_v \\ 0 \\ -x_v \end{pmatrix} \end{array} \right] g_G \dot{\theta}_H +$$

$$- mF_t \left[\begin{array}{c} 1 \\ \hline W(r_H + r_v) \end{array} \right] W \begin{pmatrix} 0 \\ 0 \\ 1 \end{pmatrix} g_G \dot{\psi}_p \tag{161}$$

The gravitational components in the gimbal system, g_G, and the components referred to the platform

$$g_p = \left[\begin{array}{c} 1 \\ \hline W(r_H + r_v) \end{array} \right] g_G \tag{162}$$

have been calculated for the static forces, f_ℓ. Thus, it is only necessary to sum these with the proper scale factors as determined by the elements of F and $\frac{\partial F}{\partial \psi_p}$ to find the coefficients which, when multiplied by the yaw and pitch angle variations, will give the variations in actuator forces.

The derivative of the triogonal transformation is obtained from the derivative of its inverse

$$\frac{\partial F}{\partial \psi_p} = -F \left(\frac{\partial F'}{\partial \psi_p} \right) F \tag{163}$$

It cannot be obtained directly, since an explicit expression for F, except in the neutral position, is too cumbersome. Since the n-th column of $F_t{}'$ is equal to

$$(F_t')_n = \left[\begin{array}{c} \begin{pmatrix} \alpha \\ \beta \\ \gamma \end{pmatrix}_n \\ \hline W(a_n) \begin{pmatrix} \alpha \\ \beta \\ \gamma \end{pmatrix}_n \end{array}\right] \tag{164}$$

and the derivative of the direction cosines is

$$\begin{pmatrix} \dot\alpha \\ \beta \\ \gamma \end{pmatrix}_n = -W^2 \begin{pmatrix} \alpha \\ \beta \\ \gamma \end{pmatrix}_n \frac{\dot\ell_n}{\ell_o} \tag{165}$$

the derivative of the n-th column of F_t' is

$$(\dot F_t')_n = -\frac{1}{\ell o} \left[\begin{array}{c} W^2 \begin{pmatrix} \alpha \\ \beta \\ \gamma \end{pmatrix}_n \dot\ell_n \\ \hline W(a_n)\ W^2 \begin{pmatrix} \alpha \\ \beta \\ \gamma \end{pmatrix}_n \dot\ell_n \end{array}\right] \tag{166}$$

The velocity, $\dot\ell_n$, is the vector velocity of the n-th actuator, so

$$\dot\ell_n = \dot x_{1p} - W(a_n)\dot x_{2p} = \left[\begin{array}{c|c} 1 & -W(a_n) \end{array}\right] \begin{pmatrix} \dot x_{1p} \\ \hline \dot x_{2p} \end{pmatrix} \tag{167}$$

Thus

$$(\dot F_t')_n = -\frac{1}{\ell o} \left[\begin{array}{c|c} W^2 \begin{pmatrix} \alpha \\ \beta \\ \gamma \end{pmatrix}_n & -W^2 \begin{pmatrix} \alpha \\ \beta \\ \gamma \end{pmatrix}_n W(a_n) \\ \hline W(a_n)W^2 \begin{pmatrix} \alpha \\ \beta \\ \gamma \end{pmatrix}_n & -W(a_n)W^2 \begin{pmatrix} \alpha \\ \beta \\ \gamma \end{pmatrix}_n W(a_n) \end{array}\right] \begin{pmatrix} \dot x_1 \\ \hline \dot x_2 \end{pmatrix}_p \tag{168}$$

The direction cosines of the six actuators, in the neutral position, are given in terms of those for actuator number one by equations 71 thru 76.

After evaluating the submatrices of $(\dot F_t')_n$ we find

$$\frac{\partial (F_t')_2}{\partial \begin{pmatrix} x_1 \\ \hline x_2 \end{pmatrix}_p} = \left[\begin{array}{c|c} E'R & 0 \\ \hline 0 & -E'R \end{array}\right] \frac{\partial (F_t')_1}{\partial \begin{pmatrix} x_1 \\ \hline x_2 \end{pmatrix}_p} \left[\begin{array}{c|c} RE & 0 \\ \hline 0 & -RE \end{array}\right] \tag{169}$$

$$\frac{\partial (F_t')_3}{\partial \begin{pmatrix} x_1 \\ \hline x_2 \end{pmatrix}_p} = \left[\begin{array}{c|c} E' & 0 \\ \hline 0 & E' \end{array}\right] \frac{\partial (F_t')_1}{\partial \begin{pmatrix} x_1 \\ \hline x_2 \end{pmatrix}_p} \left[\begin{array}{c|c} E & 0 \\ \hline 0 & E \end{array}\right] \tag{170}$$

$$\frac{\partial (F_t')_4}{\partial \begin{pmatrix} x_1 \\ \hline x_2 \end{pmatrix}_p} = \left[\begin{array}{c|c} R & 0 \\ \hline 0 & -R \end{array}\right] \frac{\partial (F_t')_1}{\partial \begin{pmatrix} x_1 \\ \hline x_2 \end{pmatrix}_p} \left[\begin{array}{c|c} R & 0 \\ \hline 0 & -R \end{array}\right] \tag{171}$$

$$\frac{\partial (F_t')_5}{\partial \begin{pmatrix} x_1 \\ \hline x_2 \end{pmatrix}_p} = \left[\begin{array}{c|c} E & 0 \\ \hline 0 & E \end{array}\right] \frac{\partial (F_t')_1}{\partial \begin{pmatrix} x_1 \\ \hline x_2 \end{pmatrix}_p} \left[\begin{array}{c|c} E' & 0 \\ \hline 0 & E' \end{array}\right] \tag{172}$$

$$\frac{\partial (F_t')_6}{\partial \begin{pmatrix} x_1 \\ \hline x_2 \end{pmatrix}_p} = \left[\begin{array}{c|c} ER & 0 \\ \hline 0 & -ER \end{array}\right] \frac{\partial (F_t')_1}{\partial \begin{pmatrix} x_1 \\ \hline x_2 \end{pmatrix}_p} \left[\begin{array}{c|c} RE' & 0 \\ \hline 0 & -RE' \end{array}\right] \tag{173}$$

For pure yaw motion

$$\dot{x}_{1p} = 0 \tag{174}$$

and

$$\dot{x}_{2p} = \dot{\psi}_p \begin{pmatrix} 0 \\ 0 \\ 1 \end{pmatrix} \tag{175}$$

Since

$$E \begin{pmatrix} 0 \\ 0 \\ 1 \end{pmatrix} = \begin{pmatrix} 0 \\ 0 \\ 1 \end{pmatrix} \tag{176}$$

$$R \begin{pmatrix} 0 \\ 0 \\ 1 \end{pmatrix} = \begin{pmatrix} 0 \\ 0 \\ 1 \end{pmatrix} \tag{177}$$

the post multipliers can be dropped. Then, if we let

$$\frac{\partial (F_t')_1}{\partial \psi_p} = \left| \begin{array}{c} \delta_1 \\ \delta_2 \\ \delta_3 \\ \hline \delta_4 \\ \delta_5 \\ \delta_6 \end{array} \right| \tag{178}$$

the derivative of F' with respect to platform yaw is

$$\left(\frac{\partial F_t'}{\partial \psi_p} \right)_{11} = \begin{bmatrix} \delta_1 & 1/2(\delta_1 - \sqrt{3}\delta_2) & -1/2(\delta_1 + \sqrt{3}\delta_2) \\ \delta_2 & -1/2(\sqrt{3}\delta_1 + \delta_2) & 1/2(\sqrt{3}\delta_1 - \delta_2) \\ \delta_3 & -\delta_3 & \delta_3 \end{bmatrix} \tag{179}$$

$$\left(\frac{\partial F_t'}{\partial \psi_p} \right)_{12} = \begin{bmatrix} -\delta_1 & -1/2(\delta_1 - \sqrt{3}\delta_2) & 1/2(\delta_1 + \sqrt{3}\delta_2) \\ \delta_2 & -1/2(\sqrt{3}\delta_1 + \delta_2 & 1/2(\sqrt{3}\delta_1 - \delta_2) \\ -\delta_3 & \delta_3 & -\delta_3 \end{bmatrix} \tag{180}$$

$$\left(\frac{\partial F_t'}{\partial \psi_p} \right)_{21} = \begin{bmatrix} \delta_4 & -1/2(\delta_4 - \sqrt{3}\delta_5) & -1/2(\delta_4 + \sqrt{3}\delta_5) \\ \delta_5 & 1/2(\sqrt{3}\delta_4 + \delta_5) & 1/2(\sqrt{3}\delta_4 - \delta_5) \\ \delta_6 & \delta_6 & \delta_6 \end{bmatrix} \tag{181}$$

$$\left(\frac{\partial F_t'}{\partial \psi_p} \right)_{22} = \begin{bmatrix} \delta_4 & -1/2(\delta_4 - \sqrt{3}\delta_5) & -1/2(\delta_4 + \sqrt{3}\delta_5) \\ -\delta_5 & -1/2(\sqrt{3}\delta_4 + \delta_5) & -1/2(\sqrt{3}\delta_4 - \delta_5) \\ \delta_6 & \delta_6 & \delta_6 \end{bmatrix} \tag{182}$$

thus

$$\left(\frac{\partial F_t'}{\partial \psi_p} \right) = \left[\begin{array}{c|c} G_{11t} & -RG_{11t} \\ \hline G_{12t} & RG_{12t} \end{array} \right] \tag{183}$$

and

$$\left(\frac{\partial F'}{\partial \psi_p} \right) = \left[\begin{array}{c|c} G_{11} & G_{12} \\ \hline -G_{11}R & G_{12}R \end{array} \right] \tag{184}$$

The elements of this matrix are found from

$$\begin{pmatrix} \delta_1 \\ \delta_2 \\ \delta_3 \end{pmatrix} = \frac{1}{\ell o} \ W^2 \begin{pmatrix} \alpha \\ \beta \\ \gamma \end{pmatrix} W(a) \begin{pmatrix} 0 \\ 0 \\ 1 \end{pmatrix} \tag{185}$$

and

$$\begin{pmatrix} \delta_4 \\ \delta_5 \\ \delta_6 \end{pmatrix} = W(a) \begin{pmatrix} \delta_1 \\ \delta_2 \\ \delta_3 \end{pmatrix} \tag{186}$$

Thus

$$\begin{pmatrix} \delta_1 \\ \delta_2 \\ \delta_3 \end{pmatrix} = \frac{1}{\ell o} \begin{bmatrix} -a_x(\alpha\beta) - a_y(\beta^2 + \gamma^2) \\ a_x(\alpha^2 + \gamma^2) + a_y(\alpha\beta) \\ -a_x(\beta\gamma) + a_y(\alpha\gamma) \end{bmatrix} \tag{187}$$

$$\begin{pmatrix} \delta_4 \\ \delta_5 \\ \delta_6 \end{pmatrix} = \begin{bmatrix} a_y\delta_3 - a_z\delta_2 \\ a_z\delta_1 - a_x\delta_3 \\ a_x\delta_2 - a_y\delta_1 \end{bmatrix} \tag{188}$$

To find the derivative of the F matrix, it is now necessary to pre- and post-multiply this by F. If we let

$$G = \frac{\partial F'}{\partial \psi_p} \tag{189}$$

then

$$\frac{\partial F}{\partial \psi_p} = -FGF \tag{190}$$

The intermediate product, GF, is given by

$$J = GF = \left[\begin{array}{c|c} J_{11} & J_{12} \\ \hline -J_{12} & -J_{11} \end{array}\right] \tag{191}$$

where

$$J_{11} = \begin{bmatrix} j_{11} & j_{12} & 0 \\ -j_{12} & -j_{11} & j_{23} \\ 0 & -j_{23} & j_{11} \end{bmatrix} \tag{192}$$

and

$$J_{12} = \begin{bmatrix} -j_{23} & 0 & j_{16} \\ 0 & -j_{16} & 0 \\ j_{16} & 0 & j_{12} \end{bmatrix} \tag{193}$$

$$j_{11} = -\frac{3}{6\gamma\nu}\left[a_y\gamma\delta_1 - a_x\gamma\delta_2 + (a_y\alpha - a_x\beta)\delta_3\right] \tag{194}$$

$$j_{12} = -\frac{1}{6\gamma\nu}\left[-(2a_y + \sqrt{3}a_x)\gamma\delta_1 + \sqrt{3}a_y\gamma\delta_2 + \right.$$
$$\left. + \{(2a_y + \sqrt{3}a_x)\,\alpha - \sqrt{3}\,a_y\beta\}\delta_3\right] \tag{195}$$

$$j_{23} = \frac{1}{6\gamma\nu}\left[a_y\gamma\delta_1 + 3a_x\gamma\delta_2 - (a_y\alpha + 3a_x\beta)\delta_3\right] \tag{196}$$

$$j_{16} = -\frac{1}{6\gamma\nu}\left[-(2a_y - \sqrt{3}\,a_x)\gamma\delta_1 - \sqrt{3}a_y\gamma\delta_2 + \right.$$
$$\left. + \{(2a_y - \sqrt{3}a_x)\alpha + \sqrt{3}a_y\beta\}\delta_3\right] \tag{197}$$

The derivative of F is then

$$P = \frac{\partial F}{\partial \psi_p} = -\left[\begin{array}{c|c} F_{11} & RF_{11} \\ \hline F_{21} & -RF_{21} \end{array}\right]\left[\begin{array}{c|c} J_{11} & J_{12} \\ \hline -J_{12} & -J_{11} \end{array}\right] \tag{198}$$

or

$$P = \left[\begin{array}{c|c} P_{11} & -RP_{11} \\ \hline P_{21} & RP_{21} \end{array}\right] \tag{199}$$

where

$$P_{11} = -(F_{11}J_{11} - RF_{11}J_{12}) \tag{200}$$

and

$$P_{21} = -(F_{21}J_{11} + RF_{21}J_{12}) \tag{201}$$

These expressions can be evaluated using equations (67), (83) and (191) to give the components of P.

Incremental Changes in Spring Constants

Because of the symmetry of the triogonal system, it was necessary to assume an arbitrary relationship between symmetrical actuators. For convenience, they were made equal. It will also be convenient to retain this relationship for deviations from the neutral position, resulting from yaw and pitch angle inputs. If we let the three specified spring constants be

$$\left(\frac{1}{k}\right)_H = \begin{pmatrix} 1/k_x \\ 1/k_\theta \\ 1/k_z \end{pmatrix}_H \tag{202}$$

as measured in the pitch system, and the resultant three actuator spring constants be

$$\left(\frac{1}{k}\right)_\ell = \begin{pmatrix} 1/k_1 \\ 1/k_2 \\ 1/k_3 \end{pmatrix} \tag{203}$$

then, for this choice of specified constants

$$\left(\frac{1}{k}\right)_\ell = 1/2\ K_1{}'\left(\frac{1}{k}\right)_H \tag{204}$$

Similar expressions are obtained for other choices of specified constants. Since the specification is assumed to be along the pitch system axes, which are fixed

to the vehicle, the instantaneous pitch angle, as well as the triogonal yaw angle affects the actuator constants. The pitch angle transformation does not appear explicitly in the definition of K_1 since to do so might require real time inversion of this matrix. Instead, the neutral value of pitch angle has been assumed to be zero, for which the pitch system axes are parallel to the platform axes. To differentiate the above equation, the effect of pitch angle must be included. To do this, we can generalize the definition of the matrix K to include the pitch system transformation. With K given by equation 63

and

$$A = H_H \cdot F \tag{205}$$

It then follows that

$$\frac{\partial K}{\partial \theta_H} = 2 \begin{bmatrix} a_{11} \frac{\partial a_{11}}{\partial \theta H} & \cdots & a_{16} \frac{\partial a_{16}}{\partial \theta_H} \\ \vdots & & \vdots \\ a_{61} \frac{\partial a_{61}}{\partial \theta_H} & \cdots & a_{66} \frac{\partial a_{66}}{\partial \theta_H} \end{bmatrix} \tag{206}$$

and

$$\frac{\partial K}{\partial \theta_p} = 2 \begin{bmatrix} a_{11} \frac{\partial a_{11}}{\partial \psi_p} & \cdots & a_{16} \frac{\partial a_{16}}{\partial \psi_p} \\ \vdots & & \vdots \\ a_{61} \frac{\partial a_{61}}{\partial \psi_p} & \cdots & a_{66} \frac{\partial a_{66}}{\partial \psi_p} \end{bmatrix} \tag{207}$$

where

$$\frac{\partial A}{\partial \theta_H} = \frac{\partial H_H}{\partial \theta_H} F = - \left[\begin{array}{c|c} W \begin{pmatrix} 0 \\ 1 \\ 0 \end{pmatrix} & 0 \\ \hline 0 & W \begin{pmatrix} 0 \\ 1 \\ 0 \end{pmatrix} \end{array} \right] A \tag{208}$$

and

$$\frac{\partial A}{\partial \psi_p} = H_H \frac{\partial F}{\partial \psi_p} = H_H \left[\begin{array}{c|c} P_{11} & -RP_{11} \\ \hline P_{21} & RP_{21} \end{array}\right] \tag{209}$$

For variations in the pitch angle, we then have

$$\frac{\partial K}{\partial \theta_H} = 2 \left[\begin{array}{ccc|ccc} -a_{11}a_{31} & -a_{12}a_{32} & -a_{13}a_{33} & -a_{11}a_{31} & -a_{12}a_{32} & -a_{13}a_{33} \\ 0 & 0 & 0 & 0 & 0 & 0 \\ a_{11}a_{31} & a_{12}a_{32} & a_{13}a_{33} & a_{11}a_{31} & a_{12}a_{32} & a_{13}a_{33} \\ \hline -a_{41}a_{61} & -a_{42}a_{62} & -a_{43}a_{63} & -a_{41}a_{61} & -a_{42}a_{62} & -a_{43}a_{63} \\ 0 & 0 & 0 & 0 & 0 & 0 \\ a_{41}a_{61} & a_{42}a_{62} & a_{43}a_{63} & a_{41}a_{61} & a_{42}a_{62} & a_{43}a_{63} \end{array}\right] \tag{210}$$

The variation of the diagonal elements of the spring constant matrix as measured in the pitch system, due to pitch angle changes, is

$$\frac{\partial}{\partial \theta_H}\left(\frac{1}{k}\right)_H = \frac{\partial K}{\partial \theta_H}\left(\frac{1}{k}\right)_\ell + K \frac{\partial}{\partial \theta_H}\left(\frac{1}{k}\right)_\ell \tag{211}$$

Since the last three columns of both K and $\frac{\partial K}{\partial \theta_H}$ are equal to the first three columns, and the spring constants of the symmetrical actuators have been chosen equal, it follows that, for the three specified spring constants

$$\frac{\partial}{\partial \theta_H}\left(\frac{1}{k}\right)_H = 2 \frac{\partial K_1}{\partial \theta_H}\left(\frac{1}{k}\right)_\ell + 2K_1 \frac{\partial}{\partial \theta_H}\left(\frac{1}{k}\right)_\ell \tag{212}$$

If these three spring constants are to remain invariant with changes in pitch angle

$$\frac{\partial}{\partial \theta_H}\left(\frac{1}{k}\right)_\ell = - K_1' \frac{\partial K_1}{\partial \theta_H}\left(\frac{1}{k}\right)_\ell \tag{213}$$

For variations of the yaw angle

$$\frac{\partial A}{\partial \psi_p} = H_H \left[\begin{array}{c|c} P_{11} & -RP_{11} \\ \hline P_{21} & RP_{21} \end{array}\right] \tag{214}$$

and

$$A = H_H \left[\begin{array}{c|c} F_{11} & RF_{11} \\ \hline F_{21} & -RF_{21} \end{array}\right] \tag{215}$$

Then

$$\frac{\partial K}{\partial \psi_p} = \left[\begin{array}{c|c} \frac{\partial K_{11}}{\partial \psi_p} & -\frac{\partial K_{11}}{\partial \psi_p} \\ \hline \frac{\partial K_{21}}{\partial \psi_p} & -\frac{\partial K_{21}}{\partial \psi_p} \end{array}\right] \tag{216}$$

Again

$$\frac{\partial}{\partial \psi_p}\left(\frac{1}{k}\right)_H = \frac{\partial K}{\partial \psi_p}\left(\frac{1}{k}\right)_\ell + K \frac{\partial}{\partial \psi_p}\left(\frac{1}{k}\right)_\ell \tag{217}$$

Since the last three columns of $\frac{\partial K}{\partial \psi_p}$ are the negative of the first three, and the spring constants of symmetrical actuators have been chosen equal

$$\frac{\partial K}{\partial \psi_p}\left(\frac{1}{k}\right)_\ell = 0 \tag{218}$$

It then follows for the three specified spring constants

$$\frac{\partial}{\partial \psi_p}\left(\frac{1}{k}\right)_H = 2K_1 \frac{\partial}{\partial \psi_p}\left(\frac{1}{k}\right)_\ell \tag{219}$$

If these are to remain invariant with changes in yaw angle, the changes in actuator spring constants are zero

$$\frac{\partial}{\partial \psi_p}\left(\frac{1}{k}\right)_\ell = 0 \tag{220}$$

Incremental Actuator Extensions

After calculating the change in gravitational force and the change in spring constant, the change in actuator extension is found from

$$\delta(\Delta\ell) = L_\ell\ \delta(f_\ell) + [f_\ell]\delta\left(\frac{1}{k}\right)_\ell \tag{221}$$

or, for the n-th actuator

$$\delta\,(\Delta \ell)_n = \left(\frac{1}{k_n}\right)\ \delta(f_n) + f_n\ \delta\left(\frac{1}{k_n}\right) \tag{222}$$

This calculation must be made in real time since the variations of actuator force and spring constant are functions of time.

In addition, the actuator lengths must be changed to produce the yaw motion. From equation 16, the squared lengths of the actuators are

$$(\ell_o)^2_n = \ell_{n_t} \cdot \ell_n \tag{223}$$

where ℓ_n is the vector actuator length

$$\ell_n = r_p + a_n - E(x_{3p})b_n \tag{224}$$

For yaw motion

$$E(x_{3p}) = \begin{bmatrix} \cos\psi_p & \sin\psi_p & 0 \\ -\sin\psi_p & \cos\psi_p & 0 \\ 0 & 0 & 1 \end{bmatrix} \tag{225}$$

Then

$$\ell_n = \begin{pmatrix} 0 \\ 0 \\ z_p \end{pmatrix} + \begin{pmatrix} a_x \\ a_y \\ a_z \end{pmatrix}_n - \begin{bmatrix} b_x\cos\psi_p + b_y\sin\psi_p \\ -b_x\sin\psi_p + b_y\cos\psi_p \\ b_z \end{bmatrix}_n \tag{226}$$

The squared length is

$$\ell_n^2 = \{a_x - b_x\cos\psi_p - b_y\sin\psi_p\}^2_n + \{a_y + b_x\sin\psi_p - b_y\cos\psi_p\}^2_n + \{z_p + a_z - b_z\}^2 \tag{227}$$

By expanding $\sin\psi_p$ and $\cos t\psi_p$, the change in length is found to be

$$\delta\ell_n = \ell_o\{C_1\psi_p - 1/2(C_1^2 - C_2)\psi_p^2 + \frac{C_1}{6}(3C_1^2 - 3C_2 - 1)\psi_p^3 + \ldots\} \qquad (228)$$

where

$$C_1 = \frac{1}{\ell o^2}(a_y b_x - a_x b_y) \qquad (229)$$

$$C_2 = \frac{1}{\ell o^2}(a_x b_x + a_y b_Y) \qquad (230)$$

The first two terms will provide an accuracy of about 0.1% for angles up to 3.5 degrees. The third term increases this to 0.001%. Only two values need be calculated, since all odd numbered actuators and all even numbered actuators change by the same amount.

Exact Calculations of Pitch Angle Effects

The relatively large values of K_1' $\frac{\partial K_1}{\partial\theta_H}$ obtained when evaluated numerically indicate that linearization about zero pitch angle will introduce considerable error for angles up to 15 degrees. Therefore, the effects of pitch angle will be calculated using the exact relationships. Linearization will still be used for yaw angle changes; however, this will be calculated for the instantaneous value of pitch angle. This is possible since the yaw angle inputs will be considerably smaller (less than 3.5 degrees).

To develop the equations for an exact solution, it is assumed that the matrix, F, includes the z-displacement to the origin of the pitch system. Then, the matrix, A, is given by

$$A = \left[\begin{array}{c|c} E_H & 0 \\ \hline 0 & E_H \end{array}\right] \left[\begin{array}{c|c} F_{11} & RF_{11} \\ \hline F_{21} & -RF_{21} \end{array}\right] \qquad (231)$$

But, since

$$E_H R = R E_H \qquad (232)$$

for pitch angle inputs

$$A = \left[\begin{array}{c|c} (E_H F_{11}) & R(E_H F_{11}) \\ \hline (E_H F_{21}) & -R(E_H F_{21}) \end{array}\right] \tag{233}$$

Thus

$$A_{11} = \begin{bmatrix} (f_{11}\cos\theta - f_{31}\sin\theta) & (f_{12}\cos\theta - f_{32}\sin\theta) & (f_{13}\cos\theta - f_{33}\sin\theta) \\ f_{21} & f_{22} & f_{23} \\ (f_{31}\cos\theta + f_{11}\sin\theta) & (f_{32}\cos\theta + f_{12}\sin\theta) & (f_{33}\cos\theta + f_{13}\sin\theta) \end{bmatrix} \tag{234}$$

and

$$A_{21} = \begin{bmatrix} (f_{41}\cos\theta - f_{61}\sin\theta) & (f_{42}\cos\theta - f_{62}\sin\theta) & (f_{43}\cos\theta - f_{63}\sin\theta) \\ f_{51} & f_{52} & f_{53} \\ (f_{61}\cos\theta + f_{41}\sin\theta) & (f_{62}\cos\theta + f_{42}\sin\theta) & (f_{63}\cos\theta + f_{43}\sin\theta) \end{bmatrix} \tag{235}$$

The matrix, K, is found by squaring each of these elements. Thus, the submatrix, K_1, is equal to

$$K_1 = \begin{bmatrix} (f_{11}\cos\theta - f_{31}\sin\theta)^2 & (f_{12}\cos\theta - f_{32}\sin\theta)^2 & (f_{13}\cos\theta - f_{33}\sin\theta)^2 \\ f_{51}{}^2 & f_{52}{}^2 & f_{53}{}^2 \\ (f_{31}\cos\theta + f_{11}\sin\theta)^2 & (f_{32}\cos\theta + f_{12}\sin\theta)^2 & (f_{33}\cos\theta + f_{13}\sin\theta)^2 \end{bmatrix} \tag{236}$$

This can be inverted by evaluating the cofactors. If we let

$$K_{10} = \begin{bmatrix} f_{11}{}^2 & f_{12}{}^2 & f_{13}{}^2 \\ f_{51}{}^2 & f_{52}{}^2 & f_{53}{}^2 \\ f_{31}{}^2 & f_{32}{}^2 & f_{33}{}^2 \end{bmatrix} \tag{237}$$

and

$$|K_{20}| = f_{51}^2 \, [f_{13}f_{33}(f_{12}^2 + f_{32}^2) - f_{12}f_{32}(f_{13}^2 + f_{33}^2)]$$

$$+ f_{52}^2 \, [f_{11}f_{31}(f_{13}^2 + f_{33}^2) - f_{13}f_{33}(f_{11}^2 + f_{31}^2)]$$

$$+ f_{53}^2 \, [f_{12}f_{32}(f_{11}^2 + f_{31}^2) - f_{11}f_{31}(f_{12}^2 + f_{32}^2)] \tag{238}$$

then, the determinant of K_1 is

$$|K_1| = |K_{10}| \cos 2\theta + |K_{20}| \sin 2\theta \tag{239}$$

The cofactors of K_1 are $(K_1)_{mn}$ and the cofactors of K_{10} are $(K_{10})_{mn}$.

Then, since

$$\left(\frac{1}{k}\right)_\ell = 1/2 \; K_1' \left(\frac{1}{k}\right)_H \tag{240}$$

the actuator spring constants can be found from the inverse of K_1

$$K_1' = K_{10}' \left\{ \cos^2\theta - \begin{bmatrix} 0 & 0 & 1 \\ 0 & 1 & 0 \\ 1 & 0 & 0 \end{bmatrix} \sin^2\theta \right\} + K_{30}' \sin 2\theta \tag{241}$$

where

$$K_{10}' = \frac{1}{|K_1|} \begin{bmatrix} (K_{10})_{11} & (K_{10})_{21} & (K_{10})_{31} \\ (K_{10})_{12} & (K_{10})_{22} & (K_{10})_{32} \\ (K_{10})_{13} & (K_{10})_{23} & (K_{10})_{33} \end{bmatrix} \tag{242}$$

$$K_{30}' = \frac{1}{|K_1|} \begin{bmatrix} (K_{20})_{11} & -(K_{20})_{21} & (K_{20})_{11} \\ (K_{20})_{12} & -(K_{20})_{22} & (K_{20})_{12} \\ (K_{20})_{13} & -(K_{20})_{23} & (K_{20})_{13} \end{bmatrix} \tag{243}$$

$$K_{20} = f_{51}^2 (K_{20})_{21} + f_{52}^2 (K_{20})_{22} + f_{53}^2 (K_{20})_{23} \tag{244}$$

Similar expressions can be found for other choices of specified spring constants. In general, each of the cofactors and the determinant of the resulting matrix, K_n, will be of the form

$$(K_n)_{pq} = C_1\cos^4\theta_H + C_2\cos^3\theta_H\sin\theta_H + $$

$$+ C_3\cos^2\theta_H\sin^2\theta_H + C_4\cos\theta_H\sin^3\theta_H + + C_5\sin^4\theta_H \tag{245}$$

or

$$(K_n)_{pq} = C_1\cos^2\theta_H + C_2\cos\theta_H\sin\theta_H + C_3\sin^2\theta_H \tag{246}$$

The derivative of A with respect to ψ_p is now

$$\frac{\partial A}{\partial \psi_p} = \left[\begin{array}{c|c} E_H & 0 \\ \hline 0 & E_H \end{array}\right] \frac{\partial F}{\partial \psi_p} = \left[\begin{array}{c|c} (E_H P_{11}) & -R(E_H P_{11}) \\ \hline (E_H P_{21}) & R(E_H P_{21}) \end{array}\right] \tag{247}$$

The derivative of K is then

$$\frac{\partial K}{\partial \psi_p} = \left[\begin{array}{c|c} \dfrac{\partial K_{11}}{\partial \psi_p} & -\dfrac{\partial K_{11}}{\partial \psi_p} \\ \hline \dfrac{\partial K_{21}}{\partial \psi_p} & -\dfrac{\partial K_{21}}{\partial \psi_p} \end{array}\right] \tag{248}$$

as before. Thus

$$\frac{\partial}{\partial \psi_p}\left(\frac{1}{k}\right)_\ell = 0 \tag{249}$$

The gravitational loading can be found as a function of time from

$$f_\ell = mF_t \left[\frac{1}{W(E_H{}'r_v)}\right] g_G \tag{250}$$

where g_G is given by equation (124) and

$$E_H{}'r_v = \begin{bmatrix} x_v\cos\theta_H - z_v\sin\theta_H \\ y_v \\ z_v\cos\theta_H + x_v\sin\theta_H \end{bmatrix} \tag{251}$$

Thus, the gravitational moments are now

$$\begin{pmatrix} g_\phi \\ g_\theta \\ g_\psi \end{pmatrix} = \begin{bmatrix} Y_v g_z - (z_v\cos\theta_H + x_v\sin\theta_H)g_y \\ (z_v\cos\theta_H + x_v\sin\theta_H)g_x - (x_v\cos\theta_H - z_v\sin\theta_H)g_z \\ (x_v\cos\theta_H - z_v\sin\theta_H)g_y - y_v g_x \end{bmatrix} \tag{252}$$

and, as before

$$f_\ell = mF_t \begin{bmatrix} g_x \\ g_y \\ g_z \\ \hline g_\phi \\ g_\theta \\ g_\psi \end{bmatrix} \tag{253}$$

The change in gravitational loading due to yaw angle is obtained by replacing r_v in the earlier equations by $E_H' r_v$. If r_H is included in the definition of F

$$\frac{\partial f_\ell}{\partial \psi_p} = m \left(\frac{\partial F_t}{\partial \psi_p}\right) \begin{bmatrix} 1 \\ \hline W(E_H' r_v) \end{bmatrix} g_G - mF_t \begin{bmatrix} 1 \\ \hline W(E_H' r_v) \end{bmatrix} W \begin{pmatrix} 0 \\ 0 \\ 1 \end{pmatrix} g_G \tag{254}$$

or

$$\frac{\partial f_\ell}{\partial \psi_p} = m\left(\frac{\partial F_t}{\partial \psi_p}\right)\begin{bmatrix} g_x \\ g_y \\ g_z \\ \hline g_\phi \\ g_\theta \\ g_\psi \end{bmatrix} +$$

$$- mF_t \begin{bmatrix} -g_y \\ g_x \\ 0 \\ \hline -(z_v\cos\theta_H + x_v\sin\theta_H)g_x \\ -(z_v\cos\theta_H + x_v\sin\theta_H)g_y \\ y_v g_y + (x_v\cos\theta_H - z_v\sin\theta_H)g_x \end{bmatrix} \tag{255}$$

The rest of the calculations remain as before.

Summary of Calculations

Mean Values

Spring Constants (Off-line). Three spring constants are to be specified either in the platform system (aircraft) or pitch system (combat vehicle). The corresponding rows of the 6 x 3 matrix

$$\begin{bmatrix} K_{11} \\ \hline K_{21} \end{bmatrix} = \frac{1}{36(\gamma\nu)^2}\begin{bmatrix} 4\lambda^2 & (\lambda - \sqrt{3}\mu)^2 & (\lambda + \sqrt{3}\mu)^2 \\ 4\mu^2 & (\sqrt{3}\lambda + \mu)^2 & (\sqrt{3}\lambda - \mu)^2 \\ \nu^2 & \nu^2 & \nu^2 \\ \hline 4\alpha^2 & (\alpha - \sqrt{3}\beta)^2 & (\alpha + \sqrt{3}\beta)^2 \\ 4\beta^2 & (\sqrt{3}\alpha + \beta)^2 & (\sqrt{3}\alpha - \beta)^2 \\ \gamma^2 & \gamma^2 & \gamma^2 \end{bmatrix} \tag{256}$$

are then selected to form the 3 x 3 spring constant matrix. For instance if k_x, k_θ, and k_z are specified, this matrix is equal to

$$K_1 = \frac{1}{36(\gamma\nu)^2} \begin{bmatrix} 4\lambda^2 & (\lambda - \sqrt{3}\mu)^2 & (\lambda + \sqrt{3}\mu)^2 \\ 4\beta^2 & (\sqrt{3}\alpha + \beta)^2 & (\sqrt{3}\alpha - \beta)^2 \\ \nu^2 & \nu^2 & \nu^2 \end{bmatrix} \tag{257}$$

The actuator spring constants are then found by inverting this matrix. For this case

$$K_1' = \frac{3\gamma\nu}{(\alpha\mu-\beta\lambda)} \begin{bmatrix} 4\alpha\beta & 4\lambda\mu & \frac{4\gamma(3\alpha\mu+\beta\lambda)}{\nu} \\ (\sqrt{3}\alpha+\beta)(\alpha-\sqrt{3}\beta) & (\sqrt{3}\lambda+\mu)(\lambda-\sqrt{3}\mu) & \frac{4\gamma[\sqrt{3}(\alpha\nu-\beta\mu)-2\beta\lambda]}{\nu} \\ -(\sqrt{3}\alpha-\beta)(\alpha+\sqrt{3}\beta) & -(\sqrt{3}\lambda-\mu)(\lambda+\sqrt{3}\mu) & -\frac{4\gamma[\sqrt{3}(\alpha\nu-\beta\mu)+2\beta\lambda]}{\nu} \end{bmatrix} \tag{258}$$

and the actuator spring constants are equal to

$$\begin{pmatrix} \frac{1}{k_1} \\ \frac{1}{k_2} \\ \frac{1}{k_3} \end{pmatrix} = \begin{pmatrix} \frac{1}{k_4} \\ \frac{1}{k_5} \\ \frac{1}{k_6} \end{pmatrix} = \frac{1}{2} K_1' \begin{pmatrix} \frac{1}{k_x} \\ \frac{1}{k_\theta} \\ \frac{1}{k_z} \end{pmatrix} \tag{259}$$

For the combat vehicle, a real time calculation of the spring constants, is required to include the effects of the instantaneous pitch angle. This involves determining the coefficients, in the cofactors of K_n, of the cosine and sine terms, for the particular choice of spring constants. In the most general case, the spring constant of actuator one is given by

$$\frac{1}{k_1} = \frac{1}{2|K_n|} \{ (K_n)_{11} (\frac{1}{k_u}) + (K_n)_{21} (\frac{1}{k})_v + (K_n)_{31} (\frac{1}{k})_w \} \tag{260}$$

where u, v, and w are the specified axes. Each of the cofactors contains terms of the form

$$(K_n)_{11} = C_{11}\cos^4\theta_H + C_{12}\cos^3\theta_H\sin\theta_H + C_{13}\cos^2\theta_H\sin^2\theta_H +$$

$$+ C_{14}\cos\theta_H\sin^3\theta_H + C_{15}\sin^4\theta_H \qquad (261)$$

Thus, for the desired specified constants, it is necessary to find the coefficients

$$d_{11} = C_{11}(\frac{1}{k_u}) + C_{21}(\frac{1}{k_v}) + C_{31}(\frac{1}{k_w}) \qquad (262)$$

$$d_{12} = C_{12}(\frac{1}{k_u}) + C_{22}(\frac{1}{k_v}) + C_{32}(\frac{1}{k_w}) \qquad (263)$$

$$d_{13} = C_{13}(\frac{1}{k_u}) + C_{23}(\frac{1}{k_v}) + C_{33}(\frac{1}{k_w}) \qquad (264)$$

$$d_{14} = C_{14}(\frac{1}{k_u}) + C_{24}(\frac{1}{k_v}) + C_{34}(\frac{1}{k_w}) \qquad (265)$$

$$d_{15} = C_{15}(\frac{1}{k_u}) + C_{25}(\frac{1}{k_v}) + C_{35}(\frac{1}{k_w}) \qquad (266)$$

then

$$\frac{1}{k_1} = \frac{1}{2|K_n|} \{d_{11}\cos^4\theta_H + d_{12}\cos^3\theta_H\sin\theta_H +$$

$$+ d_{13}\cos^2\theta_H\sin^2\theta_H + d_{14}\cos\theta_H\sin^3\theta_H + d_{15}\sin^4\theta_H\} \qquad (267)$$

The determinant, $|K_n|$, is also a function of the angle, θ_H, but the coefficients do not depend on the values of the specified constants. This evaluation must be made for all three actuator spring constants. The coefficients, C_{mn}, depend only on the choice of axes for which spring constants are specified. These need be caluclated only once for each choice of axes (of which there are 13 possible combinations, 7 of which include the x-axis).

This method of calculation eliminates the necessity of real time matrix inversion, and will give greater accuracy.

Actuator Forces (On-line). The gravity vector must first be resolved along the gimbal system axes, so

$$g_G = g \begin{bmatrix} -\cos\psi_G \sin\theta_G \\ \sin\psi_G \sin\theta_G \\ \cos\theta_G \end{bmatrix} = \begin{pmatrix} g_x \\ g_y \\ g_z \end{pmatrix} \tag{268}$$

Then, the gravitational moments about the platform system are calculated, and

$$W(r)g_G = \begin{bmatrix} yg_z - zg_y \\ zg_x - xg_z \\ xg_y - yg_x \end{bmatrix} = \begin{pmatrix} g_\phi \\ g_\theta \\ g_\psi \end{pmatrix} \tag{269}$$

where

$$r = \begin{pmatrix} x \\ y \\ z \end{pmatrix} = \begin{bmatrix} x_v \\ y_v \\ z_y + z_H \end{bmatrix} \tag{270}$$

is the displacement of the center of mass of the aircraft from the origin of the platform system in platform coordinates, and

$$r = \begin{pmatrix} x \\ y \\ z \end{pmatrix} = \begin{bmatrix} x_v \cos\theta_H - z_v \sin\theta_H \\ y_v \\ z_v \cos\theta_H + x_v \sin\theta_H \end{bmatrix} \tag{271}$$

is the displacement of the center of mass of the combat vehicle from the origin of the pitch system in platform coordinates. These components are then summed, after multiplying by the proper gain factors (elements of F matrix) to give the actuator forces,

$$f_\ell = \begin{bmatrix} f_1 \\ f_2 \\ f_3 \\ f_4 \\ f_5 \\ f_6 \end{bmatrix} = mF_t \begin{bmatrix} g_x \\ g_y \\ g_z \\ g_\phi \\ g_\theta \\ g_\psi \end{bmatrix} \tag{272}$$

Actuator Extensions (On-line). The actuator extensions are found simply by dividing each actuator force by the corresponding actuator spring constant, thus

$$(\Delta\ell)_n = \frac{f_n}{k_n} \text{ for } n = 1 \text{ to } 6. \tag{273}$$

Effective Mass Loads (Off-line). The mass load matrix is given by

$$m_\ell = F_t \left[\begin{array}{c|c} 1 & 0 \\ \hline W(r) & 1 \end{array}\right] \left[\begin{array}{c|c} m & 0 \\ \hline 0 & J \end{array}\right] \left[\begin{array}{c|c} 1 & -W(r) \\ \hline 0 & 1 \end{array}\right] F \tag{274}$$

where r is again the displacement of the center of mass from the platform origin, in platform coordinates. This is a straightforward matrix multiplication involving the location of the center of mass and the values of mass and moments of inertia. The result is a 6 x 6 matrix, containing the principal and cross-coupling mass terms. Since the model is a single DOF system, the mutual terms cannot be included. Either the principal terms or a combination of principal and mutual terms will be used for the inputs to the model. This choice will depend on experimental results.

Pitch Angle Effects (On-line)

This calculation is not required for the aircraft, as long as the displacement, r, is measured in the platform system. For the combat vehicle, the effect on gravitational forces was explained previously.

Spring Constants. For the actuator spring constants, it is necessary to evaluate the functions

$$2|K_m| \frac{1}{k_n} = \left\{ \begin{array}{l} d_{n1}\cos^4\theta_H + d_{n2}\cos^3\theta_H\sin\theta_H + d_{n3}\cos^2\theta_H\sin^2\theta_H \\ + d_{n4}\cos\theta_H\sin^3\theta_H + d_{n5}\sin^4\theta_H \end{array} \right\} \tag{275}$$

for n = 1 to 6

and

$$|K_m| = d_{o1}\cos^4\theta_H + d_{o2}\cos^3\theta_H\sin\theta_H + d_{o3}\cos^2\theta_H\sin^2\theta_H + + d_{o4}\cos\theta_H\sin^3\theta_H + d_{o5}\sin^4\theta_H \tag{276}$$

The coefficients, d_{pq}, are found off-line as explained earlier.

Effective Mass Load. No correction will be made to the effective mass load, due to pitch or yaw angle variations. These corrections would be small (maybe 10%) and, since there is already some uncertainty in the best value of mass to use in the model, it is not worthwhile.

Triogonal Yaw Angle Increment (On-line)

Again, no correction is required for the aircraft. For the combat vehicle, corrections will be made to the actuator extensions.

Spring Constant Coefficients (Off-line). The derivative of the spring constants with respect to yaw angle were found to be zero, if symmetrical actuator spring constants are made equal. Thus, no correction is required.

Actuator Forces (On-line). These coefficients are functions of the gimbal angle and must be calculated in real time. They are given by

$$\frac{\partial f_\ell}{\partial \psi_p} = m \left(\frac{\partial F_t}{\partial \psi_p}\right) \left[\bar{W}(\bar{r})^{-1}\right] g_G - mF_t \left[\bar{W}(\bar{r})^{-1}\right] W \begin{pmatrix} 0 \\ 0 \\ 1 \end{pmatrix} g_G \tag{277}$$

Since

$$W \begin{pmatrix} 0 \\ 0 \\ 1 \end{pmatrix} g_G = \begin{pmatrix} -g_y \\ g_x \\ 0 \end{pmatrix}, \tag{278}$$

$$W(r)\, W \begin{pmatrix} 0 \\ 0 \\ 1 \end{pmatrix} g_G = \begin{bmatrix} -zg_x \\ -zg_y \\ (xg_x + yg_y) \end{bmatrix} \tag{279}$$

These, plus the previously calculated values of the gravitational forces and moments, are summed according to the elements of the matrix F and its ψ_p - derivative to give the coefficients. The changes in actuator forces are then equal to

$$\delta f_n = \left(\frac{\partial f_n}{\partial \psi_p}\right) \psi_p \tag{280}$$

For these calculations, the displacement, r, is equal to

$$r = E_H' r_v \tag{281}$$

as given in equation (251). Thus

$$W(r)W \begin{pmatrix} 0 \\ 0 \\ 1 \end{pmatrix} g_G = \begin{bmatrix} -(z_v\cos\theta_H + x_v\sin\theta_H)\, g_x \\ -(z_v\cos\theta_H + x_v\sin\theta_H)\, g_y \\ y_v g_y + (x_v\cos\theta_H - z_v\sin\theta_H) g_x \end{bmatrix} \tag{282}$$

Actuator Extensions (On-line)

The actuator extensions for the combat vehicle are equal to those necessary to produce the desired yaw motion plus the gravitational extensions. The yaw inputs are

$$\delta(\Delta\ell)_n = \ell_o \{\pm C_1\psi_p - 1/2\ (C_1^{\,2} - C_2)\psi_p^{\,2}\} \tag{283}$$

The plus sign is used for odd numbered actuators, and the minus sign for even numbered actuators, where C_1 and C_2 are evaluated for actuator number one. The gravitational extensions are found by dividing the total gravitational force (results of both on-line actuator forces) by the spring constants.

$$(\Delta\ell)_n = \frac{\left[f_n + \left(\frac{\partial f_n}{\partial\psi_p}\right)\psi_p\right]}{k_n} + \delta(\Delta\ell)_n \tag{284}$$

Evaluation of Matrices

Calculation of Linear Coefficients

For both the off-line and on-line calculations, it is necessary to evaluate the elements of the matrices associated with the triogonal and pitch system transformations. The general configuration for the triogonal system has been presented in figure 1. The dimensions, in inches, for this are as follows:

$$a_1 = \begin{bmatrix} 18\sqrt{3} \\ 3.0 \\ -10.0 \end{bmatrix} \tag{285}$$

$$b_1 = \begin{bmatrix} 13.5\sqrt{3} \\ 31.5 \\ 9.875 \end{bmatrix} \tag{286}$$

$$r_p = \begin{bmatrix} 0 \\ 0 \\ 55.875 \end{bmatrix} \tag{287}$$

$$\ell_1 = \begin{bmatrix} 4.5\sqrt{3} \\ -28.5 \\ 36.0 \end{bmatrix} \tag{288}$$

$$\ell_o = 3\sqrt{241} \tag{289}$$

For the turret adapter, whose center of rotation is 60 inches below the actuator neutral position

$$r_H = \begin{pmatrix} 0 \\ 0 \\ 50.0 \end{pmatrix} \tag{290}$$

Then, the direction cosines are

$$\begin{pmatrix} \alpha \\ \beta \\ \gamma \end{pmatrix}_1 = \frac{1}{\sqrt{241}} \begin{bmatrix} 1.5\sqrt{3} \\ -9.5 \\ 12.0 \end{bmatrix} \tag{291}$$

The actuator moment arms are obtained using equation (26) and are

$$\begin{pmatrix} \lambda \\ \mu \\ \nu \end{pmatrix}_1 = \frac{1}{\sqrt{241}} \begin{bmatrix} -59.0 \\ -231\sqrt{3} \\ -175.5\sqrt{3} \end{bmatrix} \tag{292}$$

Then, from equation (83) the submatrices of the triogonal transformation are

$$F_{11} = \begin{bmatrix} -118 & -634 & 752 \\ -462\sqrt{3} & -290\sqrt{3} & 172\sqrt{3} \\ 175.5\sqrt{3} & 175.5\sqrt{3} & 175.5\sqrt{3} \end{bmatrix} \frac{\sqrt{241}}{12{,}636\sqrt{3}} \tag{293}$$

and

$$F_{21} = \begin{bmatrix} 3\sqrt{3} & 11\sqrt{3} & 8\sqrt{3} \\ -19 & 5 & 14 \\ -12 & 12 & -12 \end{bmatrix} \frac{\sqrt{241}}{12{,}636\sqrt{3}} \tag{294}$$

The ψ_p - derivatives of the first column of F_t' are

$$\begin{pmatrix} \delta_1 \\ \delta_2 \\ \delta_3 \end{pmatrix} = \frac{1}{(241)^{3/2}} \begin{bmatrix} 22.25 \\ 890.25\sqrt{3} \\ 702\sqrt{3} \end{bmatrix} \tag{295}$$

and

$$\begin{pmatrix} \delta_4 \\ \delta_5 \\ \delta_6 \end{pmatrix} = \frac{1}{(241)^{3/2}} \begin{bmatrix} 11{,}008.5\sqrt{3} \\ -38{,}130.5\sqrt{3} \\ 48{,}006.75 \end{bmatrix} \tag{296}$$

The elements of the matrix

$$J = \left(\frac{\partial F'}{\partial \psi_p}\right) F \tag{297}$$

are

$$j_{11} = -\frac{11{,}471\sqrt{3}}{169{,}182} \tag{298}$$

$$j_{12} = \frac{38\sqrt{3}}{1053} \tag{299}$$

$$j_{23} = -\frac{323\sqrt{3}}{1053} \tag{300}$$

$$j_{16} = -\frac{34\sqrt{3}}{1053} \tag{301}$$

The submatrices of the ψ_p - derivative of F are

$$P_{11} = \begin{bmatrix} -.11223802 & -.25050026 & -.13826223 \\ .22445212 & -.015025086 & -.20942704 \\ .14129392 & -.14129392 & .14129392 \end{bmatrix} \tag{302}$$

and

$$P_{21} = \begin{bmatrix} -.013097284 & -.77950916 & .79260644 \\ -.90766138 & -.46517327 & .44248811 \\ .35786481 & .35786481 & .35786481 \end{bmatrix} 10^{-2} \tag{303}$$

For the combat vehicle, using $A = H(\chi_{3H}, r_H)F$ and equations (85) and (86), then

$$A = \left[\begin{array}{c|c} \{F_{11} - W(r_H)F_{21}\} & R\{F_{11} + W(r_H)F_{21}\} \\ \hline F_{21} & -RF_{21} \end{array}\right] \tag{304}$$

$$W(r_H)F_{21} = \frac{\sqrt{241}}{12,636\sqrt{3}} \begin{bmatrix} 950 & -250 & -700 \\ 150\sqrt{3} & 550\sqrt{3} & 400\sqrt{3} \\ 0 & 0 & 0 \end{bmatrix} \tag{305}$$

Then

$$A_{11} = \frac{\sqrt{241}}{12,636\sqrt{3}} \begin{bmatrix} -1068 & -384 & 1452 \\ -612\sqrt{3} & -840\sqrt{3} & -228\sqrt{3} \\ 175.5\sqrt{3} & 175.5\sqrt{3} & 175.5\sqrt{3} \end{bmatrix} \tag{306}$$

$$A_{21} = \frac{\sqrt{241}}{12,636\sqrt{3}} \begin{bmatrix} 3\sqrt{3} & 11\sqrt{3} & 8\sqrt{3} \\ -19 & 5 & 14 \\ -12 & 12 & -12 \end{bmatrix} = F_{21} \tag{307}$$

Then

$$\left(\frac{\partial A}{\partial \theta_H}\right)_{11} = \frac{\sqrt{241}}{12,636\sqrt{3}} \begin{bmatrix} -175.5\sqrt{3} & -175.5\sqrt{3} & -175.5\sqrt{3} \\ 0 & 0 & 0 \\ -1068 & -384 & 1452 \end{bmatrix} \tag{308}$$

$$\left(\frac{\partial A}{\partial \theta_H}\right)_{21} = \frac{\sqrt{241}}{12,636\sqrt{3}} \begin{bmatrix} 12 & -12 & 12 \\ 0 & 0 & 0 \\ 3\sqrt{3} & 11\sqrt{3} & 8\sqrt{3} \end{bmatrix} \tag{309}$$

and

$$\left(\frac{\partial K}{\partial \theta_H}\right)_{11} = \frac{241\sqrt{3}}{(6318)^2} \begin{bmatrix} 31,239 & 11,232 & -42,471 \\ 0 & 0 & 0 \\ -31,239 & -11,232 & 42,471 \end{bmatrix} \tag{310}$$

$$\left(\frac{\partial K}{\partial \theta_H}\right)_{21} = \frac{241\sqrt{3}}{(6318)^2} \begin{bmatrix} 6 & 22 & 16 \\ 0 & 0 & 0 \\ -6 & -22 & -16 \end{bmatrix} \tag{311}$$

Also

$$\left(\frac{\partial A}{\partial \psi_p}\right) = \left[\begin{array}{c|c} \dfrac{\{P_{11} - W(r_H)P_{21}\}}{P_{21}} & \dfrac{-R\{P_{11} - W(r_H)P_{21}\}}{P_{21}} \end{array}\right] \tag{312}$$

$$W(r_H)P_{21} = \frac{1}{\sqrt{241}}\begin{bmatrix} \dfrac{59,350}{8,424} & \dfrac{91,250}{25,272} & -\dfrac{86,800}{25,272} \\ \dfrac{4450\sqrt{3}}{75,816} & -\dfrac{264,850\sqrt{3}}{75,816} & \dfrac{269,300\sqrt{3}}{75,816} \\ 0 & 0 & 0 \end{bmatrix} \tag{313}$$

and

$$\left(\frac{\partial A}{\partial \psi_p}\right)_{11} = \frac{1}{\sqrt{241}}\begin{bmatrix} -\dfrac{6169}{702} & -\dfrac{7897}{1053} & \dfrac{2413}{2106} \\ \dfrac{13,081\sqrt{3}}{6318} & \dfrac{21,220\sqrt{3}}{6318} & -\dfrac{34,301\sqrt{3}}{6318} \\ \dfrac{64,009\sqrt{3}}{50,544} & -\dfrac{64,009\sqrt{3}}{50,544} & \dfrac{64,009\sqrt{3}}{50,544} \end{bmatrix} \tag{314}$$

and

$$\left(\frac{\partial A}{\partial \psi_p}\right)_{21} = \begin{bmatrix} -.013097284 & -.77950916 & .79260644 \\ -.90766138 & -.46517327 & .44248811 \\ .35786481 & .35786481 & .35786481 \end{bmatrix} 10^{-2} \tag{315}$$

Then

$$\left(\frac{\partial K}{\partial \psi_p}\right)_{11} = \frac{1}{2106\sqrt{3}}\begin{bmatrix} \dfrac{1,098,082}{351} & \dfrac{1,010,816}{1053} & \dfrac{656,546}{1053} \\ -\dfrac{1,334,262}{351} & -\dfrac{2,970,800}{351} & \dfrac{1,303,438}{351} \\ \dfrac{64,009}{96} & -\dfrac{64,009}{96} & \dfrac{64,009}{96} \end{bmatrix} \tag{316}$$

and

$$\left(\frac{\partial K}{\partial \psi_p}\right)_{21} = \frac{1}{6318\sqrt{3}}\begin{bmatrix} -\dfrac{89}{8424} & -\dfrac{58,267}{25,272} & \dfrac{5386}{3159} \\ \dfrac{22,553}{8424} & -\dfrac{9125}{25,272} & \dfrac{3038}{3159} \\ -2/3 & +2/3 & -2/3 \end{bmatrix} \tag{317}$$

Then

$$K_1'\left(\frac{\partial K_1}{\partial \theta_H}\right) = \frac{\sqrt{3}}{3,369,600}\begin{bmatrix} -9,065,807 & -3,259,616 & 12,325,423 \\ -24,416,705 & -8,779,040 & 33,195,745 \\ 19,812,112 & 7,123,456 & -26,935,568 \end{bmatrix} \tag{318}$$

The relatively large values in this matrix indicate that the original intention of linearizing the results for pitch variations about zero pitch angle might introduce serious errors. This led to the decision to calculate exact values for pitch angle inputs.

Off-Line Calculations for Aircraft

The previous evaluations of the direction cosines, moment arms, and matrix F are valid for the aircraft since they are referenced to the platform. The derivatives are not required for the aircraft configuration. The additional matrices necessary for the off-line calculations are

$$K_1' = \frac{9477}{800(241)}\begin{bmatrix} -57 & 54,516 & \frac{81,856}{351} \\ -55 & -183,860 & \frac{255,040}{351} \\ 112 & 129,344 & -\frac{183,296}{351} \end{bmatrix} \tag{319}$$

Thus

$$\begin{pmatrix} \frac{1}{k_1} \\ \frac{1}{k_2} \\ \frac{1}{k_3} \end{pmatrix} = \begin{pmatrix} \frac{1}{k_4} \\ \frac{1}{k_5} \\ \frac{1}{k_6} \end{pmatrix} = \begin{bmatrix} -1.4009050 & 1339.8551 & 5.731618 \\ -1.3517505 & -4518.7790 & 17.85809 \\ 2.7526555 & 3178.9239 & -12.834522 \end{bmatrix}\begin{pmatrix} \frac{1}{k_x} \\ \frac{1}{k_\theta} \\ \frac{1}{k_z} \end{pmatrix} \tag{320}$$

The scale factors for summing gravitational components are given by equations (293) and (294).

The mass loads will depend on the aircraft. For the AH-1G, we have the following values:

$$E_H{}'r_v = \begin{pmatrix} 0 \\ 0 \\ 37.455 \end{pmatrix} \tag{321}$$

$$\left.\begin{aligned} m &= 24.61 \text{ lb sec}^2/\text{in} \\ J_x &= 30{,}360 \text{in lb sec}^2 \\ J_y &= 140{,}592 \text{ in lb sec}^2 \\ J_z &= 121{,}968 \text{ in lb sec}^2 \\ \theta_H &= -\ 20 \text{ degrees} \end{aligned}\right\} \tag{322}$$

Then

$$E_H{}'JE_H = \begin{bmatrix} -41{,}076 & 0 & -29{,}442 \\ 0 & 140{,}592 & 0 \\ -29{,}442 & 0 & 111{,}252 \end{bmatrix} \tag{323}$$

and

$$F_{11}-W(r)F_{21} = \begin{bmatrix} -.58847849 & -.3168681 & .90534657 \\ -.70564594 & -.86246023 & -.1568143 \\ .21561352 & .21561352 & .21561352 \end{bmatrix} \tag{324}$$

The mass load submatrices are

$$(m_\ell)_{11} = (m_\ell)_{22} = \begin{bmatrix} 57.921932 & 10.439513 & -15.125035 \\ 10.439513 & 32.477998 & 0.6833395 \\ -15.125035 & 0.6833395 & 52.739365 \end{bmatrix} \text{lb sec}^2/\text{in} \tag{325}$$

$$(m_\ell)_{12} = (m_\ell)_{21} = \begin{bmatrix} 12.482499 & -12.412995 & -46.441314 \\ -12.412995 & -21.711075 & -2.6121869 \\ -46.441314 & -2.6121869 & 17.620422 \end{bmatrix} \text{lb sec}^2/\text{in} \tag{326}$$

The principal mass loads are then

$$\begin{pmatrix} m_1 \\ m_2 \\ m_3 \end{pmatrix} = \begin{pmatrix} m_4 \\ m_5 \\ m_6 \end{pmatrix} = \begin{bmatrix} 57.921932 \\ 32.477998 \\ 52.739365 \end{bmatrix} \text{ lb sec}^2/\text{in} \tag{327}$$

The cross-mass terms have been calculated in case other than the principal values are used.

Off-Line Calculations for Combat Vehicle

The previously calculated values of A_{11} and A_{21} are valid for F, for which the displacement of the pitch system origin from the platform system origin is included. The values are given by equations (306) and (307). Thus, the equivalent moment arms at the neutral pitch system are given by substituting $a_z = -60$ in equation (285)

$$\begin{pmatrix} \lambda \\ \mu \\ \nu \end{pmatrix} = \frac{1}{\sqrt{241}} \begin{bmatrix} -534 \\ -306\sqrt{3} \\ -175.5\sqrt{3} \end{bmatrix} \tag{328}$$

From equations (237), (306) and (307), K_{10} is

$$K_{10} = \frac{(241)}{3(12{,}636)^2} \begin{bmatrix} 1{,}140{,}624 & 147{,}456 & 2{,}108{,}304 \\ 361 & 25 & 196 \\ 92{,}400.75 & 92{,}400.75 & 92{,}400.75 \end{bmatrix} \tag{329}$$

The determinant of K_{10} is then

$$|K_{10}| = \frac{(241)^3(41{,}925)}{4(12636)^4} \tag{330}$$

Then, the inverse of K_{10} is given by

$$(K_{10}')_o = \frac{27}{259{,}075} \begin{bmatrix} -6{,}669 & 76{,}473{,}072 & -10{,}048 \\ -6{,}435 & -37{,}739{,}520 & 226{,}880 \\ 13{,}104 & -38{,}733{,}552 & -10{,}432 \end{bmatrix} \tag{331}$$

We identify

$$(K_{30}')_o = \frac{K_{30}'}{|K_{10}|} \tag{332}$$

Then from equation (243)

$$(K_{30}')_0 = \begin{bmatrix} 1.4917264 & -14.360606.10^4 & 1.4917264 \\ -9.807656 & 5.5365515.10^4 & -9.807656 \\ -1.4965399 & .29057202.10^4 & -1.49653399 \end{bmatrix} \tag{333}$$

and the actuator spring constants are

$$K_1' = \frac{(K_{10}')_o\{\cos^2\theta_H - \begin{bmatrix} 0 & 0 & 1 \\ 0 & 1 & 0 \\ 1 & 0 & 0 \end{bmatrix} \sin^2\theta_H\} + (K_{30}')_o \sin 2\theta_H}{\{\cos 2\theta_H + \left|\frac{K_{20}}{K_{10}}\right| \sin 2\theta_H\}} \tag{334}$$

These equations are valid until

$$\tan 2\theta_H = - \frac{|K_{10}|}{|K_{20}|} = + .52214737 \tag{335}$$

or

$$\theta_H = + 13.8 \text{ degrees} \tag{336}$$

This is adequate to meet the 15 degree requirement.

The coefficients which are to be calculated off-line are

$$C_{10} = 1 \tag{337}$$

$$\frac{C_{20}}{C_{10}} = \left|\frac{K_{20}}{K_{10}}\right| = 1.9151681 \tag{338}$$

$$\begin{pmatrix} C_{11} \\ C_{12} \\ C_{13} \end{pmatrix} = (K_{10}')_o \begin{pmatrix} 1/k_x \\ 1/k_\theta \\ 1/k_z \end{pmatrix} \tag{339}$$

$$\begin{pmatrix} C_{21} \\ C_{22} \\ C_{23} \end{pmatrix} = (K_{10}')_o \begin{bmatrix} 0 & 0 & 1 \\ 0 & 1 & 0 \\ 1 & 0 & 0 \end{bmatrix} \begin{pmatrix} 1/k_x \\ 1/k_\theta \\ 1/k_z \end{pmatrix} \tag{340}$$

$$\begin{pmatrix} C_{31} \\ C_{32} \\ C_{33} \end{pmatrix} = (K_{30}')_o \begin{pmatrix} 1/k_x \\ 1/k_\theta \\ 1/k_z \end{pmatrix} \tag{341}$$

The gravitational loading and actuator extensions require no off-line calculations, other than the fixed values of F and $\partial F/\partial\psi_p$. The location of the vehicle CM and the weight must be input to complete these calculations. The actuator mass loading will be calculated in a manner similar to that for the aircraft, except that the mean value of pitch angle will be included. No correction will be made for variations in pitch and yaw angles. This again is a straightforward matrix multiplication using the input data describing the location of the CM and the mass and moments of inertia.

The final summary of the calculations required for the aircraft and combat vehicle configurations are then as follows:

Aircraft

Input

Specified spring constants and axes -

k_u, k_v, k_w

Spring constants matrix -

$$\begin{bmatrix} K_{11} \\ \hline K_{21} \end{bmatrix} = \frac{(241)}{(12{,}636)^2(3)} \begin{bmatrix} \frac{13{,}924}{} & 401{,}956 & 565{,}504 \\ 640{,}322 & 252{,}300 & 88{,}752 \\ 92{,}400.75 & 92{,}400.75 & 92{,}400.75 \\ \hline 27 & 363 & 192 \\ 361 & 25 & 196 \\ 144 & 144 & 144 \end{bmatrix} \tag{342}$$

Select rows u, v, and w to form K_m
Input K_m'

Calculate

$$\left(\frac{1}{k}\right)_\ell = \begin{bmatrix} 1/k_1 \\ 1/k_2 \\ 1/k_3 \end{bmatrix} = \begin{bmatrix} 1/k_4 \\ 1/k_5 \\ 1/k_6 \end{bmatrix} = \frac{1}{2} K_m' \begin{bmatrix} 1/k_u \\ 1/k_v \\ 1/k_w \end{bmatrix} \tag{343}$$

Test

$$k_n \geq k_{min} \qquad n = 1 \text{ to } 3$$

$$k_n \leq k_{max} \qquad n = 1 \text{ to } 3$$

Input

Mass - m

Moments of Inertia -

$J_{xx}, J_{yy}, J_{zz}, J_{xy}, J_{xz}, J_{yz}$

Displacement of CM -

$$r = E_H'(r_H + r_v) = \begin{pmatrix} x \\ y \\ z \end{pmatrix} \tag{344}$$

Pitch Angle - θ_H

Calculate

Mass loads -

$$m_\ell = \left[\begin{array}{c|c} F_{11t} & F_{21t} \\ \hline F_{11t}R & -F_{21t}R \end{array}\right] \left[\begin{array}{c|c} 1 & 0 \\ \hline W(r) & 1 \end{array}\right] \left[\begin{array}{c|c} m & 0 \\ \hline 0 & E_H'JE_H \end{array}\right] \times$$

$$\times \left[\begin{array}{c|c} 1 & -W(r) \\ \hline 0 & 1 \end{array}\right] \left[\begin{array}{c|c} F_{11} & RF_{11} \\ \hline F_{21} & -RF_{21} \end{array}\right] \tag{345}$$

where

$$\left[\begin{array}{c} F_{11} \\ \hline F_{21} \end{array}\right] = \frac{\sqrt{241}}{(12,636)\sqrt{3}} \begin{bmatrix} -118 & -634 & 752 \\ -462\sqrt{3} & -290\sqrt{3} & 172\sqrt{3} \\ \frac{175.5\sqrt{3}}{3\sqrt{3}} & \frac{175.5\sqrt{3}}{11\sqrt{3}} & \frac{175.5\sqrt{3}}{8\sqrt{3}} \\ -19 & 5 & 14 \\ -12 & 12 & -12 \end{bmatrix} \tag{346}$$

Input

Gimbal Angles - (On-line)

ψ_G, θ_G

Calculate (On-line)

$$g_G = \begin{pmatrix} g_x \\ g_y \\ g_z \end{pmatrix} = g \begin{bmatrix} -\cos\psi_G \sin\theta_G \\ \sin\psi_G \sin\theta_G \\ \cos\theta_G \end{bmatrix} \tag{347}$$

$$m_G = \begin{pmatrix} g_\phi \\ g_\theta \\ g_\psi \end{pmatrix} = \begin{bmatrix} yg_z - zg_y \\ zg_x - xg_z \\ xg_y - yg_x \end{bmatrix} \tag{348}$$

$$f_\ell = \begin{bmatrix} f_1 \\ f_2 \\ f_3 \\ f_4 \\ f_5 \\ f_6 \end{bmatrix} = m \left[\begin{array}{c|c} F_{11t} & F_{21t} \\ \hline F_{11t}R & -F_{21t}R \end{array}\right] \begin{pmatrix} g_G \\ \hline m_G \end{pmatrix} \tag{349}$$

$$(\Delta\ell)_n = \frac{f_n}{k_n} \qquad n = 1 \text{ to } 6 \tag{350}$$

Combat Vehicle

Input

Specified spring constants and axes -

k_u, k_v, and k_w

Spring constant coefficients -

$(C_q)_{mn}$ $\quad q = 1$ to 5
$m = 1$ to 3
$n = 1$ to 3

Calculate

$$d_{mn} = (C_n)_{1m}\left(\frac{1}{k_u}\right) + (C_n)_{2m}\left(\frac{1}{k_v}\right) + (C_n)_{3m}\left(\frac{1}{k_w}\right) \tag{351}$$

$n = 1$ to 5
$m = 1$ to 3

Input

Pitch Angle - (On-line)

θ_H

C_{mo} $\quad m = 1$ to 5

Calculate

$$|K| = \{C_{10}\cos^4\theta_H + C_{20}\cos^3\theta_H\sin\theta_H + C_{30}\cos^2\theta_H\sin^2\theta_H + C_{40}\cos\theta_H\sin^3\theta_H + C_{50}\sin^4\theta_H\} \tag{352}$$

$$\frac{1}{k_n} = \frac{1}{2|K|}\{d_{n1}\cos^4\theta_H + d_{n2}\cos^3\theta_H\sin\theta_H + d_{n3}\cos^2\theta_H\sin^2\theta_H + d_{n4}\cos\theta_H\sin^3\theta_H + d_{n5}\sin^4\theta_H\} \tag{353}$$

$n = 1$ to 3

$$k_{n+3} = k_n \tag{354}$$

Test

$k_n \geq k_{min}$ $\quad n = 1$ to 3

$k_n \leq k_{max}$ $\quad n = 1$ to 3

Input

Mass - m

Moments of Inertia -

J_{xx}, J_{yy}, J_{zz}, J_{xy}, J_{xz}, J_{yz}

Displacement of CM

$$r_v = \begin{pmatrix} x_v \\ y_v \\ z_v \end{pmatrix}$$

Mean pitch angle - θ_{Ho}

Calculate

$$r_o = \begin{bmatrix} x_v \cos\theta_{Ho} + z_v \sin\theta_{Ho} \\ y_v \\ z_v \cos\theta_{Ho} - x_v \sin\theta_{Ho} \end{bmatrix} = \begin{pmatrix} x_o \\ y_o \\ z_o \end{pmatrix} \tag{355}$$

$$m_\ell = \left[\begin{array}{c|c} F_{11t} & F_{21t} \\ \hline F_{11t}R & -F_{21t}R \end{array}\right] \left[\begin{array}{c|c} 1 & 0 \\ \hline W(r_o) & 1 \end{array}\right] \left[\begin{array}{c|c} m & 0 \\ \hline 0 & E_{Ho}{}'JE_{Ho} \end{array}\right] \times$$

$$\times \left[\begin{array}{c|c} 1 & -W(r_o) \\ \hline 0 & 1 \end{array}\right] \left[\begin{array}{c|c} F_{11} & RF_{11} \\ \hline F_{21} & -RF_{21} \end{array}\right] \tag{356}$$

where

$$\begin{bmatrix} F_{11} \\ \hline F_{21} \end{bmatrix} = \begin{bmatrix} -1068 & -384 & 1452 \\ -612\sqrt{3} & -840\sqrt{3} & -228\sqrt{3} \\ \frac{175.5\sqrt{3}}{3\sqrt{3}} & \frac{175.5\sqrt{3}}{11\sqrt{3}} & \frac{175.5\sqrt{3}}{8\sqrt{3}} \\ -19 & 5 & 14 \\ -12 & 12 & -12 \end{bmatrix} \frac{\sqrt{241}}{(12,636)\sqrt{3}} \tag{357}$$

Input

Gimbal Angles - (On-line)

θ_G, ψ_G

Triogonal Yaw Angle - (On-line)

ψ_p

Calculate (On-line)

$$r = \begin{pmatrix} x \\ y \\ z \end{pmatrix} = \begin{bmatrix} x_v \cos\theta_H + z_v \sin\theta_H \\ y_v \\ z_v \cos\theta_H - x_v \sin\theta_H \end{bmatrix} \tag{358}$$

$$g_G = \begin{pmatrix} g_x \\ g_y \\ g_z \end{pmatrix} = g \begin{bmatrix} -\cos\psi_G \sin\theta_G \\ \sin\psi_G \sin\theta_G \\ \cos\theta_G \end{bmatrix} \tag{359}$$

$$m_G = \begin{pmatrix} g_\phi \\ g_\theta \\ g_\psi \end{pmatrix} = \begin{bmatrix} yg_z - zg_y \\ zg_x - xg_z \\ xg_y - yg_x \end{bmatrix} \tag{360}$$

$$\frac{\partial f_\ell}{\partial \psi_p} = m \left(\frac{\partial F_t}{\partial \psi_p} \right) \left(\frac{g_G}{m_G} \right) + $$

$$+ m \left[\begin{array}{c|c} F_{11t} & F_{21t} \\ \hline F_{11t}{}^R & -F_{21t}{}^R \end{array} \right] \left[\begin{array}{c} g_y \\ -g_x \\ 0 \\ \hline zg_x \\ zg_y \\ -(xg_x + yg_y) \end{array} \right] \tag{361}$$

Where

$$\frac{\partial F_t}{\partial \psi_p} = \left[\begin{array}{c|c} P_{11t} & P_{21t} \\ \hline -P_{11t}{}^R & P_{21t}{}^R \end{array} \right] \tag{362}$$

$$
\begin{bmatrix} P_{11} \\ \hline P_{21} \end{bmatrix} = \begin{bmatrix} -1,332,504 & -1,137,168 & 195,336 \\ 313,944\sqrt{3} & 509,280\sqrt{3} & -823,224\sqrt{3} \\ 192,027\sqrt{3} & -192,027\sqrt{3} & 192,027\sqrt{3} \\ \hline -178\sqrt{3} & -10,594\sqrt{3} & 10,722\sqrt{3} \\ -21,366 & -10,950 & 10,416 \\ 8,424 & 8,424 & 8,424 \end{bmatrix} \times \frac{1}{151,632\sqrt{241}} \tag{363}
$$

$$
f_\ell = m \left[\begin{array}{c|c} F_{11t} & F_{21t} \\ \hline F_{11t}R & -F_{21t}R \end{array}\right] \begin{pmatrix} g_G \\ \hline m_G \end{pmatrix} + \psi_p \left(\frac{\partial f_\ell}{\partial \psi_p} \right) \tag{364}
$$

$$
(\Delta\ell)_n = \frac{f_n}{k_n} \qquad n = 1 \text{ to } 6 \tag{365}
$$

Table of Symbols

$$
x_1 = \begin{pmatrix} x \\ y \\ z \end{pmatrix} \qquad \text{linear position vector}
$$

$$
x_3 = \begin{pmatrix} \phi \\ \theta \\ \psi \end{pmatrix} \qquad \text{angular position vector} \begin{pmatrix} \text{relative} \\ \text{Euler angles} \end{pmatrix}
$$

$$
\dot{x}_2 = \begin{pmatrix} p \\ q \\ r \end{pmatrix} \qquad \text{angular velocity vector}
$$

x = displacement in direction of x-axis
y = displacement in direction of y-axis
z = displacement in direction of z-axis
ϕ = roll angle
θ = pitch angle
ψ = yaw angle
p = roll velocity
q = pitch velocity
r = yaw velocity

$$\dot{x}_2 = G' (x_3)\, \dot{x}_3$$

$$G'(x_3) = \begin{bmatrix} 1 & 0 & -\sin\theta \\ 0 & \cos\phi & \sin\phi\cos\theta \\ 0 & -\sin\phi & \cos\phi\cos\theta \end{bmatrix}$$

G	=	subscript denoting gimbal system
p	=	subscript denoting platform system
ℓ	=	subscript denoting triogonal system
n	=	subscript denoting actuator number
a	=	subscript denoting aircraft system
H	=	subscript denoting pitch actuator system
v	=	subscript denoting vehicle system
B	=	subscript denoting tail-boom system, relative to aircraft system
TB	=	subscript denoting tail-boom system, relative to gimbal system
'	=	prime, denoting inverse
t	=	subscript denoting transpose

$$E_1(\psi) = \begin{bmatrix} \cos\psi & \sin\psi & 0 \\ -\sin\psi & \cos\psi & 0 \\ 0 & 0 & 1 \end{bmatrix} = \text{yaw transformation matrix}$$

$$E_2(\theta) = \begin{bmatrix} \cos\theta & 0 & -\sin\theta \\ 0 & 1 & 0 \\ \sin\theta & 0 & \cos\theta \end{bmatrix} = \text{pitch transformation matrix}$$

$$E_3(\phi) = \begin{bmatrix} 1 & 0 & 0 \\ 0 & \cos\phi & \sin\phi \\ 0 & -\sin\phi & \cos\phi \end{bmatrix} = \text{roll transformation matrix}$$

$E(x_3) = E_3(\phi)E_2(\theta)E_1(\psi)$ = angular transformation matrix

$b = \begin{pmatrix} b_x \\ b_y \\ b_z \end{pmatrix}$ = location of upper end of actuator

$a = \begin{pmatrix} a_x \\ a_y \\ a_z \end{pmatrix}$ = location of lower end of actuator

$r = \begin{pmatrix} r_x \\ r_y \\ r_z \end{pmatrix}$ = vector displacement of origin of one coordinate system from origin of another coordinate system

$\ell_p = \begin{pmatrix} \ell_x \\ \ell_y \\ \ell_z \end{pmatrix}$ = vector length of actuator

$c = E\,(x_{3p})\,b$ = location of upper end of actuator, resolved into platform coordinates, origin at origin of gimbal system

ℓ = scalar length of actuator

ℓ_i = unextended scalar length of actuator

$\alpha = \dfrac{\ell_x}{\ell}$ = x - direction cosine of actuator

$\beta = \dfrac{\ell_y}{\ell}$ = y - direction cosine of actuator

$\gamma = \dfrac{\ell_z}{\ell}$ = z - direction cosine of actuator

$$W(x_1) = \begin{bmatrix} 0 & -z & y \\ z & 0 & -x \\ -y & x & 0 \end{bmatrix} = \text{rotational matrix}$$

$$\begin{pmatrix} \dot{x}_1 \\ \hline \dot{x}_2 \end{pmatrix} = \begin{pmatrix} \dot{x} \\ \dot{y} \\ \dot{z} \\ p \\ q \\ r \end{pmatrix} = \text{velocity matrix}$$

$$\begin{pmatrix} - \frac{f}{m} - \end{pmatrix} = \begin{pmatrix} f_x \\ f_y \\ f_z \\ m_\phi \\ m_\theta \\ m_\psi \end{pmatrix} = \text{force matrix}$$

$$\begin{pmatrix} \dot{x}_1 \\ \hline \dot{x}_2 \end{pmatrix}_p = F\,\dot{\ell} = \text{triogonal velocity transformation}$$

$$\begin{pmatrix} \lambda \\ \mu \\ \nu \end{pmatrix} = W(a) \begin{pmatrix} \alpha \\ \beta \\ \gamma \end{pmatrix} = \text{actuator moment arms}$$

$$f_{pn} = \begin{pmatrix} f_x \\ f_y \\ f_z \end{pmatrix}_n = \text{vector actuator force (n-th actuator)}$$

f_n = scalor actuator force (n-th actuator)

$$f_\ell = \begin{pmatrix} f_1 \\ f_2 \\ f_3 \\ f_4 \\ f_5 \\ f_6 \end{pmatrix} = \text{scalar actuator force matrix}$$

$$\left[f_\ell\right] = \begin{bmatrix} f_1 & 0 & . & . & 0 \\ 0 & f_2 & & . & . \\ \vdots & & & & . \\ 0 & 0 & . & . & f_6 \end{bmatrix} = \text{diagonal actuator force matrix}$$

$$H(x_3, r) = \left[\begin{array}{c|c} E(x_3) & -W(r)\ E(x_3) \\ \hline 0 & E(x_3) \end{array}\right] = \text{rectilinear velocity transformation matrix}$$

$$\begin{pmatrix} \dot{x}_1 \\ \hline \dot{x}_2 \end{pmatrix} = \mathcal{Z} \begin{pmatrix} \frac{f}{m} \end{pmatrix} = \text{generalized impedance matrix}$$

k_n = spring constant of n-th actuator

$$\left(\frac{1}{k}\right)_\ell = \begin{bmatrix} 1/k_1 \\ 1/k_2 \\ . \\ . \\ . \\ 1/k_6 \end{bmatrix} = \text{actuator spring constant matrix}$$

$$L_\ell = \begin{bmatrix} 1/k_1 & 0 & \cdot & \cdot & 0 \\ 0 & 1/k_2 & & & \cdot \\ \cdot & \cdot & & & \\ \cdot & \cdot & & & \cdot \\ 0 & 0 & \cdot & \cdot & 1/k_6 \end{bmatrix} = \text{diagonal actuator spring constant matrix}$$

$$\left(\frac{1}{k}\right)_p = \begin{bmatrix} 1/k_x \\ 1/k_y \\ 1/k_z \\ 1/k_\phi \\ 1/k_\theta \\ 1/k_\psi \end{bmatrix} = \text{platform spring constant matrix (principal elements)}$$

$$\left(\frac{1}{k}\right)_p = K\left(\frac{1}{k}\right)_\ell = \text{spring constant transformation matrix}$$

$$K = \begin{bmatrix} a_{11}^2 & a_{12}^2 & \cdot & \cdot & a_{16}^2 \\ a_{21}^2 & a_{22}^2 & & & \cdot \\ \cdot & & & & \cdot \\ \cdot & & & & \cdot \\ \cdot & & & & \cdot \\ a_{61}^2 & \cdot & \cdot & \cdot & a_{66}^2 \end{bmatrix}$$

$A = H(x_{3v}, r_v)H(x_{3H}, r_H)F$

- velocity transformation from triogonal system to vehicle system

g = gravitational constant = 386 in/sec^2

$$g_e = \begin{pmatrix} 0 \\ 0 \\ g \end{pmatrix} = \text{gravitational vector in earth coordinates.}$$

$$\Delta \ell = \begin{pmatrix} \Delta\ell_1 \\ \Delta\ell_2 \\ \cdot \\ \cdot \\ \cdot \\ \Delta\ell_6 \end{pmatrix} = \text{actuator extension due to gravity}$$

m = mass of vehicle

$$J = \begin{bmatrix} J_{xx} & J_{xy} & J_{xz} \\ J_{xy} & J_{yy} & J_{yz} \\ J_{xz} & J_{yz} & J_{zz} \end{bmatrix} = \text{moment of inertia matrix of vehicle}$$

$$\mathbf{m} = \begin{bmatrix} m & 0 & 0 \\ 0 & m & 0 \\ 0 & 0 & m \end{bmatrix} = \text{mass matrix of vehicle}$$

$$m_v = \left[\begin{array}{c|c} \mathbf{m} & 0 \\ \hline 0 & J \end{array}\right] = \text{inertia matrix of vehicle}$$

m_ℓ = effective inertia matrix seen by actuators

Identities

$$E'(x_3) = E_t(x_3)$$

$$\dot{E}(x_3) = -W(\dot{x}_2)E(x_3)$$

$$\dot{E}'(x_3) = E'(x_3)W(\dot{x}_2)$$

$$E(x_3)W(r)E'(x_3) = W(E(x_3)r)$$

$$W_t(r) = -W(r)$$

$$\frac{\partial}{\partial x_1} = \left[\frac{\partial}{\partial x} \middle| \frac{\partial}{\partial y} \middle| \frac{\partial}{\partial z} \right]$$

$$\frac{\partial}{\partial x_3} = \left[\frac{\partial}{\partial \phi} \middle| \frac{\partial}{\partial \theta} \middle| \frac{\partial}{\partial \psi} \right]$$

$$\frac{\partial}{\partial \ell} = \left[\frac{\partial}{\partial \ell_1} \middle| \frac{\partial}{\partial \ell_2} \middle| \cdots \middle| \frac{\partial}{\partial \ell_6} \right]$$

System Dynamics

Aircraft

Aircraft Acceleration. The external forces and moments acting on the aircraft produce accelerations as follows:

$$\left(\frac{f}{m}\right)_a = \frac{\partial}{\partial t} \left\{ m_a \begin{pmatrix} \dot{x}_1 \\ \hline \dot{x}_2 \end{pmatrix}_a \right\} - m_a \begin{bmatrix} E(x_3)\, g_e \\ \hline 0 \end{bmatrix} \tag{366}$$

Where the aircraft velocities are measured in the aircraft coordinate system, relative to earth. After carrying out the differentiation, this is equivalent to

$$\left(\frac{f}{m}\right)_a = m_a \begin{pmatrix} \ddot{x}_1 \\ \hline \ddot{x}_2 \end{pmatrix}_a + \left[\begin{array}{c|c} W(\dot{x}_{2a}) & 0 \\ \hline 0 & W(\dot{x}_{2a}) \end{array}\right] m_a \begin{pmatrix} \dot{x}_1 \\ \hline \dot{x}_2 \end{pmatrix}_a - m_a \begin{bmatrix} E(x_3)\, g_e \\ \hline 0 \end{bmatrix} \tag{367}$$

The external forces acting on the aircraft and through the triogonal system, the tail boom forces, and the weapon forces are

$$\left(\frac{f}{m}\right)_a = \left\{ \left(\frac{f}{m}\right)_P + \left(\frac{f}{m}\right)_{TB} + \left(\frac{f}{m}\right)_W \right\}_a \tag{368}$$

If the tail boom forces are applied to the aircraft about a coordinate system (fixed to the aircraft) defined by

$$x_{1B} = E(x_{3B})\, x_{1a} - r_B \tag{369}$$

the tail boom forces, referred to the aircraft c.g., are

$$\left(\frac{f}{m}\right)_{a,B} = H_t\,(x_{3B}, r_B)\left(\frac{f}{m}\right)_B \tag{370}$$

The velocities are related by

$$\begin{pmatrix} \dot{x}_1 \\ \hline \dot{x}_2 \end{pmatrix}_B = H(x_{3B}, r_B) \begin{pmatrix} \dot{x}_1 \\ \hline \dot{x}_2 \end{pmatrix}_a \tag{371}$$

The forces exerted by the platform on the aircraft, referred to the aircraft c.g., are

$$\left(\frac{f}{m}\right)_{a,p} = H_t'\,(x_{3a}, r_a)\left(\frac{f}{m}\right)_p \tag{372}$$

The weapon forces, referred to the aircraft c.g., are

$$\left(\frac{f}{m}\right)_{a,w} = H_t\,(x_{3T}, r_T)\, H_t(x_{3w}, r_w)\left(\frac{f}{m}\right)_w \tag{373}$$

Thus, the external forces acting on the aircraft are

$$\left(\frac{f}{m}\right)_a = H_t'(x_{3a}, r_a)\left(\frac{f}{m}\right)_p + H_t(x_{3B}, r_B)\left(\frac{f}{m}\right)_B + H_t(x_{3T}, r_T)\, H_t(x_{3w}, r_w)\left(\frac{f}{m}\right)_w \tag{374}$$

These, plus the gravitational force, must be equal to the rate of change of momentum as given before.

The velocity of the aircraft is equal to the relative velocity between the platform and gimbal systems plus the velocity of the gimbal system all referenced to the aircraft coordinate system. The platform velocity is

$$\begin{pmatrix} \dot{x}_1 \\ \hline \dot{x}_2 \end{pmatrix}_p = H(x_{3p}, r_p)\begin{pmatrix} \dot{x}_1 \\ \hline \dot{x}_2 \end{pmatrix}_G + \begin{pmatrix} \dot{x}_1 \\ \hline \dot{x}_2 \end{pmatrix}_{p/G} \tag{375}$$

where

$$\begin{pmatrix} \dot{x}_1 \\ \hline \dot{x}_2 \end{pmatrix}_{p/G}$$ is the platform velocity, relative to the gimbal system.

That is

$$\begin{pmatrix} \dot{x}_1 \\ \hline \dot{x}_2 \end{pmatrix}_{p/G} = F \cdot \dot{\ell} \tag{376}$$

Referred to the aircraft c.g., this is

$$\begin{pmatrix} \dot{x}_1 \\ \hline \dot{x}_2 \end{pmatrix}_a = H(x_{3a}, r_a) \left\{ H(x_{3p}, r_p) \begin{pmatrix} \dot{x}_1 \\ \hline \dot{x}_2 \end{pmatrix}_G + F \cdot \dot{\ell} \right\} \tag{377}$$

The reaction force of the tail boom actuator is applied to the gimbal system through the transformation linking the tail boom system to the gimbal system. Since

$$x_{1B} = E(x_{3B})\ x_{1a} - r_B \tag{378}$$

$$x_{1a} = E(x_{3a})\ x_{1p} - r_a \tag{379}$$

$$x_{1p} = E(x_{3p})\ x_{1G} - r_p \tag{380}$$

it follows that

$$\begin{aligned} x_{1B} &= E(x_{3B})\ E(x_{3a})\ E(x_{3p}) \cdot x_{1G} \\ &\quad - \left\{ E(x_{3B})\ E(x_{3a})\ r_p + E(x_{3B})\ r_a + r_B \right\} \end{aligned} \tag{381}$$

Thus

$$E(x_{3TB}) = E(x_{3B})\ E(x_{3a})\ E(x_{3p}) \tag{382}$$

and

$$r_{TB} = \left\{ E(x_{3B})\ E(x_{3a})\ r_p + E(x_{3B})\ r_a + r_B \right\} \tag{383}$$

The forces applied to the gimbal system, by the tail boom actuator are then

$$\left(\frac{f}{m}\right)_{G,TB} = H_t(x_{3TB}, r_{TB}) \left(\frac{f}{m}\right)_B \tag{384}$$

The total force applied to (and supplied by) the gimbal system is then

$$\left(\frac{f}{m}\right)_G = H_t\ (x_{3TB}, r_{TB}) \left(\frac{f}{m}\right)_B + H_t\ (x_{3p}, r_p) \left(\frac{f}{m}\right)_p \tag{385}$$

But, since

$$\left(\frac{f}{m}\right)_p = F_t' \cdot f_\ell \tag{386}$$

This is equal to

$$\left(\frac{f}{m}\right)_G = H_t\ (x_{3TB}, r_{TB}) \left(\frac{f}{m}\right)_B + H_t(x_{3p}, r_p)\ F_t'\ f_\ell \tag{387}$$

The final relationship required is that for the tail boom force. It is assumed that this is applied along the aircraft y axis, through the origin of the tail boom system. Then

$$\left(\frac{f}{m}\right)_{TB} = \begin{bmatrix} 0 \\ f_y \\ 0 \\ \hline 0 \\ 0 \\ 0 \end{bmatrix}_{TB} \tag{388}$$

Also, the force is proportioned to the aircraft yaw acceleration

$$\left(f_y\right)_{TB} = - \frac{\Delta J_z}{(r_{TB})_x} \begin{bmatrix} 0 \\ 0 \\ 0 \\ \hline 0 \\ 0 \\ 1 \end{bmatrix}_t \frac{\partial}{\partial t} \begin{pmatrix} \dot{x}_1 \\ \hline \dot{x}_2 \end{pmatrix}_a \tag{389}$$

This can be evaluated as

$$(f_y)_{TB} = -\frac{\Delta J_z}{(r_{TB})_x} \left[\dot{r} + p\dot{y} - q\ \dot{x}\right]_a \tag{390}$$

where

$$\dot{x}_{2a} = \begin{pmatrix} p \\ q \\ r \end{pmatrix} \tag{391}$$

<u>Interaction of systems.</u> The gimbal, triogonal, and tail boom systems are interconnected through the dynamics of the system. The mutual coupling terms can be derived by writing the expression for the output values in terms of the input values. That is

$$\left[\left(\frac{f}{m}\right)_G , f_\ell\right] = f\left[\begin{pmatrix} \dot{x}_1 \\ \dot{x}_2 \end{pmatrix}_G , \dot{\ell} , \left(\frac{f}{m}\right)_w , \left(\frac{f}{m}\right)_{TB} , g\right] \tag{392}$$

By combining the equations listed previously, the output quantities are the gimbal forces,

$$\begin{aligned} \left(\frac{f}{m}\right)_G = {} & H_{p_t} H_{a_t} \frac{\partial}{\partial t}\left\{ m_a H_a H_p \begin{pmatrix} \dot{x}_1 \\ \dot{x}_2 \end{pmatrix}_G \right\} \\ & + H_{p_t} H_{a_t} \frac{\partial}{\partial t}\left\{ m_a H_a F \dot{\ell} \right\} \\ & - H_{p_t} H_{a_t} H_{T_t} H_{w_t} \left(\frac{f}{m}\right)_w \\ & - H_{p_t} H_{a_t} m_a \begin{bmatrix} E(x_3) g_e \\ 0 \end{bmatrix} \end{aligned} \tag{393}$$

the actuator forces,

$$f_\ell = F_t H_{a_t} \frac{\partial}{\partial t}\left\{ m_a H_a H_p \begin{pmatrix} \dot{x}_1 \\ \text{---} \\ \dot{x}_2 \end{pmatrix}_G \right\}$$

$$+ F_t H_{a_t} \frac{\partial}{\partial t}\left\{ m_a H_a F \dot{\ell} \right\}$$

$$- F_t H_{a_t} H_{B_t} \left(\frac{f}{m}\right)_{TB}$$

$$- F_t H_{a_t} H_{T_t} H_{w_t} \left(\frac{f}{m}\right)_w$$

$$- F_t H_{a_t} m_a \begin{bmatrix} E(x_3)\ g_e \\ \text{------} \\ 0 \end{bmatrix} \qquad (394)$$

and the tail boom actuator velocity

$$\begin{pmatrix} \dot{x}_1 \\ \text{--} \\ \dot{x}_2 \end{pmatrix}_{B,a/G} = H_B H_a F\dot{\ell} \qquad (395)$$

The values of inertia used in the matrix, m_a, in these equations are the actual values, since the inertia augmentation loop has not been closed. The tail boom force is given by

$$\left(\frac{f}{m}\right)_{TB} = -\frac{\Delta J_z}{(r_{TB})_x} \begin{bmatrix} 0 \\ 0 \\ 0 \\ 0 \\ 0 \\ 1 \end{bmatrix}_t \frac{\partial}{\partial t} \begin{pmatrix} \dot{x}_1 \\ \text{--} \\ \dot{x}_2 \end{pmatrix}_a \qquad (396)$$

The aircraft velocities, $\begin{pmatrix} \dot{x}_1 \\ \text{--} \\ \dot{x}_2 \end{pmatrix}_a$, must be determined from the total system response, not just the external system, as represented by the dynamic equations which makes it necessary to add the feedback loops and actuator output impedances. For the triogonal actuators, this includes the spring rate simulation L_ℓ, and for the tail boom actuator, the aircraft yaw acceleration feedback as previously stated. For all actuators, it includes the compressibility and leakage components of the output impedance.

The first two terms of the force equations for the gimbal and triogonal systems represent the inertia effect of the load (acceleration and gyroscopic effects). The third term of the triogonal force equation is the inertia augmentation force, and since it is derived from the aircraft acceleration, it can be lumped into the inertia term by modifying the yaw moment of inertia. The last two terms of each give the response to the weapon and gravitational force inputs, respectively.

The tail boom actuator velocity is determined entirely by the motion of the triogonal system, since it is the only movable link coupling the two ends of the tail boom actuator.

Evaluation of the cross-coupling terms among the gimbal, triogonal, and tail boom systems can be accomplished by performing the indicated differentation of the momentum terms. Because of the highly nonlinear nature of the solution, the values will depend on the instantaneous velocities of the various parts of the system. The derivatives of the impedance transformation matrices have been evaluated for determining the linear coefficients, so that these can be used directly for numerical evaluation of the cross-coupling terms.

If it is assumed that the mass and aircraft transformation matrices are invariant, the two time derivatives are equal to

$$\frac{\partial}{\partial t}\left\{ m_a H_a H_p \begin{pmatrix} \dot{x}_1 \\ \hline \dot{x}_2 \end{pmatrix}_G \right\}$$

$$= m_a H_a H_p \left\{ \begin{pmatrix} \ddot{x}_1 \\ \hline \ddot{x}_2 \end{pmatrix}_G + \left[\begin{array}{c|c} W(\dot{x}_{2G}) & 0 \\ \hline 0 & W(\dot{x}_{2G}) \end{array}\right] \begin{pmatrix} \dot{x}_1 \\ \hline \dot{x}_2 \end{pmatrix}_G + \right.$$

$$\left. - \left[\begin{array}{c|c} E'(x_{3p}) & 0 \\ \hline 0 & E'(x_{3p}) \end{array}\right] \left[\begin{array}{c|c} W(\dot{x}_{2p}) & W(\dot{r}_p) \\ \hline 0 & W(\dot{x}_{2p}) \end{array}\right] \left[\begin{array}{c|c} E(x_{3p}) & 0 \\ \hline 0 & E(x_{3p}) \end{array}\right] \begin{pmatrix} \dot{x}_1 \\ \hline \dot{x}_2 \end{pmatrix}_G \right\}$$

(397)

Since

$$E'(x_3)\ W(r)\ E(x_3) = W\ (E'r), \tag{398}$$

the last term can be simplified somewhat and

$$\frac{\partial}{\partial t}\left\{{}^{m}H_{a}{}_{a}F\dot{\ell}\right\} = {}^{m}H_{a}{}_{a}\left\{\dot{F}\dot{\ell} + F\ddot{\ell}\right\}$$

$$= {}^{m}H_{a}{}_{a}F\left\{\overset{\bullet\circ}{\ell} - \dot{F}'F\dot{\ell}\right\} \tag{399}$$

The matrix of scalar actuator velocities can be differentiated directly since they are scalar quantities. The derivative of the transformation, F', was derived earlier in terms of the vector actuator velocities. The n-th row of this matrix is

$$(\dot{F}')_n = \left[\frac{-(\dot{\ell}_{pn})_t}{\ell_{on}} W^2 \begin{pmatrix}\alpha\\ \beta\\ \gamma\end{pmatrix}_n \;\middle|\; \frac{(\dot{\ell}_{pn})_t}{\ell_{on}} W^2 \begin{pmatrix}\alpha\\ \beta\\ \gamma\end{pmatrix}_n W(a_n) \right] \tag{400}$$

where the scaler velocity of the n-th actuator is given by equation (25).

To derive cross-coupling terms as functions of the scalar velocities, the vector velocity must be expressed as a function of the scalar velocity. For the n-th actuator, this is

$$(\dot{\ell}_p)_n = \left[1 \;\middle|\; -W(a_n)\right] F \cdot \dot{\ell} \tag{401}$$

or

$$(\dot{\ell}_p)_{n_t} = \dot{\ell}_t F_t \left[\frac{1}{W(a_n)}\right] \tag{402}$$

Thus, the n-th row of $\dot{F}'$ is equal to

$$(\dot{F}')_n = \left[-\frac{\dot{\ell}_t}{\ell_{on}} F_t \left[\frac{1}{W(a_n)}\right] W^2 \begin{pmatrix}\alpha\\ \beta\\ \gamma\end{pmatrix}_n \;\middle|\; \frac{\dot{\ell}_t}{\ell_{on}} F_t \left[\frac{1}{W(a_n)}\right] W^2 \begin{pmatrix}\alpha\\ \beta\\ \gamma\end{pmatrix}_n W(a_n) \right] \tag{403}$$

Since F_t must be evaluated numerically by finding the inverse of F', this expression cannot be reduced any further. For a given geometry, the triogonal system and its cross coupling terms can be evaluated numerically. The result will be a 6 x 6 matrix of coefficients, postmultiplied by the scalar actuator velocity matrix.

All cross-coupling terms between the gimbal and triogonal systems result from the inertia and gyroscopic effects. Between the triogonal and tail boom systems, there is a direct transfer of forces given by

$$\frac{\partial f_\ell}{\partial\left(\frac{f}{m}\right)_W} = -F_t H_{a_t} H_{T_t} H_{w_t} \tag{404}$$

and a direct transfer of velocities given by

$$\frac{\partial \begin{pmatrix} \dot{x}_1 \\ -- \\ \dot{x}_2 \end{pmatrix}_{B,a/G}}{\partial \dot{\ell}} = H_B H_a F \tag{405}$$

Again, the matrices F and F_t must be evaluated numerically.

Combat Vehicle

The dynamics of the combat vehicle are similar to that for the aircraft, except that the tail boom actuator is not used, and an additional pitch actuator system is placed between the platform system and the vehicle system. Reaction forces of the pitch system are applied to the triogonal system (platform).

Vehicle Geometry. The external forces applied to the vehicle are now given by

$$\left(\frac{f}{m}\right)_V = \left\{\left(\frac{f}{m}\right)_H + \left(\frac{f}{m}\right)_W\right\}_V \tag{406}$$

and consist only of those forces transmitted from the pitch actuator and the weapon systems.

The weapon forces, referred to the vehicle, are now

$$\left(\frac{f}{m}\right)_{V,W} = H_t\left(X_{3T}, r_T\right) H_t\left(X_{3W}, r_W\right)\left(\frac{f}{m}\right)_W \tag{407}$$

and the pitch system forces, referred to the vehicle are

$$\left(\frac{f}{m}\right)_{V,H} = H_t'\left(X_{3V}, r_V\right)\left(\frac{f}{m}\right)_H \tag{408}$$

The actuator forces are now

$$f_\ell = F_t H_t\left(X_{3H}, r_H\right)\left(\frac{f}{m}\right)_H \tag{409}$$

The velocity of the platform is again equal to the relative velocity of the platform to the gimbal system plus the velocity of the gimbal system, referenced to the platform system coordinates.

$$\left(\frac{\dot{X}_1}{\dot{X}_2}\right)_P = \left\{\left(\frac{\dot{X}_1}{\dot{X}_2}\right)_G + \left(\frac{\dot{X}_1}{\dot{X}_2}\right)_{P/G}\right\}_P \tag{410}$$

The pitch system velocity is equal to the velocity of the platform plus the velocity of the pitch system relative to the platform, referenced to the pitch system coordinates.

$$\left(\frac{\dot{X}_1}{\dot{X}_2}\right)_H = \left\{\left(\frac{\dot{X}_1}{\dot{X}_2}\right)_P + \left(\frac{\dot{X}_1}{\dot{X}_2}\right)_{H/P}\right\}_H \tag{411}$$

Thus, the velocity of the pitch system is

$$\left(\frac{\dot{X}_1}{\dot{X}_2}\right)_H = H_H\left\{\left(\frac{\dot{X}_1}{\dot{X}_2}\right)_G + F\dot{\ell}\right\} \left(\frac{\dot{X}_1}{\dot{X}_2}\right)_{H/G} \tag{412}$$

Finally, the velocity of the vehicle is

$$\left(\frac{\dot{X}_1}{\dot{X}_2}\right)_V = H_V \left(\frac{\dot{X}_1}{\dot{X}_2}\right)_H \tag{413}$$

The gravitational force applied at the vehicle CM is again equal to

$$\left(\frac{f}{m}\right)_g = m_V \left[\begin{array}{c|c} E(X_3) & 0 \\ \hline 0 & E(X_3) \end{array}\right] \left[\begin{array}{c} 0 \\ 0 \\ g \\ \hline 0 \\ 0 \\ 0 \end{array}\right] = m_V \left[\begin{array}{c} E(X_3) g_e \\ \hline 0 \end{array}\right] \tag{414}$$

where

$$E(X_3) = E(X_{3V})\, E(X_{3H})\, E(X_{3P})\, E(X_{3G}) \tag{415}$$

defines the Euler angles of the vehicle, referenced to earth.

Interaction of Systems. The output functions are now the gimbal, pitch, and triogonal system forces. Inputs are gimbal, triogonal, and pitch system velocities and weapon forces. The output functions are given by

Pitch actuator forces

$$
\begin{aligned}
\left(\frac{f}{m}\right)_H = {} & H_{V_t} \frac{\partial}{\partial t} \left\{ m_V H_V \begin{pmatrix} \dot{X}_1 \\ \dot{X}_2 \end{pmatrix}_{H/P} \right\} \\
& + H_{V_t} \frac{\partial}{\partial t} \left\{ m_V H_V H_H H_P \begin{pmatrix} \dot{X}_1 \\ \dot{X}_2 \end{pmatrix}_G \right\} \\
& + H_{V_t} \frac{\partial}{\partial t} \left\{ m_V H_V H_H F \dot{\ell} \right\} \\
& - H_{V_t} H_{T_t} H_{W_t} \left(\frac{f}{m}\right)_W \\
& - H_{V_t} m_V \begin{bmatrix} E(X_3) g_e \\ 0 \end{bmatrix}
\end{aligned}
\tag{416}
$$

Triogonal actuator forces

$$
f_\ell = F_t H_{H_t} \left(\frac{f}{m}\right)_H \tag{417}
$$

Gimbal forces

$$
\left(\frac{f}{m}\right)_G = H_{P_t} H_{H_t} \left(\frac{f}{m}\right)_H \tag{418}
$$

Since all systems are cascaded, they must supply the same forces transformed through the geometry. Again, all coupling terms are the result of inertia and gyroscopic effects except the weapon and gravitational forces. In the derivatives of the momentum, the variables are the pitch system, H_H, the platform system, H_P, the triogonal system, F, and the input velocities, $\begin{pmatrix} \dot{X}_1 \\ \dot{X}_2 \end{pmatrix}_{H/P}$, $\begin{pmatrix} \dot{X}_1 \\ \dot{X}_2 \end{pmatrix}_G$, and $\dot{\ell}$. The derivative of $\dot{\ell}$ is again $\frac{\partial}{\partial t} \dot{\ell} = \ddot{\ell}$, while the

derivatives of the gimbal and pitch system velocities are

$$\frac{\partial}{\partial t}\begin{pmatrix}\dot{X}_1\\ \hline \dot{X}_2\end{pmatrix}_G = \begin{pmatrix}\ddot{X}_1\\ \hline \ddot{X}_2\end{pmatrix}_G + \left[\begin{array}{c|c} W(\dot{X}_{2G}) & 0 \\ \hline 0 & W(\dot{X}_{2G})\end{array}\right]\begin{pmatrix}\dot{X}_1\\ \hline \dot{X}_2\end{pmatrix}_G \tag{419}$$

and

$$\frac{\partial}{\partial t}\begin{pmatrix}\dot{X}_1\\ \hline \dot{X}_2\end{pmatrix}_{H/P} = \begin{pmatrix}\ddot{X}_1\\ \hline \ddot{X}_2\end{pmatrix}_{H/P} + \left[\begin{array}{c|c} W(\dot{X}_{2_{H/P}}) & 0 \\ \hline 0 & W(\dot{X}_{2_{H/P}})\end{array}\right]\begin{pmatrix}\dot{X}_1\\ \hline \dot{X}_2\end{pmatrix}_{H/P} \tag{420}$$

Again, the derivatives of the transformations are

$$\begin{aligned} H'\dot{H} &= -\left[\begin{array}{c|c} E' & 0 \\ \hline 0 & E'\end{array}\right]\left[\begin{array}{c|c} W(\dot{X}_2) & W(\dot{r}) \\ \hline 0 & W(\dot{X}_2)\end{array}\right]\left[\begin{array}{c|c} E & 0 \\ \hline 0 & E\end{array}\right] \\ &= -\left[\begin{array}{c|c} W\left(E'\dot{X}_2\right) & W(E'\dot{r}) \\ \hline 0 & W(E'\dot{X}_2)\end{array}\right] \end{aligned} \tag{421}$$

The momentum derivatives then become

$$\begin{aligned} &\frac{\partial}{\partial t}\left\{m_V\ H_V\begin{pmatrix}\dot{X}_1\\ \hline \dot{X}_2\end{pmatrix}_{H/P}\right\} = \\ &= m_V\ H_V\left\{\begin{pmatrix}\ddot{X}_1\\ \hline \ddot{X}_2\end{pmatrix}_{H/P} + \left[\begin{array}{c|c} W(\dot{X}_{2_{H/P}}) & 0 \\ \hline 0 & W(\dot{X}_{2_{H/P}})\end{array}\right]\begin{pmatrix}\dot{X}_1\\ \hline \dot{X}_2\end{pmatrix}_{H/P}\right\} \end{aligned} \tag{422}$$

$$\frac{\partial}{\partial t}\left\{ m_V H_V H_H H_P \begin{pmatrix} \dot{X}_1 \\ \hline \dot{X}_2 \end{pmatrix}_G \right\} =$$

$$= m_V H_V H_H H_P \left\{ \begin{pmatrix} \ddot{X}_1 \\ \hline \ddot{X}_2 \end{pmatrix} + \left[\begin{array}{c|c} W(\dot{X}_{2G}) & 0 \\ \hline 0 & W(\dot{X}_{2G}) \end{array}\right] \begin{pmatrix} \dot{X}_1 \\ \hline \dot{X}_2 \end{pmatrix}_G \right. +$$

$$- \left[\begin{array}{c|c} W\left(E_P{}'\dot{X}_{2_{P/G}}\right) & W\left(E_P{}'\dot{r}_P\right) \\ \hline 0 & W\left(E_P{}'\dot{X}_{2_{P/G}}\right) \end{array}\right] \begin{pmatrix} \dot{X}_1 \\ \hline \dot{X}_2 \end{pmatrix}_G +$$

$$\left. - H_P{}' \left[\begin{array}{c|c} W\left(E_H{}'\dot{X}_{2_{H/P}}\right) & W\left(E_H{}'\dot{r}_H\right) \\ \hline 0 & W\left(E_H{}'\dot{X}_{2H/P}\right) \end{array}\right] H_P \begin{pmatrix} \dot{X}_1 \\ \hline \dot{X}_2 \end{pmatrix}_G \right\} \tag{423}$$

and

$$\frac{\partial}{\partial t}\left(m_V H_V H_H F \dot{\ell} \right) =$$

$$= m_V H_V H_H F \left\{ \ddot{\ell} - F' \left[\begin{array}{c|c} W(E_H{}'\dot{X}_{2_{H/P}}) & W(E_H{}'\dot{r}_H) \\ \hline 0 & W(E_H{}'\dot{X}_{2_{H/P}}) \end{array}\right] F \dot{\ell} \right.$$

$$\left. - (\dot{F}'F)\,\ddot{\ell} \right\} \tag{424}$$

Again, a numerical evaluation is the only practical way to determine the value of these cross-coupled terms, since they involve the matrix, F.

Passive System Mathematical Model

Purpose

The primary purpose of the mathematical model is to determine the upper and lower cylinder pressures of the triogonal actuator to produce the desired spring rate. The computer program STIFF 2 (app C) generates the required cylinder pressures as well as the actuator forces and stiffnesses for the specified gimbal rotation (pitch and yaw) because of the acting weight, the applied load and the system stiffness required.

The work detailed earlier in this report represents that portion of the analysis used in the passive system as detailed for computer programming.

Technical Approach

The following notations are used in this technical discussion:

$\underset{\sim}{F}$ = Force applied to system

K = System stiffness

$\underset{\sim}{D}$ = System deflection

$\underset{\sim}{f}$ = Actuator force

k = Actuator stiffness

$\underset{\sim}{d}$ = Actuator displacement

A = Force transformation matrix

B = Displacement transformation matrix

A^T = Matrix A transposed

B^{-1} = Matrix B inverted

Having specified the desired system stiffness (K) at the center (B) of the mounting platform, the actuator stiffnessess (k) can be derived as follows:

$$\underset{\sim}{F} = K \underset{\sim}{D} \tag{425}$$

$$\underset{\sim}{f} = k \underset{\sim}{d} \tag{426}$$

$$\underset{\sim}{f} = A \underset{\sim}{F} \tag{427}$$

$$\underset{\sim}{d} = B \underset{\sim}{D} \tag{428}$$

Substituting equations (427) and (428) in equation (425) we get

$$A \underset{\sim}{F} = k\ B\ \underset{\sim}{D}$$

$$\underset{\sim}{F} = A^{-1}\ k\ B\ \underset{\sim}{D} \tag{429}$$

From equations (425) and (429) we conclude that

$$K = A^{-1}\ k\ B \tag{430}$$

but

$$A^{-1} = B^{T} \text{ (app D)} \tag{431}$$

$$\therefore\ K = B^{T}\ k\ B \tag{432}$$

also

$$k = A\ K\ A^{T} \tag{433}$$

where $B^{-1} = A^{T}$ (app D).

By defining the system stiffness (K) at the center (B) of the mounting platform, the actuator stiffnesses (k) can be determined using equation (433). Similarly, the system stiffness (K) can be determined from equation (432), when the actuator stiffnesses are known. The above necessitates defining either of the matrices A or B, which can be obtained from the next three paragraphs.

Derivation of the Transformation Matrix $(B)^T$

The triogonal actuators represent a statically determinate system. This property makes it possible to obtain the transformation matrix (B), which is determined from the following six equations of equilibrium of forces:

$$\left.\begin{aligned}
F_x &= a_{x_1} f_1 + a_{x_2} f_2 + \text{-------} + a_{x_6} f_6 \\
F_y &= a_{y_1} f_1 + a_{y_2} f_2 + \text{-------} + a_{y_6} f_6 \\
F_z &= a_{z_1} f_1 + a_{z_2} f_2 + \text{-------} + a_{z_6} f_6 \\
M_x &= f_1(y_1 \cdot a_{z_1} - z_1 \cdot a_{y_1}) + \text{-------} + f_6(y_6 \cdot a_{z_6} - z_6 \cdot a_{y_6}) \\
M_y &= f_1(z_1 \cdot a_{x_1} - x_1 \cdot a_{z_1}) + \text{-------} + f_6(z_6 \cdot a_{x_6} - x_6 \cdot a_{z_6}) \\
M_z &= f_1(x_1 \cdot a_{y_1} - y_1 \cdot a_{x_1}) + \text{-------} + f_6(x_6 \cdot a_{y_6} - y_6 \cdot a_{x_6})
\end{aligned}\right\} \tag{434}$$

Where F_X, F_Y, F_Z, M_X, M_Y, and M_Z are the applied loads and moments to the system in the coordinate system, directions X, Y and Z, f_1--f_6 are the forces in the actuators 1 through 6, a_{x1} is the direction cosine of actuator 1 in the X direction, etc., x, y, and z are the distances from the corresponding pivot point of the actuator to the system axes on the mounting platform in the x, y, and z directions, respectively.

The above six equations can be represented in a matrix form as follows:

$$\underset{\sim}{F} = B^T \underset{\sim}{f} \tag{435}$$

Method of Analysis

Having defined the external system loads (or recoil load) and the stiffness desired in the load direction, the actuator stiffnesses can then be calculated as follows:

1. Determine the displacements and rotations of the center (B) of the mounting platform, knowing the system load (F) and flexibility (K^{-1}) at center (B) $\underset{\sim}{D} = K^{-1} \underset{\sim}{F}$

2. Obtain the actuator displacement (d) $\underset{\sim}{d} = B^T \underset{\sim}{D}$

3. Determine the actuator forces due to the system load (F) $\underset{\sim}{f}_1 = A \underset{\sim}{F}$

4. Determine the actuator forces due to the static load (P) $\underset{\sim}{f}_2 = A \underset{\sim}{P}$

5. Calculate the actuator stiffnesses $\underset{\sim}{k} = \underset{\sim}{f}_1 / \underset{\sim}{d}$

6. Knowing the effective areas (A) of the actuator, we calculate the pressure drop (Δp) across the actuator pistons $\Delta \underset{\sim}{p} = \underset{\sim}{f}_2 / \underset{\sim}{A}_o$

7. Calculate the top and bottom pressures in the actuators

$$P_t = k\ V/2Ao^2 - \Delta p/2$$

$$P_b = k\ V/2Ao^2 - \Delta p/2$$

where V = volume of the accumulator.

Capabilities of the Computer Program STIFF 2

Output Generated.

1. Actuator forces due to the static load (weight)

2. Actuator forces and displacements due to external load (recoil load)

3. Actuator stiffnesses due to the external load

4. Actuator pressures in the top and bottom cylinders due to all the applied loads

5. Top and bottom accumulator precharge pressure is generated when using oil in the actuators, and actuator precharge pressure is generated when using nitrogen

Possible Loading Conditions. This computer program is written flexibly to handle various loading conditions. Some examples are as follows:

1. For the stiffness required at the center of the mounting platform, the information given in the previous section is generated for the applied loads and the required system stiffness which are specified at the center of the mounting platform and in the direction of the platform axes.

2. For the stiffness required at the c.g. location of the vehicle, the same information given previously is generated when the applied loads and the required system stiffness are specified at the c.g. of the vehicle in the direction of the vehicle axes.

3. For the stiffness required at the weapon pivot, the recoil load and the required system stiffness are specified along the axis of the weapon, as well as the acting weight at the c.g. of the vehicle. The information generated is given in the previous section. The axis of the weapon is defined as the direction from the weapon pivot point to a specific target position.

The results are also produced by including the pitch and yaw motions of the gimbal system, while the stiffness required at the c.g. of the vehicle and at the weapon pivot are for the active system.

Input Data Required. The input data needed to use the computer program is explained as follows:

1. The mounting angle theta is between the vehicle longitudinal axis (X_V) and the mounting platform axis (X_P).

2. The acting weights are the weight of the platform, part of the actuator weights, and the payload.

3. Location of the c.g. of the acting weights are derived from the gimbal axes $(X, Y \text{ and } Z)_G$.

4. Location of weapon mounting point is derived from the c.g. location of the acting weights.

5. Location of the target is to be derived from the earth axes $(X, Y \text{ and } Z)_G$.

6. Pitch and yaw angles of the gimbal

7. Damping media are used in the actuators to get a spring constant. Either oil for the higher spring rates and damping, or nitrogen for the lower spring rates and damping can be used.

8. As detailed previously, three locations for the system stiffness are possible.

9. The system stiffness is specified in any one or all of the system directions for translation and rotation. Forces are also specified where the stiffness is given. If the system stiffness is found at the weapon mounting point, only the stiffness and force along the weapon axis are specified.

List of Constants Used in STIFF 2.

1. Coordinates of the pivot centers of actuators at yaw gimbal (XG (I), I = 1, 6)

2. Coordinates of the pivot centers of moving platform (XP(I), I = 1, 6)

3. Effective area of actuator piston (AP = 21.205 $in.^2$)

4. Total volume of accumulator plus actuator fully extended (V_o = 421 $in.^3$)

5. Effective volume of the actuator and the maximum and minimum actuator stiffness is shown in table 1.

The STIFF 2 input map is shown in table 2.

MAIN HYDRAULIC POWER UNIT

Priority

Design and part selection for the hydraulic power unit was given first priority since this is a long lead time item. Further urgency is given to this unit since the Government is required to provide a suitable room in which the unit can be installed. The physical arrangement and clearance dimensions for such a room, to house the equipment described in this report, is shown on drawing D-2637.[1]

Flow Requirements

The basic criteria for specifying this power unit is the total flow required to drive the various subsystems at their maximum performance velocities. These velocities (or rpm) are derived elsewhere in this report and are used here to predict the maximum required flow rate. Flow rate for a given actuator velocity can be obtained from the formula

$$Q_{valve}(\text{gpm}) = \frac{\text{Velocity}^{\text{"/sec}} \times \text{piston area}^{\text{sq in}} \times 60^{\text{sec/min}}}{231^{\text{cu in/gal}}} \tag{436}$$

Then for pitch

$$Q_V = \frac{25.74 \times 50.265 \times 60}{231} = 336 \text{ gpm} \tag{437}$$

This will be the flow required on the larger area of the piston and through the servovalve. Considering that this pitch motion is a simple harmonic motion, the actual pumping capacity can be reduced by providing appropriate accumulators on the line. The use of accumulators will reduce the actual pump flow to

$$Q_{pump}(\text{gpm}) = \frac{2 \times Q_{valve}}{\pi} \text{ or}$$

$$= \frac{2 \times 336}{\pi} = 214 \text{ gpm} \tag{438}$$

The flow for yaw will be calculated in a somewhat different manner since a piston type hydraulic motor is involved rather than a hydraulic cylinder.

---

[1]Drawings cited throughout this report are on file at the Ware Simulation Center, Rock Island Arsenal, Rock Island, IL, and are available for reference.

In the piston type, the motor flow is dependent on the motor displacement, maximum motor rpm, and volumetric efficiency of the motor, or

$$Q_v(\text{gpm}) = \frac{q^{\,''^3/\text{rev}} \times \text{rpm}}{231^{\,''^3/\text{gal}} \times e} \qquad (439)$$

where

q = motor displacement/rev = 2310 in^3/rev (taken from Haggulund's catalog motor model 8385)

e = volumetric efficiency = .8 (from catalog)

$$Q_v(\text{gpm}) = \frac{2310 \times 3.15}{231 \times .8} = 39.37 \qquad (440)$$

This will be the maximum flow required at the motor and through the servovalve. The use of appropriate accumulators on the line will reduce the actual pump flow to

$$Q_p(\text{gpm}) = \frac{2 \times 39.37}{\pi} = 25 \text{ gpm [from equation (438)]} \qquad (441)$$

The flow requirements for the 6-DOF suspension when using it as a spring rate device are fully developed later in this report. The flow entered in table 3 is based on the availability of the 480-gpm pump unit when simultaneous maximum performance of all units is required. Limitations of various factors which influence the actual flow rate will be explained later.

The flow for the tail boom simulator is calculated for a hydraulic cylinder from equation (436) or

$$Q_v = \frac{10.2^{\text{in/sec}} \times 1.6567^{\text{sq in}} \times 60^{\text{sec/min}}}{231^{\text{cu in/gal}}} = 4.4 \text{ gpm} \qquad (442)$$

This will be the maximum flow required at the cylinder and through the servovalve. The use of accumulators on this line is not appropriate, so the pump flow requirement will also be 4.4 gpm.

Similarly the flow for the combat vehicle pitch is

$$Q_v = \frac{64.4^{\text{in/sec}} \times 7.568^{\text{sq in}} \times 60^{\text{sec/min}}}{231^{\text{cu in/gal}}} = 127 \text{ gpm} \qquad (443)$$

maximum flow at the cylinder and through the servovalve. The use of appropriate accumulators on the line will reduce the actual pump flow to

$$Q_p(\text{gpm}) = \frac{2 \times 127}{\pi} = 81 \text{ gpm} \qquad (444)$$

Again, the flow for the combat vehicle yaw, is

$$Q_v = \frac{22.5^{in/sec} \times 10.652^{sq\ in} \times 60^{sec/min}}{231^{cu\ in/gal}} = 62.25 \text{ gpm} \tag{445}$$

maximum flow at each of six cylinders and through each of six servovalves. Since all six actuators must be moving simultaneously, the total flow requirement will be 6 x 62.25 gpm or 373.5 gpm. The use of accumulators will reduce the actual pump flow to

$$Q_p(\text{gpm}) = \frac{2 \times 373.5}{\pi} = 238 \text{ gpm} \tag{446}$$

Three vibration systems are provided, two small units to simulate miscellaneous vibrations and one large unit to simulate rotor vibrations as discussed in detail later in this report.

The cylinder for the small units has an effective area of .283 sq in., and its piston moves at a maximum velocity of 31.4 in./sec, thus from equation (436).

$$Q_v = \frac{31.4^{\ in/sec} \times .283^{\ sq\ in} \times 60^{\ sec/min}}{231^{\ cu\ in/\ gal}} = 2.31 \text{ gpm} \tag{447}$$

The cylinder for the large unit has an effective area of 1.89 sq in., and its piston moves at a maximum velocity of 47.3 in./sec, thus from equation (436)

$$Q_v = \frac{47.3^{in/sec} \times 1.89^{sq\ in} \times 60^{sec/min}}{231^{cu\ in/gal}} = 23.2 \text{ gpm} \tag{448}$$

Thus the total valve flow is

$$2 \times 2.31 + 23.2 = 27.8 \text{ gpm} \tag{449}$$

The use of appropriate accumulators on the line will reduce the actual pump flow to

$$Q_p(\text{gpm}) = \frac{2 \times 27.8}{\pi} = 18 \text{ gpm} \tag{450}$$

From the above equation, the oil pump flow will be required for maximum performance of the various motions as shown in table 3.

Accumulator sizing is explained in appendix E, and accumulators for servosystems are given in table 4.

Component Selection

Six potential suppliers were contacted for equipment recommendations, pricing, and delivery schedules. Of these only one, Airline Hydraulics Corporation, a distributor of Vicker's, Inc., equipment, has produced an acceptable proposal. On this basis, we have continued to negotiate with them.

Our design incorporates two power units, each with a rated flow of 120 gpm at 3000 psi, or a total pump flow of 240 gpm. From the information in table 3, it is apparent that this flow is adequate for the highest performance of any system operating alone. Combinations of simultaneous motions are possible at lower performance levels. These maximum performance levels can be determined by use of the various performance graphs included later in this report.

A block diagram of the overall hydraulic system (including the power units) is shown in figure 2. The schematic arrangement of the unit, as it is being developed, is shown on drawing C-2624 with its list of materials on drawing B-2631. A common 600 gallon-capacity tank will be provided to serve the total hydraulic system (both present and future equipment). Also, common pressure and return manifolds will be provided to serve both the present and future hydraulic equipment. As noted above, two identical 120 gpm-pump units will be furnished now with provisions for adding two additional, identical units in the future.

The selected Vickers, Inc., variable delivery, pressure compensated, axial piston pumps, Model PVA-120, requires that its suction inlet be pressurized to 100 psi to provide maximum life and efficiency and the quietest operation. This inlet pressure will be supplied to each main pump by its own auxiliary centrifugal pump rated at 200 gpm and 125-psi pressure. This pump will have its own motor rated at

$$\text{H.P.} = \frac{\text{Flow}^{\text{gpm}} \times \text{Pressure}^{\text{psi}}}{1714} \div \frac{1}{\text{efficiency}}$$

$$= \frac{200 \text{ gpm} \times 125 \text{ psi}}{1714} \times \frac{1}{73\%} = 20 \text{ H.P.} \tag{451}$$

Output of this pump will be fed through full flow 10μ pressure filters and then to the suction inlet of its main pump. A pressure relief valve is provided in this line to protect against excessive pressure and to proportion the auxiliary pump flow to the suction requirements of the main pump. A pressure switch is provided in this line to interlock main pump motor starter to line pressure so that the main pump cannot be started unless suction pressure is available. An electric switch on the filters signals the operator control panel to indicate condition (cleanliness) of the filters.

Each main pump is rated for 120 gpm, 3000 psi at 1200 rpm and will have its own motor rated at

$$\text{H.P.} = \frac{120^{\text{gpm}} \times 3000^{\text{psi}}}{1714} \times \frac{1}{94\%} = 224 \text{ H.P. [from equation (451)]} \tag{452}$$

The nearest standard motor of 250 HP will be provided. The motor will be wound as a part winding start motor to reduce the inrush current to 65% of normal inrush (for across-the-line starting). Suitable part winding starting equipment will be provided in the unit control center (units 1M and 2M).

The output of this pump will be fed to the pressure distribution manifold with the aid of the following devices: (1) a pressure relief valve to protect against excessive pressure, (2) a check valve to prevent pressure interaction between the pumps connected to the distribution manifold, and (3) a pressure guage for convenience in adjusting pump pressure and relief valve settings.

Oil returning from the various operating systems will be collected in a common return manifold. From this manifold, it will be circulated through the cooling coils and returned to the common supply tank. Suitable valving, controls, and sensors are provided to maintain the set operating temperature of the oil.

To prevent surges and the possibility of cavitation of the hydraulic fluid on the return side of the servovalves, the return manifold is pressurized to 75 psi by a check valve set for this pressure. Accumulators are provided on both the pressure and return manifolds to smooth the flow of oil. Calculations for sizing these accumulators are given in appendix E.

Cooling System

Some means must be provided for dissipating the heat produced by extended high performance operation of the hydraulic equipment. Since cooling water is not available at the installation, we have investigated the possibility of using oil-to-air cooling equipment. We have pursued this with several manufacturers. The best proposal was received from DeAnnuntis and Associates, Inc., representing the Trane Co. Two systems were proposed, one for a 95°F ambient air temperature and one for 105°F. Pertinent data from DeAnnuntis is given in appendix E.

Control Center

Closely associated with the hydraulic power unit is the electric control center. We are planning to furnish a unit type control center which will provide for distribution of the electric power. This control center, to be installed in the pump room, will have the starters for the main pump motors, the auxiliary pump motors, and the cooling fan motors. Empty plug-in spaces will be provided for later installation of starting equipment for the future pump units. The physical layout of the pump unit, the individual compartment diagrams, and the overall schematic for the system, are shown in appendix E.

Starters for the main pump motors are mounted in compartments 1M and 2M. They are connected as two winding motors to provide reduced starting current and consequent lower line currents (dwg A-2639, app E). Provisions are made for starting and stopping these motors at the control center or at the control console (see dwg 2CD-127). An interlock is provided to prevent operation of these motors until adequate suction pressure is available. Circuit breakers and overload relays are provided to protect the motors and line equipment from excess current demands or short circuits. Provision is made in each of these compartments for connecting three size 500-MCM power leads provided by the Government from their 440 V, three phase, 60-Hz supply. Compartments 5M and 6M are reserved for future addition of identical starting equipment.

Starters for the auxiliary pump motors are mounted in compartments 3B and 3D. These units are plug-in devices which connect to the rear mounted bus bar system. They are connected as across-the-line starters (dwg A-2640, app E). Provisions are made for starting and stopping these motors at the control center or at the control console (dwg 2CD-127). Circuit breakers and overload relays are provided to protect the motors and line equipment from excess current demands or short circuits. Compartments 3F and 3H are reserved for future addition of identical starting equipment.

Compartment 3K is empty and will not be used.

Compartment 3M contains a relay panel with the contactor (CR) for energizing the 110 V circuits, a relay (AR) which controls the oil cooler fan motors and fuses for the various remote equipment lines (dwg A-2641, app E).

Starters for the oil cooler fan motors are mounted in compartments 4B and 4D. These units are plug-in devices which connect to the rear mounted bus bar system. They are connected as across-the-line starters (dwg A-2642, app E). These motors cannot be started manually but are connected to run automatically when the main pumps are running and the tank oil temperature reaches 130°F. Circuit breakers and overload relays are provided to protect the motors and line equipment from excess current demands or short circuits. Provision is made in compartment 4B for connecting three size 2 AWG power leads provided by the Government from their 440 V, three phase, 60-Hz supply. Compartments 4F and 4H are reserved for future identical starting equipment.

Compartment 4K is empty and will not be used.

Compartment 4M contains a transformer panel to supply the 110 V needed by the entire system (dwg A-2643, app E). This unit is a plug-in device which connects to the rear mounted bus bar system. A 5KVA transformer is connected across two phases of the 440 V supply through contacts of relays 1MCR and 2MCR. The coils of these relays are connected across different phases of the supply line. This arrangement provides a simple means of phase failure protection to the entire system. Failure of any 440 V phase drops out the appropriate relay opening the 440 V connection to the transformer and interrupting the 110 V output. Without this 110 V output all the motor starter relays drop out stopping the motors. Relay (CR) also drops out thus shutting off all power to the electronic circuits including the servo systems.

The power control console (dwg 2CD-127) contains indicator lights to show:

- Main pump motors--RUN, and STOP
- Auxiliary pump motors--RUN, and STOP
- Hydraulic oil--TEMP LOW, TEMP OK, and TEMP HIGH
- Hydraulic oil--LEVEL LOW, LEVEL OK, and LEVEL HIGH
- FILTERS DIRTY, FILTERS OK

MAIN PITCH SYSTEM

Main Pitch Actuator

Our investigation of the main pitch gimbal actuation system indicates that the required performance can be achieved with the existing mechanical system and hydraulic actuator.

Design calculations have been made to determine pertinent design values for various parameters of the main pitch drive system (app F). The calculations were made for both the AH-1G and the AAH helicopter. The moment of inertia calculations include the additional 3000 lb weight of the new yaw drive motor. The hydraulic force required to move the maximum load at the specified acceleration is 57,436 lb (AAH Helicopter). The existing actuator system provides 108,000 lb. The existing structure was designed to withstand this hydraulic load.

The existing hydraulic piping and control wiring must be completely changed to accommodate the new high flow servosystem. The hydraulic schematic of the new piping is shown on dwg A-2627, appendix F, and the physical layout is shown on drawing J-2603.

To meet the valve-flow requirement of 336 gpm, we propose to use a Moog 79-400 valve with a 73-233 Electro-Hydraulic Servo Valve as the pilot stage (Pc no. J-2603-9). This valve combination is rated 400 gpm at 1000 psi pressure drop. After investigating several other commercially available valves (Sanders Associates and MTS, Inc.) and our own design, the use of the Moog valve proved to be the most cost effective approach. Technical data on the Moog valve is given in appendix F.

System Analysis

A block diagram has been generated for the servo control systems to be incorporated in the design of the Helicopter Fuselage Mount Simulator. The general form for this block diagram is shown in figure 3 in which the main pitch control system is described. The general form for the transfer characteristics of these systems is shown in figure 4.

Main Pitch Actuator

The Main Pitch Actuator Feedback Control system transfer characteristic has been developed based on the general form shown in figure 4. A frequency response analysis was performed to determine open loop gain versus system stability for payload ranges varying from the AAH helicopter fuselage to the AH-1G helicopter fuselage. Specific values of constants shown in figure 4 for the main pitch actuator control system are listed in table 5.

As a guideline for setting a mimimum open-loop gain constant to resist a firing load of 9000 lb, so that the maximum position error will be well within ±2°, an estimate of the maximum required open-loop gain constant of the main pitch actuator control system was made by the following equation derived in appendix G:[2]

$$K > \frac{T_d C}{r^2 A^2 (\theta_d)_{ss}} \tag{453}$$

---

[2]This equation was derived under the assumptions of: (1) The actuator-load damping would mainly depend on the viscous damping, (2) the actuator-load structural stiffness is at least five times higher than the actuator hydraulic stiffness (app H).

where

K = main pitch control system open-loop gain constant n sec^{-1}.

It is shown in appendix G that the required minimum open-loop gain constant was 4.1/sec.

To perform the frequency analysis, the transfer function of each system component must first be determined. When we consider that our primary interests in the analysis lie in the frequency range from d.c. to 100 Hz, the system components which will contribute significant dynamic characteristics to the open-loop response are the hydraulic valve and the actuator.

A Moog three stage, 4 way, hydraulic, flow-control valve has been selected for the main pitch actuator. A typical model of this valve rated 400 gpm at 1000 psi valve drop was tested by Moog with spool displacement feedback to provide excellent valve closed-loop frequency response flat from d.c. to 100 Hz. The phase response was measured and found to have phase shift of -8° at 10 Hz, -45° at 67 Hz and -90° at 120 Hz.

The other component block to be considered in the frequency analysis is the pitch actuator and load dynamics. Its transfer function was found to have a second order time-lag characteristic equation between valve flow and actuator velocity. The natural frequency of this quadratic was calculated to be 3.63 Hz for the AAH fuselage payload and 5 Hz for the AH-1G fuselage payload. The damping factor of the quadratic was derived in terms of actuator viscous friction, valve leakage and load inertia. At this time, there is no information on the actuator viscous damping. It is very difficult either to calculate or to test the actuator-plus-load running friction, although we know that the actuator-load running friction is not equal to zero. By neglecting the viscous term in the derived transfer function, the damping factor due only to valve leakage and load inertia was calculated to be 0.04 for the AAH load and 0.03 for the AH-1G load. In the final system design, the actuator-load damping factor will be larger than 0.03 because of the actuator viscous friction. If the overall damping is below a selected nominal value of 0.3 (assumed), a means to increase the actuator damping such as an external leakage bypass across the acuator must be implemented. It is safe to assume, for the purpose of performing the frequency analysis, that the actuator transfer function is a quadratic having a damping factor of 0.3 for the worst case.

With the hydraulic valve minor loop characteristics obtained from the manufacturer (table 6) and the actuator dynamics, as discussed in the previous paragraphs, two frequency responses were calculated for the main pitch position control system under two different loading conditions, that is, with the AAH or the AH-1G fuselage as payloads. The open loop transfer characteristic for the AAH fuselage payload described in the block diagram of figure 5 is plotted in figure 6 where a Kv in excess of 5.25 per second is provided and phase and amplitude margins are well within the required design specification when a simple lag/lead network is placed in the forward open loop characteristic.

In each of the systems we have designed for a phase margin greater than 40° where phase margin is defined as "the angle by which the phase of the open loop

ratio of a stable system differs from 180° at gain crossover" (from Chestnut and Mazer, Vol. 1, pg 341).[3] A phase margin of 40° will produce a closed loop peak of +3.3 db while a phase margin of 30°, as referenced in the contract, would cause a +6 db peak in the closed loop characteristic which we would not consider as being a good design. A similar transfer characteristic is also plotted in figure 6 for the AH-1G payload described in the block diagram of figure 7.

The closed loop transfer characteristic for both the AAH and AH-1G payload are shown in figure 8 where the computed system bandwidth is approximately 10 times the specified bandwidth for the helicopter load.

Included in the plot of the closed loop characteristic of figure 8 is the maximun velocity that the system can achieve. This shows that a peak amplitude of ±28° can be obtained from D.C. to 0.13 Hz while at the specified frequency bandwidth of 0.3 Hz a peak amplitude of ±11.9° can be achieved before velocity limiting is reached. The frequency response test must be performed at an amplitude of 1° not to exceed velocity limitations when operating out to 20 Hz. Figure 9 shows the operating limits imposed on the system by the physical parameters of the system. The chart indicates that the required operation of 10° amplitude at 0.3 Hz will be met. At higher frequencies, the performance is flow limited out to about 4 Hz. Beyond this frequency, the performance is acceleration (force) limited. The acceleration limit shown on the chart is based on conditions with the AH-1G fuselage mounted on the simulator and the gun firing. The acceleration limits will be different for other conditions.

Pitch Actuator Control System Circuit Diagram

The circuit schematic of the main pitch control system has been completed. This design includes nonlinear gain compensation for unequal piston area. It also includes automatic error zeroing for start-up, reduced loop gain for smooth start-up, and error and full gain monitoring to control firing.

MAIN YAW SYSTEM

Main Yaw Actuator

The required yaw torque in the activated system is much higher than in the original system since the hydro/mechanical brake is no longer available for holding the load under firing conditions.

Design calculations were made to determine pertinent design values for various parameters of the main yaw drive system (app I). Also, calculations were

---

[3]Harold Chestnut and Robert W. Mazer, Servomechanics and Regulating System Design, second edition, Library of Congress 59-9339, John Wiley and Sons, New York, February, 1961.

made for both the AH-1G and the AAH helicopter. The moment of inertia calculations include the additional 3000 lb weight of the new yaw drive motor. The torque required to move the maximum load at the specified acceleration is 62,967 ft lb (AAH helicopter). The existing hydraulic motor, rated at 10,400 ft lb torque, is not adequate for the new requirements. See appendix I for detailed descriptions of several Hagglund motors.

To provide this larger torque capacity, it is necessary to replace the existing rotary torque actuator with one of larger capacity. The use of a larger capacity rotary torque actuator of the type currently mounted on the yaw gimbal (Ohio Oscillator Co. Model H-250) was ivestigated. Also, a similar rotary actuator made by Flo-Torq was investigated. In both cases, our required torque is higher than available in the normal production models made by these companies. Furthermore, they depend on rather large pitch spur gears to transmit torque. This gearing introduces an intolerable backlash of about 1/2 degree. Both these suppliers have declined to quote on furnishing nonstandard units.

We propose to use a Hagglund Model 8385 hydraulic motor for this application. The mounting arrangement of this motor on the yaw gimbal is shown on drawing D-2604. This motor has a rated capacity of 83,160 ft lb at 3000 psi at speeds from zero to 16 rpm. An additional advantage accrues from the use of this motor since its construction eliminates the need for rotary hydraulic joints in the pipelines leading to the valve or motor ports. This unit is available in Hagglund's U. S. stock for prompt delivery.

The existing hydraulic piping and control wiring must be completely changed to accommodate the new high flow servo system. The hydraulic schematic of the new piping is shown on dwg A-2630 (app I).

To meet the valve flow requirement of 40 gpm, we propose to use a Moog 79-060 valve with a 73-232 electro-hydraulic servovalve as a pilot stage (pc. D-2604-6). This valve is rated 60 gpm at 1000 psi pressure drop and is the same valve to be used on the 6-DOF actuators. This 60-gpm valve is proposed because a suitable 40-gpm valve is not available. Duplicating the 6-DOF valving results in a small initial cost saving and saves on the requirements for maintenance parts.

We have investigated several other commercially available valves (Sanders Associates and MTS, Inc.) as well as our own design and have concluded that the use of the Moog valve is the most cost effective approach.

The existing hydro-mechanical brake system will be retained as a safety back up when the yaw servo is not energized. Its torque rating of 300,000 ft lb is more than adequate to resist any contemplated loading. The existing structural members were designed for a maximum loading torque of 252,000 ft lb and are more than adequate for the contemplated servo actuation.

The sections of this report covering the 6-DOF system and the combat-vehicle turret adapter will show that a torque of 196,650 ft lb is required to yaw the combat vehicle turret under specified conditions. As noted earlier, this main yaw system can provide only 83,160 ft lb of torque so it will not be used for high performance yawing of the combat-vehicle turret. The solution to this situation is discussed later in this report.

System Analysis

The main yaw control system was determined in a preliminary analysis. This is a standard position type of control servo where shaft angle is fed back to compare with the input command of angular position. The block diagram for this system is shown in figure 10.

The equations of system dynamics have been developed and are shown in figure 11. The specific values of constants shown in this figure for the main yaw control system are listed in table 7. The block labeled Hydraulic Valve Minor Loop Response is representative of the servovalve and spool valve general form that is shown in figure 4.

The open loop frequency response for the main yaw control system has been designed for a K_v of 6.3/sec. In appendix G, it is shown that $K_v > 1.25$/sec to satisfy positional accuracy during disturbing forces. The open loop response with a K_v in excess of the design value, as recorded in the block diagrams of figures 12 and 13, is plotted in figure 14 for both the AAH and AH-1G payload. The servo valve minor loop characteristics used in this analysis were obtained from the manufacturer and are listed in table 8.

The calculated open loop response recorded in figure 14 shows that the phase margin for the AAH helicopter fuselage is 57° and amplitude margin is -6.5 db while the same compensation will give a 64° phase margin and -7 db amplitude margin for the AH-1G fuselage all of which are within the specifications required.

The calculated closed loop response as recorded in figure 15 shows that a peak of +1.5 db appears around 0.15 Hz. The characteristic remains within ±1.5 db over the range of d.c. to 0.33 Hz for the AAH payload and d.c. to 0.25 for the AH-1G. These are very close to the required bandwidth of 0.3 Hz and would be difficult to improve upon since the natural frequency of both systems is relatively low. This can be more accurately determined once the hardware is assembled and tested. Some improvement may now be achieved by adjustment of compensation networks.

Included in the plot of the closed loop characteristic of figure 15 is the maximum velocity that the system can achieve. This shows that a peak amplitude of ±75° can be obtained from d.c. to 0.07 Hz, while at the specified frequency bandwidth of 0.3 Hz, a peak amplitude of 17.5° can be achieved before velocity limiting is reached. The frequency response test must be performed at an amplitude of less than 3.5° not to exceed velocity limitations when operating out to 20 Hz.

The operating limits imposed on the system by its physical parameters is shown in figure 16. The chart indicates that the required operation of 10° amplitude at 0.3 Hz will be met, but at higher frequencies the performance is flow limited to about 0.75 Hz. Beyond this frequency, the performance is acceleration (force) limited. The acceleration limit shown on the chart is based on conditions wth the AH-1G fuselage mounted on the simulator and the gun firing. The acceleration limits will be different for other conditions.

Two lines are shown for velocity limits. One shows the limits at 40-gpm oil flow which is the volume assigned to this unit to meet the specified performance. The other line shows the limits at 60-gpm oil flow which is the valve capability and could be met when other systems are not demanding their full quota of oil.

System Circuit Diagram

The overall configuration of the main yaw system has been generated and card slots provided for the required electronics components to be mounted in the control console. All wiring details for this system have been completed.

TRIOGONAL SUSPENSION SYSTEM

6-DOF Suspension

The activation of the 6-DOF suspension is primarily a function of the control system. A complete analysis of the control system is given later in this report.

Two mechanical changes are required to make the suspension responsive to the control system. To bring the flow rate at maximum velocity within the flow capabilities of the hydraulic pump unit, we will insert a sleeve (dwg B-2616) and new piston (dwg B-2615) into the existing six actuators.

As an alternative, consideration was given to replacing the existing actuators with similar actuators having the required smaller bores. This approach was abandoned because of:

- Significant changes in mounting dimensions requiring design and production of several adapter pieces
- Smaller oil passages leading to high flow velocities and pressure drops
- No significant savings in machine down time
- Higher basic cost--$360 each actuator for new sleeve and piston compared to $650 for each new actuator plus the additional costs of the required adapters

The other change involves the addition of an electrohydraulic servovalve to control the flow. The selection of this valve, as for the other systems, depends on the required flow rate through the valve which then depends on the maximum velocity and area of the actuator piston.

6-DOF Springs

When used in the spring rate mode, the force and displacement to the payload can be expressed by the pressure and flow supplied to the support system as follows:

$$P = P_o \sin \omega t$$

$$q = q_o \cos \omega t$$

where

P = Instantaneous system pressure

P_o = Peak system pressure

q = Instantaneous system flow

q_o = Peak system flow

Using the following equations, solve for flow

$$F\ X = \frac{P_o\ q_o}{\omega} \tag{454}$$

$$\omega = \sqrt{\frac{K}{M}} \tag{455}$$

$$X = \frac{F}{K} \tag{456}$$

where

F = Applied force

X = Displacement

K = System spring rate

M = System mass

Then

$$q_o = \frac{F\left(\frac{F}{K}\right)\sqrt{\frac{K}{M}}}{P_o} = \frac{F^2\sqrt{\frac{K}{M}}}{KP_o} \text{ cu in/sec} \tag{457}$$

or

$$\frac{F^2}{\sqrt{K}} = P_o\sqrt{M} \times q_o \tag{458}$$

In equation (458), the actual flow in the system depends on four variables which may change from one test setup to another. Plotting these values is a convenient way to show their relationship, and to do this the following conditions were set up for the AH-1G aircraft system:

Suspended weight of the system is 12,000 lb, then

$$M = \frac{12000}{386.4} = 31 \ \#sec^2/in \tag{459}$$

Actuator pressure is

$$P_a = \frac{12000 \text{ lbs } (.21561)}{10.64 \text{ sq in}} = 243.2 \text{ psi} \tag{460}$$

$$\therefore \frac{F^2}{\sqrt{K}} = (243.2)\sqrt{31}\ q_o = 1354\ q_o \tag{461}$$

Since the servovalves were selected on the basis of turret yaw capability and can pass a rated flow of 60 gpm each, this value (60 x 6 = 360 gpm) was assigned to q_o and a plot made of "F" vs "K" to define the maximum operating limits of this system (fig. 17).

In the combat vehicle system, a suspended weight of 13,000 lb was used so that

$$M = \frac{13000}{386.4} = 33.64 \tag{462}$$

$$P_T = \frac{13000 \times (.21561)}{10.64} = 263.4 \tag{463}$$

$$\frac{F^2}{\sqrt{K}} = 263.4\sqrt{33.64}\ q_o = 1528\ q_o \tag{464}$$

The plot made of "F" vs "K" for q_o = 360 gpm defines the operating limits of this system when full valve flow is available. Another plot was made with q_o = 49.2 gpm to define the operating limits of this system when available flow is curtailed due to maximum simultaneous operation of the combat vehicle yaw motion.

6-DOF Yaw

The 6-DOF actuators will also be used to provide high performance yaw motion to the combat vehicle turrets. This application is discussed later in this report, where justification for use of a 60-gpm servovalve is presented. This servovalve will be a Moog 79-060 valve with a 73-232 electrohydraulic servovalve as the pilot stage as previously described in this report.

6-DOF Piping

The hydraulic schematic of the proposed piping is shown in figure 18. A new physical arrangement of the piping on the actuators is being worked out in conjunction with an overall pitch/yaw gimbal piping arrangement. A major part of this effort involves the use of rotary hydraulic joints to bring oil pressure onto the gimbals and to take off the return flow.

Two critical rotary transition points exist; one is at the main pitch gimbal axis, and the other is at the main yaw axis. A maximum flow of 269 gpm is required onto the yaw gimbal to supply the 6-DOF actuators when they are being used to provide yaw and spring motion to the combat vehicle turret. This flow must be brought from the stationary structure onto the movable pitch gimbal and then onto the movable yaw gimbal. The use of hose in this application does not appear practical:

- The required 2 1/2 in. I.D. x 3000 psi rated hose is not really flexible enough to accommodate the degree of gimbal rotation required

- The minimum bend radious of 36 in. would require a hose loop of at least 6 feet diameter between the structure and the pitch gimbal and between the pitch gimbal and the yaw gimbal

- The two hoses required (supply and return lines) at each of these places would be unsightly

We investigated commercially available joints made by Chickson and Barco. The available joints of the required capacity are not suitable for this application for the following reasons:

- Physical size too large for available space

- No pilot or mounting arrangements are provided so that complicated brackets would be required to support the joints and to provide concentricity with the gimbal axis

- Position of the pipe ports leads to a poor arrangement of our connecting pipes

- Any cost saving over special joints is doubtful

The design of a rotary joint suitable for use on both the pitch axis and the yaw axis of the simulator is shown in drawing D-2614. This joint contains passages for both the supply oil at 3000 psi and the return oil at 100 psi. Note that the high pressure passage is inside the low pressure passage so that any leakage of high pressure oil will flow into the return line. This joint also provides a pilot and mounting holes for easy attachment to the simulator.

6-DOF Position Indication

The present limit switches mounted on each actuator and now used to control position indicating lights will be reconnected to provide shut-off signals if maximum excursion of the actuator is approached. Full range continous position indication will be provided electronically and indicated by calibrated meters at the control console. Exact position of each of the six actuators will be indicated at all times.

Study of Spring/Damping Simulator

During the development of the system design, considerable effort has been expended to determine the best design for the spring/damping simulator. This study has mainly been performed on an analog computer available in the FIRL Labs for this type of design optimization. The basic concept has been reduced to practice in actual hardware (FIRL property; not purchased on the project), and portions of the test results are included in this report. The fabrication and tests to verify the concept were not charged to the project. The block diagram for the system to verify the concept is shown in figure 19. Data obtained from closed-loop tests were transferred back through a Nicholas chart to provide the open-loop characteristic. The open-loop gain was then set for the desired closed-loop damping, the results of which are recorded in figure 20. The system operated at a supply pressure of 1000 psi and supported a load of 200 lb. The hardware is shown in the photograph included as figure 21 where the load is resting on a support beam with the actuator close to fully extended. One of the pressure transducers is visible while the second is hidden by the upper framework. The overall sketch for the test stand is shown in figure 22. A long lever arm is used to lift the 200-lb weight from the load supporting actuator. Rapid upward motion of the lever arm located on the opposite side of the fulcrum from the load causes a force step input to the servoactuator.

Referring back again to figure 20, the recorded actuator position, shows an overdamped characteristic when a step input of position command is electronically injected into the system. One of the theories to be proved was the ability to change the system characteristic by the insertion of a lag network in the forward loop of the electronic amplifier system used to sum the position input command and feedback position and to drive the servovalve. The data obtained from tests provided an open-loop characteristic recorded in figure 23 as described by three test points. Two lag network designs were tried in which one had a break frequency of 0.7 cps, and the other at 1.0 cps. The closed-loop theoretical response for the break located at 0.7 cps is recorded in figure 24 in which both the frequency and step responses are recorded. This network was connected into the forward loop of the test system, and the step response for this hardware system is shown in figure 25. The underdamped characteristic is in quite good agreement with the theoretical response recorded in figure 24. It is quite evident that the overdamped system of figure 20 could then be easily controlled to have a predicted underdamped characteristic as recorded in figure 25. Since the

deflection of the actuator used to simulate a spring must be a function of applied force to the spring, tests were performed to verify the previously established characteristic as a change of force function on the actuator. The overdamped system of figure 20 is recorded in figure 26 for the condition of lifting the 200-lb weight and then letting it suddenly hang from the actuator, thus producing a step change in force. The response characteristic shows static change in actuator position as the weight is lifted and, on application of the weight, an overdamped response of change in position is recorded. The underdamped system is shown in figure 27, thus further verifying the system concept.

System Analysis

Up to this report period, the system analysis of the triogonal actuator control systems has been performed in the following four areas:

1. Stability analysis of one basic triogonal actuator position servo at maximum specified spring-rate condition
2. Development of the spring-rate adaptive control system block diagram for actuator pressure sensing
3. The closed-loop performance of the preliminary design, adaptive spring-rate control system due to a step force input
4. Frequency response analysis of the linearized adaptive spring-rate control system at four different spring rates.

Detailed discussions on these four analyses are reported in the following paragraphs.

Position Servo Analysis

It is essential to examine and design each of the triogonal actuator position servos properly so that they will be stable and can be controlled by the model following adaptive-control system at maximum specified sring-rate conditions. The basic triogonal actuator position servosystem, as shown in the system block diagram in figure 28 contains:

- A position input summing amplifier
- A gain control multiplier
- A phase control multiplier
- A minor-loop input amplifier
- A servovalve drive amplifier

- A three-stage, four-way flow control servovalve
- A valve spool displacement feedback LVDT
- The triogonal actuator with external bypass
- The actuator position feedback LVDT

The combined frequency response of the servovalve minor-loop components was provided by the servovalve manufacturer, since we considered purchasing a complete valve package with spool displacement LVDT feedback. The manufacturer's test data on one of the selected 60-gpm valve (Moog 79-060) is recorded in table 9.

The linearized actuator transfer function between valve flow and actuator velocity was derived as a quadratic with a natural frequency of

$$f = \frac{1}{2\pi}\sqrt{\frac{2\ K_{HA}}{M}}\ \text{(with actuator bypass)} \tag{465}$$

where

K_{HA} = Actuator hydraulic stiffness

M = Mass of actuator piston and load

The damping ratio is mainly dependent on the actuator bypass leakage flow which was designed (app H) to have a nominal value of 5.3 gpm at 1000 psi pressure drop.

The expression for the actuator damping ratio ξ, is

$$\zeta = \frac{1}{4}\sqrt{\frac{2\ K_{HA}}{M}}\left(\frac{A^2}{K_{HA}C} + \frac{CM}{A^2}\right) \tag{466}$$

where

A = Effective area of piston of one side

C = Leakage coefficient of the bypass

When we consider the values of these parametes for the payload of the AAH helicopter fuselage (heaviest one) as follows:

$$K_{HA} = \frac{2B\ (A_S + A_L)}{L}$$

$B = 200{,}000$ psi

$A_S = A_L = 10.652\ in^2$

$L = 9$ in

$K_{HA} = 945{,}000$ lb per in

$$M = \frac{(16{,}000 + 2500 + 1500)(.21561)(3)}{368} = 33.5\ \frac{\text{lb-sec}^2}{\text{in}}\ \text{(worst case)}$$

$$C = \frac{5.8\ \text{gpm}}{1000\ \text{psi}} = 2.23 \times 10^{-2}\ \text{cis/psi}$$

the calculated natural frequency, f, and damping ratio, ξ, for the actuator transfer function are

$f = 38$ Hz

$\xi = 0.7$

The open-loop gain constant required for the highest specified spring-rate was calculated (app H) as 36. Using an open-loop gain constant of 45 and the dynamic characteristics of the valve and actuator as stated above and plotted in figure 29, a closed-loop frequency response for the triogonal position servo was calculated and plotted as shown in figure 30. The graph obviously shows that the position loop is very stable even at the condition of simulating a maximum spring-rate of 250,000 lb/in. where a phase margin of 65° and amplitude margin of -12 db are observed in figure 29.

Adaptive Control System Block Diagram

In the proposed model following spring rate adaptive-control system, the system concept was derived to account for the sensing of the spring force applied to the spring model and the actual load mass. However, in real practice, the only force or pressure which can be easily measured will be the force or pressure developed across the actuator.

Referring to the system block diagram in figure 31, it can be shown that the force signal at F_3 will be the applied force, F, if the transfer function of F_3/F_2 is

$$\frac{F_3}{F_2} = \frac{1}{G_1\ G_x} \qquad (467)$$

where

G_1 = Transfer function between servo output position, X, and force developed at F_2.

G_x = Closed-loop transfer function between applied force and servo output displacement, X.

Since

$$G_x = \frac{\dfrac{1}{MS^2 + DS}}{1 + \dfrac{G_1}{MS^2 + DS}} \qquad (468)$$

with

M = Effective actuator load mass

D = Effective actuator load damping coefficient

S = Laplace transform operator

$$G_1 G_x = \frac{G_1}{MS^2 + DS + G_1} \qquad (469)$$

or

$$\frac{F_3}{F_2} = \frac{MS^2 + DS + G_1}{G_1} \qquad (470)$$

The above equation indicates the simulation of a second order leading network in order to obtain the equivalent forcing function of F at F_3. One of the methods employed at the present time is to obtain an approximate leading transfer function of F_3/F_2 with a second order lag at frequencies 22 times above the break frequency of $\sqrt{G_1/M}$ which is

$$\frac{F_3}{F_2} = \frac{MS^2 + DS + G_1}{G_1\ (MS^2 + DS + 500\ G_1)} \qquad (471)$$

The new system block diagram of the adaptive spring-rate control system is shown in figure 32. This has been proven successful in the computer analysis described later.

Adaptive Spring-Rate Control System with Step Force Inputs

To verify the revised system block diagram and its controllability in spring-rate and damping, an analog computer simulation of the adaptive control system was performed. A spring-mass model identical to the model in the adaptive control loop was simulated so that the performance of the adaptive spring system could be compared to this external simple spring model. Recording of the simulation was made on strip chart channels as follows:

Channel 1 - System error, X-Xc

2 - Actuator displacement, X

3 - Adaptive loop spring model displacement, Xc

4 - External Spring model displacement, Xm

5 - Input signal (either force input or spring rate input to both spring models)

The simulation showed that high open-loop gain with lead compensation is required in the adaptive loop to provide fast response at maximum specified spring-rate and a low damping condition.

The test was performed by applying a small step force input superimposed on a static force applied to the actuator and to the external spring model. Eight recordings were made on four different spring-rates and two dampng ratio settings. These recordings are listed in table 10, with the results shown in figures 33 to 40.

When we compare the steady-state displacements of the actuator to those of the external model, we conclude that the control of spring-rate by the adaptive system is excellent. When we compare the transient portion of these recorded displacements, the control of the damping is cosidered good.

Effect of Variation in Damping in Hydraulic Actuator

A nominal or design value of damping will be selected for the actuators used in the triogonal system. A computer study was made to determine the effect on the spring rate simulation if the damping value in the actual hardware varied from the nominal. Referring to figure 32 the value of D in the force compensation network was held constant at the nominal value. All other values of D that are representative of the hardware were changed simultaneously from a nominal damping factor of 0.7 to 0.5 and 2.1. The theoretical force response of the actuator is shown in figure 41 for a step change in flow input where the damping factor is 0.5. In figure 42 the damping was changed to 0.7 and the force response has less overshoot. The heavily damped characteristic is shown in figure 43 where the damping factor is 2.1.

The theoretical effect on the adaptive spring rate control system was studied for the spring rate of 130,000 lb/in. with two selected system damping ratios. A damping ratio of 0.376 is recorded in figure 44. It is shown that the actuator displacement characteristic is not greatly affected by a change in damping factor of 0.5 to 2.1. The damping ratio for the system was then selected as 1.24 and the results for damping factor changes from 0.5 to 2.1 are shown in figure 45. The actuator displacement is quite similar for the factor of 0.5 and 0.7. When the damping factor was moved to 2.1, one portion of the characteristic exhibited a higher frequency discontinuity in the overdamped rsponse. This much change in damping factor may be too extreme since it reflects a 300% increase over the nominal. A more realistic variation would be 30% for which the effect would be negligible. These effects can only be made firm once the hardware has been assembled and tests performed to verify the theoretical analysis.

Adaptive Spring-Rate Control System-Dynamic Studies

To see the stability and dynamic performance of the adaptive spring-rate control system over the range of the spring-rate control from 1000 lb/in. to 100,000 lb/in., three step responses were recorded from the analog computer simulation of the spring-rate control system. These responses were measured for a step change in spring-rate from a selected level setting for the adaptive spring model under a constant load force. Because of the constant load force, the model and the actuator displacement will change when the spring-rate changes. By comparing the actuator displacement to an external spring-mass model displacement, the dynamic performance of the adaptive control system can be realized.

The strip-chart recordings of the displacement responses of the actuator and model at 1000 lb/in. spring-rate with a step change of 100 lb/in. is shown in figure 46.

The recording for the case of 10,000 lb/in. spring rate with a step change of 1000 lb/in. is shown in figure 47.

The recording for the case of 100,000 lb/in. spring-rate with a step change of 20,000 lb/in. is shown in figure 48.

Other constant parameter values used in this simulation are as follows:

Effective actuator load mass = 4.33 lb-sec^2/in.

Static load force = 2000 lb - 3000 lb

Actuator bypass leakage flow = 30 gpm at 1000 psi load pressure

Spring model damping factor = 0.35

During this study, it was found that a previously selected leakage flow of six gpm produced too great a damping coefficient for the lowest spring rate of 1000 lb/in. Since damping is a function of actuator velocity, and increased damping can be achieved by velocity feedback, a study was made to determine the

effect of positive velocity feedback for the purpose of decreasing the damping coefficient. This is effective, but to reach the damping factor of 0.5 as recorded in figure 39, leakage had to be increased to 30 gpm at 1000 psi load pressure. However, a more normal static load condition would require

Total load	=	16,000 lb
Actuator load	=	2,667 lb
Maximum actuator load	=	5,334 lb
Piston area	=	10.652 in^2
Differential pressure	=	501 psi
Flow	=	21 gpm

Revised Adaptive Spring-Rate Control System Block Diagram

The linearized transfer function of a hydraulic actuator between input flow, Q, and the actuator velocity, sX, has been derived in app H as the following quadratic function:

$$\frac{sX}{Q} = \frac{1/A}{\frac{M}{K_{HA}} s^2 + \left(\frac{D_a}{K_{HA}} + \frac{MC}{A^2}\right)s + 1 + \frac{D_a C}{A^2}} \tag{472}$$

The transfer function between the force, F_2, developed by the actuator and the actuator velocity can be expressed as

$$\frac{sX}{F_2} = \frac{1}{Ms + D_a} \tag{473}$$

From the above two equations, the transfer function between flow and force developed can be obtained by

$$\frac{F_2}{Q} = \frac{\frac{sX}{Q}}{\frac{sX}{F_2}} = \frac{(Ms + D_a)\ \ (1/A)}{\frac{M}{K_{HA}} s^2 + \left(\frac{D_a}{K_{HA}} + \frac{MC}{A^2}\right) s + 1 + \frac{D_a C}{A^2}} \tag{474}$$

Based on the above three actuator transfer functions, the system block diagram of the adaptive spring-rate control system was developed as shown in figure 32. However, equation (473) is correct only when there is no external input forces so the force developed, F_2, is for accelerating the load mass, M, and for overcoming the viscous damping force, $D_a sX$. When there is an external force, F, input to the actuator system, equation (473), should be modified as

$$\Sigma F = F_2 - F = M s^2 X + D_a sX \tag{475}$$

Equation (474) should then be modified in relation to equation (475). Instead of combining equations (472) and (475) to get the transfer between Q and F_2, the

actuator transfer function block diagram has been separated into three transfer blocks and a summing junction expressed by the equations

$$Q_L = A\ sX \tag{476}$$

$$Q_v - Q_L = Q_{cL} \tag{477}$$

$$Q_{cL} = \frac{A}{K_{HA}} sF_2 + \frac{C}{A} F_2 \tag{478}$$

where

Q_L = Actuator velocity flow

Q_v = Servovalve output flow

Q_{cL} = Actuator compressibility and leakage flow

Subsequently, the force detection circuit in the adaptive loop (described earlier in this report) should be modified due to the change in G_1 which is the transfer function between the servo output position, X, and the force developed at F_2. In simulating an actuator spring-rate of less than or equal to 100,000 lb/in., the force detection circuit transfer function of $1/G_1G_x$ was derived to have a simple expression as follows:

$$\frac{1}{G_1G_x} = \frac{M}{K_H} s^2 + \frac{MC}{A^2} s + 1 \qquad (\text{for } K \leqq 100{,}000) \tag{479}$$

With this transfer function and the revised actuator transfer function block diagram arrangement, a revised system block of the adaptive spring-rate control system was developed. The block diagram in figure 49 is to replace the one previously derived as shown in figure 32.

Numerous analog computer runs from the revised adaptive control system were made to study its simulated performance. From the computer results, no change was observed in capability to obtain 1000 lb/in. spring-rate to greater than 100,000 lb/in. with good accuracy and excellent stability. Some very minor improvement was observed in the dynamic response at the 1000 lb/in. spring rate. The apparent leakage flow is the limiting factor of good transient response at the low spring-rate setting. A computer study on higher leakage bypass flow was made and is discussed in the next paragraphs.

System Response Curves Measured from the Computer Simulated Adaptive Control System at Larger Actuator Bypass Opening

The stiffness of a position-controlled hydraulic actuator servo system can be related mathematically to the system open loop-gain constant, K_v, the

actuator piston area, A, and the actuator bypass leakage coefficient, C, as follows:

$$\frac{F}{X} = \frac{K_V A^2}{C} \left(1 + \frac{D_a C}{A^2} \right) \tag{480}$$

where

F = Applied force

X = Actuator displacement

D_a = Actuator viscous damping coefficient

From the above equation, many values of C can be used for a given spring stiffness as long as K_V changes with it (app H). However, the speed of the actuator displacement response due to a step change in force input is proportional to the servo open loop-gain constant, K_V. Although the adaptive controller may force the actuator servo to produce a displacement response similar to that of the model, the position servo loop should have a loop gain high enough or approximately equivalent to that required to produce the appropriate response time or damping of the actuator response. This means that for a higher position gain constant, K_V, at low spring-rate simulation, a higher leakage bypass is needed. The approximate value of the leakage coefficient, C, of the actuator bypass for a certain desirable damping was derived in the revised appendix H with a mathematical expression as follows:

$$C = \frac{A^2}{D} = \frac{A^2}{2\zeta\sqrt{KM}} \quad \text{(approximately)} \tag{481}$$

where

A = Actuator effective area
D = Adaptive model damping coefficient
K = Simulated spring-rate
ζ = Spring-mass damping factor
M = Effective mass of the actuator load

The value of C used in the previous design for a spring-rate higher than 60,000 lb/in. to a maximum of 200,000 lb/in. was 5.3 gpm per 1000 psi load pressure or more realistically 0.80 gpm per 150 psi. Later it was found that the leakage flow should be at least 21 gpm at 501 psi for a spring-rate of 1000 lb/in. which again is more realistically expressed as 6.3 gpm per 150 psi. To have a good model following-transient response for spring-rates between 300 to 30,000 lb/in., it was found that the leakage bypass should be opened more. In a recent analog computer study, excellent response curves were generated for low spring-rate simulations when the leakage coefficient of the bypass was set for 30 gpm per 150 psi load pressure. These curves are displayed in figures 50 to 58. The other major parameter values used in this computer simulation (fig. 49) were as follows:

$M = 2.63\ \text{lb-sec}^2/\text{in}$

$C = .77\ \text{cis/psi}$

$A = 10.652\ \text{sq. in}$

$D_a = 21\ \text{lb-sec/in (assumed)}$

$K_H = .945 \times 10^6\ \text{lb/in}$

$k_1 = 10{,}000$

$k_2 = .1\ \text{sec}$

$\omega_v = 515\ \text{rad/sec}$

$\zeta_v = .6$

In equation (481), the value of C can be determined for a selected range of spring rates, K, and an average value of actuator load mass, M, from the two extremes in loading due to changes in actuator orientation. If necessary, a compromise can be made between the bypass leakage coefficient and the actuator piston area, A, to reduce the bypass flow rate.

Because of a substantial increase in bypass flow required for the low spring rate low-damping simulation, the leakage flow can no longer be negligible in equations (454) and (458) and in figure 19, and it should be modified to include a constant leakage flow for a nonfiring constant load mass. Based on the bypass leakage used in the computer simulation, the leakage flow per actuator is approximately one third of the maximum servovalve output flow at 150 psi load pressure and the maximum load pressure will be limited to approximately 500 psi, which is higher than the required actuator pressure of 243.2 psi calculated for the AH-1G fuselage system as described earlier in this report. In the combat vehicle system, the total flow requirement for maximum specified simulated velocity was calculated to be 62.3 gpm per actuator (app J), and the maximum actuator pressure required to develop the maximum acceleration was approximately 1520 psi which could not be reached if the computer simulation bypass is used. So either a higher flow-rate servovalve should be used for each of the 6-DOF actuators or a compromise in design of the actuator piston area and bypass as discussed in the previous paragraph will be needed for the combat vehicle motion system. When a 60 gpm-servovalve design is used for the 6-DOF actuator-suspension system, the lowest obtainable spring-rate with good system response for maximum combat vehicle yaw motion is predicted approximately at 20,000 lb/in. The leakage bypass should then be set at 7 gpm per 150 psi actuator pressure for the combat vehicle. Spring-rate lower than 20,000 lb/in. can be achieved at a reduced performance on combat vehicle yaw motion with a larger actuator leakage bypass.

TAIL ROTOR SIMULATOR

Mechanical Suspension

The purpose of the tail rotor simulator is to introduce the loads and forces into the cut-off frame of the helicopter that would normally appear there in a flying helicopter when the various weapons are fired. To accomplish this, a controllable force should be applied in the proper direction and magnitude to the end bulkhead of the cut-off helicopter. Two main objectives are to be met by the simulator: (1) The moment of inertia of the actual tail boom is to be simulated, and (2) the counter-recoil forces normally supplied by the tail rotor through pilot or stability augmentation system control are to be provided when firing the weapons.

It is difficult to reproduce the exact weight, c.g., and mass moment of inertia simultaneously unless the original geometry and mass distribution is preserved. However, the effect of the tail boom moment of inertia can be simulated if an external force is applied so that the firing load imparts the same acceleration to the cut-off helicopter as it would give to the full length helicopter. By including the effect of the stability augmentation system in this force calculation, this acceleration will be further tailored to simulate both the moment of inertia and the tail rotor thrust effect encountered during firing of the weapon.

This tail rotor simulator is an entirely new system developed for this specific application. Design calculations were made to determine pertinent design values for various parameters of this system. These values are tabulated in drawing A-2634, appendix K.

The physical arrangement of the structure required to support the force producing actuator is shown on drawing D-2606.[4] The design of the upper support link has been changed to a fabricated pipe arch to permit its mounting to the underside of the yaw gimbal to straddle actuators number 2 and 3 to accommodate the mounting position of the AH-1G helicopter. This attachment point allows the tail rotor simulator and the aircraft to move as a unit when the main pitch and yaw angles are changed. This main support linkage is designed as a pin jointed "dog-leg" with spherical bearings to relieve the local moment loads. This allows the helicopter section to move freely in the fore and aft direction, in the vertical direction, and in pitch. The attachment of the hydraulic actuator to the support link is made through a universal joint which gives the helicopter freedom to roll (dwg D-2645). Pure lateral freedom is provided through the actuator when no yaw restraining signals are present. The actuator will produce a controlled yaw motion and the structure is designed to resist the applied moments and forces.

---

[4]Drawings cited throughout this report are on file at the Ware Simulation Center, Rock Island Arsenal, Rock Island, IL.

The actuator is controlled by the servo system to produce the proper simulation forces. The hydraulic schematic is shown in drawing A-2635, appendix K. To meet the valve flow requirement of 4.4 gpm, we propose to use a standard commercial Moog valve model 73-233 rated 10 gpm at 1000 psi pressure drop.

System Analysis

The physical concept for the system analysis is shown in figure 59 where the various elements are denoted by

I_{ad} - Yaw moment of inertia of the mounting adapter

I_f - Yaw moment of inertia of the fuselage

K_F - Fuselage stiffness

K_{SP} - Spring rate of 6-DOF

An assumption has been made that the stiffness of the support links and joints is much greater than either K_F or K_{SP}. A four-way servovalve is used to control pressure difference and flow in the piston and the bypass C.

From the physical layout, a block diagram has been developed as shown in figure 60.

The tail boom control system is designed to provide force control over a frequency range of approximately 0.005 Hz to 70 Hz. In any force system, provision must be made to maintain a steady state position so that the moving system does not change position due to unbalanced forces acting on the device. This was accomplished by providing a D.C. or static position feedback that automatically reduces in gain as the frequency of motion increases. Conversely, the force feedback system must have little or no D.C. gain but must be of constant gain over a selected frequency spectrum. The concept has been developed in which each system has been analyzed separately. The position servo is shown in the block diagram of figure 61 while the force servo is shown in the block diagram of figure 62. As noted in the plot of frequency response, figure 63, the force servo is relatively flat from 0.005 Hz to 70 Hz while the position servo falls off in amplitude very rapidly above 0.001 Hz and remains at least -10 db below the D.C. nominal at any frequency above 0.01 Hz. The large negative and positive peaks in the position system are due to system dynamics that appear in the feedback path of the position system. These are not of importance since over the majority of the frequency range the position gain is 1/10 of the force gain thus insuring force control.

COMBAT VEHICLE SYSTEM

Mechanical Suspension

This overall simulator was designed as a variable flexibility, or variable damping ratio device for testing interactions between aircraft and weapon systems. A useful extension of this application is for testing interactions between combat vehicles and weapon systems. Because of the differences in mounting requirements and performance characteristics, some new adapters and operating equipment are required to take advantage of this extended usefulness.

The general arrangement of such a combat vehicle suspension system is shown on drawing D-2609. Design calculations were made to determine pertinent design values for various parameters of the system. These values for pitch motion are listed in drawing A-2633, appendix J.

The adapter consists of a turret mounting plate and tube which is adjustable in the vertical direction. The tube is mounted in a roll gimbal ring, then mounted on a pitch gimbal ring through trunnions and self aligning ball-joint bearings (Torrington 35SF14). The pitch gimbal and the self aligning ball-joint bearings are mounted on the suspension ring through trunnions.

The main suspension ring is designed to be attached directly to the clevis brackets of the 6-DOF suspension system rather than to the existing aircraft mounting platform. This provides a greater available clearance to the floor and helps to keep the total moving weight down.

The connection between the tube and the roll gimbal is a pair of taper wedge friction clamps designed to resist the torsional and thrust loads applied to it while permitting infinite axial adjustment of the turret and the pitch axis within the 24-inch range provided.

The combat vehicle system is provided with its own actuator to produce desired pitch displacements. The actuator is controlled by the servosystem. The hydraulic schematic is shown in drawing A-2636, appendix J. To meet the valve flow requirement of 126.6 gpm, we propose to use a Moog 79-200 valve with a 73-233 electro-hydraulic servovalve as the pilot stage. This valve combination is rated 200 gpm at 1000 psi pressure drop. We have investigated several other commercially available valves (Sanders Associates and MTS, Inc.) including our own design and have concluded that the use of the Moog valve is the most cost effective approach.

This actuator/valve combination is also required to provide for variable spring rates in pitch. As noted previously, a valve flow of 126.6 gpm is required to provide maximum pitch displacement performance. With a 200-gpm valve, an additional flow of 73.4 gpm can be accommodated to provide spring characteristics.

By using the formulae developed earlier in this report, the following is concluded:

Suspended weight of combat vehicle is 13,000 lb.

$$M = \frac{13000}{386.4} = 33.64 \tag{482}$$

$$P_t = \frac{6076^{\#}\text{(actuator load)}}{7.568^{''2}\text{(actuator area)}} = 803 \text{ psi} \tag{483}$$

$$\frac{F^2}{\sqrt{K}} = 803 \sqrt{33.64}\ q_o = 4657.4\ q_o \tag{484}$$

The plot of "F" vs "K" for q_o = 73 gpm is shown in figure 64 to define the operating limits of this system for the specified conditions when simultaneously pitching at maximum performance. Note that the spring system is not flow limited at any combination of firing forces and spring rates within the system operating range.

As was mentioned earlier in this report, the main yaw system does not have the performance capabilities required to meet the maximum performance specified for combat vehicle yaw motion. A solution to this problem is available with the existing equipment. The triogonal actuator suspension system is very efficient in the yaw mode and can be programmed to provide the high frequency yaw motion to the turret while retaining its effectiveness as a spring simulator. When using this yaw mode, the existing hydraulic brake will be applied to the main yaw system effectively eliminating it from the movable systems.

Calculated pertinent parameters for combat vehicle yaw drive are tabulated as input to the SDFS computer program and shown in appendix J. Tabulations of the parameters associated with the main yaw drive for full combat vehicle performance are also shown in appendix J.

The output of this program is summarized in appendix J and confirms that the altered 6-DOF actuators are adequate to provide the maximum yaw performance as specified for the combat vehicle. To meet the valve flow requirement of 62.3 gpm, a Moog 79-060 valve will be used with a 73-232 electrohydraulic servovalve as a pilot stage. This valve is rated 60 gpm at 1000 psi pressure drop and is the same valve used on the main yaw drive. It is fully described earlier in this report. This valve will have a flow rate of 70.5 gpm at the minimum pressure drop of 1380 psi needed to provide maximum yaw performance as shown in the calculations given in appendix J. This then provides a valve flow of 8.2 gpm to be used in providing the spring rate operation. The plot of "F" vs "K" for q_s = 49.2 gpm, shown in figure 19 of this report, defines the operating limits of this system when maximum performance operation of the combat vehicle is combined with spring rate requirements.

System Analysis

The combat vehicle system is controlled in pitch by the turret pitch control system. Since the main pitch control could not satisfy the velocity requirements for the combat vehicle, a smaller actuator has been provided that can achieve the amplitude and frequency requirements. This system will also provide a spring rate characteristic similar in design to each of the 6-DOF actuators. The block diagram for the Turret Pitch Position Servo System is shown in figure 65 and the transfer characteristic is recorded in figure 66. The characteristics for the servovalve were obtained from the manufacturer and are tabulated in table 12 for the band of frequencies that are pertinent to the servo system design. The open loop frequency response is shown in figure 67 for a K_v of 70 per second and a compensation network with a lag at 0.4 Hz and a lead at 0.8 Hz. The amplitude margin is -9.5 db and phase margin is 65 degrees. The closed loop response is shown in figure 68 indicating a well damped system with a bandwidth of 13 Hz (-3 db pt). Once the actual hardware system confirms these characteristics, the open loop gain can be raised by +3 db.

The spring rate control system will be similar in design to each of the 6-DOF spring rate actuators. The maximum stiffness will be determined by the amount of open loop, K_v, that can be put into the system.

The operating limits imposed on the turret pitch system by physical parameters of the system are shown in figure 69. These limits were calculated based on the data given previously. The chart indicates that the required operation of 3° amplitude at 3.5 Hz will be met. The acceleration limit shown on the chart is based on the MICV-65 turret mounted on the simulator and the gun firing.

Operating limits for the main yaw drive system are shown in figures 16 and 70. The specified operating point for the combat vehicle falls outside the achievable capabilities of the yaw system.

The operating limits for the combat vehicle using the 6-DOF actuators to provide yaw is shown in figure 71. The specified operating point in yaw can be achieved using the actuators as described earlier in this report.

VIBRATION SYSTEMS

Introduction

Three vibrational systems will be supplied to provide environmental vibrations normally caused by parts of the system not included in the simulation. These are the main rotor, the tail rotor, and one auxiliary rotor (undesignated source). These components normally exert forces on the aircraft fuselage due to vibration of their masses. The vibrational systems will provide equivalent forces.

Each vibration system will generate the desired force by vibrating a mass at the proper amplitude and frequency. A force will thus be exerted on the aircraft equal to the reaction force

$$f = m\ddot{x}$$

where $\ddot{x}$ is the acceleration of the mass, m. The mass and acceleration values will be chosen to match the forces normally produced by the actual components. Each system will be a hydraulic servo system (single axis) which can be attached to the airframe at the desired location.

The servo systems will be excited by tape recordings, made under operational conditions, of the acceleration of the components being simulated by other inputs. The desired force is this acceleration multiplied by the mass of the component.

A preliminary investigation was made to determine if this approach was feasible and to evaluate some of the major requirements. Two basic designs were examined: (1) A relatively small system suitable for the tail-rotor and auxiliary vibrators, and (2) a much larger one suitable for the main rotor. A design for the combat vehicle was not evaluated because the 40,000 lb peak force requirement does not appear practical.

Main Rotor System

Vibration specifications for the main rotor give a double amplitude of 0.4 in. between 5 and 10 Hz, 2 g from 10 to 28 Hz, 0.05 in. double amplitude from 28 to 44 Hz, and 5 g from 44 to 5000 Hz. The weight of the main rotor system is 942.3 lb. Thus, the required force varies from a minimum of 480 lb at 5 Hz to a maximum of 4700 lb between 44 and 5000 Hz. To avoid adding excessive weight to the helicopter fuselage, the mass of the vibration system should be kept to a minimum, but this requires a relatively large displacement for the servo system. As a compromise, a vibrating weight of 250 lb was selected for the study. The required peak-to-peak amplitude of vibration is then 1.506 in.

Design Limitations

The output force is limited by several factors in different parts of the frequency range which are shown in figure 72. At low frequencies, the maximum amplitude of the vibrating mass produces a limit which varies as the square of the frequency. The values given will match the low-frequency requirements or the main rotor. In the mid-frequency range the output force will be limited by the supply pressure of 3000 PSI. The actuator area must be chosen large enough to provide the maximum required force. At high frequencies, the force is limited by a combination of saturation of the servovalve amplifier, the servovalve coil time constant, the servovalve spool resonance, and the flow capability of the servovalve. In this region, the limiting force varies inversely as the fourth power of frequency.

Design Parameters

The design parameters for this study were determined as follows:

$mg = 250$ lb

$$x_o = \left(\frac{M_a}{M}\right) y_o = \frac{942.3}{250} (0.2) = 0.753 \text{ inch} \tag{485}$$

$$A = \frac{f_{max}}{P_{max}} = \frac{4700}{2500} = 1.89 \text{ in}^2$$

$$q_v = 76 \text{ in}^3/\text{sec @1000 psi (20 gpm valve)} \tag{486}$$

The 20 gpm valve provides a flow of

$$q_o = \sqrt{3}\, q_v = 132 \text{ in}^3/\text{sec @ 3000 psi} \tag{487}$$

The high frequency limit is then given by

$$\frac{f_{max}}{E_v} = \frac{q_o A \omega_\gamma^2}{R i_o T C_c} \cdot \frac{1}{\omega^4} \tag{488}$$

where

ω_γ = 628 rad/sec (valve spool resonance)

T = 4.5 ms (valve coil time constant)

i_o = 10 M_a (valve rated current)

R = 500 ohm (valve coil resistance)

C_c = $1.42 10^{-5}$ in^5/lb (compliance)

E_v = 10 volt (amplifier saturation voltage)

Then, the maximum force is

$$f_{max} = \frac{1.97\ 10^{12}}{f^4} \tag{489}$$

where f is the frequency in Hz. The maximum frequency at which full output (4700 lb) can be obtained is then

f_{max} = 138 Hz

Tail Rotor System

The vibration specifications for the tail rotor are assumed to be identical to those for the main rotor. The parameters specified in the proposal have been used for the feasibility analysis. These are

$m_g = 12.5$ lb

$x_o = 0.5$ in.

$A = 0.283$ in.^{2}

The peak velocity is then

$$\dot{x}_{max} = 62.8(0.5) = 31.4 \text{ in/sec} \tag{490}$$

and the peak flow is

$$q_{max} = A\dot{x}_{max} = 8.80 \text{ in}^3\text{/sec} = 2.31 \text{ gpm} \tag{491}$$

A 4 gpm (1000 psi) valve was chosen, for which the spool resonant frequency is

$$\omega_v = 2\pi(220) = 1380 \text{ rad/sec} \tag{492}$$

The valve coil time constant is again

$T = 4.5 \cdot 10^{-3}$ sec

so that the maximum available force at high frequencies is now

$$f_{max} = \frac{2.16 \cdot 10^{12}}{f^4} \tag{493}$$

The highest frequency at which the required force of 154 lb can be produced is then

$$f_{max} = 340 \text{ Hz} \tag{494}$$

Stability Analyses

The response of the vibration servos will be affected by the impedance of the airframe at the mounting location, but it is reasonable to assume that over the range of frequencies for which the servo is designed to operate, the airframe will look like a pure mass, the value of which is much greater than that of the vibration system. The equivalent circuit for the vibration system is shown in figure 73. The feedback signal for the servo system is derived from a force transducer located between the actuator cylinder and the mounting frame.

The loop gain for this system is given by

$$K_{oL} = \frac{M^1 K_c K_e K_i K_a}{K_x} \cdot \frac{S^2}{\left\{ 1 + \frac{A_S}{K_q K_x} \left[1 + SM^1 \frac{g_v + S_{C_c}}{A^2} \right] \right\}} \tag{495}$$

where

$M^1 = \frac{M M_a}{(M+M_a)}$ is the equivalent mass of the system

M = the mass of the vibrator

M_a = the mass of the airframe

K_i = the current gain of the servovalve amplifier

K_C = the gain of the compensation network

K_E = the gain of the error amplifier

A = the piston area

X_o = the half stroke

$K_q = \frac{\left(\partial_q / \partial_i \right) P_s}{\left[1 + 2\zeta_\gamma \left(\frac{S}{\omega_\gamma} \right) + \left(\frac{S}{\omega_\gamma} \right)^2 \right]}$ = the servovalve flow gain

q_v = the leakage flow constant

C_c = the compliance of the trapped fluid

$K_x = \frac{K_{xo}}{(1+T_x S)}$ = the LVDT gain

T_x = the LVDT time constant

$K_a = \frac{K_{ao}}{(1+T_a S)}$ = the force transducer gain

T_a = the force transducer time constant

ω_v = the valve spool resonant frequency

ζ_v = the valve spool damping factor

$\left(\frac{\partial_q}{\partial_i} \right)_{P_s} = \frac{q_o}{i_o}$ = low frequency valve gain at zero load pressure

Excluding the compensation network, this is proportional to the square of the frequency at low frequencies and inversely proportional to the cube of frequency at high frequencies. Furthermore, for low values of leakage, a large resonant peak may result from the load resonant frequency, but this can be reduced by the proper choice of actuator position feedback.

If the proper frequency dependence of the various gain factors appearing in the expression for loop gain are inserted, the denominator polynomial, excluding the compensation network, becomes

$$P(S) = 1 + \frac{A_S}{K_{xo}\left(\frac{\partial q}{\partial i}\right)}\left[1+\frac{SM\left(q_\gamma+SC_c\right)}{A^2}\right]\left[1+2\zeta\left(\frac{S}{\omega_\gamma}\right)+\left(\frac{S}{\omega_\gamma}\right)^2\right]\left(1+T_x S\right) \tag{496}$$

It is desired to select a value for the position transducer gain, K_{xo}, that will result in a reasonable degree of damping for the roots of this polynomial. Also, it is desirable to retain as low a value of leakage, q_v, as possible, unless suitable damping cannot be obtained without adding additional leakage. This has been possible, and the leakage constant has been assumed equal to zero.

For this value, the roots of the denominator polynomial occur at frequencies of

$$f_x = \begin{cases} 8.8\angle\pm 17.2° \\ 73.5\angle\pm 74.8° \\ 92.4\angle\pm 87.6° \end{cases} \quad \text{Hz} \tag{497}$$

The last two are underdamped more than desired but should cause no problem since they occur in the middle of the response band.

Main Rotor

For the main rotor vibrator, the following parameters have been chosen:

$Mg = 250$ lb ($M=0.648$ lb sec^2/in)

$A = 1.89$ in^2

$X_o = 0.756$ in

$\left(\frac{\partial q}{\partial i}\right)_{P_\gamma = 3000} = 13.2$ in^3/Ma sec (Moog 35S-020)

f_γ = 100 Hz

C_c = $1.429 \cdot 10^{-5}$ in^5/lb

g_γ = 0

T_x = $1.59 \cdot 10^{-3}$ sec (f_x = 100 Hz)

With these values, the load resonance will be reasonably well damped by choosing a position feedback gain equal to

$$K_{xo} = 29.6 \text{ Ma/in} \tag{498}$$

This results in a resonance peak of about 11 db at 82.8 Hz in the loop gain.

To stabilize the loop, a compensation network equal to

$$K_c = \frac{7.76\ (1+ 1.924 \cdot 10^{-3} S)^4}{(1+0.318S)\ (1+7.31 \cdot 10^{-3} S)\ (1+.0531 \cdot 10^{-3} S)^2} \tag{499}$$

is used. This results in a closed loop bandwidth extending from 3 Hz to 500 Hz. These curves are shown in figure 74.

Tail Rotor

For the tail rotor vibrator, the parameters are as follows:

M_g = 12.5 lb (M = .0324 lb sec^2/in)

A = 0.283 in^2

X_o = 0.5 in

$\left(\frac{\partial_q}{\partial_i}\right)_{P_\gamma = 3000}$ = 2.67 in^3/Ma sec

f_γ = 220 Hz

C_c = $1.905 \cdot 10^{-6}$ in^5/lb sec

q_γ = 0

T_x = $1.59 \cdot 10^{-3}$ sec

For these values, the position feedback gain has been made equal to

$$K_{xo} = 46.4 \text{ Ma/in} \tag{500}$$

This gives denominator roots at frequencies of

$$f_x = \begin{cases} 106.4 \angle \pm 61.9° \\ 149.5 \angle \pm 82.4° \\ 208.7 \angle \pm 62.2° \end{cases} \quad \text{Hz} \tag{501}$$

The compensation network in this case has been chosen to be

$$K_c = \frac{12.12\ (1+1.065\cdot 10^{-3}S)^3\ (1+0.763\cdot 10^{-3}S)^2}{(1+ .318S)\ (1+3.58\cdot 10^{-3}S)^2\ (1+.053\cdot 10^{-3}S)^2} \tag{502}$$

This again results in a closed loop bandwidth from 3 Hz to 500 Hz. These curves are shown in figure 75.

Final Designs

The final designs for the main rotor and tail rotor systems are shown in figures 76 and 77. The auxiliary system will be identical to the tail rotor system. Compensation has been added in the force feedback loop to correct for the high frequency response of the force transducers, and extend the bandwidth out to the predicted 500 Hz.

SYSTEM AND SUBSYSTEM ELECTRONIC POWER CONTROLS

The control of power supplies needed for all of the servosystems is shown in the schematic diagram of 26D-108. The power supplies, with the exception of the 5 V-regulated supply, will all be located in cabinet 3. The 5-V supply is located in cabinet 1 so that it will have short lead lengths to the computer interface logic circuits. The power to the supplies is controlled by a line contactor that is operated by a key switch (dwg A-2626, app E). Each supply will have an indicator type of fuse to protect the supply on the 120 V, 60 Hz power side. The power supply indicator lights are all 28-V lamps that are controlled through transistors with the exception of the 28-V supply, thus permitting use of one type of lamp and lamp housings that look uniform. The power supply leads to the servo systems have been divided to prevent coupling between systems where relatively long supply leads are necessary. The return for the 28-V unregulated supply is separate from the regulated supplies used for signal circuits, thus decreasing the chance of noise. The return for the -84-V supply used for the feedback circuits is connected to the signal common at each control location, thus making the common junction as close as possible to the input of the summing amplifier. An interlock circuit is provided to connect power to either the tail boom servo or the turret servo since both systems never operate simultaneously. Power select switches are also supplied for the vibration servos. These are independent of each other and can be selected in any desired combination. Panel lights indicate which system is powered.

SYSTEM START UP AND FAIL-SAFE INTERLOCKS

Start Up and Fail-Safe System

The preliminary design has been completed for the limit circuits so that electronic limit of command signals will be provided and followed up by limit switch circuits. The electronic position limit is provided to prevent the system from reaching the limit switch. Since start-up system has been designed so that the actuators must be within the operating range located between the limit switches, the servo system error must be below a specified amount and all power supplies must be on. To prevent undesirable motions in the actuators at turn-on caused by pressure build-up in the system, an automatic gain control has been designed. At turn-on, the gain is in the order of 1/10 the normal gain, thus decreasing system bandwidth which then limits velocity. During a nominal 5-second period, the gain will rise smoothly to the normal set value.

Firing Interlock

The circuit schematic diagram (dwg 26D-109) for the fail-safe firing interlock has been completed. The visual indicator with engraved notation of "Standby to Fire" is designed to operate through the interlock of

1. Emergency pushbutton.
2. Main pump control relay contacts.
3. Gun aiming position sensor.
4. Servo system "full gain" relay contacts.
5. Servo system hydraulic control relay contacts.

When all subsystems are activated, thus closing the firing control relay, the "Gun on Target" and "Standby to Fire" indicator lights will be on. The firing can then be initiated by closing the firing circuit through a manually operated pushbutton in series with the firing relay contacts.

The panel layout for the firing interlock system has been completed and is shown in drawing 26D-127.

ELECTRONIC WIRING AND PACKAGING

Wiring

Preliminary circuit board wiring design was done for the pitch and yaw servo system. The computer interface circuit boards are under consideration. A total of 76 cards or 60% of the buffering and logics boards will be purchased items from the Digital Equipment Corporation.

Most of the internal wiring diagrams of the control consoles have been completed. Wiring of the three control panels and one relay panel are also completed for construction.

Packaging

The latest estimate is that three 52 inch height-control consoles will be needed to house all of the electronics, power supplies, pump motor controls, and indicators. A total of 14 card racks will be needed to hold the boards. The tentative arrangement of the control consoles are

<u>Control console 1</u>

Pitch servo card rack
Yaw servo card rack
Computer interface card racks
Turret pitch system card rack
Tail boom control system card rack
Terminal panel
Control panel

<u>Control console 2</u>

Six triogonal actuator card racks
Terminal panel
Control panel

<u>Control console 3</u>

Vibration system card racks
Relay panel
Circuit breaker
D.C. power supply
Terminal panel
Control panel

Main pump motor "Start/Stop" pushbuttons
Auxiliary pump motor "Start/Stop" pushbuttons
Indicating lights
Main terminal board for incoming wire connections

The packaging for the card racks is shown in the drawing 26D-130. The control panel for the pitch, yaw, triogonal actuator, turret and tail boom systems is shown in drawings 26D-121 and 26D-124.

Conclusions

A design has been completed for an activated 6-DOF simulator. The simulator was designed to mount portions of vehicles and withstand the force of small arms and automatic cannons firing from these vehicles. This design includes: (1) A complete mathematical model of the simulator, (2) design and sizing of the required hydraulic and electrical controls, (3) design of an active pitch and yaw system for the simulator, (4) modeling and fabrication of the spring rate and damping controls for the triogonal actuator system, (5) design of a tail rotor simulator to be added to helicopter fuselages suspended from the 6-DOF simulator, (6) design of a combat vehicle adapter for suspending small turrets (less than 65-inch ring) from the simulator, and (7) design of vibration systems to simulate various field environments such as rotor beat or over-the-road motion.

Limits on the capabilities of the simulator are established throughout this design report. In some complex cases, such as the spring rates achievable by the simulator with systems of different inertias mounted to the simulator, definitive limits could not be defined. However, a computer program has been written based on the math model developed earlier in this report that will solve for the spring rate limitations.

This design indicates that the passive 6-DOF simulator can be modified to provide a tool for testing weapon systems under realistic conditions. A spring rate and damping ratio can be set into the simulator so that mounted vehicles will respond to weapon firings in a manner duplicating that encountered in the field. In addition, vibrations may be propagated through mounted systems with a spectrum similar to that measured in these vehicles under field conditions.

The activated 6-DOF simulator can then provide an effective laboratory setting for testing weapon systems under controlled, repeatable conditions. Types of tests that can be performed with the simulator include research and development testing prior to field testing to remove initial design deficiencies, initial production testing of weapons under controlled mounting and vibration conditions, product improvement testing to compare system changes fairly and accurately, and system identification testing to establish causes of weapon system failures correctly and to develop accurate models of these systems.

Table 1. Actuator variations

Damping media	Effective volume of the actuator ($in.^3$)	Actuator stiffness (lb/in.) Maximum	Minimum
Oil	117.5	23,000	800
Nitrogen	326.0	5,000	300

Table 2. STIFF 2 program input map

Card no.	Variable	Description	Format
1 2 3	TITLE	For title and other information	10A6 10A6 10A6
4	THETA	Mounting angle of vehicle with platform (pitch), degrees (if THETA is greater than 99 END)	E10.0
5	W	Weight of platform, part of actuator and payload, pound	
	XW(I) I=1,3	Location of c.g. of weight with respect to center of gimbal (X,Y, and Z) inch	4E10.0
6	XGUN(I) I=1,3	Location of weapon mounting point to c.g. of weight (X,Y and Z) inch	3E10.0
7	TRGT(I) I-1,3	Location of target with respect to earth axes	3E10.0
8	RY RZ	Pitch angle of gimbal, degrees Yaw angle of gimbal, degrees	2E10.0
9	Media	Damping media, input 1 for oil or 2 for nitrogen	I2
10	LOC	Location where the system stiffness is specified	I2
		LOC = 1 Stiffness given at center of the mounting platform, in the direction of the platform axes	

Table 2. (cont)

Card no.	Variable	Description	Format
		LOC = 2 Stiffness given at the c.g. location of the vehicle and in the direction of the vehicle axes*	
		LOC = 3 Stiffness given at the weapon pivot point in the direction of the weapon axes*	
11	SK(I) I-1,6	System stiffness required (Note: If LOC = 3, SK(1) only is specified which is the stiffness along the weapon axis.)	6E10.0
12	SF(I)	System force, which is the force applied in the direction in which the system stiffness SK is specified (Note: If LOC = 3, SF(1) is the recoil load of the weapon.)	6E10.0

Return to card 4.

---

*LOC 2 and 3 are intended to be used in the active system; this portion is not finalized.

Table 3. Pump oil flow (gpm) required for various motions at maximum performance

Motion	Aircraft	Combat vehicle
Main pitch	214	--
Main yaw	25	--
6-DOF springs	218[a]	31[b]
Tail boom	5	--
Turret pitch	--	81 gpm-pitch + 46 gpm spring
Turret yaw (6 DOF)	--	238
Vibrators	18	18
Total gpm for simultaneous maximum performance	480	414

[a]Based on 480 gpm power unit. Performance limited to maximum flow rate of 269 gpm at the pump.

[b]Based on simultaneous maximum yaw performance. Performance limited to maximum flow rate of 269 gpm at the pump.

Table 4. Accumulators for servo systems

	Subsystem	Frequency (Hz)	Q_v (gpm)	V_x (gal.)	V_1 (gal.)	Accumulator provided (gal.)
1	Main pitch	0.3	336	1.76	37.0	40.0
2	Main yaw	0.3	40	0.21	4.4	5.0
3	6-DOF spring	1.0[a]	360	0.566	11.89	12.0
4	Turret pitch	3.5	127	0.057	1.2	5.0
5	Turret yaw (6-DOF)	3.5	374	0.168	3.5	12.0
6	Tail boom	0.3	5[b]	0	0	0
7	Shakers	10.0	28	0.0004	0.1	0.25

[a]Based on AH-1G aircraft with 1200 #/in. spring rate.

[b]Full flow provided by pump.

Table 5. List of parameter values for calculating the main pitch control system frequency responses

Parameter	Symbol	Value	Unit
Effective actuator piston area	A	37.7	sq in.
Input summing amplifier gain	b_1	1	volt/volt
Foward compensation amplifier gain	b_2	.9	volt/volt
Amplifier gain (adjustable)	b_3	1.1	volt/volt
Hydraulic valve spool displacement feedback gain	b_5	10	volts/in.
Pitch gimbal position feedback gain	b_6	0.6	volts/deg
Leakage coefficient of the spool valve	C_2	2.54×10^{-2}	cis/psi
Actuator-load viscous damping coefficient	D	$\leq 2 \times 10^{7}$ *	lb-in.-sec
Total mass moment of inertia (with AAH payload)	J (AAH)	82,522	lb-in.-sec^2
Total mass moment of inertia (with AH-1G payload)	J (AH-1G)	43,430	lb-in.-sec^2
Spool valve flow gain	K_3	6170	cis/in.
Stiffness of actuator rod attachment joints	K_A	2,500,000*	lb/in.
Actuator hydraulic stiffness	K_{HA}	104,500	lb/in.
Effective radius of pitch angular rotation	r	78	in.
Valve spool displacement LVDT time constant	T	.0016	seconds
Angle between actuator axis and tangent of pitching arc	θ_T	33° (max.)	degree
Assumed damping factor of the actuator and load	ζ_A	.3*	--
Forward compensation network		$\frac{.053\ s + 1}{.106\ s + 1}$	

*Assumed values

Table 6. Servovalve characteristics of main pitch control system

Frequency (Hz)	Transfer function	
	Magnitude (dB)	Phase (degrees)
1.00E-01	0.00E.01	-1.5
3.00E-01	0.00E-01	-2.0
5.00E-01	0.00E-01	-3.0
7.00E-01	0.00E-01	-3.5
9.00E-01	0.00E-01	-3.7
1.00E+00	0.00E-01	-3.9
1.50E+00	0.00E-01	-4.3
2.00E+00	0.00E-01	-4.5
3.00E+00	0.00E-01	-5.0
3.10E+00	0.00E-01	-5.1
3.20E+00	0.00E-01	-5.1
3.30E+00	0.00E-01	-5.2
3.40E+00	0.00E-01	-5.2
3.50E+00	0.00E-01	-5.3
3.60E+00	0.00E-01	-5.3
3.70E+00	0.00E-01	-5.4
3.80E+00	0.00E-01	-5.4
3.90E+00	0.00E-01	-5.5
4.00E+00	0.00E-01	-5.5
5.00E+00	0.00E-01	-6.0
8.00E+00	0.00E-01	-6.5
1.00E+01	0.00E-01	-7.0
1.50E+01	0.00E-01	-11.5

Table 7. List of parameter values used for calculating the main yaw control system frequency responses

Parameter	Symbol	Value	Unit
Design system open-loop gain constant	G open	6.3	per sec
Forward path amplifier gain	$b_1 b_2 b_3$	1.1	volt/volt
Yaw gimbal position feedback gain	b_6	.4	volts/deg
Leakage coefficient of valve and motor	C	.0231	cis/psi
Hydraulic motor displacement	d_m	368	cu in./rad
Motor-load viscous damping coefficient	D_m	$\leqq$ 48,000	lb-ft-sec
Total mass moment of inertia (with AAH payload)	J_M (AAH)	47,545	lb-ft-sec^2
Total mass moment of inertia (with AH-1G payload)	J_M (AH-1G)	16,105	lb-ft-sec^2
Motor hydraulic stiffness	K_{HM}	1.232×10^6	lb-ft/rad
Spool valve flow gain	K_3	924	cis/in.
Compensation lead time constants	T_1, T_2	.795, 5.46	sec
Compensation lag time constants	T_3, T_4	1.59, 15.9	sec

Forward compensation $\dfrac{(T_1 s + 1)\,(T_2 s + 1)}{(T_3 s + 1)\,(T_4 s + 1)}$

Table 8. Servovalve characteristics of main yaw control system

Frequency (Hz)	Transfer function Magnitude (dB)	Phase (degrees)
1.00E+00	0.00E-01	-3.0
3.00E+00	0.00E-01	-4.0
5.00E+00	0.00E-01	-4.5
8.00E+00	0.00E-01	-5.0
1.00E+01	0.00E-01	-5.0
1.50E+01	0.00E-01	-8.0
2.00E+01	0.00E-01	-10.0
2.50E+01	0.00E-01	-13.0
3.00E+01	0.00E-01	-17.5
4.00E+01	0.00E-01	-28.0
7.00E+01	7.00E-01	-61.0

Table 9. Manufacturer's test data

Frequency (Hz)	Amplitude ratio (dB)	Phase-shift (degrees)
10	0	-5
20	0	-10
40	0	-28
70	+0.7 (peak)	-61
82	0	-90
100	-1.5	-134

Table 10. Recordings on four spring-rates and two damping ratio settings

Static force (lb)	Spring-rate (lb/in.)	Damping ratio
30,000	200,000	0.3
30,000	200,000	1.0
20,000	130,000	0.376
20,000	130,000	1.24
10,000	60,000	0.55
10,000	60,000	1.8
1,000	1,000	0.5
1,000	1,000	1.0

Table 11. Moog servovalve 73-233 manufacturer's data

Frequency (Hz)	Transfer function Magnitude (dB)	Transfer function Phase (degrees)
1.00E+00	0.00E-01	-3.0
1.50E+00	0.00E-01	-3.0
2.00E+00	0.00E-01	-4.0
3.00E+00	0.00E-01	-5.0
5.00E+00	0.00E-01	-5.5
7.00E+00	0.00E-01	-6.0
1.00E+01	0.00E-01	-7.0
1.50E+01	-5.00E-02	-10.0
2.00E+01	-2.00E-01	-13.0
3.00E+01	-4.00E-01	-20.0
4.00E+01	-5.00E-01	-25.0
5.00E+01	-8.00E-01	-32.0
6.00E+01	-1.30E+00	-40.0
7.00E+01	-2.10E+00	-47.0
8.00E+01	-2.80E+00	-55.0
9.00E+01	-3.70E+00	-61.0
1.00E+02	-4.50E+00	-68.0
1.30E+02	-6.50E+00	-92.0
1.50E+02	-7.60E+00	-107.0
2.00E+02	-9.40E+00	-140.0

Table 12. Servovalve characteristics for turret control system

Frequency (Hz)	Transfer function Magnitude (dB)	Transfer function Phase (degrees)
5.00E+00	0.00E-01	-10.0
7.50E+00	0.00E-01	-11.0
1.00E+01	0.00E-01	-12.0
1.50E+01	2.00E-01	-16.0
2.00E+01	4.50E-01	-26.0
3.00E+01	-7.50E-01	-45.0
4.00E+01	-3.00E+00	-64.0
5.00E+01	-5.20E+00	-87.0
7.00E+01	-1.00E+01	-135.0

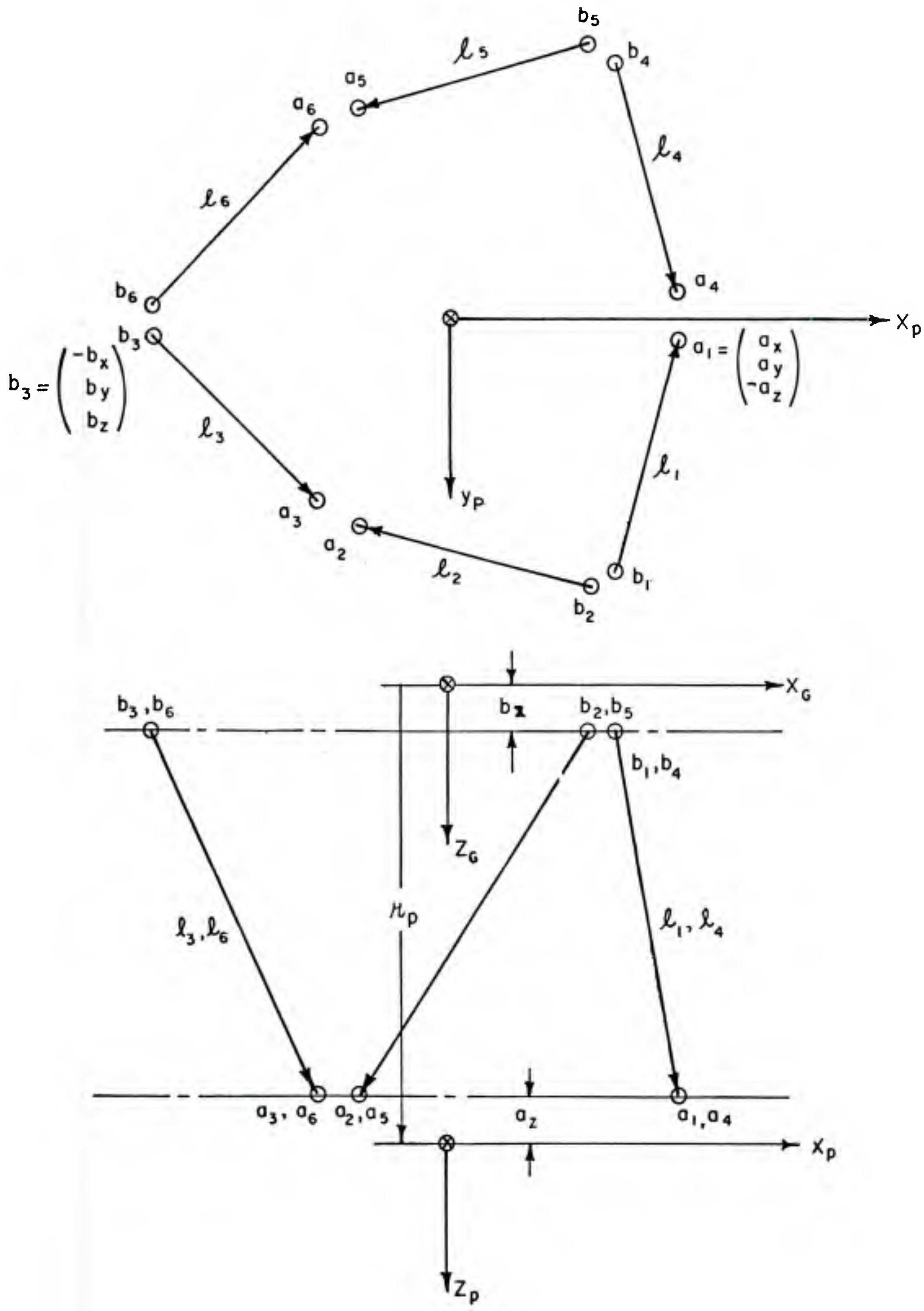

Figure 1. Triogonal system

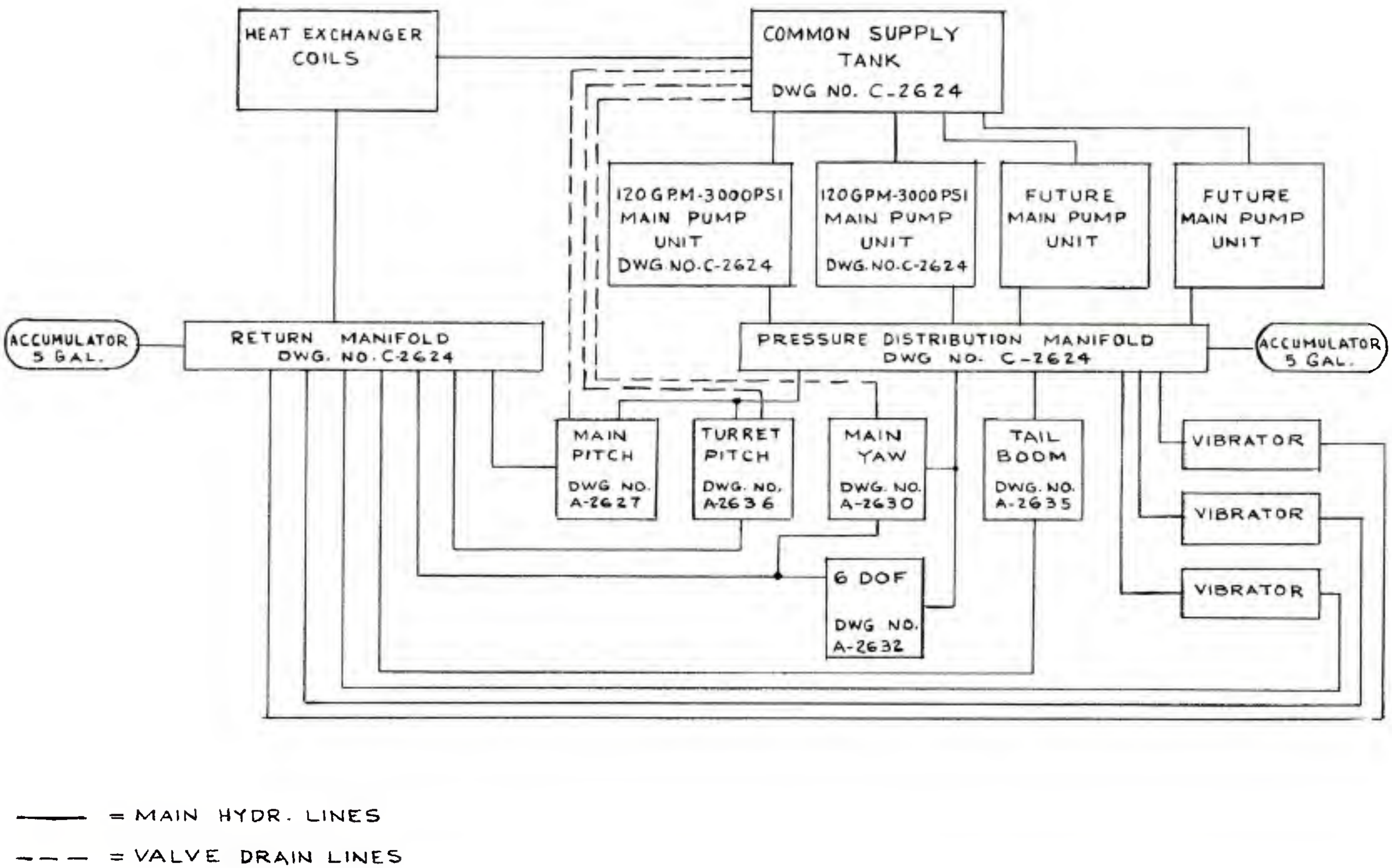

Figure 2. Block diagram overall hydraulic system

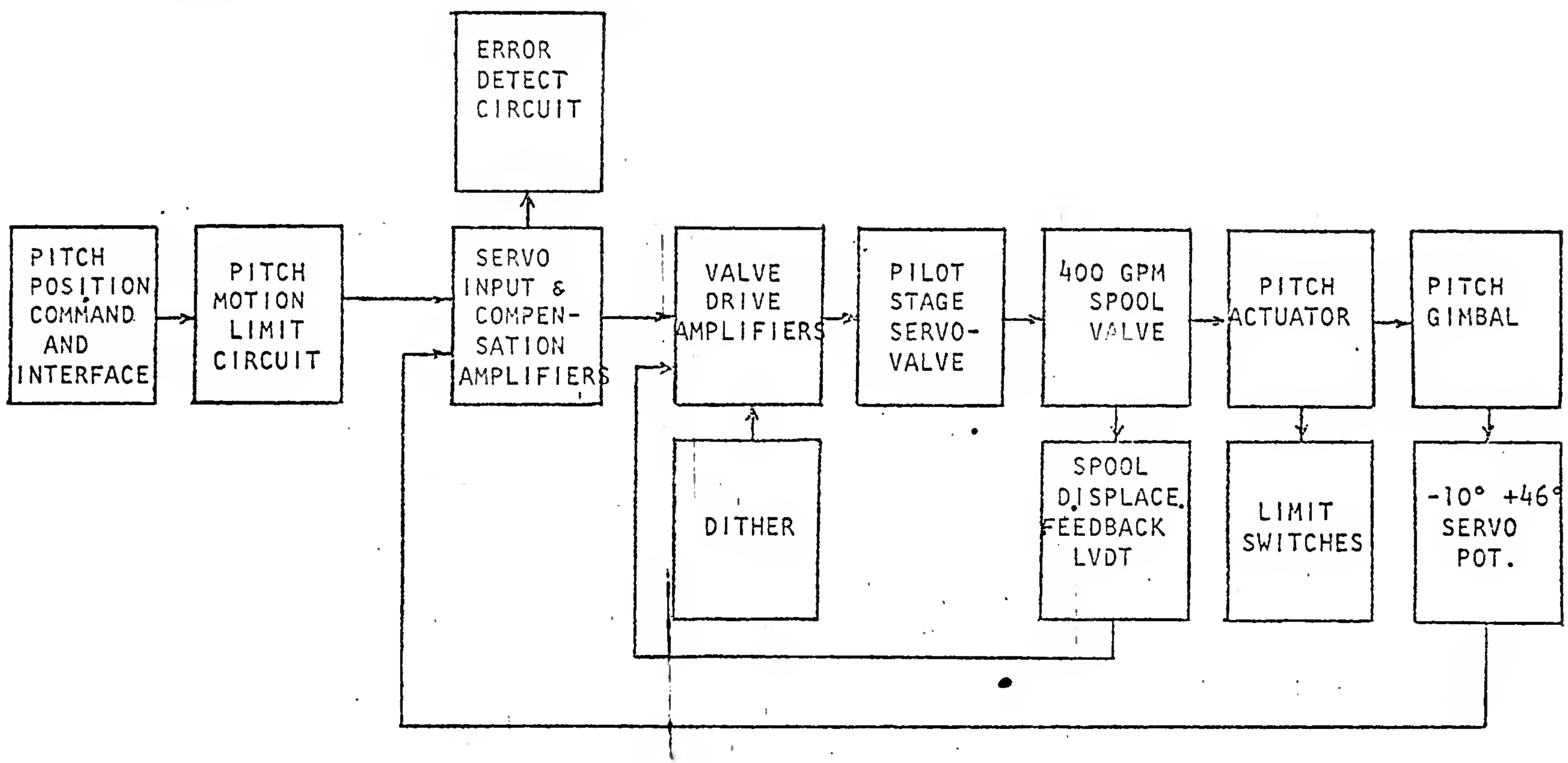

Figure 3. Main pitch-actuator feedback control system block diagram

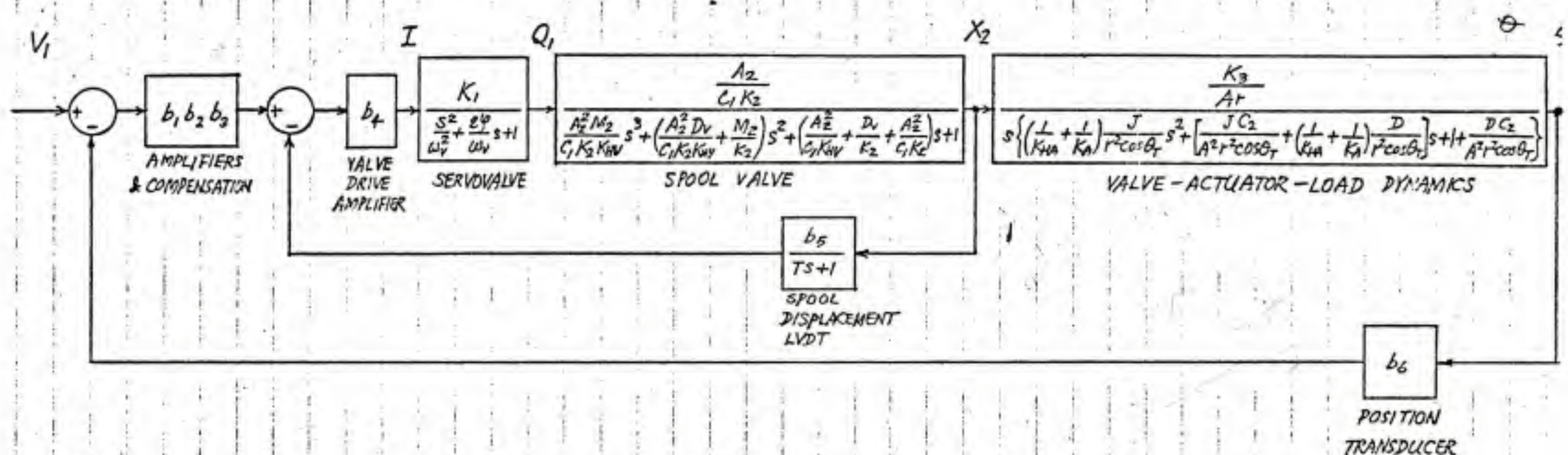

Figure 4. Transfer characteristics of main pitch-actuator feedback control system

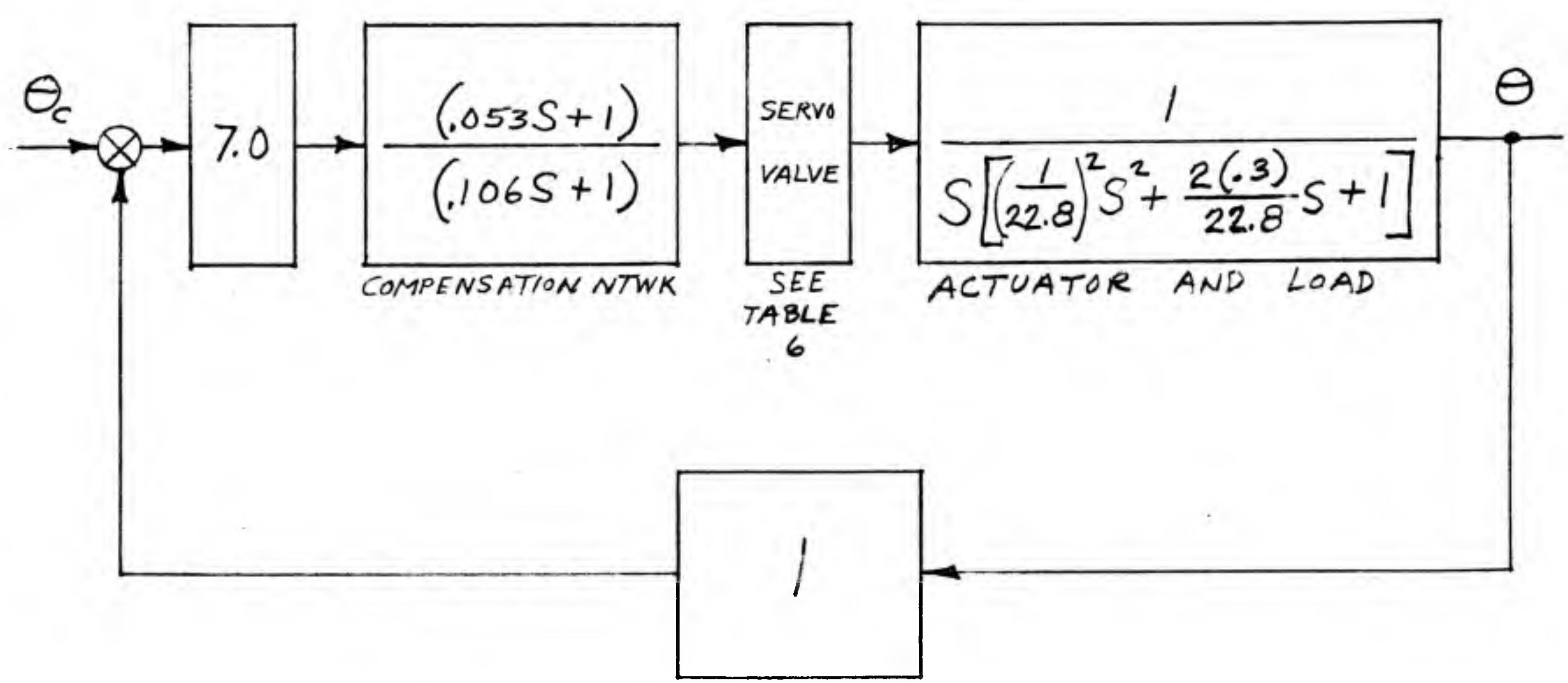

Figure 5. Main pitch control system AAH payload

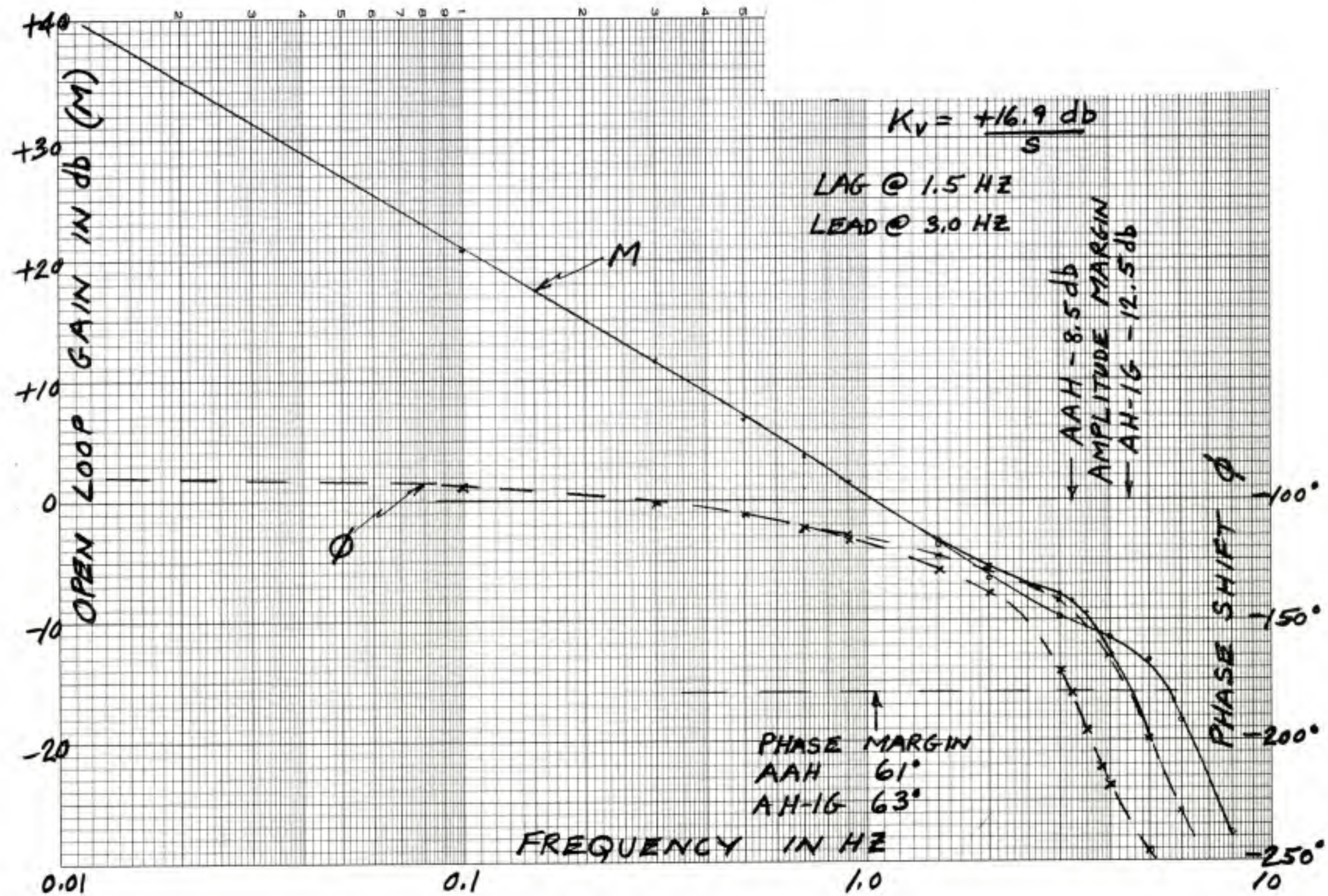

Figure 6. Main pitch control system open loop

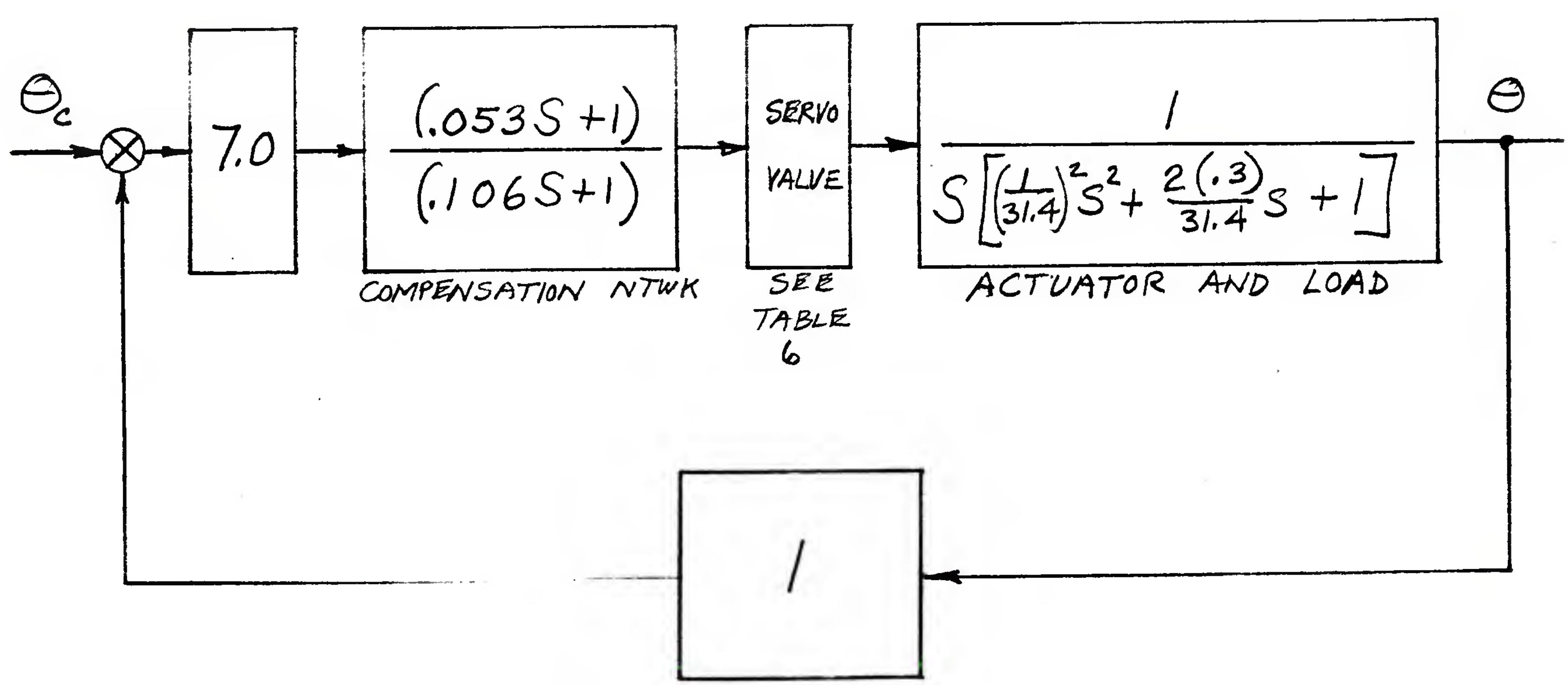

Figure 7. Main pitch control system AH-1G payload

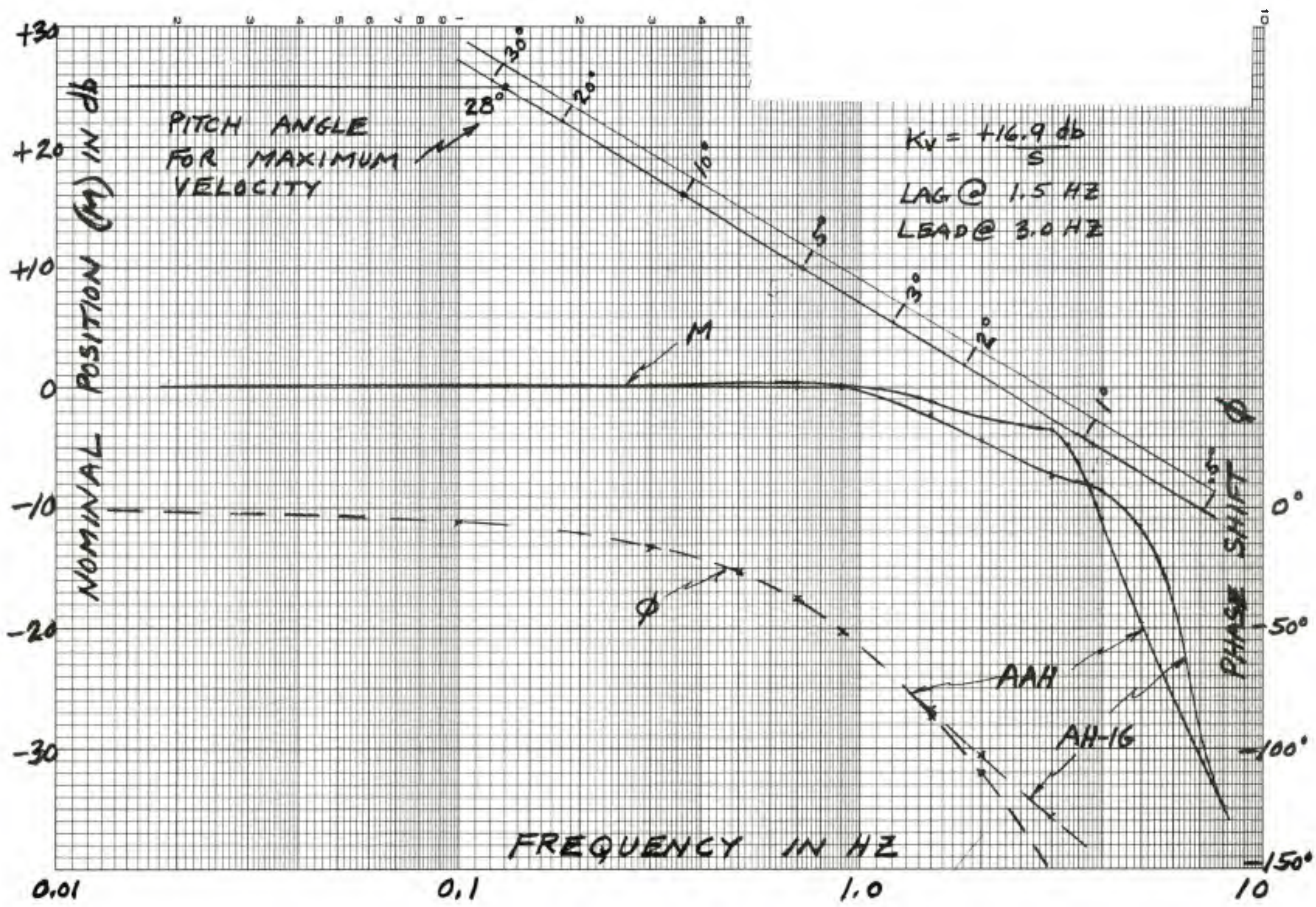

Figure 8. Main pitch control system closed loop

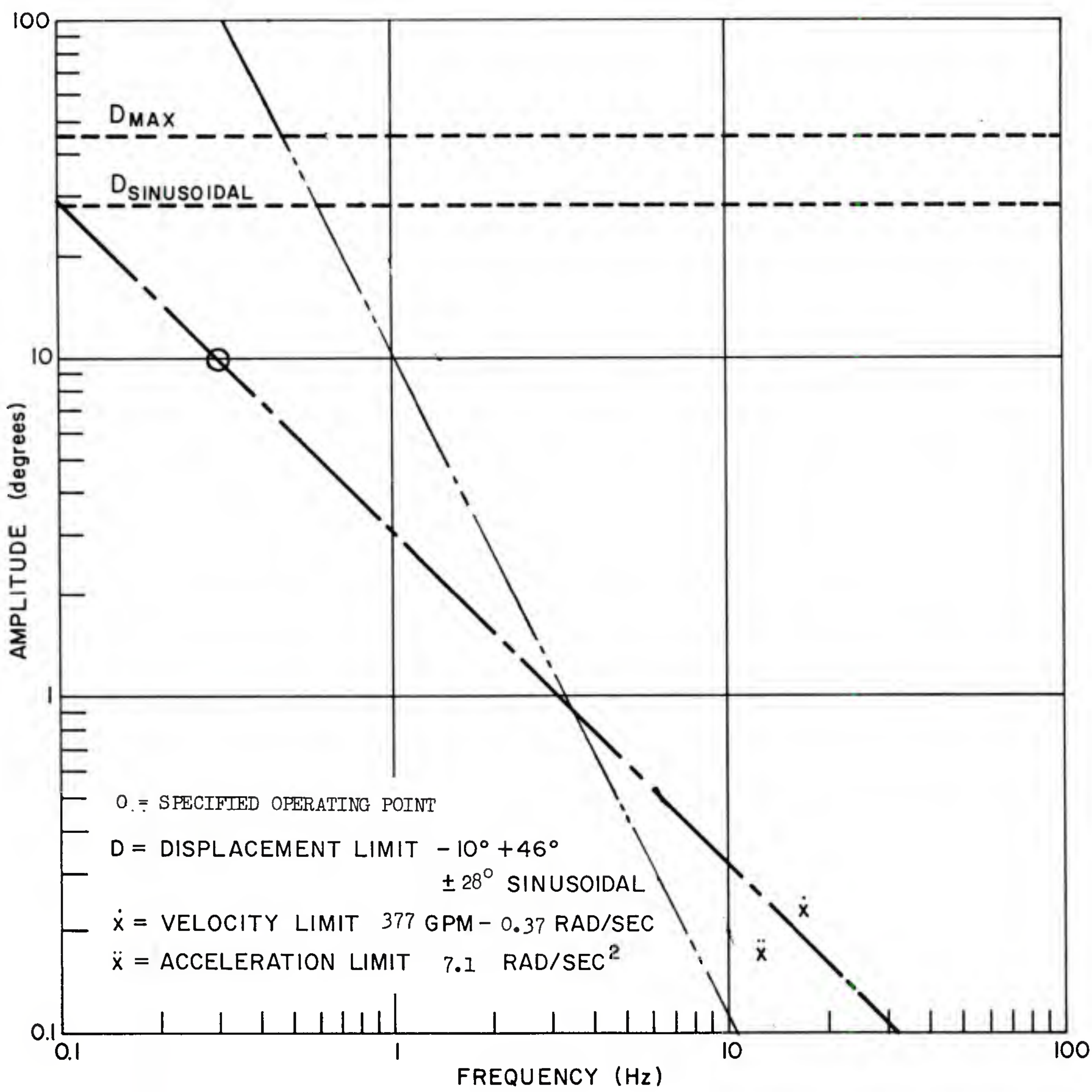

Figure 9. Main pitch operating limits

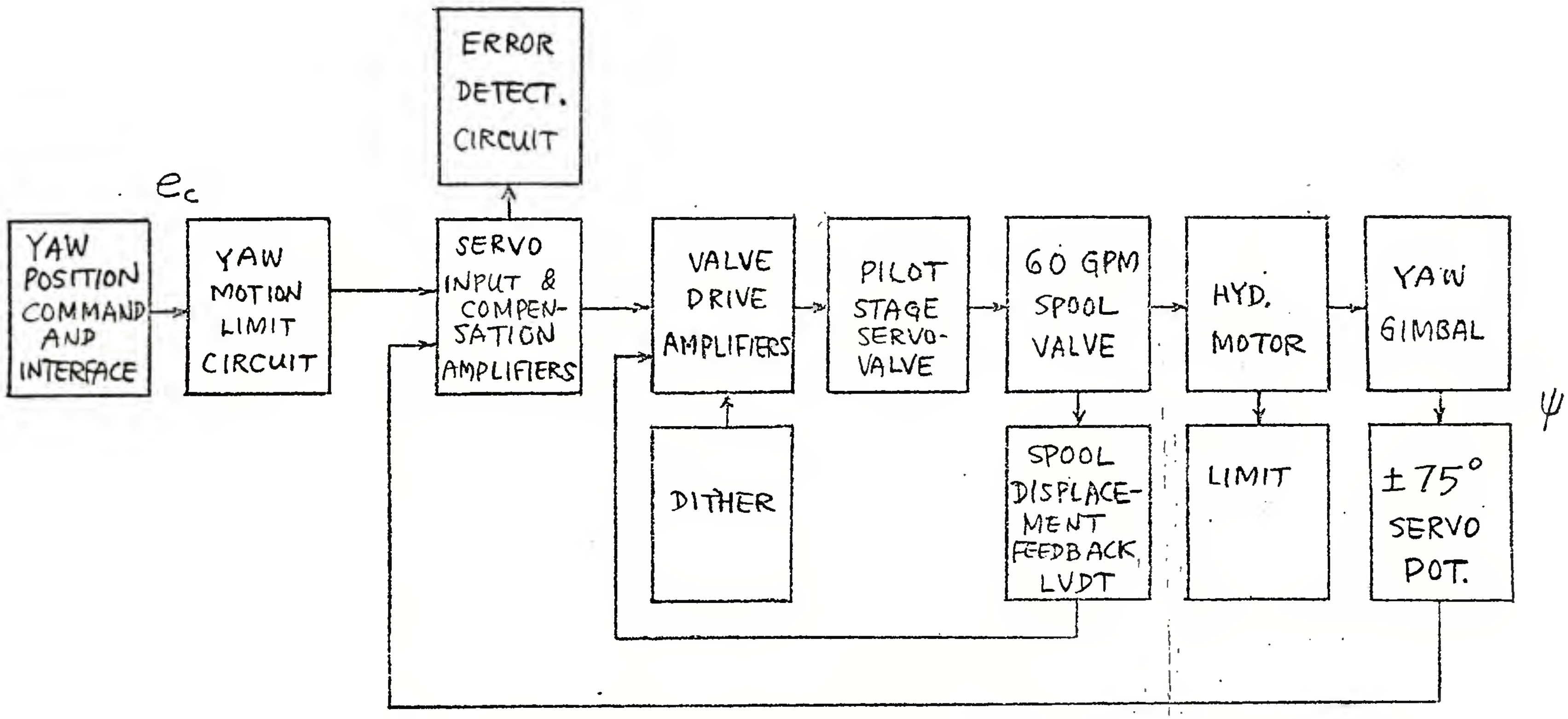

Figure 10. Main yaw feedback control system block diagram

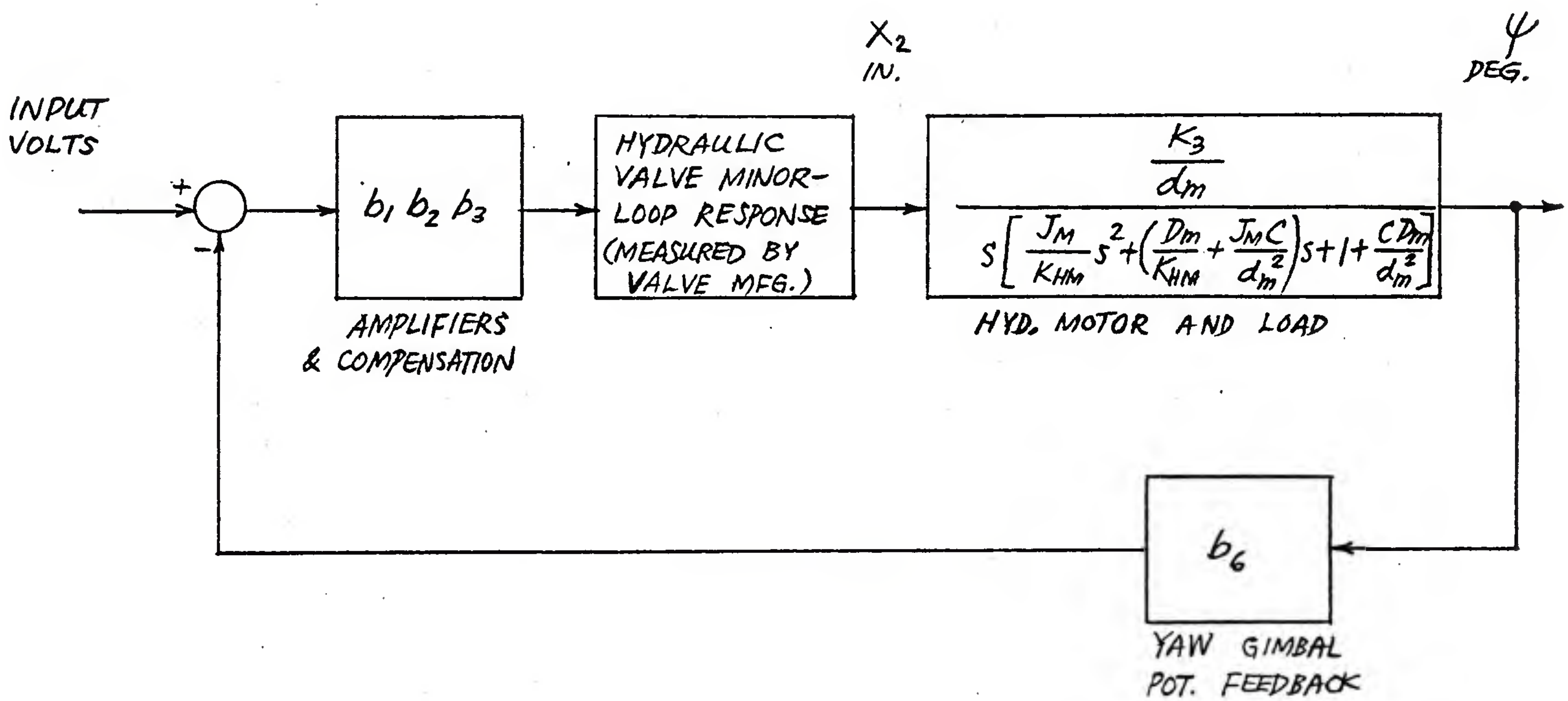

Figure 11. Transfer function block diagram of the main yaw feedback control system

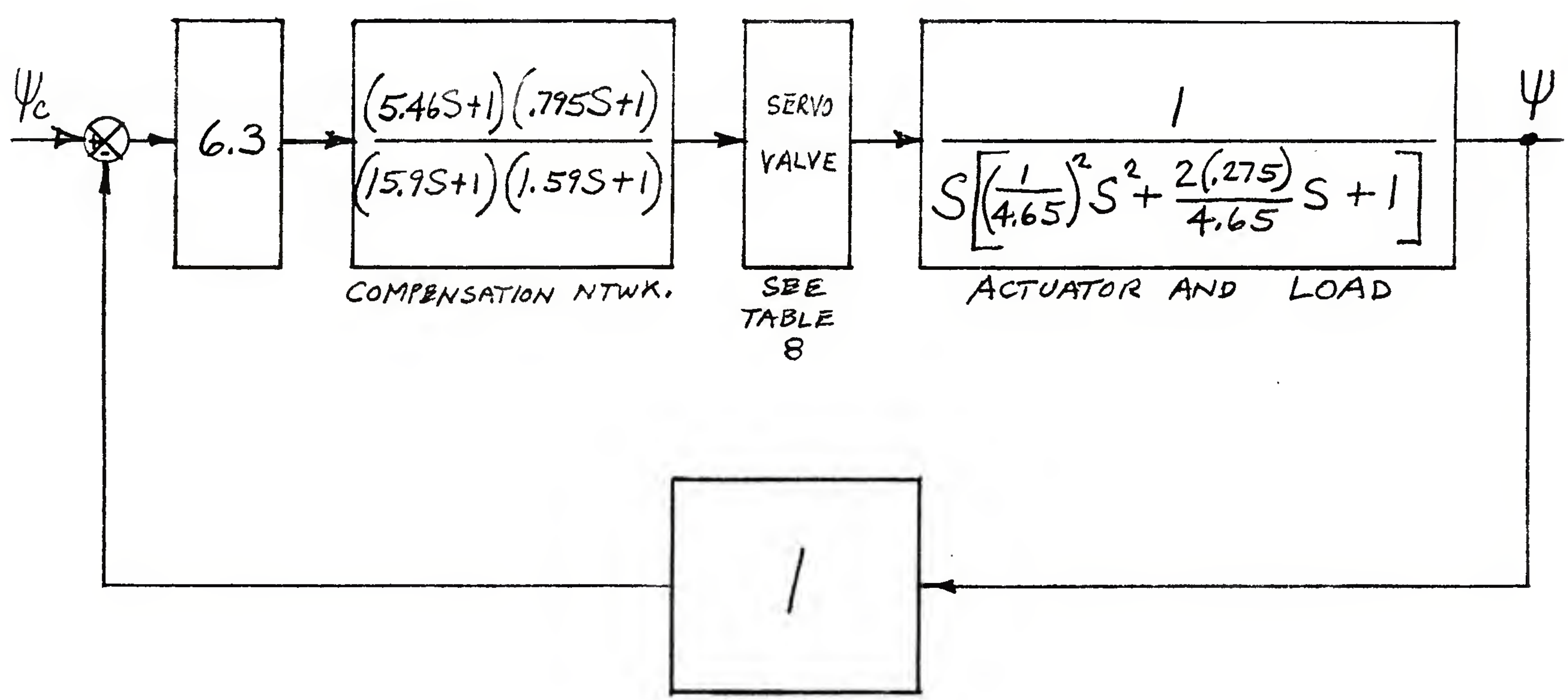

Figure 12. Main yaw control system AAH payload

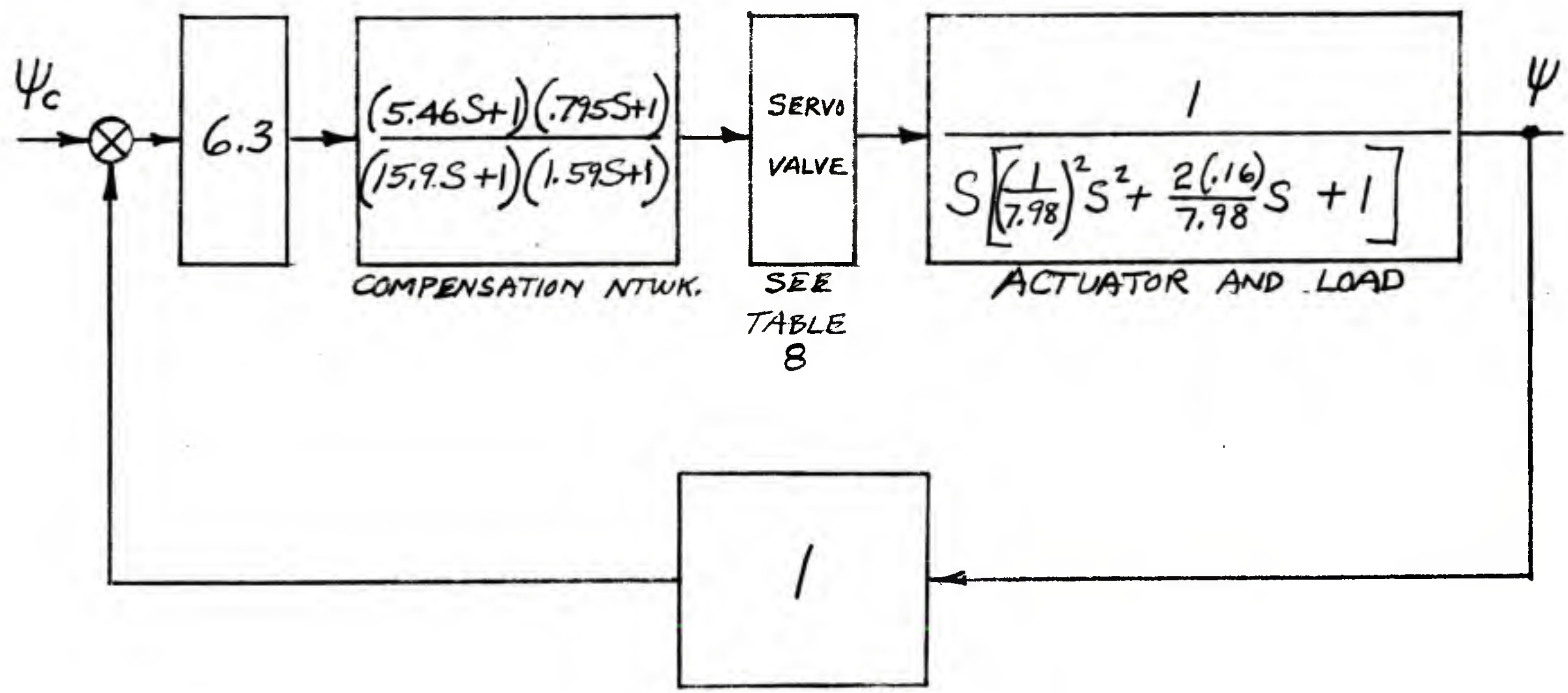

Figure 13. Main yaw control system AH-1G payload

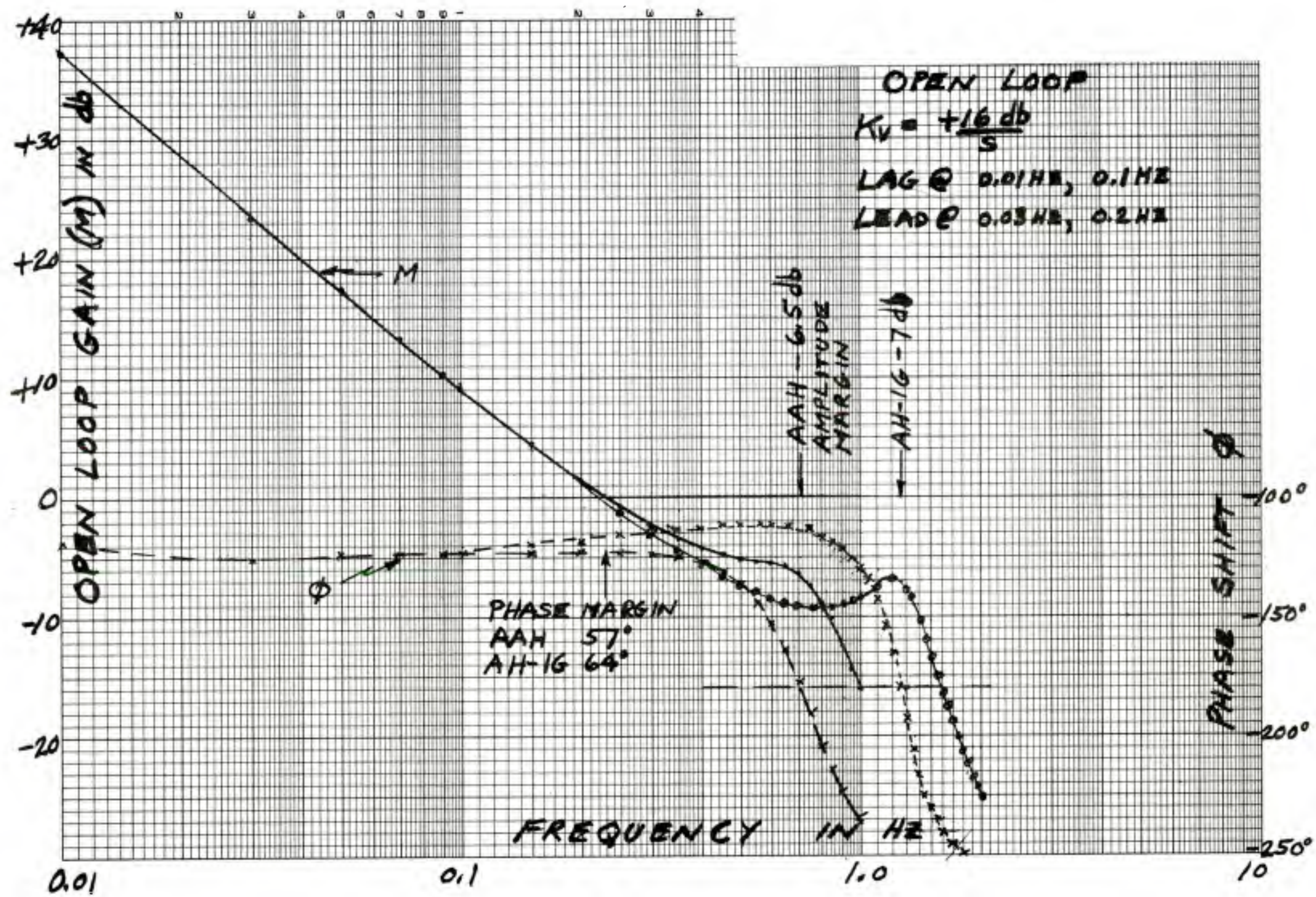

Figure 14. Main yaw control system open loop

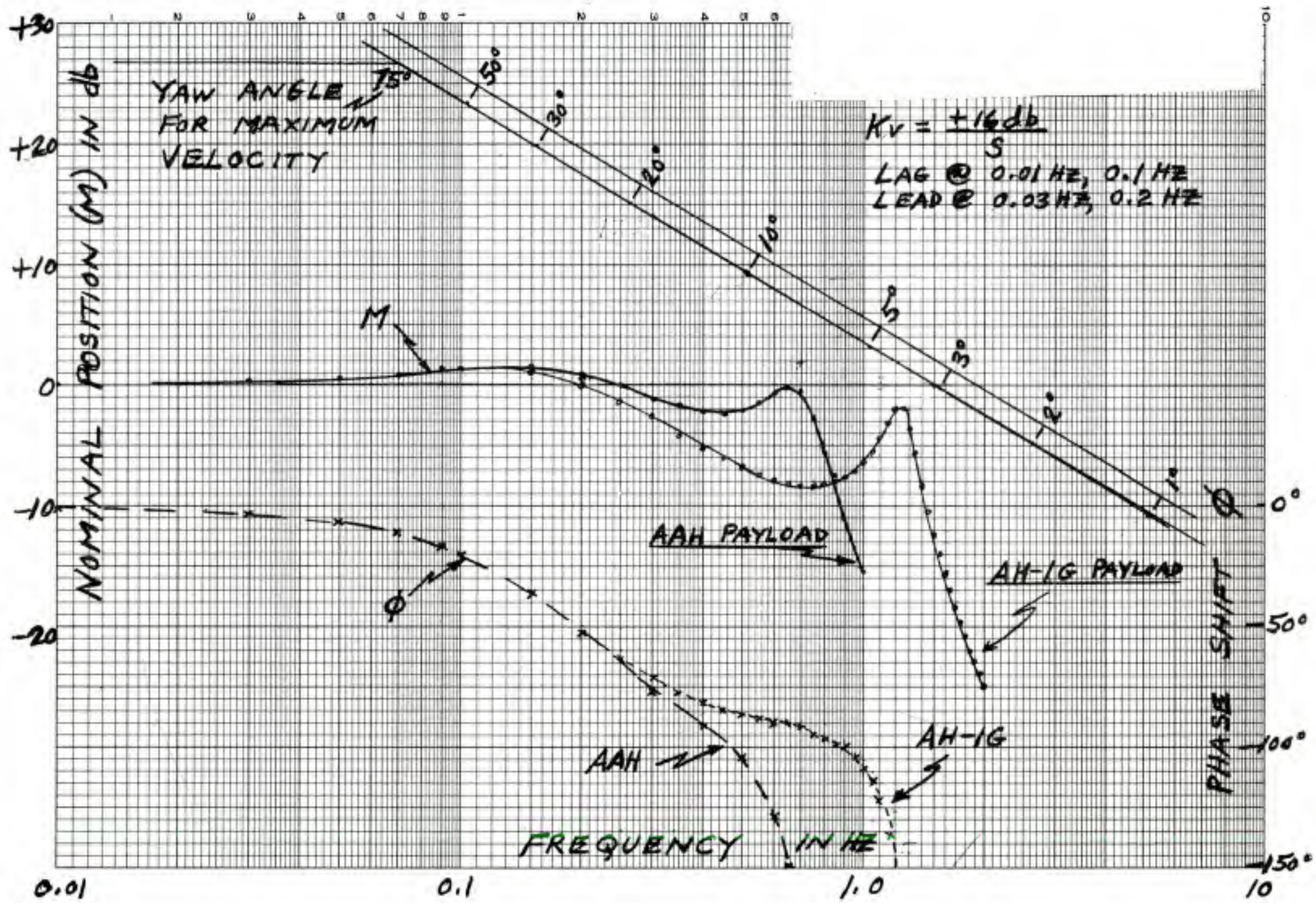

Figure 15. Main yaw control system closed loop

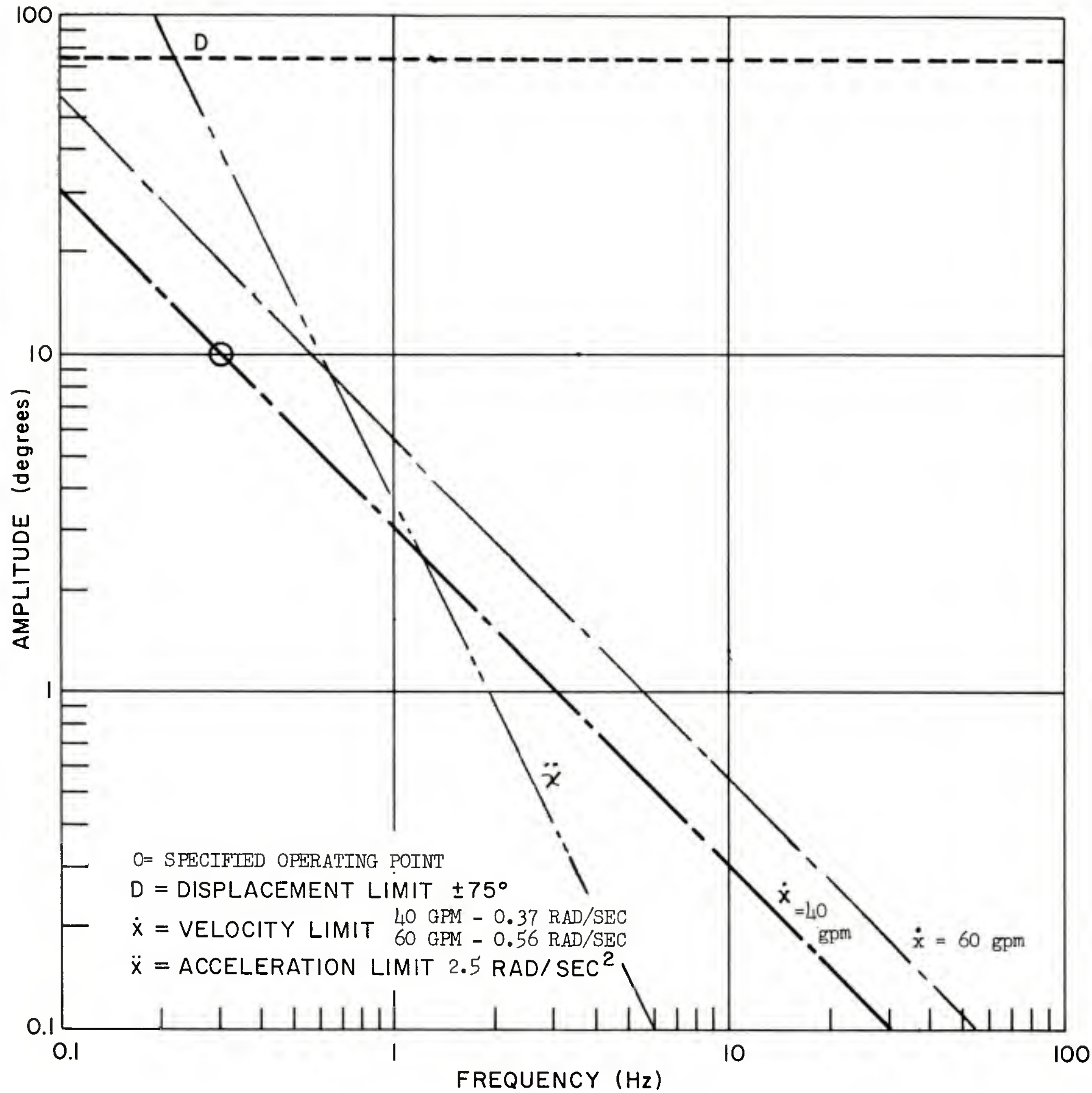

Figure 16. Main yaw operating limits (AH-1G aircraft)

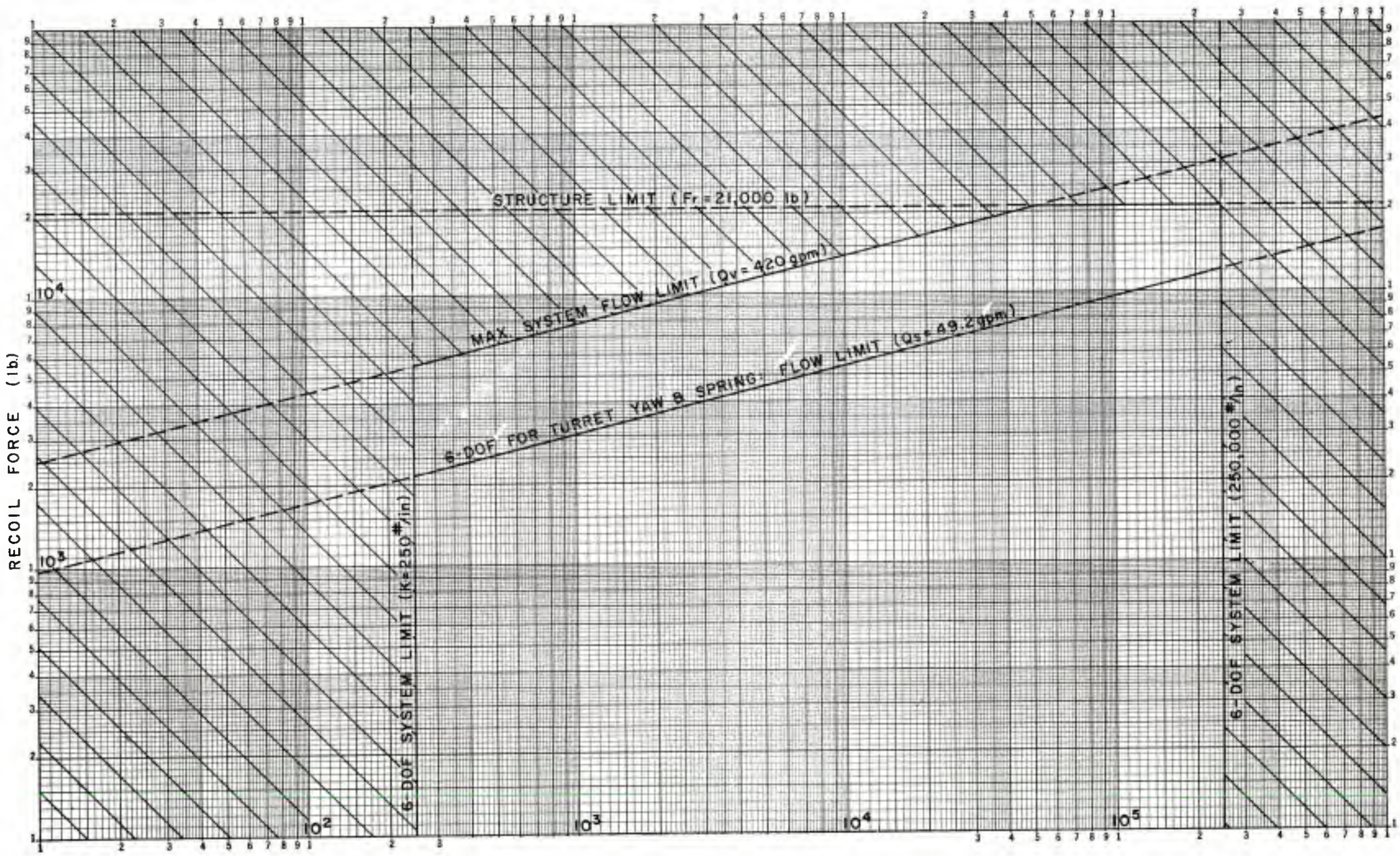

Figure 17. 6-DOF system spring rate $(\frac{\text{lb}}{\text{in.}})$

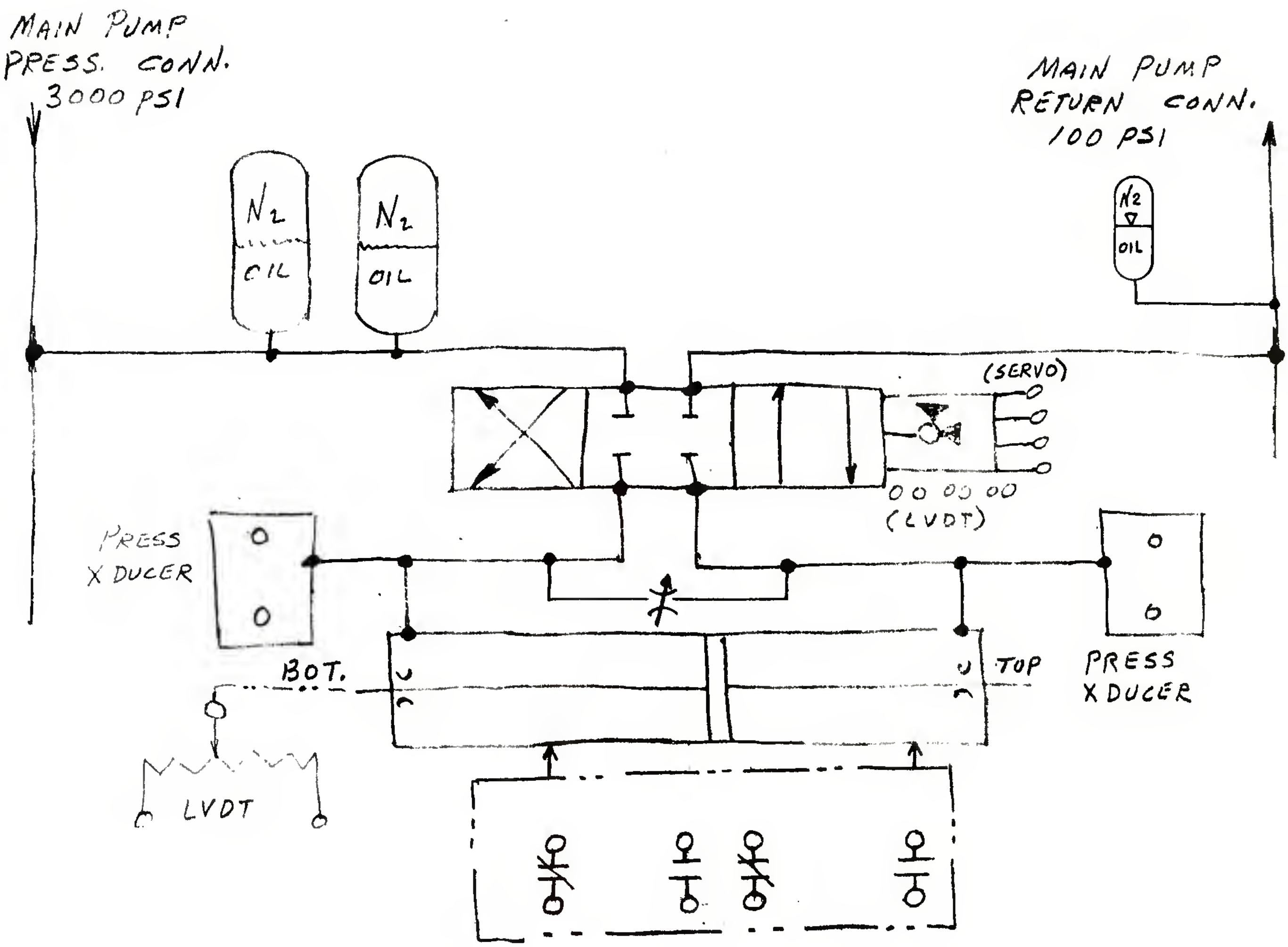

Figure 18. Hydraulic schematic modified 6-DOF suspension (typical)

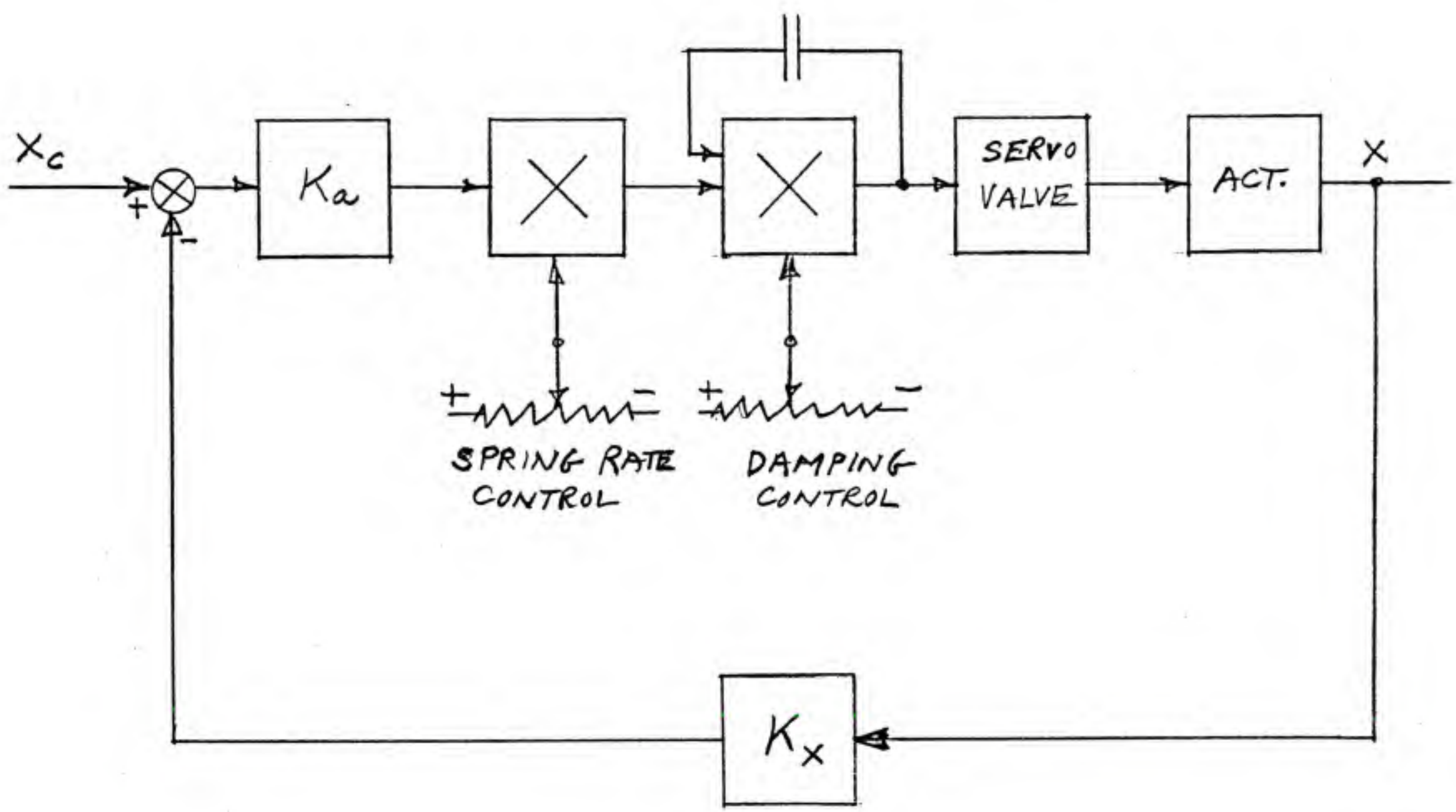

Figure 19. Control circuit to verify spring rate and damping control

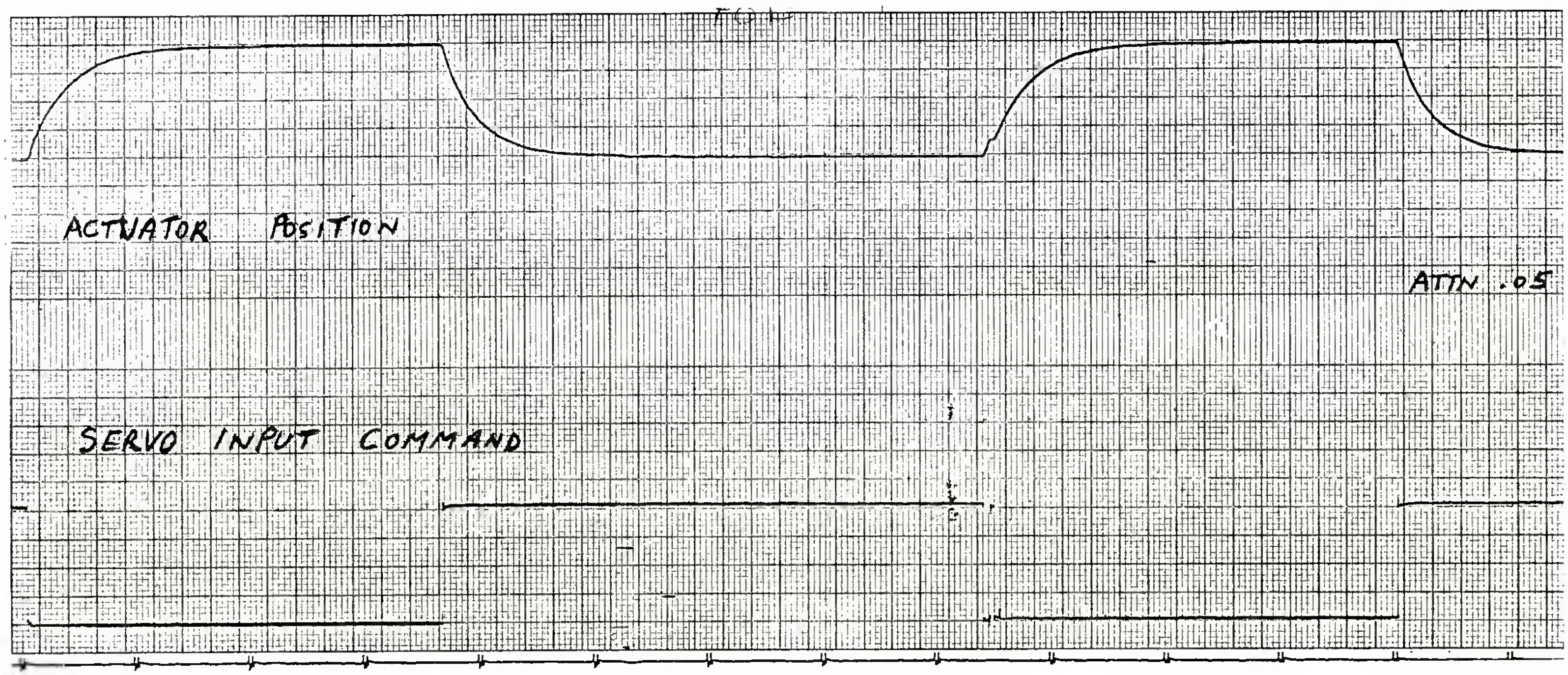

Figure 20. Servo system with bypass on actuator open 1 1/2 turns

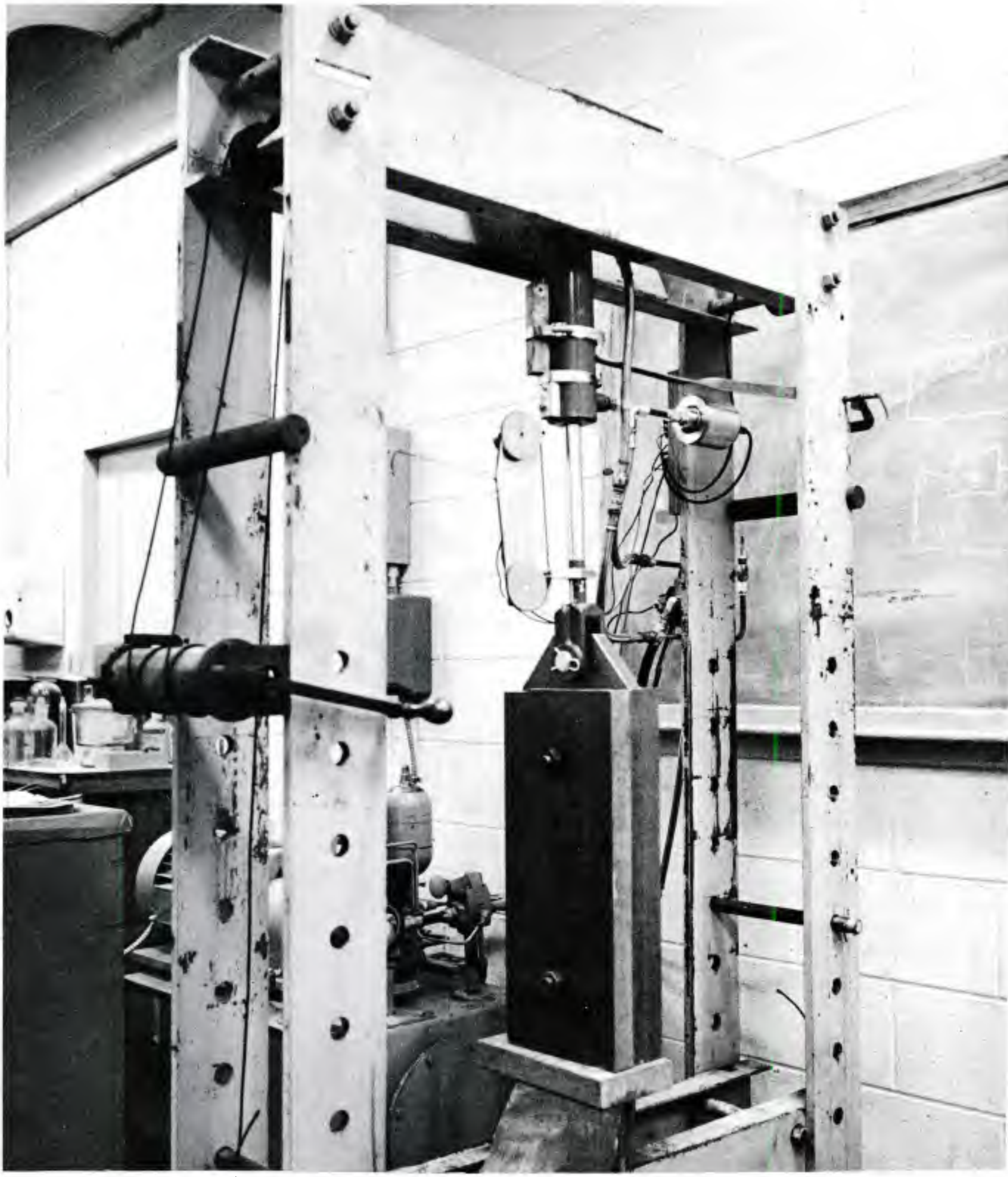

Figure 21. Spring and damping test set-up

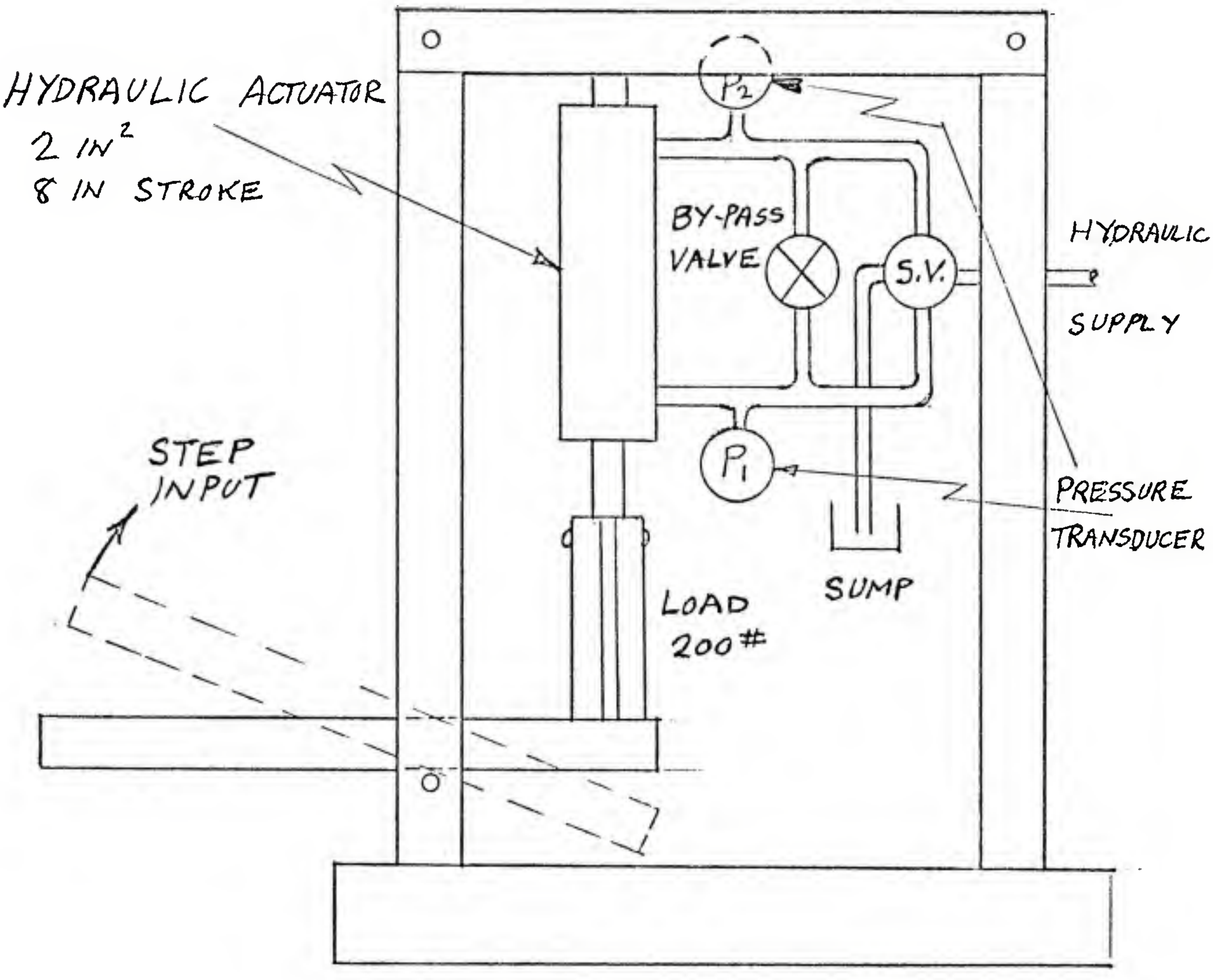

Figure 22. Test stand

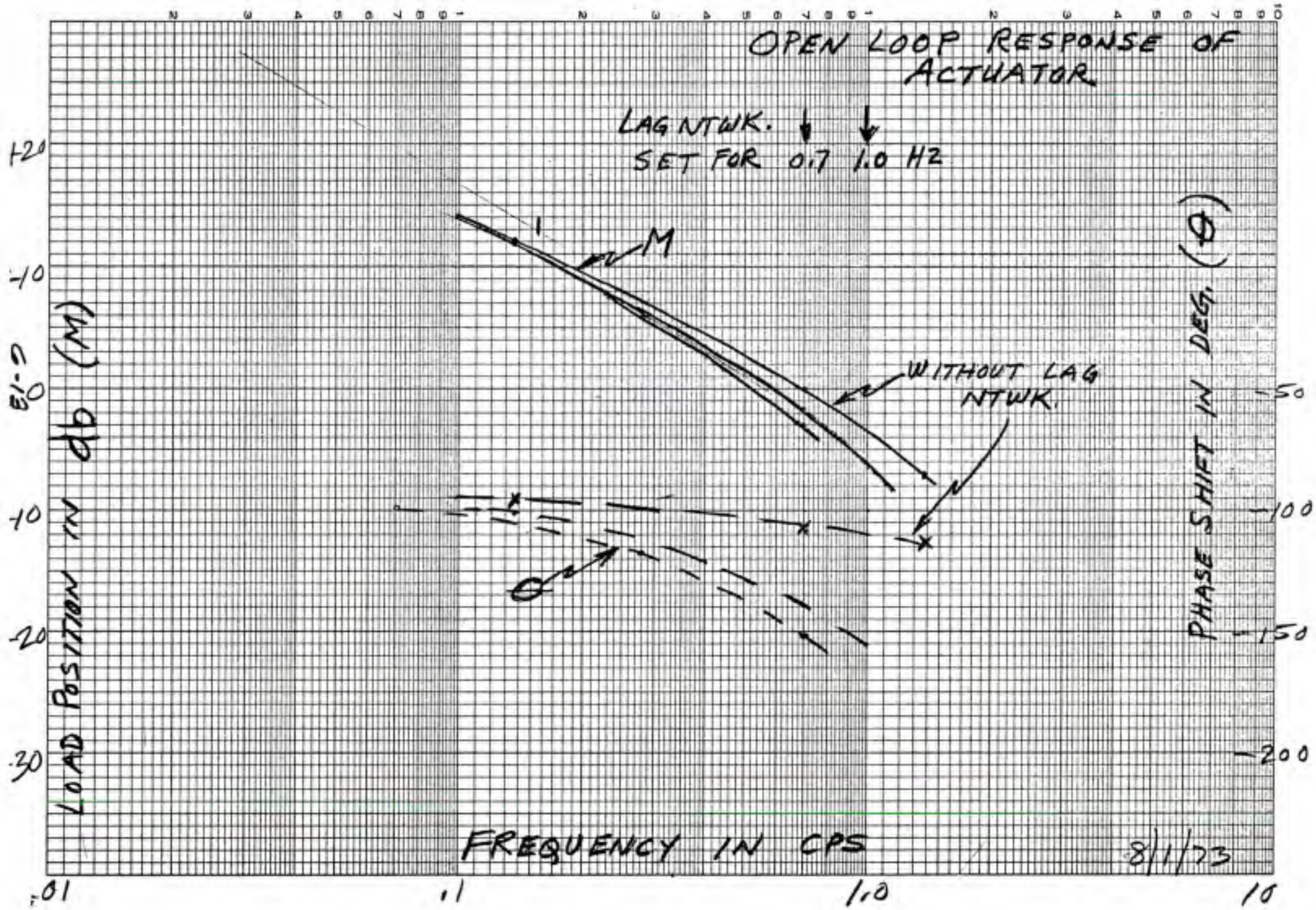

Figure 23. Open loop response of actuator

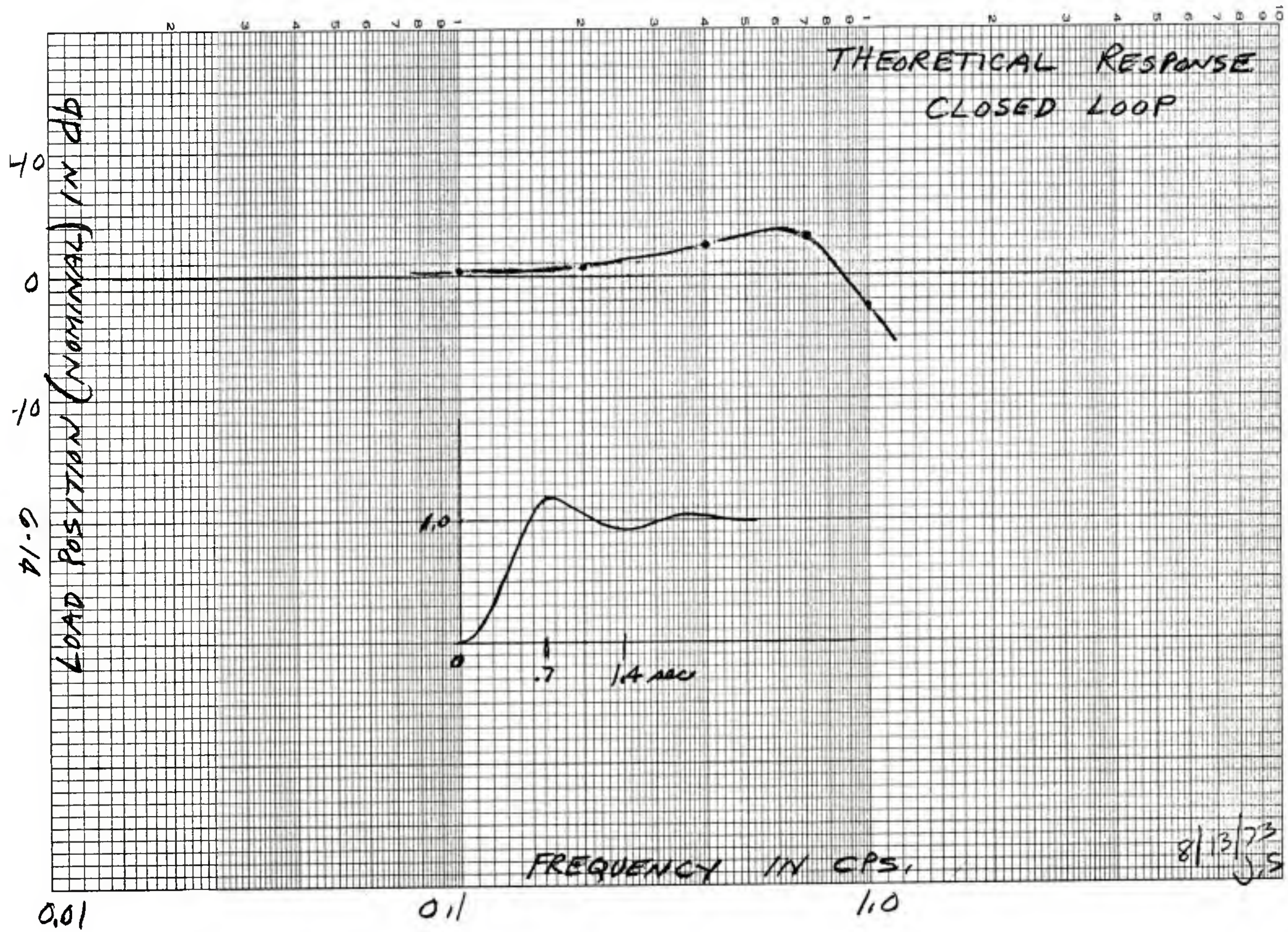

Figure 24. Theoretical response closed loop

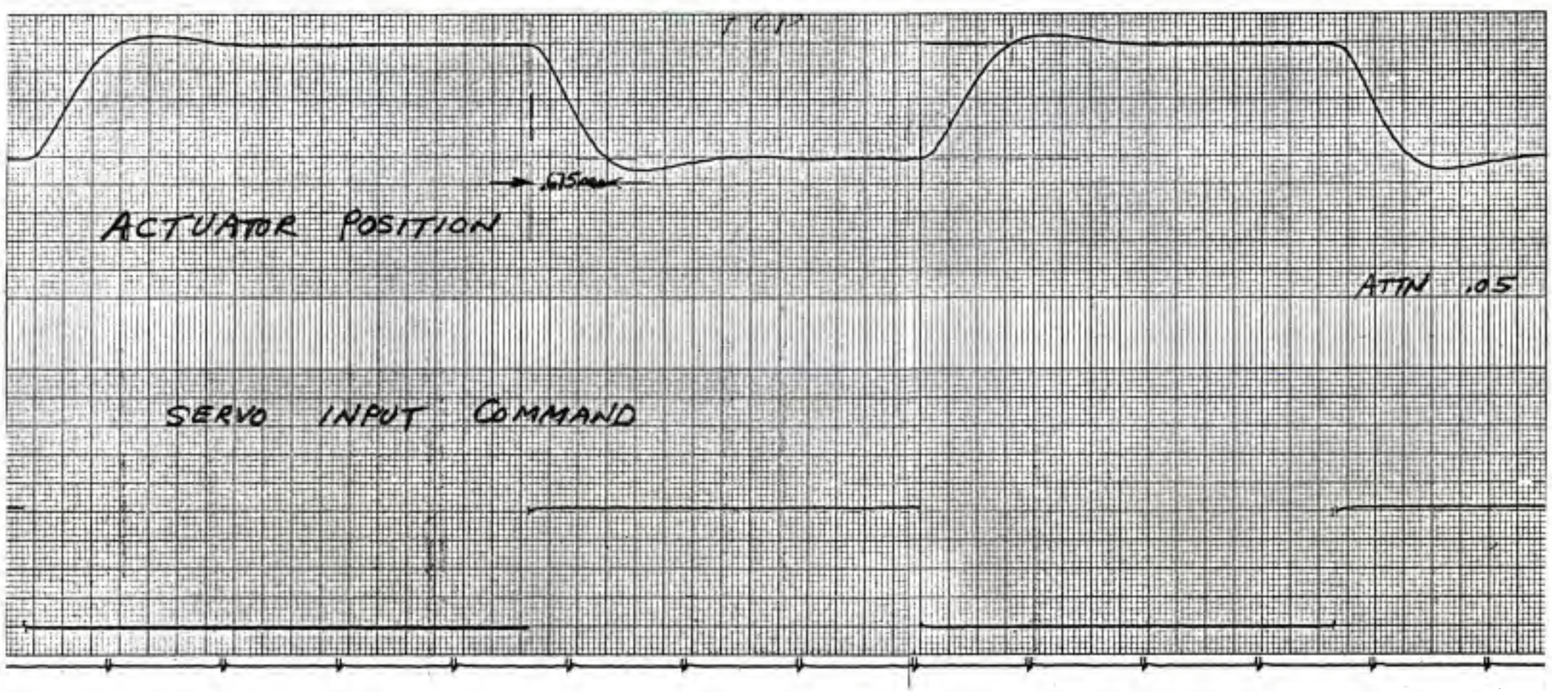

Figure 25. Servo system with bypass on actuator open 1 1/2 turns; lag network added to forward loop; overdamped system controlled to produce underdamped characteristic

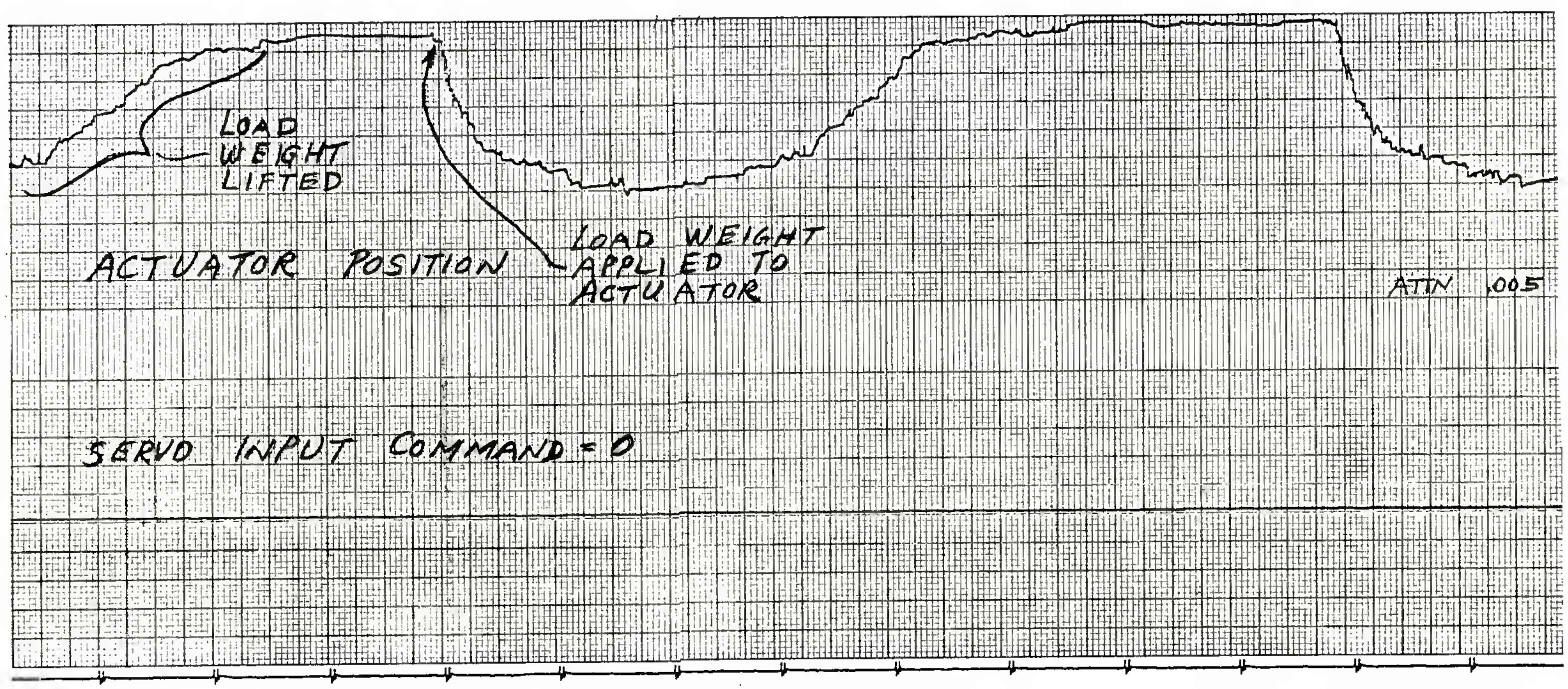

Figure 26. Servo system with bypass on actuator open 1 1/2 turns; lag network added to forward loop; step change in force and response characteristic

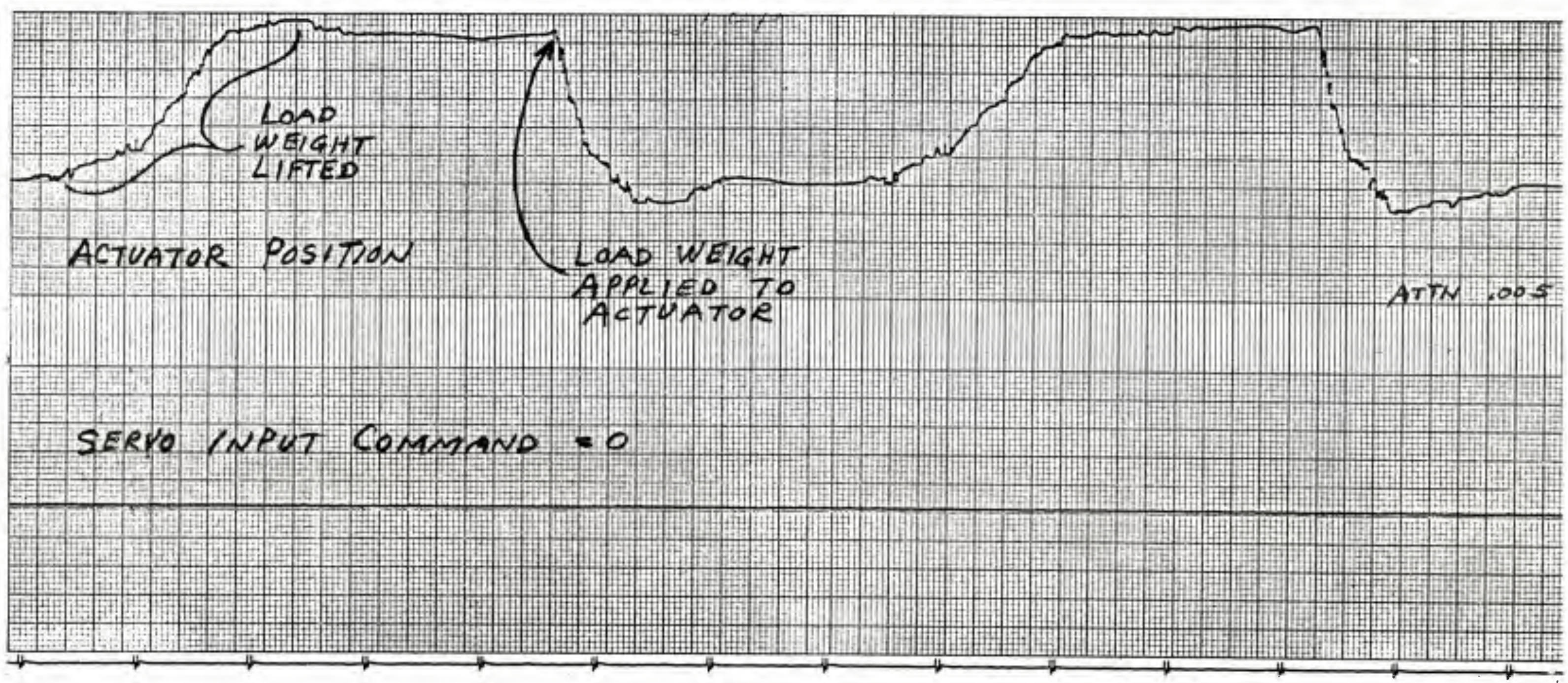

Figure 27. Servo system with bypass on actuator open 1 1/2 turns; lag network added to forward loop; underdamped system

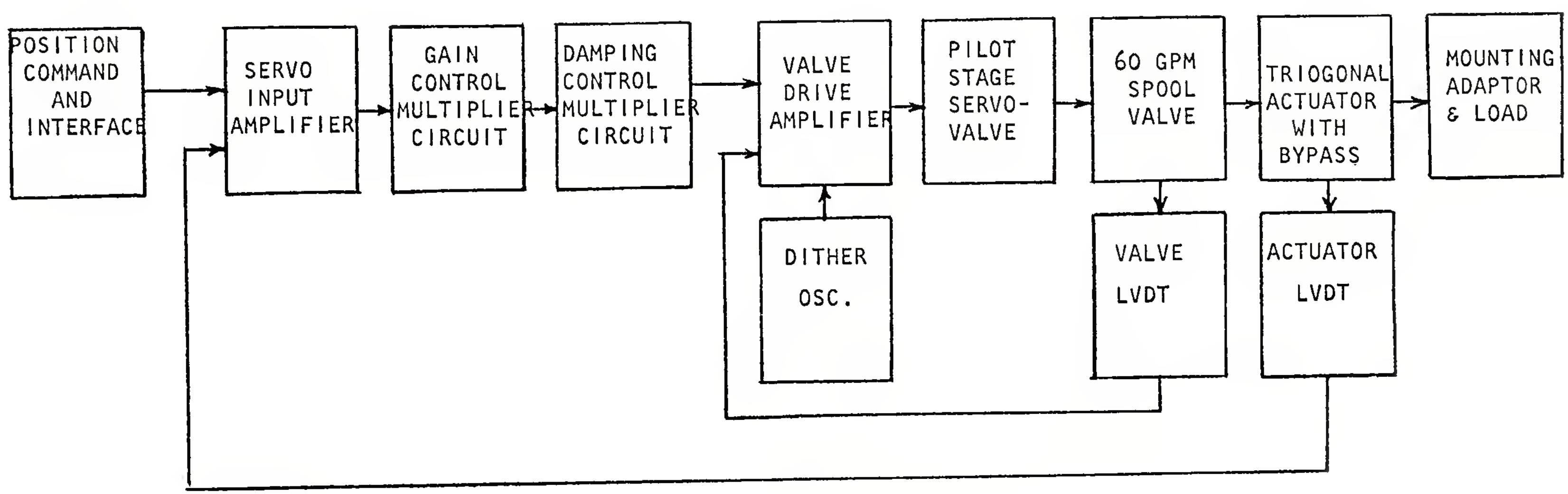

Figure 28. Triogonal actuator position servo system block diagram

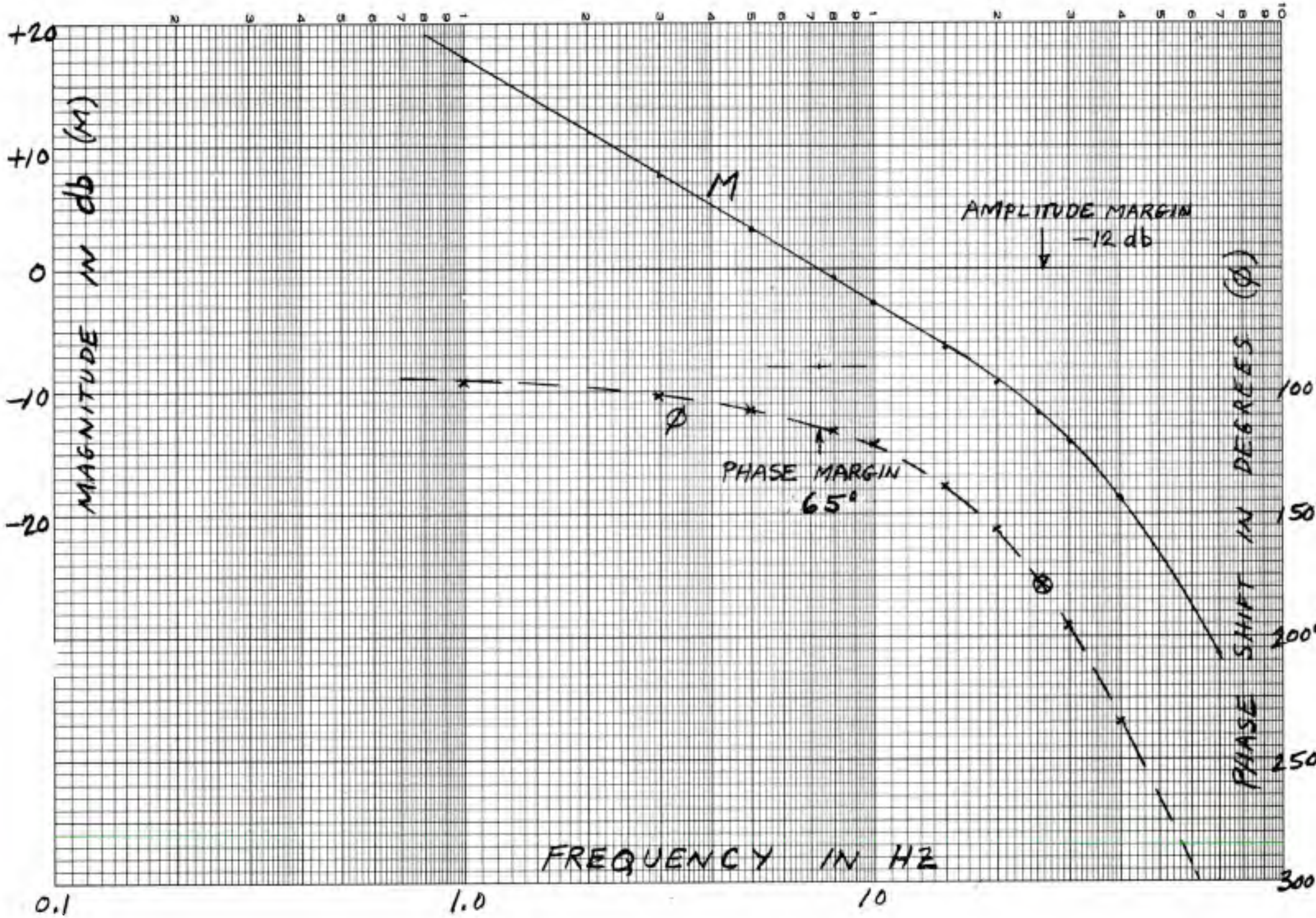

Figure 29. Open loop gain constant (45) and the dynamics of the value and actuator

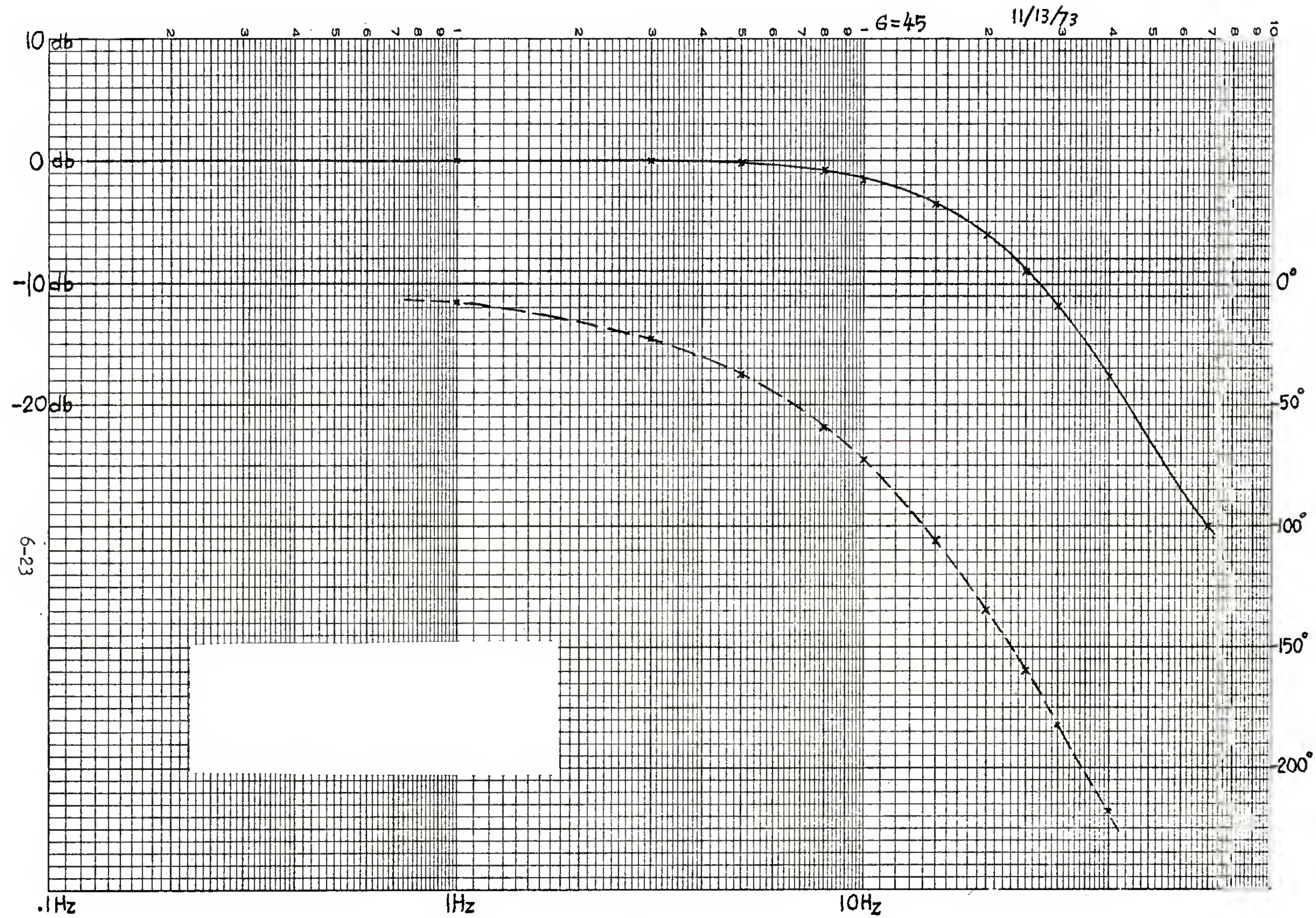

Figure 30. Calculated frequency response of the triogonal actuator position servo system

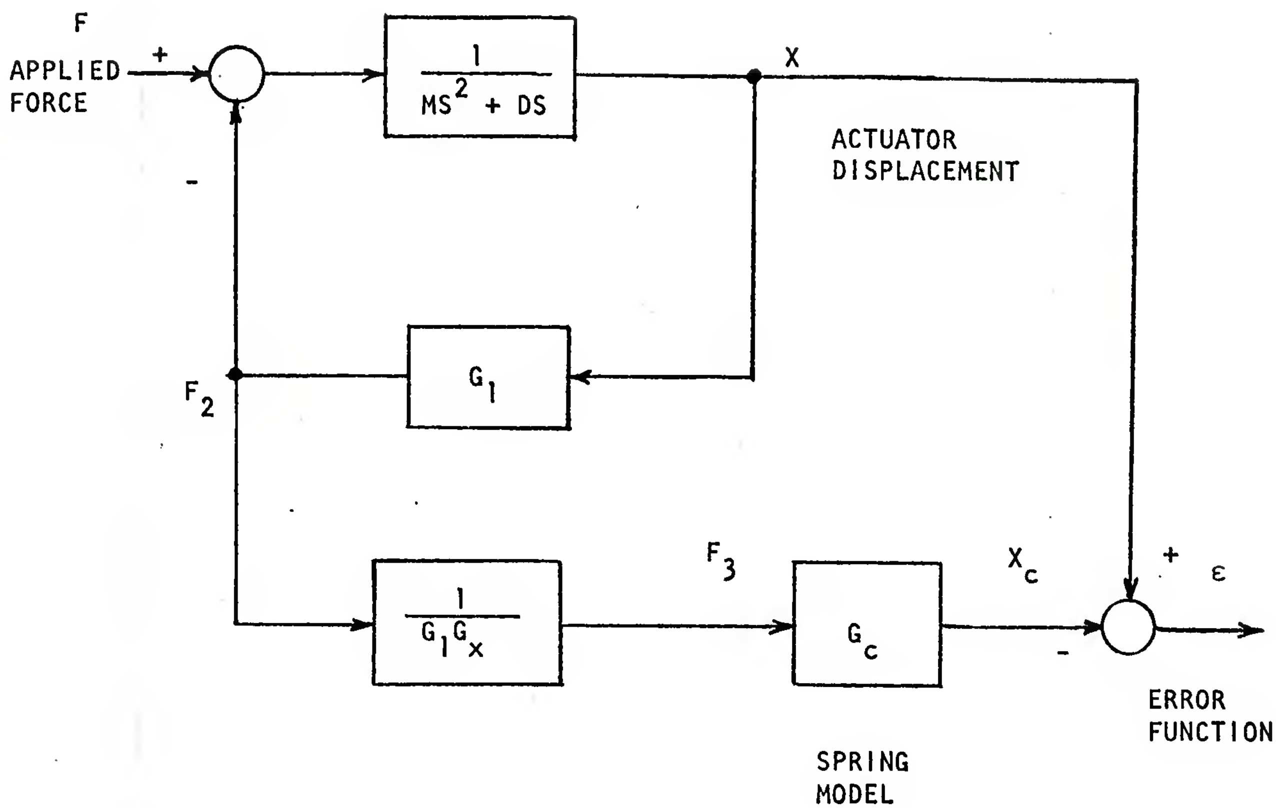

Figure 31. Force sensing schematic block diagram of the adaptive spring-rate control system

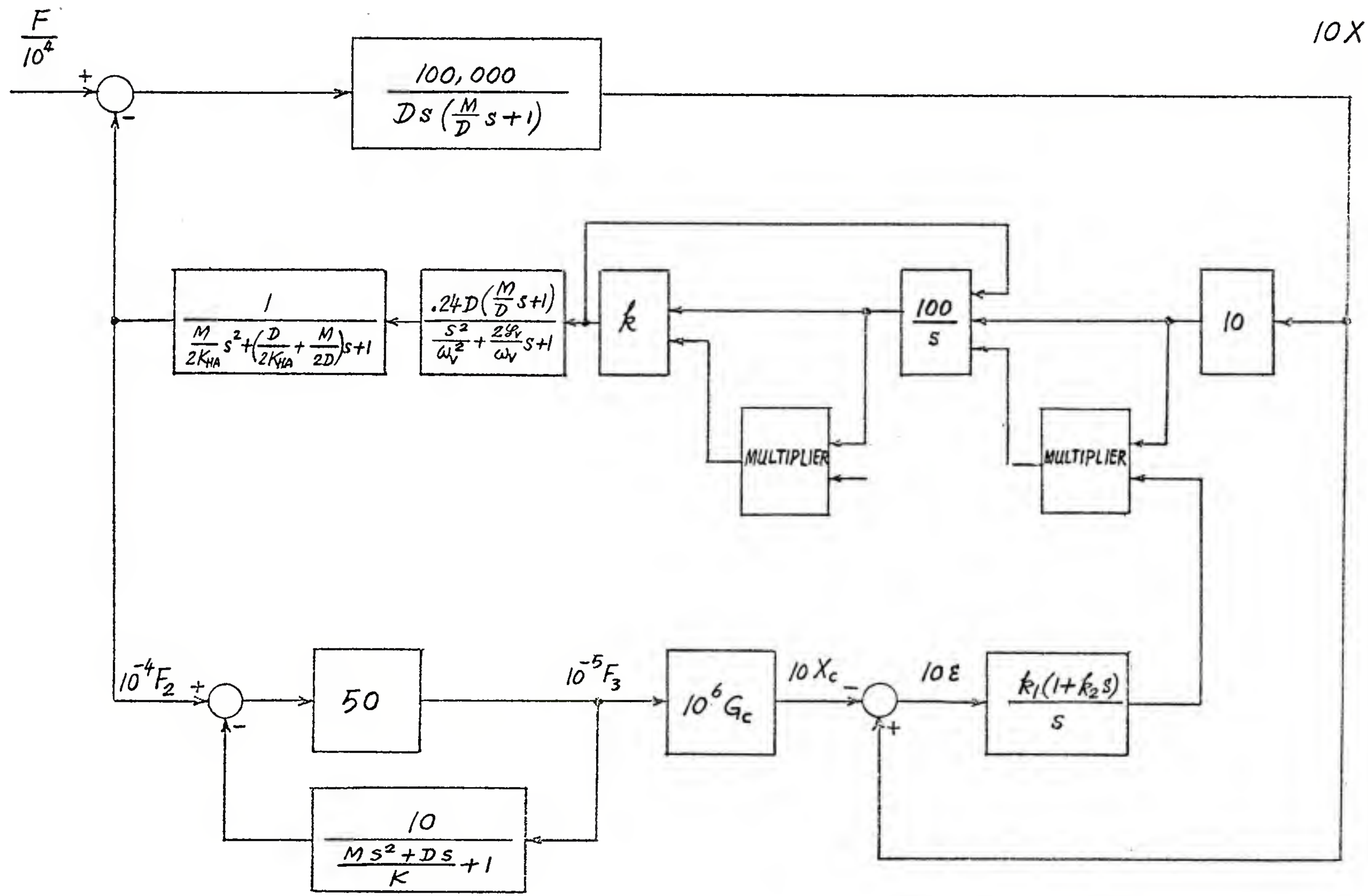

Figure 32. System block diagram of the adaptive spring-rate control system

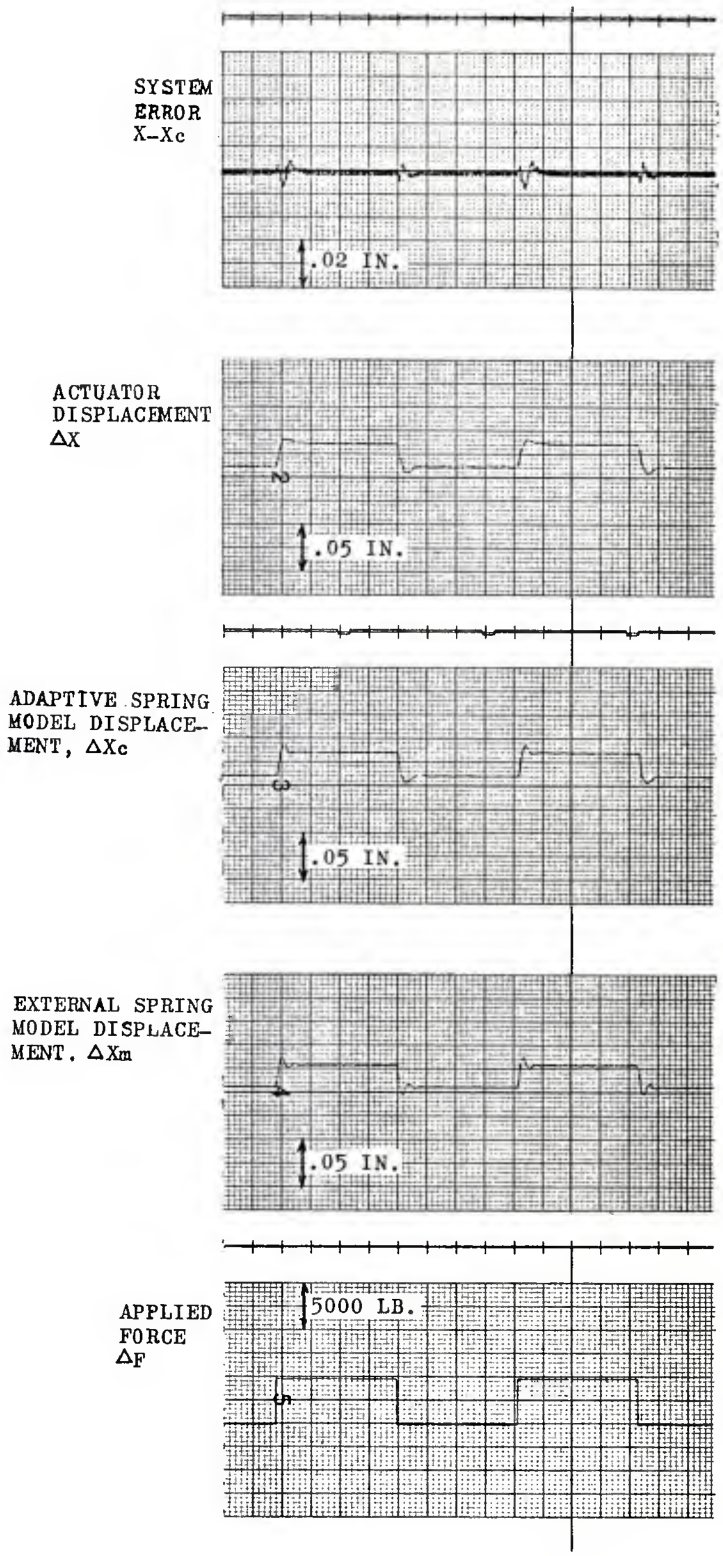

Figure 33. Position response of the simulated adaptive spring-rate control system with step force input; $K = 200{,}000 \frac{lb}{in.}$, $\zeta = 0.3$

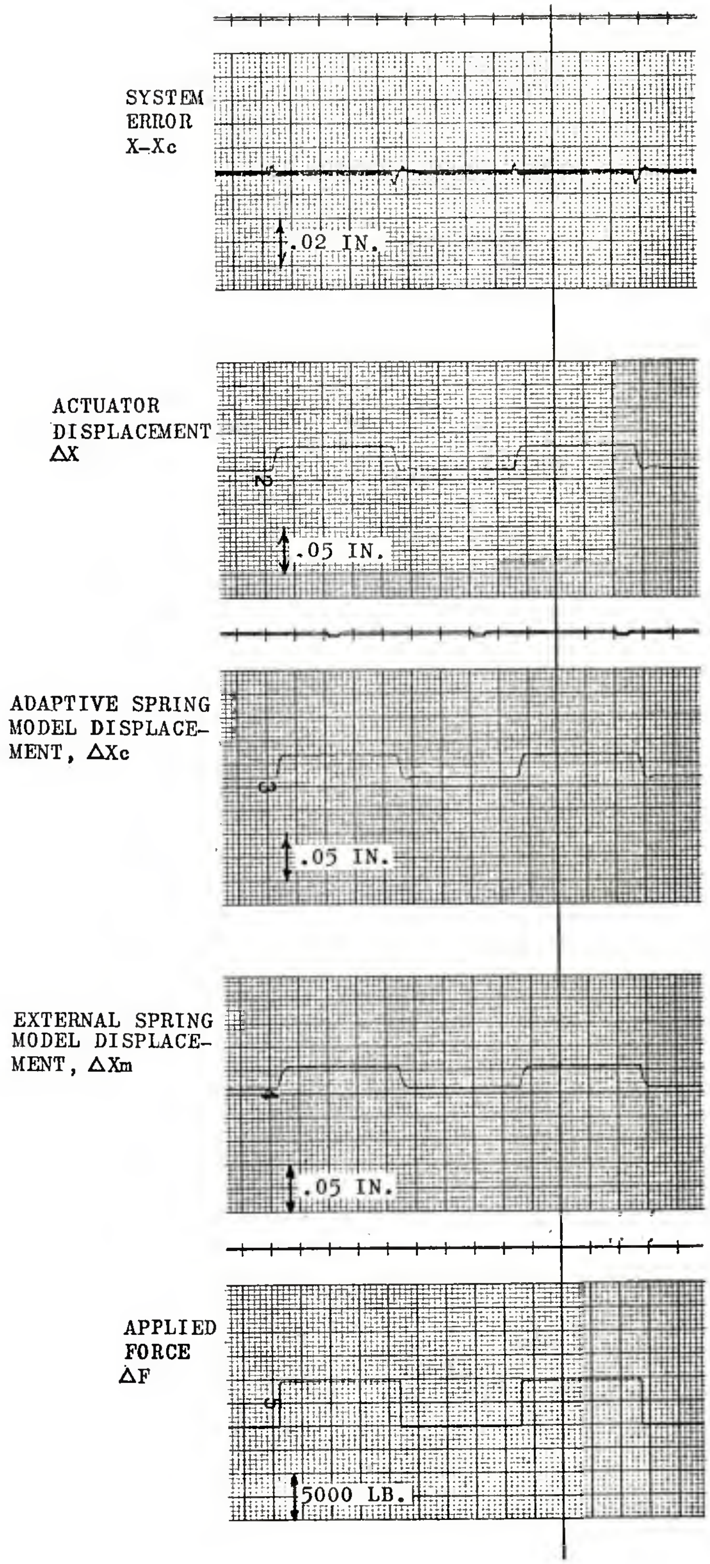

Figure 34. Position response of the simulated adaptive spring-rate control system with step force input; $K = 200{,}000\ \frac{lb}{in.}$, $\zeta = 1.0$

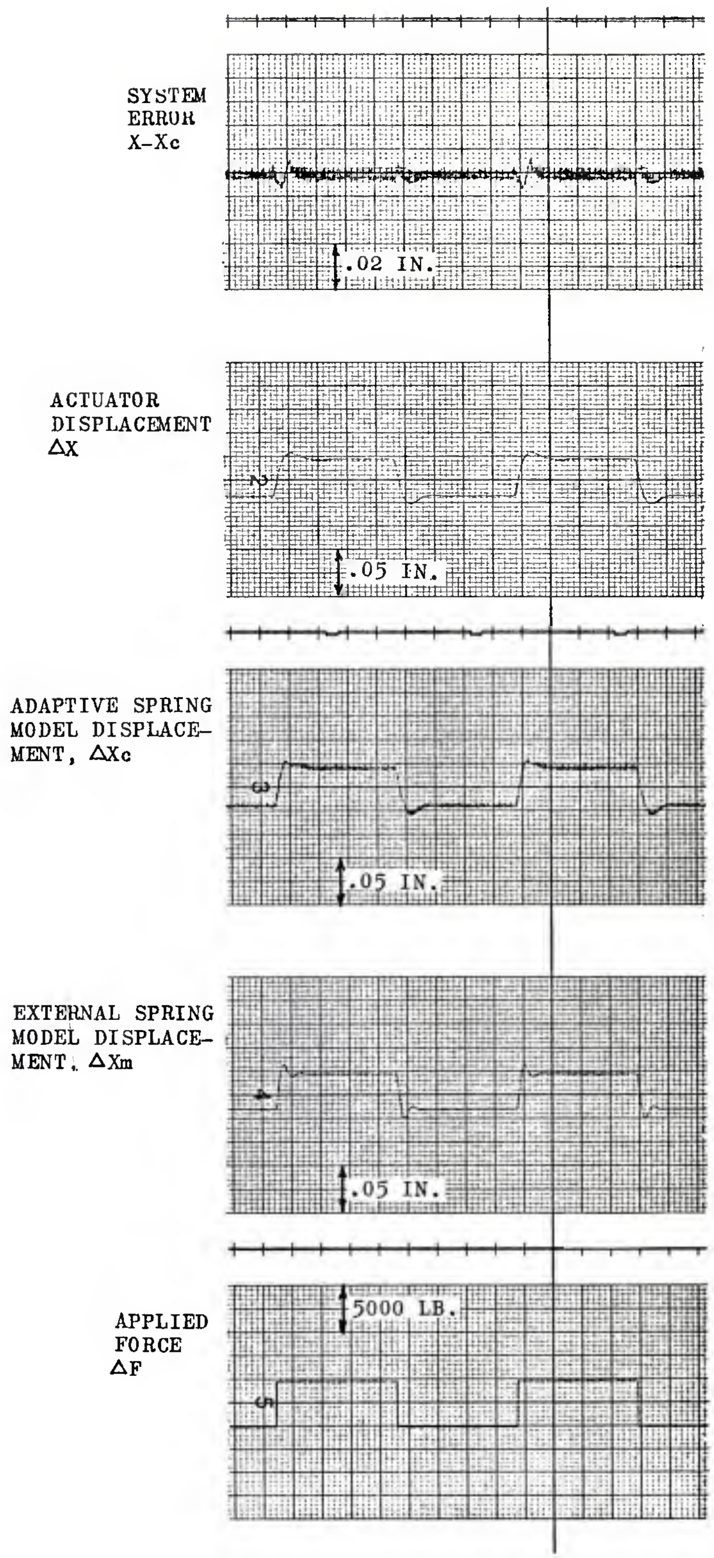

Figure 35. Position response of the simulated adaptive spring-rate control system with step force input; $K = 130{,}000 \frac{\text{lb}}{\text{in.}}$, $\zeta = 0.376$

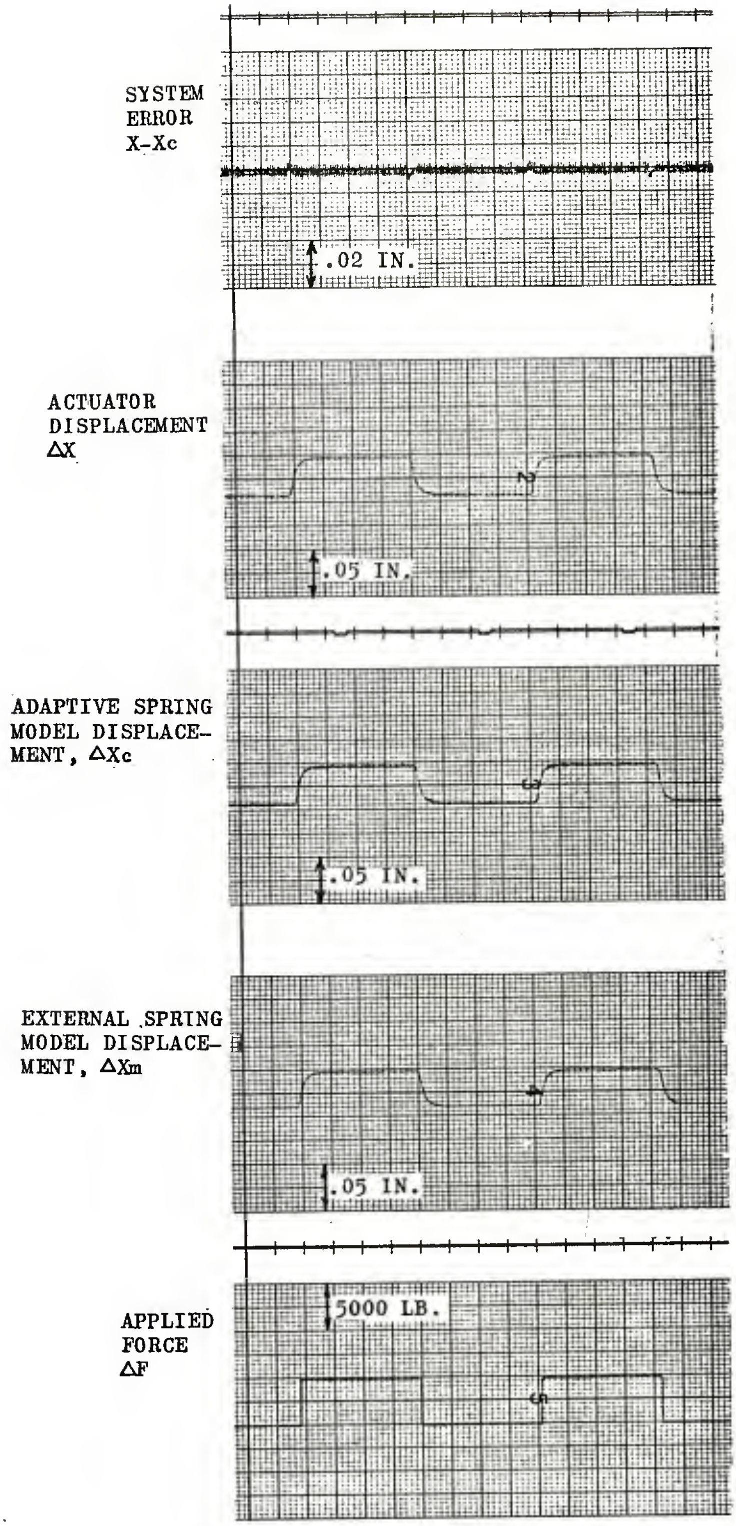

Figure 36. Position response of the simulated adaptive spring-rate control system with step force input; $K = 130{,}000\ \frac{\text{lb}}{\text{in.}}$, $\zeta = 1.24$

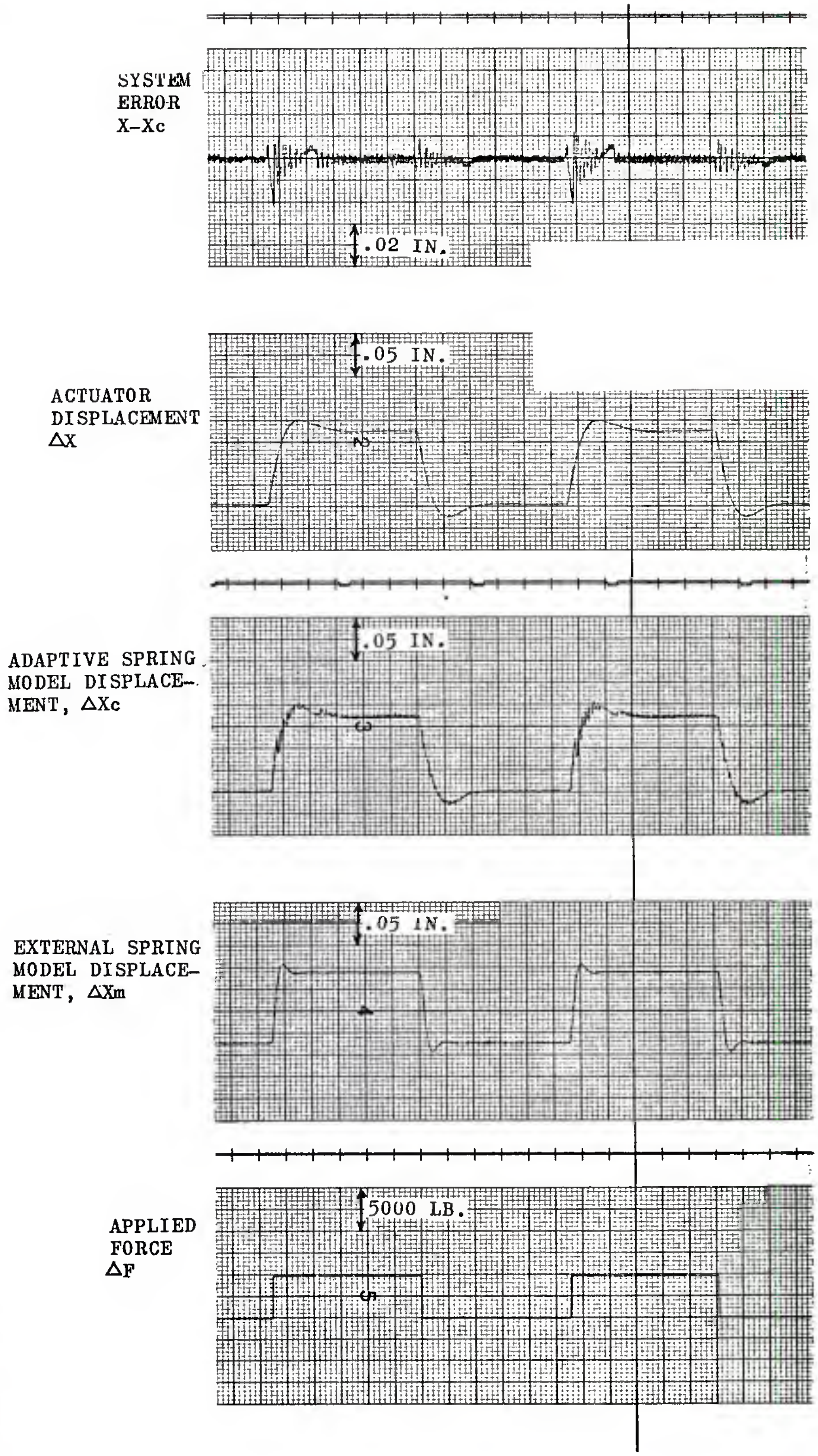

Figure 37. Position response of the simulated adaptive spring-rate control system with step force input; $K = 60{,}000\ \frac{\text{lb}}{\text{in.}}$, $\zeta = 0.55$

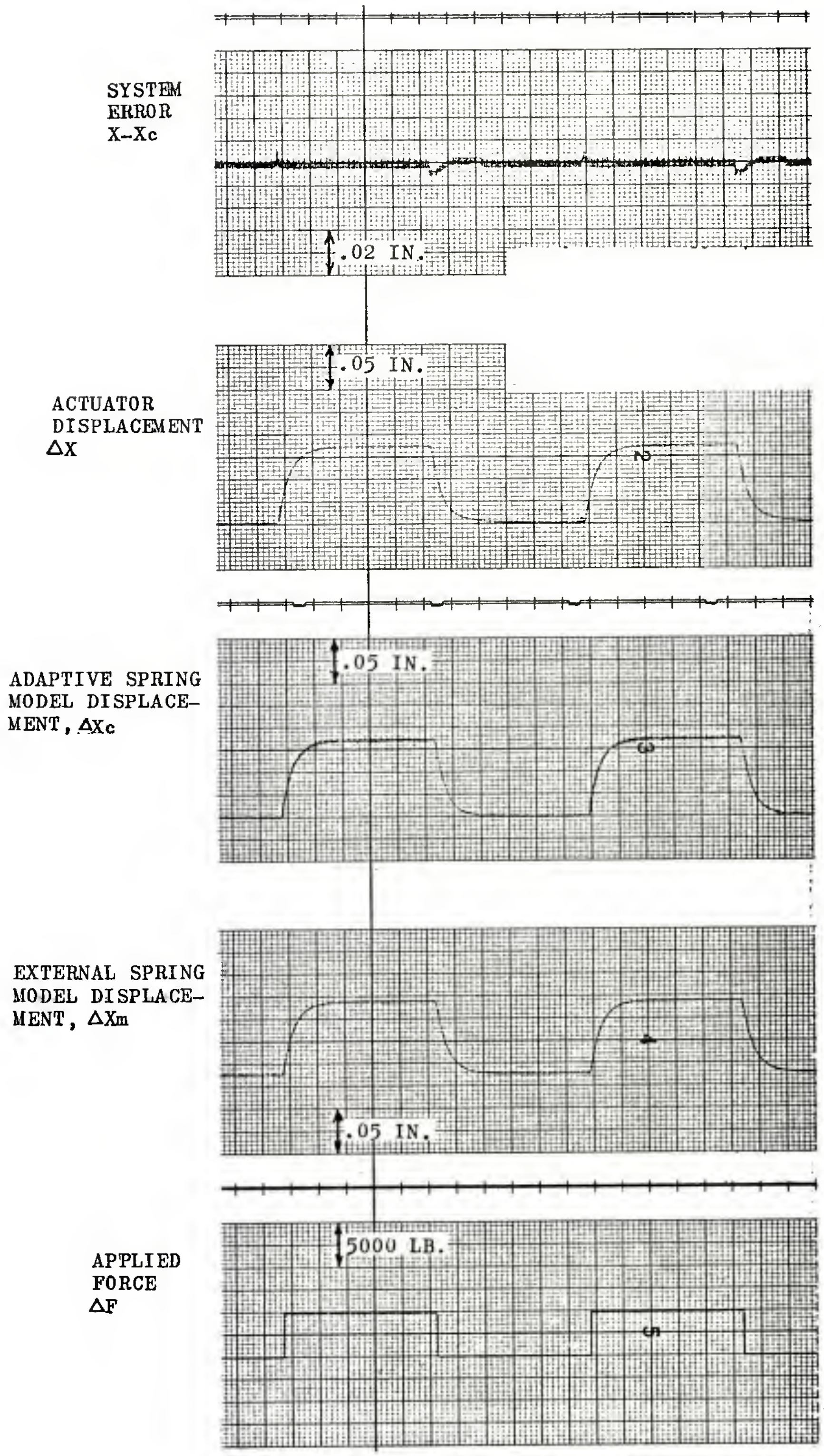

Figure 38. Position response of the simulated adaptive spring-rate control system with step force input; $K = 60{,}000\ \frac{lb}{in.}$, $\zeta = 1.8$

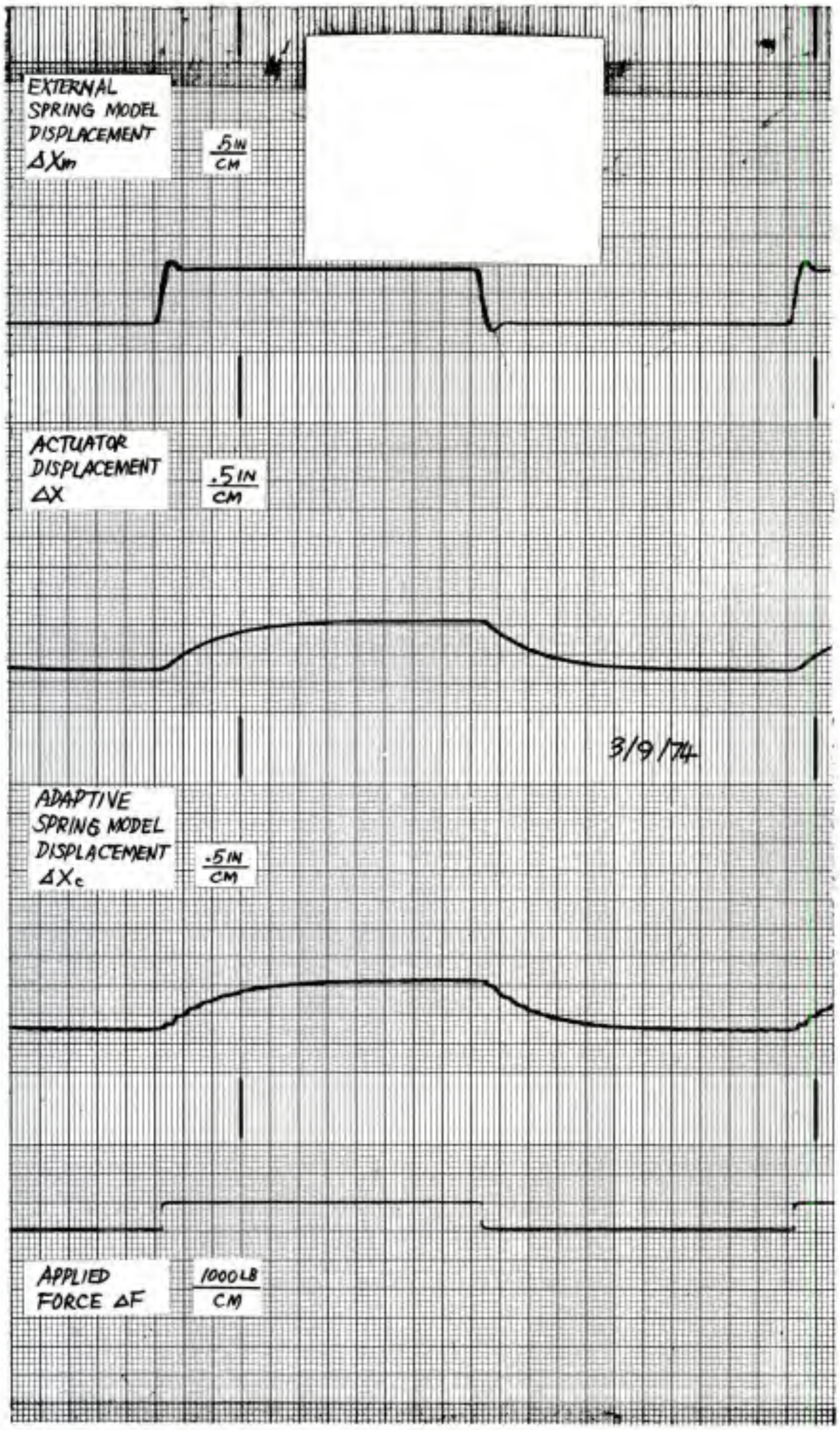

Figure 39. Position response of the simulated adaptive spring-rate control system with step force input; $K = 1000 \frac{lb}{in.}$, $\zeta = 0.5$

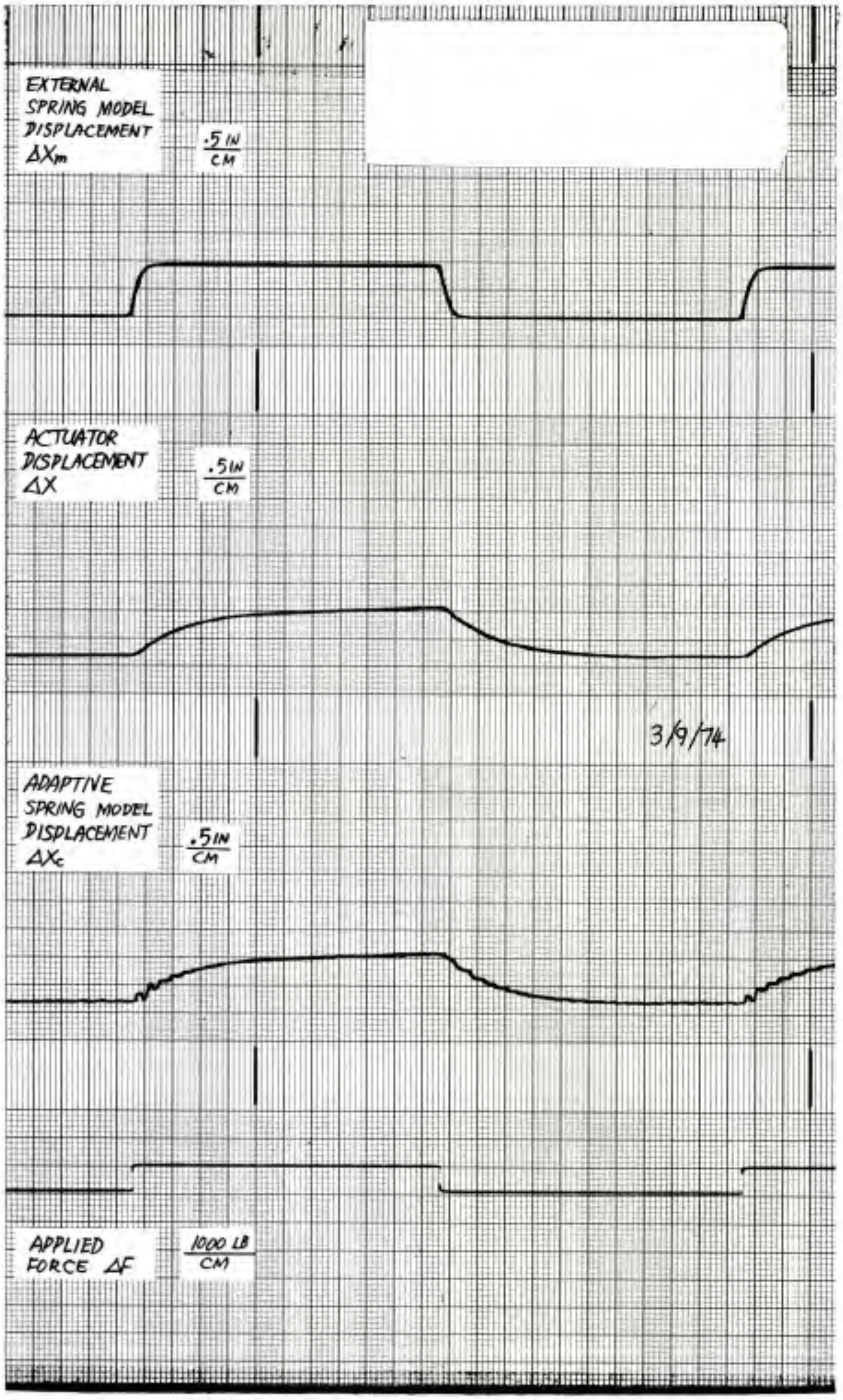

Figure 40. Position response of the simulated adaptive spring-rate control system with step force input; K = 1000 $\frac{lb}{in.}$, 1.0

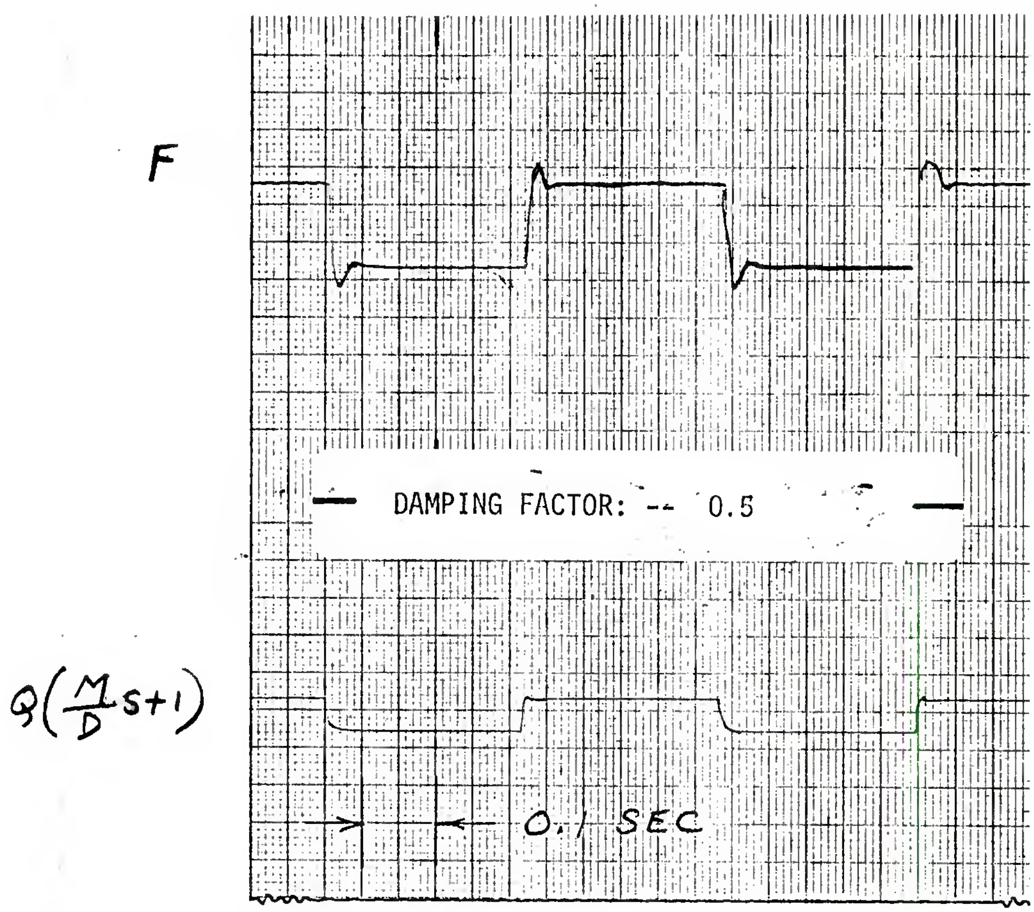

Figure 41. Theoretical force response of the actuator with 0.5 damping factor

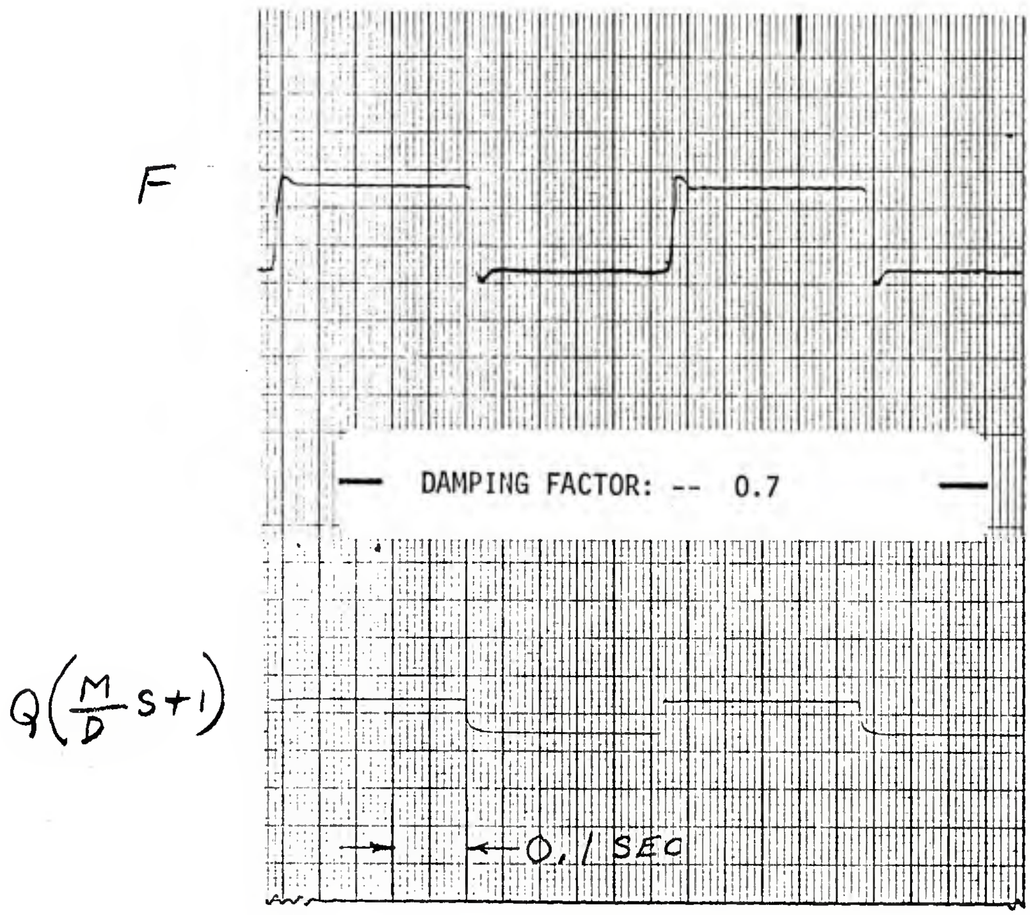

Figure 42. Theoretical force response of the actuator with 0.7 damping factor

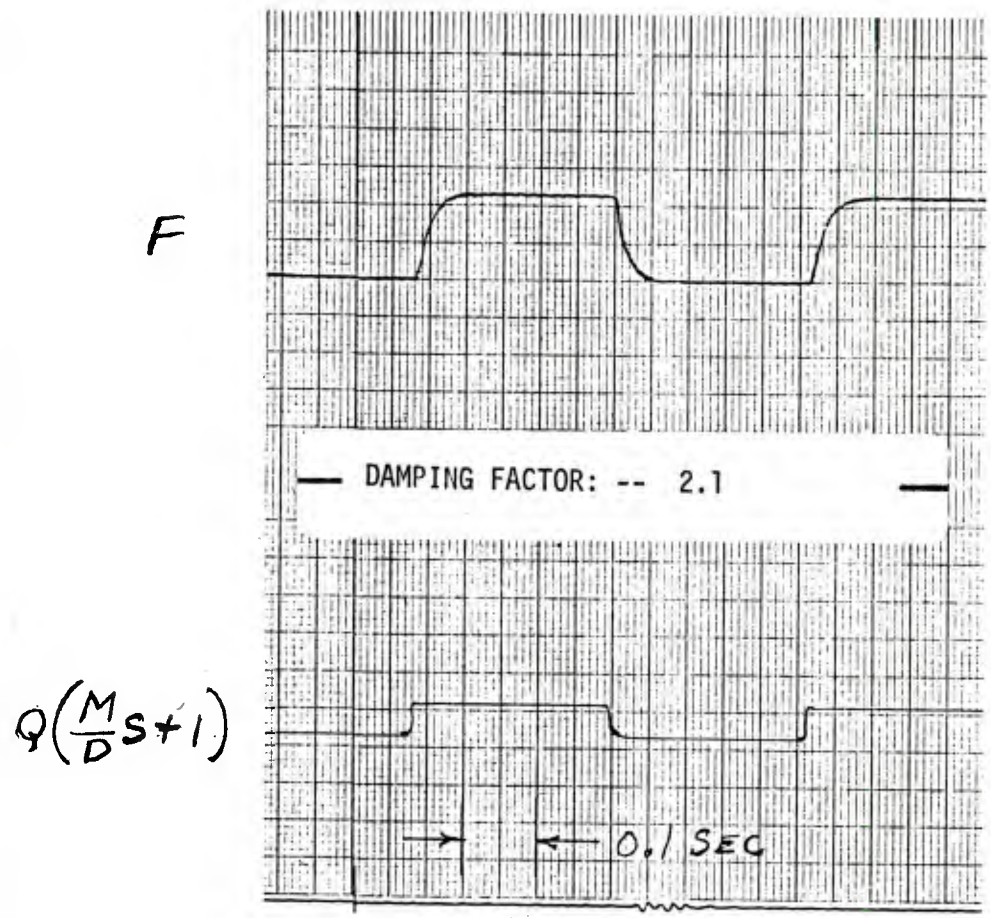

Figure 43. Theoretical force response of the actuator with 2.1 damping factor

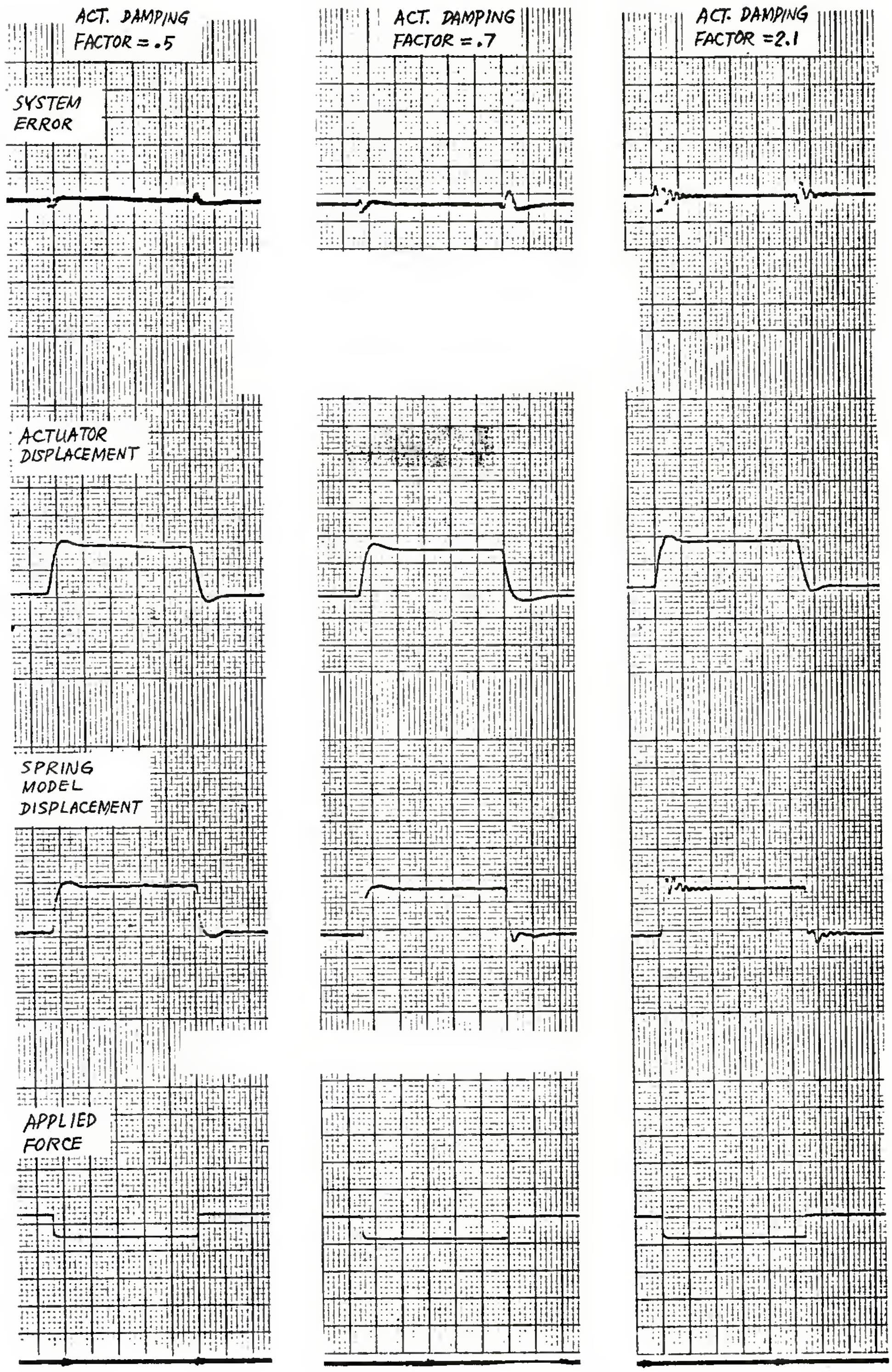

Figure 44. Effects of actuator damping coefficient on the position response of the simulated adaptive spring-rate control system with a step force input; $K = 130{,}000\ \frac{\text{lb}}{\text{in.}}$, $\zeta = 0.376$

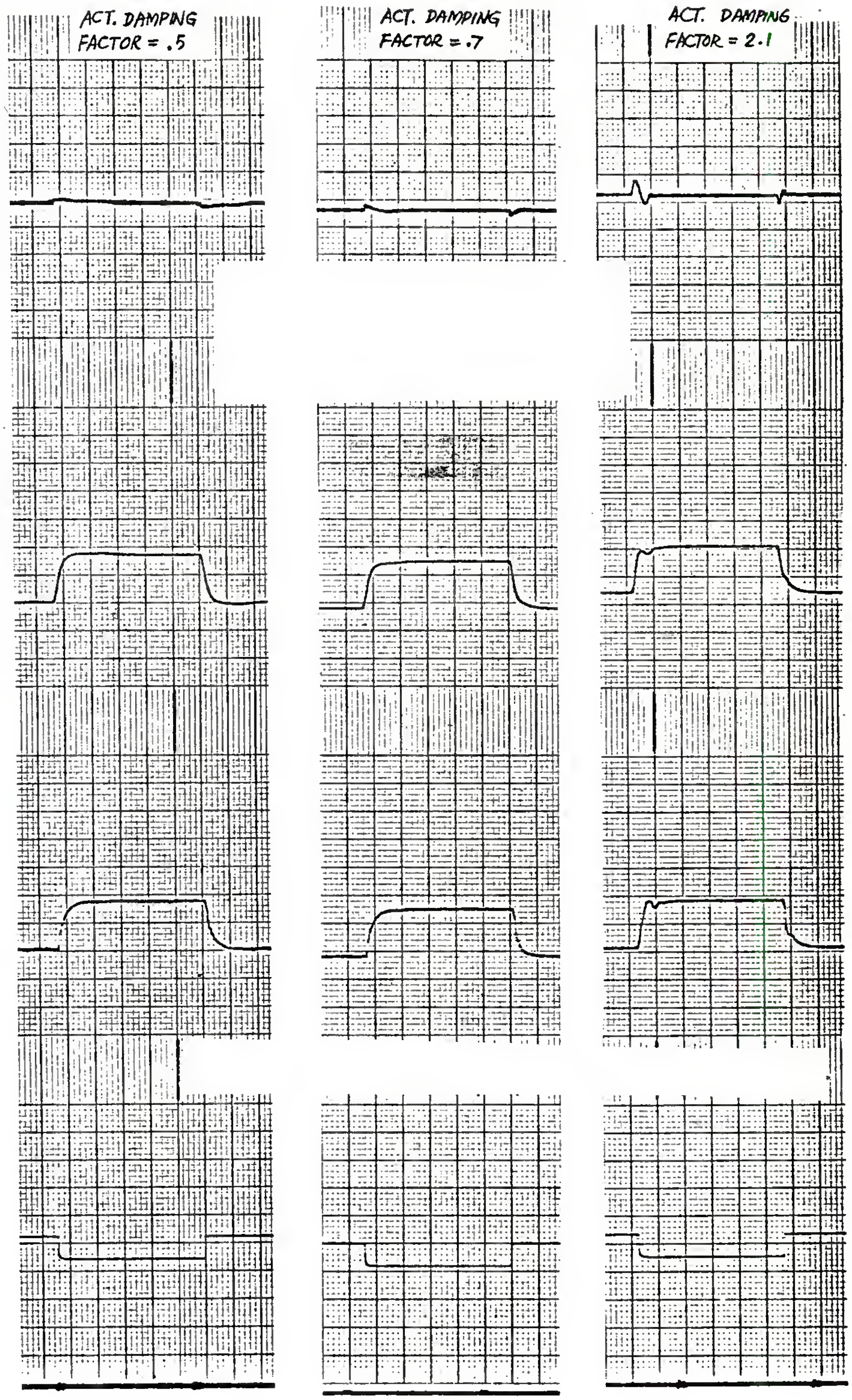

Figure 45. Effects of actuator damping coefficient on the position response of the simulated adaptive spring-rate control system with a step force input; K = 130,000 $\frac{\text{lb}}{\text{in.}}$, ζ = 1.24

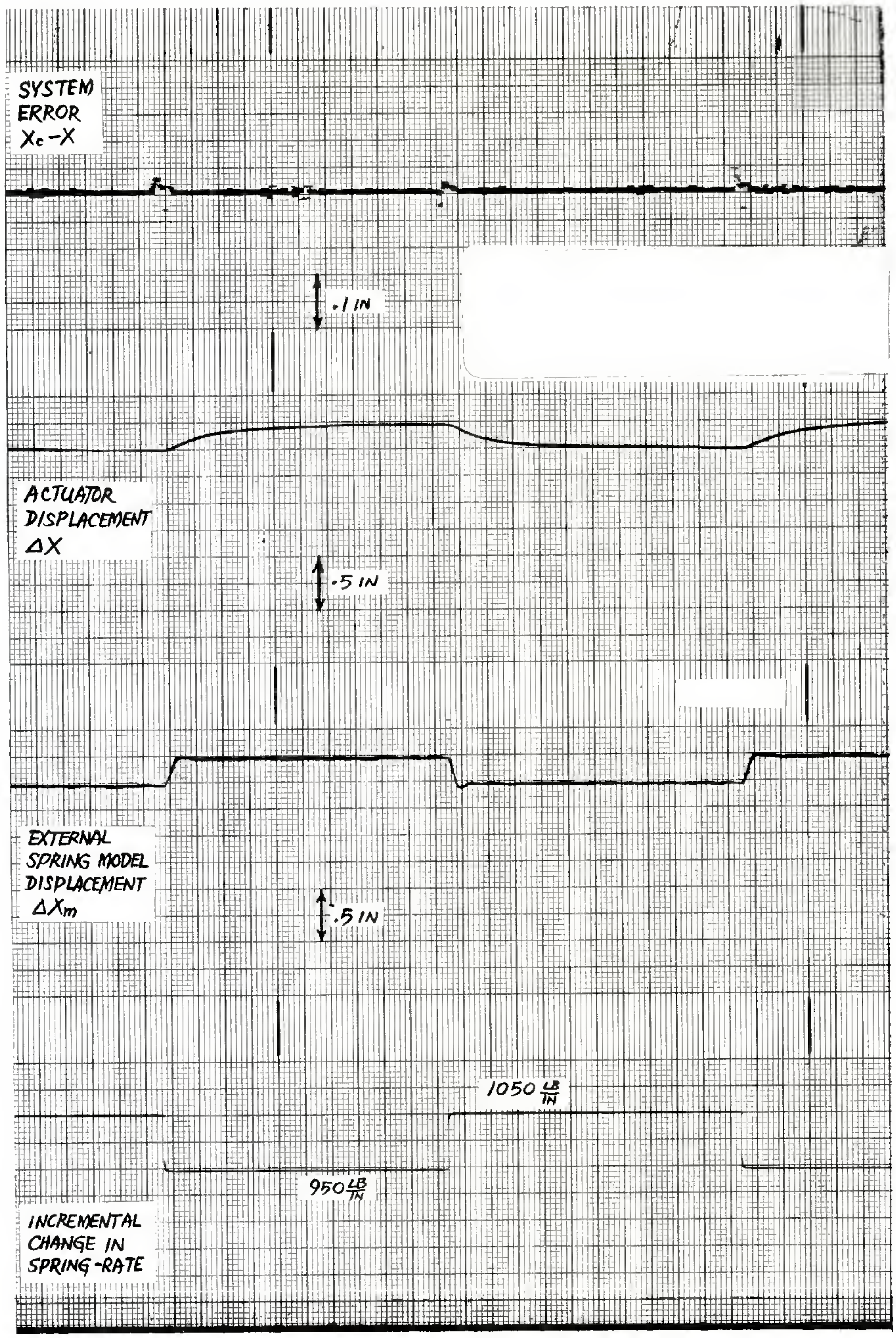

Figure 46. Analog computer simulation of the adaptive spring-rate control system with input = 1000 ± 50 $\frac{\text{lb}}{\text{in.}}$

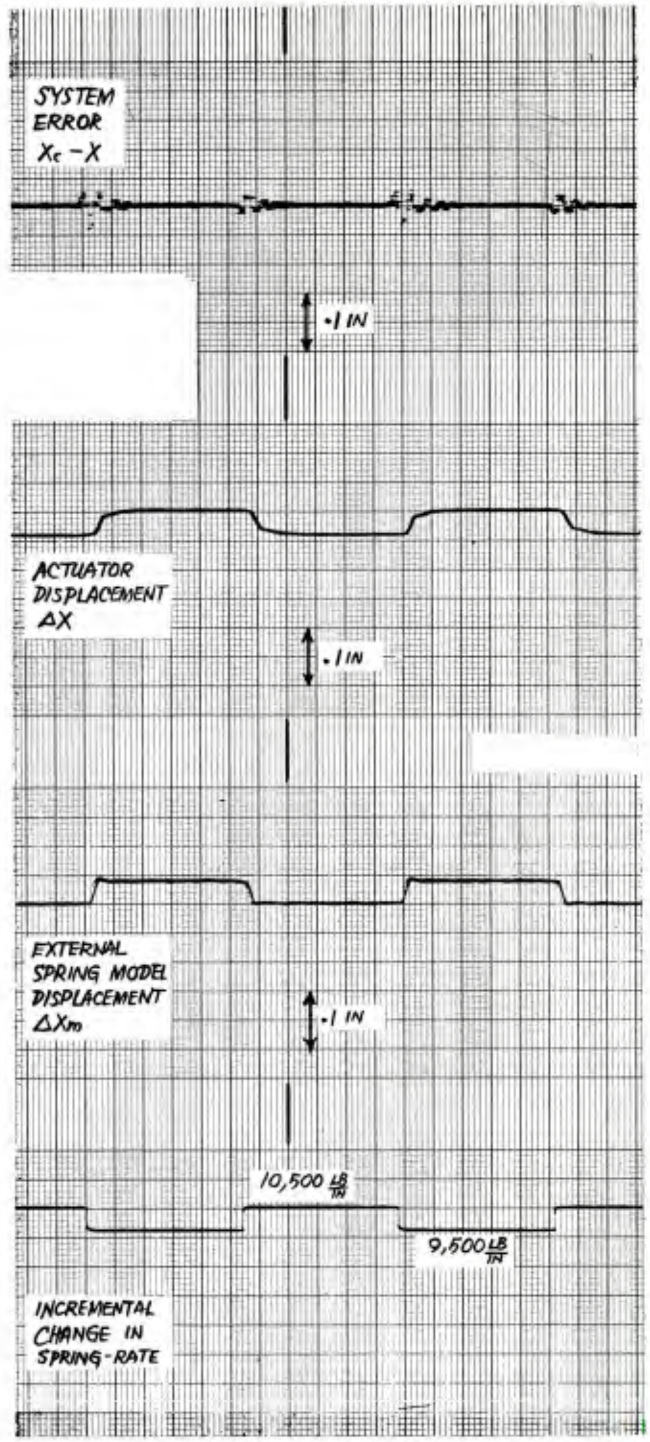

Figure 47. Analog computer simulation of the adaptive spring-rate control system with input = 10,000 ± 500 $\frac{\text{lb}}{\text{in.}}$

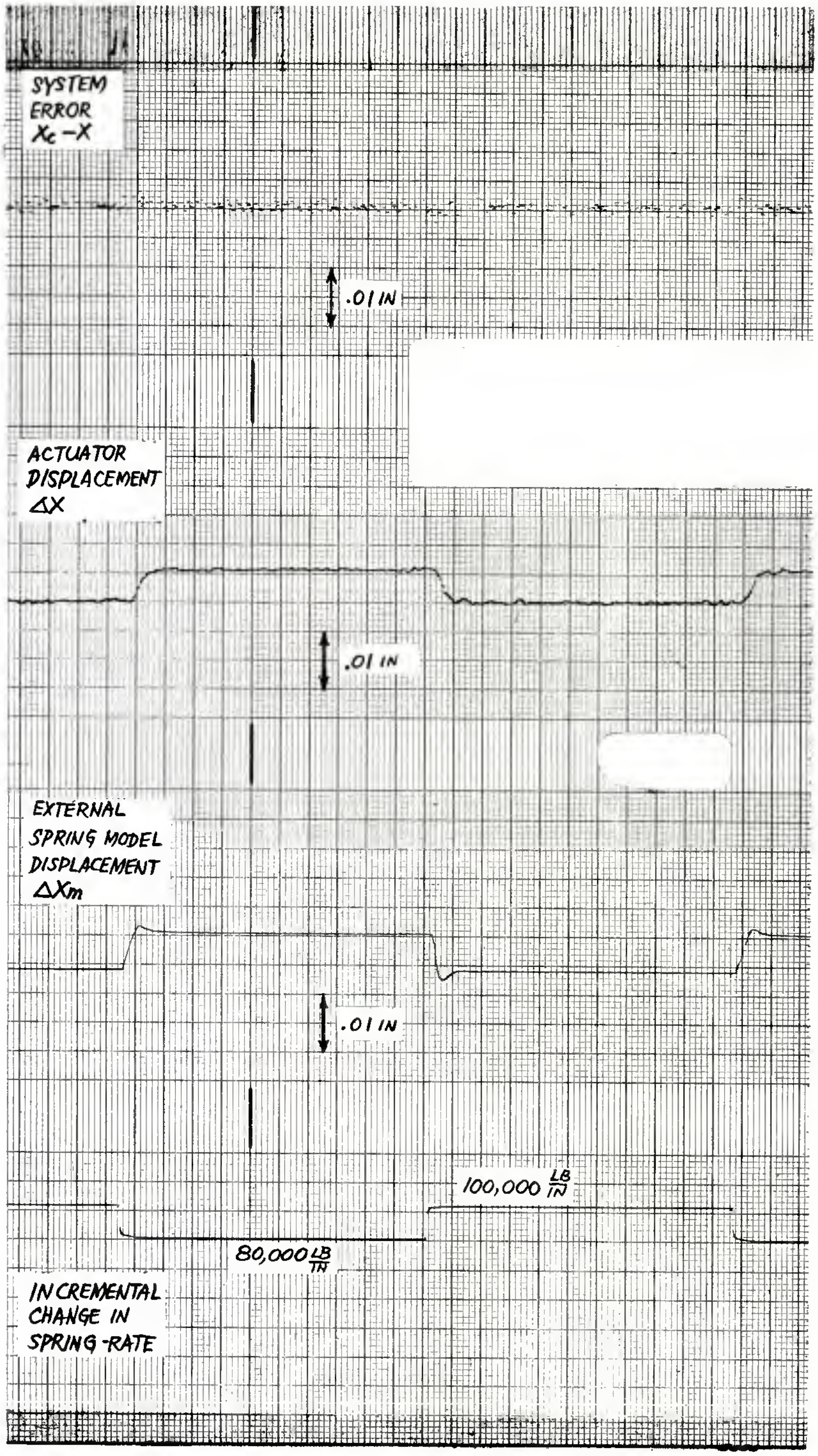

Figure 48. Analog computer simulation of the adaptive spring-rate control system with input = 90,000 ± 10,000 $\frac{lb}{in}$.

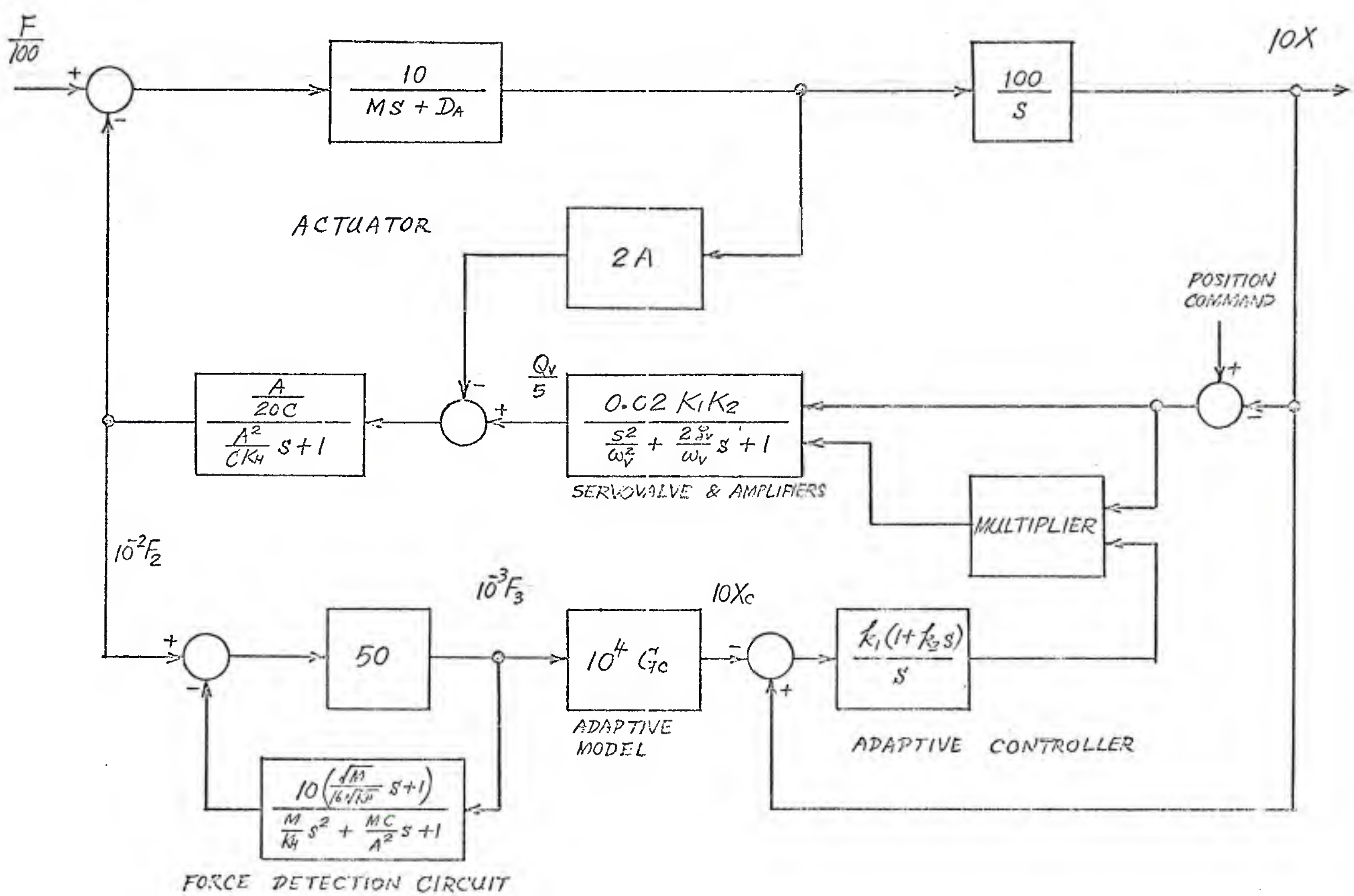

Figure 49. Revised system block diagram of the adaptive spring-rate control system

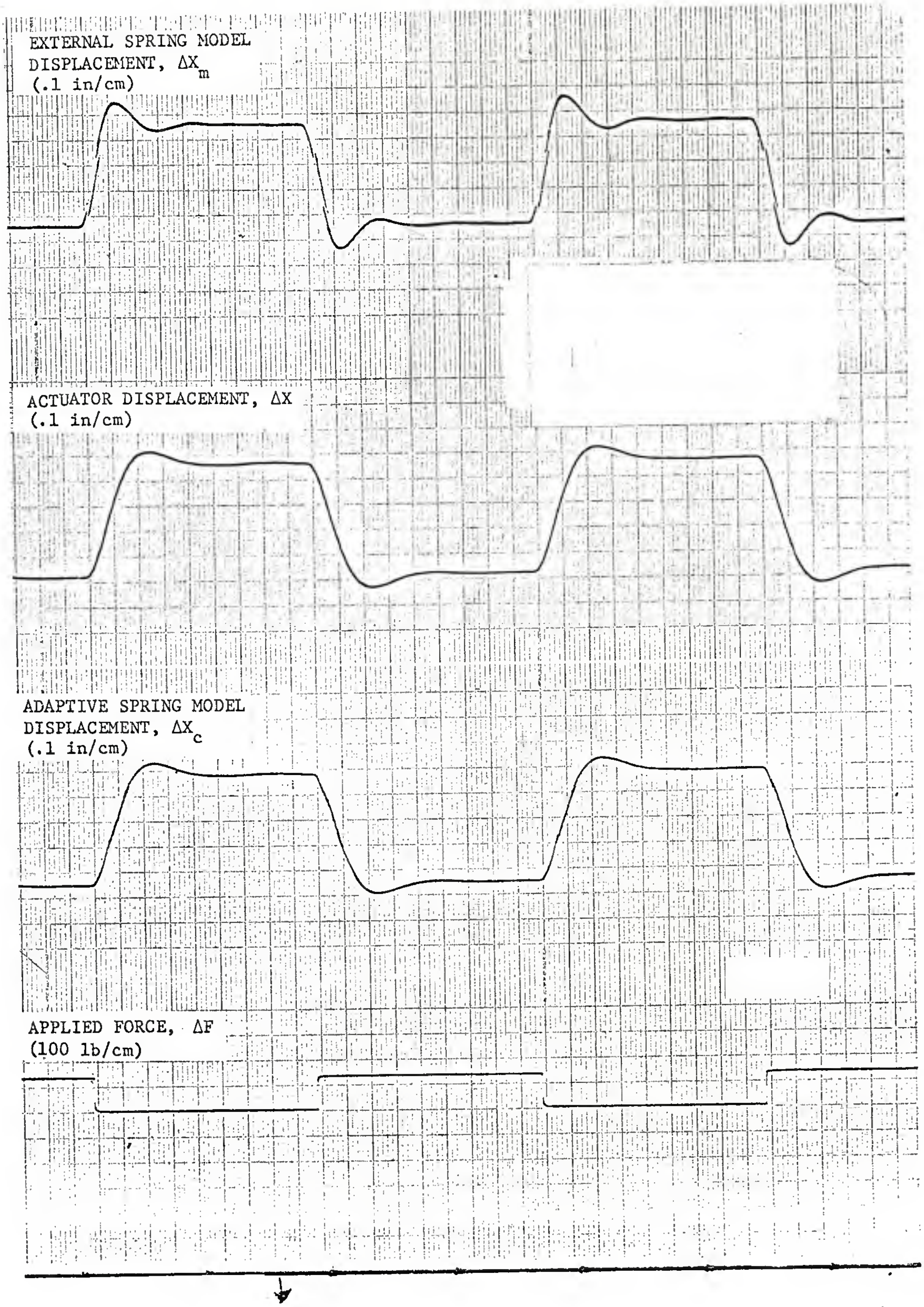

Figure 50. Position response of the adaptive spring-rate control system with step force input; $K = 300 \frac{lb}{in.}$, $\zeta = 0.468$

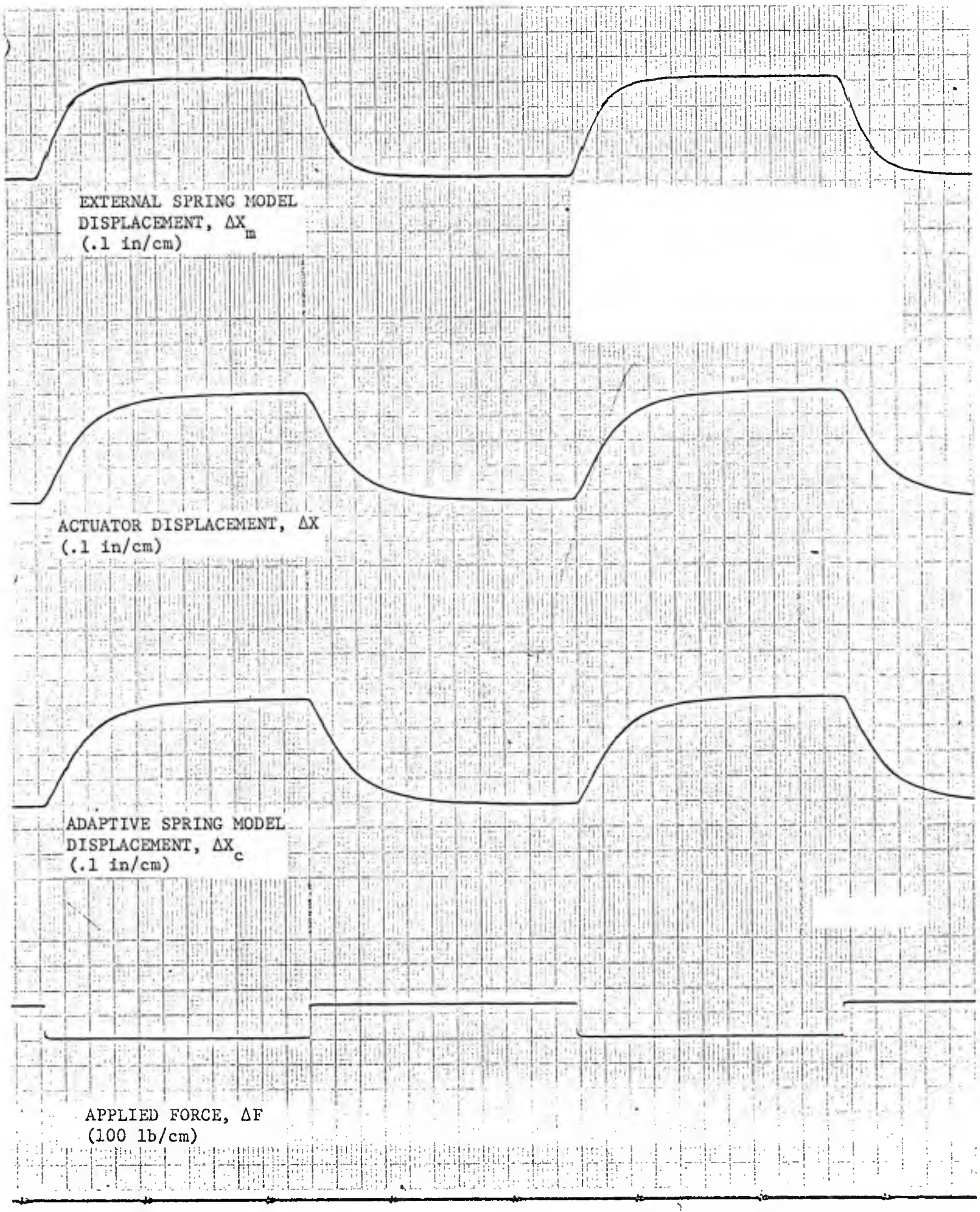

Figure 51. Position response of the adaptive spring-rate control system with step force input; $K = 300 \frac{\text{lb}}{\text{in.}}$, $\zeta = 1.4$

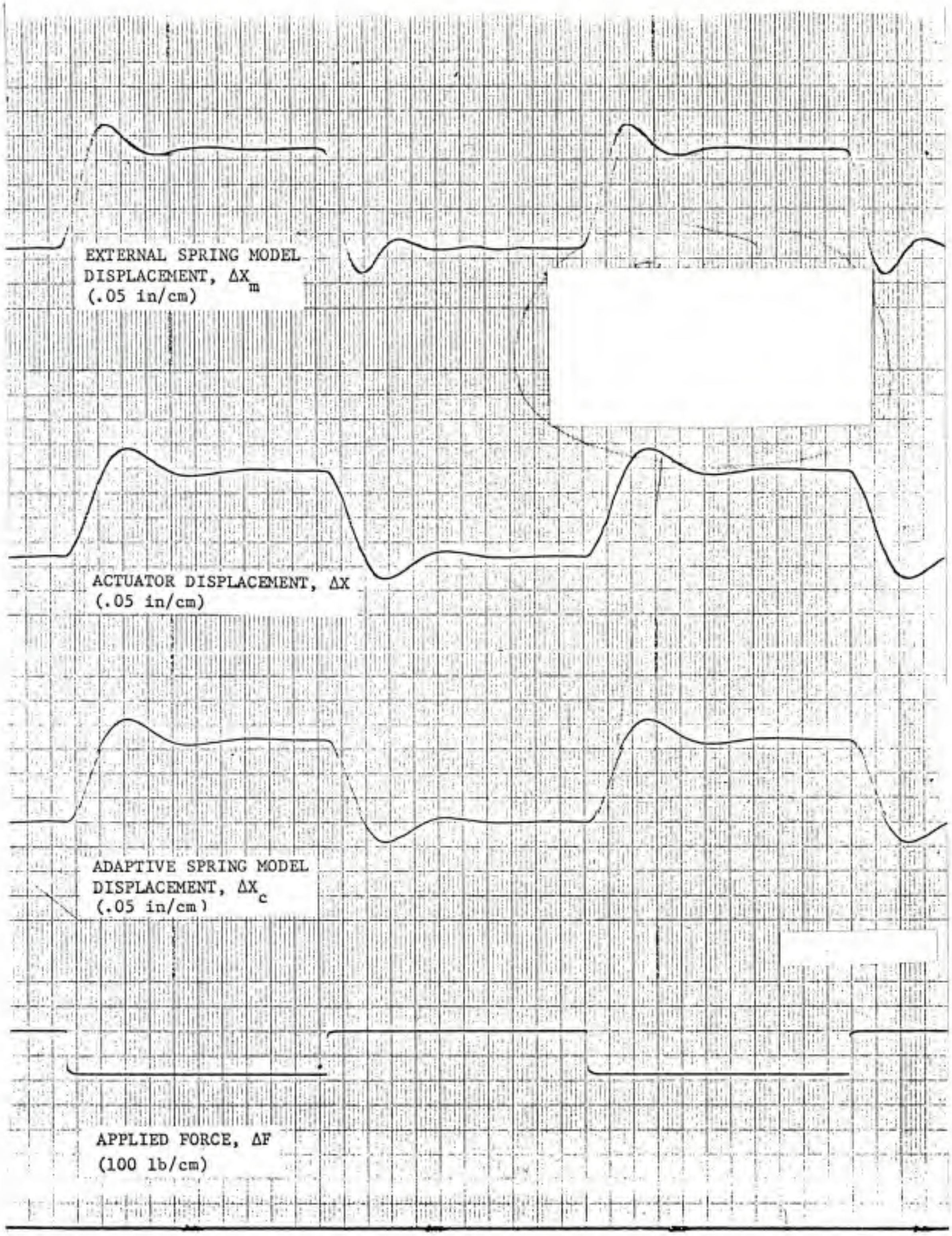

Figure 52. Position response of the adaptive spring-rate control system with step force input; $K = 1000 \frac{\text{lb}}{\text{in.}}$, $\zeta = 0.384$

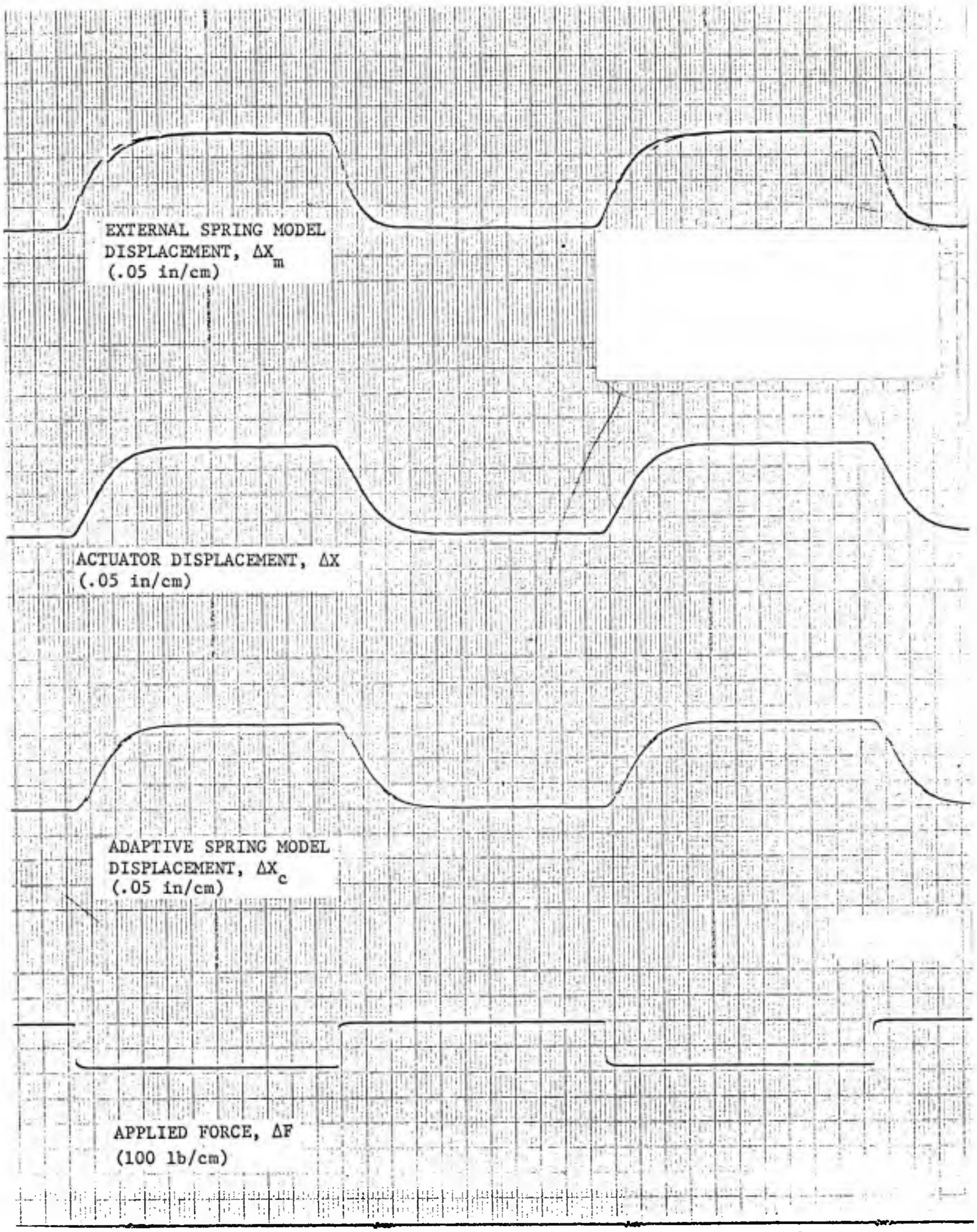

Figure 53. Position response of the adaptive spring-rate control system with step force input; $K = 1000 \frac{\text{lb}}{\text{in.}}$, $\zeta = 1.0$

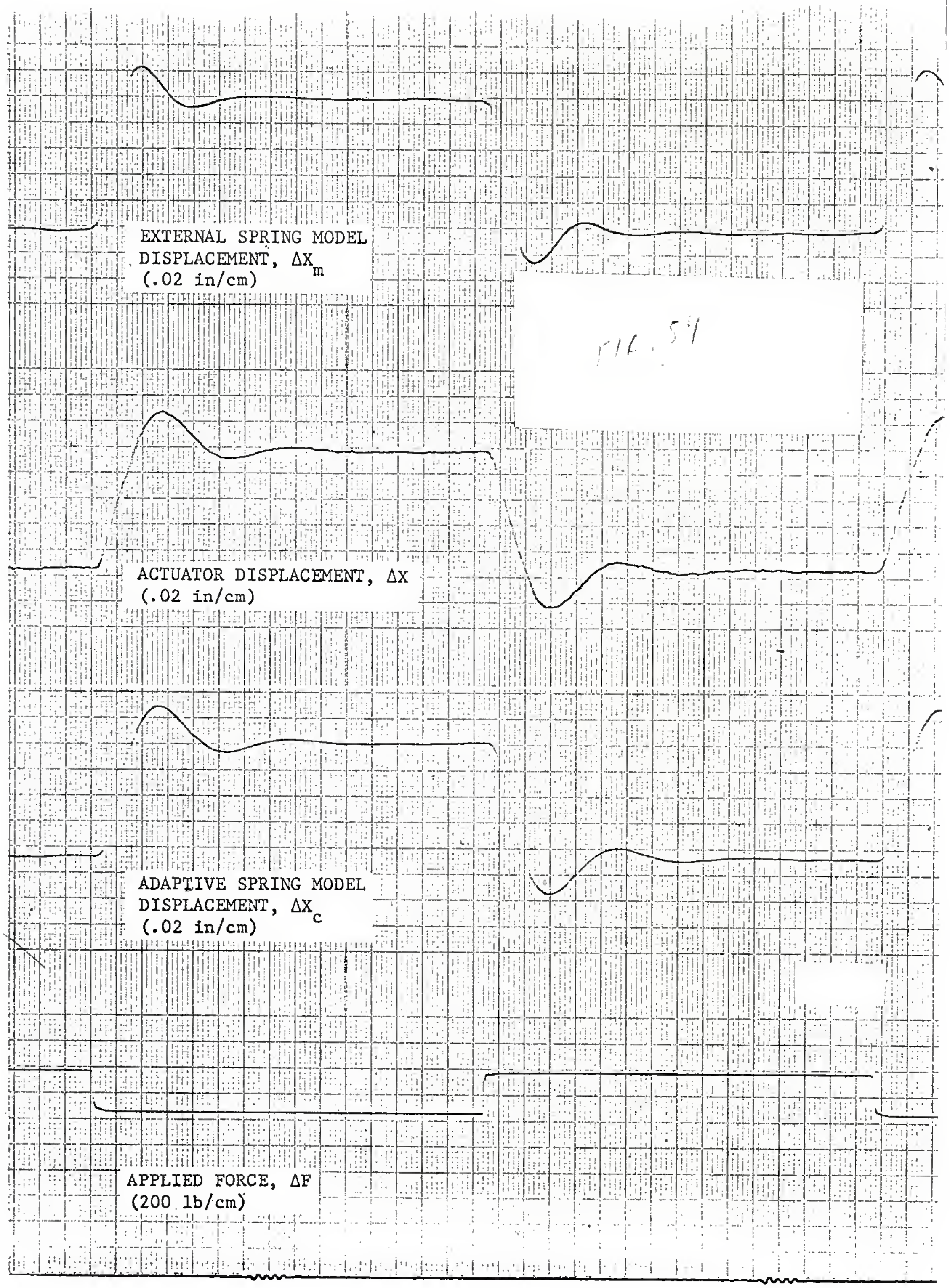

Figure 54. Position response of the adaptive spring-rate control system with step force input; $K = 3000 \frac{\text{lb}}{\text{in.}}$, $\zeta = 0.444$

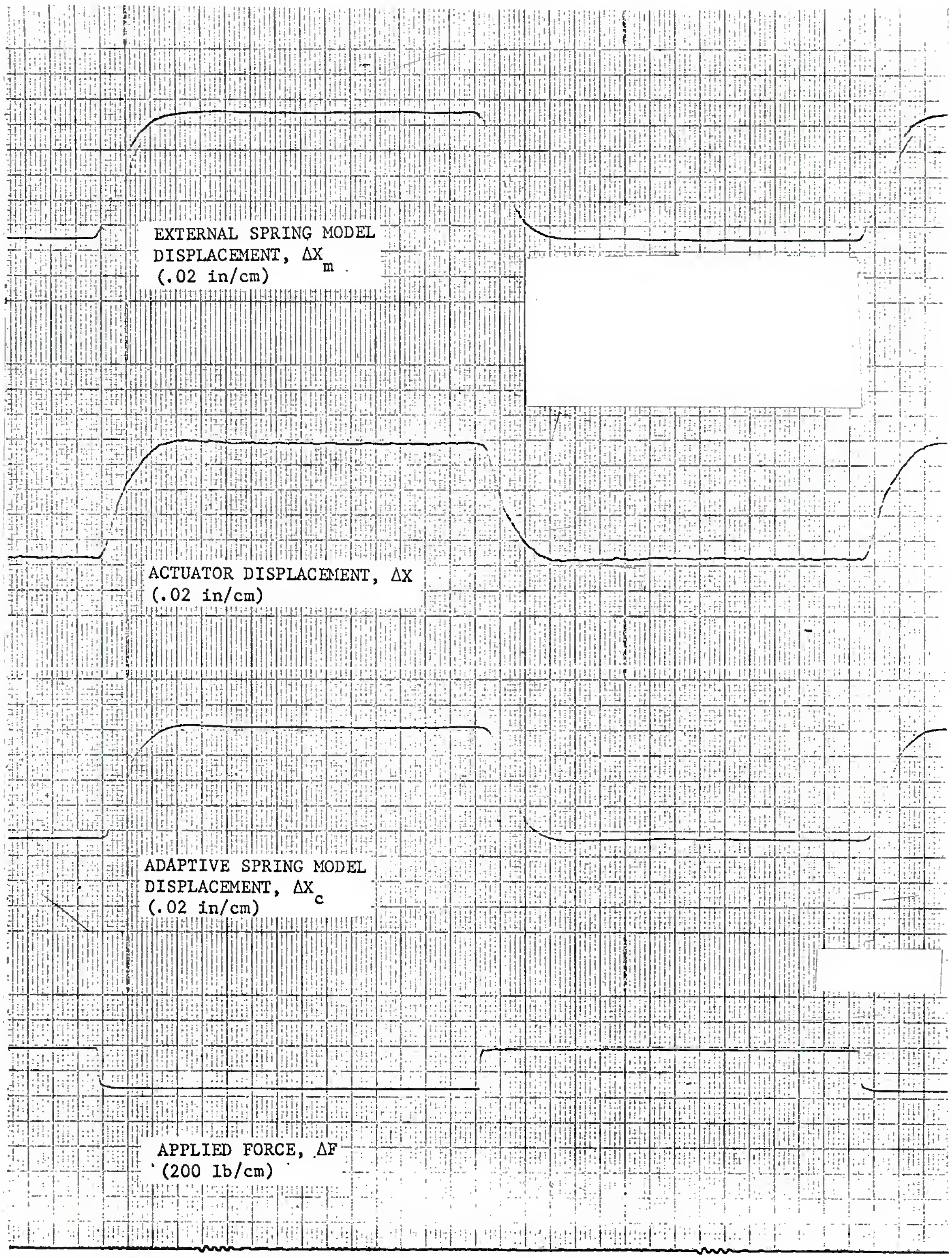

Figure 55. Position response of the adaptive spring-rate control system with step force input; $K = 3000 \frac{\text{lb}}{\text{in.}}$, $\zeta = 1.0$

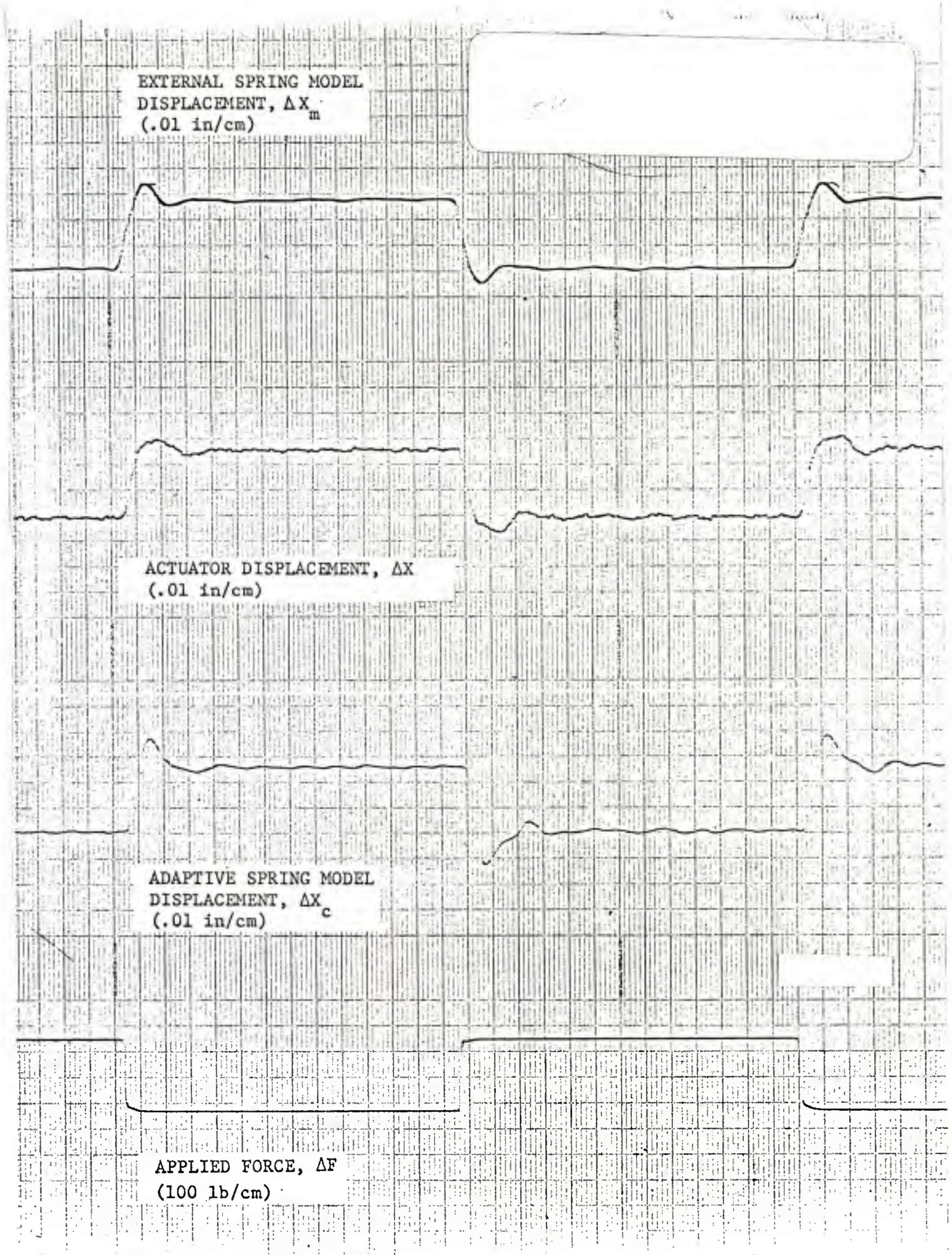

Figure 56. Position response of the adaptive spring-rate control system with step force input; $K = 10{,}000 \ \frac{\text{lb}}{\text{in.}}$, $\zeta = 0.487$

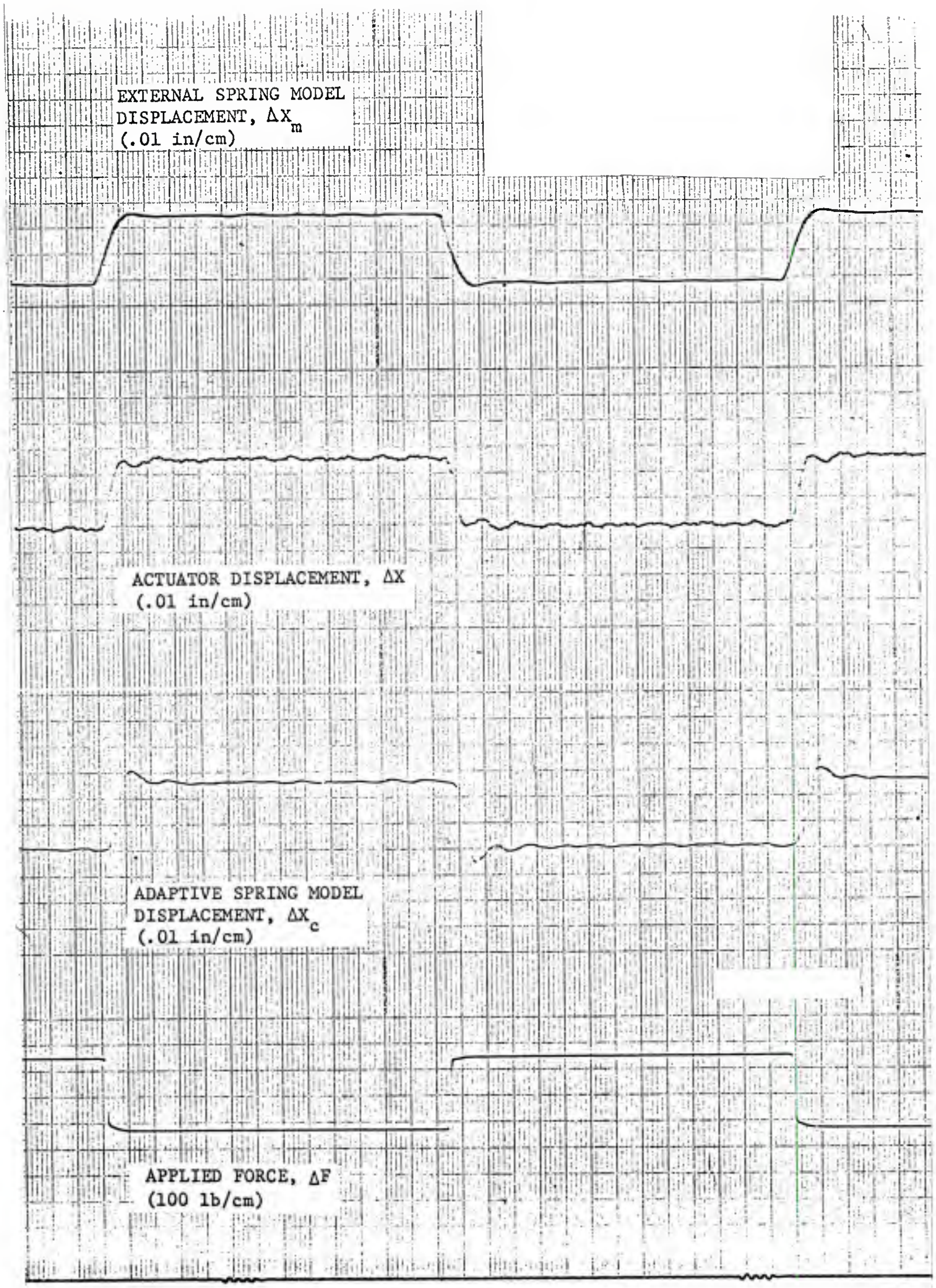

Figure 57. Position response of the adaptive spring-rate control system with step force input; $K = 10{,}000 \frac{\text{lb}}{\text{in.}}$, $\zeta = 0.81$

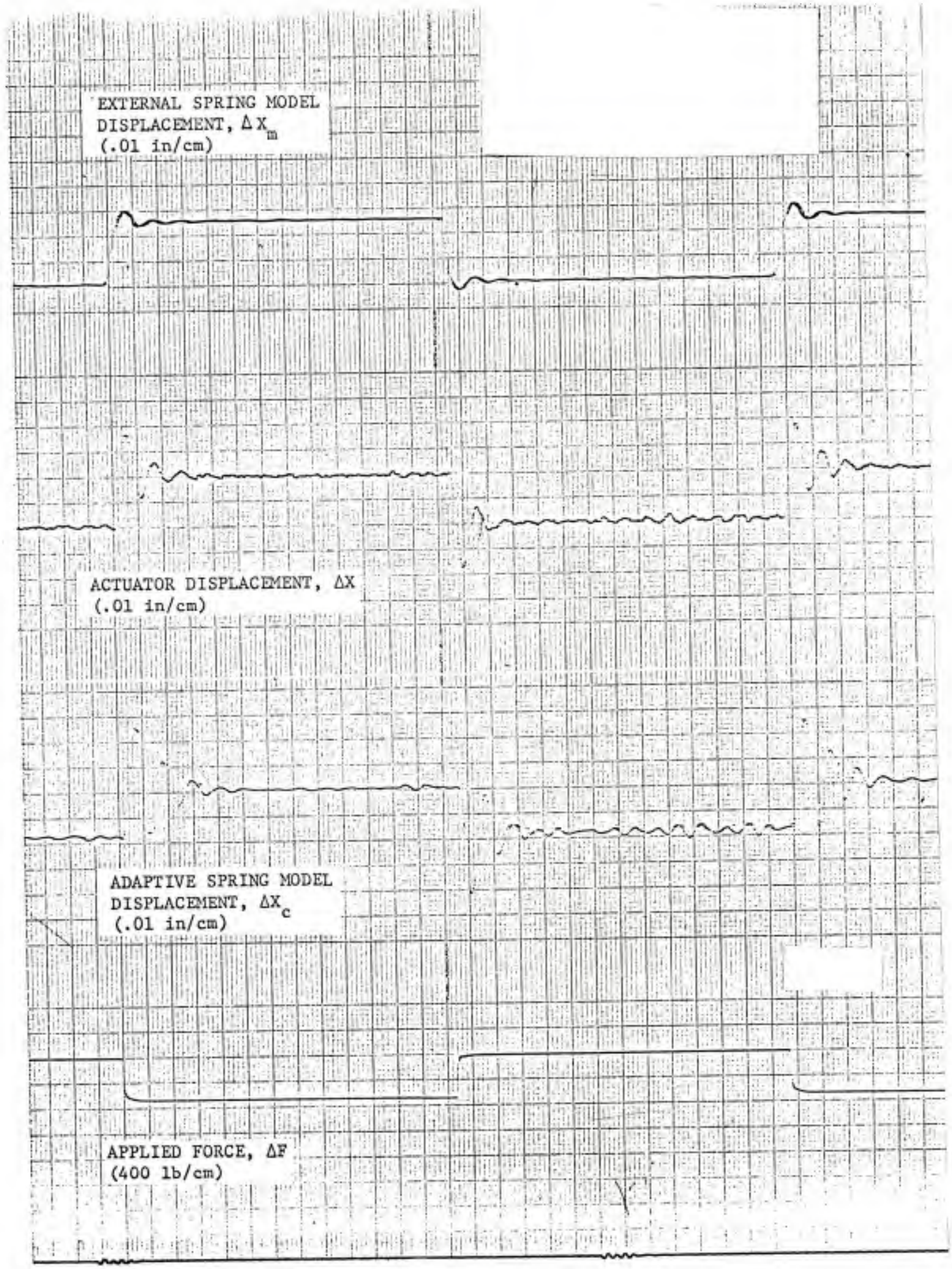

Figure 58. Position response of the adaptive spring-rate control system with step force input; $K = 30{,}000 \frac{\text{lb}}{\text{in.}}$, $\zeta = 0.468$

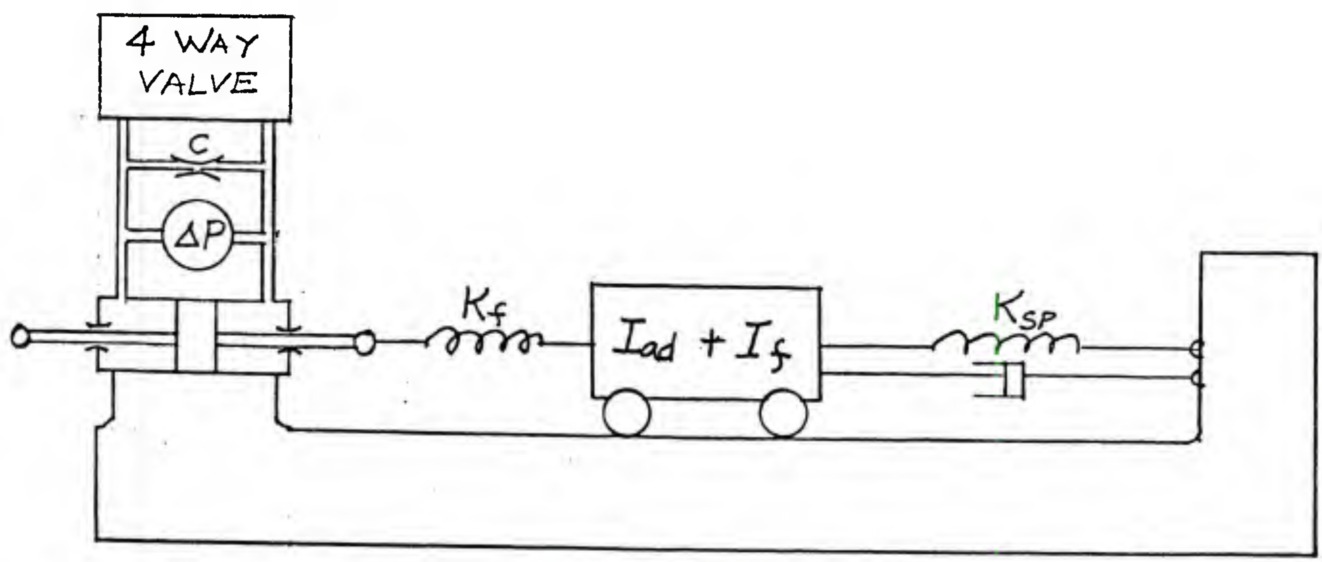

Figure 59. Physical concept tail-boom control system

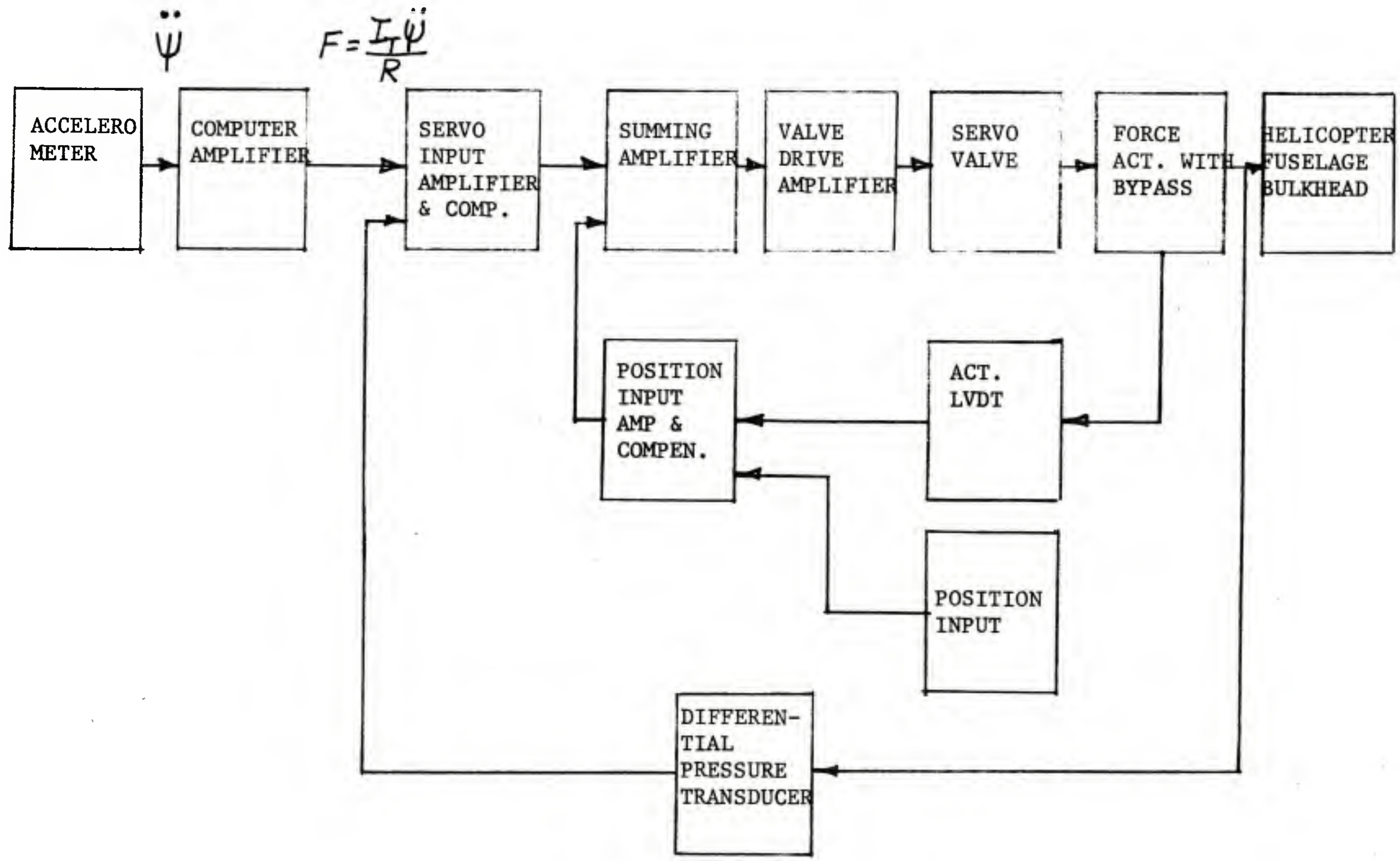

Figure 60. Tail-boom control system block diagram

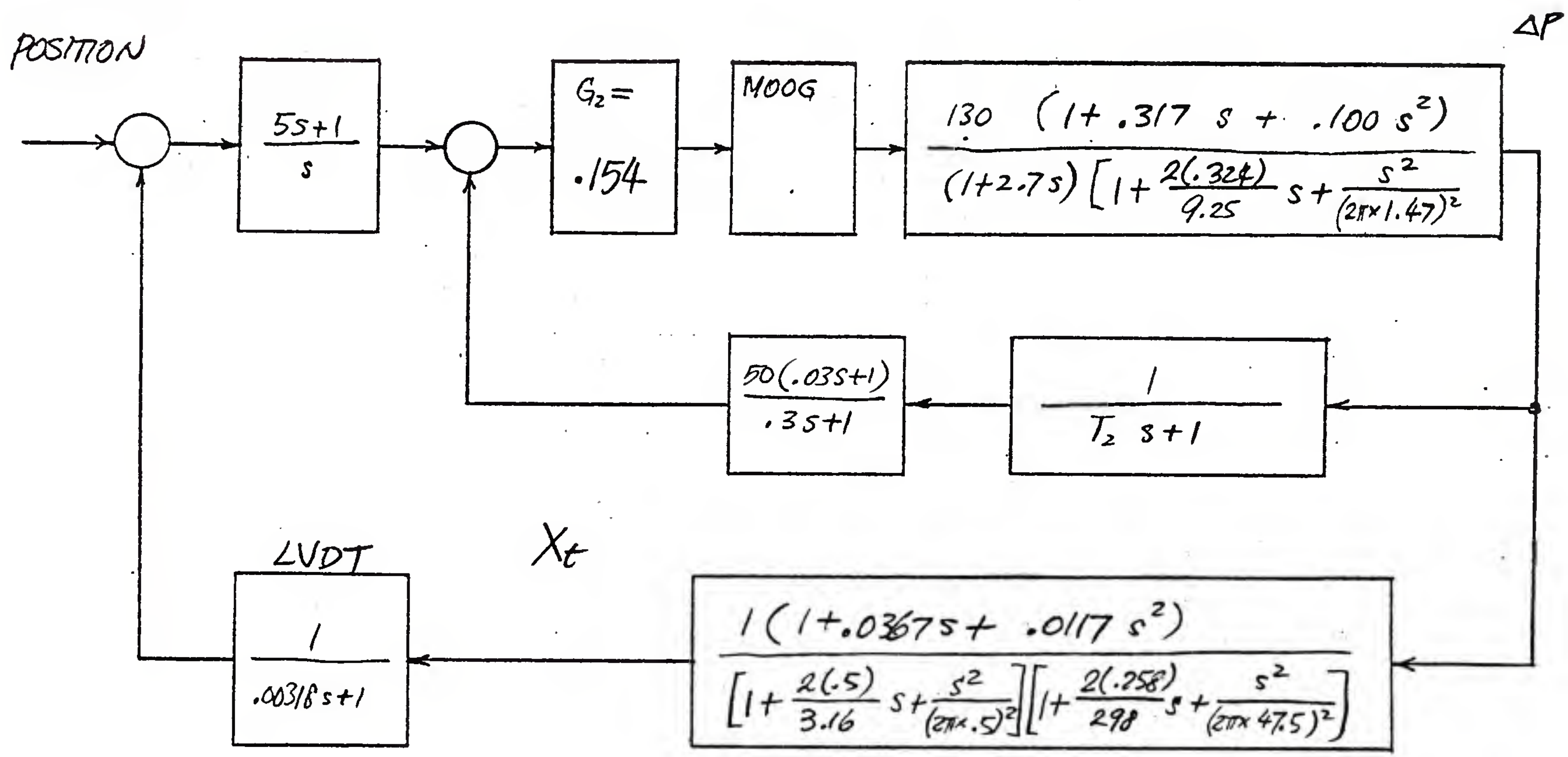

Figure 61. Block diagram for position servo tail-boom control

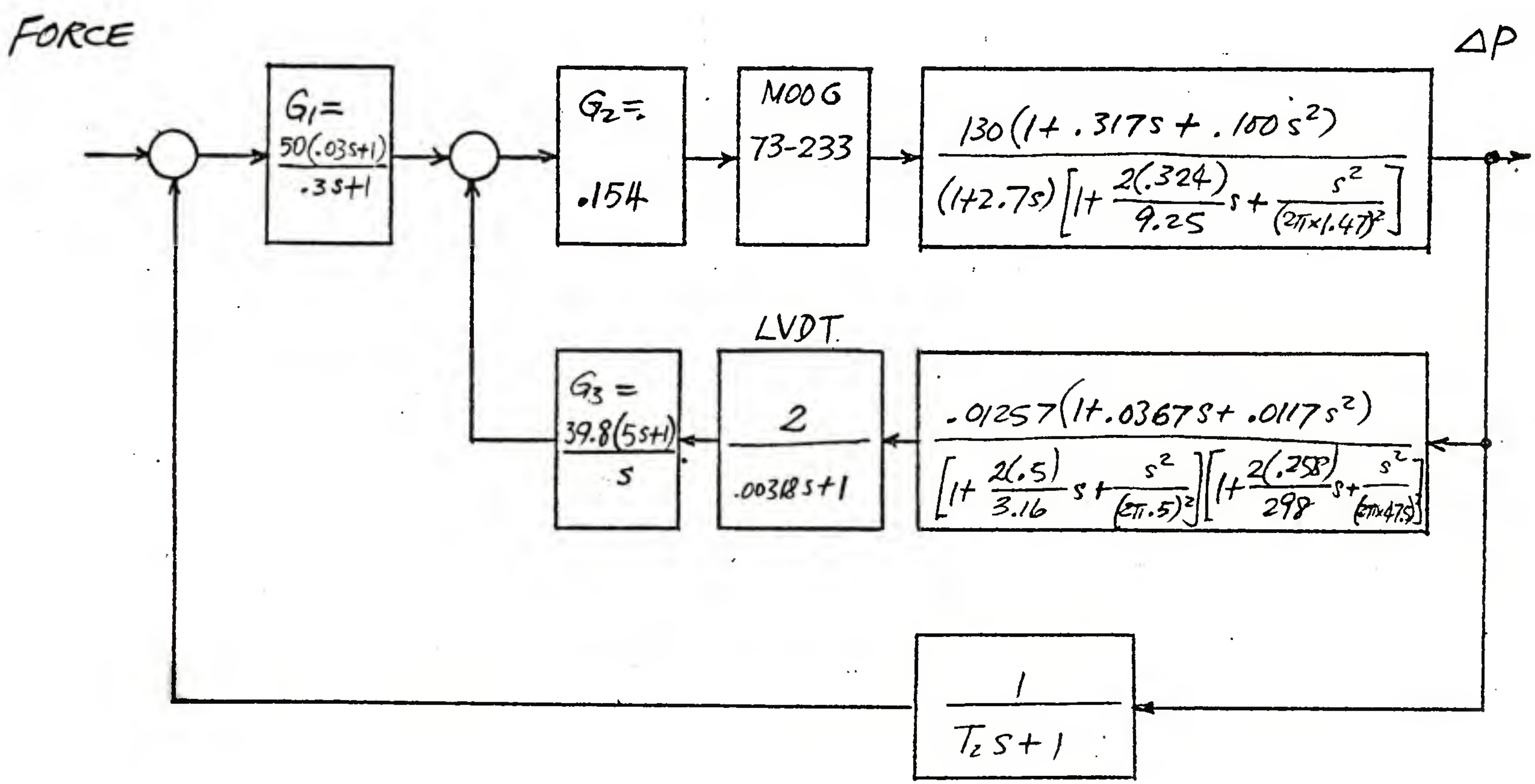

Figure 62. Block diagram for force servo tail-boom control

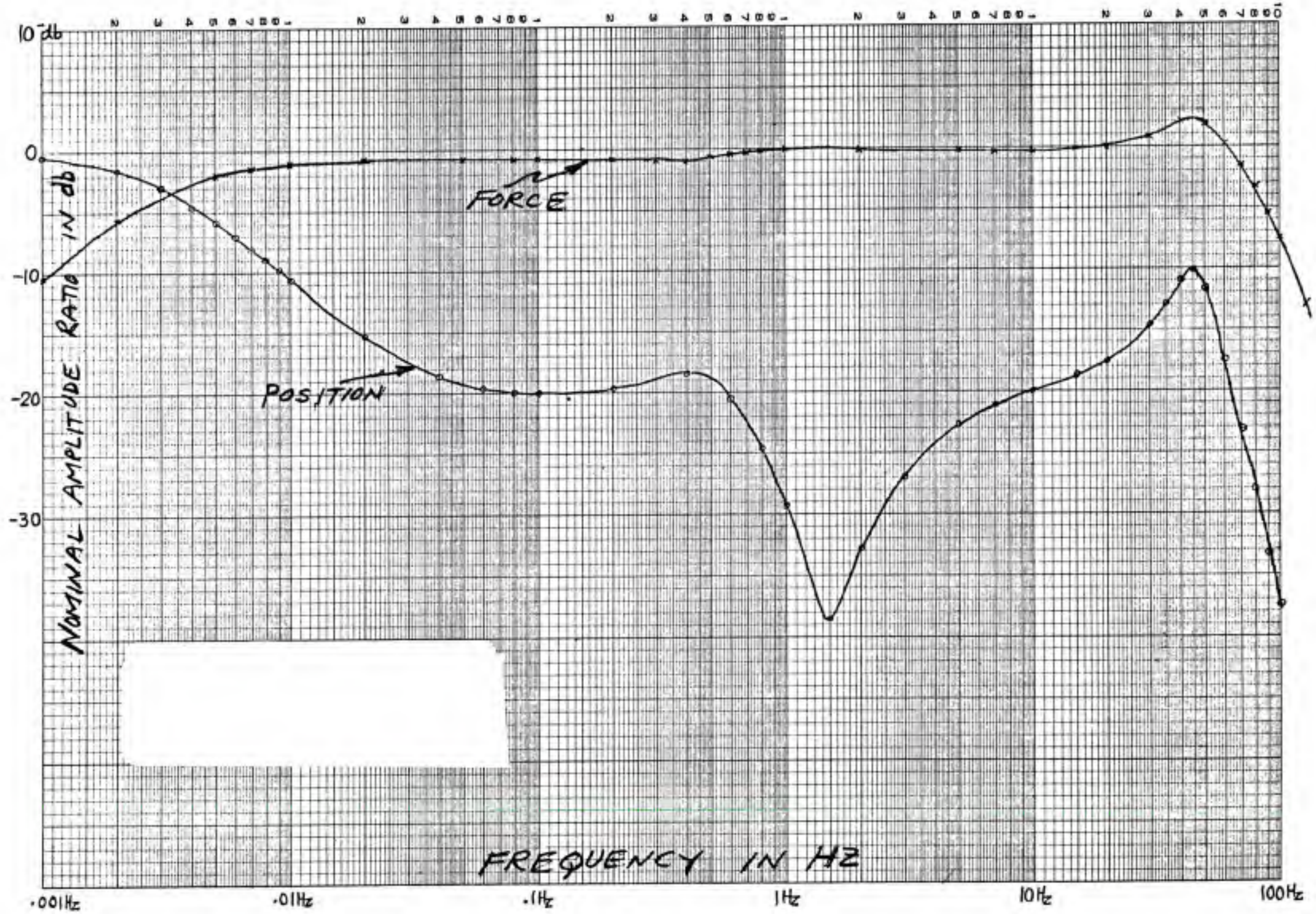

Figure 63. Tail-boom control frequency response of force and position

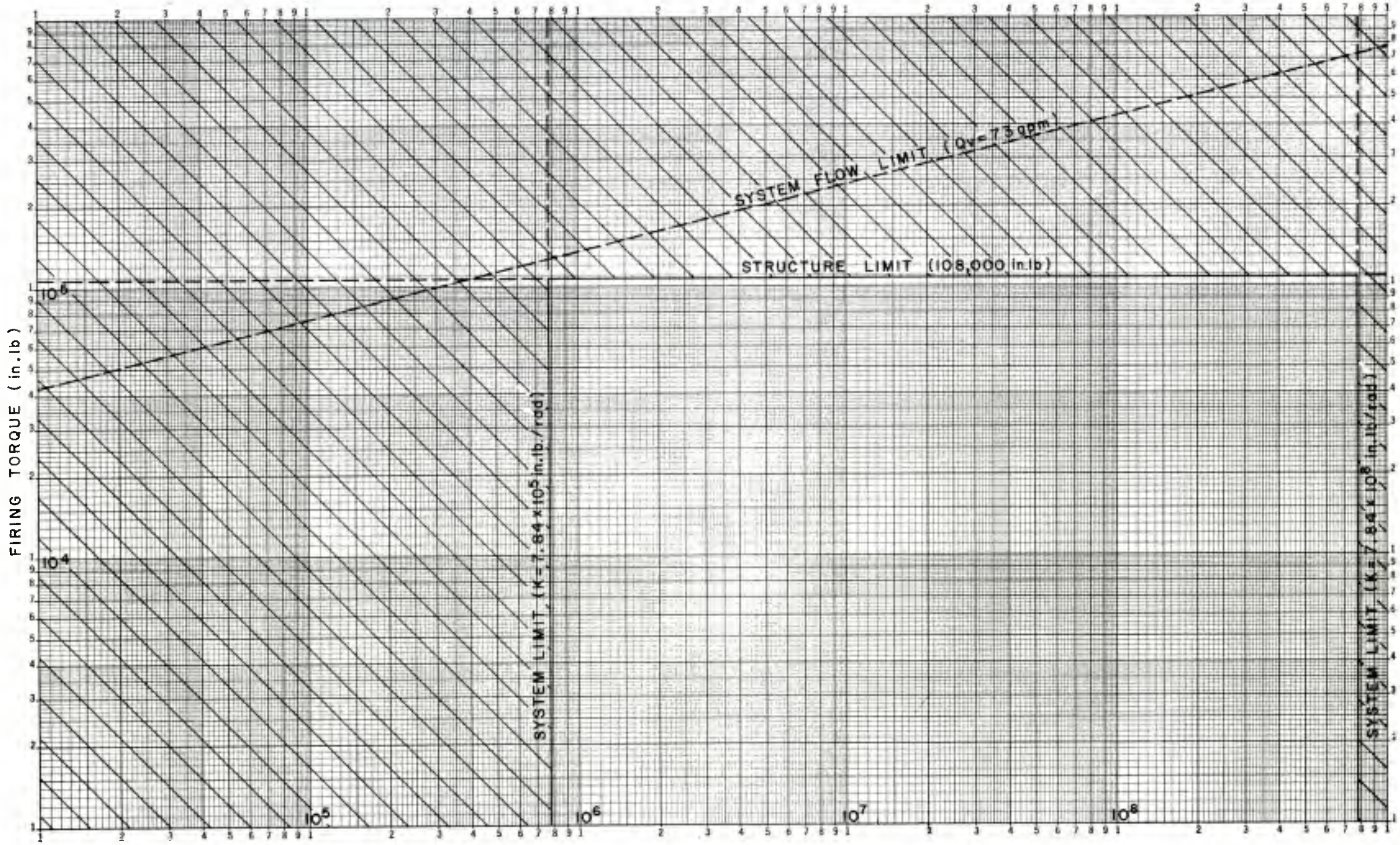

Figure 64. Combat vehicle pitch spring rate (in. lb/rad)

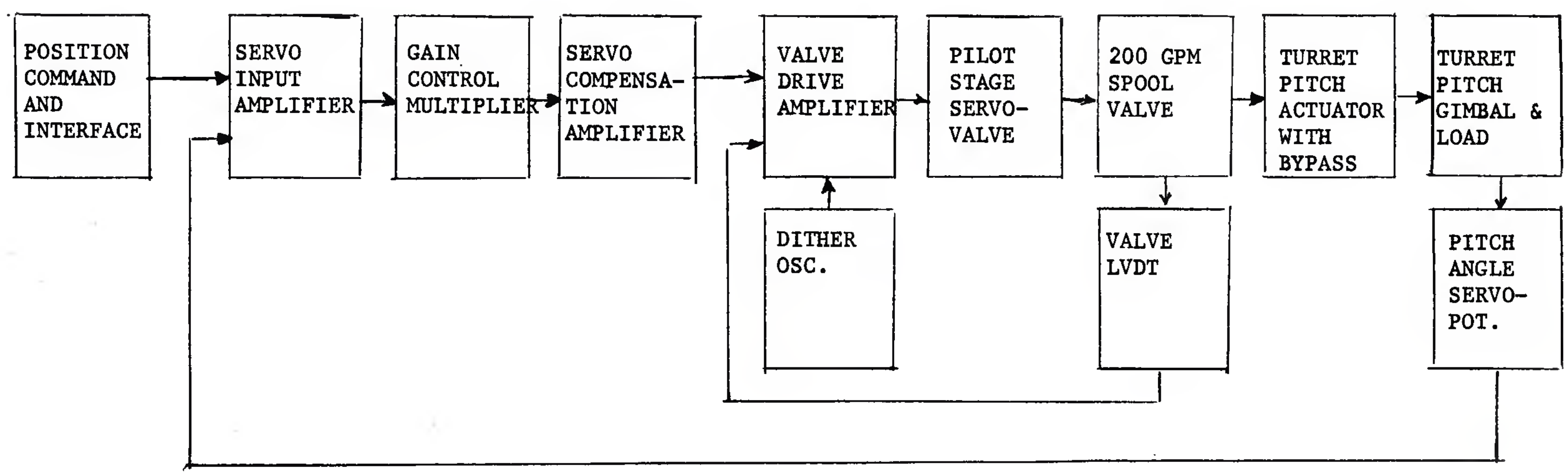

Figure 65. Turret pitch actuator position servo system block diagram

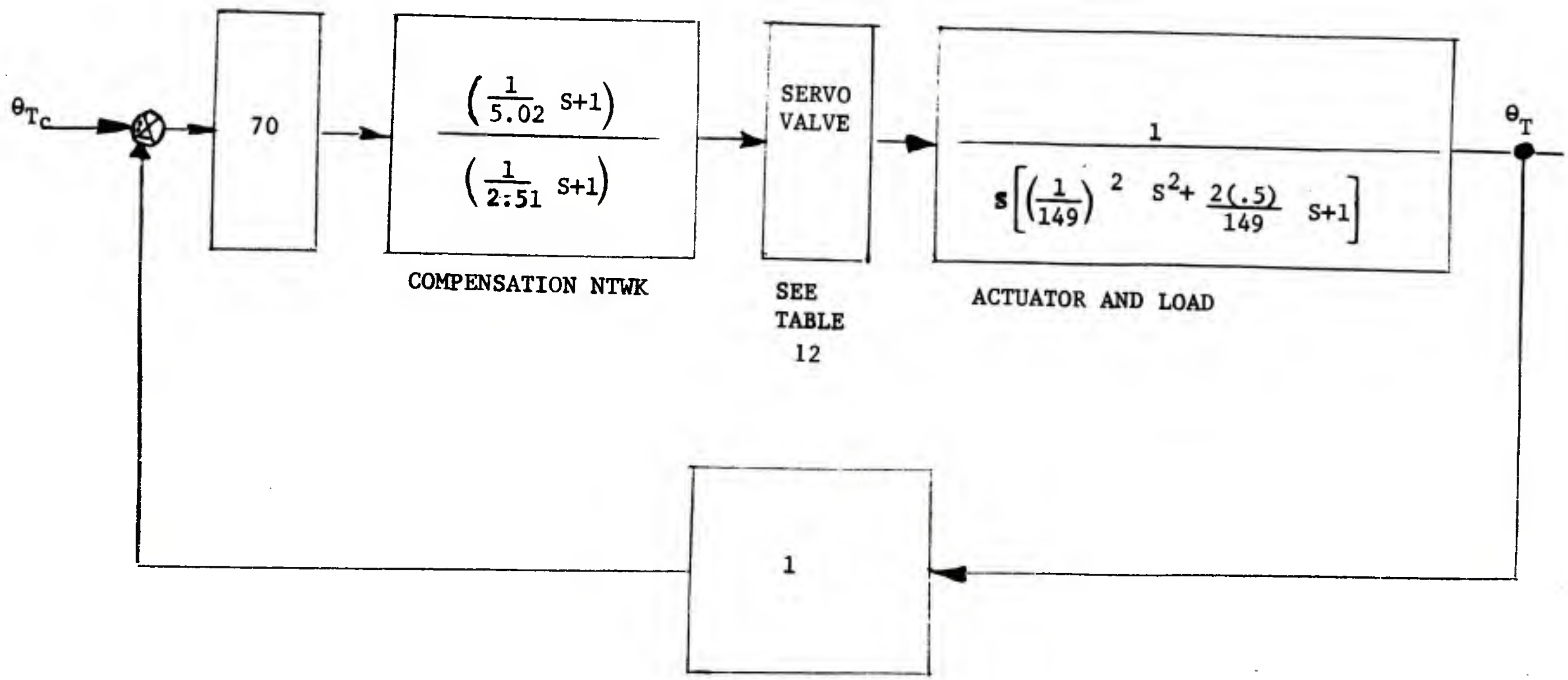

Figure 66. Turret pitch position control system

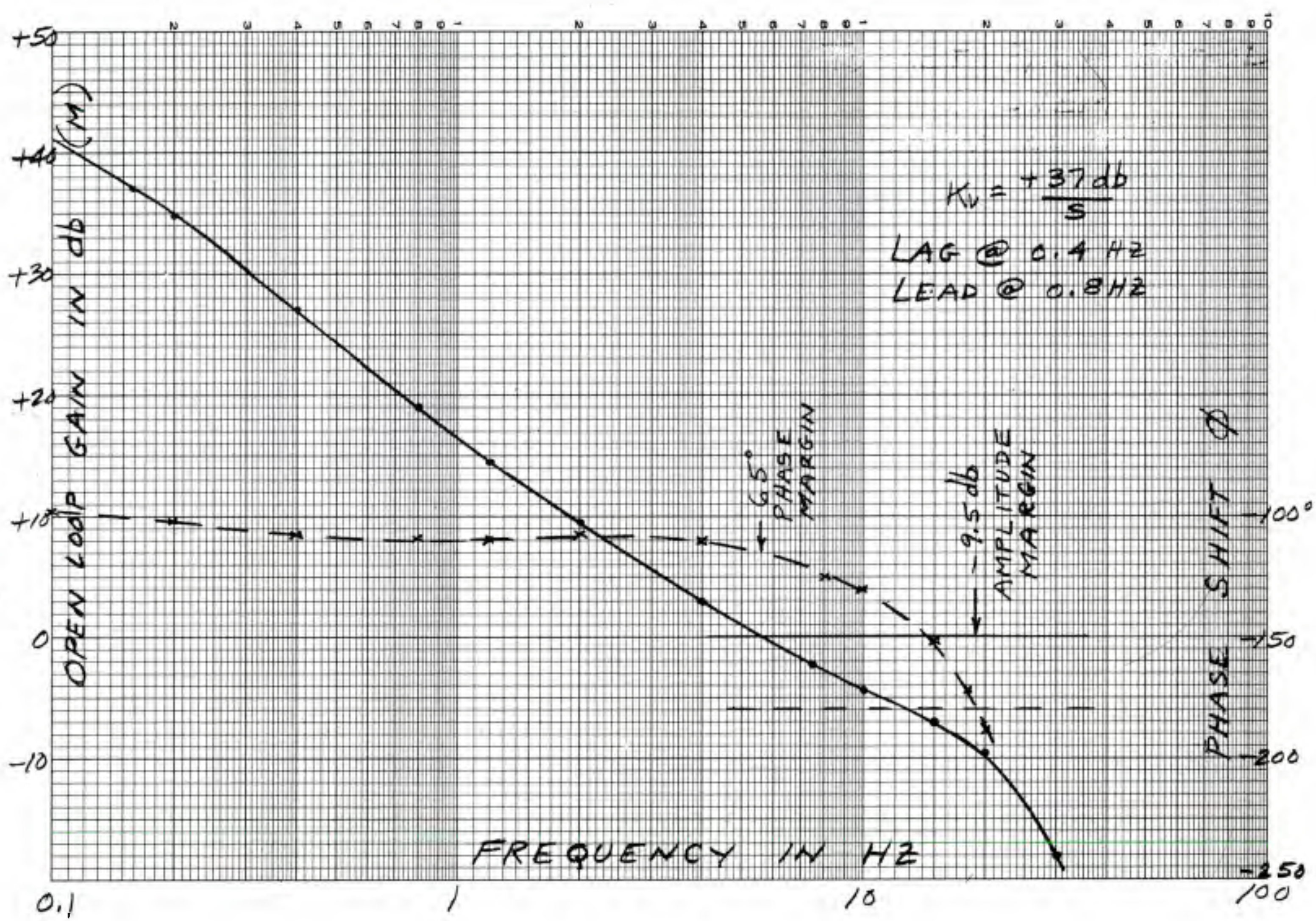

Figure 67. Turret pitch control system open loop

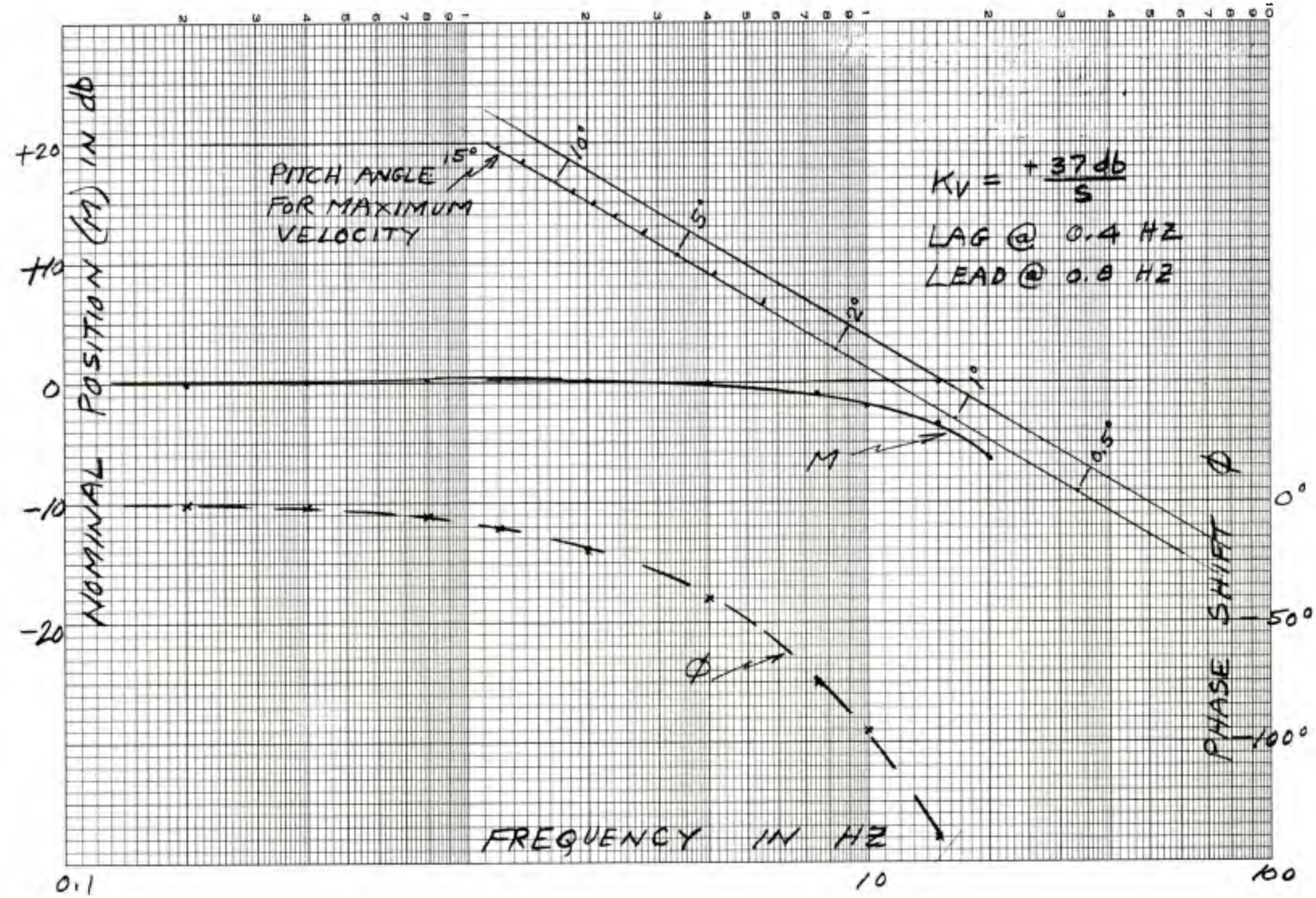

Figure 68. Turret pitch control system closed loop

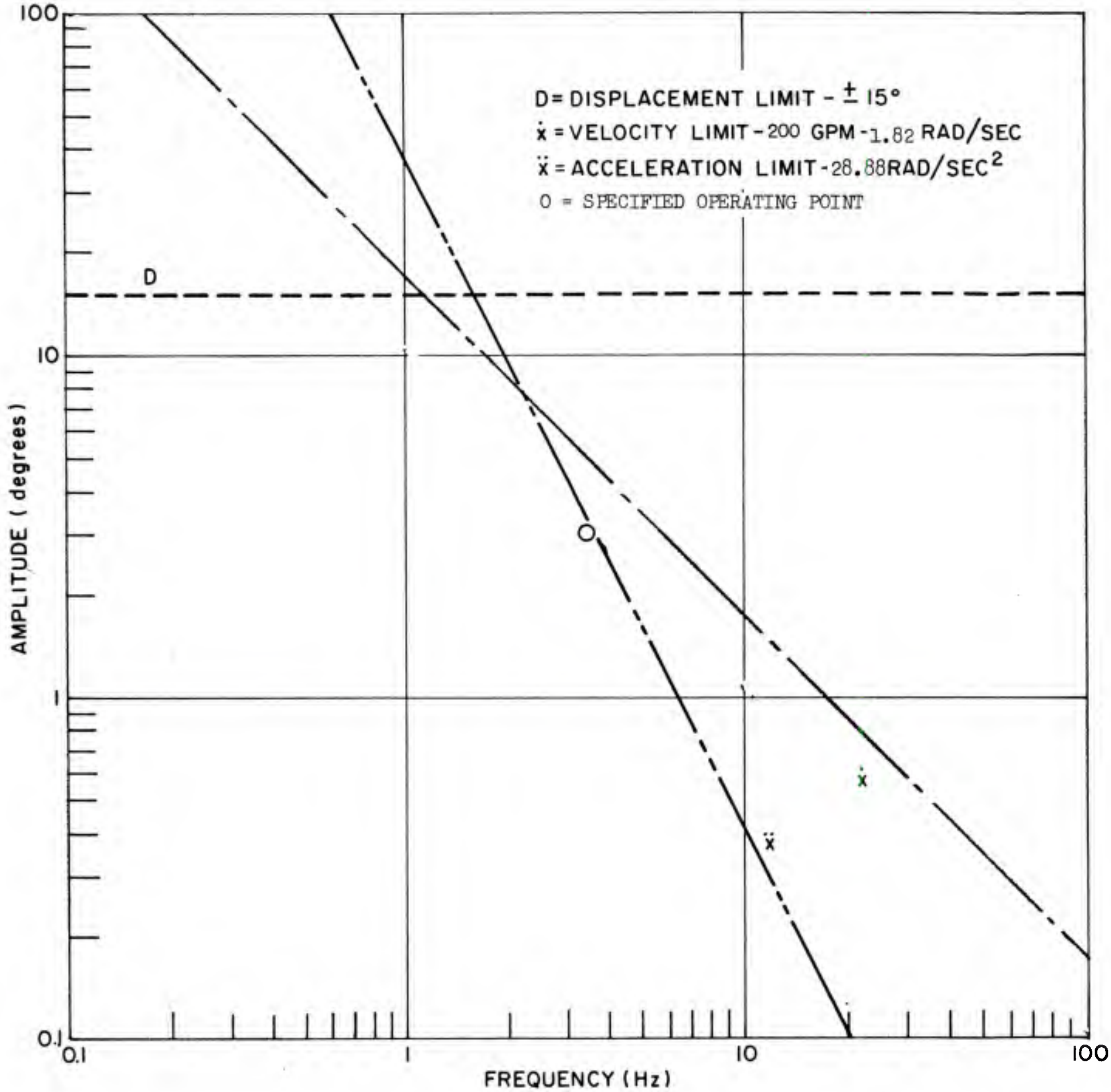

Figure 69. Pitch drive operating limits combat vehicle

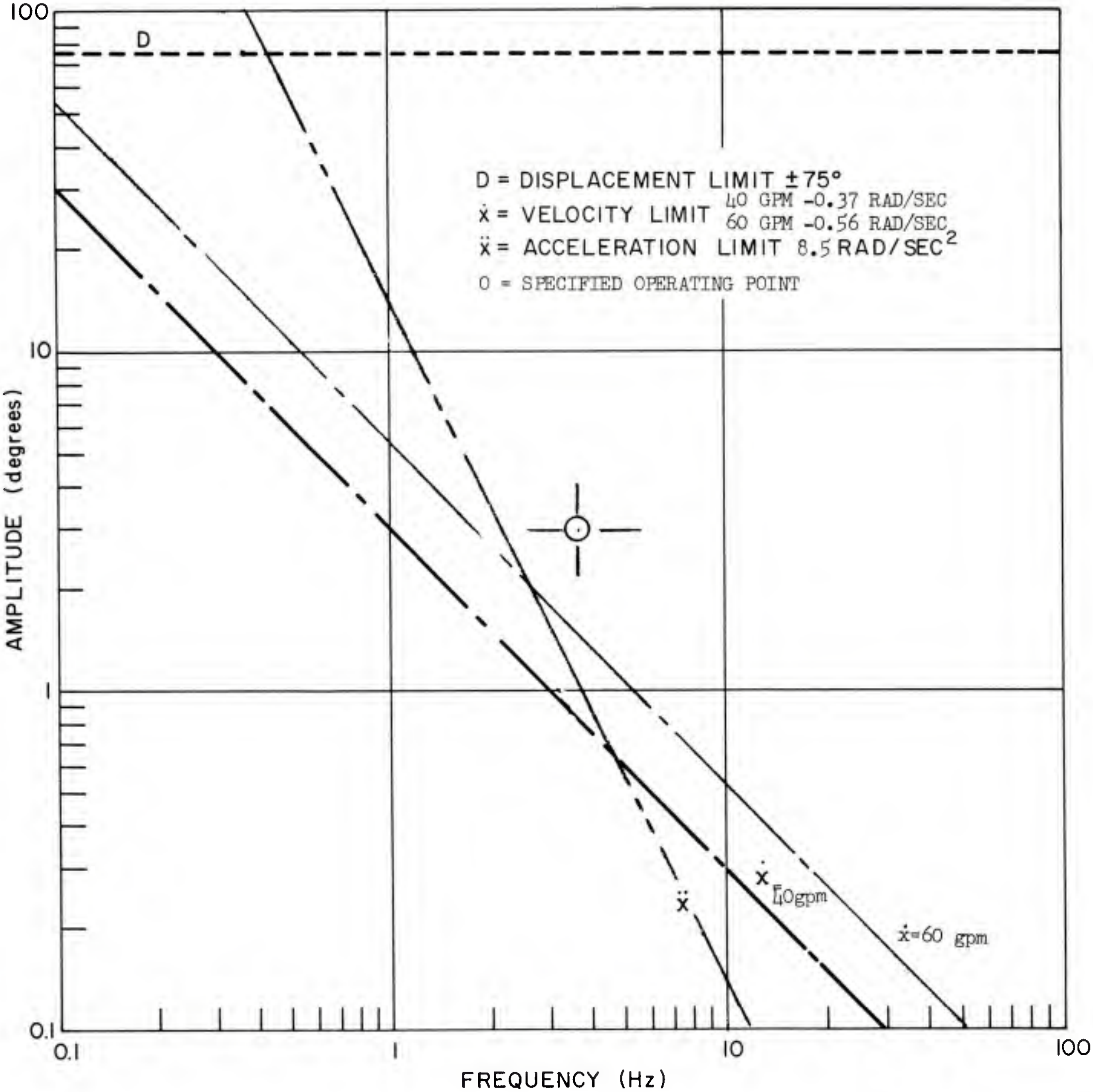

Figure 70. Main yaw drive operating limits combat vehicle

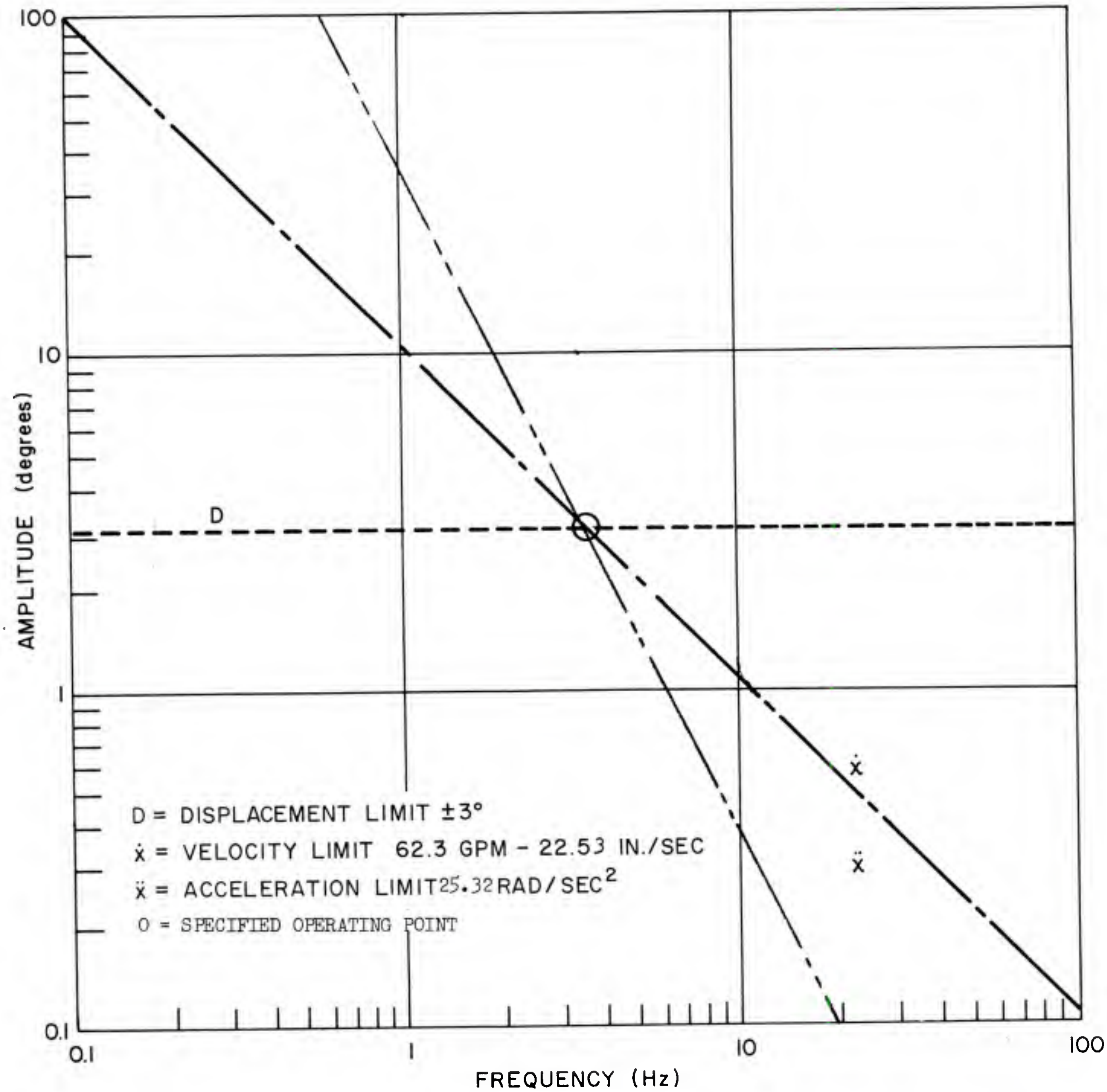

Figure 71. 6-DOF yaw drive operating limits combat vehicle

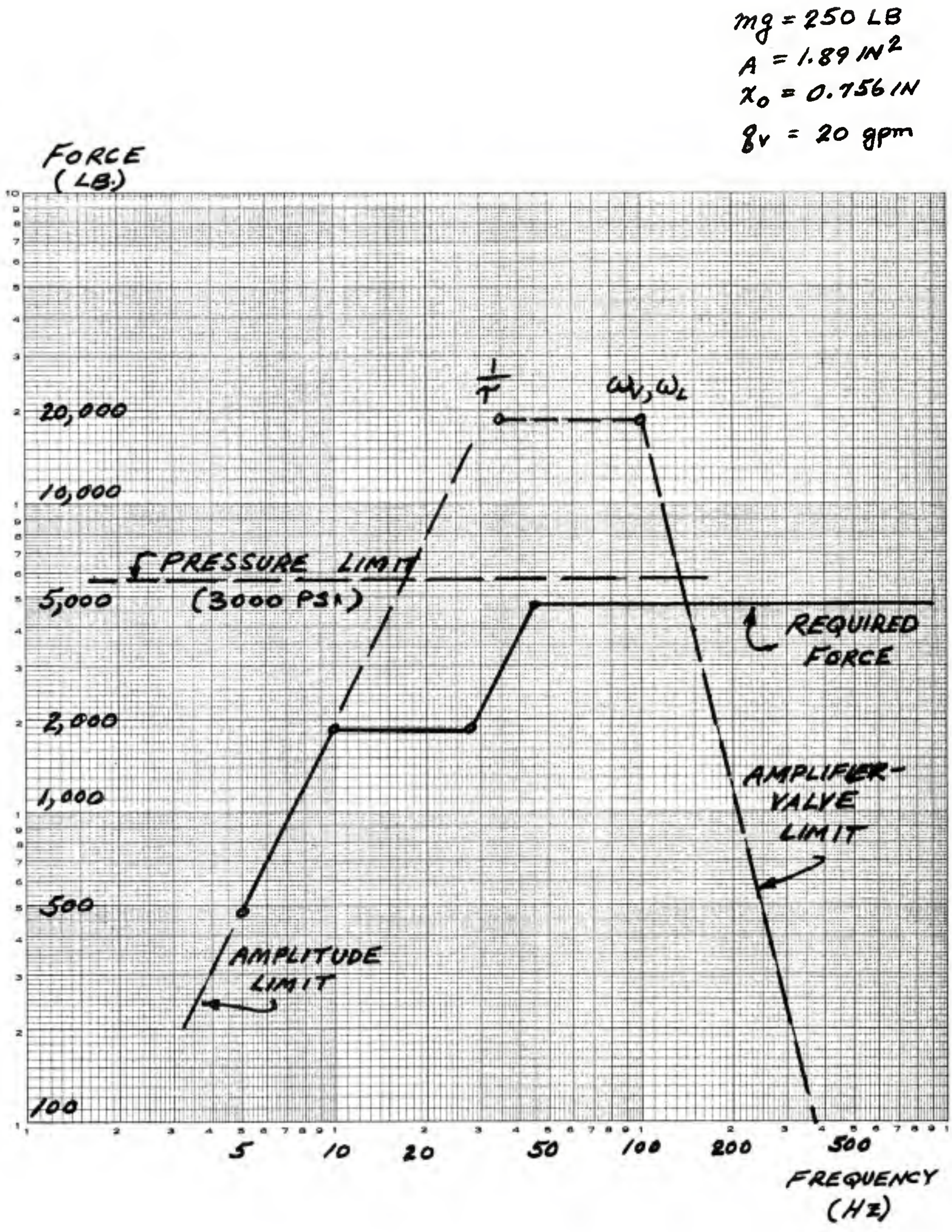

Figure 72. Output force limits (main rotor)

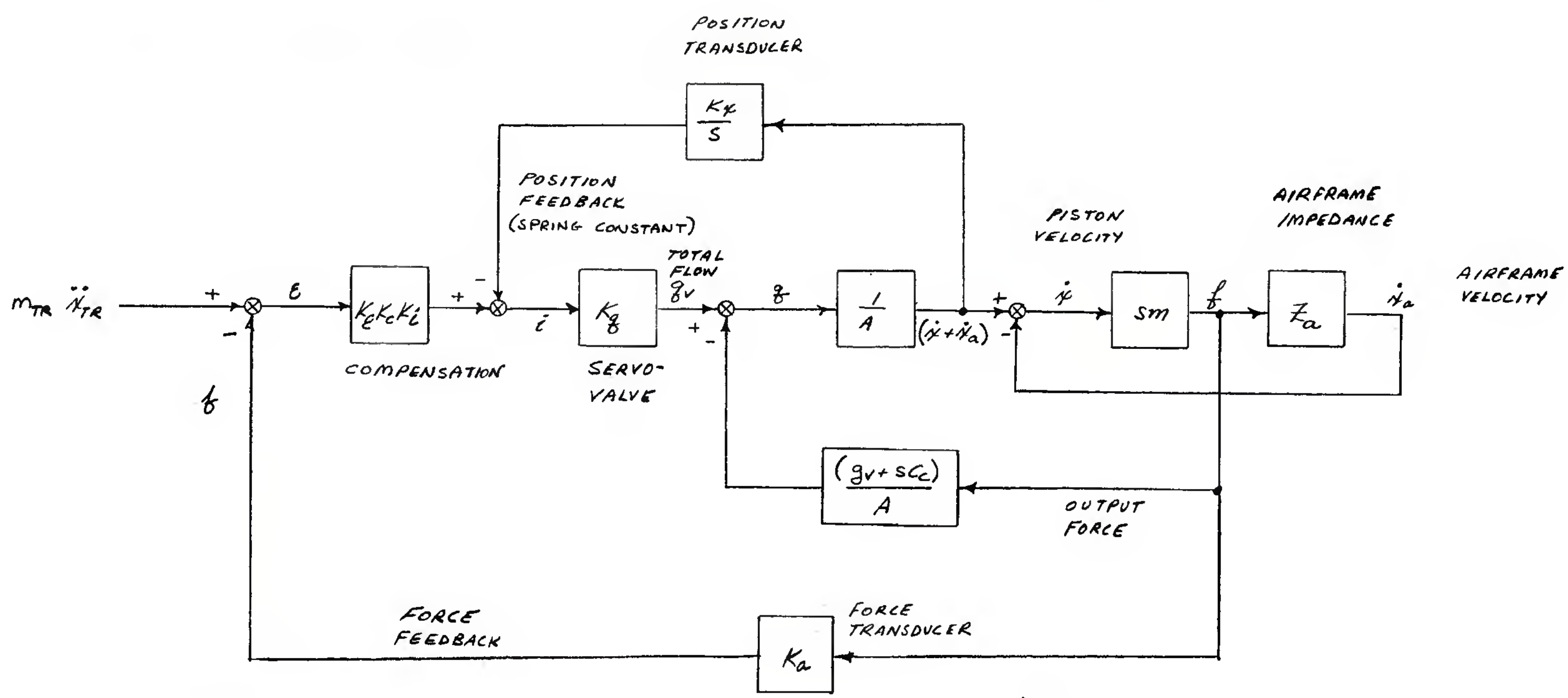

$$K_{OL} = \frac{m' K_i K_c K_\varepsilon K_a}{K_x} \cdot \frac{s^2}{\left\{1 + \frac{A s}{K_q K_x}\left[1 + \frac{s m' (g_v + s C_c)}{A^2}\right]\right\}}$$

$$K_q = \frac{\partial q / \partial i}{\left[1 + 2\zeta_v \left(\frac{s}{\omega_v}\right) + \left(\frac{s}{\omega_v}\right)^2\right]}$$

$$m' = \frac{m\, m_a}{(m + m_a)}$$

Figure 73. Vibrator-equivalent circuit

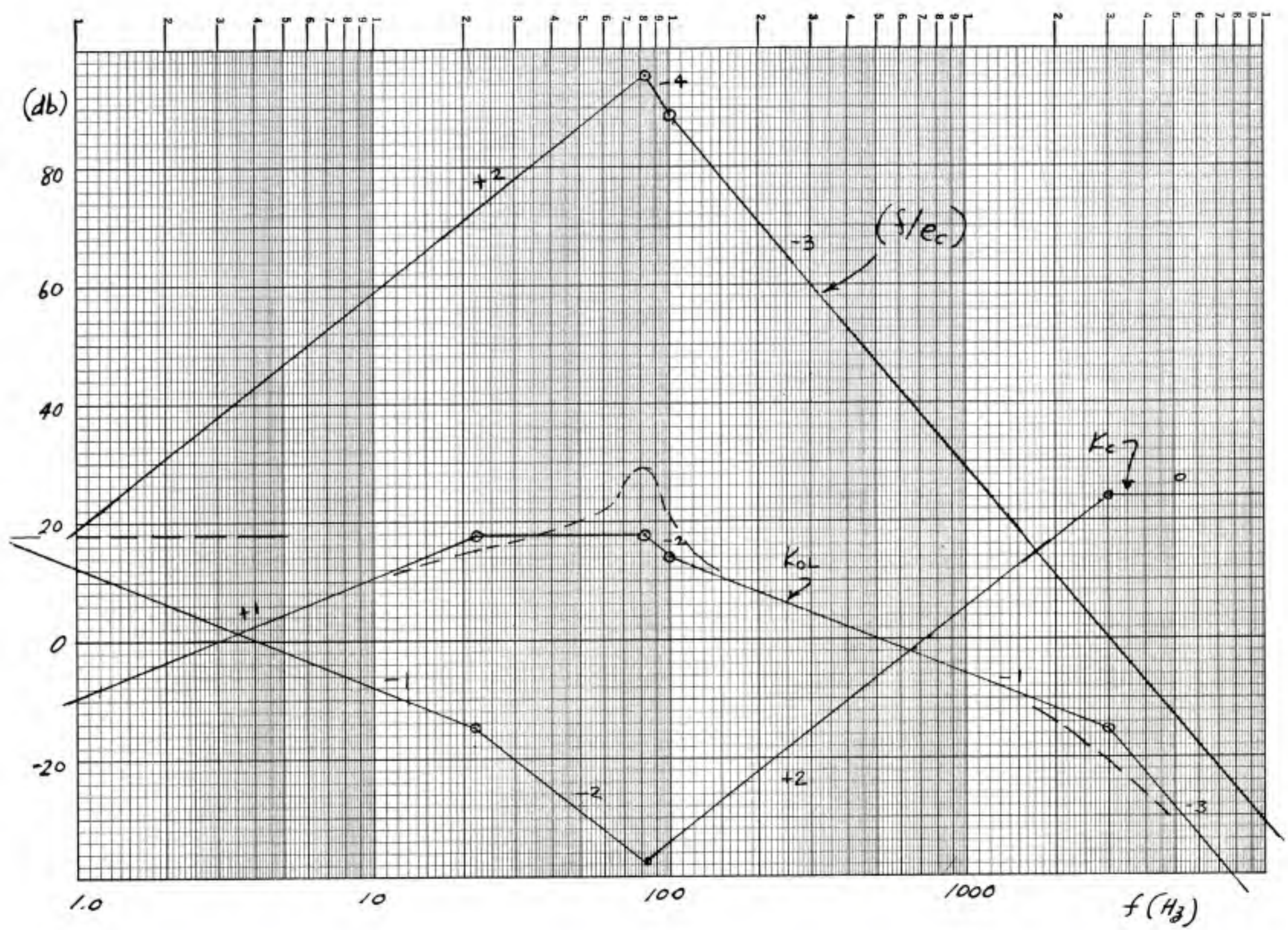

Figure 74. Main rotor system response

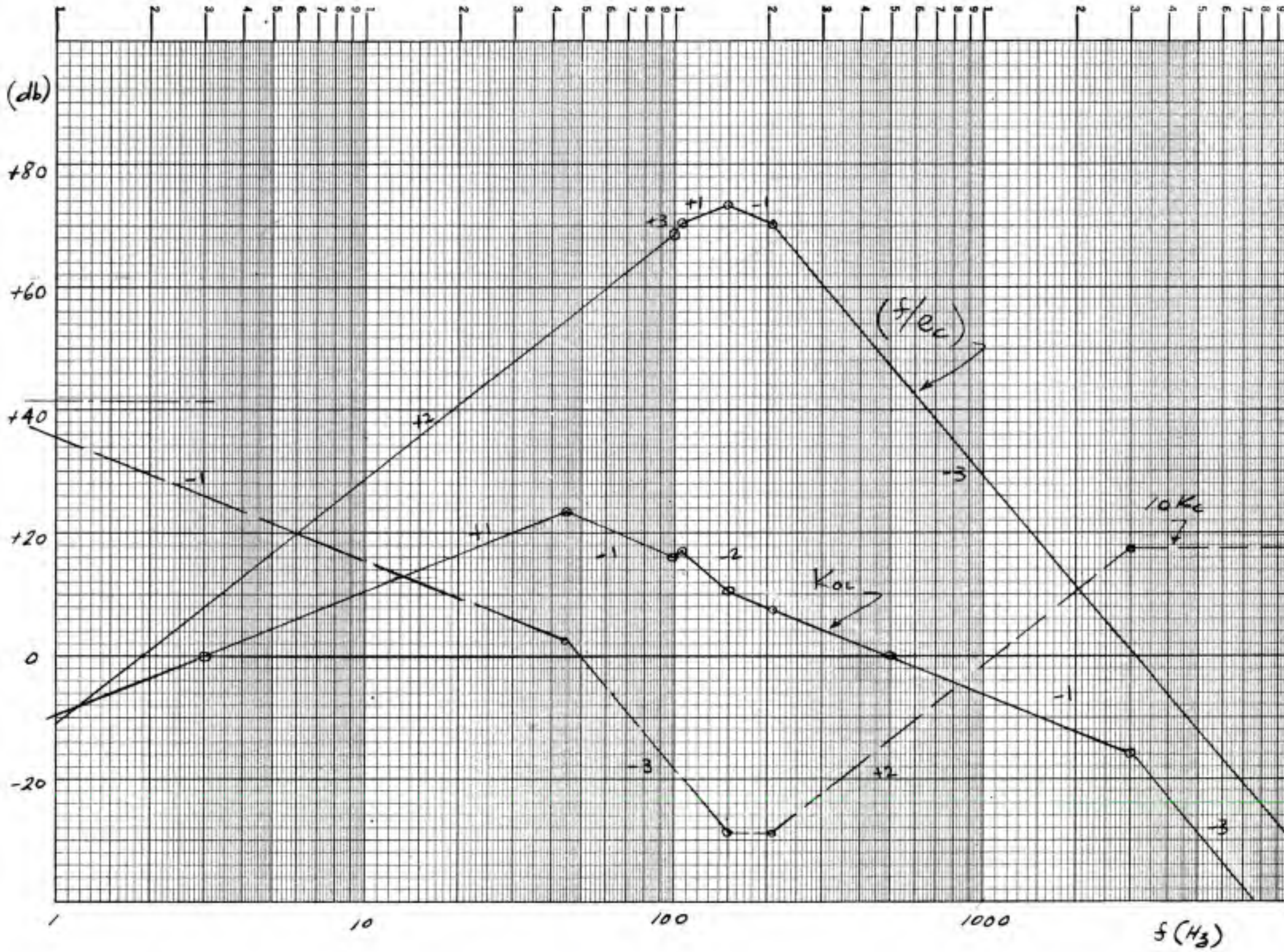

Figure 75. Tail rotor system response

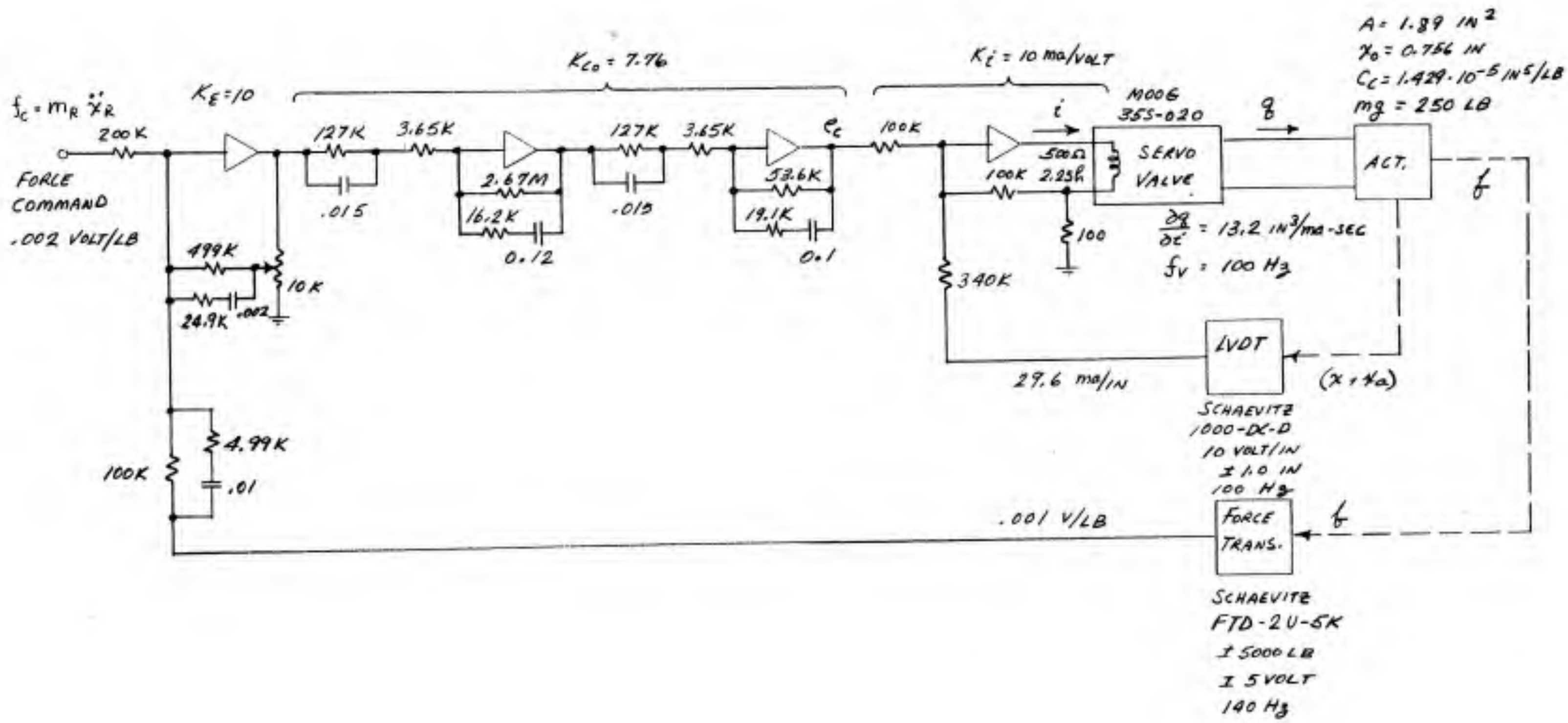

Figure 76. Vibrator servo system (MR)

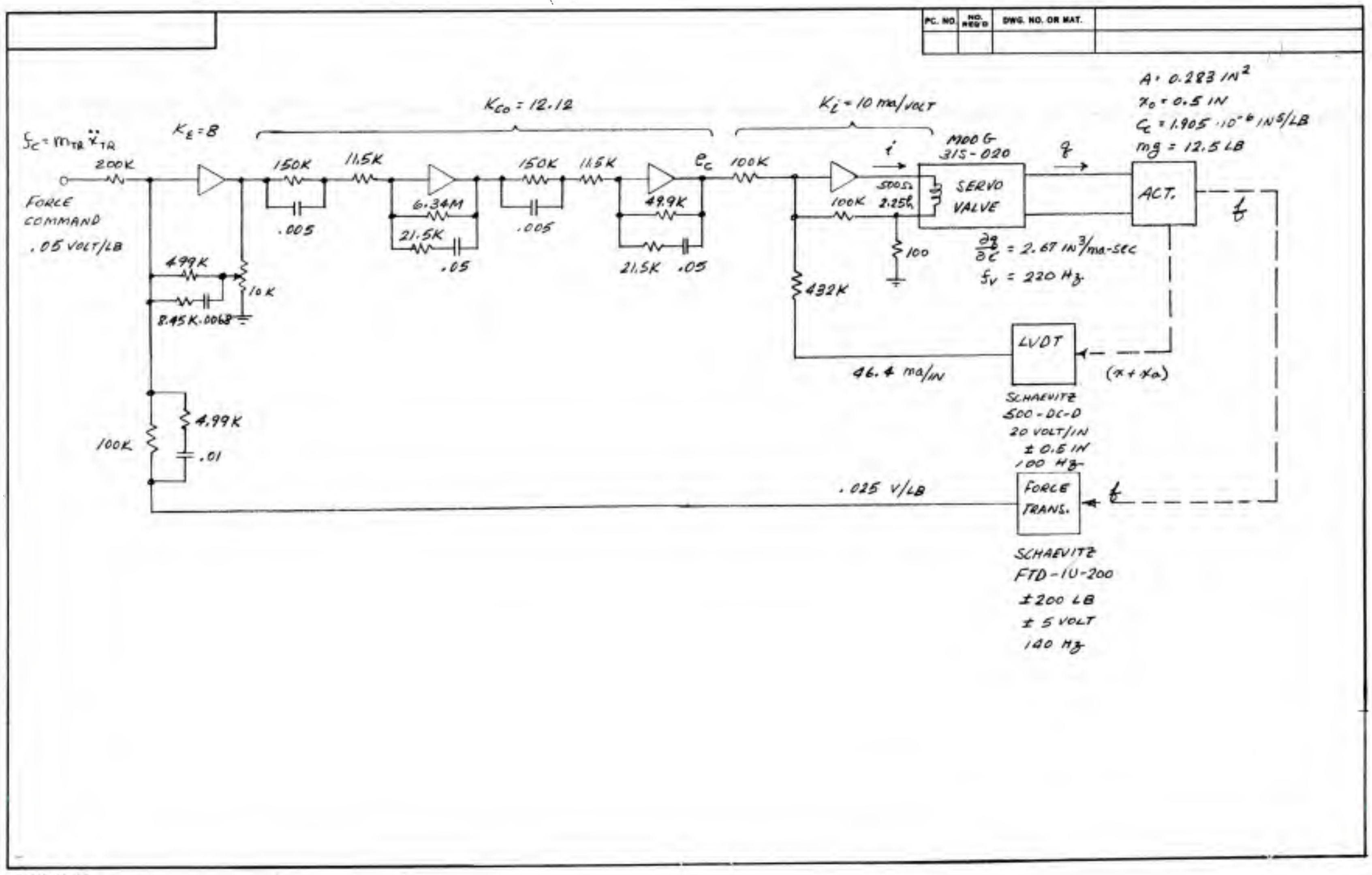

Figure 77. Vibrator servo system (TR)

APPENDIX A
COMPUTER CONTROL OF 6-DOF SIMULATOR
AND COMPUTER PROGRAM

Computer Control of 6-DOF Simulator

Introduction

The digital computer (Nova 2/10) performs two functions in the control of the 6-DOF Simulator: (1) It calculates manual input values of effective mass, spring constant, and actuator lengths off-line. These can then be used for static operation. (2) It calculates the same quantities and inputs the results directly to the servo systems via the D/A converters. These are periodically updated to reflect changes in the gimbal pitch and yaw angles and in the pitch angle of the combat vehicle adapter.

The entire program is resident in core. Specific sections are addressed by appropiate inputs at the teletype keyboard. The off-line results are output to the teletype printer. The program sections are:

1. Load mass matrix
2. Spring constants
3. Elastance matrix at input system
4. Actuator static forces and lengths
5. On-line program

The sections must be addressed in order; however, any previously executed section can be readdressed. Succeeding sections must then again be taken in order. Addressing is accomplished by typing the above code number, following the query "*".

```
 28   TYPE " <15> "
      ACCEPT "*",Q
      IF (Q-1) 28,231,29
 29   IF (Q-Q0-1) 231,231,232
232   IF (Q-6) 28,231,28
231   GOTO (2,30,80,90,200) Q
```

Actuator Mass Load Matrix

The mass load is calculated from the equation developed in the Math Model earlier in this report.

$$M_P = F_t H_t MHF \tag{A-1}$$

in which F is the triogonal transformation (from actuators to platform axes), H is the rectilinear transformation of the platform axes to the component axes, and M is the mass matrix along the component axes about its CM. Since M is defined about the CM, the two off-diagonal 3 x 3 submatrices are zero. The diagonal submatrices are

$$M_{11} = \begin{bmatrix} m & 0 & 0 \\ 0 & m & 0 \\ 0 & 0 & m \end{bmatrix} \tag{A-2}$$

and

$$M_{22} = \begin{bmatrix} J_{xx} & J_{xy} & J_{xz} \\ J_{xy} & J_{yy} & J_{yz} \\ J_{xz} & J_{yz} & J_{zz} \end{bmatrix} \tag{A-3}$$

The equation, (A-1), is evaluated for each of the distinct components of the system, i.e., actuators, platform, platform adapter, and vehicle, and the results are added to give the total mass load. Since the triogonal transformation is common to all components, the summation is performed in the platform coordinate system and then transformed to the actuators. The value due to the actuators remains fixed since the actuators are never changed, and this data is stored permanently in the program (array AM).

```
      DATA AM/1.900.5,3*0.,.7996739,2*0.,1.90045,0.,-.7996739,
     1 4*0.,1.658009,4*0.,-.7996739,0.,813.2535,2*0.,.7996739,
     2 3*0.,813.2535,6*0.,1750.554/
```

Similarly, since the triogonal system is assumed to be always in its neutral position, the transformation, F, remains constant and is stored as the array, F.

```
      DATA F/5.107058E-2,-.530741,.2156135,3.685701E-3,
     1 -1.347696E-2,-8.511763E-3,-.4851705,-.2211421,.2156135,
     2 1.351424E-2,3.546568E-3,8.511763E-3,.4340999,.3095989,
     3 .2156135,9.828537E-3,9.93039E-3,-8.511763E-3,
     4 5.107058E-2,.530741,.2156135,-3.685701E-3,-1.347696E-2,
     5 8.511763E-3,-.4851705,.2211421,.2156135,-1.351424E-2,
     6 3.546568E-3,-8.511763E-3,.4340999,-.3095989,.2156135,
     7 -9.828537E-3,9.93039E-3,8.511763E-3/
```

The rectilinear transformations, H, for each o the three load compnents, i.e., platform, platform adapter, and vehicle, are developed by the program from the locations of the centers of mass and the Euler angles of the corresponding coordinate systems. These are shown as

$$H = \left[\begin{array}{c|c} E(x_3) & -W(r)\ E(x_3) \\ \hline 0 & E(x_3) \end{array}\right] \tag{A-4}$$

The matrix, E, is the angular transformation of the Euler angles

$$x_3 = \begin{pmatrix} \phi \\ \theta \\ \psi \end{pmatrix} \tag{A-5}$$

and W is the rotational matrix of the distance to the center of mass

$$r = \begin{pmatrix} x \\ y \\ z \end{pmatrix} \tag{A-6}$$

given by

$$W(r) = \begin{pmatrix} 0 & -z & y \\ z & 0 & -x \\ -y & x & 0 \end{pmatrix} \tag{A-7}$$

The elements of the angular transformation are

$$\left.\begin{aligned}
e_{11} &= \cos\theta\cos\psi \\
e_{21} &= \sin\phi\sin\theta\cos\psi - \cos\phi\sin\psi \\
e_{31} &= \cos\phi\sin\theta\cos\psi + \sin\phi\sin\psi \\
e_{12} &= \cos\theta\sin\psi \\
e_{22} &= \cos\phi\cos\psi + \sin\phi\sin\theta\sin\psi \\
e_{32} &= \cos\phi\sin\theta\sin\psi - \sin\phi\cos\psi \\
e_{13} &= -\sin\theta \\
e_{23} &= \sin\phi\cos\theta \\
e_{33} &= \cos\phi\cos\theta
\end{aligned}\right\} \tag{A-8}$$

These two transformations are returned by the subroutines ROT (W, X, Q) and ANGLE (E, X, Q), respectively. The value of the integer, Q, specifies the column of the array, X, from which values for r and x_3 are taken. The rectilinear transformation, H, is returned by the subroutine TRANS (C, E, W, Q). The result is the array, C. The integer, Q, now either specifies the order of multiplication of W and E, depending on whether r is measured in the original system or the transformed system, or it specifies that r is equal to zero.

Initially, the configuration data is requested by the program. Development of the mass load proceeds as follows:

```
2    WRITE (10,4)
4    FORMAT (15H0CONFIGURATION   //)
     ACCEPT "LOCATION OF CM <15>","  PLATFORM: <15>",
    1 (X(R,1),R=1,3),"  PLATFORM ADAPTER: <15>",(X(R,2),R=1,3),
    2 "  VEHICLE: <15>",(X(R,3),R=1,3),"PLATFORM ADAPTER <15>",
    3 "  LOCATION OF VEHICLE INTERFACE: <15>",(X(R,7),R=1,3),
    4 "  EULER ANGLES: <15>",(X(R,7),R=4,6),"WEIGHTS <15>",
    5 "  PLATFORM: ",WGT(1),"  PLATFORM ADAPTER: ",WGT(2),
    6 "  VEHICLE: ",WGT(3),"MOMENTS OF INERTIA <15>",
    7 "  PLATFORM: <15>",(MOI(R,1),R=1,6),
    8 "  PLATFORM ADAPTER: <15>",(MOI(R,2),R=1,6),
    9 "  VEHICLE: <15>",(MOI(R,3),R=1,6)
```

First, the locations of the centers of mass of the platform, platform adapter, and vehicle are inputed. These are typed in the order x, y, z, separated by commas and terminated with a carriage return (↵). The values for the platform and platform adapter are measured, in inches, from the origin of the platform coordinate system (in the plane of the lower pivot points of the actuators) to the appropriate CM, in the platform system. The location of the vehicle CM is measured from the origin of the platform adapter/vehicle interface, in the vehicle coordinate system. For the AH-1G, this origin is 10 inches below the origin of the platform system, along the z-azis. In this case

$$r_V = \begin{pmatrix} 12.8104 \\ 0 \\ 35.1962 \end{pmatrix} \tag{A-9}$$

Next the platform adapter/vehicle interface data are requested. This consists of the location of the origin, which, as stated for the AH-1G is

$$r_I = \begin{pmatrix} 0 \\ 0 \\ 10 \end{pmatrix} \tag{A-10}$$

and the Euler angles (which rotate the platform axes into the vehicle axes). For the AH-1G, the vehicle system is pitched 20 degrees below the platform system, so that

$$x_{3v} = \begin{pmatrix} 0 \\ -20 \\ 0 \end{pmatrix} \tag{A-11}$$

The third block of data requested consists of the weights of the platform, platform adapter, and vehicle (in pounds). For the AH-1G, these are 800, 1700 and 9500 lb, respectively.

Finally, the moments of inertia of platform, platform adapter, and vehicle are requested. These are typed in the order J_{xx}, J_{yy}, J_{zz}, J_{xy}, J_{xz}, J_{yz}.

They are measured in units of in. lb sec^2. The subroutine INERTIA (J, MOI, Q) forms the full 3 x 3 matrix (equation 3) from these values. The integer, Q, specifies the column of the array, MOI, from which values are taken.

With this data, the calculation can proceed. The mass matrix, M, is initialed to the values for the actuators.

```
      DO 6 R=1,6
      DO 6 S=1,6
      M(R,S)=AM(R,S)
6     CONTINUE
```

The derivation of these values is given in appendix B.

Next, the H transformation from interface to vehicle is formed.

```
CALL ROT(W,X,3)
CALL ANGLE(E,X,7)
CALL TRANS(C,E,W,1)
```

This returns the array

$$C = \left[\begin{array}{c|c} E(x_{3v}) & -W(r_v)\ E(x_{3v}) \\ \hline 0 & E(x_{3v}) \end{array}\right] \tag{A-12}$$

Then the transformation from platform to interface is formed.

```
CALL ROT(W,X,7)
CALL UNIT(E)
CALL TRANS(D,E,W,1)
```

This returns the array

$$D = \left[\begin{array}{c|c} 1 & -W(r_I) \\ \hline 0 & 1 \end{array}\right] \tag{A-13}$$

The complete transformation is then formed by multiplying the two.

```
CALL MULT(C,D,H,6)
```

Since

$$E(x_3)\ W(r) = W\ [E(x_3)r]\ E(x_3) \tag{A-14}$$

this returns the array

$$H = \left[\begin{array}{c|c} E(x_3) & -W[E(x_3)\ r_I + r_v]\ E(x_{3v}) \\ \hline 0 & E(x_{3v}) \end{array}\right] \qquad \text{(A-15)}$$

which is the rectilinear transformation from platform to vehicle.

The integer, Q, is set to 3, upon entering the loop beginning with statement 11, which then returns the inertia matrix for the vehicle. The mass matrix (6 x 6) is then formed, referred to vehicle axes.

```
      Q=3
11    CALL INERTIA(J,MOI,Q)
      CALL ZERO(C,6)
      DO 14 R=1,3
      DO 14 S=1,3
      C(R+3,S+3)=J(R,S)
      IF (R-S) 14,12,14
12    C(R,S)=WGT(Q)/386.063
14    CONTINUE
```

This is then transformed to the platform axes by forming the product

$$M = H_t CH \qquad \text{(A-16)}$$

and adding this value to the previous value of M.

```
      CALL MULT(C,H,H1,6)
      CALL TRNSP(C,H,6)
      CALL MULT(C,H1,H,6)
      DO 16 R=1,6
      DO 16 S=1,6
      M(R,S)=M(R,S)+H(R,S)
16    CONTINUE
```

The integer, Q, is now decremented by one, giving a new value of 2, and the program advances to statement 17. This returns the transformation from platform to the CM of the platform adapter.

```
      Q=Q-1
      IF (Q) 21,21,17
17    CALL ROT(W,X,Q)
      CALL UNIT(E)
      CALL TRANS(H,E,W,1)
```

The program now loops back to statement 11

```
      GOTO 11
```

and forms the mass matrix for the platform adapter. This is transformed to the platform axes and again added to the previous values. Once more the integer, Q, is decremented, this time to a value of one, and the procedure is repeated for the platform. The mass load matrix now contains the contributions from all four basic components of the system, actuators, vehicle, platform adapter, and platform. However, it is still referred to the platform coordinate system. By decrementing the value of Q once more (to a value of zero), the program advances to statement 21. This premultiplies it by F, in order to refer the values to the triogonal system.

```
21    CALL TRNSP(C,F,6)
      CALL MULT(C,M,H,6)
      CALL MULT(H,F,M,6)
```

To preserve symmetry in the calculations, the actuators were numbered so that 4, 5 and 6 are mirror images of 1, 2 and 3 in the X-Z plane. The physical actuators are numbered clockwise, with number 1 located in the positive Y direction. The array ACTN, also stored in common, is used to rearrange the matrix M into the matrix H1.

```
      DATA ACTN/2,3,6,5,4,1/

      DO 23 R=1,6
      DO 23 S=1,6
      H1(R,S)=M(ACTN(R),ACTN(S))
23    CONTINUE
```

This matrix is then typed, in the order corresponding to the physical numbering system, and control of the program is returned to the operator.

```
      WRITE (10,24)((H1(R,S),S=1,6)R=1,6)
24    FORMAT (40H0ACTUATOR LOAD MASS MATRIX (LB-SEC↑2/IN)  //
     1 (6F10.4))
      Q0=1
      GOTO 28
```

Spring Constants

The second part of the program calculates the values of actuator spring constant, off-line. This generally follows the development of the math model as described earlier in this report. However, no restriction is placed on the location and orientation of the axes for which values are specified, except that they form a nonsingular set. Three values must be specified, which are the reciprocals of the principal elastances along three axes chosen from the lists of the spring constants of the math model as described earlier in this report. Their order of input depends on which value is most critical, since the values are subject to the physical limitations of the actuators and servo systems.

The initial part of this section determines the minimum and maximum values of spring constant possible for each of the actuators, based on the load mass determined in section 1. The maximum value is the smaller of 200,000 lb/in.

or $\omega^2 M$, where

$$\omega = 2\pi\,(10) = 62.8 \text{ rad/sec} \tag{A-17}$$

and M is the principal load mass element for that actuator. The minimum value is the larger of 250 lb/in. or $\omega^2 M/1500$.

```
      DO 35 R=1,6
      K(R+15)=3947.842*M(R,R)
      K(R+9)=K(R+15)/1500
      IF (K(R+15)-2.0E5) 33,33,32
32    K(R+15)=2.0E5
33    IF (K(R+9)-250.) 34,35,35
34    K(R+9)=250.
35    CONTINUE
```

In addition, it has been assumed that the symmetry about the X-Z plane is preserved for spring constants, that is

$$k_{N+3} = k_N \tag{A-18}$$

Thus, the smaller maximum and larger minimum are chosen for each pair of actuators.

```
      DO 39 R=1,3
      IF (K(R+15)-K(R+18)) 37,37,36
36    K(R+15)=K(R+18)
37    IF (K(R+9)-K(R+12)) 38,39,39
38    K(R+9)=K(R+12)
39    CONTINUE
```

The location and orientation of the coordinate system for which spring constants are to be specified ("Input System") is then requested.

```
      ACCEPT "ORIGIN OF INPUT SYSTEM: ",(X(R,4),R=1,3),
     1 "EULER ANGLES OF INPUT SYSTEM: ",(X(R,4),R=4,6)
```

These are typed in as measured in the vehicle system, using the origin of the interface as reference. For instance, if the CM of the aircraft is chosen, and values are specified along the aircraft axes, the following would be typed for the AH-1G

```
ORIGIN OF INPUT SYSTEM: 12.8104, 0., 35.1962
EULER ANGLES OF INPUT SYSTEM: 0., 0., 0.
```

Next, the matrix, A, is formed, which is the transformation from the input system to the triogonal system as previously described.

$$A = H\,(x_{3I},\ r_I)\,F \tag{A-19}$$

```
      CALL ANGLE(E,X,4)
      CALL ROT(W,X,4)
      CALL TRANS(C,E,W,2)
      CALL ANGLE(E,X,7)
      CALL ROT(W,X,7)
      CALL TRANS(D,E,W,2)
      CALL MULT(C,D,H,6)
      CALL MULT(H,F,A,6)
```

This is calculated by multiplying the transformation from interface to input system by that from platform to interface, and then multiplying the result by the triogonal transformation (actuator to platform). The index 2 is used in both calls to TRANS, since the distances in both cases are measured in the original system (not the one resulting from rotation by the Euler angles).

In order to continue, it is now necessary to specify which axes are to be chosen for the input values of spring constant. These are typed in the order of importance (U, V, W) with the code

$x = 1$

$y = 2$

$z = 3$

$\phi = 4$ (roll)

$\theta = 5$ (pitch)

$\psi = 6$ (yaw)

```
      WRITE (10,42)
42    FORMAT (12H0INPUT AXES= ,Z)
      READ (11) N(1),N(2),N(3)
```

For instance, if the axes are x, θ, and z, the following would be typed:

INPUT AXES = 1, 5, 3 ↓

The 3 x 3 matrix, G, is now formed which relates the actuator spring constants to the specified spring constants.

```
      DO 43 R=1,3
      DO 43 S=1,3
      G(R,S)=A(N(R),S)*A(N(R),S)+A(N(R),S+3)*A(N(R),S+3)
43    CONTINUE
```

This calculation deviates slightly from that given in the math model, since the restriction on the location of the input coordinate system has been removed. The A matrix, in the general case, will not necessarily exhibit the symmetry specified in the math model. The inverse of this matrix is then returned by calling the subroutine INV.

```
      CALL INV (I,G,GØ)
```

The variable, GO, is the determinant, $|G|$. From the inverse, I, it is possible to calculate the actuator elastances directly from the specified elastances.

$$\begin{pmatrix} e_1 \\ e_2 \\ e_3 \end{pmatrix} = I \begin{pmatrix} e_u \\ e_v \\ e_w \end{pmatrix} \tag{A-20}$$

The input elastances, e_u, e_v and e_w, must be chosen to give physically realizable values fo the actuators. The major portion of this part of the program is used for determining the limits on the input values which correspond to the limits previously imposed on the actuator values. For the specification of e_v, the most important of the three input values, the equations relating actuator values to input values are used.

$$\begin{pmatrix} e_u \\ e_v \\ e_w \end{pmatrix} = G \begin{pmatrix} e_1 \\ e_2 \\ e_3 \end{pmatrix} \tag{A-21}$$

Since the elements of the matrix, G, are obtained by summing squares of the elements of the matrix, A, they must be positive. It then follows that the maximum and minimum values of input values are obtained by substituting maximum and minimum actuator values if there are no other restrictions. For the initial input specification

$$e_u = g_{11}\, e_1 + g_{12}\, e_2 + g_{13}\, e_3 \tag{A-22}$$

Thus the minimum and maximum limits on the equivalent spring constant are

```
K(7)=1/(G(1,1)/K(10)+G(1,2)/K(11)+G(1,3)/K(12))
K(8)=1/(G(1,1)/K(16)+G(1,2)/K(17)+G(1,3)/K(18))
```

These values are typed out with the appropriate dimensions, depending upon whether k_u is a linear or angular constant, and an input value is requested.

```
        IF (N(1)-3) 44,44,45
44      TYPE K(8)," >KU> ",K(7)," LB/IN"
        GOTO 46
45      TYPE K(8)," >KU> ",K(7)," IN-LB/RAD"
46      ACCEPT "KU= ",K(9)
```

The operator then selects a value within these limits and types it.

With this value of e_u and the actuator limiting values, it is now possible to find the limits on e_v. From equation 20

$$\left.\begin{aligned} e_1 &= i_{11}\, e_u + i_{12}\, e_v + i_{13}\, e_w \\ e_2 &= i_{21}\, e_u + i_{22}\, e_v + i_{23}\, e_w \\ e_3 &= i_{31}\, e_u + i_{32}\, e_v + i_{33}\, e_w \end{aligned}\right\} \qquad \text{(A-23)}$$

or, by solving for e_w,

$$\left.\begin{aligned} e_w &= \frac{1}{i_{13}}\,(e_1 - i_{11}\, e_\mu) - \frac{i_{12}}{i_{13}}\, e_v \\ e_w &= \frac{1}{i_{23}}\,(e_2 - i_{21}\, e_\mu) - \frac{i_{22}}{i_{23}}\, e_v \\ e_w &= \frac{1}{i_{33}}\,(e_3 - i_{31}\, e_\mu) - \frac{i_{32}}{i_{33}}\, e_v \end{aligned}\right\} \qquad \text{(A-24)}$$

For the maximum and minimum limits of e_1, e_2 and e_3, and the specified value of e_u, these provide six curves relating e_w to e_v. The intersections of these curves determine the limits of e_v.

Initially, the slopes of the curves are determined, B(R,1). If the coefficient of e_1, e_2, or e_3 is positive, the corresponding terms, B(R,2) and B(R,3) are determined from the miminum and maximum values of the actuator spring constant, respectively. If negative, they are interchanged.

```
            DO 49 R=1,3
            B(R,1)=-I(R,2)/I(R,3)
            IF (I(R,3)) 48,47,47
      47    B(R,2)=1/(K(R+9)*I(R,3))
            B(R,3)=1/(K(R+15)*I(R,3))
            GOTO 49
      48    B(R,2)=1/(K(R+15)*I(R,3))
            B(R,3)=1/(K(R+9)*I(R,3))
      49    CONTINUE
```

These would be the intercepts on the w-axis if e_v were zero. To develop the equations necessary to determine the limits, it is necessary to rearrange the three equations, (A-24), in order of decreasing slopes. A typical result is shown in figure A-1. These are labeled e_{w1}, e_{w2} and e_{w3}, respectively. The superscripts, + and −, are used to designate the maximum and minimum values of

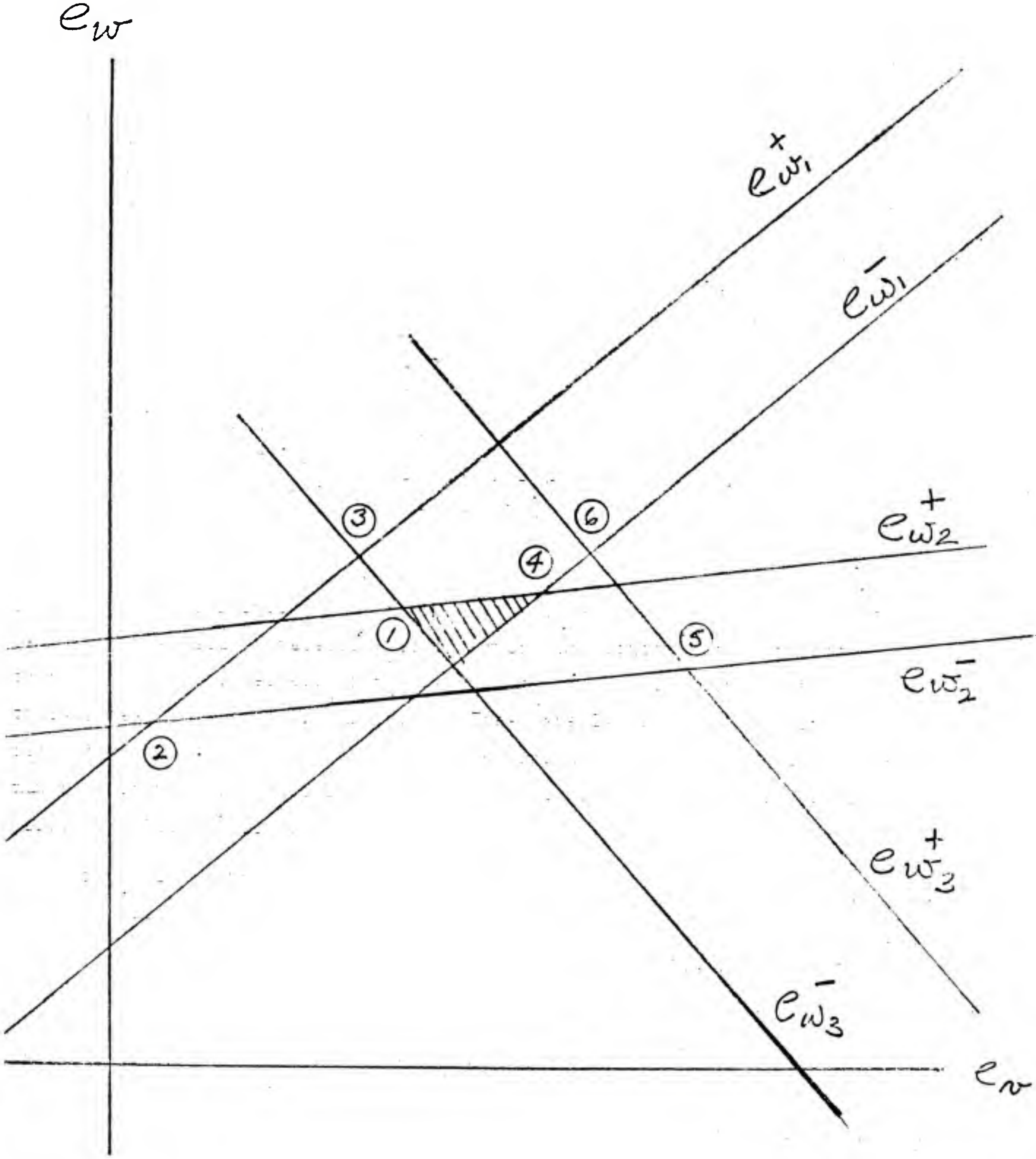

Figure A-1. Equation (A-24)

each of the three equations. Thus, the actual value must lie between the two curves for each equation.

In the illustration, the values of e_v and e_w must lie in the shaded area to be within the limits of all three equations. Thus, since e_v is the next value to be specified, it must be between the values determined by intersections 1 and 4. The minimum is the largest of the three labeled 1, 2, and 3. These are the intersections of maximum value of the curve with the largest slope (1+) and the minimum values of the other two (2- and 3-), and the intersection of the maximum value of the curve with the intermediate slope (2+) and the minimum value of the curve with the minimum slope (3-). These are numbered as follows:

Intersection	Curves
1	2+, 3-
2	1+, 2-
3	1+, 3-

Similarly, the three intersections which determine the maximum value of e_v are numbered as follows:

Intersection	Curves
4	2+, 1-
5	3+, 2-
6	3+, 1-

These six intersections comprise all of those possible between the maximum value of one curve and the minimum value of another.

Since B(R,2) and B(R,3) have been defined such that B(R,2) corresponds to the minimum and B(R,3) the maximum elastance curve, regardles of the sign of I(R,3), these intersections are found as follows: To avoid confusion, the equations will be rewritten with the symbols used in the program. For R = 1, 2, and 3

$$\left.\begin{aligned} e_{wr}^{+} &= B(R,3) - \frac{I(R,1)}{I(R,3)}\,e_u - \frac{I(R,2)}{I(R,3)}\,e_v \\ e_{wr}^{-} &= B(R,2) - \frac{I(R,1)}{I(R,3)}\,e_u - \frac{I(R,2)}{I(R,3)}\,e_v \end{aligned}\right\} \qquad \text{(A-25)}$$

The six intersections are then

$$\left.\begin{array}{l}
1. \quad e_v\,[I(2,2)I(3,3) - I(2,3)I(3,2)] \\
\quad = e_u\,[I(2,3)I(3,1) - I(2,1)I(3,3)] + \\
\quad + I(2,3)I(3,3)\,[B(2,3) - B(3,2)] \\
\\
2. \quad e_v[I(1,3)I(3,2) - I(1,2)I(3,3)] \\
\quad = e_u[I(1,1)I(3,3) - I(1,3)I(3,1)] + \\
\quad + I(3,3)I(1,3)\,[B(3,2) - B(1,3)] \\
\\
3. \quad e_v[I(1,2)I(2,3) - I(1,3)I(2,2)] \\
\quad = e_u[I(1,3)I(2,1) - I(1,1)I(2,3)] + \\
\quad + I(1,3)I(2,3)\,[B(1,3) - B(2,2)] \\
\\
4. \quad e_v[I(2,2)I(3,3) - I(2,3)I(3,2)] \\
\quad = e_u[I(2,3)I(3,1) - I(2,1)I(3,3)] + \\
\quad + I(2,3)I(3,3)\,[B(2,2) - B(3,3)]
\end{array}\right\} \qquad (A-26)$$

5. $e_v[I(1,3)I(3,2) - I(1,2)I(3,3)]$

$= e_u[I(1,1)I(3,3) - I(1,3)I(3,1)] +$

$+ I(3,3)I(1,3)\ [B(3,3) - B(1,2)]$

6. $e_v[I(1,2)I(2,3) - I(1,3)I(2,2)]$

$= e_u(I(1,3)I(2,1) - I(1,1)I(2,3)] +$

$$+ I(1,3)I(2,3)\ [B(1,2) - B(2,3)] \qquad \text{(A-26)}$$

By introducing the cofactors of the matrix, I, these can be rewritten as

$$G(1,1)e_v = B(1,4) + G(2,1)e_u$$

$$G(1,2)e_v = B(2,4) + G(2,2)e_u$$

$$G(1,3)e_v = B(3,4) + G(2,3)e_u$$

$$G(1,1)e_v = B(1,5) + G(2,1)e_u$$

$$G(1,2)e_v = B(2,5) + G(2,2)e_u$$

$$G(1,3)e_v = B(3,5) + G(2,3)e_u \qquad \text{(A-27)}$$

The program next calculates the six intercepts

```
B(1,4)=G0*I(2,3)*I(3,3)*(B(2,3)-B(3,2))
B(2,4)=G0*I(3,3)*I(1,3)*(B(3,2)-B(1,3))
B(3,4)=G0*I(1,3)*I(2,3)*(B(1,3)-B(2,2))
B(1,5)=G0*I(2,3)*I(3,3)*(B(2,2)-B(3,3))
B(2,5)=G0*I(3,3)*I(1,3)*(B(3,3)-B(1,2))
B(3,5)=G0*I(1,3)*I(2,3)*(B(1,2)-B(2,3))
```

The six values of e_v from these equations, for the specified value of e_u, are now calculated and assigned to the array, L. These values are repeated for L(7) through L(12) for later calculations (statement 61).

```
      DO 50 R=1,3
      DO 50 S=1,2
      L(R+3*(S-1))=(B(R,S+3)+G(2,R)/K(9))/G(1,R)
      L(R+3*(S+1))=L(R+3*(S-1))
50    CONTINUE
```

To separate these values of e_u into those representing maximum and minimum limits, it is necessary to determine the order of magnitude of the slopes. Six cases are possible, defined by assigning a value to the variable, Q, as follows:

Q	Order
0	B(1,1) ≥ B(2,1) ≥ B(3,1)
1	B(1,1) ≥ B(3,1) > B(2,1)
2	B(3,1) > B(1,1) ≥ B(2,1)
3	B(3,1) > B(2,1) > B(1,1)
4	B(2,1) ≥ B(3,1) > B(1,1)
5	B(2,1) > B(1,1) ≥ B(3,1)

```
      IF (B(1,1)-B(2,1)) 56,51,51
51    IF (B(1,1)-B(3,1)) 55,52,52
52    IF (B(2,1)-B(3,1)) 54,53,53
53    Q=0
      GOTO 61
54    Q=1
      GOTO 61
55    Q=2
      GOTO 61
56    IF (B(2,1)-B(3,1)) 60,57,57
57    IF (B(1,1)-B(3,1)) 59,58,58
58    Q=5
      GOTO 61
59    Q=4
      GOTO 61
60    Q=3
```

The values of e_u corresponding to maximum limits of e_v are then L(1 + Q), L(2 + Q), and L(3 + Q). Those corresponding to minimum limits are L(4 + Q), L(5 + Q), and L(6 + Q). The smallest of the maximum and the largest of the minimum are found by using the Fortran functions, AMIN1 and AMAX1.

```
61      DO 62 R=1,6
        K(R+21)=L(R+Q)
62      CONTINUE
        K(7)=1/AMIN1(K(22),K(23),K(24))
        K(8)=1/AMAX1(K(25),K(26),K(27))
```

The limits of k_v are then typed and a value requested.

```
        IF (N(2)-3) 63,63,64
63      TYPE K(8)," >KV> ",K(7)," LB/IN"
        GOTO 65
64      TYPE K(8)," >KV> ",K(7)," IN-LB/RAD"
65      ACCEPT "KV= ",K(10)
```

The operator then types his choice.

Now, given the values of k_u and k_v, three values of the maximum and minimum limits for k_w can be found directly from the equations, (A-25). The smallest maximum and largest minimum are again selected by the Fortran routines AMIN1 and AMAX1.

```
        DO 66 R=1,3
        K(R+21)=B(R,2)-I(R,1)/(I(R,3)*K(9))+B(R,1)/K(10)
        K(R+24)=K(R+21)+B(R,3)-B(R,2)
66      CONTINUE
        K(7)=1/AMIN1(K(22),K(23),K(24))
        K(8)=1/AMAX1(K(25),K(26),K(27))
```

The limits for k_w are then typed, and an input value is requested.

```
        IF (N(3)-3) 67,67,68
67      TYPE K(8)," >KW> ",K(7)," LB/IN"
        GOTO 69
68      TYPE K(8)," >KW> ",K(7)," IN-LB/RAD"
69      ACCEPT "KW= ",K(11)
```

This choice is then typed by the operator.

The actuator spring constants are now calculated from the three input values and equations, (A-20).

```
        DO 70 R=1,3
        SK(R)=1/(I(R,1)/K(9)+I(R,2)/K(10)+I(R,3)/K(11))
        SK(R+3)=SK(R)
70      CONTINUE
```

These values are then typed by the printer, and control is again transferred to the operator.

```
        WRITE (10,71)
71      FORMAT (17H0SPRING CONSTANTS  //)
        WRITE (10,72) SK(2),SK(3),SK(6)
72      FORMAT ("  K1="F10.2"  K2="F10.2"  K3="F10.2"  LB/IN")
        WRITE (10,73) SK(5),SK(4),SK(1)
73      FORMAT ("  K4="F10.2"  K5="F10.2"  K6="F10.2"  LB/IN")
        Q0=2
        GOTO 28
```

Elastance at Input Coordinate System

The first section of part 3 of the program calculates the full 6 x 6 matrix of elastance values as measured at the input system. As previously described from the Math Model, the impedance (elastance) of the input system is given by

$$Z = AZ_{\ell}A_{t} \tag{A-28}$$

The impedance of the actuators is a diagonal matrix of the individual actuator elastances. The program calculates the input elastance as follows, after which it types the values and returns control to the operator.

```
80      WRITE (10,81)
81      FORMAT (19H0ELASTANCE AT INPUT  //)
        DO 82 R=1,6
        DO 82 S=1,6
        H(R,S)=0.
        DO 82 P=1,6
        H(R,S)=H(R,S)+A(R,P)*A(S,P)/SK(P)
82      CONTINUE
        WRITE (10,83)((H(R,S),S=1,6)R=1,6)
83      FORMAT (6E12.6)
        Q0=3
        GOTO 28
```

Actuator Static Forces and Lengths

The next section, statements 90 to 98 and 207 to 226, calculates the actuator forces due to gravity and the resultant extensions due to the finite spring constants. These extensions are inputed (manually) to the servo systems to return the triogonal system to neutral. This same calculation is used as part of the on-line program (in which the results are inputed to the servo systems automatically) and will be discussed later in detail. Statements 90 to 98 serve to input data required for the off-line calculation and to type out the results. On entering this section, the gimbal pitch and yaw angles are requested.

```
90      TYPE " <15> "
        ACCEPT "GIMBAL PITCH ANGLE: ",X(5,5),
       1 "GIMBAL YAW ANGLE: ",X(6,5)
```

These are typed by the operator, converted to radians, and assigned to the variables A2 and A1. The integer, Q0, is assigned the value 4 to identify the off-line calculation, and N(4) is assigned the value zero to signify that the platform adapter pitch angle is fixed.

```
Q0=4
N(4)=0
A2=DTR*X(5,5)
A1=DTR*X(6,5)
GOTO 207

PARAMETER DTR=.1745329E-1
```

On completing the calculations, the program returns to statement 92, types out the results, and returns control to the operator.

```
92    WRITE (10,93)
93    FORMAT (23H0ACTUATOR STATIC FORCES //)
      WRITE (10,94) ACTF(2),ACTF(3),ACTF(6)
94    FORMAT ("   F1="F9.2"   F2="F9.2"   F3="F9.2"   LB")
      WRITE (10,95) ACTF(5),ACTF(4),ACTF(1)
95    FORMAT ("   F4="F9.2"   F5="F9.2"   F6="F9.2"   LB")
      WRITE (10,96)
96    FORMAT (17H0ACTUATOR LENGTHS  //)
      WRITE (10,97) LGTH(2),LGTH(3),LGTH(6)
97    FORMAT ("   L1="F8.6"   L2="F8.6"   L3="F8.6"   IN")
      WRITE (10,98) LGTH(5),LGTH(4),LGTH(1)
98    FORMAT ("   L4="F8.6"   L5="F8.6"   L6="F8.6"   IN")
      GOTO 28
```

On-Line Program

The remainder of part 3 of the program performs the on-line calculations. On entering this section at statement 200, the operator is queried as to whether the platform adapter pitch angle is fixed or variable.

```
200   WRITE (10,201)
201   FORMAT (16H0ON-LINE PROGRAM  //)
      Q0=5
      ACCEPT "PITCH ANGLE FIXED (0) OR VARIABLE (1) ?",N(4)
```

This is the angle between the platform and the vehicle (platform adapter pitch angle), not the gimbal pitch angle. It will normally be fixed for the helicopter and variable for the combat vehicle. The operator responds with either a zero or one. If zero (fixed angle), the program jumps to statement 206. If one (variable angle), it calculates portions of the matrix, A, not involving the platform adapter pitch angle.

Starting with statement 202, the transformation from input system to platform system is formed. This is the same calculation as in part 2 of the program.

```
        IF (N(4)) 206,206,202
202     CALL ANGLE(E,X,4)
        CALL ROT(W,X,4)
        CALL TRANS(C,E,W,2)
```

The next four statements define the angular transformation for the roll and pitch angles of the vehicle. This is expanded to the 6 x 6 angular transformation

$$D = \left[\begin{array}{c|c} E & 0 \\ \hline 0 & E \end{array}\right] \tag{A-29}$$

```
X(4,8)=X(4,7)
X(5,8)=X(5,7)
X(6,8)=0.
CALL ANGLE(E,X,8)
CALL TRANS(D,E,W,3)
```

The matrices C and D are then multiplied, to produce the matrix, H.

```
CALL MULT(C,D,H,6)
```

The angular transformation for the vehicle yaw angle is next formed.

```
X(4,8)=0.
X(5,8)=0.
X(6,8)=X(6,7)
CALL ANGLE(E,X,8)
```

This is combined with the rotational matrix for the interface location to form the partial transformation, C, which in turn is postmultiplied by the triogonal transformation.

```
CALL ROT(W,X,7)
CALL TRANS(C,E,W,2)
CALL MULT(C,F,H1,6)
```

At this point, statement 206, the program is resumed for fixed as well as variable pitch angle. The three time variable angles, gimbal pitch and yaw, and platform adapter pitch, are next read in by the A/D converter.

```
206   DO 208 R=0,2
A        LDA      0,T.+2,3        ;R
A        DOAS     0,ADCV
A        SKPDN    ADCV
A        JMP      .-1
A        DIC      0,ADCV
A        STA      0,T.+1,3        ;S
      ANG(R+1)=S
208   CONTINUE
```

The DO-loop sequentially sets R equal to 0, 1, and 2. These values are loaded into the A register of the A/D converter (channel number), and the conversion is started. The program waits until the done flag is set, when the converted value is loaded into accumulator zero. This is then temporarily stored in the runtime

stack at the location allocated for the variable, S. Finally, it is assigned to the appropriate element of the array, ANG.

The gimbal pitch and yaw angles are next converted to radians. These are scaled for full scale values of ± 50° in pitch and ± 75° in yaw. Calculation of the gravitational forces follows the development of the Math Model. The basic equation relating the actuator force to the various components which comprise the load is

$$f_\ell = mF_t H_t(x_3, r)\begin{pmatrix} g_v \\ - \\ 0 \end{pmatrix} \tag{A-30}$$

where $H(x_3, r)$ is the transformation from the platform system to the CM of the particular component, F is the triogonal transformation, and g_v is the gravitational vector at the CM of the component. It is given by

$$g_v = E(x_3)\, E(x_{3G})\, g_e \tag{A-31}$$

where x_{3G} is the set of gimbal Euler angles and g_e is the earth's gravitational vector.

$$g_e = \begin{pmatrix} 0 \\ 0 \\ g \end{pmatrix} \tag{A-32}$$

The gravitational vector referred to the gimbal system is

$$g_G = E(x_{3G})\, g_e = g\begin{bmatrix} -\cos\psi_G \sin\theta_G \\ \sin\psi_G \sin\theta_G \\ \cos\theta_G \end{bmatrix} \tag{A-33}$$

Since the rectilinear transformation is given by

$$H(x_3, r) = \left[\begin{array}{c|c} E(x_3) & -W(r)\,E(x_3) \\ \hline 0 & E(x_3) \end{array}\right] \tag{A-34}$$

its transpose is

$$H_t(x_3, r) = \left[\begin{array}{c|c} E'(x_3) & 0 \\ \hline E'(x_3)W(r) & E'(x_3) \end{array}\right] \tag{A-35}$$

Equation 30 can then be simplified to

$$f_\ell = mF_t \left[\begin{array}{c|c} 1 & 0 \\ \hline E'(x_3)\ W(r)\ E(x_3) & 1 \end{array}\right] \begin{pmatrix} g_G \\ \hline 0 \end{pmatrix} \tag{A-36}$$

or

$$f_\ell = mF_t \left[\begin{array}{c} 1 \\ \hline W[E'(x_3)r] \end{array}\right] g_G \tag{A-37}$$

as measured in the platform system, the forces and moments are

$$f_p = m \left[\begin{array}{c} 1 \\ \hline W[E'(x_3)\ r] \end{array}\right] g_G \tag{A-38}$$

Thus, the three forces are simply

$$\begin{pmatrix} f_x \\ f_y \\ f_z \end{pmatrix} = mg_G \tag{A-39}$$

and the moments are

$$\begin{pmatrix} m_\phi \\ m_\theta \\ m_\psi \end{pmatrix} = mW\ [E'(x_3)\ r]\ g_G \tag{A-40}$$

The gimbal gravitational unit vector is calculated first. This is assigned to the first three elements of the second row of the matrix, B.

```
      A2=ANG(1)/2346.835
      A1=ANG(2)/1564.557
207   CA1=COS(A1)
      SA1=SIN(A1)
      SA2=SIN(A2)
      B(2,1)=-CA1*SA2
      B(2,2)=SA1*SA2
      B(2,3)=COS(A2)
```

At this point, the program jumps to statement 219 if the pitch angle is fixed; otherwise, it continues with statement 211. Statements 211 to 219 complete

the calculation of the A matrix, using the variable pitch angle, ANG(3). New values of actuator spring constant are then calculated to reflect the change in pitch angle.

The platform adapter pitch angle, as measured by the A/D converter is first converted to degrees. Full scale represents ± 15 degrees. The angular transformation for this value is then formed and the full 6 x 6 angular transformation is generated.

```
      IF (N(4)) 219,219,211
211   A3=ANG(3)/136.5333
      X(5,8)=A3
      X(6,8)=Ø.
      CALL ANGLE(E,X,8)
      CALL TRANS(C,E,W,3)
```

This is then postmultiplied by the matrix, H1, and premultiplied by the matrix, H, to form the matrix A which is used for time varying pitch angles. The corresponding G matrix and its inverse are then also calculated.

```
      CALL MULT(C,H1,D,6)
      CALL MULT(H,D,A,6)
      DO 213 R=1,3
      DO 213 S=1,3
      G(R,S)=A(N(R),S)*A(N(R),S)+A(N(R),S+3)*A(N(R),S+3)
213   CONTINUE
      CALL INV(I,G,GØ)
```

The new values of actuator spring constant are calculated from this matrix, I, and the previously inputed spring constants for the input system. If the variable pitch angle forces the actuator spring constants to exceed their physical limits, they are modified to these values.

```
      DO 214 R=1,3
      SK(R)=1/(I(R,1)/K(9)+I(R,2)/K(1Ø)+I(R,3)/K(11))
214   CONTINUE
      DO 25Ø R=1,3
      IF (SK(R)-K(R+15)) 216,216,215
215   SK(R)=K(R+15)
216   IF (SK(R)-K(R+9)) 217,218,218
217   SK(R)=K(R+9)
218   SK(R+3)=SK(R)
25Ø   CONTINUE
```

At this point, the measured platform adapter pitch angle is added to the fixed value previously typed in during part 1. This allows for any initial pitch angle between the vehicle coordinate system and the platform system, when the platform adapter pitch angle, as measured by the A/D converter, is zero. This initial value must be inputed in part 1 before going to the on-line program, in response to the query: "Platform Adapter Euler Angles." If the pitch angle is fixed, statement 219 selects only the fixed value from part 1.

```
      A2=X(5,7)+A3
      GOTO 220
219   A2=X(5,7)
```

From this point on, the program continues for both fixed and variable pitch angles. For fixed angles, it uses the values of actuator spring constant calculated in part 2.

The transpose of the angular transformation from platform to interface

```
220   X(4,8)=X(4,7)
      X(5,8)=A2
      X(6,8)=X(6,7)
      CALL ANGLE(E,X,8)
```

is postmultiplied by the distance from the interface origin to the vehicle CM, and the result added to the distance from the platform to the interface.

```
      CALL DIST(E,X(1,3),X(2,3),X(3,3),X(1,8),X(2,8),X(3,8))
      DO 221 R=1,3
      X(R,8)=X(R,8)+X(R,7)
221   CONTINUE
```

This gives the distance from the platform to the vehicle CM in platform coordinates which is shown as

$$r = E' \; (x_{3V}) \; r_V + r_I \tag{A-41}$$

The rotational matrix of this is then formed.

```
      CALL ROT(W,X,8)
```

When multiplied by the gimbal gravitational vector and the weight of the vehicle, this will give the platform moments due to the vehicle. Multiplying the gimbal gravitational vector by the weight of the vehicle gives the platform forces. These forces and moments are stored in the array, PLF.

```
      DO 233 R=1,6
      PLF(R)=0.
233   CONTINUE
      Q=3
223   CALL DIST(-W,B(2,1),B(2,2),B(2,3),B(2,4),B(2,5),B(2,6))
      DO 222 R=1,6
      PLF(R)=PLF(R)+B(2,R)*WGT(Q)
222   CONTINUE
```

The integer, Q, equal to 3 identifies the vehicle in the above equations. It is now decremented by one to the value 2, and the rotational matrix for the platform adapter is formed.

```
      Q=Q-1
      IF (Q) 224,235,234
234   CALL ROT(W,Y,Q)
      GOTO 223
```

The program then loops back to statement 223. This causes the contribution of the platform adapter to be added to the platform forces and moments. The integer, Q, is again decremented by one to the value one (signifying the platform) and the program loops once more. This adds the contribution of the platform.

At this point, Q is decremented to zero, and the program jumps to statement 235. This adds the contribution of the actuators, decrements the value of Q to minus one and jumps to statement 224.

```
235    X(1,8)=0.
       X(2,8)=0.
       X(3,8)=ALOC
       CALL ROT(W,X,8)
       WGT(0)=AWGT
       GOTO 223

       DATA AWGT,ALOC/529.2845,-13.22399/
```

The platform forces and moments are now multiplied by the triogonal transformation to give the actuator forces.

```
224    DO 226 R=1,6
       ACTF(R)=0.
       DO 255 S=1,6
       ACTF(R)=ACTF(R)+F(S,R)*PLF(S)
255    CONTINUE
```

These are divided by the actuator spring constants to give the actuator extensions.

```
       LGTH(R)=ACTF(R)/SK(R)
226    CONTINUE
```

At this point, if the variable, Q0, is equal to 4, which signifies the off-line calculation, the program returns to statement 92. Otherwise it continues. To output the data in the order in which the actuators are pysically numbered, the index, R, is equated sequentially to the values stored in the array ACTN.

```
       IF (Q0-4) 256,92,256
256    DO 246 S=1,6
       R=ACTN(S)
```

The range of the spring constants is now determined. If it is equal to or greater than 10,000 lb/in., the program jumps to statement 228; otherwise, the value is scaled for a full scale value of 10,000 and stored in the array, IVAL. The corresponding bit of the variable, RANGE, is cleared, to indicate that this value is measured with the low range. If the spring constant is greater than 10,000, it is scaled for a full scale value of 200,000 lb/in., and the corresponding bit of RANGE is set to one.

```
      IF (SK(R)-10000.) 227,228,228
227   IVAL(R+1)=.4096*SK(R)
      CALL ICLR(RANGE,S)
      GOTO 229
228   IVAL(R+1)=.02048*SK(R)
      CALL ISET(RANGE,S)
```

The six least significant bits of the variable, RANGE, are used to indicate range values. The first, bit 15, applies to actuator number one. The sixth, bit 10, applies to actuator number 6.

As a precaution against exceeding the D/A input range due to converting from real to integer values, the integer result is checked against the full scale input values.

```
229   IF (IVAL(R+1)-7777K) 240,240,230
230   IVAL(R+1)=7777K
```

The actuator lengths are then scaled to a full scale value of ± 5 inches, and again, the integer values limited to the full scale input values.

```
240   IVAL(R+7)=-409.6*LGTH(R)
      IF (IVAL(R+7)-3777K) 242,242,241
241   IVAL(R+7)=3777K
242   IF (IVAL(R+7)-174000K) 243,244,244
243   IVAL(R+7)=174000K
```

Next, the mass load inputs to the servos are calculated, scaled to a full scale value of 1.5 lb sec^2/in., and limited to the maximum permissible value.

```
244   IVAL(R+13)=-3072/M(R,R)
      IF (IVAL(R+13)-174000K) 245,246,246
245   IVAL(R+13)=174000K
246   CONTINUE
```

After all six spring constant ranges have been established in the DO-loop terminated by statement 246, the variable, RANGE, is stored in the first element of IVAL.

```
      IVAL(1)=RANGE
```

The 19 values in the array, IVAL, are then outputed to the D/A converter, using the integer S (for which the location in the run-time stack is known) as temporary storage, both for the subaddress and for the data. Initially, the D/A subaddress is loaded into the D/A "A" register.

```
                DO 249 R=1,19
                S=IADDR(R)
      A           DOA       0,65

      DATA IADDR/21K,224K,22K,222K,24K,223K,23K,227K,25K,225K,
     1 27K,226K,26K,232K,30K,230K,32K,231K,31K/
```

These are loaded in the order:

DIOS SLOT NO.	FUNCTION
5	RANGE
11B	k_6
7A	k_1
7B	k_2
11A	k_5
9B	k_4
9A	k_3
17B	ℓ_6
13A	ℓ_1
13B	ℓ_2
17A	ℓ_5
15B	ℓ_4
15A	ℓ_3
23B	m_6
19A	m_1
19B	m_2
23A	m_5
21B	m_4
21A	m_3

Physically, the D/A outputs are arranged in the same order as the actuators are numbered. The data is updated in the order in which calculations are performed (symmetrical system).

Next the data is loaded into the D/A "B" register.

```
        S=IVAL(R)
A        DOB      Ø,65
249     CONTINUE
```

The Fortran compiler automatically loads the value of S into accumulator zero before storing it in the run-time stack when executing the instructions

```
S = IADDR(R)
```

and

```
S = IVAL(R)
```

Thus, there is no need to load accumulator zero with these values again, before outputing it to the D/A converter (device code 65).

This completes the on-line routine, except to loop back to the beginning (statement 206) to start another cycle. The escape routine

```
A        SKPDN   TTI
A        JMP     LOOP
A        NIOC    TTI
       GOTO 28
```

allows the operator to break the loop and regain control, by stiking any key on the teletype. This sets the "done" flag causing the program to jump to statement 28, after clearing the teletype. If the "done" flag has not been set, the program jumps to the label "LOOP", which returns the program to statement 206.

```
A LOOP:
       GOTO 206
       END
```

```
C        MAIN PROGRAM - 6 DOF SIMULATOR (RIA) - PART 1
      PARAMETER DTR=.1745329E-1
      COMMON/FXV/F(6,6),AM(6,6),AWGT,ALOC,IADDR(19),ACTN(6)
      DIMENSION A(6,6),ACTF(6),B(3,6),C(6,6),D(6,6),
     1 E(3,3),G(3,3),H(6,6),H1(6,6),H2(3,3),I(3,3),IVAL(19),
     2 J(3,3),K(27),L(12),LGTH(6),M(6,6),MOI(6,3),N(4),
     3 PLF(6),ANG(3),SK(6),W(3,3),WGT(0:3),X(6,8)
      INTEGER ANG,Q,Q0,P,R,S,ACTN,RANGE
      REAL I,J,K,L,LGTH,M,MOI
      EXTERNAL MULT,ROT,ANGLE,INERTIA,INV,DIST,ISET,ICLR,
     1 TRANS,TRNSP,ZERO,UNIT
      DATA F/5.107058E-2,-.530741,.2156135,3.685701E-3,
     1 -1.347696E-2,-8.511763E-3,-.4851705,-.2211421,.2156135,
     2 1.351424E-2,3.546568E-3,8.511763E-3,.4340999,.3095989,
     3 .2156135,9.828537E-3,9.93039E-3,-8.511763E-3,
     4 5.107058E-2,.530741,.2156135,-3.685701E-3,-1.347696E-2,
     5 8.511763E-3,-.4851705,.2211421,.2156135,-1.351424E-2,
     6 3.546568E-3,-8.511763E-3,.4340999,-.3095989,.2156135,
     7 -9.828537E-3,9.93039E-3,8.511763E-3/
      DATA AM/1.90045,3*0.,.7996739,2*0.,1.90045,0.,-.7996739,
     1 4*0.,1.658009,4*0.,-.7996739,0.,813.2535,2*0.,.7996739,
     2 3*0.,813.2535,6*0.,1750.554/
      DATA AWGT,ALOC/529.2845,-13.22399/
      DATA IADDR/21K,224K,22K,222K,24K,223K,23K,227K,25K,225K,
     1 27K,226K,26K,232K,30K,230K,32K,231K,31K/
      DATA ACTN/2,3,6,5,4,1/
      TYPE "           SIX DOF SIMULATOR <15> "
 28   TYPE " <15> "
      ACCEPT "*",Q
      IF (Q-1) 28,231,29
 29   IF (Q-Q0-1) 231,231,232
232   IF (Q-6) 28,231,28
231   GOTO (2,30,80,90,200) Q
  2   WRITE (10,4)
  4   FORMAT (15H0CONFIGURATION  //)
      ACCEPT "LOCATION OF CM <15>","  PLATFORM: <15>",
     1 (X(R,1),R=1,3),"  PLATFORM ADAPTER: <15>",(X(R,2),R=1,3),
     2 "   VEHICLE: <15>",(X(R,3),R=1,3),"PLATFORM ADAPTER <15>",
     3 "   LOCATION OF VEHICLE INTERFACE: <15>",(X(R,7),R=1,3),
     4 "   EULER ANGLES: <15>",(X(R,7),R=4,6),"WEIGHTS <15>",
     5 "   PLATFORM: ",WGT(1),"  PLATFORM ADAPTER: ",WGT(2),
     6 "   VEHICLE: ",WGT(3),"MOMENTS OF INERTIA <15>",
     7 "   PLATFORM: <15>",(MOI(R,1),R=1,6),
     8 "   PLATFORM ADAPTER: <15>",(MOI(R,2),R=1,6),
     9 "   VEHICLE: <15>",(MOI(R,3),R=1,6)
```

```
      DO 6 R=1,6
      DO 6 S=1,6
      M(R,S)=AM(R,S)
 6    CONTINUE
      CALL ROT(W,X,3)
      CALL ANGLE(E,X,7)
      CALL TRANS(C,E,W,1)
      CALL ROT(W,X,7)
      CALL UNIT(E)
      CALL TRANS(D,E,W,1)
      CALL MULT(C,D,H,6)
      Q=3
11    CALL INERTIA(J,MOI,Q)
      CALL ZERO(C,6)
      DO 14 R=1,3
      DO 14 S=1,3
      C(R+3,S+3)=J(R,S)
      IF (R-S) 14,12,14
12    C(R,S)=WGT(Q)/386.Ø63
14    CONTINUE
      CALL MULT(C,H,H1,6)
      CALL TRNSP(C,H,6)
      CALL MULT(C,H1,H,6)
      DO 16 R=1,6
      DO 16 S=1,6
      M(R,S)=M(R,S)+H(R,S)
16    CONTINUE
      Q=Q-1
      IF (Q) 21,21,17
17    CALL ROT(W,X,Q)
      CALL UNIT(E)
      CALL TRANS(H,E,W,1)
      GOTO 11
21    CALL TRNSP(C,F,6)
      CALL MULT(C,M,H,6)
      CALL MULT(H,F,M,6)
      DO 23 R=1,6
      DO 23 S=1,6
      H1(R,S)=M(ACTN(R),ACTN(S))
23    CONTINUE
      WRITE (1Ø,24)((H1(R,S),S=1,6)R=1,6)
24    FORMAT (4ØHØACTUATOR LOAD MASS MATRIX (LB-SEC↑2/IN)  //
     1 (6F1Ø.4))
      QØ=1
      GOTO 28
```

```
C        MAIN PROGRAM - PART 2
 30     TYPE " <15> "
        DO 35 R=1,6
        K(R+15)=3947.842*M(R,R)
        K(R+9)=K(R+15)/1500
        IF (K(R+15)-2.0E5) 33,33,32
32      K(R+15)=2.0E5
 33     IF (K(R+9)-250.) 34,35,35
 34     K(R+9)=250.
35      CONTINUE
        DO 39 R=1,3
        IF (K(R+15)-K(R+18)) 37,37,36
36      K(R+15)=K(R+18)
37      IF (K(R+9)-K(R+12)) 38,39,39
38      K(R+9)=K(R+12)
39      CONTINUE
        ACCEPT "ORIGIN OF INPUT SYSTEM: ",(X(R,4),R=1,3),
       1 "EULER ANGLES OF INPUT SYSTEM: ",(X(R,4),R=4,6)
        CALL ANGLE(E,X,4)
        CALL ROT(W,X,4)
        CALL TRANS(C,E,W,2)
        CALL ANGLE(E,X,7)
        CALL ROT(W,X,7)
        CALL TRANS(D,E,W,2)
        CALL MULT(C,D,H,6)
        CALL MULT(H,F,A,6)
        WRITE (10,42)
42      FORMAT (12H0INPUT AXES= ,Z)
        READ (11) N(1),N(2),N(3)
        DO 43 R=1,3
        DO 43 S=1,3
        G(R,S)=A(N(R),S)*A(N(R),S)+A(N(R),S+3)*A(N(R),S+3)
43      CONTINUE
        CALL INV(I,G,G0)
        K(7)=1/(G(1,1)/K(10)+G(1,2)/K(11)+G(1,3)/K(12))
        K(8)=1/(G(1,1)/K(16)+G(1,2)/K(17)+G(1,3)/K(18))
        IF (N(1)-3) 44,44,45
44      TYPE K(8)," >KU> ",K(7)," LB/IN"
        GOTO 46
45      TYPE K(8)," >KU> ",K(7)," IN-LB/RAD"
46      ACCEPT "KU= ",K(9)
        DO 49 R=1,3
        B(R,1)=-I(R,2)/I(R,3)
        IF (I(R,3)) 48,47,47
47      B(R,2)=1/(K(R+9)*I(R,3))
        B(R,3)=1/(K(R+15)*I(R,3))
        GOTO 49
48      B(R,2)=1/(K(R+15)*I(R,3))
        B(R,3)=1/(K(R+9)*I(R,3))
49      CONTINUE
        B(1,4)=G0*I(2,3)*I(3,3)*(B(2,3)-B(3,2))
        B(2,4)=G0*I(3,3)*I(1,3)*(B(3,2)-B(1,3))
        B(3,4)=G0*I(1,3)*I(2,3)*(B(1,3)-B(2,2))
        B(1,5)=G0*I(2,3)*I(3,3)*(B(2,2)-B(3,3))
        B(2,5)=G0*I(3,3)*I(1,3)*(B(3,3)-B(1,2))
        B(3,5)=G0*I(1,3)*I(2,3)*(B(1,2)-B(2,3))
```

```
      DO 50 R=1,3
      DO 50 S=1,2
      L(R+3*(S-1))=(B(R,S+3)+G(2,R)/K(9))/G(1,R)
      L(R+3*(S+1))=L(R+3*(S-1))
50    CONTINUE
      IF (B(1,1)-B(2,1)) 56,51,51
51    IF (B(1,1)-B(3,1)) 55,52,52
52    IF (B(2,1)-B(3,1)) 54,53,53
53    Q=0
      GOTO 61
54    Q=1
      GOTO 61
55    Q=2
      GOTO 61
56    IF (B(2,1)-B(3,1)) 60,57,57
57    IF (B(1,1)-B(3,1)) 59,58,58
58    Q=5
      GOTO 61
59    Q=4
      GOTO 61
60    Q=3
61    DO 62 R=1,6
      K(R+21)=L(R+Q)
62    CONTINUE
      K(7)=1/AMIN1(K(22),K(23),K(24))
      K(8)=1/AMAX1(K(25),K(26),K(27))
      IF (N(2)-3) 63,63,64
63    TYPE K(8)," >KV> ",K(7)," LB/IN"
      GOTO 65
64    TYPE K(8)," >KV> ",K(7)," IN-LB/RAD"
65    ACCEPT "KV= ",K(10)
      DO 66 R=1,3
      K(R+21)=B(R,2)-I(R,1)/(I(R,3)*K(9))+B(R,1)/K(10)
      K(R+24)=K(R+21)+B(R,3)-B(R,2)
66    CONTINUE
      K(7)=1/AMIN1(K(22),K(23),K(24))
      K(8)=1/AMAX1(K(25),K(26),K(27))
      IF (N(3)-3) 67,67,68
67    TYPE K(8)," >KW> ",K(7)," LB/IN"
      GOTO 69
68    TYPE K(8)," >KW> ",K(7)," IN-LB/RAD"
69    ACCEPT "KW= ",K(11)
      DO 70 R=1,3
      SK(R)=1/(I(R,1)/K(9)+I(R,2)/K(10)+I(R,3)/K(11))
      SK(R+3)=SK(R)
70    CONTINUE
      WRITE (10,71)
71    FORMAT (17H05PRING CONSTANTS  //)
      WRITE (10,72) SK(2),SK(3),SK(6)
72    FORMAT ("  K1="F10.2"  K2="F10.2"  K3="F10.2"  LB/IN")
      WRITE (10,73) SK(5),SK(4),SK(1)
73    FORMAT ("  K4="F10.2"  K5="F10.2"  K6="F10.2"  LB/IN")
      Q0=2
      GOTO 28
```

```
C        MAIN PROGRAM - PART 3
 80    WRITE (10,81)
 81    FORMAT (19H0ELASTANCE AT INPUT  //)
       DO 82 R=1,6
       DO 82 S=1,6
       H(R,S)=0.
       DO 82 P=1,6
       H(R,S)=H(R,S)+A(R,P)*A(S,P)/SK(P)
 82    CONTINUE
       WRITE (10,83)((H(R,S),S=1,6)R=1,6)
 83    FORMAT (6E12.6)
       Q0=3
       GOTO 28
 90    TYPE " <15> "
       ACCEPT "GIMBAL PITCH ANGLE: ",X(5,5),
      1 "GIMBAL YAW ANGLE: ",X(6,5)
       Q0=4
       N(4)=0
       A2=DTR*X(5,5)
       A1=DTR*X(6,5)
       GOTO 207
 92    WRITE (10,93)
 93    FORMAT (23H0ACTUATOR STATIC FORCES //)
       WRITE (10,94) ACTF(2),ACTF(3),ACTF(6)
 94    FORMAT ("  F1="F9.2"  F2="F9.2"  F3="F9.2"  LB")
       WRITE (10,95) ACTF(5),ACTF(4),ACTF(1)
 95    FORMAT ("  F4="F9.2"  F5="F9.2"  F6="F9.2"  LB")
       WRITE (10,96)
 96    FORMAT (17H0ACTUATOR LENGTHS  //)
       WRITE (10,97) LGTH(2),LGTH(3),LGTH(6)
 97    FORMAT ("  L1="F8.6"  L2="F8.6"  L3="F8.6"  IN")
       WRITE (10,98) LGTH(5),LGTH(4),LGTH(1)
 98    FORMAT ("  L4="F8.6"  L5="F8.6"  L6="F8.6"  IN")
       GOTO 28
200    WRITE (10,201)
201    FORMAT (16H0ON-LINE PROGRAM  //)
       Q0=5
       ACCEPT "PITCH ANGLE FIXED (0) OR VARIABLE (1) ?",N(4)
       IF (N(4)) 206,206,202
202    CALL ANGLE(E,X,4)
       CALL ROT(W,X,4)
       CALL TRANS(C,E,W,2)
       X(4,8)=X(4,7)
       X(5,8)=X(5,7)
       X(6,8)=0.
       CALL ANGLE(E,X,8)
       CALL TRANS(D,E,W,3)
       CALL MULT(C,D,H,6)
       X(4,8)=0.
       X(5,8)=0.
       X(6,8)=X(6,7)
       CALL ANGLE(E,X,8)
       CALL ROT(W,X,7)
       CALL TRANS(C,E,W,2)
       CALL MULT(C,F,H1,6)
```

```
206     DO 208 R=Ø,2
A         LDA      Ø,T.+2,3          ;R
A         DOAS     Ø,ADCV
A         SKPDN    ADCV
A         JMP      .-1
A         DIC      Ø,ADCV
A         STA      Ø,T.+1,3          ;S
        ANG(R+1)=S
208     CONTINUE
        A2=ANG(1)/2346.835
        A1=ANG(2)/1564.557
207     CA1=COS(A1)
        SA1=SIN(A1)
        SA2=SIN(A2)
        B(2,1)=-CA1*SA2
        B(2,2)=SA1*SA2
        B(2,3)=COS(A2)
        IF (N(4)) 219,219,211
211     A3=ANG(3)/136.5333
        X(5,8)=A3
        X(6,8)=Ø.
        CALL ANGLE(E,X,8)
        CALL TRANS(C,E,W,3)
        CALL MULT(C,H1,D,6)
        CALL MULT(H,D,A,6)
        DO 213 R=1,3
        DO 213 S=1,3
        G(R,S)=A(N(R),S)*A(N(R),S)+A(N(R),S+3)*A(N(R),S+3)
213     CONTINUE
        CALL INV(I,G,GØ)
        DO 214 R=1,3
        SK(R)=1/(I(R,1)/K(9)+I(R,2)/K(1Ø)+I(R,3)/K(11))
214     CONTINUE
        DO 25Ø R=1,3
        IF (SK(R)-K(R+15)) 216,216,215
215     SK(R)=K(R+15)
216     IF (SK(R)-K(R+9)) 217,218,218
217     SK(R)=K(R+9)
218     SK(R+3)=SK(R)
25Ø     CONTINUE
        A2=X(5,7)+A3
        GOTO 22Ø
219     A2=X(5,7)
22Ø     X(4,8)=X(4,7)
        X(5,8)=A2
        X(6,8)=X(6,7)
        CALL ANGLE(E,X,8)
        CALL DIST(E,X(1,3),X(2,3),X(3,3),X(1,8),X(2,8),X(3,8))
        DO 221 R=1,3
        X(R,8)=X(R,8)+X(R,7)
221     CONTINUE
        CALL ROT(W,X,8)
```

```
      DO 233 R=1,6
      PLF(R)=0.
233   CONTINUE
      Q=3
223   CALL DIST(-W,B(2,1),B(2,2),B(2,3),B(2,4),B(2,5),B(2,6))
      DO 222 R=1,6
      PLF(R)=PLF(R)+B(2,R)*WGT(Q)
222   CONTINUE
      Q=Q-1
      IF (Q) 224,235,234
234   CALL ROT(W,X,Q)
      GOTO 223
235   X(1,8)=0.
      X(2,8)=0.
      X(3,8)=ALOC
      CALL ROT(W,X,8)
      WGT(0)=AWGT
      GOTO 223
224   DO 226 R=1,6
      ACTF(R)=0.
      DO 255 S=1,6
      ACTF(R)=ACTF(R)+F(S,R)*PLF(S)
255   CONTINUE
      LGTH(R)=ACTF(R)/SK(R)
226   CONTINUE
      IF (Q0-4) 256,92,256
256   DO 246 S=1,6
      R=ACTN(S)
      IF (SK(R)-10000.) 227,228,228
227   IVAL(R+1)=.4096*SK(R)
      CALL ICLR(RANGE,S)
      GOTO 229
228   IVAL(R+1)=.02048*SK(R)
      CALL ISET(RANGE,S)
229   IF (IVAL(R+1)-7777K) 240,240,230
230   IVAL(R+1)=7777K
240   IVAL(R+7)=-409.6*LGTH(R)
      IF (IVAL(R+7)-3777K) 242,242,241
241   IVAL(R+7)=3777K
242   IF (IVAL(R+7)-174000K) 243,244,244
243   IVAL(R+7)=174000K
244   IVAL(R+13)=-3072/M(R,R)
      IF (IVAL(R+13)-174000K) 245,246,246
245   IVAL(R+13)=174000K
246   CONTINUE
      IVAL(1)=RANGE
      DO 249 R=1,19
      S=IADDR(R)
A       DOA      0,65
      S=IVAL(R)
A       DOB      0,65
249   CONTINUE
A       SKPDN    TTI
A       JMP      LOOP
A       NIOC     TTI
      GOTO 28
A LOOP:
      GOTO 206
      END
```

```
      SUBROUTINE TRANS(C,E,W,Q)
      DIMENSION C(6,6),E(3,3),W(3,3),H(3,3)
      INTEGER Q,R,S
      EXTERNAL MULT,ZERO
      GOTO (1,2,3) Q
1     CALL MULT(W,E,H,3)
      GOTO 4
2     CALL MULT(E,W,H,3)
      GOTO 4
3     CALL ZERO(H,3)
4     DO 5 R=1,3
      DO 5 S=1,3
      C(R,S)=E(R,S)
      C(R+3,S)=0.
      C(R,S+3)=-H(R,S)
      C(R+3,S+3)=E(R,S)
5     CONTINUE
      RETURN
      END

      SUBROUTINE TRNSP(C,D,Q)
      INTEGER Q,R,S
      DIMENSION C(Q,Q),D(Q,Q)
      DO 1 R=1,Q
      DO 1 S=1,Q
      C(R,S)=D(S,R)
1     CONTINUE
      RETURN
      END

      SUBROUTINE ZERO(E,Q)
      INTEGER Q,R,S
      DIMENSION E(Q,Q)
      DO 1 R=1,Q
      DO 1 S=1,Q
      E(R,S)=0.
1     CONTINUE
      RETURN
      END

      SUBROUTINE MULT(C1,D1,H5,Q)
      INTEGER P,Q,R,S
      DIMENSION C1(Q,Q),D1(Q,Q),H5(Q,Q)
      DO 1 R=1,Q
      DO 1 S=1,Q
      H5(R,S)=0.
      DO 1 P=1,Q
      H5(R,S)=H5(R,S)+C1(R,P)*D1(P,S)
1     CONTINUE
      RETURN
      END
```

```
      SUBROUTINE ROT(W,X,Q)
      INTEGER Q
      DIMENSION W(3,3),X(6,8)
      W(1,1)=0.
      W(2,1)=X(3,Q)
      W(3,1)=-X(2,Q)
      W(1,2)=-X(3,Q)
      W(2,2)=0.
      W(3,2)=X(1,Q)
      W(1,3)=X(2,Q)
      W(2,3)=-X(1,Q)
      W(3,3)=0.
      RETURN
      END

      SUBROUTINE INERTIA(J,MOI,Q)
      INTEGER Q
      DIMENSION J(3,3),MOI(6,3)
      J(1,1)=MOI(1,Q)
      J(2,1)=MOI(4,Q)
      J(3,1)=MOI(5,Q)
      J(1,2)=MOI(4,Q)
      J(2,2)=MOI(2,Q)
      J(3,2)=MOI(6,Q)
      J(1,3)=MOI(5,Q)
      J(2,3)=MOI(6,Q)
      J(3,3)=MOI(3,Q)
      RETURN
      END

      SUBROUTINE INV(I,G,G2)
      INTEGER R,S
      REAL I
      DIMENSION I(3,3),G(3,3),H(6,6)
      DO 1 R=1,3
      DO 1 S=1,3
      H(R,S)=G(R,S)
      H(R+3,S)=G(R,S)
      H(R,S+3)=G(R,S)
      H(R+3,S+3)=G(R,S)
1     CONTINUE
      DO 2 R=1,3
      DO 2 S=1,3
      I(4-S,4-R)=H(2*R-1,2*S-1)*H(2*R,2*S)-H(2*R-1,2*S)*H(2*R,2*S-1)
2     CONTINUE
      G2=I(1,1)*G(1,1)+I(2,1)*G(1,2)+I(3,1)*G(1,3)
      DO 3 R=1,3
      DO 3 S=1,3
      I(R,S)=I(R,S)/G2
3     CONTINUE
      RETURN
      END
```

```
      SUBROUTINE DIST(E1,X1,Y1,Z1,XØ,YØ,ZØ)
      DIMENSION E1(3,3)
      XØ=E1(1,1)*X1+E1(2,1)*Y1+E1(3,1)*Z1
      YØ=E1(1,2)*X1+E1(2,2)*Y1+E1(3,2)*Z1
      ZØ=E1(1,3)*X1+E1(2,3)*Y1+E1(3,3)*Z1
      RETURN
      END

      SUBROUTINE ANGLE(E,X,Q)
      INTEGER Q
      DIMENSION E(3,3),X(6,8)
      DTR=1.745329E-2
      PHI=DTR*X(4,Q)
      THETA=DTR*X(5,Q)
      PSI=DTR*X(6,Q)
      SPHI=SIN(PHI)
      CPHI=COS(PHI)
      STHETA=SIN(THETA)
      CTHETA=COS(THETA)
      SPSI=SIN(PSI)
      CPSI=COS(PSI)
      E(1,1)=CTHETA*CPSI
      E(2,1)=SPHI*STHETA*CPSI-CPHI*SPSI
      E(3,1)=CPHI*STHETA*CPSI+SPHI*SPSI
      E(1,2)=CTHETA*SPSI
      E(2,2)=CPHI*CPSI+SPHI*STHETA*SPSI
      E(3,2)=CPHI*STHETA*SPSI-SPHI*CPSI
      E(1,3)=-STHETA
      E(2,3)=SPHI*CTHETA
      E(3,3)=CPHI*CTHETA
      RETURN
      END

      SUBROUTINE UNIT(E)
      INTEGER R
      DIMENSION E(3,3)
      EXTERNAL ZERO
      CALL ZERO(E,3)
      DO 1 R=1,3
      E(R,R)=1.
1     CONTINUE
      RETURN
      END
```

APPENDIX B
6-DOF MATH MODEL
ACTUATOR LOAD MASS DUE TO ACTUATORS

EFFECTIVE MASS OF ACUTATORS

Because of the motion of the platform, the actuators experience not only motion in their axial direction, but also motion in the transverse direction and rotation about the upper pivot point. Since they have finite mass and moments of inertia, this motion requires forces to be exerted by the platform on the actuators. Since each actuator can provide only axial forces, the nonaxial forces must be provided by the other five actuators.

To derive an expression for the mass load of the actuator system upon itself, it is necessary to first determine the actuator motion in terms of the platform motion. This then determines the forces exerted on each actuator which can then be translated into the platform coordinate system and summed for all six actuators. Then by transforming the impedance of the platform into the triogonal coordinate system, the equivalent mass load on each actuator can be found.

To determine the forces exerted on the individual actuator, it is necessary to determine the linear and angular velocities. For this purpose, a coordinate system will be affixed to each actuator with the x axis along the actuator axis. An angular transformation will be defined, $E(x_3)$, which rotates the platform axes into each of these systems. Then, since the projection of a unit vector along the actuator into the platform system must yield the direction cosines, we have

$$\begin{pmatrix} 1 \\ 0 \\ 0 \end{pmatrix} = E(x_3)\delta \tag{B-1}$$

or

$$\delta = E'(x_3) \begin{pmatrix} 1 \\ 0 \\ 0 \end{pmatrix} \tag{B-2}$$

where the direction cosines are

$$\delta = \begin{pmatrix} \alpha \\ \beta \\ \gamma \end{pmatrix} \tag{B-3}$$

For the conventional order of rotation, the angular transformation is

$$E'(x_3) = E_1'(\psi)\ E_2'(\theta)\ E_3'(\phi) \tag{B-4}$$

It then follows that the direction cosines are equal to

$$\delta = \begin{bmatrix} \cos\psi \cos\theta \\ \sin\psi \cos\theta \\ -\sin\theta \end{bmatrix} \tag{B-5}$$

These equations can be solved for the pitch and yaw angles to give

$$\begin{aligned} \sin\theta &= -\gamma \\ \cos\theta &= \sqrt{1-\gamma^2} \\ \sin\psi &= \beta/\sqrt{1-\gamma^2} \\ \cos\psi &= \alpha/\sqrt{1-\gamma^2} \end{aligned} \tag{B-6}$$

By differentiating these, we have

$$\begin{aligned} \dot{\theta} &= -\mathring{\gamma}/\sqrt{1-\gamma^2} \\ \dot{\psi} &= (\alpha\mathring{\beta} - \beta\mathring{\alpha})/(1-\gamma^2) \end{aligned} \tag{B-7}$$

The angular velocities of the actuator are

$$\dot{x}_2 = G'(x_3)\,\mathring{x}_3 \tag{B-8}$$

or

$$\dot{x}_3 = G(x_3)\,\mathring{x}_2 \tag{B-9}$$

where

$$G(x_3) = \begin{bmatrix} 1 & \sin\phi\tan\theta & \cos\phi\tan\theta \\ 0 & \cos\phi & -\sin\phi \\ 0 & \sin\phi\sec\theta & \cos\phi\sec\theta \end{bmatrix} \tag{B-10}$$

Since the actuators are mounted to the gimbal system and platform by means of ball joints, no axial torque can be applied to either the cylinder or piston. Then the roll velocity is zero which is shown as

$$p = 0 \tag{B-11}$$

The time derivatives of the Euler Angles are then

$$\dot{\phi} = q \sin \phi \tan \theta + r \cos \phi \tan \theta$$

$$\dot{\theta} = q \cos \phi - r \sin \phi$$

$$\dot{\psi} = (q \sin \phi + r \cos \phi) \sec \theta \tag{B-12}$$

Thus

$$\dot{\phi} = \dot{\psi} \sin \theta = - \gamma\dot{\psi} \tag{B-13}$$

The actuator angular velocities are then

$$\dot{x}_2 = \frac{1}{\sqrt{1 - \gamma^2}} \begin{bmatrix} 0 \\ -\dot{\gamma} \cos \phi + (\alpha\dot{\beta} - \beta\dot{\alpha}) \sin \phi \\ (\alpha\dot{\beta} - \beta\dot{\alpha}) \cos \phi + \dot{\gamma} \sin \phi \end{bmatrix} \tag{B-14}$$

The choice of roll angle is arbitrary. Normally, it should be chosen so that the y and z axes are principal axes of the actuator. For an axially symmetric actuator, any value can be used. If we choose $\phi = 0$, then

$$\dot{x}_2 = \frac{1}{\sqrt{1 - \gamma^2}} = \begin{bmatrix} 0 \\ -\dot{\gamma} \\ (\alpha\dot{\beta} - \beta\dot{\alpha}) \end{bmatrix} \tag{B-15}$$

The actuator consists of two parts which move relative to each other, the cylinder and the piston. The axial velocity of the cylinder is zero, while that of the piston is equal to the scalar velocity of the actuator. The angular velocities of both are equal. To find the forces exerted by the platform on the actuator, we can isolate the two parts as shown in figure B-1. If we sum forces and moments about the CM of each, we have (for a linearized analysis):

$$f_{ax} + f_{cx} = M_a \ddot{x}_a$$

$$f_{ay} + f_{cy} = M_a \ddot{y}_a$$

$$f_{az} + f_{cz} = M_a \ddot{z}_a$$

$$0 = J_{ax} \dot{p} \tag{B-16}$$

$$f_{cz}(\ell_o - d_c - d_a) - f_{az}(d_a) + M_{cy} = J_{ay}\dot{q}$$

$$f_{ay}(d_a) - f_{cy}(\ell_o - d_c - d_a) + M_{cz} = J_{az}\dot{r}$$

$$f_{bx} - f_{cx} = M_b \ddot{x}_b$$

$$f_{by} - f_{cy} = M_b \ddot{y}_b$$

$$f_{bz} - f_{cz} = M_b \ddot{z}_b$$

$$0 = J_{bx}\dot{p} \qquad \text{(B-16) cont}$$

$$f_{bz}(d_b) + f_{cz}(d_c - d_b) - M_{cy} = J_{by}\dot{q}$$

$$-f_{cy}(d_c - d_b) - f_{by}(d_b) - M_{cz} = J_{bz}\dot{r}$$

The linear velocities are given in terms of the velocity of the platform pivot point by

$$\dot{x}_a = \dot{x}$$

$$\dot{y}_a = \left(\frac{\ell_o - d_a}{\ell_o}\right)\dot{y}$$

$$\dot{z}_a = \left(\frac{\ell_o - d_a}{\ell_o}\right)\dot{z}$$

$$\dot{x}_b = 0$$

$$\dot{y}_b = \left(\frac{d_b}{\ell_o}\right)\dot{y}$$

$$\dot{z}_b = \left(\frac{d_b}{\ell_o}\right)\dot{z} \qquad \text{(B-17)}$$

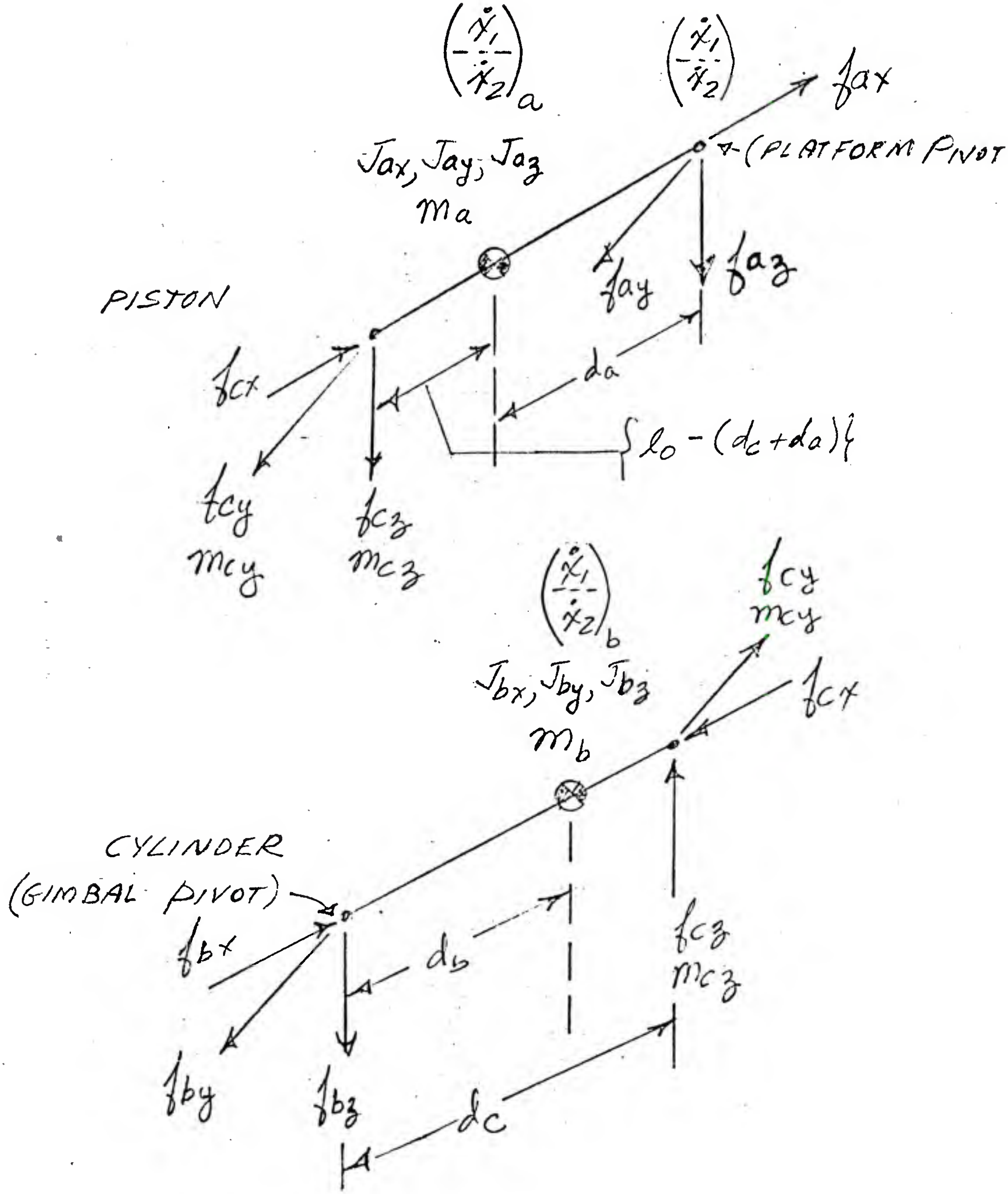

Figure B-1. Actuator dynamics

By solving these equations for the forces exerted by the platform on the actuator, we have

$$f_{ax} = M_a \ddot{x}$$

$$f_{ay} = M \ddot{y} + \frac{J_z}{\ell_o} \dot{r}$$

$$f_{az} = M \ddot{z} - \frac{J_y}{\ell_o} \dot{q} \qquad \text{(B-18)}$$

where

$$M = M_a \left(\frac{\ell_o - d_a}{\ell_o} \right)^2 + M_b \left(\frac{d_b}{\ell_o} \right)^2$$

$$J_y = (J_{ay} + J_{by})$$

$$J_z = (J_{az} + J_{bz}) \qquad \text{(B-19)}$$

Thus, the actuator forces are

$$f_a = \begin{bmatrix} m_a & 0 & 0 \\ 0 & m & 0 \\ 0 & 0 & m \end{bmatrix} \ddot{x}_1 + \frac{J}{\ell_o} \begin{bmatrix} 0 & 0 & 0 \\ 0 & 0 & 1 \\ 0 & -1 & 0 \end{bmatrix} \ddot{x}_2 \qquad \text{(B-20)}$$

where it has been assumed

$$J_y = J_z \qquad \text{(B-21)}$$

These forces are still expressed in the actuator coordinate system. In the platform system, they are

$$f_p = E'(x_3)\ f_a \qquad \text{(B-22)}$$

If the forces are translated to the origin of the platform system, the moments required to compensate for the translation are

$$M_p = W(a)\ f_p \qquad \text{(B-23)}$$

The total forces and moments are the sums of these for all six actuators.

The accelerations, $\ddot{x}_1$ and $\ddot{x}_2$ are still expressed in the actuator coordinate system. The angular velocities were found to be

$$\dot{x}_2 = \frac{1}{\sqrt{1-\gamma^2}} \begin{bmatrix} 0 \\ -\gamma \\ (\alpha\,\dot{\beta} - \beta\,\dot{\alpha}) \end{bmatrix} = \frac{1}{\sqrt{1-\gamma^2}} \begin{bmatrix} 0 & 0 & 0 \\ 0 & 0 & -1 \\ -\beta & \alpha & 0 \end{bmatrix} \dot{\delta} \qquad \text{(B-24)}$$

The rate of change of direction cosines is

$$\dot{\delta} = - W^2\ (\delta)\ \frac{\dot{\ell}_p}{\ell_o} \qquad \text{(B-25)}$$

Thus

$$\dot{x}_2 = \frac{1}{\ell_o \sqrt{1-\gamma^2}} \begin{bmatrix} 0 & 0 & 0 \\ 0 & 0 & +1 \\ +\beta & -\alpha & 0 \end{bmatrix} W^2(\delta)\ \dot{\ell}_p \qquad \text{(B-26)}$$

The linear velocities are given in terms of the vector actuator velocity by

$$\dot{x}_1 = E(x_3)\ \dot{\ell}_p \qquad \text{(B-27)}$$

But the vector actuator velocity is related to the platform velocity by

$$\dot{\ell}_p = \dot{x}_{1p} - W(a)\ \dot{x}_{2p} \qquad \text{(B-28)}$$

Thus

$$\dot{x}_1 = E(x_3) \left\{ \dot{x}_{1p} - W(a)\ \dot{x}_{2p} \right\} \qquad \text{(B-29)}$$

For small (linearized) motions, the accelerations are related in the same manner as the velocities. Thus, by combining the above relationships, the platform forces and moments are related to the platform accelerations by

$$\left(\frac{f}{m}\right)_p = \sum_{n=1}^{6} \left[\begin{array}{c|c} m_{An} & -m_{An}\,W_{(an)} \\ \hline W_{(an)}\,m_{An} & -W_{(an)}\,m_{An}\,W_{(an)} \end{array}\right] \left(\frac{\ddot{x}_1}{\ddot{x}_2}\right)_p \qquad \text{(B-30)}$$

where, for each actuator

$$m_A = E'(x_3)\left\{\begin{bmatrix} m_a & 0 & 0 \\ 0 & m & 0 \\ 0 & 0 & m \end{bmatrix} E(x_3) + \right.$$

$$\left. - \frac{J}{\ell_o^{\,2}} \cdot \frac{1}{\sqrt{1-\gamma^2}} \begin{bmatrix} 0 & 0 & 0 \\ 0 & 0 & 1 \\ 0 & -1 & 0 \end{bmatrix} \begin{bmatrix} 0 & 0 & 0 \\ 0 & 0 & -1 \\ -\beta & \alpha & 0 \end{bmatrix} W^2\ (\delta) \right\}$$

$$E(x_3') = \frac{1}{\sqrt{1-\gamma^2}} \begin{bmatrix} \alpha\sqrt{1-\gamma^2} & +\beta\sqrt{1-\gamma^2} & +\gamma\sqrt{1-\gamma^2} \\ -\beta & \alpha & 0 \\ -\alpha\gamma & -\beta\gamma & \left(1-\gamma^2\right) \end{bmatrix}$$

$$W^2(\delta) = \begin{bmatrix} (\alpha^2-1) & \alpha\beta & \alpha\gamma \\ \alpha\beta & (\beta^2-1) & \beta\gamma \\ \alpha\gamma & \beta\gamma & (\gamma^2-1) \end{bmatrix} \tag{B-31}$$

Thus

$$m_A = (m_a - m)\ \{1 + W^2\ (\delta)\ \} + m +$$

$$- \frac{J}{\ell_o^{\,2}} \frac{E'(x_3)}{\sqrt{1-\gamma^2}} \begin{bmatrix} 0 & 0 & 0 \\ -\beta & \alpha & 0 \\ 0 & 0 & 1 \end{bmatrix} W^2\ (\delta) \tag{B-32}$$

This reduces to

$$m_A = m + (m_a - m)\ \{1 + W^2\ (\delta)\} +$$

$$- \frac{J}{\ell_o^{\,2}\ (1-\gamma^2)} \begin{bmatrix} \beta^2 & \alpha\beta & \alpha\gamma \\ -\alpha\beta & \alpha^2 & \beta\gamma \\ 0 & 0 & (1-\gamma^2) \end{bmatrix} W^2\ (\delta) \tag{B-33}$$

which further reduces to

$$m_A = m + (m_a - m)\ \{1 + W^2\ (\delta)\}\ -\ \frac{J}{\ell_o^2}\ W^2\ (\delta) \tag{B-34}$$

After collecting terms, we have

$$m_A = m_a + \{m_a - m - \frac{J}{\ell_o^{\ 2}}\}\ W^2\ (\delta) \tag{B-35}$$

The four submatrices of the mass matrix can then be found by summing

$$W^2(\delta),\ W(a)\ W^2(\delta),\ \text{and}\ W(a)\ W^2(\delta)\ W(a) \tag{B-36}$$

over the six actuators. These values are

$$\sum_{n=1}^{6} W^2(\delta_n) = -3 \begin{bmatrix} (1+\gamma^2) & 0 & 0 \\ 0 & (1+\gamma^2) & 0 \\ 0 & 0 & 2(1-\gamma^2) \end{bmatrix}$$

$$\sum_{n=1}^{6} W(a_n)\ W^2(\delta_n) = 3\ \left\{a_z\ (1+\gamma^2)\ + \gamma(\alpha a_x + \beta a_y)\right\} \begin{bmatrix} 0 & 1 & 0 \\ -1 & 0 & 0 \\ 0 & 0 & 0 \end{bmatrix}$$

$$\sum_{n=1}^{6} W(a_n)\ W^2(\delta_n)\ W(a_n) = 3 \begin{bmatrix} a_{11} & 0 & 0 \\ 0 & a_{11} & 0 \\ 0 & 0 & a_{33} \end{bmatrix} \tag{B-37}$$

where

$$a_{11} = a_x^{\ 2}(1-\gamma^2) + a_y^{\ 2}(1-\gamma^2) + a_z^{\ 2}(1+\gamma^2) + 2\gamma a_z(\alpha a_x + \beta a_y)$$

$$a_{33} = 2\ \left\{a_x^{\ 2}\ (1-\beta^2) + a_y^{\ 2}\ (1-\alpha^2) + 2\alpha\beta\ a_x a_y\right\} \tag{B-38}$$

At the platform pivot plane, these evaluate to

$$\sum_{n=1}^{6} W^2\ (\delta_n) = -\frac{3}{241}\begin{bmatrix} 385 & 0 & 0 \\ 0 & 385 & 0 \\ 0 & 0 & 194 \end{bmatrix}$$

$$= \begin{bmatrix} -4.792531 & 0 & 0 \\ 0 & -4.7925311 & 0 \\ 0 & 0 & -2.4149378 \end{bmatrix}$$

$$\sum_{n=1}^{6} W(a_n)\ W^2(\delta_n) = \frac{1890}{241}\begin{bmatrix} 0 & +1 & 0 \\ -1 & 0 & 0 \\ 0 & 0 & 0 \end{bmatrix}$$

$$= \begin{bmatrix} 0 & +7.8423237 & 0 \\ -7.8423237 & 0 & 0 \\ 0 & 0 & 0 \end{bmatrix}$$

$$\sum_{n=1}^{6} W(a_n)\ W^2(\delta_n)\ W(a_n) = \frac{1}{241}\begin{bmatrix} 285471 & 0 & 0 \\ 0 & 285471 & 0 \\ 0 & 0 & 864121.5 \end{bmatrix}$$

$$= \begin{bmatrix} 1184.5270 & 0 & 0 \\ 0 & 1184.5270 & 0 \\ 0 & 0 & 3585.5664 \end{bmatrix} \qquad \text{(B-39)}$$

Also

$$\sum_{n=1}^{6} W(a_n) = 0$$

$$-\sum_{n=1}^{6} W^2(a_n) = \begin{bmatrix} 2943 & 0 & 0 \\ 0 & 2943 & 0 \\ 0 & 0 & 5886 \end{bmatrix} \text{ in}^2 \tag{B-40}$$

The neutral geometry of the RIA 6-DOF actuator is shown in figure B-2. In addition, two accumulators are attached to each cylinder. The calculated values for the piston and cylinder are then

M_a = .2352934 lb sec^2/in.

d_a = 17.242 in.

$J_{ay} = J_{az}$ = 29.82127 in. lb sec^2

M_b = 1.0168095 lb sec^2/in.

d_b = 20.2079 in.

J_{by} = 79.6253 in. lb sec^2

J_{bz} = 88.49286 in. lb sec^2

Since the orientation of the accumulators on the cylinders has not been specified, an average value of 84.0586 in. lb sec^2 will be used for both J_{by} and J_{bz}. Then the total transverse inertia is

$J = J_a + J_b$ = 113.8799 in. lb sec^2

The transverse mass is

$$M = 0.284759 \text{ lb sec}^2\text{/in.} \tag{B-41}$$

Then, for

ℓ_o = 46.572524 in

$$(m_a - m - \frac{J}{\ell_o^2}) = -\ .101969 \text{ lb sec}^2\text{/in.} \tag{B-42}$$

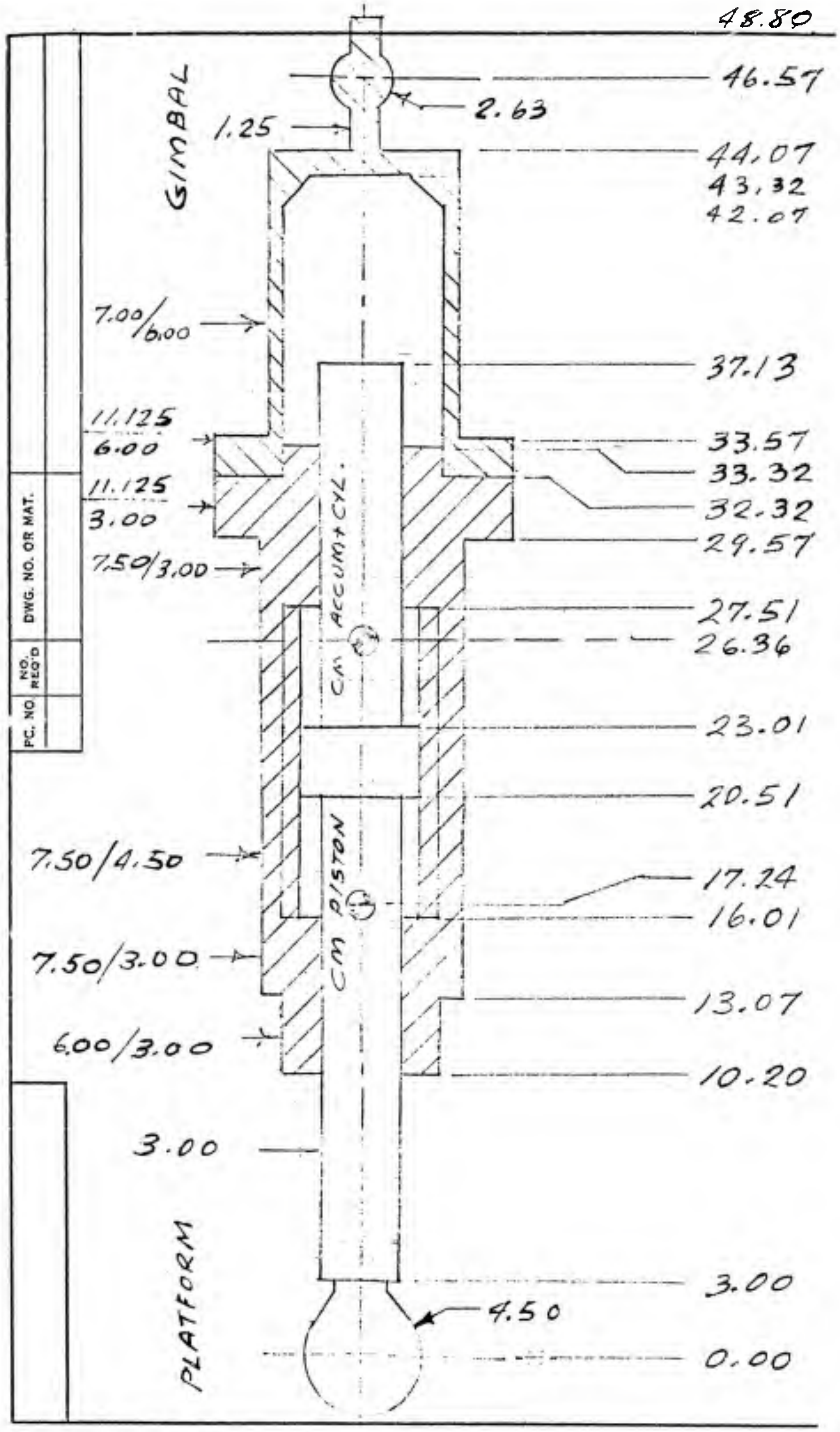

Figure B-2. Actuator neutral position

The load mass submatrices (as measured in the platform system) are then

$$M_{11} = \begin{bmatrix} 1.900450 & 0 & 0 \\ 0 & 1.900450 & 0 \\ 0 & 0 & 1.658009 \end{bmatrix} \text{ lb sec}^2/\text{in.}$$

$$M_{12} = M_{21_t} = \begin{bmatrix} 0 & .7996739 & 0 \\ -.7996739 & 0 & 0 \\ 0 & 0 & 0 \end{bmatrix} \text{ lb sec}^2$$

$$M_{22} = \begin{bmatrix} 813.2535 & 0 & 0 \\ 0 & 8132535 & 0 \\ 0 & 0 & 1750.554 \end{bmatrix} \text{ in. lb sec}^2 \qquad \text{(B-43)}$$

APPENDIX C
LISTING OF COMPUTER PROGRAM STIFF 2

LISTING OF COMPUTER PROGRAM "STIFF 2"

```
      DIMENSION   TITLE(30),AD(6),AAK(6,6),AF(6),AK(6),AT(6,6),A(6,6),
     1AK1(6,6),B(6,6),C(3),C1(3),DX(6,6),DP(6),F(3),FA(6),F1(6),PR(6),
     2PTOP(6),PBOT(6),R1T(3,3),R1T2(3,3),R1T3(3,3),ROT2(3,3),ROT3(3,3),
     3ROT(3,3),SD(6),SF(6),SL(6),SK(6,6),SK1(6,6),SSK(6,6),SX(3,6),TRGT(
     43),XP(3,6),XG(3,6),XP1(3,6),XGUN(3),XGUN1(3),XW(3),XW1(3),SKO(6,6)
     5,XTRGT(3),DT(3),R6T(6,6),RSK(6,6),SK01(6,6),R5TT(6,6),S1KO(6,6)
     6,SFO(6),SFO1(6),ROTT(6,6),ROTT1(6,6),                 PRT(6),PRB(6)
     7,SFC(6),R6T1(6,6),SD1(6)
      IT=0
      READ (5,14) TITLE
   14 FORMAT (10A6)
C     C O N S T A N T S
      PI=3.141592654
      RAD=PI/180.
C COORDINATES OF PIVOT  CENTERS AT PITCH GIMBAL  (DIRECTION,JOINT)
      XG (1,1) = 15.5885
      XG (1,2) =-38.9711
      XG (1,3) =-38.9711
      XG (1,4) = 15.5885
      XG (1,5) = 23.3827
      XG (1,6) = 23.3827
      XG (2,1) = 36.0
      XG (2,2) =  4.5
      XG (2,3) = -4.5
      XG (2,4) =-36.0
      XG (2,5) =-31.5
      XG (2,6) = 31.5
C COORDINATES OF PIVOT CENTERS AT MOUNTING PLATFORM
      XP (1,1) =-12.9903
      XP (1,2) =-18.1865
      XP (1,3) =-18.1865
      XP (1,4) =-12.9903
      XP (1,5) = 31.1769
      XP (1,6) = 31.1769
      XP (2,1) = 28.5
      XP (2,2) = 25.5
      XP (2,3) =-25.5
      XP (2,4) =-28.5
      XP (2,5) = -3.0
```

```
      XP (2,6) =  3.0
      DO 1 I=1,6
      XG (3,I) = 9.875
    1 XP (3,I) =45.875
C   AP= EFFECTIVE AREA OF ACTUATOR PISTON, IN2
      AP = 21.205
C   VO = TOTAL VOLUME(ACCUMULATOR+ ACTUATOR FULLY EXTENDED)
      VO = 421.
C   C= COORDINATE OF CENTER OF PLATFORM
      C(1) = 0.0
      C(2) = 0.0
      C(3) = XP(3,1)
      DO 3 I=1,3
      DO 3 J=1,6
    3 SX(I,J)=-XG (I,J)+XP (I,J)
      DO 4 I=1,6
      SL(I) = 0.0
C CALCULATE ACTUATOR LENGTH
      DO 5 J=1,3
    5 SL(I) =SL(I)+SX(J,I)**2
    4 SL(I) =SQRT(SL(I))
C CALCULATE DIRECTION COSINES
      DO 6 I=1,6
      DO 6 J=1,3
    6 DX(J,I)= SX(J,I)/SL(I)
      DO 7 J=1,6
      DX(4,J)= DX(3,J)*(XP (2,J)-C (2)  )-DX(2,J)*(XP (3,J)-C (3)  )
      DX(5,J)=-DX(3,J)*(XP (1,J)-C (1)  )+DX(1,J)*(XP (3,J)-C (3)  )
    7 DX(6,J)= DX(2,J)*(XP (1,J)-C (1)  )-DX(1,J)*(XP (2,J)-C (2)  )
      DO 23 I=1,6
      DO 23 J=1,6
      B(J,I) = DX(I,J)
   23 A(I,J) = DX(I,J)
      CALL MATIN(A,ID,6)
      DO 24 I=1,6
      DO 24 J=1,6
   24 AT(I,J) = A(J,I)
C   THETA = MOUNTING ANGLE OF VEHICLE WITH PLATFORM, DEG.
 1000 READ(5,2) THETA
      IT=IT+1
      IF(THETA.GT.99.) GO TO 9999
      WRITE(6,15) IT,TITLE
   15 FORMAT(1H1,' CASE',I3,10A6/8X,10A6//10A6// )
C   W= WEIGHT OF PLATFORM, PART OF ACTUATORS AND PAYLOAD, LB
C   XW= C.G. LOCATION OF WEIGHT W.R.T. CENTER OF GIMBAL   , IN.
      READ(5,2) W,(XW(I),I=1,3)
C   XGUN = POSITION OF WEAPON MOUNTING POINT W.R.T. C.G. OF WEIGHT
      READ(5,2) (XGUN(I),I=1,3)
C   TRGT = POSITION OF TARGET W.R.T. CENTER OF PITCH GIMBAL
      READ(5,2) (TRGT(I),I=1,3)
C   RY AND RZ ARE THE GIMBAL PITCH AND YAW
      READ (5,2) RY,RZ
    2 FORMAT(6E10.0)
      RY = RY+THETA
      RADY = RY*RAD
      RTHETA =THETA*RAD
      RADZ =RZ*RAD
```

```
      CALL RT2(ROT2,RADY)
      CALL RT3 (ROT3,RADZ)
      CALL MATMAT (ROT3,ROT2,ROT,3,3)
      CALL MATMAT (ROT ,XP  ,XP1,6,3)
      CALL MATVEC(ROT,C,C1,3)
      WRITE(6,81) W
   81 FORMAT(9X,'ACTING WEIGHT                   =',F16.1,'  LBS'//)
      WRITE(6,26)
   26 FORMAT(9X'COORDINATES, INCH      '7X'X',11X'Y',11X'Z'/)
      WRITE(6,29) ((XW(I),I=1,3),(XGUN(I),I=1,3),(TRGT(I),I=1,3))
   29 FORMAT(9X'C.G. OF WEIGHT         '3F12.3/9X'WEAPON MOUNTING POINT'
     1 3F12.3/9X,'TARGET                ' 3F12.3/)
C    MEDIA 1 = OIL
C    MEDIA 2 = NITROGEN
      READ(5,22)   MEDIA
   22 FORMAT(I2)
      WRITE(6,96) THETA
   96 FORMAT(/ /4X'MOUNTING ANGLE OF VEHICLE WITH PLATFORM, DEG. .......'
     1 F10.2)
      WRITE(6,80) RY,RZ
   80 FORMAT(//9X'GIMBAL ROTATION, DEG.'/
     1           9X'----- --------- ----'//13X'PITCH'F10.2,'  (INCL. MOU
     1NTING ANGLE)'/13X'YAW   'F10.2/)
C    V= EFFECTIVE VOLUME OF ACCUMULATOR, IN3
      IF(MEDIA.EQ.1) GO TO 200
      AKMAX = 5000.
      AKMIN  =300.
      V=326.
      GO TO 201
  200 AKMAX = 23000.
      AKMIN  =800.
      V = 117.5
  201 CONTINUE
C   AKMAX,AKMIN = ACTUATOR STIFFNESS MAX. AND MIN. RESP.
      IF(MEDIA.EQ.1)   WRITE(6,82) V, AKMAX,AKMIN
      IF(MEDIA.EQ.2)   WRITE(6,182) V, AKMAX,AKMIN
   82 FORMAT(  /3X'DAMPING MEDIA........ OIL '//
     1          3X'EFFECTIVE VOLUME OF ACCUMULATOR  = 'F10.1,'  IN3    '/
     2          3X'MAXIMUM ACTUATOR STIFFNESS       = 'F10.1,'  LB/IN'/
     3          3X'MINIMUM ACTUATOR STIFFNESS       = 'F10.1,'  LB/IN'/)
  182 FORMAT(///3X'DAMPING MEDIA........ NITROGEN'//
     1          3X'EFFECTIVE VOLUME OF ACCUMULATOR  = 'F10.1,'  IN3    '/
     2          3X'MAXIMUM ACTUATOR STIFFNESS       = 'F10.1,'  LB/IN'/
     3          3X'MINIMUM ACTUATOR STIFFNESS       = 'F10.1,'  LB/IN'/)
  999 FORMAT(2X///)
   99 FORMAT(/I6/)
C    CALCULATE FORCE AND MOMENT COMPONENTS
      DO 8 I=1,3
    8 F(I)= 0.0
      F(3)= W
      RAD1Y = -RADY
      RAD1Z  = -RADZ
      CALL RT2(R1T2,RAD1Y)
      CALL RT3(R1T3,RAD1Z)
      CALL MATMAT(R1T3,R1T2,R1T,3,3)
      CALL MATVEC(R1T,F,F1,3)
      CALL MATVEC(ROT,XW,XW1,3)
```

```
      CALL MATVEC(ROT,XGUN,XGUN1,3)
      F1(4) =  F(3)*(XW1(2)- C1(2))- F(2)*(XW1(3)- C1(3))
      F1(5) =  F(1)*(XW1(3)- C1(3))- F(3)*(XW1(1)- C1(1))
      F1(6) =  F(2)*(XW1(1)- C1(1))- F(1)*(XW1(2)- C1(2))
C   FA=ACTUATOR FORCE,LB
  100 FORMAT(6F15.6)
      CALL MATVEC(A,F1,FA,6)
C   I N I T I A L I Z A T I O N
      DO 52 I=1,6
      SD(I)=0.0
      SFO(I)=0.0
      SFC(I)=0.0
      DO 52 J=1,6
      ROTT(I,J)=0.0
      ROTT1(I,J)=0.0
      SKO(I,J) = 0.0
      SK(I,J) = 0.0
      AK1(I,J) = 0.0
   52 SK1(I,J) = 0.0
      DO 112 I=1,3
      DO 112 J=1,3
      ROTT1(I,J)=R1T(J,I)
      ROTT1(I+3,J+3)=R1T(J,I)
      ROTT(I,J)=R1T(I,J)
  112 ROTT(I+3,J+3) =R1T(I,J)
C LOC  = CODE FOR LOCATION OF DESIRED STIFFNESS
C    1. AT MTG. PLATFORM,  2. AT C.G. OF VEHICLE, 3. AT WEAPON MTG. PT.
      READ(5,22) LOC
C   SK = STIFFNESS REQUIRED IN WEAPON COORDINATE SYSTEM
   67 READ (5,2) (SK(I,I),I=1,6)
      IF(LOC.LT.3) GO TO 70
      DO 45 I=1,3
   45 XTRGT(I)=TRGT(I)-(XGUN1(I)+XW1(I))
      STRGT=0.0
      DO 46 I=1,3
   46 STRGT=STRGT+XTRGT(I)**2
      STRGT=SQRT(STRGT)
      DO 47 I=1,3
      DT(I)=XTRGT(I)/STRGT
   47 SKO(I,I) = SK(1,1)*DT(I)**2
      CALL MATMAT(ROTT1,SKO,S1KO,6,6)
      CALL MATMAT(S1KO,ROTT,SKO,6,6)
       READ(5,2) RECOIL
      DO 75 I=1,3
   75 SFO1(I)=RECOIL*DT(I)
      CALL MATVEC(ROTT,SFO1,SFC,6)
      WRITE(6,103) RECOIL
  103 FORMAT(/3X,'RECOIL LOAD                             =',F10.1,'  LBS'//)
      WRITE(6,66)
   66 FORMAT(14X,'REQUIRED STIFFENESS AT WEAPON MOUNTING POINT'/)
C TRANSFER WEAPON STIFFNESS TO PLATFORM SYSTEM
      X1=XGUN(1)+XW(1) -C(1)
      Y1=XGUN(2)+XW(2) -C(2)
      Z1=XGUN(3)+XW(3) -C(3)
      CALL R6T2(R6T,0.,X1,Y1,Z1)
      DO 121 I=1,6
      DO 121 J=1,6
```

```
  121 R6TT(I,J)=R6T(J,I)
      CALL MATMAT(R6T,SKO,RSK,6,6)
      CALL MATMAT(RSK,R6TT,SKO1,6,6)
      CALL MATVEC(R6T,SFO,SF,6)
      DO 27 I=1,6
      DO 27 J=1,6
      IF (SKO1(I,J).LT. 1.0) GO TO 27
      IF(SF(I).LT. 1.0) GO TO 27
      SK1(I,J) = 1./SKO1(I,J)
   27 CONTINUE
      GO TO 71
C    SFO = EXTERNAL FORCES
   70 READ(5,2) (SFO(I),I=1,6)
      IF(LOC.EQ.2) GO TO 122
      DO 123 I=1,6
  123 SF(I)=SFO(I)
  122 WRITE(6,72)
   72 FORMAT(/14X,' EXTERNAL LOADS '/)
      WRITE(6, 94) (SFO(I),I=1,6)
   94 FORMAT( 31X'X',12X'Y',12X'Z'//4X'FORCE, LB.           ',3F12.1/
     1 4X'MOMEMT, IN.LB.     ',3F12.1/)
      IF(LOC.EQ.1) GO TO 74
      IF(LOC.EQ.2) WRITE(6,65)
   65 FORMAT(14X,'REQUIRED STIFFNESS AT C.G. OF VEHICLE '/)
      GO TO 97
   74 WRITE(6,64)
   64 FORMAT(14X,'REQUIRED STIFFNESS AT MOUNTING PLATFORM'/)
      DO 150 I=1,6
  150 SKO(I,I)=SK(I,I)
      GO TO 28
   97 RTHETA = -RTHETA
      X1 = XW1(1)-C1(1)
      Y1 = XW1(2)-C1(2)
      Z1 = XW1(3)-C1(3)
      CALL R6T2(R6T,RTHETA,X1,Y1,Z1)
      CALL MATVEC(R6T,SFO,SF,6)
      DO 300 I=1,6
      IF(SK(I,I).LT.1.0) GO TO 300
      SD1(I)=SFO(I)/SK(I,I)
  300 CONTINUE
      WRITE(6,13)(SD1(I),I=1,6)
      CALL R6T3(R6T1,RTHETA,X1,Y1,Z1)
      CALL MATVEC(R6T1,SD1,SD,6)
      WRITE(6,13)(SD(I),I=1,6)
      GO TO 373
   28 DO 21 I=1,6
      DO 21 J=1,6
   21 SKO1(I,J)=SKO(I,J)
   31 DO 73 I=1,6
      DO 73 J=1,6
      IF (SKO1(I,J).LT. 1.0) GO TO 73
      SK1(I,J) = 1./SKO1(I,J)
   73 CONTINUE
  373 CONTINUE
   71 WRITE(6,104)(SK(I,I),I=1,6)
  104 FORMAT( 31X'X',12X'Y',12X'Z'//4X'TRANSLATION, LB/IN',3F12.1/
     1 4X'ROTATION,IN.LB/RAD',3F12.1/)
```

```
   20 FORMAT(6F12.1/)
      IF(LOC.EQ.2) GO TO 245
      CALL MATVEC(SK1,SF,SD,6)
C TRANSFORMATION OF FORCES TO CENTER OF GIMBAL
  245 DO 42 I=1,6
   42 SFC(I)=SF(I)+F1(I)
      SFC(4)=SFC(4)-SFC(2)*C(3)
      SFC(5)=SFC(5)+SFC(1)*C(3)
      SFC(6)=SFC(6)
      WRITE(6,124)
  124 FORMAT(/14X'FORCES AT PITCH GIMBAL IN ITS COORDINATE SYSTEM'/)
      WRITE(6,94) (SFC(I),I=1,6)
      CALL MATVEC(B,SD,AD,6)
      CALL MATVEC(A,SF,AF,6)
      DO 30 I=1,6
      AK(I)=AF(I)/AD(I)
   30 AK1(I,I)=1./AK(I)
      CALL MATMAT(AT,AK1,AAK,6,6)
      CALL MATMAT(AAK,A ,SSK,6,6)
      WRITE(6,15) IT,TITLE
      WRITE (6,77)
   77 FORMAT(18X'ACTUATOR FORCES AND DISPLACEMENTS DUE TO'// 8X'ACTUATOR
     1','4X'WEIGHT,LB      RECOIL LOAD,LB.    DIPL.(RECOIL LD.),IN '/)
      WRITE (6,78) (I, FA(I),AF(I),AD(I),I=1,6)
   78 FORMAT( 9XI1,2F17.1,F22.5)
      DO 9 I=1,6
    9 DP(I) =FA(I)/AP
C   AK = ACTUATOR STIFFNESS,LB/IN
  102 FORMAT(3E15.6)
C  CHECK IF ACTUATOR STIFFNESS IS WITHIN RANGE
      DO 10 I=1,3
      IF (AK(I).GT.AKMIN)GO TO 11
      WRITE (6,13) AK(I),AKMIN
      GO TO 10
   13 FORMAT(6F15.4)
   11 IF (AK(I).LT.AKMAX)GO TO 10
      WRITE (6,13) AK(I),AKMAX
   10 CONTINUE
C   CALCULATE ACTUATOR PRESSURES
      DO 12 I=1,6
      PTOP(I)=(AK(I)*V/(2.*AP**2))-0.5*DP(I)
   12 PBOT(I)= PTOP(I)+DP(I)
      WRITE(6,107)
  107 FORMAT (//18X' ACTUATOR STIFFNESS AND PRESSURES'/
     1           18X' -------- --------- --- ---------'// 8X'ACTUATOR
     2STIFFNESS          TOP PRESSURE     BOT. PRESSURE'/21X 'LB/IN',14X
     2'PSI' 14X'PSI'/)
      WRITE(6,101) (I,AK(I),PTOP(I),PBOT(I),I=1,6)
  101 FORMAT(9X,I1,3F17.1)
C   PR = PRECHARGE PRESSURE, PSI     (FOR NITROGEN ONLY)
      IF(MEDIA.EQ.1) GO TO 203
      DO 205 I=1,6
  205 PR(I) = PTOP(I)*V/V0
      WRITE(6,202)
  202 FORMAT(//24X'ACTUATOR PRECHARGE'/24X'-------- ---------'
     1 //19X'ACTUATOR    '7X'PRECHARGE (PSI)'/ )
      DO 206 I=1,6
```

```
      IF(FA(I).LT. 0.0) GO TO 207
      WRITE(6,209) I,PR(I)
  209 FORMAT(20X,I1,'  (TOP)',F17.1)
      GO TO 206
  207 WRITE(6,208) I,PR(I)
  208 FORMAT(20X,I1,'  (BOTTOM)',F14.1)
  206 CONTINUE
      GO TO 230
  203 DO 250 I=1,6
      PRT(I)=PTOP(I)*V/235.
  250 PRB(I)=PBOT(I)*V/235.
      WRITE(6,222)
  222 FORMAT(//24X'ACCUMULATOR PRECHARGE'/24X'----------- ----------'
     1 //15X'NO.',8X'TOP',10X'BOTTOM'/)
      WRITE(6,290)(I,PRT(I),PRB(I),I=1,6)
  290 FORMAT(16X,I1,2F14.1)
  230 WRITE(6,530)
  530 FORMAT(//1H1//)
      WRITE(6,531)
  531 FORMAT(/ 20X'RESULTANT FLEXIBILITY AT THE REQUIRED LOCATION'/)
      WRITE(6,511) ((SSK(I,J),J=1,6),I=1,6)
  511 FORMAT( 2X,6E12.6/)
      CALL MATIN(SSK,ID,6)
      WRITE(6,210)
  210 FORMAT(/ 20X'RESULTANT STIFFNESS AT THE REQUIRED LOCATION'/)
      WRITE(6,211) ((SSK(I,J),J=1,6),I=1,6)
  211 FORMAT( 2X,6F12.1/)
      GO TO 1000
 9999 STOP
      END
```

```
R6T3
5/12/74-13:04:10 (,0)

INE R6T3       ENTRY POINT 000103

USED: CODE(1) 000124; DATA(0) 000026; BLANK COMMON(2) 000000

L REFERENCES (BLOCK, NAME)

 COS
 SIN
 NERR3$

 ASSIGNMENT  (BLOCK, TYPE, RELATIVE LOCATION, NAME)

 000017 105G       0001    000020 110G       0001    000043 123G       0001    000044 126G
 000004 INJP$      0000 I  000001 J

  1*            SUBROUTINE  R6T3(ROT2,Q,X,Y,Z)
  2*            DIMENSION ROT2(6,6)
  3*            DO 1 I=1,6
  4*            DO 1 J=1,6
  5*          1 ROT2(I,J)=0.0
  6*            ROT2(1,1)=COS(Q)
  7*            ROT2(1,3)=SIN(Q)
  8*            ROT2(2,2)=1.0
  9*            ROT2(3,1)=-SIN(Q)
 10*            ROT2(3,3)=COS(Q)
 11*            DO 2 I=1,3
 12*            DO 2 J=1,3
 13*          2 ROT2(I+3,J+3) = ROT2(I,J)
 14*            ROT2(1,5)=-Z
 15*            ROT2(1,6)= Y
 16*            ROT2(2,4)= Z
 17*            ROT2(2,6)=-X
 18*            ROT2(3,4)=-Y
 19*            ROT2(3,5)= X
 20*            RETURN
 21*            END

) OF COMPILATION:          NO  DIAGNOSTICS.
```

```
.R6T2,.R6T2
)3/06/74-16:28:25 (,0)

INE R6T2        ENTRY POINT 000103

._USED: CODE(1) 000124; DATA(0) 000026; BLANK COMMON(2) 000000

L REFERENCES (BLOCK, NAME)

 COS
 SIN
 NERR3$

 ASSIGNMENT (BLOCK, TYPE, RELATIVE LOCATION, NAME)

 000017 105G      0001  000020 110G      0001  000043 123G      0001   000044 126G
 000004 INJP$     0000 I 000001 J

   1*          SUBROUTINE  R6T2(ROT2,Q,X,Y,Z)
   2*          DIMENSION ROT2(6,6)
   3*          DO 1 I=1,6
   4*          DO 1 J=1,6
   5*        1 ROT2(I,J)=0.0
   6*          ROT2(1,1)=COS(Q)
   7*          ROT2(1,3)=SIN(Q)
   8*          ROT2(2,2)=1.0
   9*          ROT2(3,1)=-SIN(Q)
  10*          ROT2(3,3)=COS(Q)
  11*          DO 2 I=1,3
  12*          DO 2 J=1,3
  13*        2 ROT2(I+3,J+3) = ROT2(I,J)
  14*          ROT2(4,2)=-Z
  15*          ROT2(4,3)= Y
  16*          ROT2(5,1)= Z
  17*          ROT2(5,3)=-X
  18*          ROT2(6,1)=-Y
  19*          ROT2(6,2)= X
  20*          RETURN
  21*          END

 OF COMPILATION:         NO  DIAGNOSTICS.
```

```
.MATIN,.MATIN
3/06/74-16:28:26 (,0)

INE MATIN      ENTRY POINT 000341

 USED: CODE(1) 000361; DATA(0) 000070; BLANK COMMON(2) 000000

L REFERENCES (BLOCK, NAME)

 NERR3$

 ASSIGNMENT  (BLOCK, TYPE, RELATIVE LOCATION, NAME)

 000062 100L        0001     000065 105L        0001     000015 107G        0001     000021 114G
 000042 125G        0001     000113 152G        0001     000155 163G        0001     000163 170G
 000235 207G        0001     000262 217G        0001     000304 231G        0001     000133 310L
 000300 710L        0001     000317 715L        0001     000312 720L        0001     000321 740L
 000022 DETERM      0000 I 000024 I           0000 I 000032 ICOLUM      0000 I 000000 INDEX
 000031 IROW        0000 I 000023 J           0000 I 000032 JCOLUM      0000 I 000031 JROW
 000026 L           0000 I 000030 L1          0000 R 000027 PIVOT       0000 R 000033 SWAP


            SUBROUTINE MATIN(Z,ID,N)
      C     MATRIX INVERSION ONLY                                            00001
      C                                                                      00001
            DIMENSION INDEX( 6 ,3), Z(N,N)
            EQUIVALENCE (IROW,JROW), (ICOLUM,JCOLUM), (AMAX, T, SWAP)        00001
      C                                                                      00001
      C     INITIALIZATION                                                   00001
      C                                                                      00001
            DETERM=1.0
            DO 20 J=1,N                                                      00001
         20 INDEX(J,3) = 0                                                   00001
            DO 550 I=1,N                                                     00001
      C                                                                      00001
      C     SEARCH FOR PIVOT ELEMENT                                         00001
      C                                                                      00001
            AMAX=0.0
            DO 105 J=1,N                                                     00001
            IF(INDEX(J,3).EQ.1)GO TO 105                                     00001
            DO 100 K=1,N                                                     00001
            IF(INDEX(K,3)-1) 80, 100, 715                                    00001
         80 IF(AMAX.GE.ABS(Z(J,K)))GO TO 100
            IROW=J                                                           00001
            ICOLUM=K                                                         00001
            AMAX = ABS(Z(J,K))
        100 CONTINUE                                                         00001
        105 CONTINUE                                                         00001
            INDEX(ICOLUM,3) = INDEX(ICOLUM,3) +1                             00001
            INDEX(I,1)=IROW                                                  00001
            INDEX(I,2)=ICOLUM                                                00001
```

```
C
C      INTERCHANGE ROWS TO PUT PIVOT ELEMENT ON DIAGONAL
C
       IF(IROW.EQ.ICOLUM)GO TO 310
       DETERM=-DETERM
       DO 200 L=1,N
       SWAP=Z(IROW,L)
       Z(IROW,L)=Z(ICOLUM,L)
  200  Z(ICOLUM,L)=SWAP
C
C      DIVIDE PIVOT ROW BY PIVOT ELEMENT
C      DIVIDE PIVOT ROW BY PIVOT ELEMENT
C
  310  PIVOT   =Z(ICOLUM,ICOLUM)
       Z(ICOLUM,ICOLUM)=1.0
       DO 350 L=1,N
  350  Z(ICOLUM,L)=Z(ICOLUM,L)/PIVOT
C
C      REDUCE NON-PIVOT ROWS
C
       DO 550 L1=1,N
       IF(L1.EQ.ICOLUM)GO TO 550
       T=Z(L1,ICOLUM)
       Z(L1,ICOLUM)=0.0
       DO 450 L=1,N
  450  Z(L1,L)=Z(L1,L)-Z(ICOLUM,L)*T
  550  CONTINUE
C
C      INTERCHANGE COLUMNS
C
       DO 710 I=1,N
       L=N+1-I
       IF(INDEX(L,1).EQ.INDEX(L,2))GO TO 710
       JROW=INDEX(L,1)
       JCOLUM=INDEX(L,2)
       DO 705 K=1,N
       SWAP=Z(K,JROW)
       Z(K,JROW)=Z(K,JCOLUM)
       Z(K,JCOLUM)=SWAP
  705  CONTINUE
  710  CONTINUE
       DO 730 K = 1,N
       IF(INDEX(K,3).EQ.1)GO TO 720
       GO TO 715
  720  CONTINUE
  730  CONTINUE
       ID =1
       GO TO 740
  715  ID =2
  740  RETURN
C      LAST CARD OF PROGRAM
       END
```

OF COMPILATION: NO DIAGNOSTICS.

```
.MATMAT,.MATMAT
3/06/74-16:28:28 (,0)

INE MATMAT     ENTRY POINT 000112

 USED: CODE(1) 000132; DATA(0) 000042; BLANK COMMON(2) 000000

L REFERENCES (BLOCK, NAME)

 NERR3$

 ASSIGNMENT  (BLOCK, TYPE, RELATIVE LOCATION, NAME)

 000043 105G        0001    000046 110G        0001    000050 114G        0000 I 000000 I
 000001 J           0000 I 000002 K


  1*            SUBROUTINE MATMAT(A,B,C,M,N)
  2*            DIMENSION A(N,N),B(N,M),C(N,M)
  3*            DO 1 I=1,N
  4*            DO 1 J=1,M
  5*            C(I,J) =0.0
  6*            DO 1 K=1,N
  7*          1 C(I,J) =C(I,J) + A(I,K)*B(K,J)
  8*            RETURN
  9*            END

) OF COMPILATION:        NO  DIAGNOSTICS.
```

```
.RT2,.RT2
03/06/74-16:28:29 (,0)

TINE RT2        ENTRY POINT 000033

E USED: CODE(1) 000042; DATA(0) 000012; BLANK COMMON(2) 000000

AL REFERENCES (BLOCK, NAME)

 COS
 SIN
 NERR3$

E ASSIGNMENT  (BLOCK, TYPE, RELATIVE LOCATION, NAME)

 000001 INJP$

               SUBROUTINE RT2(ROT2,Q)
               DIMENSION ROT2(3,3)
               ROT2(1,1) = COS(Q)
               ROT2(1,2) = 0.
               ROT2(1,3) =  SIN(Q)
               ROT2(2,1) = 0.
               ROT2(2,2) = 1.
               ROT2(2,3) = 0.
               ROT2(3,1) =-SIN(Q)
               ROT2(3,2) = 0.
               ROT2(3,3) = COS(Q)
               RETURN
               END

 OF COMPILATION:         NO  DIAGNOSTICS.
```

```
.RT3,.RT3
3/06/74-16:28:30 (,0)

INE RT3        ENTRY POINT 000033

 USED: CODE(1) 000042; DATA(0) 000012; BLANK COMMON(2) 000000

L REFERENCES (BLOCK, NAME)

 COS
 SIN
 NERR3$

 ASSIGNMENT  (BLOCK, TYPE, RELATIVE LOCATION, NAME)

 000001 INJP$

   1*            SUBROUTINE RT3(ROT3,R)
   2*            DIMENSION ROT3(3,3)
   3*            ROT3(1,1) = COS(R)
   4*            ROT3(1,2) = -SIN(R)
   5*            ROT3(1,3) = 0.
   6*            ROT3(2,1) = SIN(R)
   7*            ROT3(2,2) = COS(R)
   8*            ROT3(2,3) = 0.
   9*            ROT3(3,1) = 0.
  10*            ROT3(3,2) = 0.
  11*            ROT3(3,3) = 1.
  12*            RETURN
  13*            END

) OF COMPILATION:       NO  DIAGNOSTICS.
```

```
•MATVEC••MATVEC
13/06/74-16:28:31 (•0)

TINE MATVEC     ENTRY POINT 000062

E USED: CODE(1) 000077; DATA(0) 000025; BLANK COMMON(2) 000000

AL REFERENCES (BLOCK, NAME)

  NERR3$

E ASSIGNMENT  (BLOCK, TYPE, RELATIVE LOCATION, NAME)

  000025 105G      0001   000031 111G     0000 I 000000 I        0000   000003 INJP$


 1*            SUBROUTINE MATVEC(A,B,C,N)
 2*            DIMENSION A(N,N),B(N),C(N)
 3*            DO 1 I = 1,N
 4*            C(I) = 0.
 5*            DO 1 J = 1,N
 6*          1 C(I) = C(I) + A(I,J)*B(J)
 7*            RETURN
 8*            END

) OF COMPILATION:         NO  DIAGNOSTICS.
```

```
                                    6- D O F   S I M U L A T O R
                                    ****************************
              VEHICLE .............  AH 1G  HELICOPTER
        0.
       3000.0         0.0         0.0       45.875
         0.0         0.0         0.0
       1000.         0.0         50.
         0.0         0.0
       2
       1
       1207.5      0.0
        1000.
```

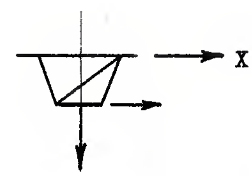


```
        0.0
       3000.0         0.0         0.0       45.875
        1000.
         0.0         0.0         0.0
       0.0         0.0
       2
       1
        0.0         0.0        3585.2
       0.0         0.0         1000.
```

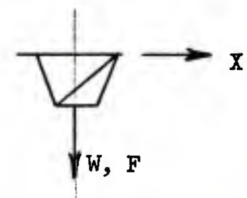


```
       0.
       3000.0         0.0         0.0       45.875
         0.0         0.0         0.0
       1000.         0.0         0.
         0.0         0.0
       2
       1
       1207.5                                         1758500.
       1000.                                           1000.
```

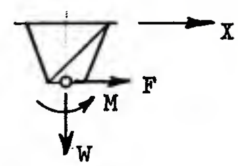

CASE 1 6- D O F S I M U L A T O R
****

VEHICLE .... AH 1G HELICOPTER

ACTING WEIGHT = 3000.0 LBS

COORDINATES, INCH	X	Y	Z
C.G. OF WEIGHT	.000	.000	45.875
WEAPON MOUNTING POINT	.000	.000	.000
TARGET	1000.000	.000	50.000

MOUNTING ANGLE OF VEHICLE WITH PLATFORM, DEG. ...... .00

GIMBAL ROTATION, DEG.
------ --------- ----

PITCH .00 (INCL. MOUNTING ANGLE)
YAW .00

DAMPING MEDIA......... NITROGEN

EFFECTIVE VOLUME OF ACCUMULATOR = 326.0 IN3
MAXIMUM ACTUATOR STIFFNESS = 5000.0 LB/IN
MINIMUM ACTUATOR STIFFNESS = 300.0 LB/IN

EXTERNAL LOADS

	X	Y	Z
FORCE, LB.	1000.0	.0	.0
MOMEMT, IN.LB.	.0	.0	.0

REQUIRED STIFFNESS AT MOUNTING PLATFORM

	X	Y	Z
TRANSLATION, LB/IN	1207.5	.0	.0
ROTATION, IN.LB/RAD	.0	.0	.0

CASE 1

6- D O F S I M U L A T O R
****

VEHICLE .... AH 1G HELICOPTER

ACTUATOR FORCES AND DISPLACEMENTS DUE TO

ACTUATOR	WEIGHT,LB	RECOIL LOAD,LB.	DIPL.(RECOIL LD.),IN
1	646.8	-485.2	-.50819
2	646.8	434.1	.36959
3	646.8	434.1	.36959
4	646.8	-485.2	-.50819
5	646.8	51.1	.13860
6	646.8	51.1	.13860

ACTUATOR STIFFNESS AND PRESSURES
-------- --------- --- ---------

ACTUATOR	STIFFNESS LB/IN	TOP PRESSURE PSI	BOT. PRESSURE PSI
1	954.7	330.8	361.3
2	1174.5	410.5	441.0
3	1174.5	410.5	441.0
4	954.7	330.8	361.3
5	368.5	118.3	148.8
6	368.5	118.3	148.8

ACCUMULATOR PRECHARGE
----------- ---------

ACCUMULATOR	PRECHARGE (PSI)
1 (TOP)	256.2
2 (TOP)	317.9
3 (TOP)	317.9
4 (TOP)	256.2
5 (TOP)	91.6
6 (TOP)	91.6

RESULTANT STIFFNESS AT CENTER OF PLATFORM

1207.5	-.0	-.0	-.0	-.0	.0
-.0	803.1	-.0	13058.6	.0	-17930.4
-.0	-.0	2984.8	-.0	26618.2	-.0
-.0	13058.6	-.0	1843334.9	.0	-116455.2
-.0	.0	26618.2	.0	1084776.9	.1
.0	-17930.4	-.0	-116455.2	.1	1915275.2

CASE 2 6- D O F S I M U L A T O R

VEHICLE .... AH 1G HELICOPTER

ACTING WEIGHT = 3000.0 LBS

COORDINATES, INCH	X	Y	Z
C.G. OF WEIGHT	.000	.000	45.875
WEAPON MOUNTING POINT	1000.000	.000	.000
TARGET	.000	.000	.000

MOUNTING ANGLE OF VEHICLE WITH PLATFORM, DEG. ...... .00

GIMBAL ROTATION, DEG.

PITCH .00 (INCL. MOUNTING ANGLE)
YAW .00

DAMPING MEDIA......... NITROGEN

EFFECTIVE VOLUME OF ACCUMULATOR = 326.0 IN3
MAXIMUM ACTUATOR STIFFNESS = 5000.0 LB/IN
MINIMUM ACTUATOR STIFFNESS = 300.0 LB/IN

EXTERNAL LOADS

	X	Y	Z
FORCE, LB.	.0	.0	1000.0
MOMEMT, IN.LB.	.0	.0	.0

REQUIRED STIFFNESS AT MOUNTING PLATFORM

	X	Y	Z
TRANSLATION, LB/IN	.0	.0	3585.2
ROTATION,IN.LB/RAD	.0	.0	.0

CASE 2

6- D O F S I M U L A T O R
****

VEHICLE .... AH 1G HELICOPTER

ACTUATOR FORCES AND DISPLACEMENTS DUE TO

ACTUATOR	WEIGHT,LB	RECOIL LOAD,LB.	DIPL.(RECOIL LD.),IN
1	646.8	215.6	.21561
2	646.8	215.6	.21561
3	646.8	215.6	.21561
4	646.8	215.6	.21561
5	646.8	215.6	.21561
6	646.8	215.6	.21561

ACTUATOR STIFFNESS AND PRESSURES

ACTUATOR	STIFFNESS LB/IN	TOP PRESSURE PSI	BOT. PRESSURE PSI
1	1000.0	347.3	377.8
2	1000.0	347.3	377.8
3	1000.0	347.3	377.8
4	1000.0	347.3	377.8
5	1000.0	347.3	377.8
6	1000.0	347.3	377.8

ACCUMULATOR PRECHARGE

ACCUMULATOR	PRECHARGE (PSI)
1 (TOP)	268.9
2 (TOP)	268.9
3 (TOP)	268.9
4 (TOP)	268.9
5 (TOP)	268.9
6 (TOP)	268.9

RESULTANT STIFFNESS AT CENTER OF PLATFORM

1207.5	-.0	-.0	-.0	-7842.5	.0
-.0	1207.5	.0	7842.7	.0	-.1
-.0	-.0	3585.2	-.0	.0	-.0
-.0	7842.7	-.0	1758542.3	.0	-1.3
-7842.5	.0	.0	.0	1758533.9	.1
.0	-.1	-.0	-1.3	.0	2300516.7

CASE 3

6- D O F   S I M U L A T O R
****

VEHICLE .... AH 1G HELICOPTER

ACTING WEIGHT = 3000.0 LBS

COORDINATES, INCH	X	Y	Z
C.G. OF WEIGHT	.000	.000	45.875
WEAPON MOUNTING POINT	.000	.000	.000
TARGET	1000.000	.000	.000

MOUNTING ANGLE OF VEHICLE WITH PLATFORM, DEG. .... .00

GIMBAL ROTATION, DEG.
------ --------- ----

PITCH .00 (INCL. MOUNTING ANGLE)
YAW .00

DAMPING MEDIA......... NITROGEN

EFFECTIVE VOLUME OF ACCUMULATOR = 326.0 IN3
MAXIMUM ACTUATOR STIFFNESS = 5000.0 LB/IN
MINIMUM ACTUATOR STIFFNESS = 300.0 LB/IN

EXTERNAL LOADS

	X	Y	Z
FORCE, LB.	1000.0	.0	.0
MOMEMT, IN.LB.	.0	1000.0	.0

REQUIRED STIFFNESS AT MOUNTING PLATFORM

	X	Y	Z
TRANSLATION, LB/IN	1207.5	.0	.0
ROTATION, IN.LB/RAD	.0	1758500.0	.0

CASE 3

6- D O F S I M U L A T O R

****

VEHICLE .... AH 1G HELICOPTER

ACTUATOR FORCES AND DISPLACEMENTS DUE TO

ACTUATOR	WEIGHT,LB	RECOIL LOAD,LB.	DIPL.(RECOIL LD.),IN
1	646.8	-481.6	-.50248
2	646.8	444.0	.37759
3	646.8	444.0	.37759
4	646.8	-481.6	-.50248
5	646.8	37.6	.12489
6	646.8	37.6	.12489

ACTUATOR STIFFNESS AND PRESSURES

ACTUATOR	STIFFNESS LB/IN	TOP PRESSURE PSI	BOT. PRESSURE PSI
1	958.5	332.2	362.7
2	1176.0	411.0	441.5
3	1176.0	411.0	441.5
4	958.5	332.2	362.7
5	301.0	93.9	124.4
6	301.0	93.9	124.4

ACCUMULATOR PRECHARGE

ACCUMULATOR	PRECHARGE (PSI)
1 (TOP)	257.2
2 (TOP)	318.3
3 (TOP)	318.3
4 (TOP)	257.2
5 (TOP)	72.7
6 (TOP)	72.7

RESULTANT STIFFNESS AT CENTER OF PLATFORM

1207.1	-.0	-20.1	-.0	515.5	.0
-.0	753.4	-.0	13248.6	.0	-19596.6
-20.1	-.0	2910.4	-.0	29222.1	-.0
-.0	13248.6	-.0	1847402.1	.0	-108162.6
515.5	.0	29222.1	.0	1007732.1	.1
.0	-19596.6	-.0	-108162.7	.1	1867540.6

INPUT DATA

```
 1.                                   6- D O F   S I M U L A T O R
 2.                                   ****************************
 3.             VEHICLE .............  AH 1G  HELICOPTER
 4.      20.
 5.       9500.0        0.0         0.0      93.33
 6.         0.0        0.0         0.0
 7.       1000.        0.0         0.
 8.          0.0        0.0
 9.      1
10.      1
11.       10000.                30000.                 15000000.
12.      -8457.                -3078.                 -401327.
13.      100.

TIME: 0.0922 SECONDS.
```

CASE 1

6- D O F S I M U L A T O R
****

VEHICLE .... AH 1G HELICOPTER

ACTING WEIGHT = 9500.0 LBS

COORDINATES, INCH	X	Y	Z
C.G. OF WEIGHT	.000	.000	93.330
WEAPON MOUNTING POINT	.000	.000	.000
TARGET	1000.000	.000	.000

MOUNTING ANGLE OF VEHICLE WITH PLATFORM, DEG. 20.00

GIMBAL ROTATION, DEG.
------ --------- ----

PITCH 20.00 (INCL. MOUNTING ANGLE)
YAW .00

DAMPING MEDIA......... OIL

EFFECTIVE VOLUME OF ACCUMULATOR = 117.5 IN3
MAXIMUM ACTUATOR STIFFNESS = 23000.0 LB/IN
MINIMUM ACTUATOR STIFFNESS = 800.0 LB/IN

EXTERNAL LOADS

	X	Y	Z
FORCE, LB.	-8457.0	.0	-3078.0
MOMEMT, IN.LB.	.0	-401327.0	.0

REQUIRED STIFFNESS AT MOUNTING PLATFORM

	X	Y	Z
TRANSLATION, LB/IN	10000.0	.0	30000.0
ROTATION,IN.LB/RAD	.0	15000000.0	.0

FORCES AT PITCH GIMBAL IN ITS COORDINATE SYSTEM

	X	Y	Z
FORCE, LB.	-11706.2	.0	5849.1
MOMEMT, IN.LB.	.0	-1092538.9	.0

CASE 1 — 6- D O F S I M U L A T O R
****

VEHICLE .... AH 1G HELICOPTER

ACTUATOR FORCES AND DISPLACEMENTS DUE TO

ACTUATOR	WEIGHT,LB	RECOIL LOAD,LB.	DIPL.(RECOIL LD.),IN
1	2954.4	2016.1	.17099
2	-1016.8	-8320.2	-.83285
3	-1016.8	-8320.2	-.83285
4	2954.4	2016.1	.17099
5	3836.9	4313.1	.42394
6	3836.9	4313.1	.42394

ACTUATOR STIFFNESS AND PRESSURES
-------- --------- --- ---------

ACTUATOR	STIFFNESS LB/IN	TOP PRESSURE PSI	BOT. PRESSURE PSI
1	11790.7	1470.9	1610.2
2	9990.0	1329.2	1281.3
3	9990.0	1329.2	1281.3
4	11790.7	1470.9	1610.2
5	10173.9	1238.8	1419.8
6	10173.9	1238.8	1419.8

ACCUMULATOR PRECHARGE
----------- ---------

NO.	TOP	BOTTOM
1	735.4	805.1
2	664.6	640.6
3	664.6	640.6
4	735.4	805.1
5	619.4	709.9
6	619.4	709.9

RESULTANT FLEXIBILITY AT THE REQUIRED LOCATION

.781673-04	.000000	.315871-05	.228706-13	.435845-06	-.439648-13
.113687-12	.828593-04	-.170530-11	-.282288-06	.426326-13	.412051-07
.315871-05	-.170530-11	.263319-04	.399680-13	-.128639-07	.159872-13
.157652-13	-.282288-06	.435207-13	.529893-07	-.333067-15	-.340362-08
.435845-06	.355271-13	-.128639-07	-.277556-15	.575809-07	.111022-15
-.404121-13	.412051-07	.159872-13	-.340362-08	.000000	.410364-07

RESULTANT STIFFNESS AT THE REQUIRED LOCATION

13429.0	-.0	-1660.8	-.0	-102018.7	.0
-.0	12293.7	.0	65045.4	-.0	-6949.3
-1660.8	.0	38186.4	-.0	21101.7	-.0
-.0	65045.4	-.0	19316977.2	.1	1536864.1
-102018.7	-.0	21101.7	.1	18143777.5	-.2
.0	-6949.3	-.0	1536864.1	-.1	24503048.2

@FIN

APPENDIX D
USE OF PIPDYNE COMPUTER PROGRAM TO VERIFY THAT $A^T = B^{-1}$ AND $B^T = A^{-1}$

Summary

The relationship between the system stiffness and the actuator stiffnesses of the mathematical model is

$$K = A^{-1} k B \tag{D-1}$$

or

$$K = B^T k B \tag{D-2}$$

where

$$B^T = A^{-1} \tag{D-3}$$

The following analysis is given to verify that $A^T = B^{-1}$ and $B^T = A^{-1}$.

Test Model

The triogonal actuator system, which is composed of six actuators elements 1 through 6 is shown in figure D-1. A joint is located at each end of the actuators; the top joints 8 through 13 are the boundary joints. Joints 1 through 7 are located on the mounting platform, of which joint 1 is used to introduce the loads to the system. Elements 6 through 18 represent the mounting platform which interconnects joints 1 through 7 to form a rigid structure.

Use of Computer Program

A computer program to solve a three-dimensional frame structure may be used. Here, FIRL computer program called PIPDYN is used.

Input Data Required

1. Joint Coordinates

The coordinates of joints 1 through 13 are given in the X, Y, Z system shown on figure D-1.

2. Material Properties

The material used is steel, for which

Youngs Modulus = 30×10^6 psi, and

Poisson's Ratio = 0.3

3. Member Properties

The members representing the mounting platform (7 through 18) are assumed to be of solid circular cross section of 10 in diameter.

Members 1 through 6 representing the actuators are assumed to have the same stiffnesses (k) of 10,000 lb/in. each and are represented by a solid circular cross section.

The following approach is used to obtain the diameter of members representing the actuators.

$$k = \frac{AE}{L} \tag{D-4}$$

$$\therefore \quad A = \frac{kL}{E}$$

$$d = \sqrt{\frac{4A}{\pi}} = \sqrt{\frac{4kL}{\pi E}} \tag{D-5}$$

where

K = actuator stiffness = 10,000 lb/in.

L = actuator length = 46.57 in.

E = Youngs modulus = 30×10^6 psi

Therefore

The diameter (d) of the member = 0.1406 in.

4. Releases

The following constraints are imposed on the test model in order to represent the actual triogonal system.

The joint located at the top end of each actuator (boundary joints) is released in rotation about the three system axes. The joint located at the bottom of each actuator is released in rotation about two of the system axes, the third rotation is constrained to avoid singularity.

5. Loading

Two loading conditions are imposed on the system and are applied at joint (1).

Loading (1) - Forces

A unit force = 10,000 lb is applied in each direction of the system axes X, Y and Z. Similarly a unit moment = 10,000 in./lb is applied about each direction of the system axes X, Y and Z.

A total of 6 loads are applied at joint 1.

Loading (2) - Displacements

A unit displacement = 1.0 in. is applied in each direction of the system axes X, Y and Z. Similarly, a unit rotation = 1.0 radian is applied about each direction of the system axes X, Y and Z.

A total of 6 loads are applied at joint 1. Note that joint 1 is completely constrained from translation and rotation except in that direction in which a translation or a rotation loading is applied.

Computer Results

The computer results are given in attachment (2).

The two loading cases are designated by:

Loading 1 - Force transformation, and

Loading 2 - Displacement transformation

Extraction of Results for Computer Output

Three sets of results are extracted from the computer output to verify the three following relations.

Force Displacement for the Triogonal System

Equation (425) of the mathematical model given earlier in this report is

$$\underset{\sim}{F} = K \underset{\sim}{D} \qquad \text{(D-6)}$$

The computer output listed in table D-1 determines matrix K which is given in table D-2. This matrix is obtained by getting the displacements and rotations of joint 1 in each of the system coordinate directions due to the applied loading 1.

Actuator System, Force Transformation Matrix

Equation (427) of the mathematical model given earlier in this report is

$$\underset{\sim}{f} = A \underset{\sim}{F} \tag{D-7}$$

Matrix A^T is given in table D-3, which is obtained from the computer output, loading 1, which is the actuator force (along its local axis - F2, at end 2) with a sign reversed to represent the actuator force component in the direction of the applied load.

Actuator System, Displacement Transformation Matrix

Equation (428) of the mathematical model given earlier in this report is

$$\underset{\sim}{d} = B \underset{\sim}{D} \tag{D-8}$$

Matrix B^T is given in table D-4 which is obtained from the computer output, loading 2, which is the actuator displacement (along its local axis - X2, at end 2) with a sign reversed to represent the actuator component in the direction of the applied displacement.

Conclusions

The following results can be concluded, simply by inspection of matrices A and B^{-1} (tables D-3 and D-6) and matrices B and A^{-1} (tables D-4 and D-5), that

$$A^T = B^{-1} \tag{D-9}$$

and

$$B^T = A^{-1} \tag{D-10}$$

Also by comparing matrix (A^{-1} x B) table D-7 and the stiffness matrix (K) (table D-2), we can justify equation D-1 given in the summary of this appendix, which is applied for the stiffness of equal actuators.

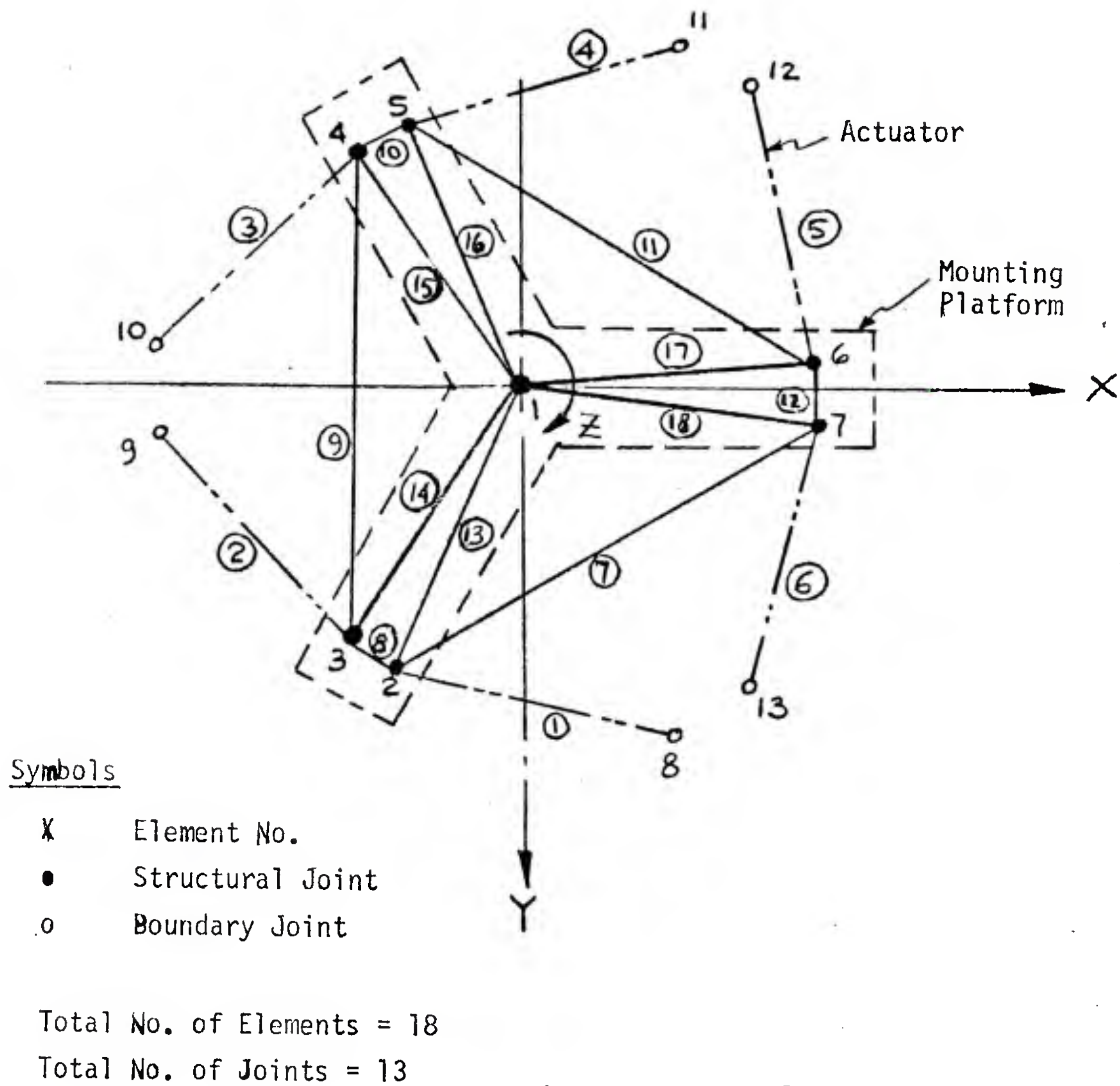

Figure D-1. Test model, triogonal actuator system (plan)

Table D-1. System flexibility matrix*

.85320	.00000	.00000	.00000	.00380	.00000
.00000	.85320	.00000	-.00380	.00000	-.00000
.00000	.00000	.27976	.00000	.00000	.00000
.00000	-.00380	.00000	.00059	.00000	.00000
.00380	.00000	.00000	.00000	.00059	.00000
.00000	-.00000	.00000	.00000	.00000	.00044

*Ref. computer results, attachment 2 - loading 1

Table D-2. System stiffness matrix (K)

1.20682	.00000	-.00000	.00000	-7.80397	.00000
.00000	1.20682	.00000	7.80405	.00000	.00001
-.00000	.00000	3.57445	.00000	-.00010	.00000
.00000	7.80405	.000001751	.90138	.00000	.00005
-7.80398	.00000	-.00010	.000001751	.89470	.00000
.00000	.00001	.00000	.00005	.000002294	.29361

Table D-3. Actuator system, force transformation matrix $(A)^{T}$*

-.48517	.43410	.43410	-.48517	.05107	.05107
-.22114	.30960	-.30960	.22114	.53074	-.53074
.21561	.21561	.21561	.21561	.21561	.21561
.01351	.00983	-.00983	-.01351	-.00369	.00369
.00355	.00993	.00993	.00355	-.01348	-.01348
.00851	-.00851	.00851	-.00851	.00851	-.00851

*Ref computer results attachment 2 - loading 1

Table D-4. Actuator system, displacement transformation matrix $(B)^{T}$*

-.61322	.44641	.44641	-.61322	.16682	.16682
-.16142	-.45036	.45036	.16142	.61178	.61178
.77074	.77074	.77074	.77074	.77074	.77074
21.95092	19.63575	-19.63575	-21.95092	-2.31516	2.31516
10.00000	14.01000	14.01000	10.00000	-24.01006	-24.01006
19.52949	19.52950	19.52950	-19.52949	19.52951	-19.52951

*Ref. computer results attachment 2 - loading 2

Table D-5. A^{-1} matrix

-.61359	.44636	.44636	-.61359	.16722	.16722
-.16098	.45096	-.45096	.16098	.61194	-.61194
.77300	.77300	.77300	.77300	.77300	.77300
22.03258	19.71328	-19.71328	22.03258	-2.31930	2.31930
10.03938	14.05508	14.05508	10.03938	-24.09446	-24.09446
19.59343	-19.57708	19.57708	-19.59343	19.58389	-19.58389

Table D-6. B^{-1} matrix

-.48537	.43418	.43418	-.48537	.05119	.05119
-.22112	.30979	-.30979	.22112	.53090	-.53090
.21624	.21624	.21624	.21624	.21624	.21624
.01356	.00987	-.00987	-.01356	-.00369	.00369
.00357	.00996	.00996	.00357	-.01353	-.01353
.00853	-.00853	.00853	-.00853	.00853	-.00853

Table D-7. $A^{-1} \times B$ matrix (equivalent to $B^T \times B$)

1.20684	.00000	-.00000	-.00000	-7.79466	-.00000
-.00000	1.20690	.00000	7.80899	-.00000	.00002
-.00000	.00000	3.57469	.00000	-.00009	.00000
-.00000	7.80515	.000011752	.18031	.00000	-.00049
-7.80288	.00000	.00001	-.000001751	.62956	.00003
.00000	.00305	-.00000	.68668	.000022294	.88837

APPENDIX E
MAIN HYDRAULIC POWER UNIT

Adiabatic condition:

$$V_1 = \frac{V_x(P_3/P_1)^{1/n}}{1 - (P_3/P_2)^{1/n}}$$

Where:

V_1 = Size of accumulator necessary, cu. in. This is the maximum volume occupied by the gas at precharge pressure.

V_x = Volume of fluid discharged from accumulator, cu. in. It is the additional volume of fluid demanded by the system.

P_1 = Gas precharge of accumulator, psi. This pressure must be less than or equal to minimum system pressure (P_3).

P_2 = Maximum system design operating pressure, psi.

V_2 = Compressed volume of gas at maximum system pressure, cu. in.

P_3 = Minimum system pressure at which the additional volume of fluid is needed, psi.

V_3 = The expanded volume of gas at minimum system pressure, cu. in.

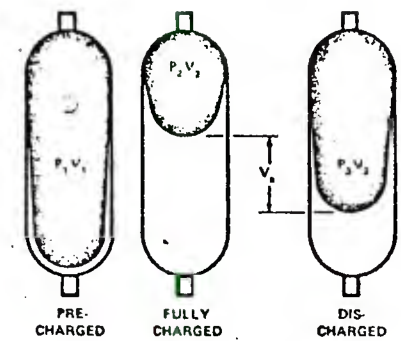

Q_V = REQ'D VALVE FLOW (IN^3/SEC)

Q_P = PUMP FLOW PROVIDED $= \frac{2Q_V}{\pi}$ (IN^3/SEC)

$$\therefore \quad V_x = \frac{Q_V - Q_P}{\text{FREQUENCY}} = \left(Q_V - \frac{2Q}{\pi}\right)/f = \frac{.3634\,Q_V}{f} \quad (IN^3)$$

LET: $P_1 = 1{,}500$ PSI, $P_2 = 3{,}000$ PSI & $\frac{P_3}{P_2} = .9$

$$\therefore \quad P_3 = 2{,}700 \text{ PSI}, \quad \frac{P_3}{P_1} = \frac{2700}{1500} = 1.8$$

$$n = 1.4 \text{ (FOR } N_2\text{)}, \quad \frac{1}{n} = .714$$

$$V_1 = \frac{V_x (1.8)^{.714}}{1-(.9)^{.714}} = \frac{1.5217\,V_x}{.0725} \doteq 21\,V_x = \frac{7.6314\,Q_V}{f} \quad (IN^3)$$

CONVERT TO GALLONS:

$$V_1 = 21\,V_x = \frac{(21)(.3634)\,Q_V\,\frac{60}{231}\text{ (GPM)}}{f\,(60)\text{ (CPM)}} = \frac{.033\,Q_V}{f} \quad (GAL)$$

ACCUMULATOR — AT POWER UNIT :—

SIZING — FOR LINE SHOCK DAMPENER ONLY :—

$$V = \frac{\left[\frac{W}{2g}v^2\right]\left[\frac{n-1}{P_1}\right]}{\left[\frac{12}{\left[\frac{P_2}{P_1}\right]^{\left[\frac{n-1}{n}\right]}-1}\right]}$$

Where:

V = Required accumulator capacity, cu. in.

P_2 = Maximum shock pressure, psi.

W = Total weight of fluid in the pipe line, lb

g = Acceleration due to gravity, 32.2 ft/sec².

n = 1.4 for nitrogen.

v = Flow velocity, ft/sec.

P_1 = System pressure at normal flow rate, psi.

$P_1 = 3000$ PSI

$P_2 = 1.5(P_1) = 4{,}500$ PSI

$v = 20$ FT/SEC. (240 GPM IN 3.85 IN² PIPE)

$W = \gamma \cdot A \cdot L = 53\left(\frac{\#}{ft^3}\right) \times \frac{3.85}{144}(ft^2) \times 70' \doteq 100\ \#$

$$V = \left[\frac{100}{2g}(20)^2\right]\left[\frac{.4}{3000}\right]\left[\frac{12}{(1.5)^{.285}-1}\right] \doteq 8.\ (IN^3)$$

FOR PUMP PULSATION DAMPENER :—

PERMISSIBLE FLUCTUATION = ± 5% OF 3000 PSI

$V_1 = \frac{.6(DISPL.)(1.05)^{.714}}{1-(.95)^{.714}}$, $DISPL. = \frac{240 \times 231}{1200\ RPM} = 46.2\ (IN^3)$

$\therefore V_1 = \frac{27.72(1.036)}{1-(.964)} \doteq 800\ (IN^3)$

ACCUMULATOR SIZE = $\frac{808}{231} = 3.5$ GAL (MIN.)

NEAREST STOCK SIZE : 5 GAL.

DeAnnuntis & Associates, Inc.
CONSULTING ENGINEERS
WESTERN SAVINGS BANK BUILDING • PHILADELPHIA, PA. 19107

REGISTERED PROFESSIONAL ENGINEERS
PEnnypacker 5-7814

William J. DeAnnuntis, P. E.

FLUID COOLER REQUIREMENTS

THE FRANKLIN INSTITUTE
20th and Cherry Streets
Philadelphia, Pa.

CONDITIONS*	CASE I	CASE II
Ambient Air Temp.	95.0°F.	105.0°F.
GPM of Oil	250	250
Entering Oil Temp.	130.00°F.	130.00°F.
Leaving Oil Temp.	116.35°F.	116.35°F.
MBH	687.0	687.0
Elevation	1000 Ft.	1000 Ft.

*Conditions: Cool 250 GPM of MIL-O-5606 fluid from 130°F. to a minimum of 116.35°F. at 95°F. ambient air (Case I) and 105°F. (Case II). The fluid shall be pumped from a 600-gallon tank at atmospheric pressure.

DeAnnuntis & Associates, Inc.
CONSULTING ENGINEERS
WESTERN SAVINGS BANK BUILDING • PHILADELPHIA, PA. 19107

REGISTERED PROFESSIONAL ENGINEERS
PENNYPACKER 5-7814

William J. DeAnnuntis, P. E.

FLUID COOLER SELECTION

THE FRANKLIN INSTITUTE
20th and Cherry Streets
Philadelphia, Pa.

EQUIP. SELECTION	CASE I	CASE II
Trane Model No.	GC08-B2-14.5-5	GC08-B2-21-5
Velocity (FPS)	70	73
Std. Coil Face Vel.(FPM)	500	550
Oil Press. Drop (PSI)	3	4
Velocity (FPS)	2.23	2.23
BHP (Per Fan)	5 (Approx.)	12 (Approx.)
R.P.M.	550	670
Fans	(2) 60" Dia. 6 Blade Adj. Pitch	(2) 60" Dia. 6 Blade Adj.Pitch
Coil Face Area	116 Ft.^{2}	168 Ft.^{2}
Fin Series (Fins/Ft.)	S-16 (108)	S-16 (108)
Spiral Turbulators	Yes	Yes
Tubes	5/8" Dia. x 0.024" Copper	5/8" Dia.x 0.024" Copper
Header Type	HR	HR
Arrangement	No. 4	No. 4
Mean T.D. (°F.)	21.7	14.5
Coil	4 Row - 2 Pass	4 Row - 2 Pass
Fan Motors	(2) 7½ H.P.	(2) 15 H.P.
Coils	(4) 24" x 174"	(4) 24" x 252"

Includes: Base unit, Drive Arrangement No. 4, 4 Coils 24" x Length, 4 Row, 2 Pass HR Coils, Adjustable Pitch Fans, Fan Guards and Orifices, Motors TEFC Type, Single Speed 1800 RPM, Belts & Sheaves.

NOTE: OPTIONAL EQUIP.: MOTORIZED DAMPERS, CAPACITY CONTROLS, CATWALK, LADDER, FAN GUARDS.

OIL COOLER SYSTEM

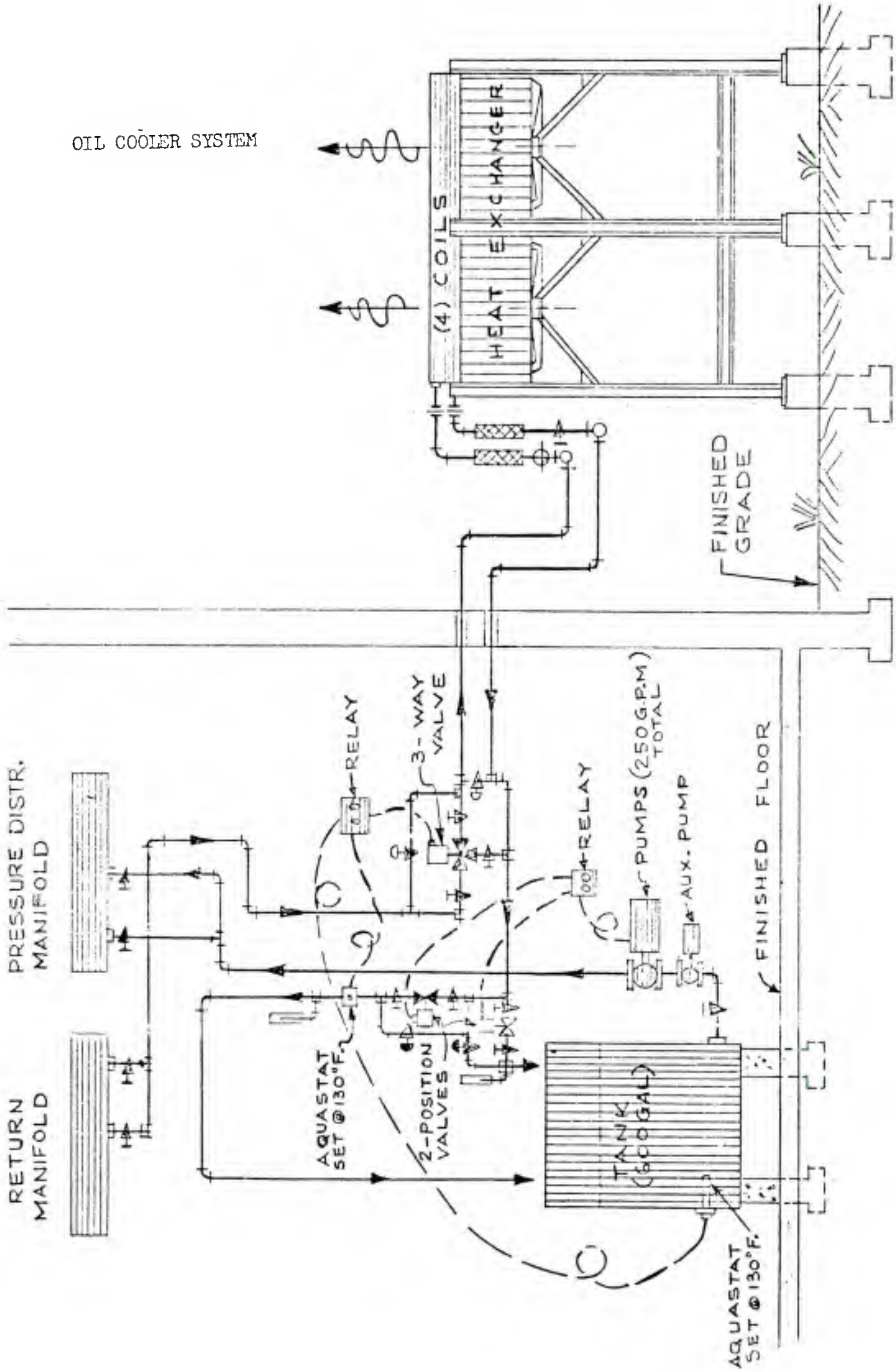

Drawing A-2662

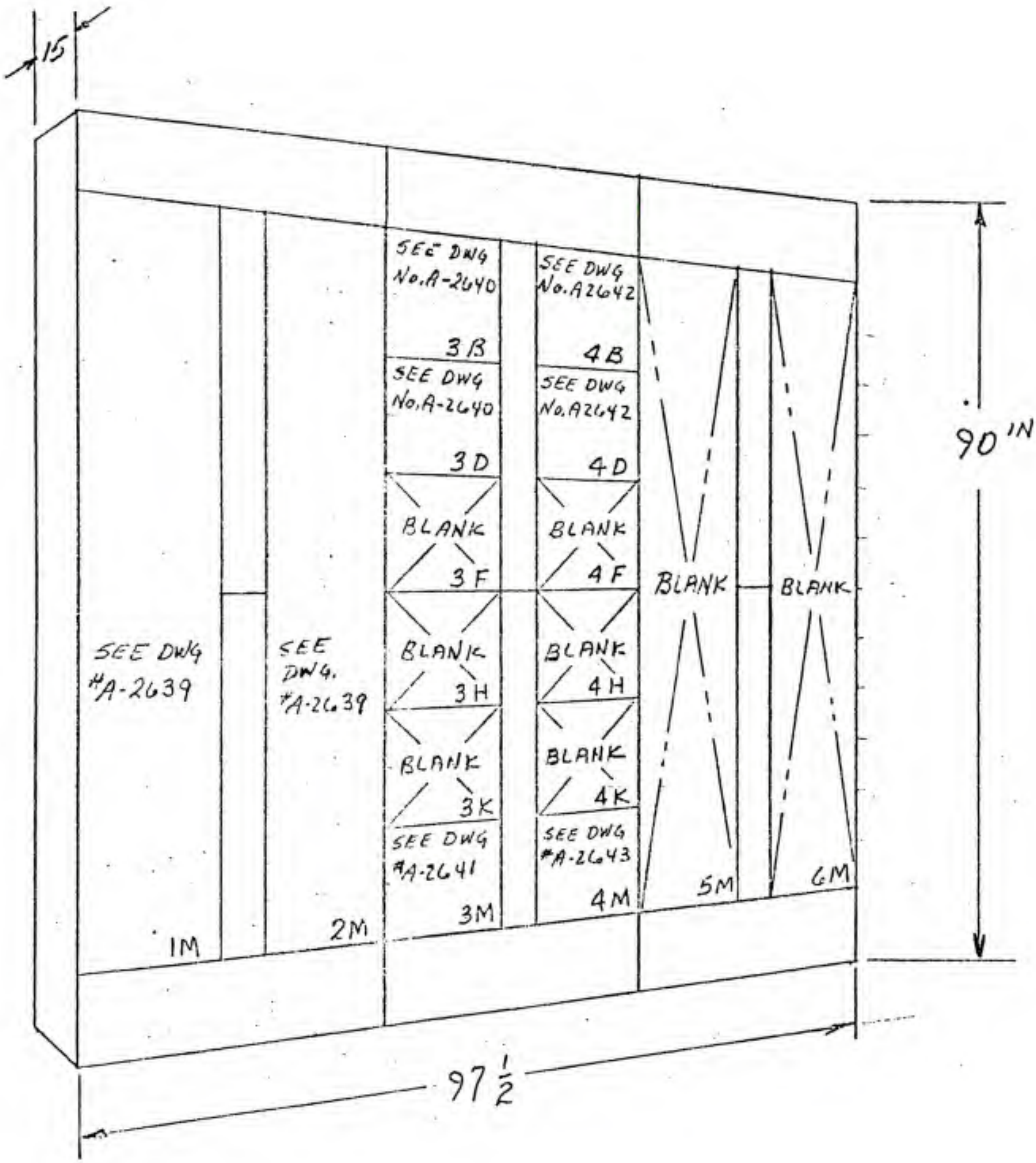

Drawing B-2638. Arrangement - unit control center

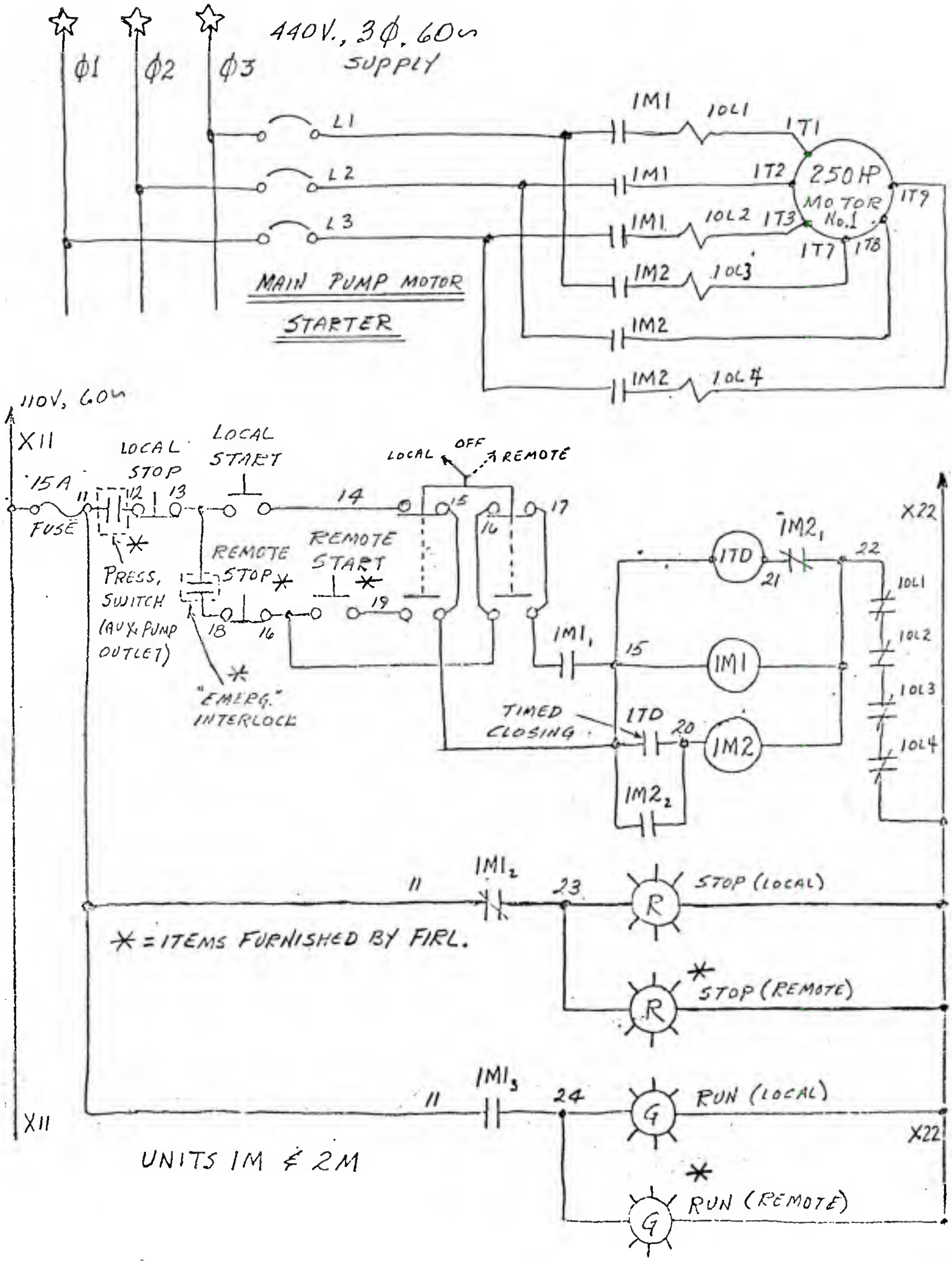

Drawing A-2639

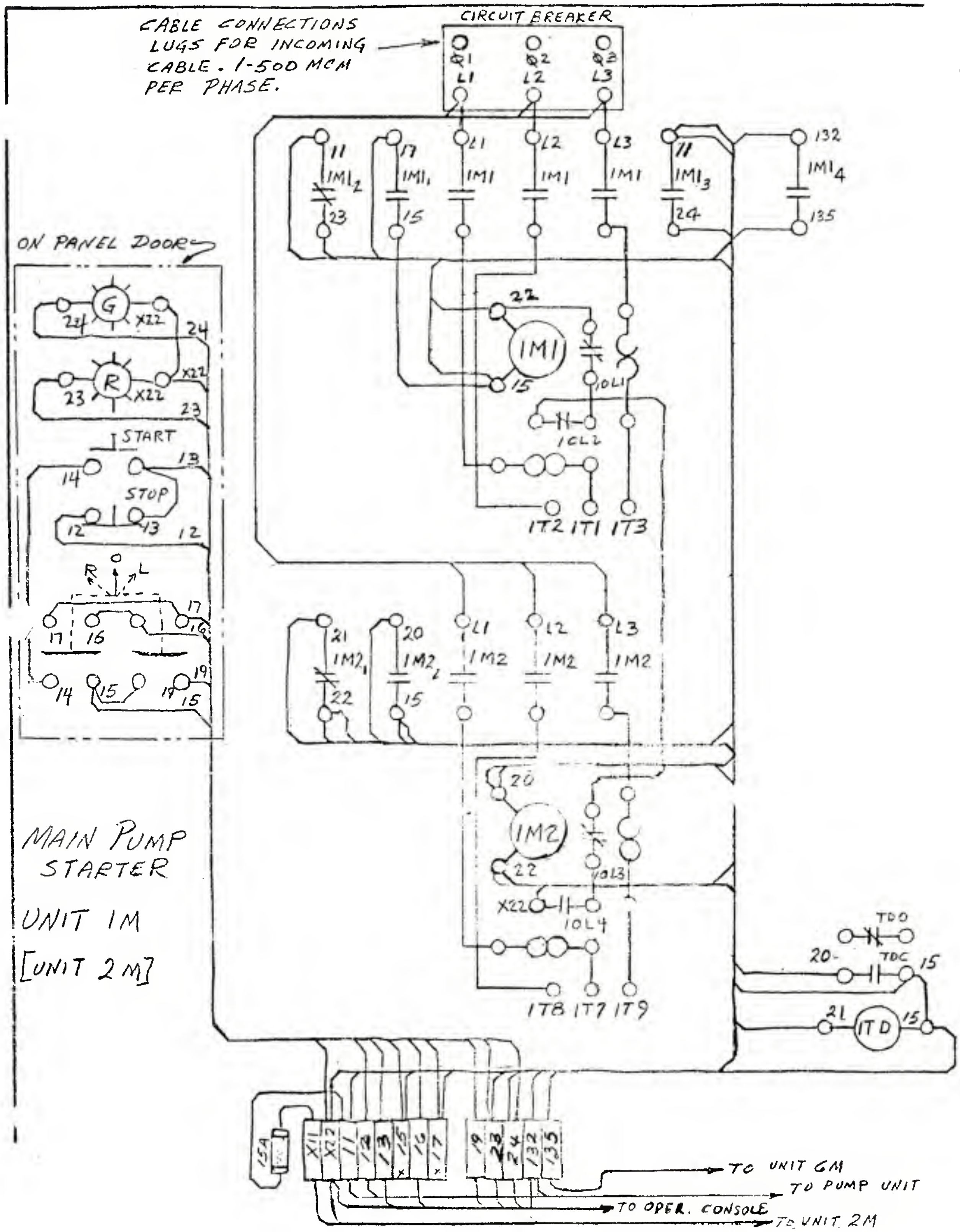

Drawing A-2639

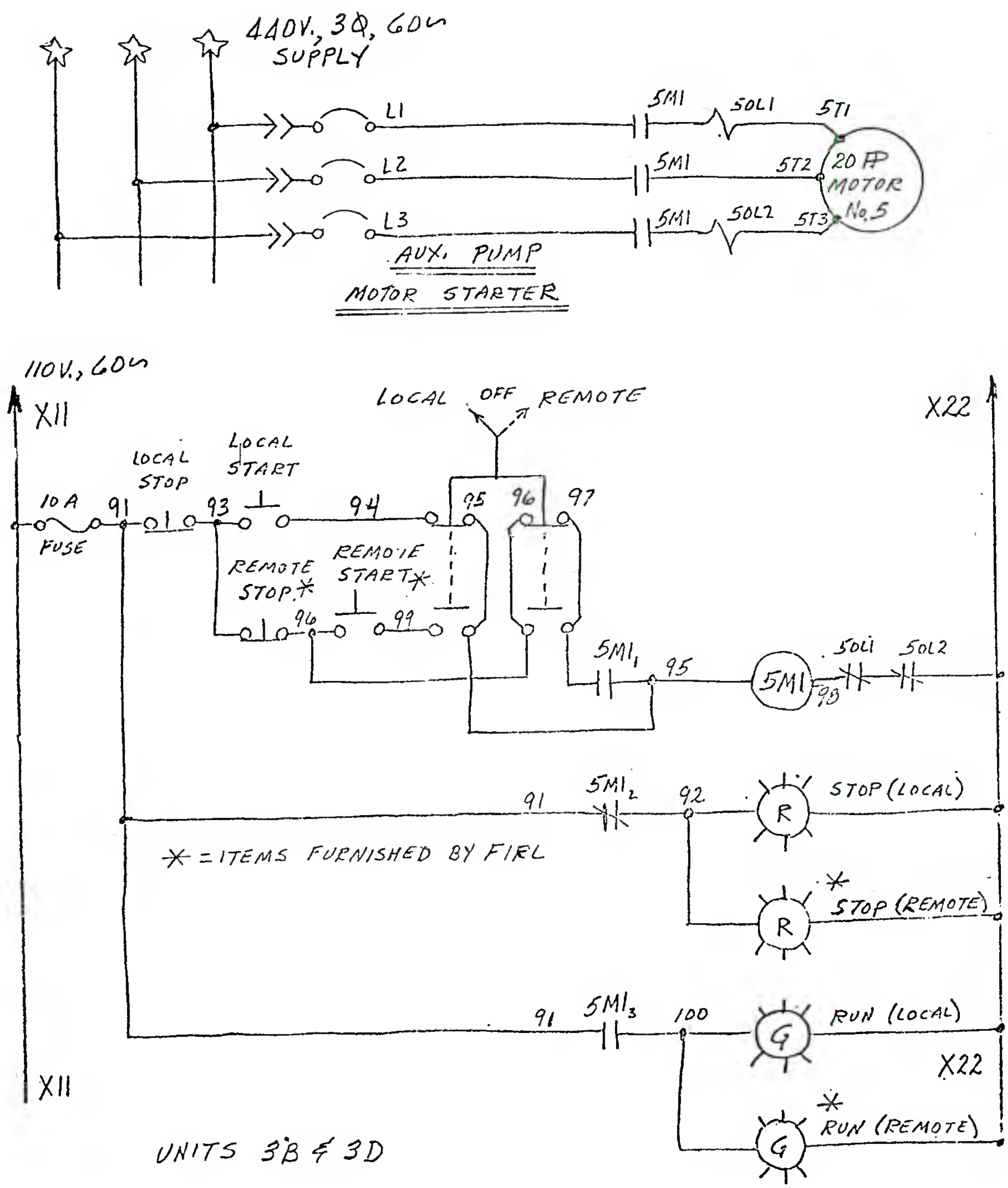

Drawing A-2640

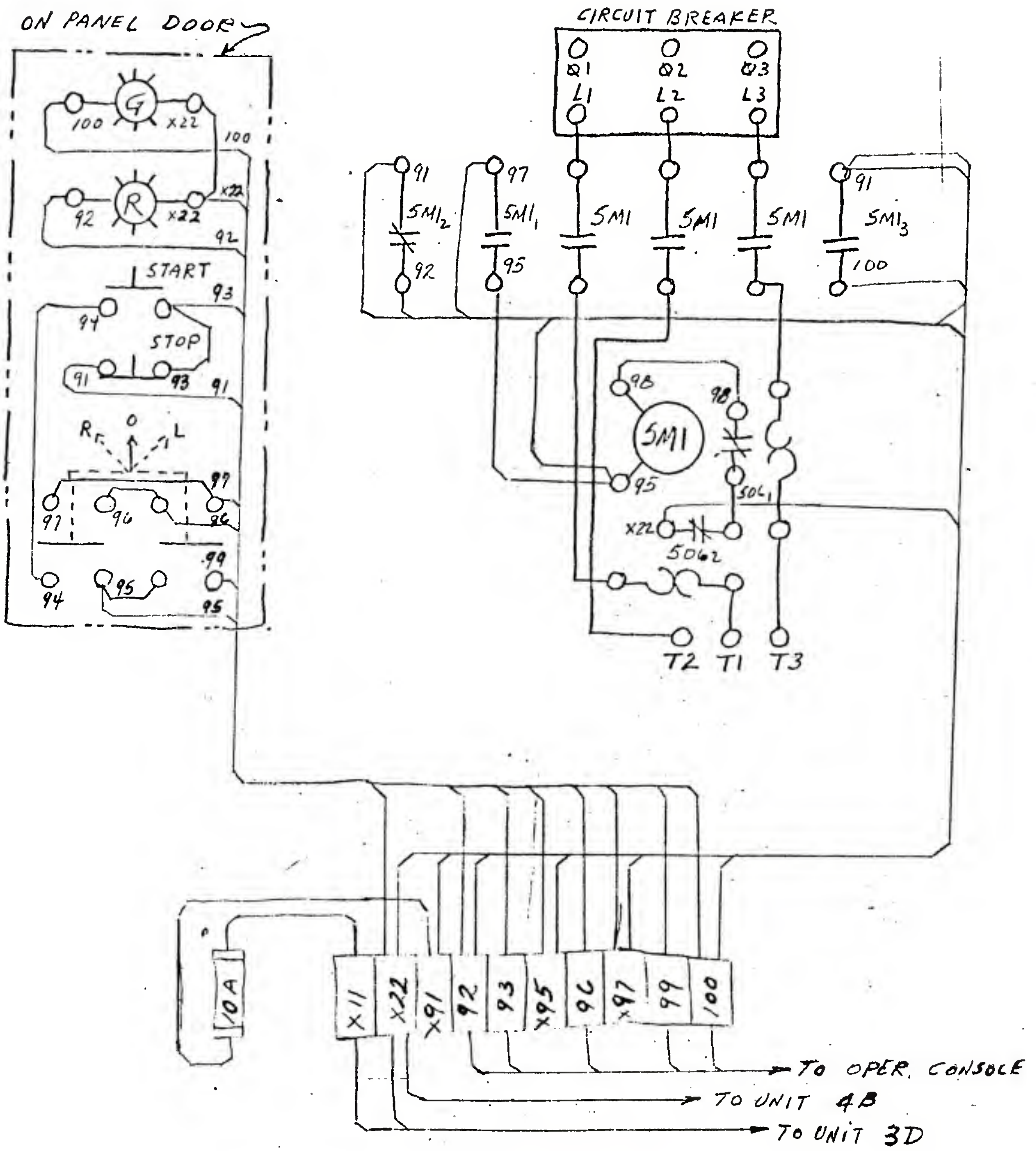

Drawing A-2640. Auxiliary pump starter - unit 3B (unit 3D)

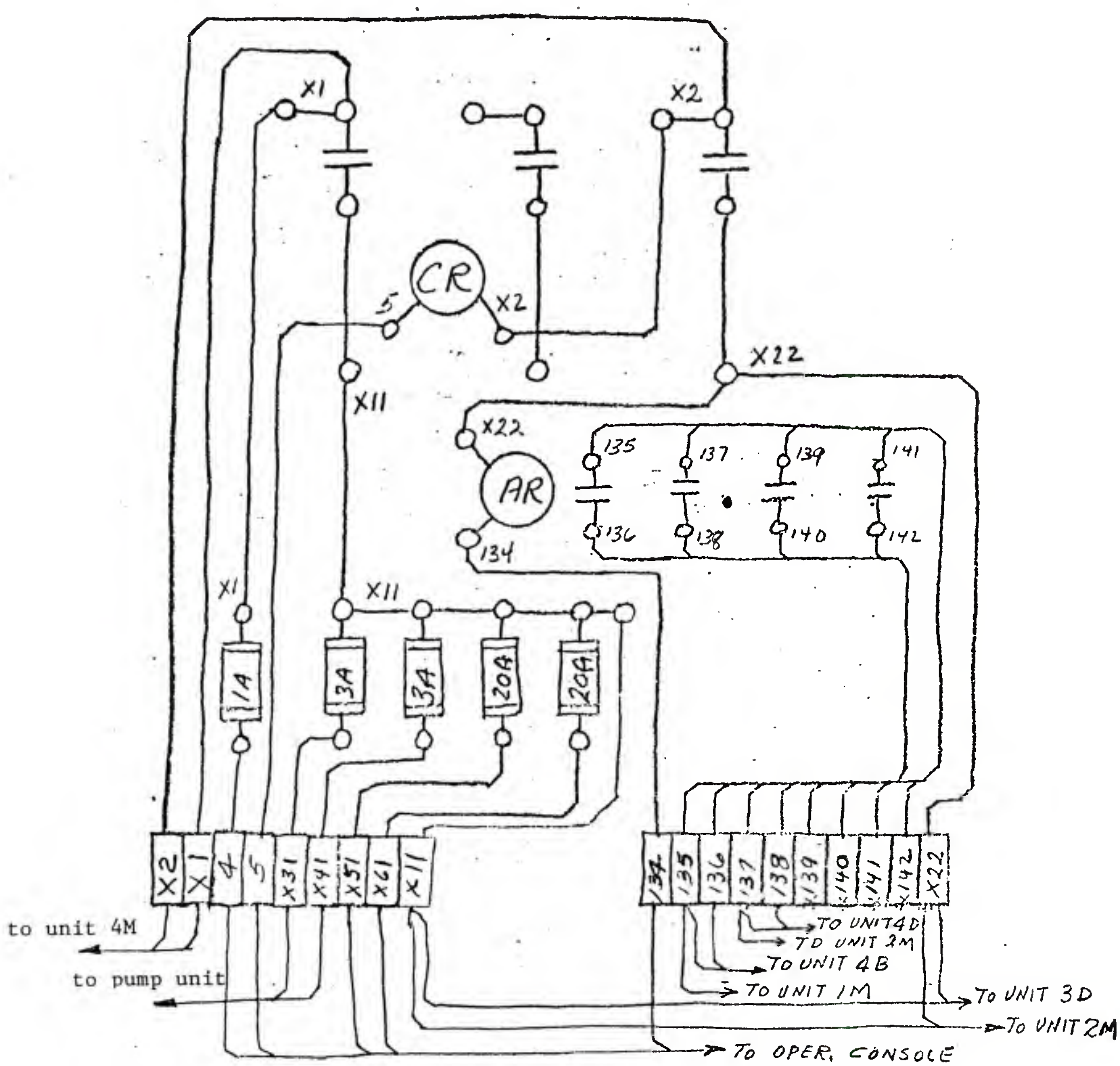

Drawing A-2641. Relay panel - unit 3M

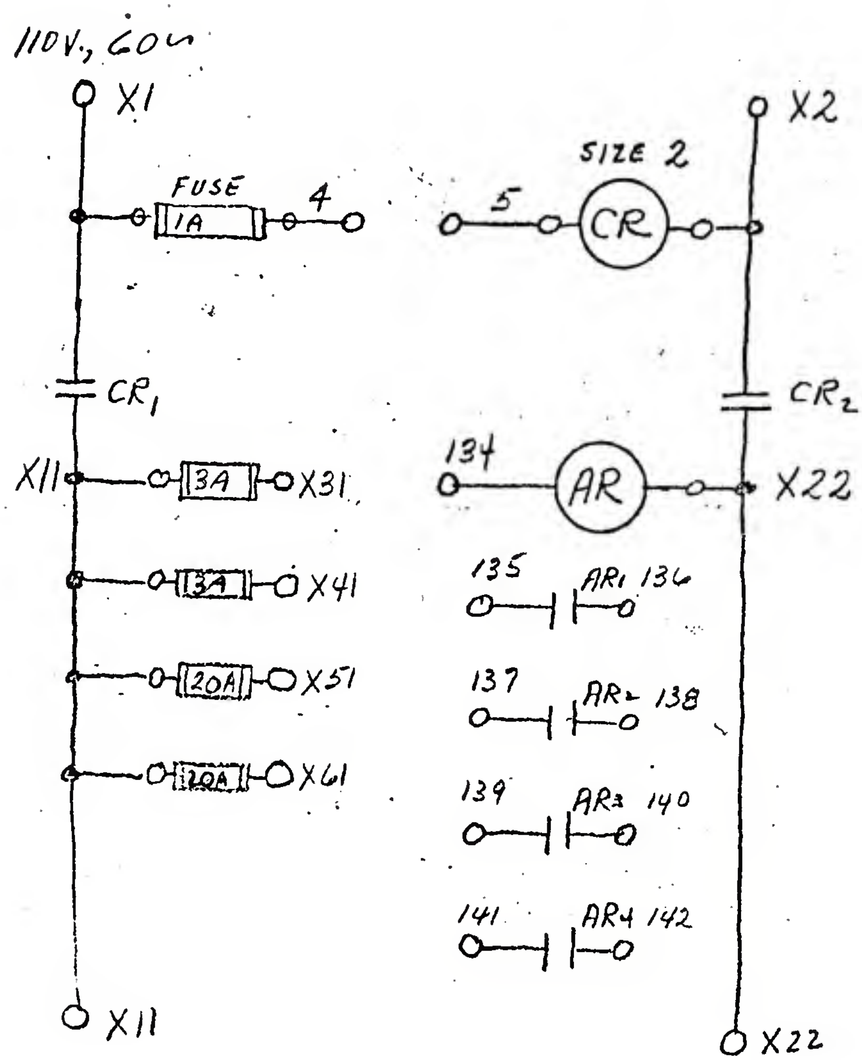

Drawing A-2641. Relay panel - unit 3M

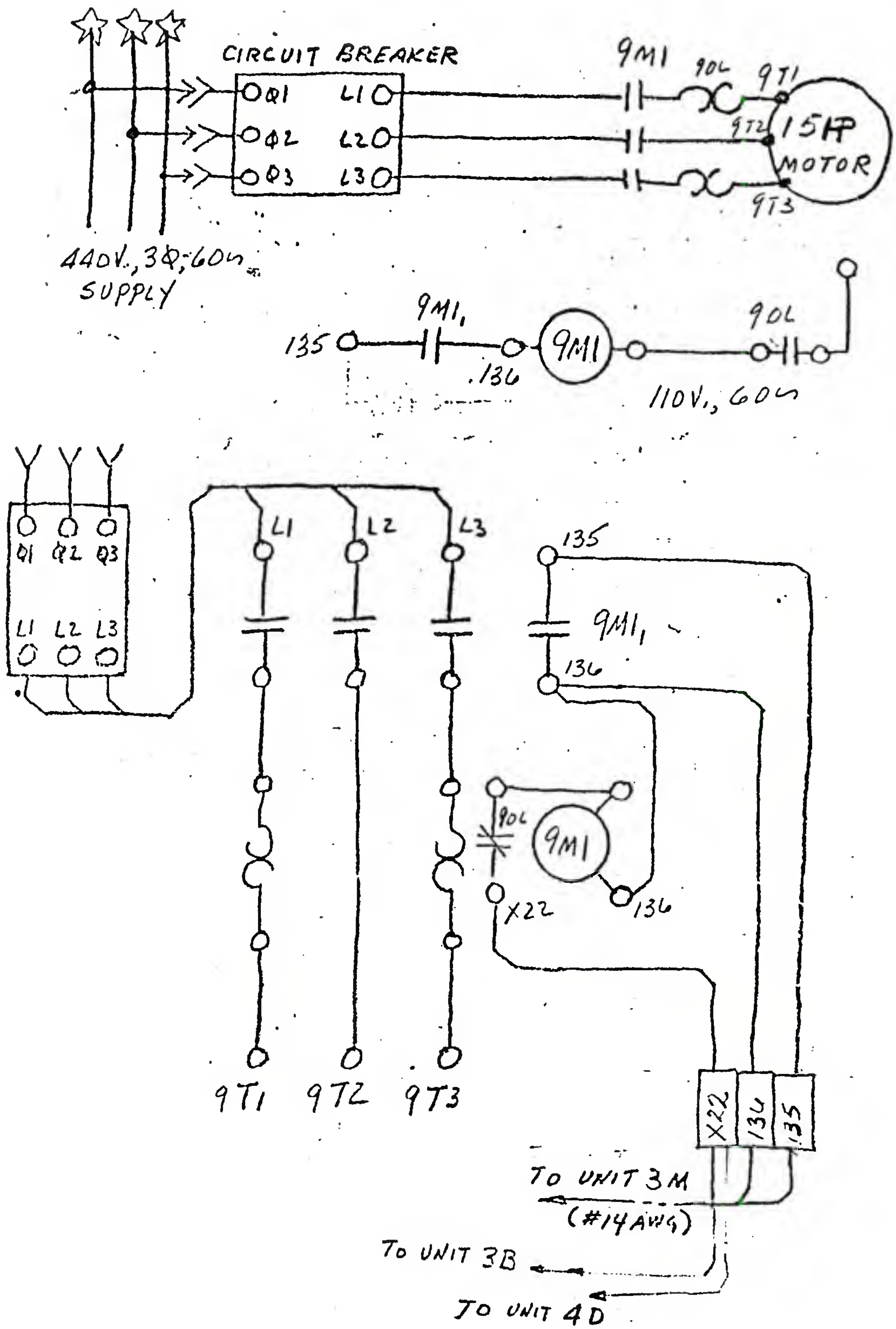

Drawing A-2642. Motor starter - unit 4B (unit 4D)

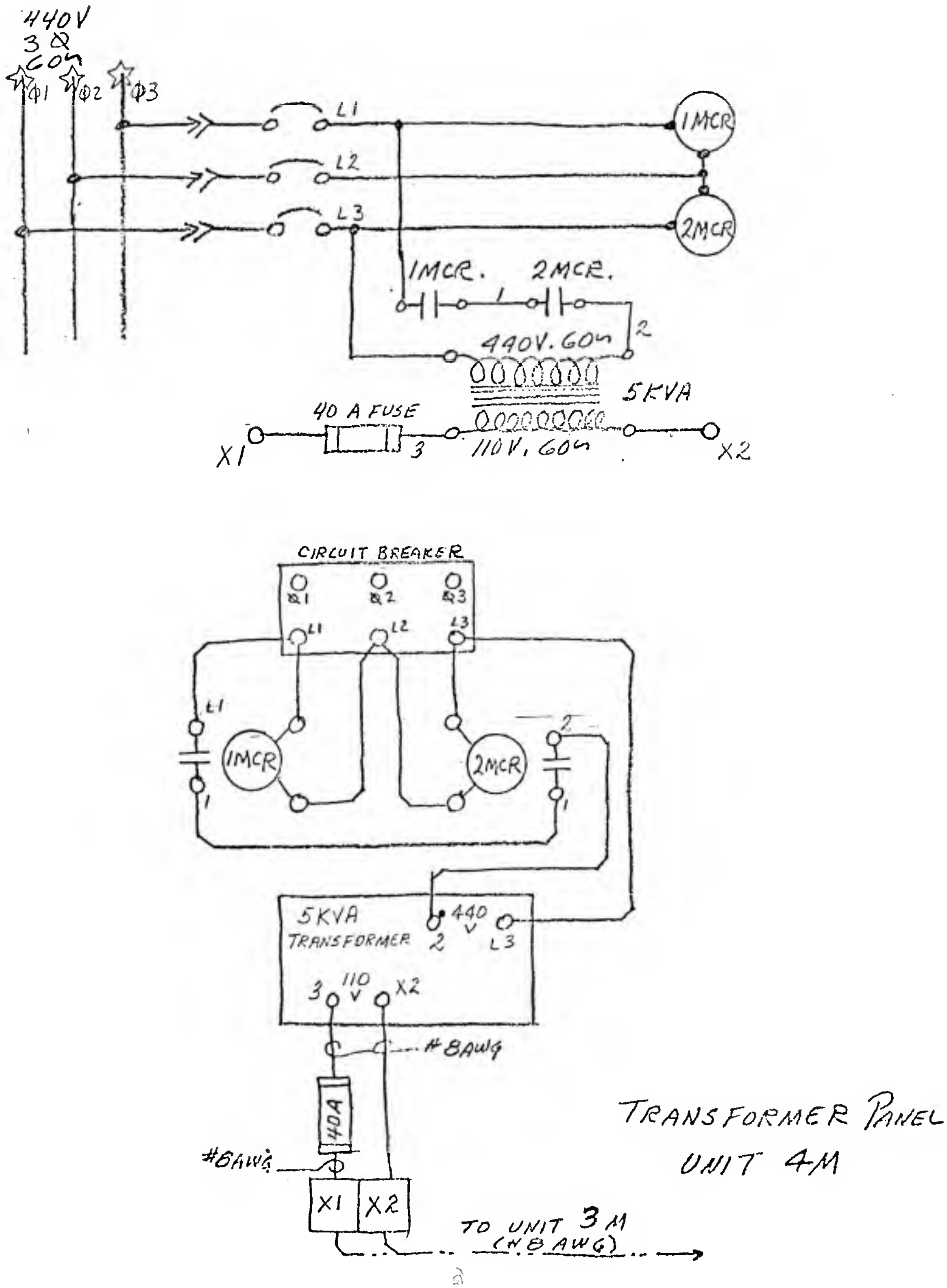

Drawing A-2643

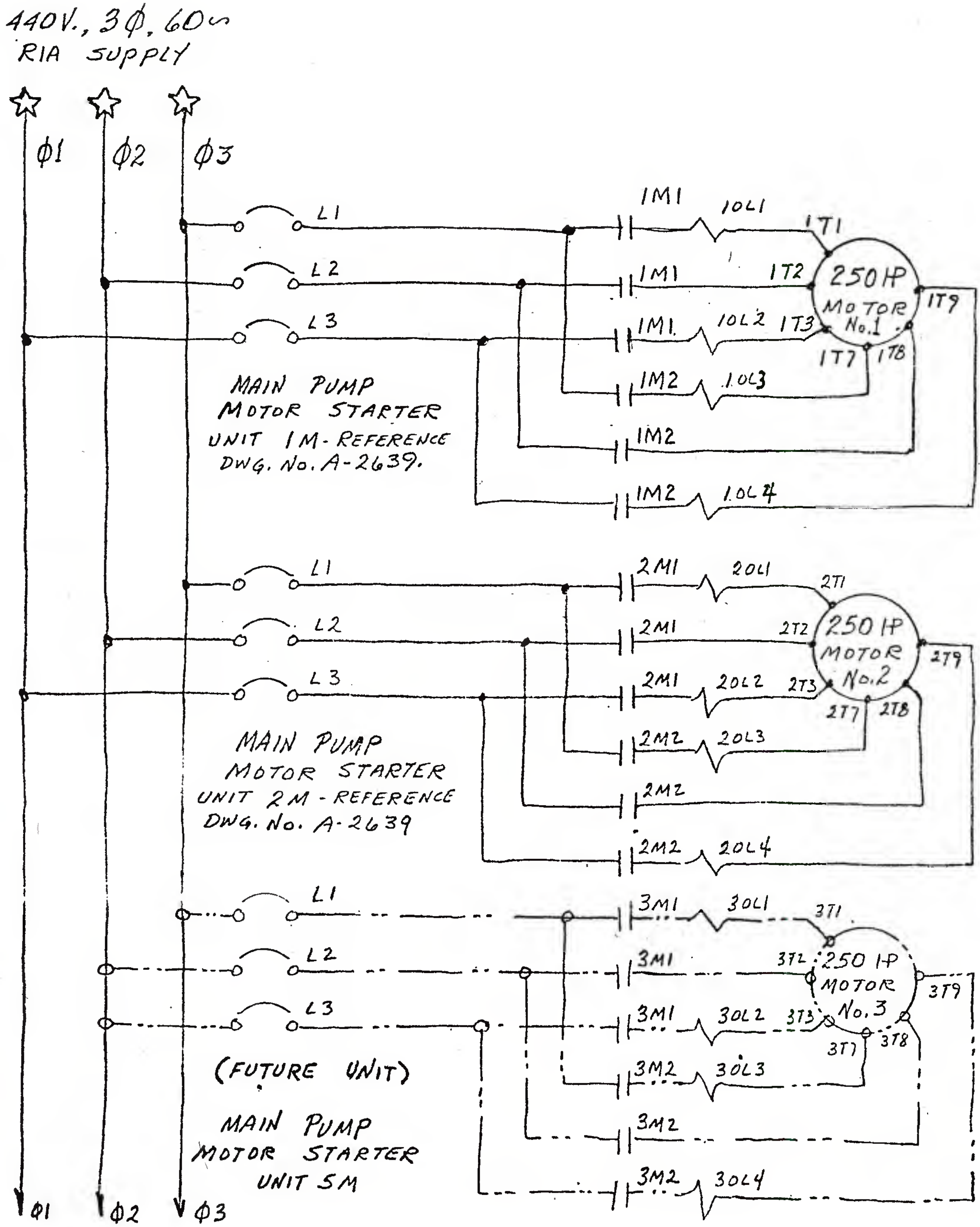

Drawing A-2626. Electrical schematic controls - modified helicopter fuselage mount simulator

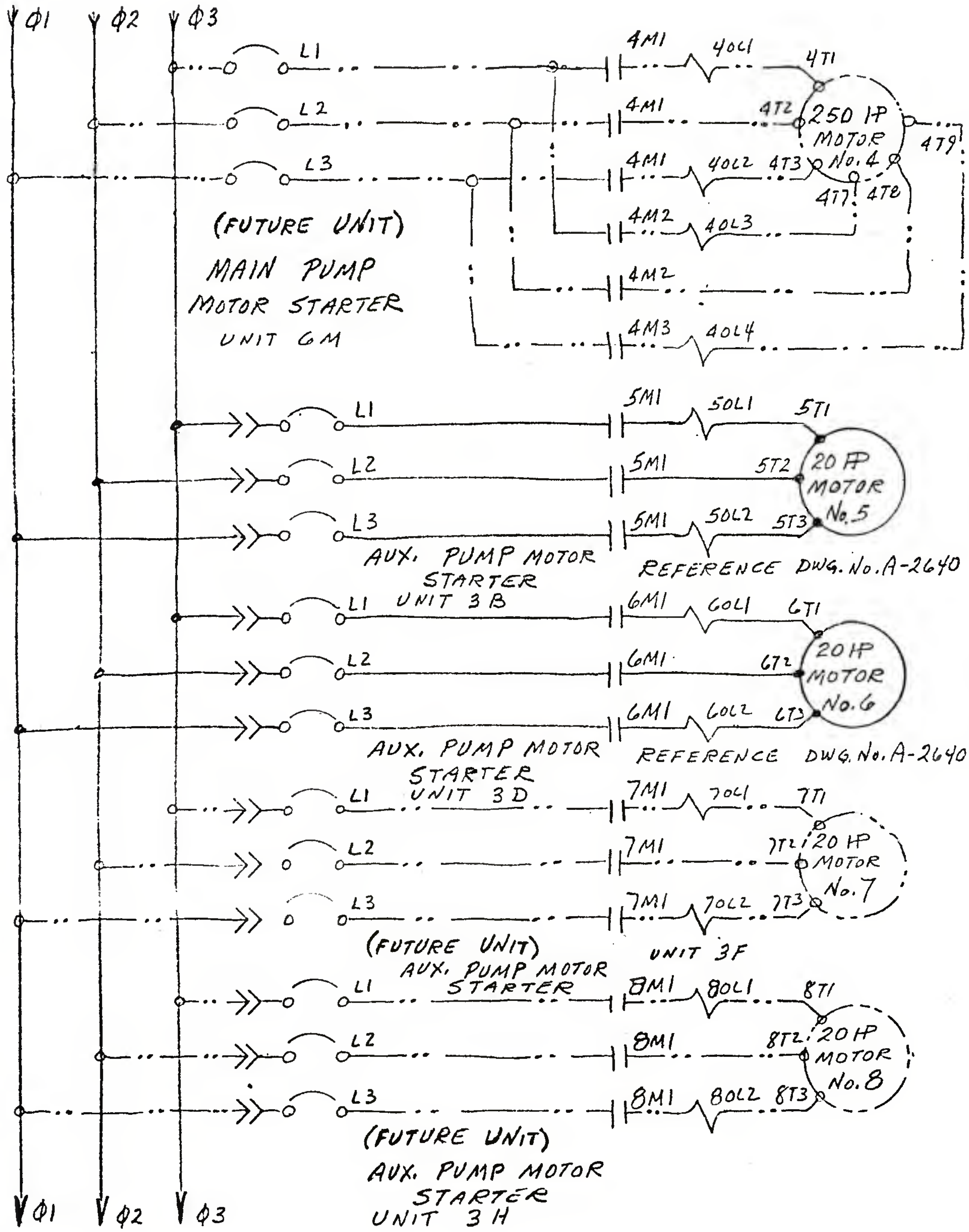

Drawing A-2626

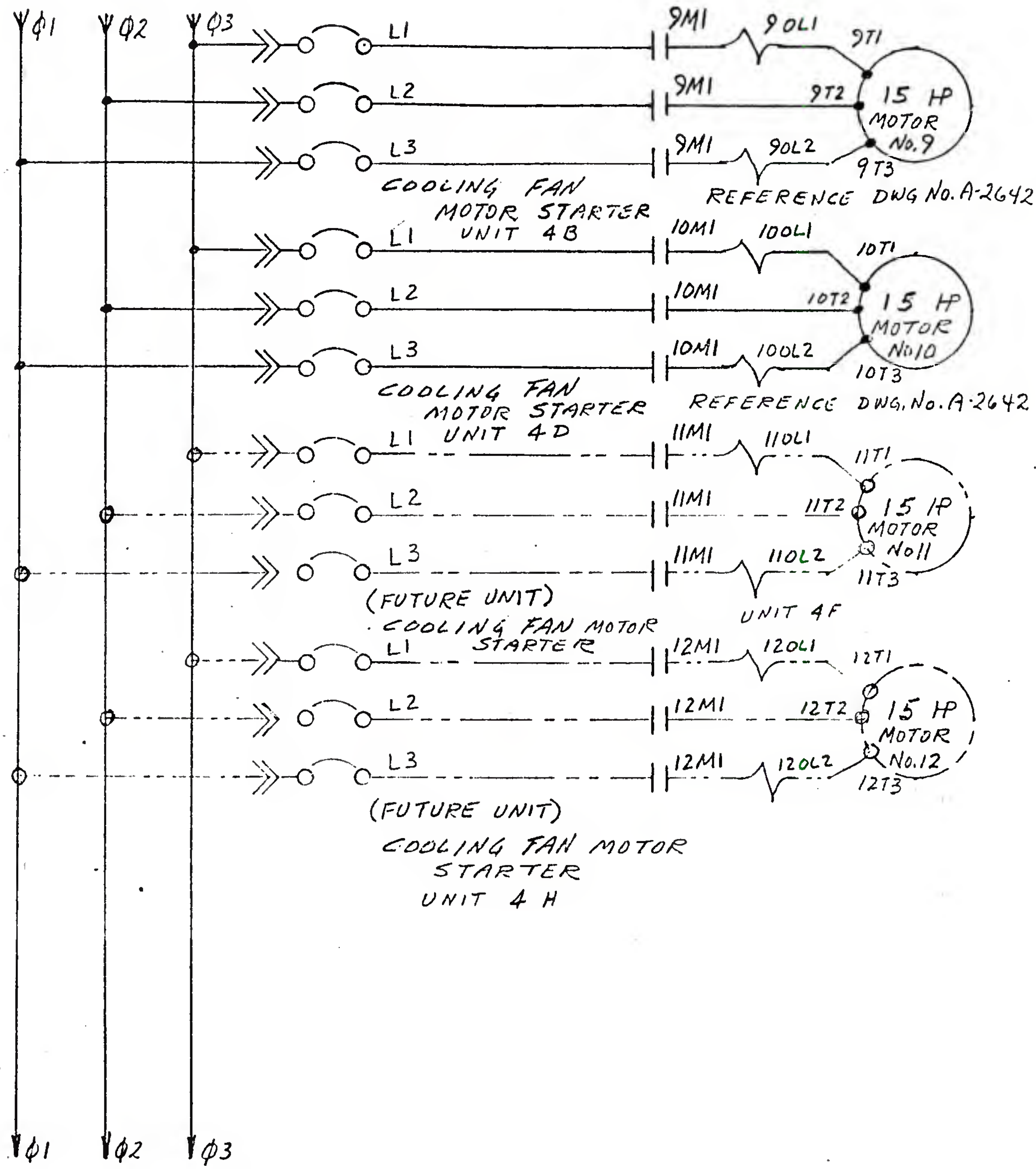

Drawing A-2626

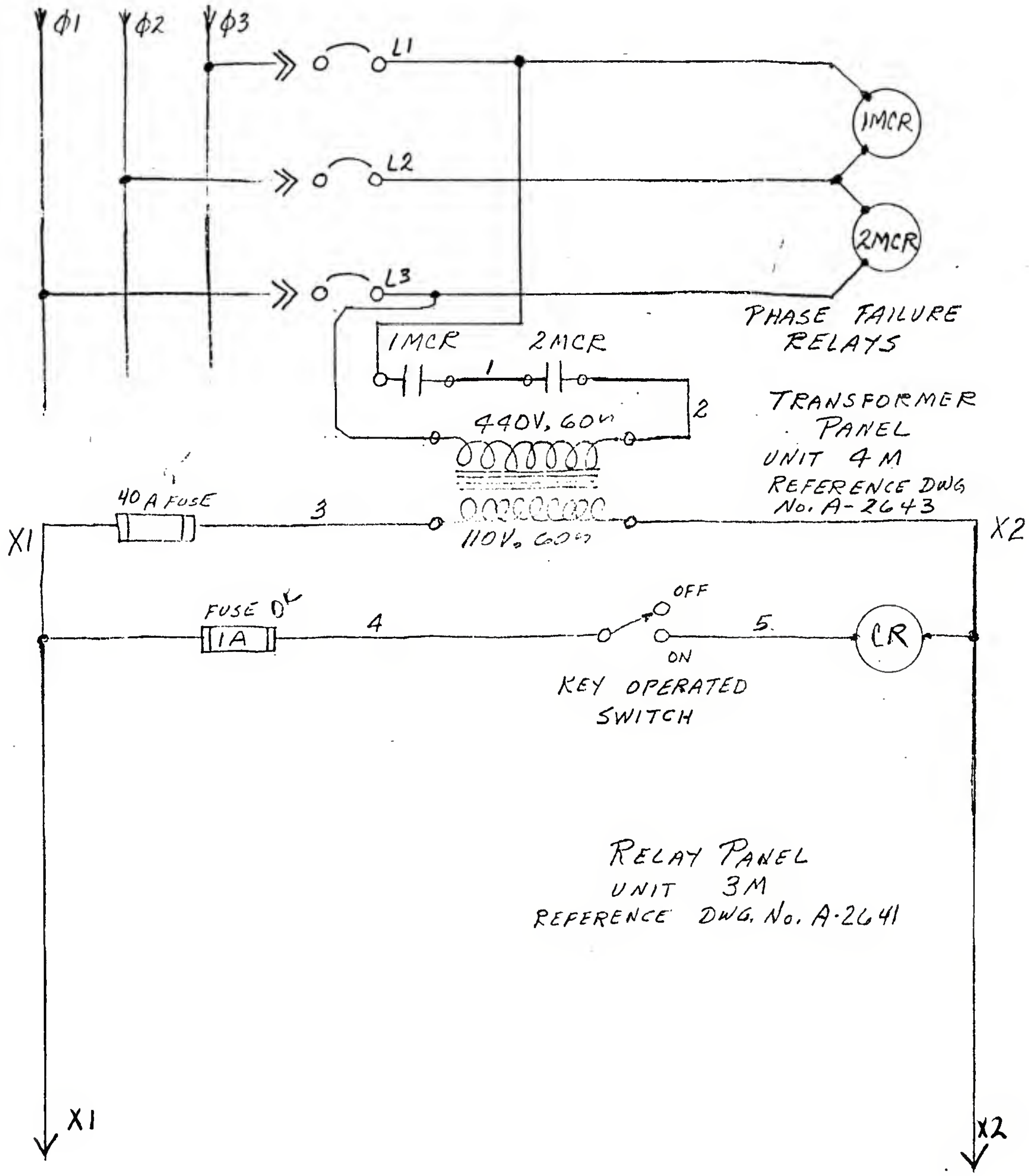

Drawing A-2626

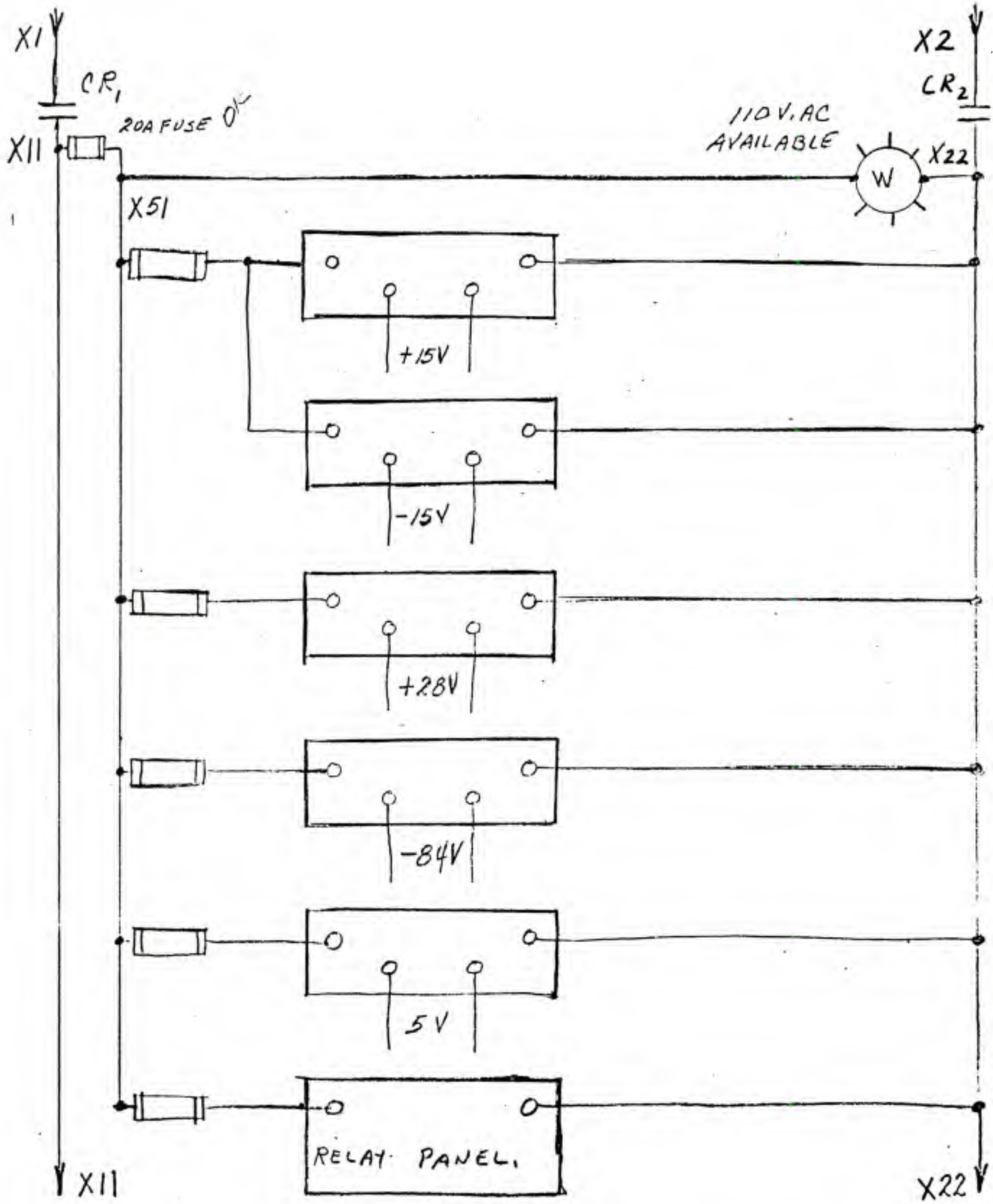

Drawing A-2626

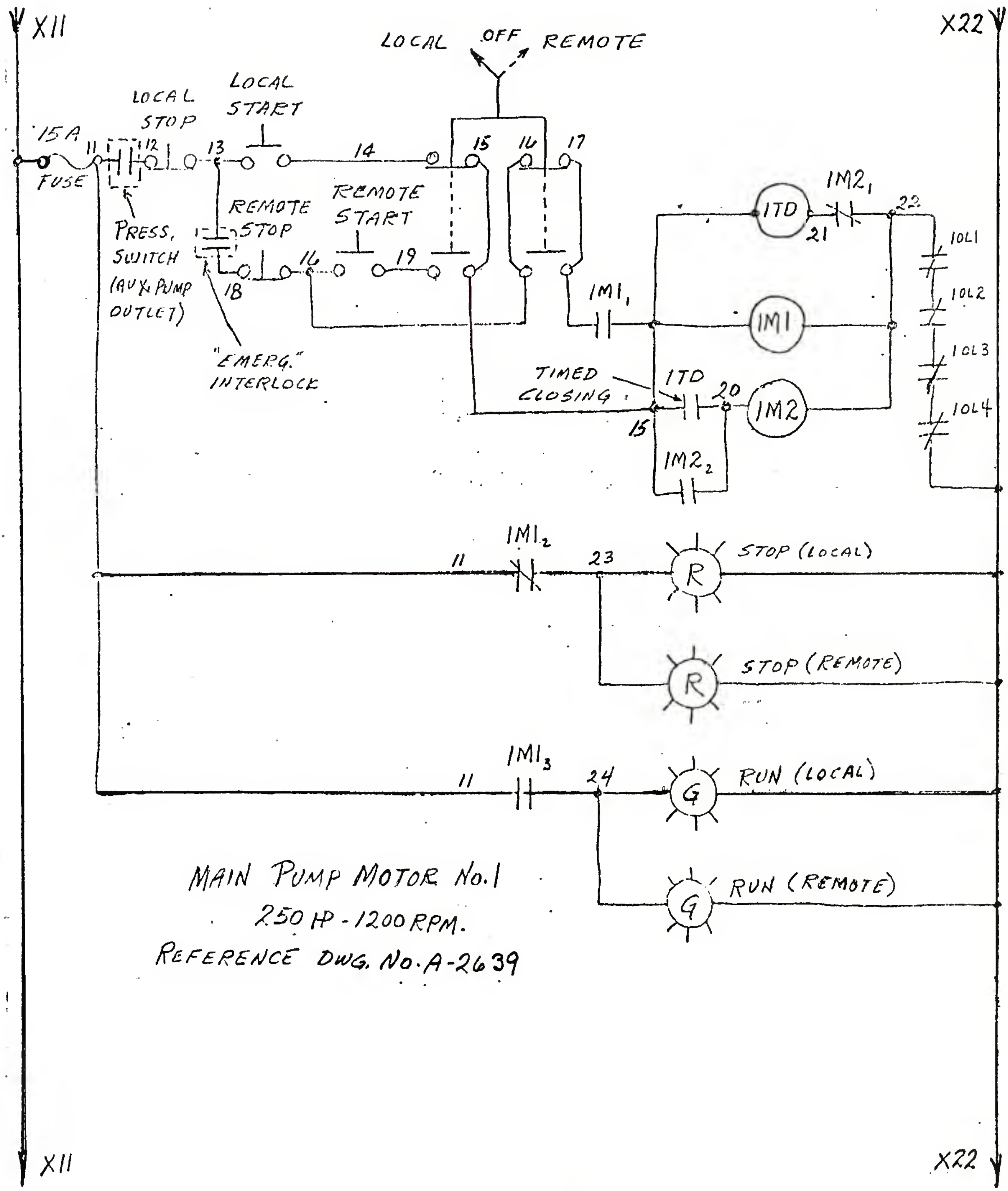

Drawing A-2626

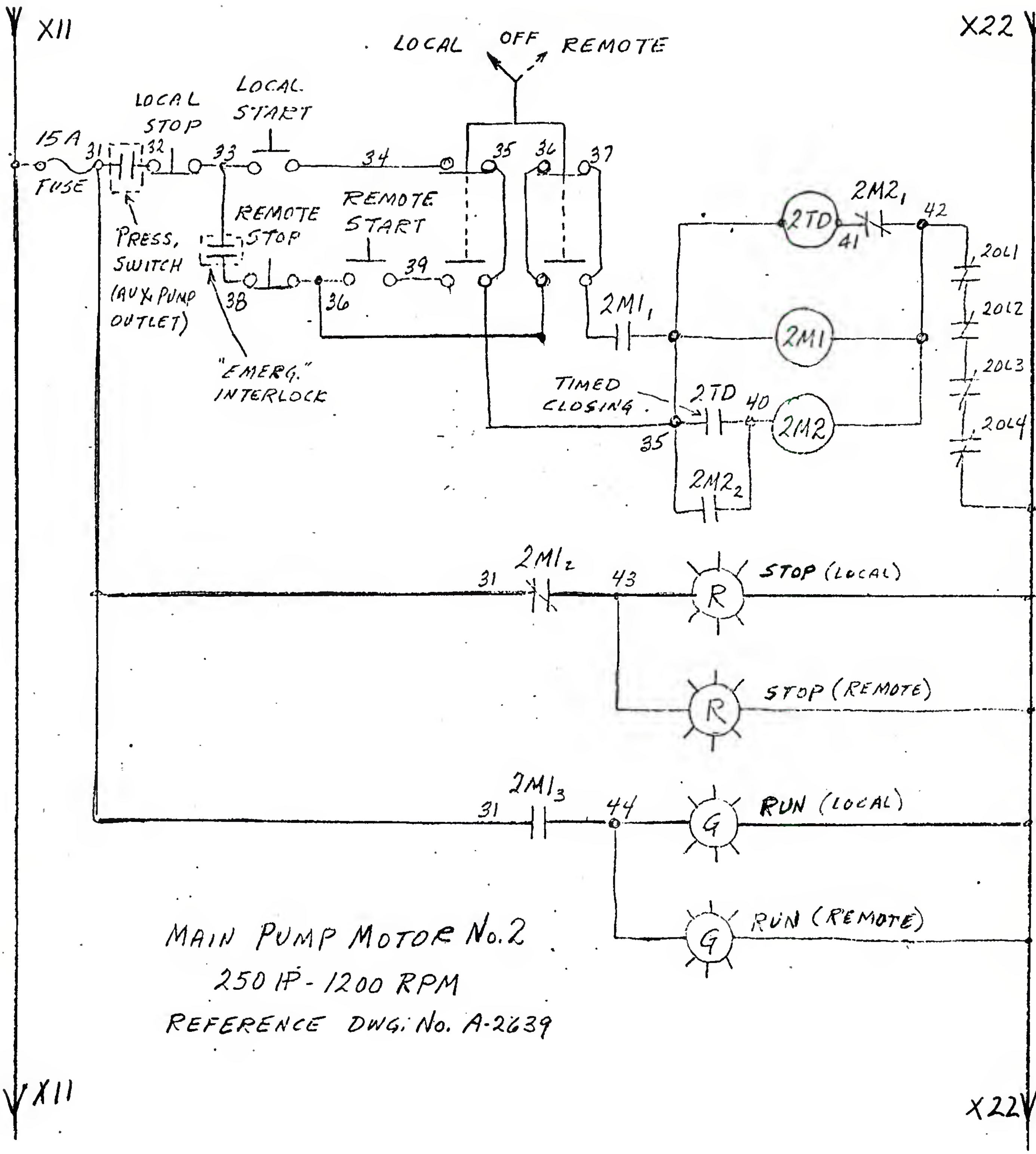

Drawing A-2626

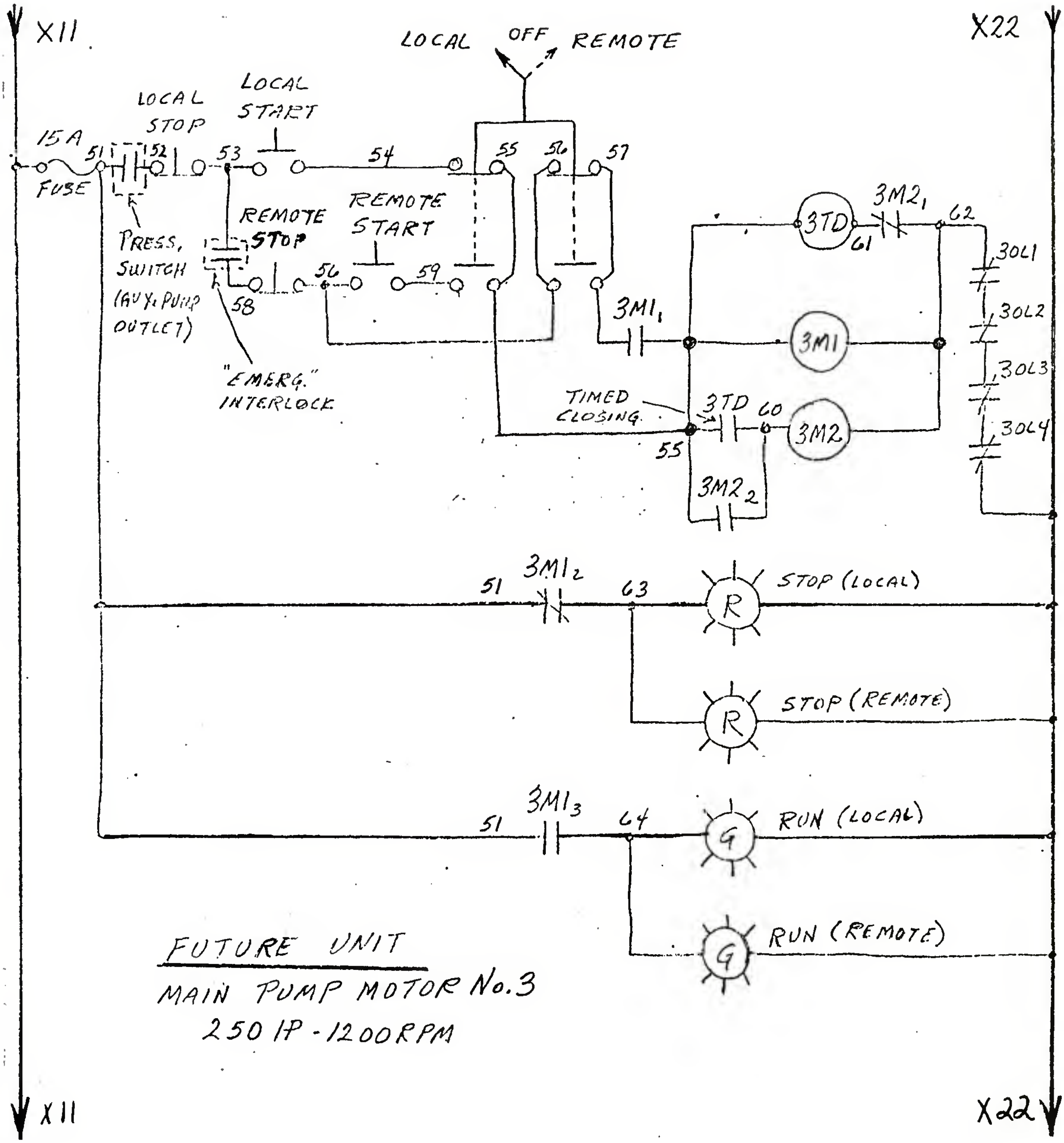

Drawing A-2626

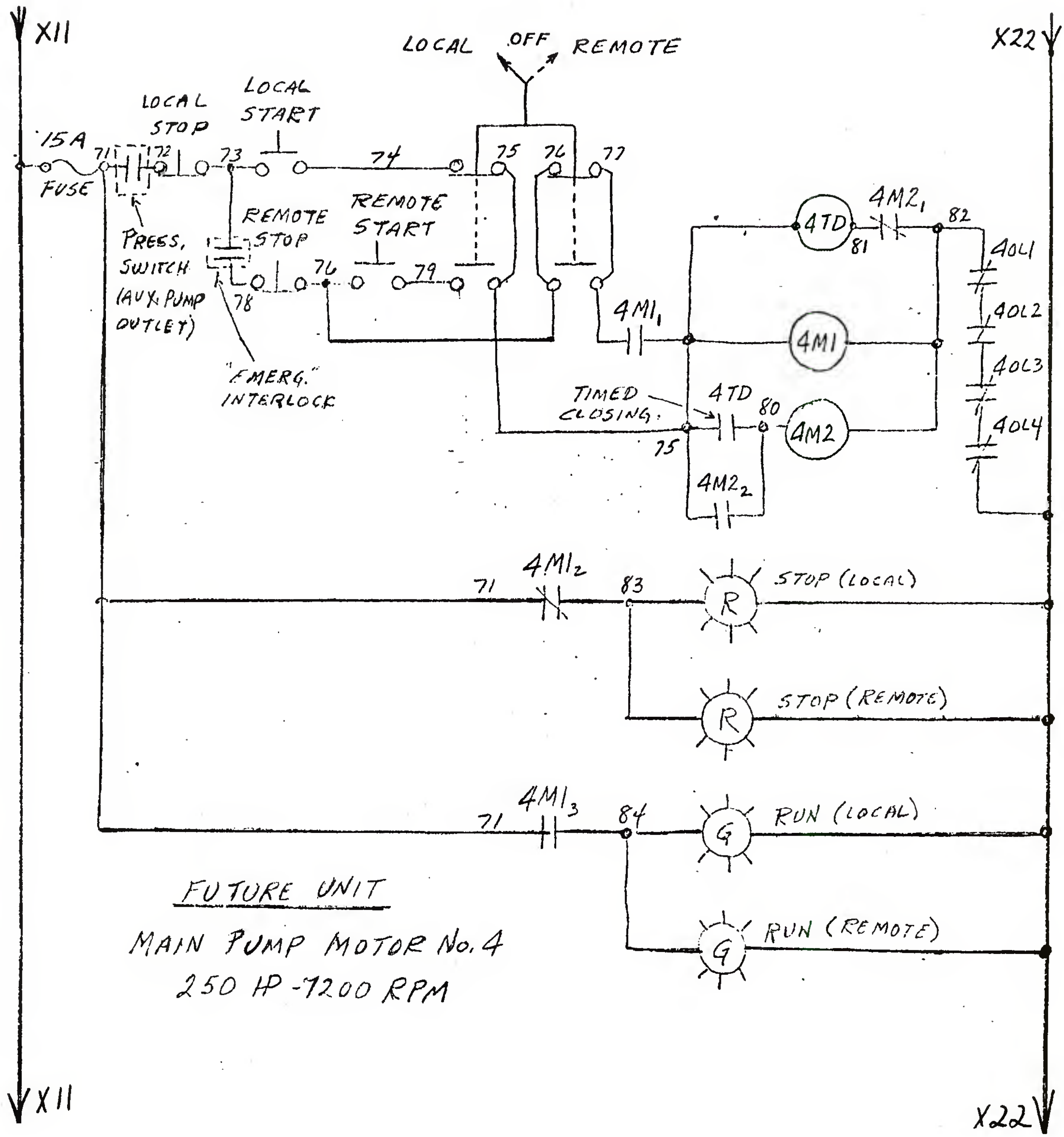

Drawing A-2626

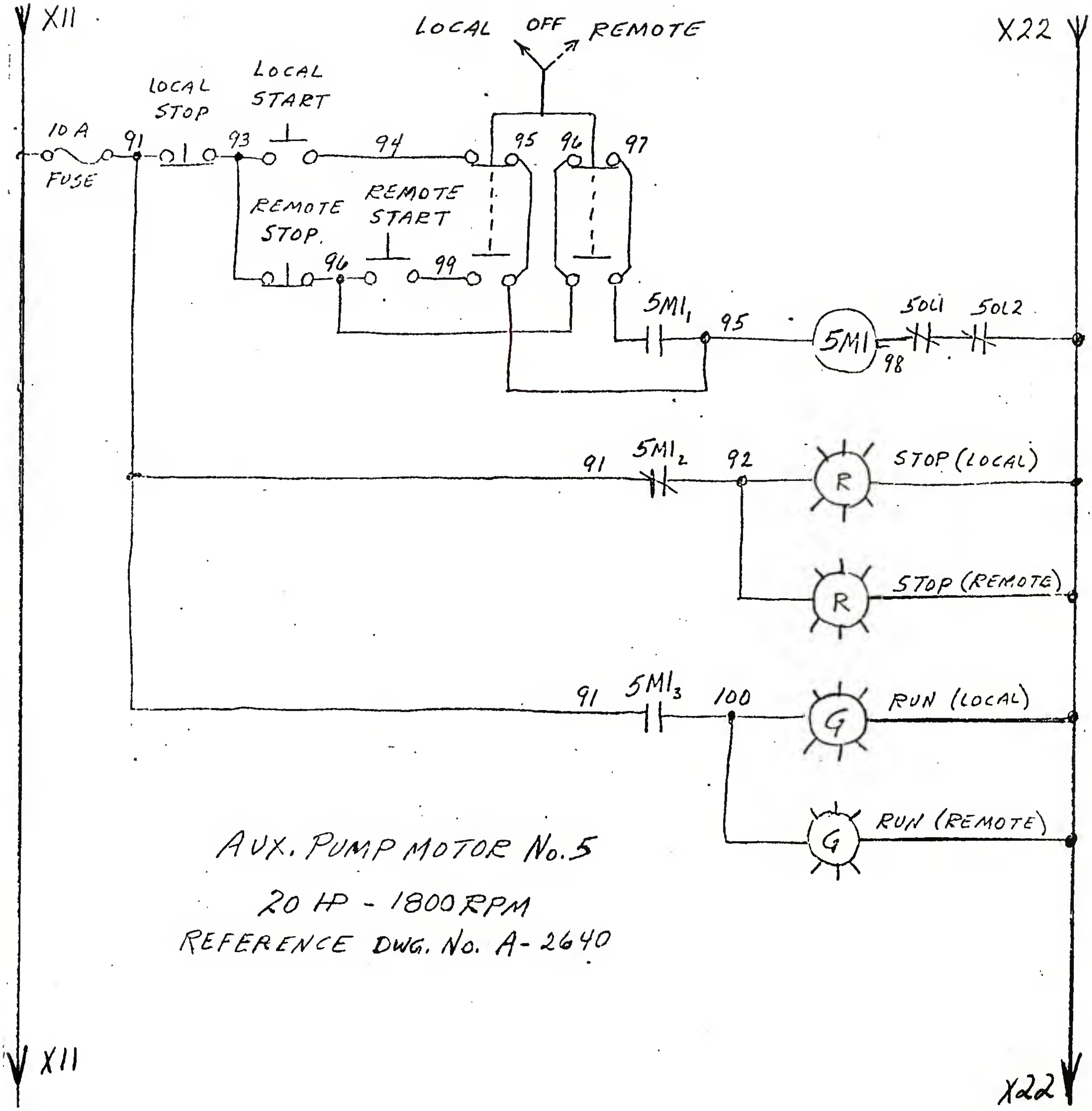

Drawing A-2626

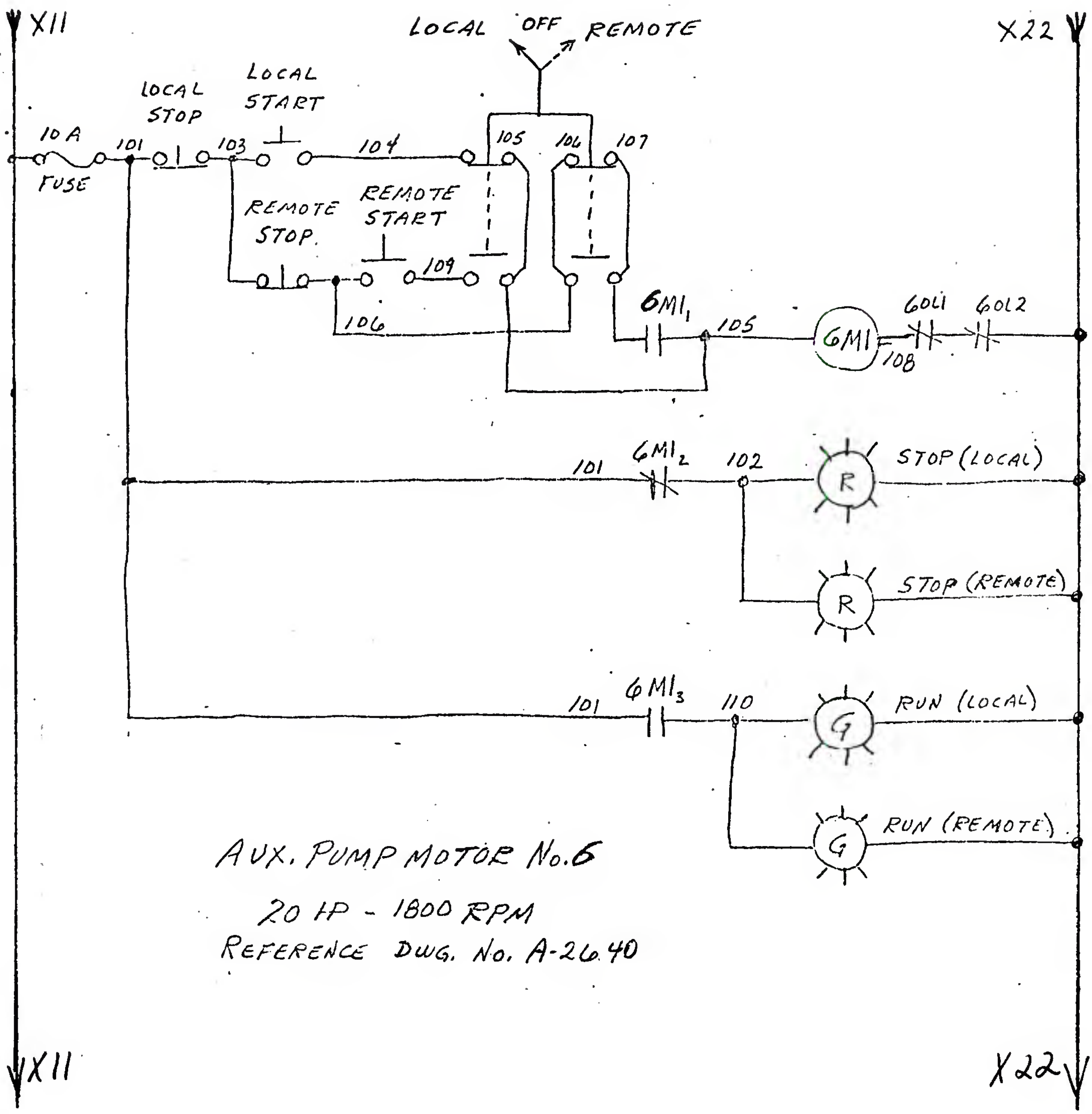

Drawing A-2626

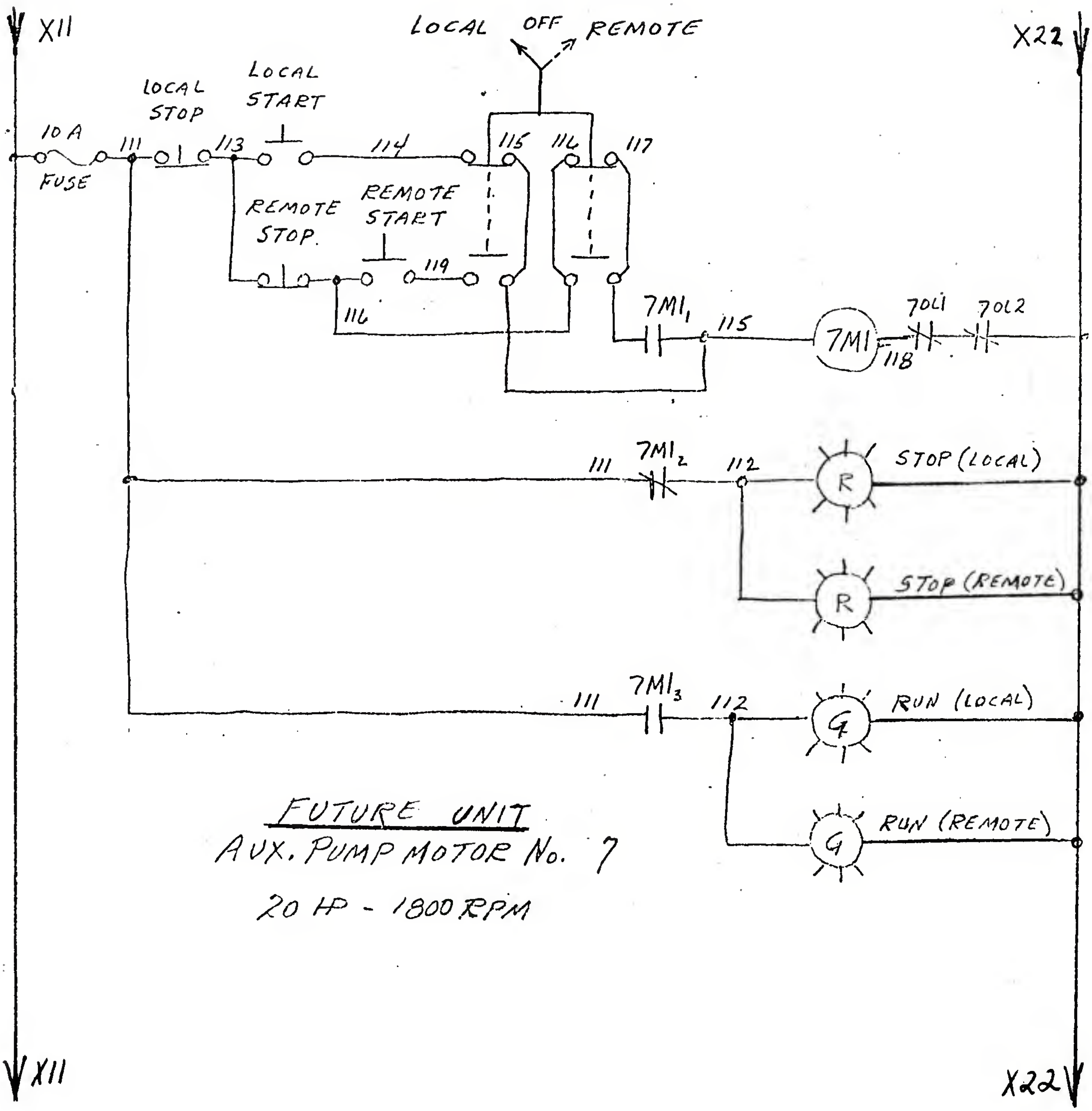

Drawing A-2626

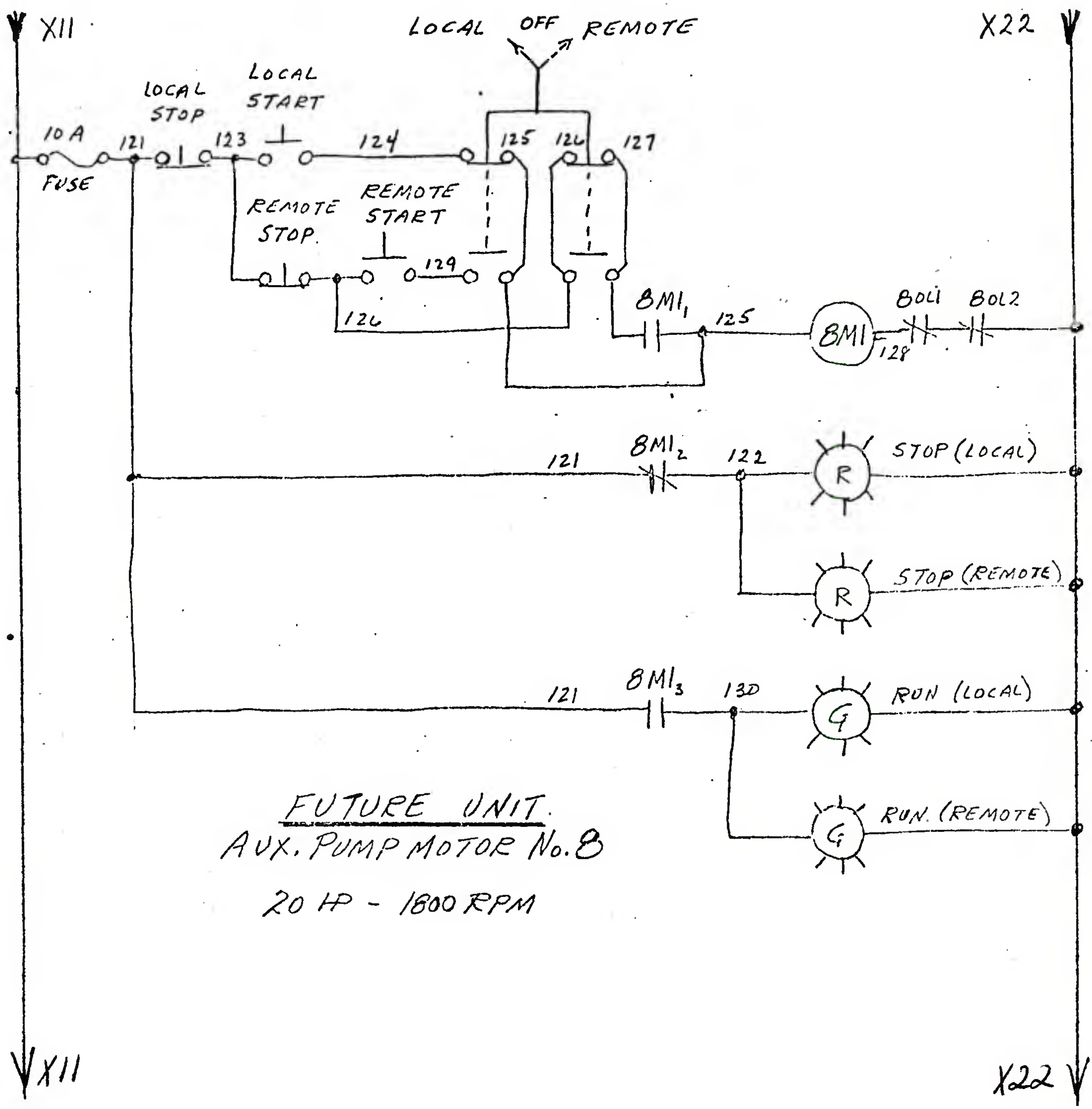

Drawing A-2626

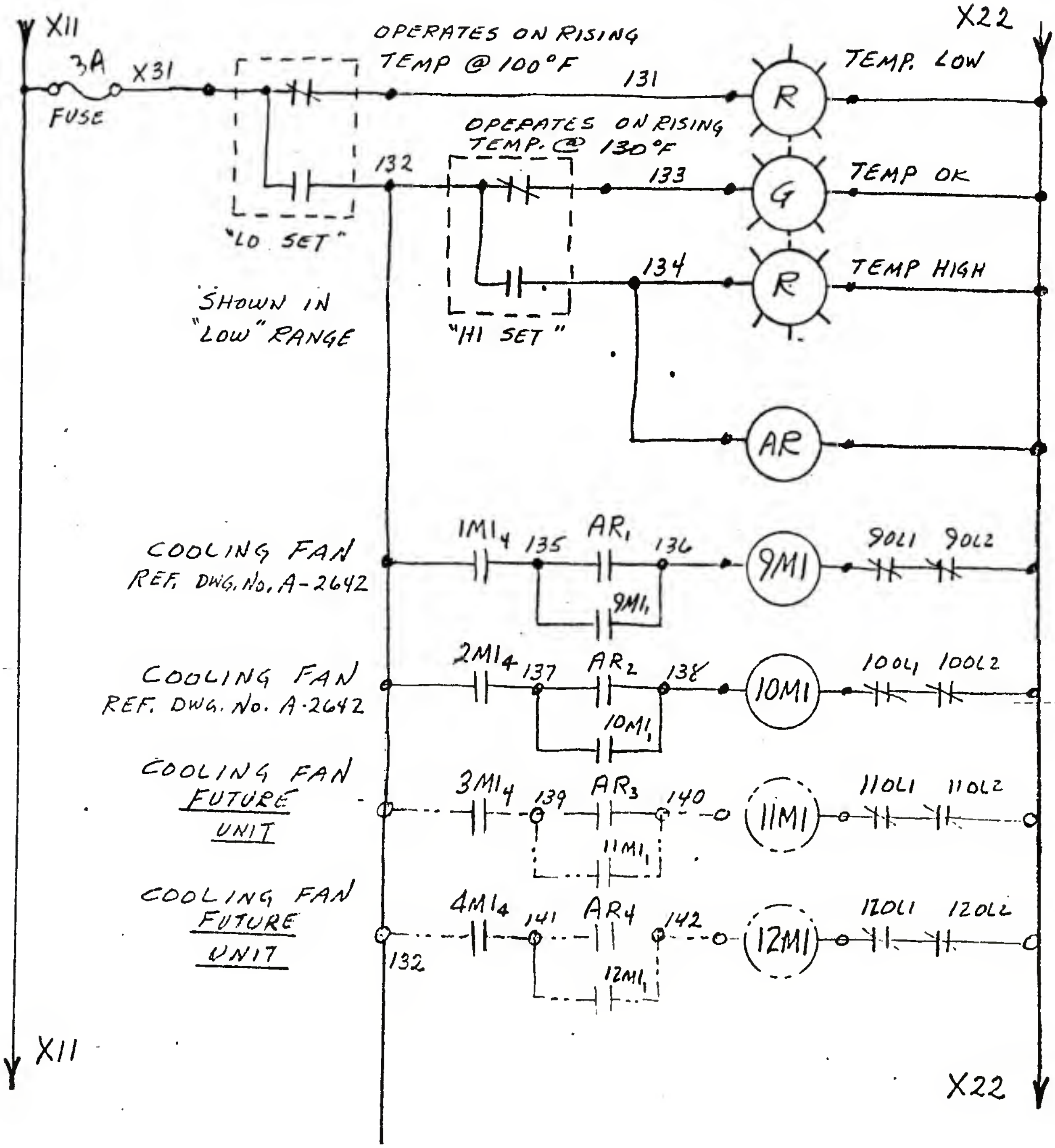

Drawing A-2626

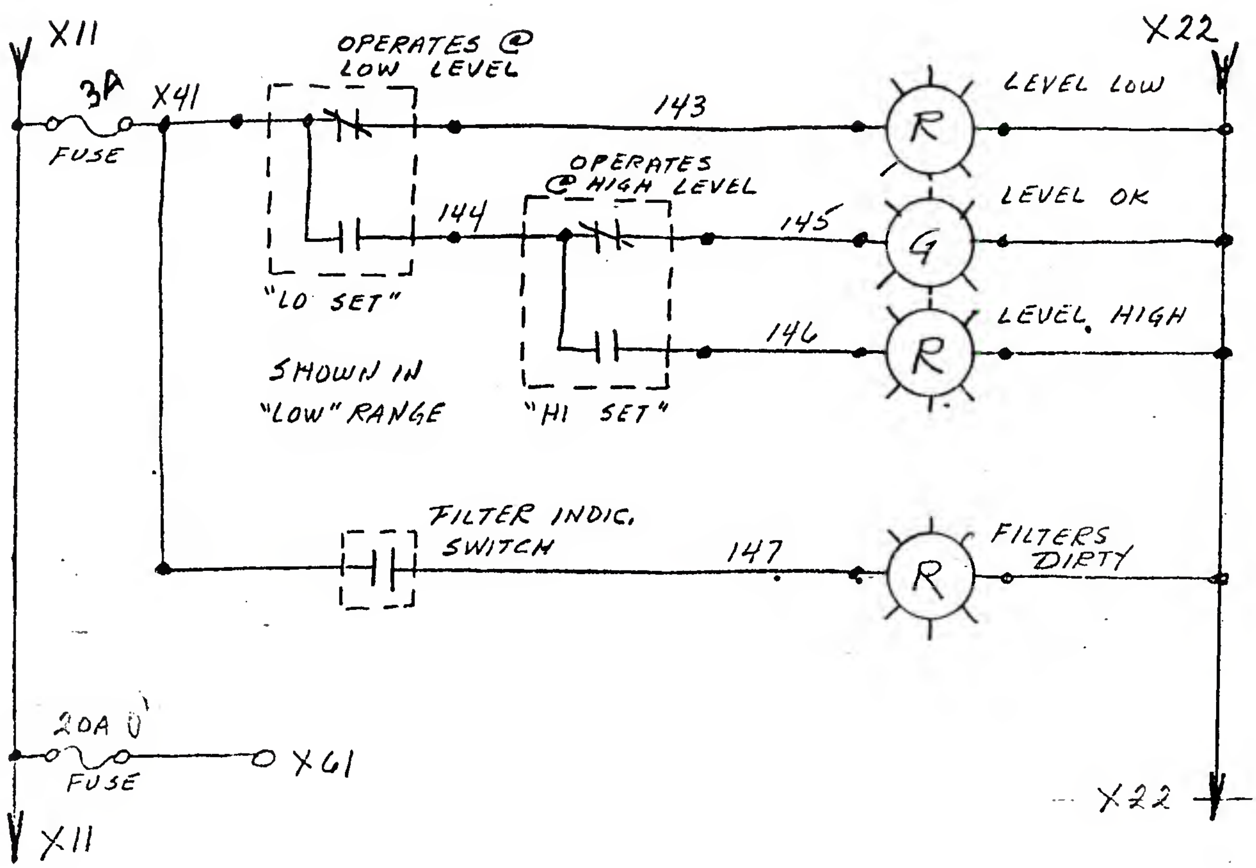

Drawing A-2626

APPENDIX F
MAIN PITCH SYSTEM

TITLE ACTIVATION OF 6-DOF SIMULATOR

MAIN PITCH	DRIVE SYSTEM: AH-1G			
PARAMETER		REFERENCE	DESIGN VALUE	UNIT
MASS MOMENT OF INERTIA	I	AH-1G	43,430 *	$LB\text{-}FT\text{-}SEC^2$
UNBALANCE	T_m	$37{,}520 \times 2.284' \times \cos 45°$	60,606 *	LB-FT
FIRING TORQUE	T_{fr}	$9000\# \times 11'$	99,000	LB-FT
MAX. AMPLITUDE	X	EXISTING	+45 / -10	DEGREE
PEAK MOTION: AMPLITUDE	χ	SPEC.	10	DEGREE
PEAK MOTION: FREQUENCY	f	SPEC.	.3	Hz
PEAK MOTION: VELOCITY	$\dot{\chi}$	$(2\pi)^2(f)(\chi)/360$	.33	RAD/SEC
PEAK MOTION: ACCEL.	$\ddot{\chi}$	$2\pi(f)(\dot{\chi})$	.62	RAD/SEC^2
ACTUATOR 8" BORE × 4" ROD: ARM	R	EXISTING	6.5'	FT.
STROKE	L	EXISTING	72"	IN.
REQ'D TORQUE	T	$1.5(I\ddot{\chi} + T_m + T_{fr})$	279,800	LB-FT
HYD. FORCE	F_H	$\frac{T}{R} = 43{,}046$ REQ'D.	108,000 * AVAILABLE	LB.
PISTON AREA	A_s	$> \frac{F_H}{3000} = 14.56$ REQ'D.	37.7 AVAILABLE	IN^2
	A_L		50.265	IN^2
PISTON SPEED	V	$12R(\dot{\chi})$	25.74	IN/SEC
VALVE FLOW	Q_v	$\frac{A_L(V)(60)}{231}$	336	GPM
PUMP FLOW	Q_p	$> \frac{2}{\pi} Q_v$	214	GPM
HYDRAULIC STIFFNESS	K_H	$2\times10^5 \; \frac{2(A_s+A_L)}{L/12} R^2$	247×10^6	LB-FT/RAD.
ESTIMATED NATURAL FREQ.	f_n	$\frac{1}{2\pi}\sqrt{\frac{K_H}{1.2\,I}}$	11.	Hz

Form 207 IBM 6-71

* SEE DWG A-2625 SHEET 2.

Drawing No. A-2628
Sheet 1 of 4

TITLE ACTIVATION – MAIN PITCH DRIVE

Estimated Mass Moment of Inertia About Main Pitch (Y) Axis.

Item	Weight (lb)	C.G. Offset R(ft)	$\frac{WR^2}{g}$ (lb-ft-sec^2)	I_o (lb-ft-sec^2)
Pitch & Yaw Gimbals Ass'y.	20,000	0	0	9,500
(6) Suspension Actuators	2,520	2.5	490	87
Mounting Adaptor	2,500	4.0	1,242	324
AH-1G Helicoptor	9,500	7.78	17,857	13,401
YAW DRIVE MOTOR ASSY	3,000	-1.5	211	318
Total	37,520	2.284	19,800	23,630
Mass Moment of Inertia (lb-ft-sec^2)			43430	

$$C.G. = \frac{(2520)(2.5)+(2500)(4)+(9500)(7.78)-(3000)(1.5)}{37,520} = 2.284'$$

MAX. UNBALANCE TORQUE (T_m) :–

$$T_m = (37520)(2.284)(\cos 45°) \doteq 60,606 \text{ (FT-lb)}$$

$$F_H(\text{AVAIL}) = (A_S \times 3000 \text{ PSI}) - (A_L \times 100 \text{ PSI}) = (37.7 \times 3000) - (50.265 \times 100)$$

$$= 113,100 - 5026.5 = 108,000 \text{ lb.}$$

Drawing No. A-2628
Sheet 2 of 4

Form 207 10M 6-71

TITLE **ACTIVATION OF 6-DOF SIMULATOR**

MAIN PITCH — DRIVE SYSTEM: AAH

PARAMETER			REFERENCE	DESIGN VALUE	UNIT
MASS MOMENT OF INERTIA		I	AAH HELICOPTER	82,498 △	$LB\text{-}FT\text{-}SEC^2$
UNBALANCE		T_m	$(44020)(3.096)\cos 45°$	96,365 △	LB-FT
FIRING TORQUE		T_{fr}	$9000\# \times 11'$	99,000	LB-FT
MAX. AMPLITUDE		X	EXISTING ACTUATOR	$+45°$ $-10°$	DEGREE
PEAK MOTION	AMPLITUDE	x	SPEC.	10°	DEGREE
PEAK MOTION	FREQUENCY	f	SPEC.	.3	HZ
PEAK MOTION	VELOCITY	$\dot{x}$	$(2\pi)^2(f)(x)/360$	.33	RAD/SEC
PEAK MOTION	ACCEL.	$\ddot{x}$	$2\pi(f)(\dot{x})$	.62	RAD/SEC^2
ACTUATOR 8" BORE × 4" ROD	ARM	R	EXISTING	6.5'	FT.
ACTUATOR 8" BORE × 4" ROD	STROKE	L	EXISTING	72"	IN.
ACTUATOR 8" BORE × 4" ROD	REQ'D TORQUE	T	$1.5(I\ddot{x} + T_m + T_{fr})$	369,770	LB-FT
ACTUATOR 8" BORE × 4" ROD	HYD. FORCE	F_H	$\frac{T}{R} = 56,888$ REQ'D.	108,000 * AVAILABLE	LB.
ACTUATOR 8" BORE × 4" ROD	PISTON AREA	A_S	$> \frac{F_H}{3000} = 19.15$ REQ'D.	37.7 AVAILABLE	IN^2
ACTUATOR 8" BORE × 4" ROD	PISTON AREA	A_L		50.265	IN^2
ACTUATOR 8" BORE × 4" ROD	PISTON SPEED	V	$12R(\dot{x})$	25.74	IN/SEC
ACTUATOR 8" BORE × 4" ROD	VALVE FLOW	Q_V	$\frac{A_L(V)(60)}{231}$	336	GPM
ACTUATOR 8" BORE × 4" ROD	PUMP FLOW	Q_P	$> \frac{2}{\pi} Q_V$	214	GPM
ACTUATOR 8" BORE × 4" ROD	HYDRAULIC STIFFNESS	K_H	$2\times10^5 \frac{2(A_S+A_L)}{L/12} R^2$	247×10^6	LB-FT/RAD.
ESTIMATED NATURAL FREQ.		f_n	$\frac{1}{2\pi}\sqrt{\frac{K_H}{1.2\ I}}$	7.95	HZ

Form 207 10M 6-71

* SEE DWG A-2628, SHEET 2

△ SEE DWG A-2628, SHEET 4

Drawing No. A-2628
Sheet 3 of 4

TITLE ACTIVATION – MAIN PITCH DRIVE

Estimated Mass Moment of Inertia About Main Pitch (Y) Axis.

Item	Weight (lb)	C.G. Offset R(ft)	$\frac{WR^2}{g}$ (lb-ft-sec^2)	I_o(lb-ft-sec^2)
Pitch & Yaw Gimbals Ass'y.	20,000	0	0	9,500
(6) Suspension Actuators	2,520	2.5	490	87
Mounting Adaptor	2,500	4.0	1,242	324
AAH Helicoptor	16,000	7.78 *	30,076	40,250
YAW DRIVE MOTOR ASS'Y	3,000	-1.5	211	318
Total	44,020	3.096	32,019	50,479
Mass Moment of Inertia (lb-ft-sec^2)			82,498	

$$C.G. = \frac{(2520)(2.5)+(2500)(4)+(16000)(7.78)-(3000)(1.5)}{44,020} = 3.096'$$

$$T_M = (44020)(3.096)(\cos 45°) = 96,365 \text{ (FT-lb)}$$

* ASSUMED SAME AS AH-1G HELICOPTOR, ACTUAL C.G. OFF-SET DEPEND UPON DETAILED DESIGN OF SUSPENSION ADAPTOR FOR THE PARTICULAR AIRCRAFT.

Drawing No. A-2628
Sheet 4 of 4

TITLE HYDR. SCHEMATIC
MODIFIED MAIN PITCH ACTUATOR.

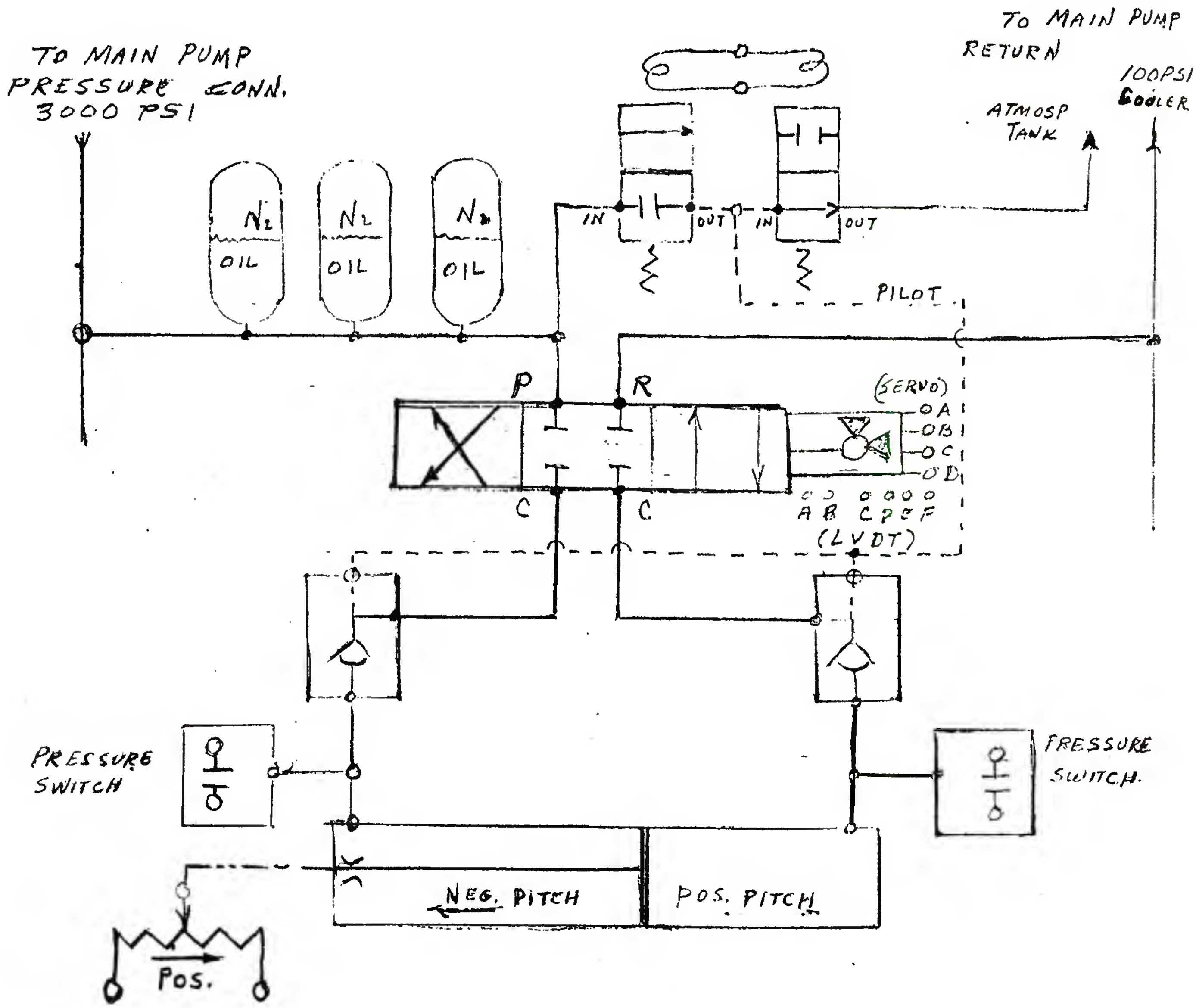

Drawing No. A-2627

Form 207 10M 6-71

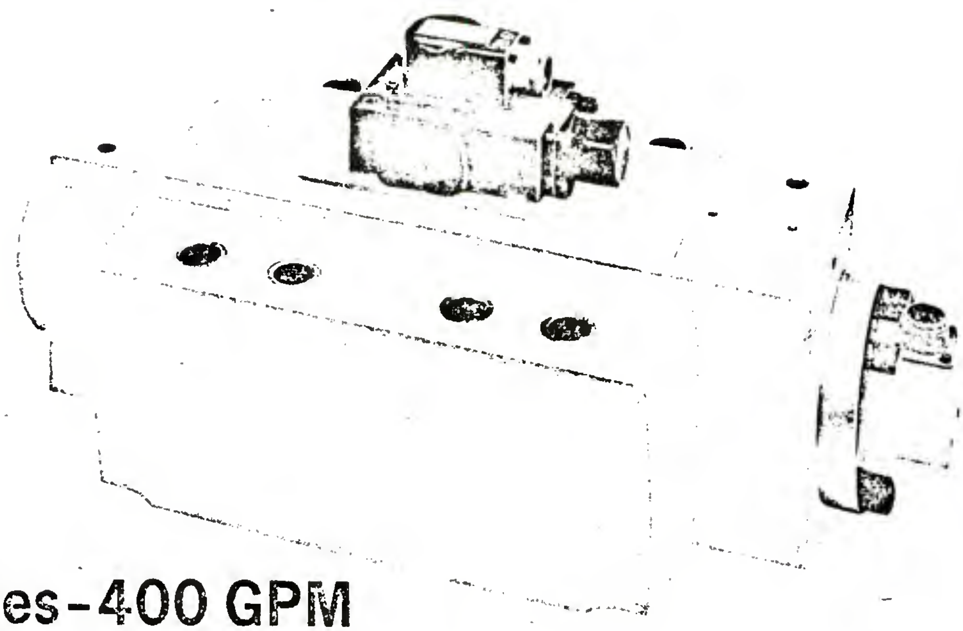

Moog 79 Series-400 GPM High Flow Servovalves

Moog® 79 Series — 400 GPM Servovalves control position, velocity or force of massive machine elements, with fast response at high flows. They are 3-stage servovalves using standard 2-stage Moog industrial valves for pilot operation. Operating in conjunction with an electronic position feedback loop, the pilot valve controls position of the 3rd stage spool, which in turn meters the high output flow.

Because of the high position loop gain around the 3rd stage, hysteresis and threshold properties meet or exceed the specifications of the best 2-stage servovalves. Application areas include automatic gage control for steel mills, vibration testing or large equipment, position control on huge machinery, or wherever precise control is required in the range of 0 to 600 HP.

A single servoamplifier can be used to provide closed loop operation for the third stage spool position and the required amplification and electronic mixing functions for the outer or major loops. Moog Series 82 Servocontrollers are highly recommended for this purpose.

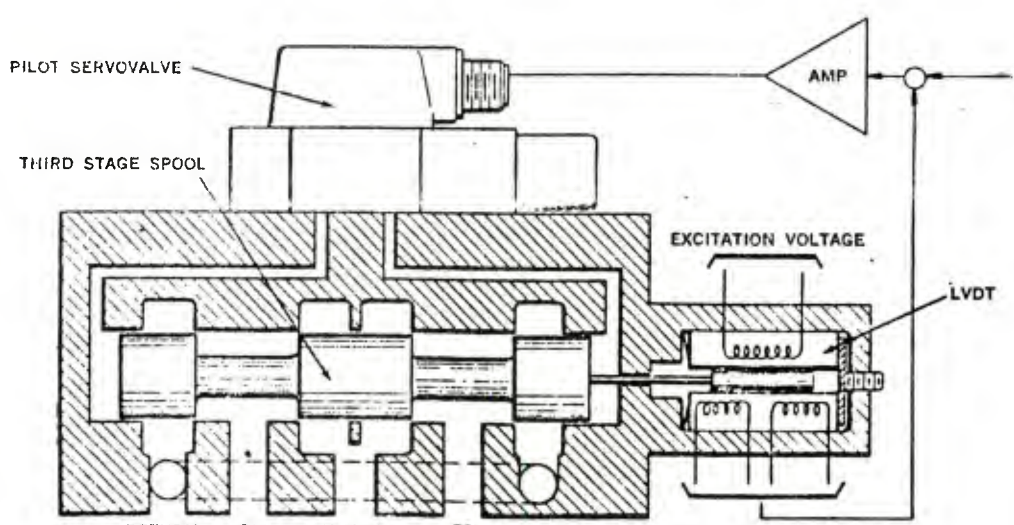

SCHEMATIC DIAGRAM
79 SERIES 3 STAGE SERVOVALVE WITH ELECTRICAL FEEDBACK

The following options are available:

- Choice of Moog Series 73, 74 or 76 Servovalve for pilot operation with flow rates for optimum performance in the particular application.
- Choice of LVDT or DCDT spool position feedback transducer.
- Provision for mounting auxiliary spool position transducer for monitoring.
- Provision for operating the pilot valve from a separate hydraulic power source.

General Characteristics

Flow Rating	400 gpm at 1000 psi valve drop
Operating Pressure	300 to 3000 psi
Inlet proof pressure	4500 psi
Return proof pressure	3000 psi
Fluid	Petroleum base hydraulic fluid Others on special order
Filtration	10 microns recommended
Internal leakage at null	less than 2% of rated flow
External leakage	none
Pressure gain at null	Greater than 30% supply pressure for 1% input
Weight	157 lbs.
Null Shift*	less than 1% for 80% to 110% supply pressure variation 0% to 20% back pressure variation 100°F temperature change
Hysteresis*	less than 1%
Threshold*	less than 0.5%

*Values for third stage spool position loop gain of 250 sec^{-1}

FLOW LOAD CHARACTERISTICS
(Supply pressure greater than 1000 PSI)

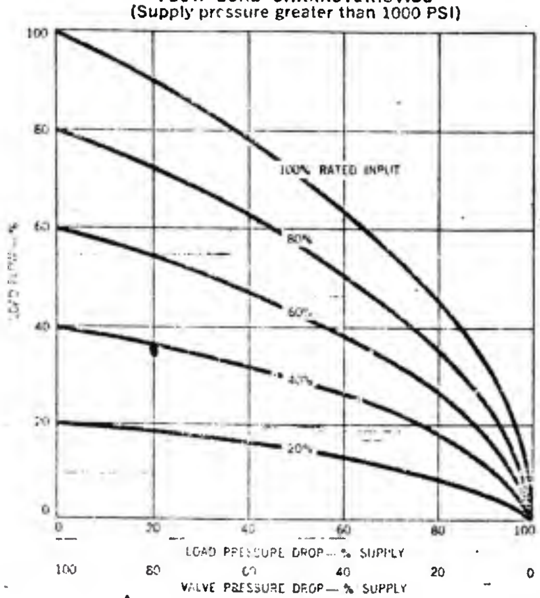

FREQUENCY RESPONSE CHARACTERISTICS
SMALL AMPLITUDE RESPONSE

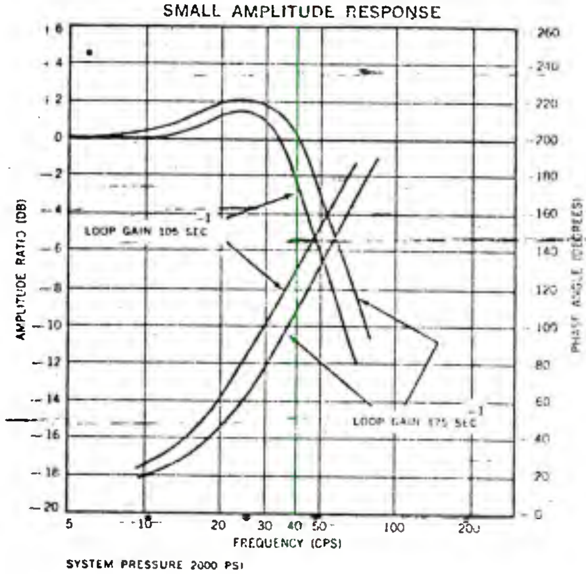

FLOW VS. SPOOL POSITION
(At Various Valve Pressure Drops)

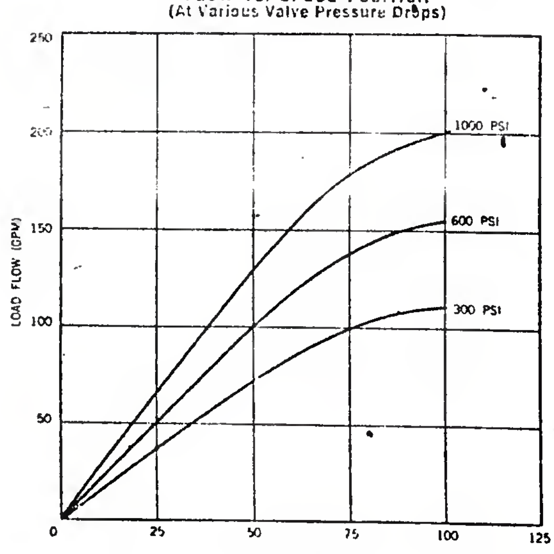

FULL AMPLITUDE RESPONSE

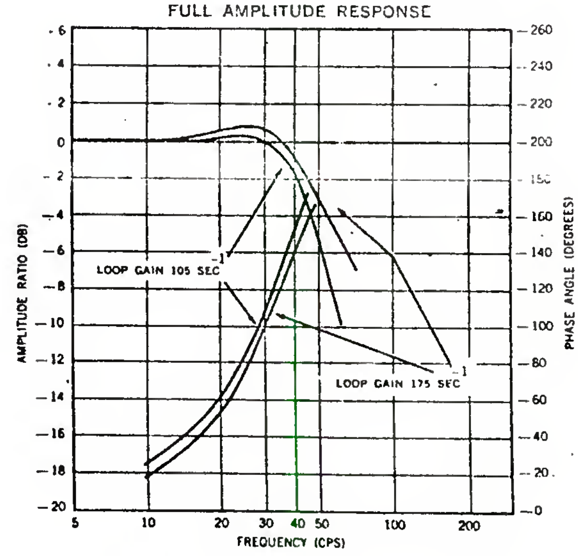

SYSTEM RESPONSE

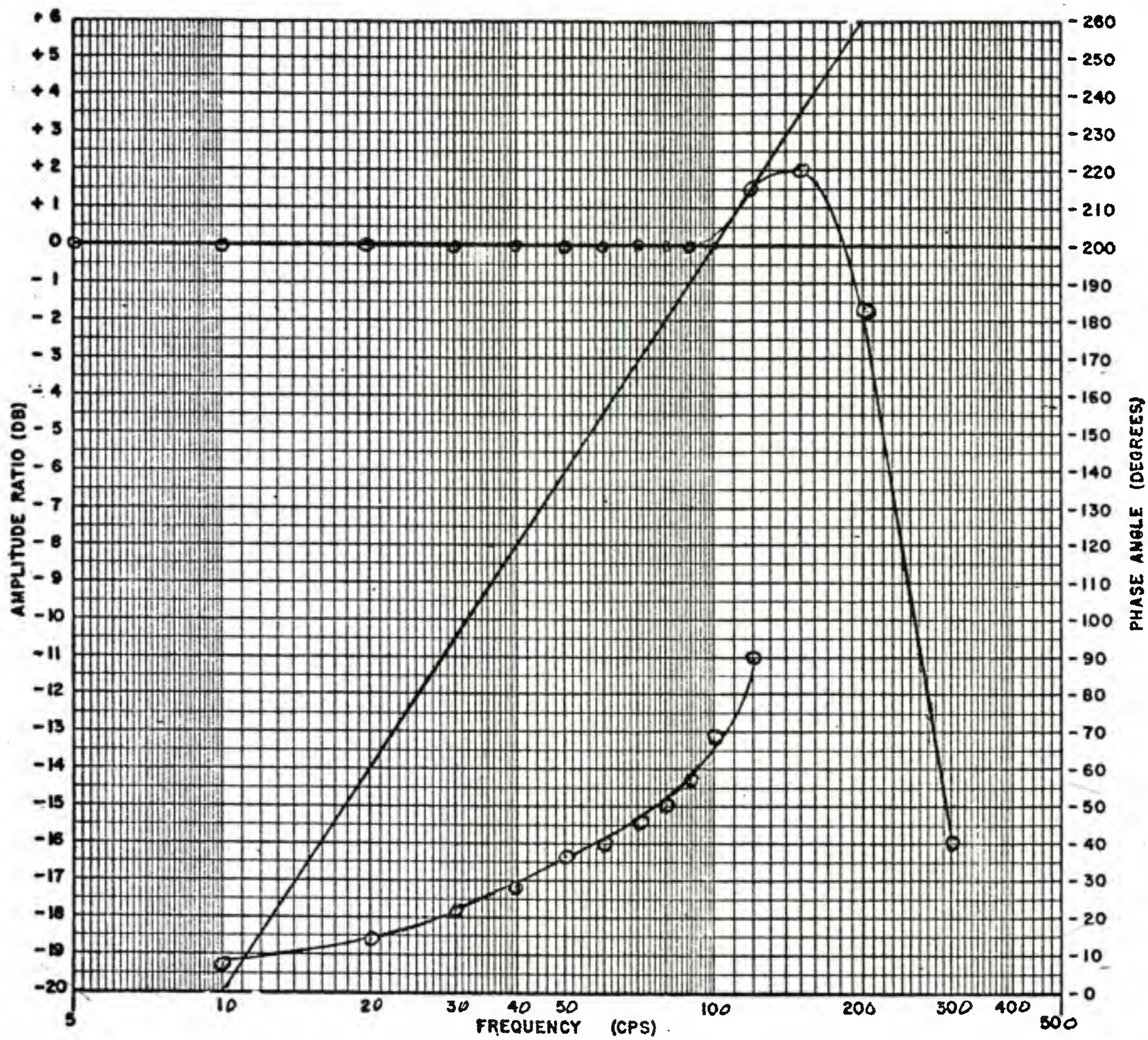

MODEL 79-400 SERIAL Typical

DATE 8/28/73 BY P.E.C.

73-233 pilot valve

RECEIVED

OCT 18 1973

MOOG

MOOG INC., EAST AURORA, NEW YORK

SYSTEM PRESSURE 3000 PSI

INPUT SIGNAL ±3% of 400 gpm @ 1000 PV MA.(P-P)

OUTPUT 3rd stage spool position.

$K_{loop} = 450\ sec^{-1}$
with lead-lag compensation

APPENDIX G
DETERMINATION OF SERVO OPEN-LOOP GAIN
REQUIRED FOR RESISTING LOAD DISTURBANCES

When we consider an angular position feedback control system with a simple block diagram as shown in figures G-1 and G-2, the output position error, θ_d, caused by a disturbing torque, T_d, can be obtained from the closed-loop transfer function of figure G-2 as follows:

$$\frac{\theta_d}{T_d} = \frac{G_2}{1 + G_1 G_2} \tag{G-1}$$

where

G_1 = transfer function between output position and torque developed

G_2 = transfer function between load torque and output position

For the case of an electrohydraulic actuator system, G_1 and G_2 can be derived from a typical position control system block diagram shown in figure G-3. When we combine the two feedback branches, with $\theta_{in} = 0$, the transfer function of G_1 is

$$G_1 = \frac{r}{\frac{A}{K_H} S + \frac{C}{A}} \left[\frac{K_1 K_2}{\frac{S^2}{\omega^2} + \frac{2\phi}{\omega} S + 1} + rAS \right] \tag{G-2}$$

$$G_2 = \frac{1}{JS^2 + DS} \tag{G-3}$$

where

A = effective actuator piston area

C = leakage coefficient of the actuator and servovalve spool

D = actuator-load viscous damping coefficient

J = total load mass moment of inertia

K_H = actuator hydraulic stiffness

K_1 = amplifier scale factor in ma per radian

K_2 = servovalve gain constant in cis per ma

r = effective radius of angular motion

S = Laplace transform operator

ϕ = servovalve transfer function damping factor

ω = servovalve transfer function natural frequency

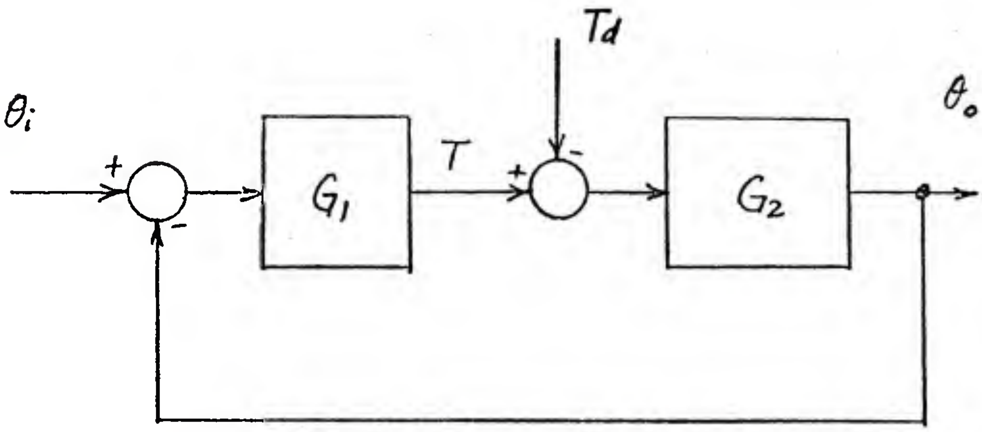

Figure G-1. Angular position control feedback servo system

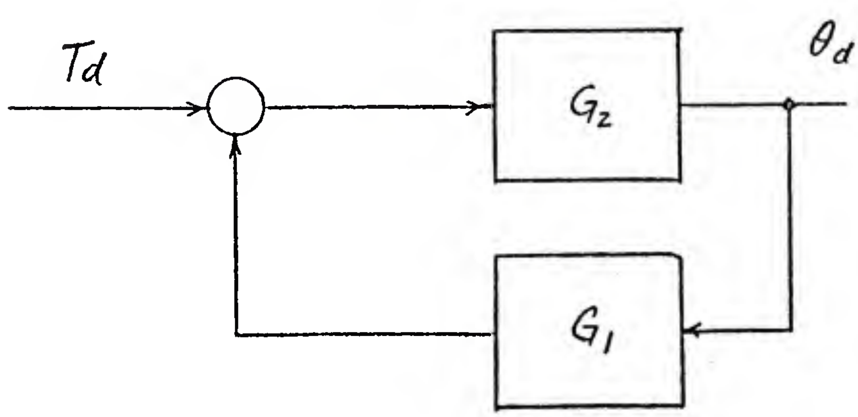

Figure G-2. Closed-loop transfer function

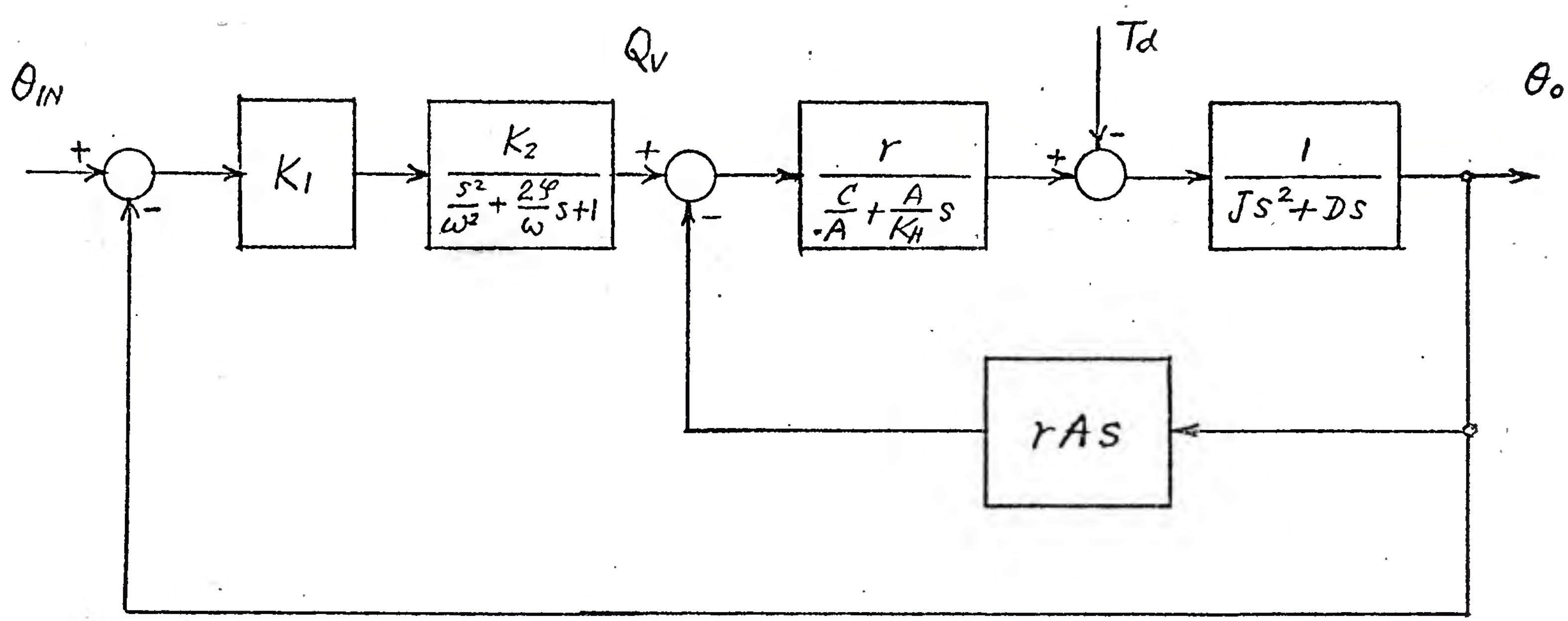

CHECK: If $Td = 0$

$$\frac{\theta_o}{Q_v} = \frac{\left(\frac{r}{\frac{C}{A} + \frac{As}{K_H}}\right)\left(\frac{1}{Js^2 + Ds}\right)}{1 + \frac{r^2 A s}{\left(\frac{C}{A} + \frac{A}{K_H}s\right)\left(Js^2 + Ds\right)}}$$

$$= \frac{1}{rAs\left[\frac{J}{r^2 K_H} s^2 + \left(\frac{D}{r^2 K_H} + \frac{JC}{r^2 A^2}\right) s + 1 + \frac{DC}{r^2 A^2}\right]}$$

Figure G-3. Position control system

The closed-loop transfer function of position due to a disturbing torque, T_d, is therefore

$$\frac{\theta_d}{T_d} = \frac{\left(\frac{A}{K_H} S + \frac{C}{A}\right)\left(\frac{S^2}{\omega^2} + \frac{2\phi}{\omega} S + 1\right)}{\left(JS^2+DS\right)\left(\frac{A}{K_H} S+\frac{C}{A}\right)\left(\frac{S^2}{\omega^2}+\frac{2\phi}{\omega} S+1\right) + r^2AS\left(\frac{S^2}{\omega^2}+\frac{2\phi}{\omega} S+1\right) + rK_1K_2} \tag{G-4}$$

When applying the final value theorem to determine the steady-state error in position, $\left(\theta_d\right)_{SS}$, due to a step disturbing torque, T_d, the steady-state error is

$$\left(\theta_d\right)_{SS} = \lim_{S\to 0} S\left(\frac{\theta_d}{T_d}\right)\left(\frac{T_d}{S}\right) = \frac{T_d\ C}{rAK_1K_2} \tag{G-5}$$

To express the steady-state error in terms of the servo system open-loop gain constant, K_1K_2 in the above expression can be substituted by K_o which is derived from figure G-3 as follows:

Since

K_o = open-loop gain constant

$$= \frac{K_1K_2}{rA\left(1 + \frac{DC}{r^2A^2}\right)} \tag{G-6}$$

thus

$$rAK_1K_2 = r^2A^2\left(1 + \frac{DC}{r^2A^2}\right)K_o \tag{G-7}$$

or

$$\left(\theta_d\right)_{SS} = \frac{T_d\ C}{r^2A^2\left(1 + \frac{DC}{r^2A^2}\right)K_o} \tag{G-8}$$

or

$$K_o = \frac{T_d\ C}{r^2A^2\left(1 + \frac{DC}{r^2A^2}\right)\left(\theta_d\right)_{SS}} \tag{G-9}$$

For a specified value of step disturbing torque, T_d, and an acceptable position error, θ_d, the required servo system open-loop gain constant, K_o, to resist the disturbing torque is

$$\boxed{K_o > \frac{T_d\ C}{r^2A^2\left(\theta_d\right)_{SS}}} \tag{G-10}$$

since

$$\frac{T_d\ C}{r^2A^2\left(\theta_d\right)_{SS}} > \frac{T_d\ C}{r^2A^2\left(1 + \frac{DC}{r^2A^2}\right)\left(\theta_d\right)_{SS}} \tag{G-11}$$

Calculation of the Main Pitch Control System Open-Loop Gain

For a maximum firing torque of 99,000 ft-lb as calculated in appendix F of this report, the required servo open-loop constant, K_v, to resist this disturbing torque for a position error of 1 degree or less is

$$K_v = \frac{(99{,}000)(12)C}{r^2\ \ A^2\ (1/57.3)} \tag{G-12}$$

where

C = assumed to have a leakage coefficient equivalent to a damping factor of 0.8 for the actuator

= 0.508 cis/psi

A = 37.7 sq in.

r = 78 in

K_v = 4.1/sec

The value of K_v used in the system design is 7 which is larger than the required loop gain calculated above.

Calculation of the Main Yaw Control System Open-Loop Gain

The required open-loop gain constant for the Main Yaw control system was calculated with the following parameter values:

T_d = 10,625 ft-lb (app I)

C = 0.0231 cis/psi (table 7)

dm = 368 in.^{3}/rad

$(\theta_d)_{ss} = \frac{1}{57.3}$ radian

$$K_v = \frac{(10,625)\ (12)\ (.0231)\ (57.3)}{(368)\ (368)}$$

$$= 1.25\ 1/\text{sec} \tag{G-13}$$

The value of K_v used in the system design is 6.3 which is much greater than the required value of K_v calculated above.

APPENDIX H
CALCULATION OF THE REQUIRED OPEN-LOOP GAIN AND BYPASS LEAKAGE COEFFICIENT OF THE TRIOGONAL ACTUATOR SERVO SYSTEM

The steady-state error in position due to a constant, frequency independent disturbing force in a position control servo system can be derived as

$$X_{d\ static} = \frac{F_d}{DK_v} \tag{H-1}$$

where

X_d = position error due to disturbance

F_d = disturbing force

D = damping coefficient of the actuator-load

The damping coefficient D in equation (H-1) can be derived from the characteristic equation of the hydraulic valve-actuator-load transfer function. The transfer function was developed in a previous analysis in a form of

$$\frac{X}{Q_2} = \frac{1}{As\left[\left(\frac{1}{K_{HA}} + \frac{1}{K_A}\right) MS^2 + \left(\frac{MC}{A^2} + \frac{D}{K_A}\right)s + 1 + \frac{DC}{A^2}\right]} \tag{H-2}$$

where

X = actuator displacement

Q_2 = actuator input flow rate

A = effective piston area

K_{HA} = actuator hydraulic stiffness

K_A = actuator attachment joints and structural stiffness

C = leakage coefficient of the hydraulic valve and actuator bypass

s = Laplace transform operator

If D is mainly due to the actuator bypass leakage flow, it would have a value approximately equal to $D = \frac{A^2}{C}$

The last term in equation (H-2) will be equal to one such as

$$\frac{DC}{A^2} = \frac{A^2}{C} \text{ X } \frac{C}{A^2} = 1 \tag{H-3}$$

The second order function in the denominator of (H-2) can then be solved for the damping ratio, ζ, and the natural frequency, ω_n. Since $K_A >> K_{HA}$, the terms in K_A may be ignored. Then

$$\omega_n = \sqrt{\frac{2K_{HA}}{M}} \qquad \text{(H-4)}$$

and

$$\frac{2\zeta}{\omega_n} = \frac{1}{2}\left(\frac{M}{D} + \frac{D}{K_{HA}}\right) \qquad \text{(H-5)}$$

Using (H-4), equation (H-5) can be solved for D.

$$D = \sqrt{2K_{HA}M}\ \left[\zeta \pm \sqrt{\zeta^2 - \frac{1}{2}}\right] \qquad \text{(H-6)}$$

The design values of K_{HA}, M, A, F_d/X_d for each 6-DOF actuator are

$K_{HA} = 0.945 \times 10^6$ lb/in.

$M = 33.5$ lb-sec^2/in.

$A = 20.652$ in.^{2}

$\frac{F_d}{X_d} = K_{ACT} = 2 \times 10^5$ lb/sec

Therefore, the bypass leakage coefficient C can be determined from equations (H-3) and (H-6).

$$C = \frac{A^2}{\sqrt{2K_{HA}M}\ \left[\zeta \pm \sqrt{\zeta^2 - \frac{1}{2}}\right]} \qquad \text{(H-7)}$$

For $\zeta = 0.707$ and the values given above

$$C = 2.04 \times 10^{-2} \text{cis/psi} = \frac{5.30 \text{ gpm}}{1000 \text{ psi}} \qquad \text{(H-8)}$$

The required servo-open loop gain K_V in equation (H-1) is given by

$$K_V = \frac{F_d}{DX_d} \qquad \text{(H-9)}$$

From equation (H-6) and the design values

$$K_V = 36 \tag{H-10}$$

Revision

Equation (H-1) was derived assuming no disturbing force applied to the actuator. For the 6-DOF simulator a disturbing force (gun-firing) will be present. The following derivation was developed to further clarify equation (H-1).

When we consider a position feedback control system with a simple block diagram as shown in figures H-1 and H-2, the output position, X, due to a disturbing impact load force, F, can be obtained from the closed-loop transfer function of figure H-2 as follows:

$$\frac{X}{F} = \frac{G_2}{1 + G_1 G_2} \tag{H-11}$$

where

G_1 = transfer function between output position and force developed

G_2 = transfer function between load force and output position

For the case of an electrohydraulic actuator system, G_1 and G_2 can be derived from a typical position control system block diagram shown in figure H-3. When we combine the two feedback branches, with $X_{in.} = 0$, the transfer function of G_1 is

$$G_1(s) = \frac{1}{\frac{A}{K_{HA}} s + \frac{C}{A}} \quad \frac{K_1 K_2}{\frac{s^2}{\omega^2} + \frac{2\zeta}{\omega} s + 1} + As \tag{H-12}$$

and

$$G_2(s) = \frac{1}{Ms^2 + Ds} \tag{H-13}$$

where

A = effective actuator piston area

C = leakage coefficient of the actuator and servovalve

D = actuator--load viscous damping coefficient (e.g., piston, joints and load frictions, load damper, and windage friction, etc.)

M = total moving load mass

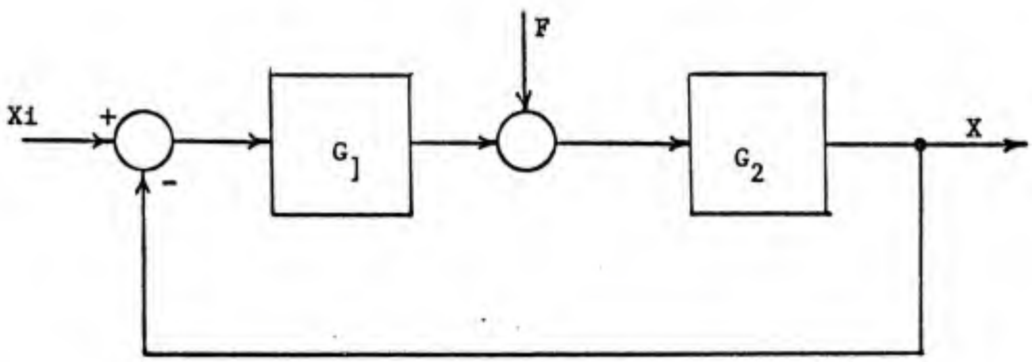

Figure H-1. Block diagram of the position feedback control system, view 1

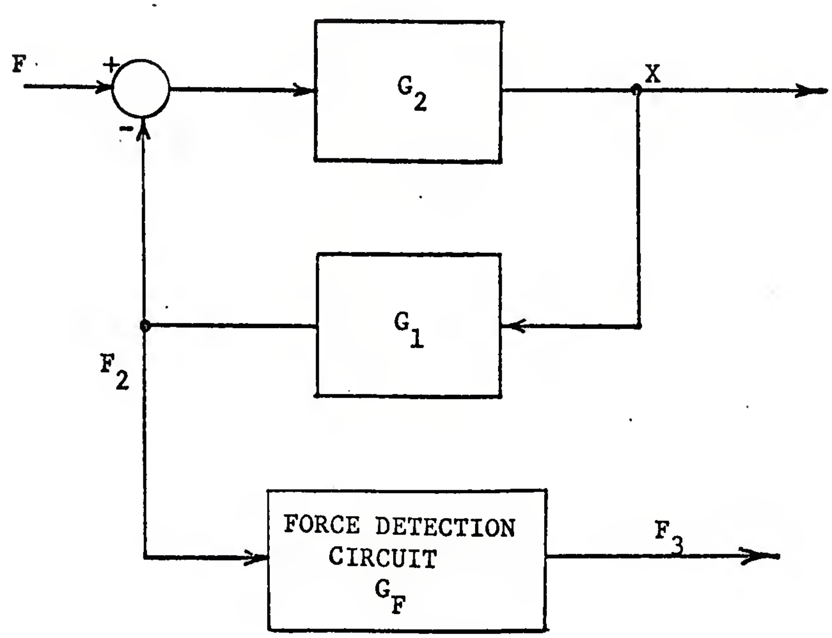

Figure H-2. Block diagram of the position feedback control system, view 2

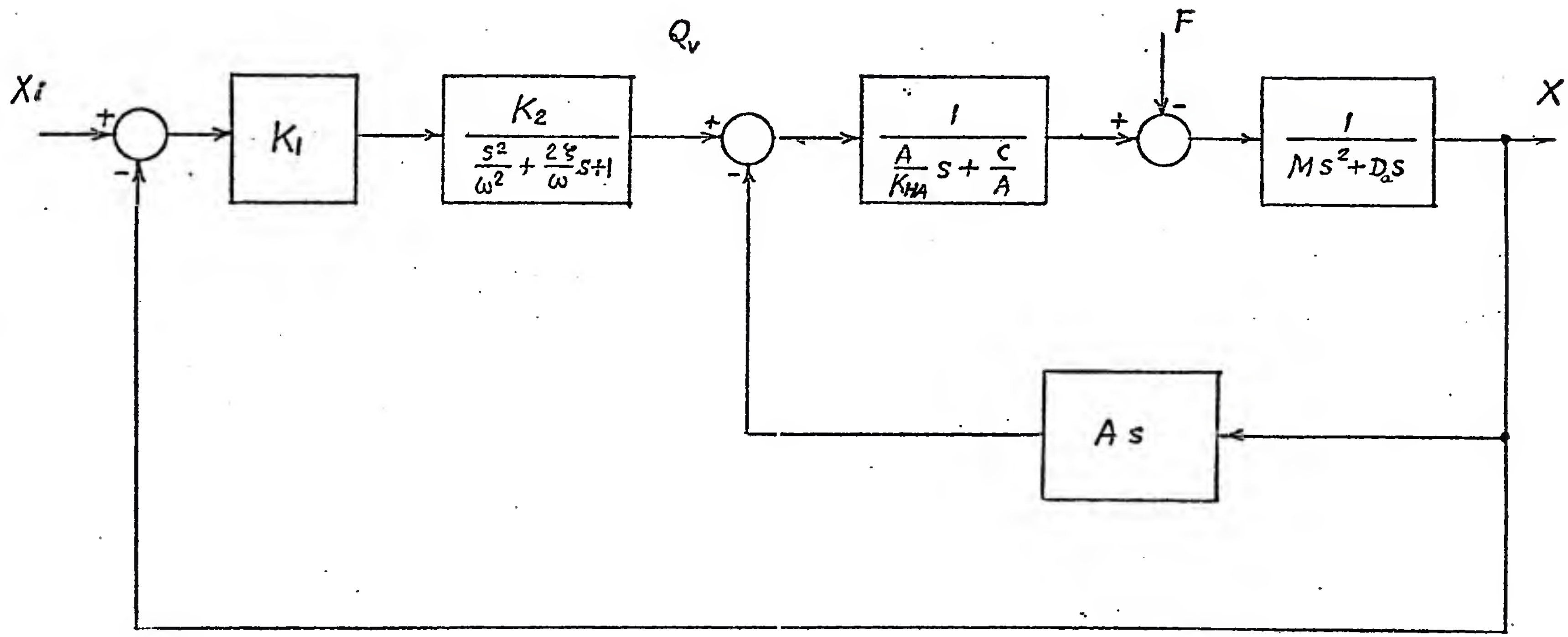

Figure H-3. Block diagram of an electrohydraulic actuator position servo

K_{HA} = actuator hydraulic stiffness

K_1 = amplifier scaling factor in ma per inch

K_2 = servovalve gain constant in cis per ma

s = Laplace transform operator

ζ = servovalve transfer function damping factor

ω = servovalve transfer function natural frequency

The closed-loop transfer function of position due to a disturbing force F is, therefore

$$\frac{X_d}{F} = \frac{(\frac{A}{K_H}s + \frac{C}{A})(\frac{S}{\omega^2} + \frac{2\zeta}{\omega}s + 1)}{(Ms^2 + Ds)(\frac{A}{K_H}s + \frac{C}{A})(\frac{S^2}{\omega^2} + \frac{2\zeta}{\omega}s + 1) + As(\frac{S^2}{\omega^2} + \frac{2\zeta}{\omega}s + 1) + K_1K_2} \quad \text{(H-14)}$$

When applying the final value theorm to determine the steady-state error in position $(X)_{ss}$ due to a step disturbing force F, the steady-state error is

$$(X)_{ss} = \lim_{s\to o} s\,(\frac{X_d}{F})(\frac{F}{s}) = \frac{FC}{AK_1K_2} \quad \text{(H-15)}$$

To express the steady-state error in terms of the servo system open-loop gain constant, K_V, the parameters K_1 and K_2 in equatin (H-5) can be related to K_V, from figure 3, as follows:

$$K_v = \frac{K_1K_2}{A(1 + \frac{DC}{A^2})} \quad \text{(H-16)}$$

Substituting equation (H-16) into (H-15) gives

$$(X)_{ss} = \frac{FC}{A^2K_V(1 + \frac{DC}{A^2})} \quad \text{(H-17)}$$

The required servo system open-loop gain constant to resist a specified maximum disturbing force F for an acceptable steady-state position error $(X)_{ss}$ is

$$K_V = \frac{FC}{A^2(1 + \frac{DC}{A^2}(X)_{ss}} \quad \text{(H-18)}$$

For $D = A^2/C$ equation (H-18) becomes

$$K_V = \frac{F}{2DX_{ss}} \tag{H-19}$$

This is a lower bound on equation (H-19) and, therefore, equation (H-9) merely provided a larger gain than required for the open-loop gain.

APPENDIX I

MAIN YAW SYSTEM

TITLE ACTIVATION OF 6-DOF SIMULATOR

MAIN YAW DRIVE SYSTEM:

PARAMETER			REFERENCE	DESIGN VALUE		UNIT
	MASS MOMENT OF INERTIA	I	AAH AIRCRAFT	47,625 *		LB-FT-SEC^2
			AH-1G AIRCRAFT	15,778 **		
	UNBALANCE	T_m	AAH -	8000 *		LB-FT
			AH1G -	11,350 **		
	FIRING TORQUE	T_{fr}	$3000\# \times \frac{42.5}{12}$	10,625 *		LB-FT
	MAX. AMPLITUDE	X	SPEC.	± 75		DEGREE
PEAK MOTION	AMPLITUDE	x	SPEC.	± 10		DEGREE
PEAK MOTION	FREQUENCY	f	SPEC.	.3		Hz
PEAK MOTION	VELOCITY	$\dot{x}$	$(2\pi)^2(f)(x)/360$	.33		RAD/SEC
PEAK MOTION	ACCEL.	$\ddot{x}$	$2\pi(f)(\dot{x})$	.62		RAD/SEC^2
	REQ'D TORQUE	T	$1.5(I\ddot{X} + T_m + T_{fr})$	AAH	72,229	LB-FT
				AH1	41,036	
	MAX. RPM	ω	$\dot{x}(60/2\pi)$	3.15		RPM
DRIVE MOTOR HAGGLUND #8385	MAX. TORQUE	T_{max}	$\frac{3080}{100} \times 3000 \times (e)$ EFF=.9	83,160 AVAILABLE		LB-FT
DRIVE MOTOR HAGGLUND #8385	MOTOR FLOW	g	CATALOG	2310.		IN^3/REV.
DRIVE MOTOR HAGGLUND #8385	VALVE FLOW	Q_V	$\frac{g\omega}{231(e)} = 40$ REQ'D.	60 RATED		GPM
DRIVE MOTOR HAGGLUND #8385	PUMP FLOW	Q_P	$\frac{2}{\pi} Q_V$	25		GPM
DRIVE MOTOR HAGGLUND #8385	HYDRAULIC STIFFNESS	K_H	SEE DWG. A-2629 SH. 2 OF 4	1.232×10^6		LB-FT/RAD.
	ESTIMATED NATURAL FREQUENCY	f_n	$\frac{1}{2\pi}\sqrt{\frac{K_H}{1.2\,I}}$	AAH	.74	Hz
				AH-1G	1.27	

Form 207 10M 1-73 * SEE DWG. A-2629, SHT. 3
** SEE DWG. A-2629, SHT. 4

Drawing No. A-2629
Sheet 1 of 4

TITLE MAIN YAW DRIVE

EST. HYDAULIC STIFFNESS OF DRIVE MOTOR:

HAGGLUNDS MODEL # 8385

TRAPPED VOLUME (V) = 2310 (IN^3) = $A \cdot L$

TORQ / PSI $(A \cdot R) = \frac{3080 \times 12}{100} = 369.6$ (IN^3)

$$\therefore \frac{R}{L} = \frac{A \cdot R}{A \cdot L} = .16$$

$$K_H = R^2 \frac{AB}{L} = \frac{R}{L} \cdot (AR) \cdot B \quad , \quad B = 250{,}000 \text{ PSI}$$

$$K_H = (.16)(369.6)(250{,}000) = 14.784 \times 10^6 \left(\frac{\text{IN-lb}}{\text{RAD.}}\right)$$

$$\text{OR} = 1.232 \times 10^6 \left(\frac{\text{FT}\cdot\text{lb}}{\text{RAD.}}\right)$$

Form 207 10M 1-73

Drawing No. A-2629
Sheet 2 of 4

TITLE YAW DRIVE

ESTIMATED MASS MOMENT OF INERTIA
ABOUT HELICOPTOR YAW (Z) AXIS:-

ITEM	WEIGHT (lb.)	C.G. OFFSET R (FT.)	$\frac{WR^2}{g}$ (lb-FT-SEC²)	I_o
YAW GIMBAL	7,500	0	0	1900
YAW DRIVE MOTOR	3,000	0	0	435
(6) SUSPENSION ACTUATORS	2,520	0	0	580
MOUNTING ADAPTORS	2,500	0	0	185
HELICOPTOR AAH	16,000	.5	125	44,400
TOTAL	31,520		125	47,500
			47,625	

UNBALANCE MOMENT (T_m) = 16,000 # x .5' = 8,000 (FT-lb).

FIRING TORQUE (T_{fr}) = 3000 # x $\frac{42.5''}{12}$ = 10,625 (FT-lb) MAX.

Drawing No. A-2629
Sheet 3 of 4

Form 10 10M 6-71

TITLE YAW DRIVE

ESTIMATED MASS MOMENT OF INERTIA
ABOUT HELICOPTOR YAW (Z) AXIS:-

ITEM	WEIGHT (lb.)	C.G. OFFSET R (FT.)	$\frac{WR^2}{g}$ (lb-FT-SEC²)	I_o
YAW GIMBAL	7,500	0	0	1900
YAW DRIVE MOTOR	3,000	0	0	435
(6) SUSPENSION ACTUATORS	2,520	0	0	580
MOUNTING ADAPTORS	2,500	0	0	185
HELICOPTOR AH-1G	9,500	1.19'	418	12,260
TOTAL			418	15,360
			15,778	

UNBALANCE MOMENT (T_m) = 9500# × 1.19' = 11305 (FT-lb)

FIRING TORQUE (T_{fr}) = 3000# × $\frac{42.5''}{12}$ = 10,625 (FT-lb) MAX.

Drawing No. A-2629
Sheet 4 of 4

Form 207 10M 6-71

OPERATING PRINCIPLES

The pistons (1) are contained in a stationary cylinder housing (2) and are connected to rollers (3) which bear on the cam ring (4). The rotary valve (5) distributes oil from the inlet (A) to each cylinder in sequence. The oil pressure displaces the pistons outward, forcing the rollers against the cam ring, causing it and the outer casing of the motor to rotate. Fixed side guides (6) absorb reaction forces on the rollers, thus unloading the pistons from any side (tangential) forces. Oil escapes from the motor through outlet (C). An even number of opposed pistons assures hydraulic balance and unloads the main bearing from any piston forces.

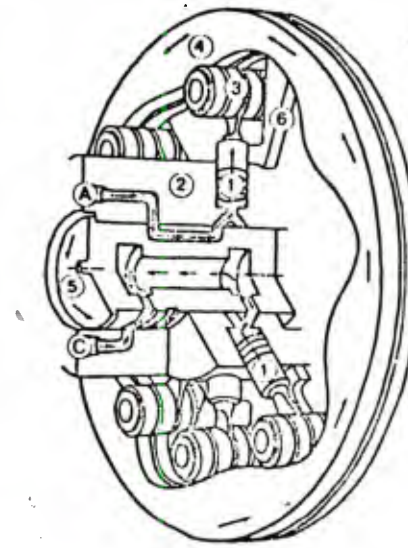

OUTSTANDING FEATURES

- FULL RATED STARTING TORQUE
- CONSTANT TORQUE — 0 TO FULL RPM
- LOW SPEED CONTROL UNDER 1 RPM AT FULL TORQUE
- INSTANT REVERSING
- TWO SPEED RANGES
- INTEGRAL CONTROL VALVES
- INTEGRAL HYDRAULIC BRAKES
- FREE WHEELING

MOTOR CHARACTERISTICS

MOTOR TYPE	WEIGHT	NORMAL SPEED RANGE				HIGHER SPEED RANGE		
		GALS. OIL PER REV.	CU. IN. PER/REV.	TORQUE FT. LB. 100 PSI	RPM	GALS. OIL PER REV.	TORQUE FT. LB. 100 PSI	RPM
1155	216	.22	50.8	69	0-300	—	—	—
2150	728	.62	143.2	190	0-100	.31	95	0-120
2165	728	1.05	242.5	321	0-60	.52	160	0-110
3160	639	.90	207.9	273	0-200	.45	136	0-200
4150	958	1.24	286.4	380	0-115	.62	190	0-115
4160	958	1.80	415.8	545	0-80	.90	272	0-80
4170	958	2.44	563.6	743	0-65	1.22	372	0-65
6170	1365	2.92	674.5	890	0-55	1.46	445	0-55
6185	1435	4.32	997.9	1315	0-36	2.16	657	0-36
8285	3080	8.64	1996.0	2630	0-16	4.32	1315	0-32
8385	3080	10.00	2310.0	3080	0-16	5.00	1540	0-32

Note: Maximum pressures. Types 1155 and 3160 — 5000 PSI. Types 2150 and 4150 — 3500 PSI. Type 4160 — 3250 PSI. All others — 3000 PSI.

TYPICAL TORQUE EXAMPLES — BASED ON MOTOR 4170

TYPICAL STARTING TORQUE AT 0 RPM FOR ALL HÄGGLUNDS HYDRAULIC MOTORS WITH MAXIMUM DISPLACEMENT

—— Theoretical ——— Actual

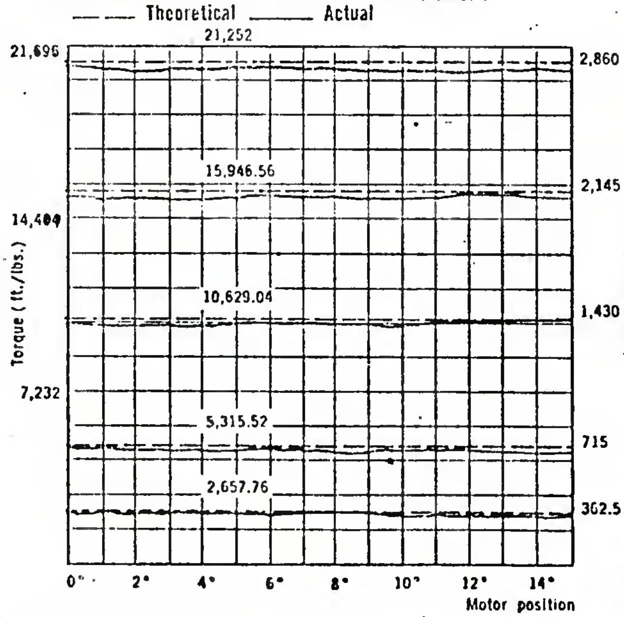

TYPICAL STARTING TORQUE AT 0 RPM FOR ALL HÄGGLUNDS HYDRAULIC MOTORS WITH HALF DISPLACEMENT

—— Theoretical ——— Actual

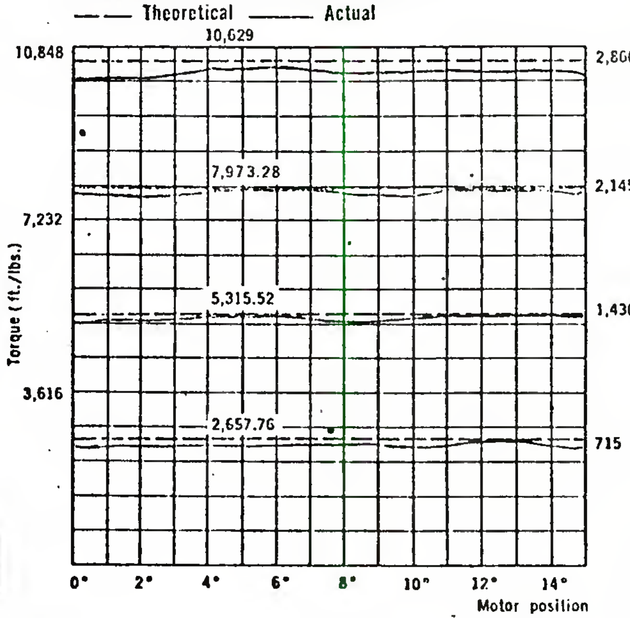

PERFORMANCE CHARACTERISTICS

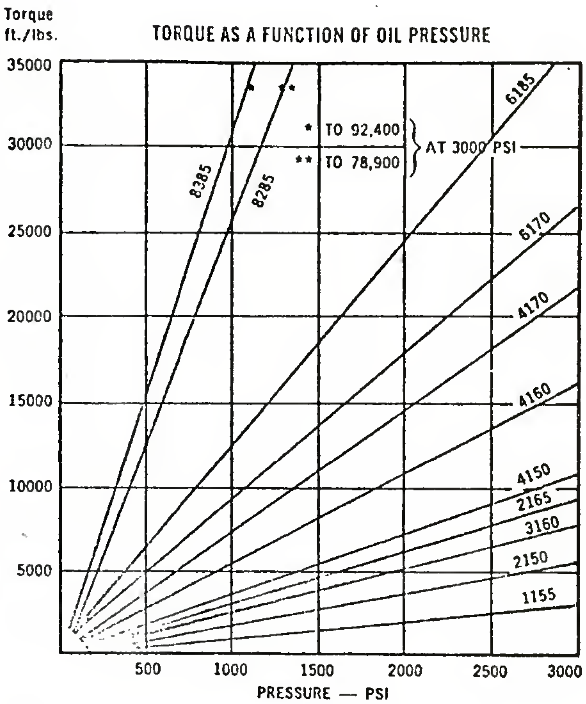

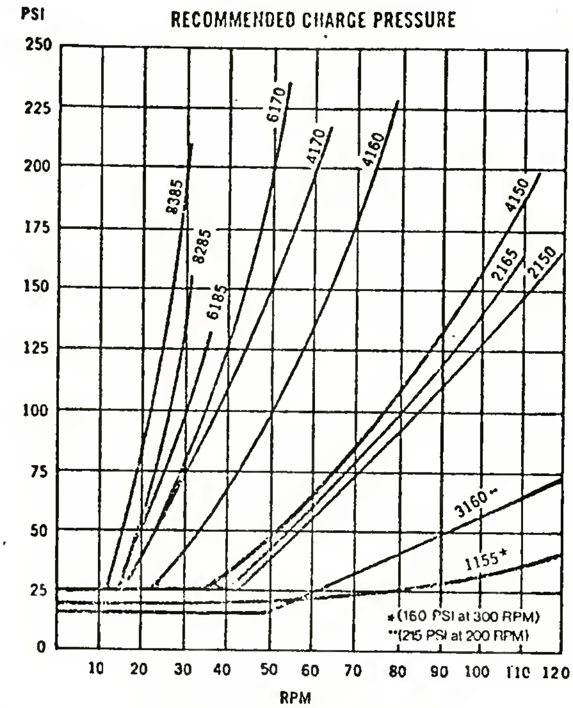

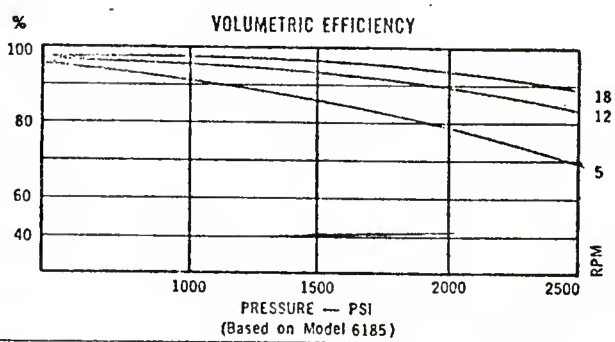

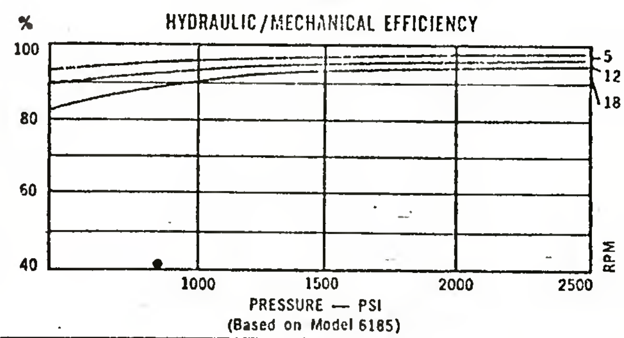

DIMENSIONS IN INCHES

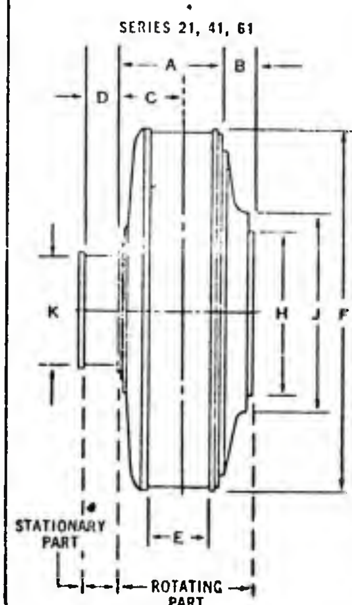

Motor Type*	A	B	C	D	E	F	H	J	K
2150	9.213	1.634	5.551	2.559	5.118	25.275	10.236	13.386	9.606
2165	9.213	1.634	5.551	2.559	5.118	25.275	10.236	13.386	9.606
4150	9.331	2.795	5.787	2.756	5.276	30.236	12.598	15.748	10.669
4160	9.331	2.795	5.787	2.756	5.276	30.236	12.598	15.748	10.669
4170	9.331	2.795	5.787	2.756	5.276	30.236	12.598	15.748	10.669
6170	9.606	2.992	5.827	3.150	5.750	33.779	15.354	18.504	10.669
6185	9.606	2.992	5.827	3.937	5.750	33.779	15.354	18.504	10.787
8285	13.667	3.184	9.055	2.126	7.815	43.307	17.323	NA	NA
8385	13.667	3.184	9.055	2.126	7.815	43.307	17.323	NA	NA

*Request installation data sheets for 1155 and 3160 wheel motors.

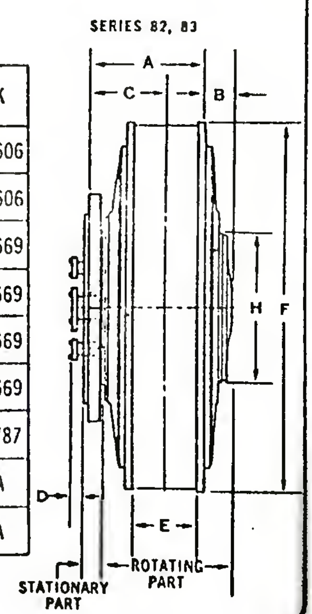

TITLE HYDR.- SCHEMATIC MODIFIED MAIN YAW ACTUATOR

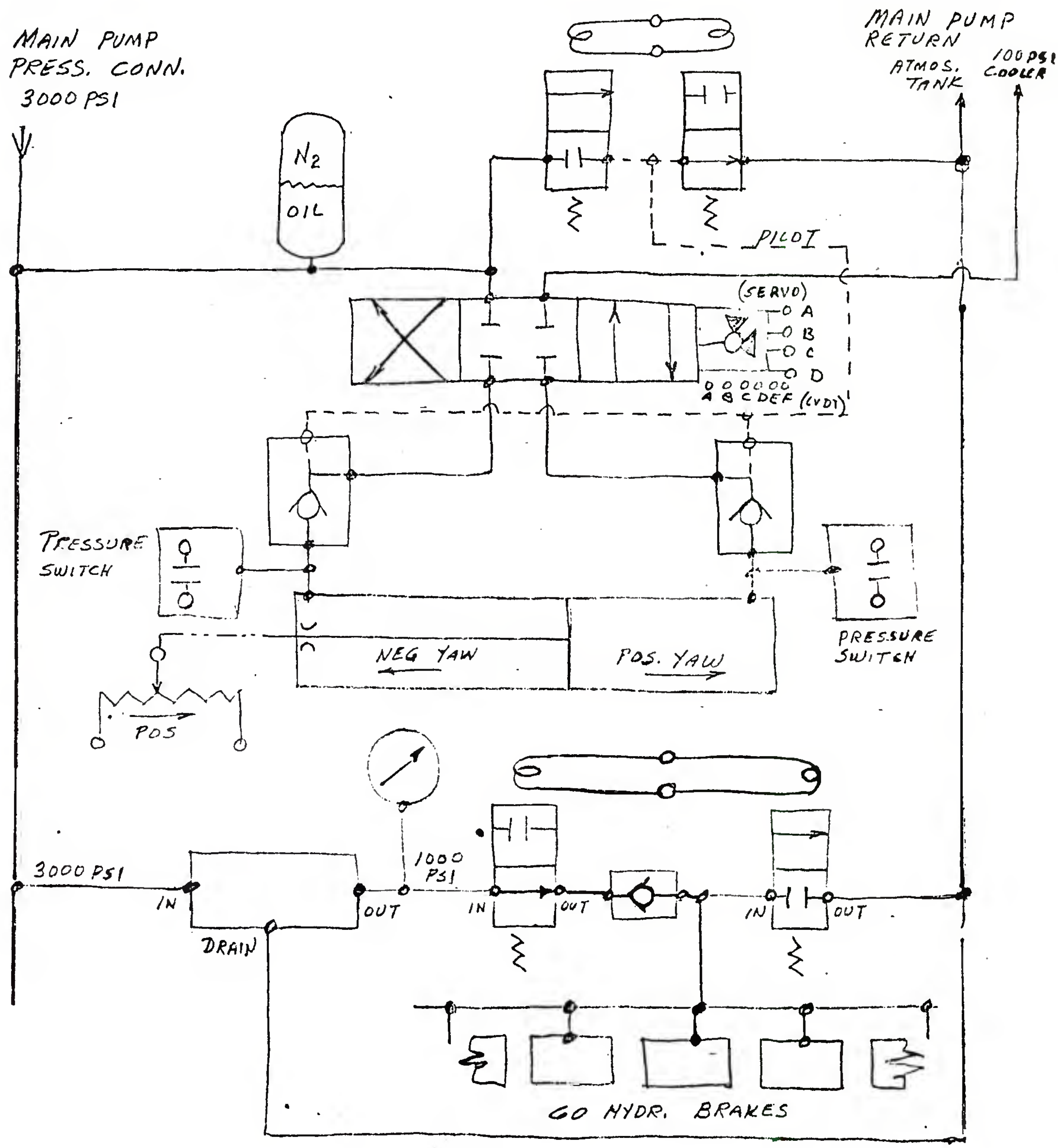

SERVOVALVE DYNAMIC RESPONSE

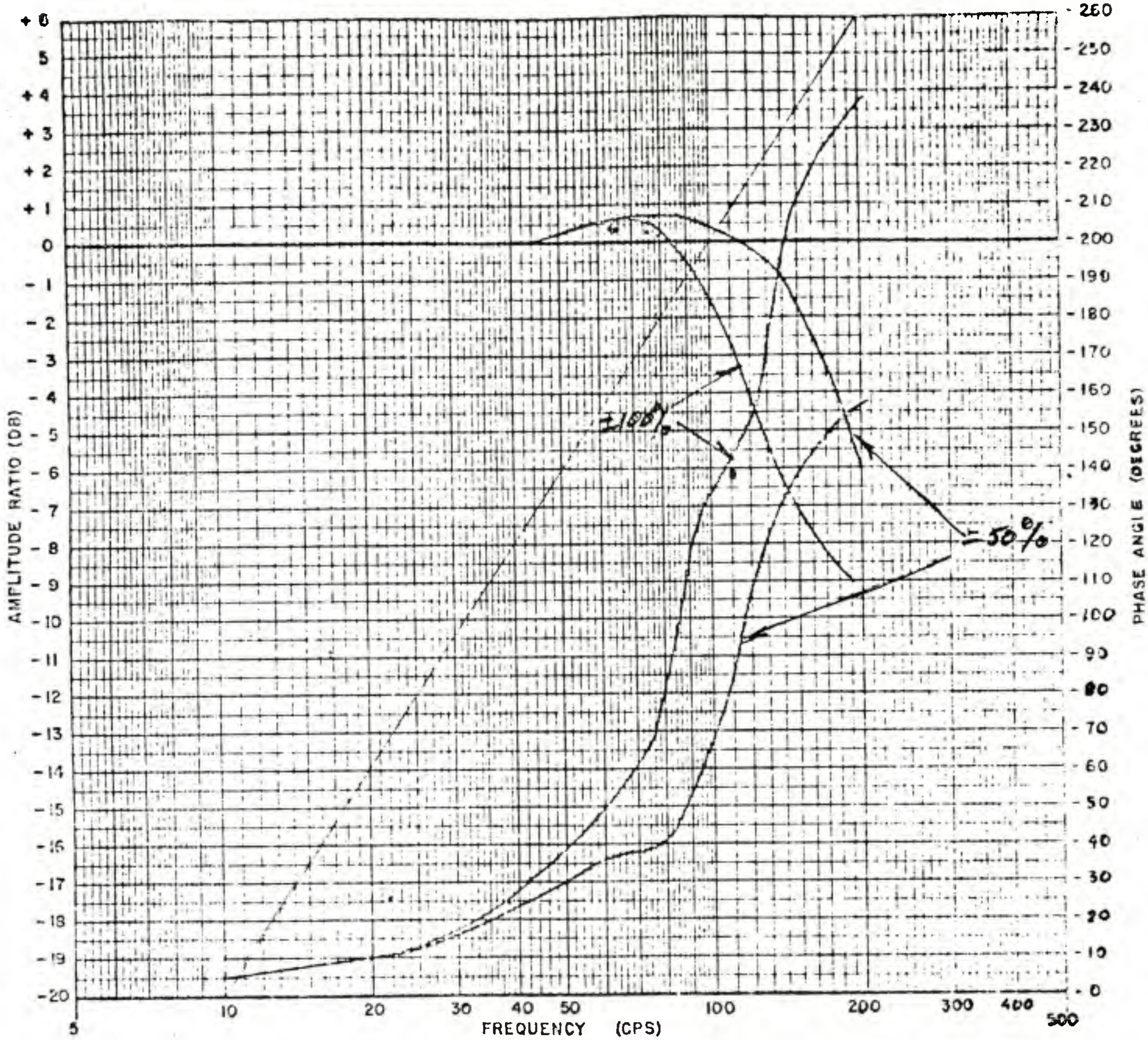

MODEL 79-060 SERIAL TYPICAL

DATE ______ BY ______

SYSTEM PRESSURE 3000 PSI

INPUT SIGNAL % RATED

OUTPUT THIRD STAGE SPOOL POSITION

RECEIVED

OCT 18 1973

MOOG

MOOG INC., EAST AURORA, NEW YORK

10K

100K

0.068

LEAD COMPENSATION

LOOP GAIN 740 sec^{-1}

5

APPENDIX J
COMBAT VEHICLE SYSTEM

TITLE ACTIVATION OF 6-DOF SIMULATOR

TANK PITCH	DRIVE SYSTEM:

PARAMETER			REFERENCE	DESIGN VALUE	UNIT
MASS MOMENT OF INERTIA		I	MICV 65 + 10%	2,000	$LB\text{-}FT\text{-}SEC^2$
UNBALANCE		T_m	$6076(1')(\sin 15^\circ)$	1573	LB-FT
FIRING TORQUE		T_{fr}	$3000 \times 3'$	9,000	LB-FT
MAX. AMPLITUDE		X		$\pm 15^\circ$	DEGREE
PEAK MOTION	AMPLITUDE	x	SPEC.	3.0	DEGREE
	FREQUENCY	f	SPEC.	3.5	Hz
	VELOCITY	$\dot{x}$	$(2\pi)^2(f)(x)/360$	1.15	RAD/SEC
	ACCEL.	$\ddot{x}$	$2\pi(f)(\dot{x})$	25.32	RAD/SEC^2
ACTUATOR 4" BORE × 2½" ROD	ARM	R	56"	4.67	FT.
	STROKE	L	$2(\sin 15^\circ)(56) = 29''$	30"	IN.
	REQ'D TORQUE	T	$1.5(I\ddot{x} + T_m + T_{fr})$	91,820	LB-FT
	HYD. FORCE	F_H	$\frac{T}{R} = 19{,}676$ REQ'D.	21,947 AVAIL	LB.
	PISTON AREA	A_s	$> \frac{F_H}{3000} = 6.56$ REQ'D.	7.568 AVAIL	IN^2
		A_L	$= A_s$	7.568	IN^2
	PISTON SPEED	V	$12R(\dot{x})$	64.4	IN/SEC
	VALVE FLOW	Q_v	$\frac{A_L(V)(60)}{231}$	126.6	GPM
	PUMP FLOW	Q_p	$> \frac{2}{\pi} Q_v$	81	GPM
	HYDRAULIC STIFFNESS	K_H	$2\times10^5 \frac{2(A_s+A_L)}{L/12} R^2$	53.35×10^6	LB-FT/RAD.
ESTIMATED NATURAL FREQ.		f_n	$\frac{1}{2\pi}\sqrt{\frac{K_H}{1.2\,I}}$	23.7	Hz

Form 207 10-1 6-71

Drawing No. A-2633

Estimated Mass Moment of Inertia
About Tank Pitch Axis

Item	Weight (lb)	C.G. Offset R(ft)	$\frac{WR^2}{g}$ (lb-ft-sec^2)	I_o (lb-ft-sec^2)
(Pitch & Roll Gimbal)	4,000	0	0	465
Tank Coupla (MICV65 + 10%)	6,076	1'	189	1,155
SUPPORT TUBE	1120	1'	35	521
Total	10,076	----	380	1,620
Mass Moment of Inertia (lb-ft-sec^2)			2,000	

TITLE HYDR. SCHEMATIC
COMBAT VEHICLE PITCH ACTUATOR

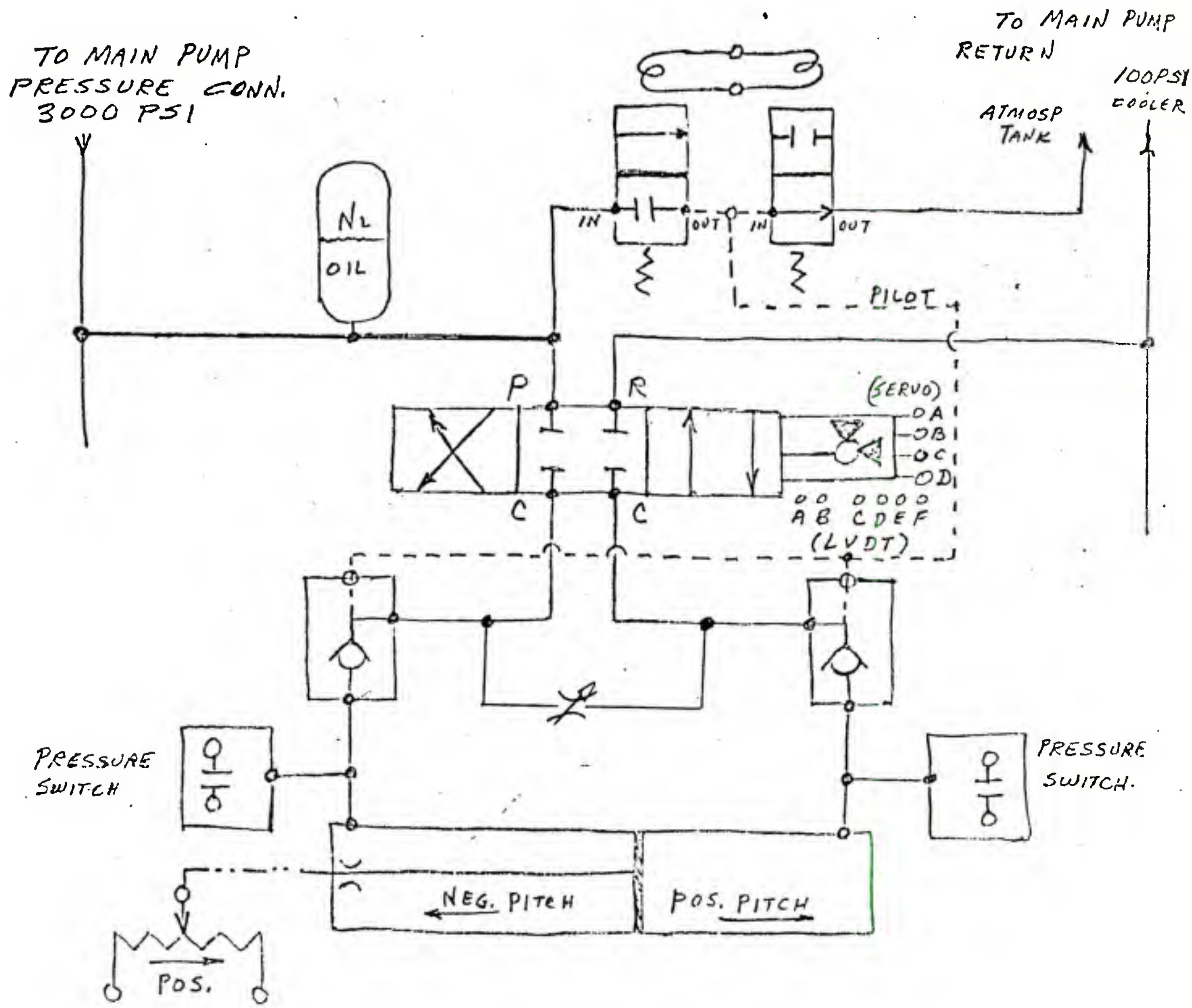

Form 207 10M 6-71

Drawing No. A-2636

Moog 79 Series-200 GPM High Flow Servovalves

Moog 79 Series — 200 GPM Servovalves control position, velocity or force of massive machine elements, with fast response at high flows. They are 3-stage servovalves using standard 2-stage Moog industrial valves for pilot operation. Operating in conjunction with an electronic position feedback loop, the pilot valve controls position of the 3rd stage spool, which in turn meters the high output flow.

Because of the high position loop gain around the 3rd stage, hysteresis and threshold properties meet or exceed the specifications of the best 2-stage servovalves. The excellent dynamic response of the 79 Series — 200 GPM servovalves makes them well suited for structural or fatigue testing applications where high frequency and full amplitude output are required.

A single servoamplifier can be used to provide closed loop operation for the third stage spool position and the required amplification and electronic mixing functions for the outer or major loops. Moog Series 82 Servocontrollers are highly recommended for this purpose.

Moog 79 Series — 200 GPM Servovalves are available in two configurations: Standard and High Response. In the Standard configuration, pilot valve flow operates on the full area of the third stage spool. In the High Response configuration, pistons of smaller area are incorporated on the ends of the third stage spool to optimize response as a function of pilot valve flow.

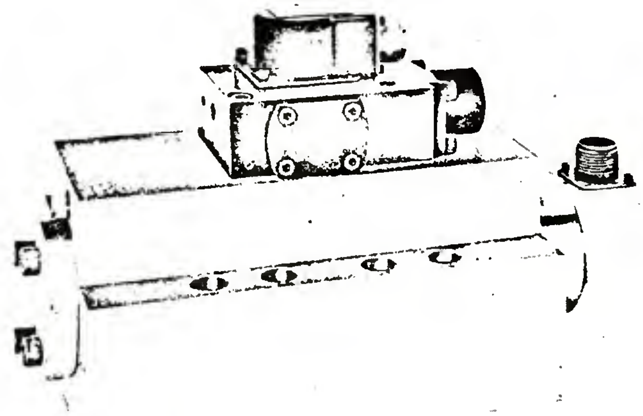

The following options are available in both configurations:

- Choice of Moog Series 73, 74 or 76 Servovalve for pilot operation with flow rates for optimum performance in the particular application.
- Choice of LVDT or DCDT spool position feedback transducer.
- Provision for mounting auxiliary spool position transducer for monitoring.
- Provision for operating the pilot valve from a separate hydraulic power source.

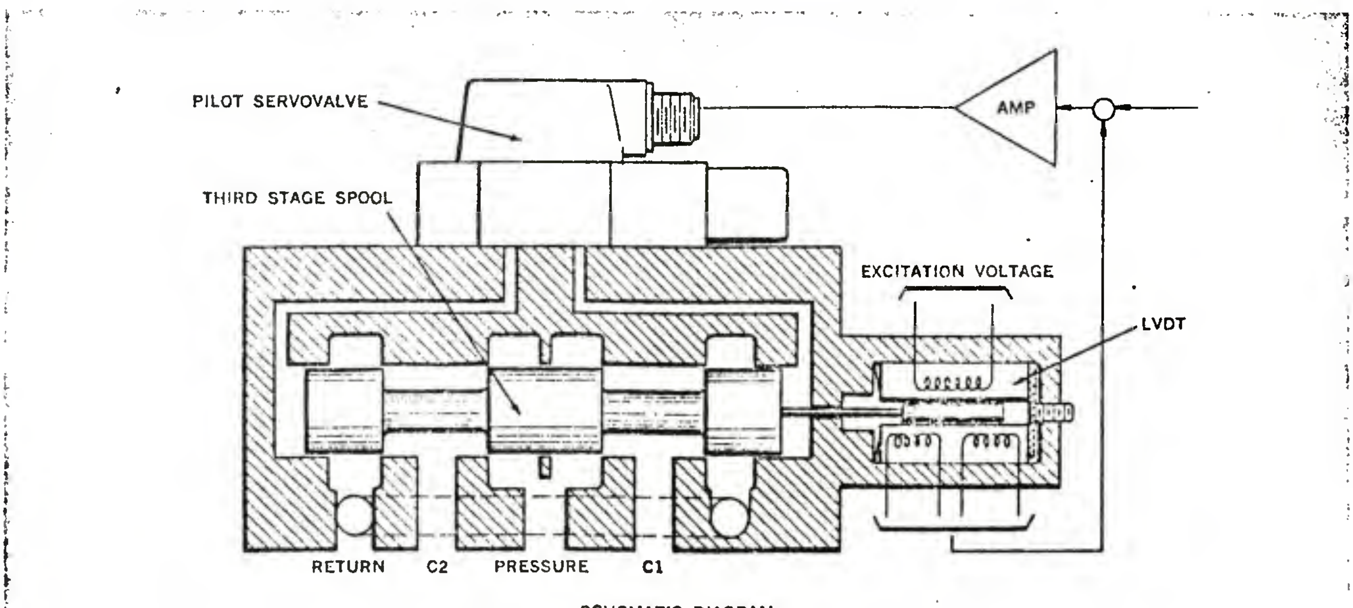

SCHEMATIC DIAGRAM
79 SERIES 3 STAGE SERVOVALVE WITH ELECTRICAL FEEDBACK

General Characteristics

Flow Rating	200 gpm at 1000 psi valve drop
Operating Pressure	300 to 3000 psi
Inlet proof pressure	4500 psi
Return proof pressure	3000 psi
Fluid	Petroleum base hydraulic fluid Others on special order
Filtration	10 microns recommended
Internal leakage at null	less than 2% of rated flow
External leakage	none
Pressure gain at null	Greater than 30% supply pressure for 1% input
Weight	47 lbs.
Null Shift*	less than 1% for 80% to 110% supply pressure variation 0% to 20% back pressure variation 100°F temperature change
Hysteresis*	less than 1%
Threshold*	less than 0.5%

*Values for third stage spool position loop gain of 250 sec^{-1}

FLOW LOAD CHARACTERISTICS
(Supply pressure greater than 1000 PSI)

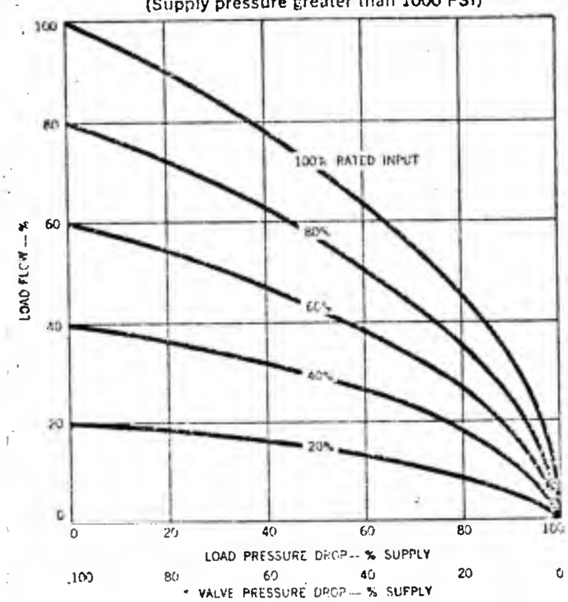

FLOW VS. SPOOL POSITION
(at various valve pressure drop)

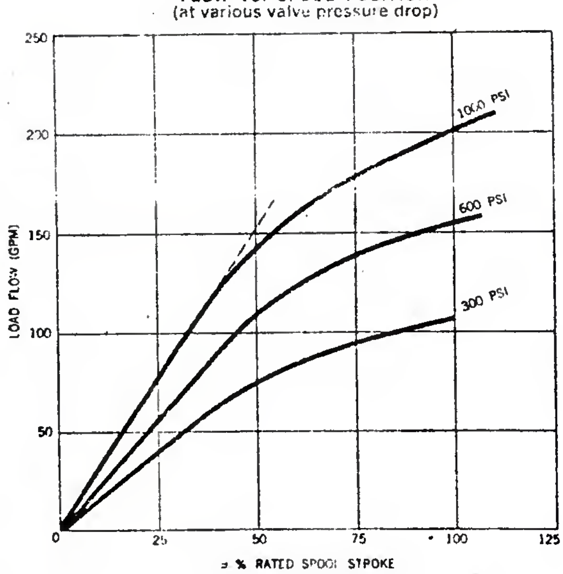

FREQUENCY RESPONSE CHARACTERISTICS

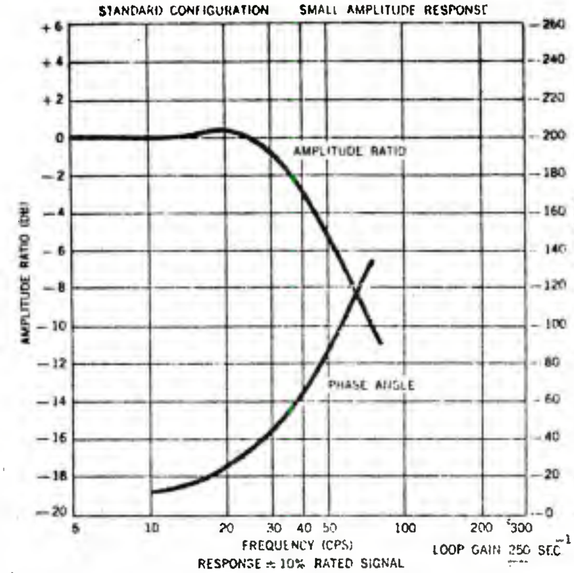

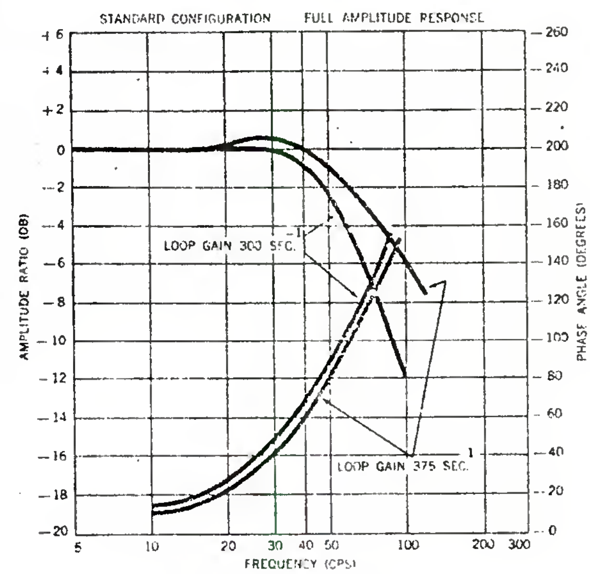

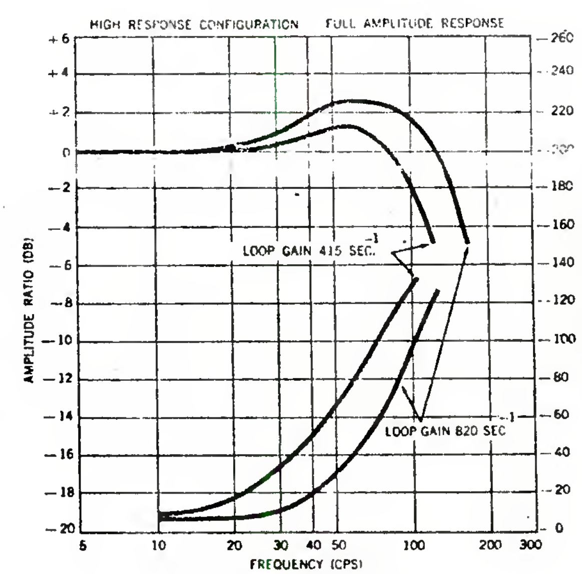

SYSTEM RESPONSE

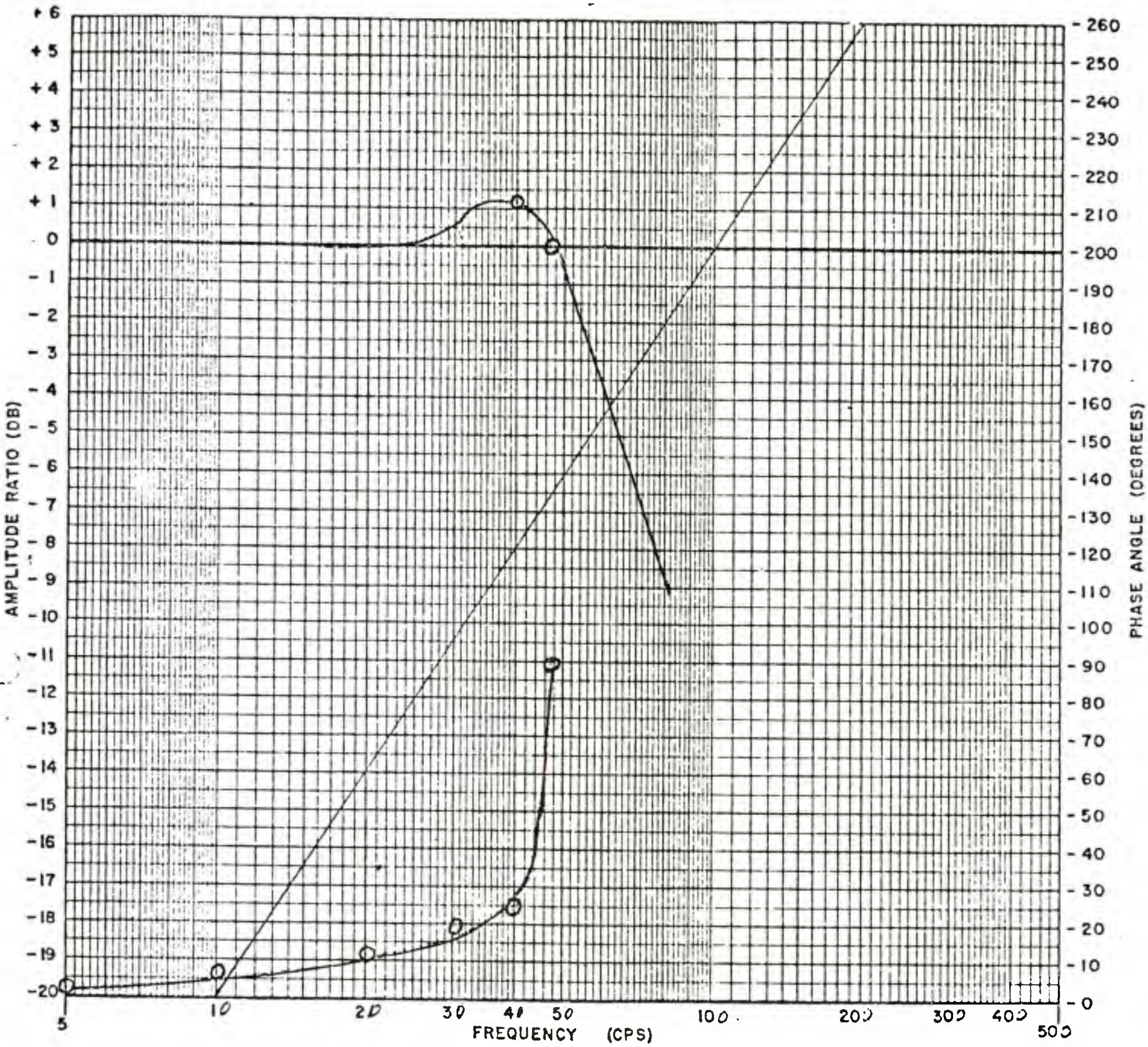

MODEL 79-200 SERIAL TYPICAL Improved Response

DATE 8/7/73 BY P. E. C.

73-232 pilot valve

SYSTEM PRESSURE 3000 PSI

INPUT SIGNAL ± 100% rated ~~MA(P-P)~~

OUTPUT Spool Position - 2nd Stage

$K_{loop} = 1075\ sec^{-1}$

MOOG
MOOG INC., EAST AURORA, NEW YORK

RECEIVED

OCT 18 1973

TITLE **6-DOF FOR TANK YAW DRIVE**

SUSPENDED WT. = 13,000 (lb.)

MASS MOMENT OF INERTIA (I_z) = 30,000 (lb-in-sec²)

REQ'D ACCELERATION ($\ddot{\psi}$) = 25.32 (RAD/SEC²)

FIRING LOAD: 3000 (lb) AT 3' ARM

$F_x = 3000$ (lb)

$M_z = 108,000$ (in-lb)

TORQUE (T) = $I_z \ddot{\psi} + M_z$ = 867,600 (in-lb)

EQUIV. $\ddot{\psi}$ FOR SAME I_z ($\ddot{\psi}_1$):

$$\ddot{\psi}_1 = \frac{T}{I_z} = \frac{867600}{30,000} = 28.92 \text{ (RAD/SEC}^2\text{)}$$ SAY 29.

ASSUMING (2) CONCENTRATED WT. AT ± X" (6500 # EA.)

$$I_z = (2)\left(\frac{6500}{g}\right)(x^2) = 30,000 \text{ (lb-in-sec}^2\text{)}$$

$$x = \sqrt{\frac{30,000 \times g}{(2)(6500)}} = 29.86"$$ (SAY 30")

ACCELERATION IN X-AXIS DUE TO FIRING:—

$$F = M\ddot{x} = 3,000 \#$$

$$\ddot{x} = \frac{3000 \times g}{13,000 \#} = .23g = 89.17 \text{ (in/sec}^2\text{)}$$ SAY 90.

Form 207 10M 1-73

TITLE 6-DOF FOR TANK YAW DRIVE

INPUT OF "SDFS" PROGRAM:-

	LUMPED WEIGHT			
NO.	X	Y	Z	Wt (lb)
1	+ 30"	0	+36"	6,500
2	- 30"	0	+36	6,500

PLATFORM DISPLACEMENT			
	X	Y	Z
TRANSLATION (IN.)	0	0	0
ROTATION (DEGREE)	0	0	3.0

ACCELERATIONS ACTING ON Wt.			
	X	Y	Z
TRANSLATION (IN/SEC^2)	90.	0	0
ROTATION (RAD/SEC^2)	0	0	29.

Form 207 10M 1-73

6 - D . O . F .
FOR TANK YAW DRIVE

COORDINATES OF FIXED FRAME

ACTUATOR	X (IN.)	Y (IN.)	Z (IN.)
1	15.58846	36.00000	-36.00000
2	-38.97114	4.50000	-36.00000
3	-38.97114	-4.50000	-36.00000
4	15.58846	-36.00000	-36.00000
5	23.38269	-31.50000	-36.00000
6	23.38269	31.50000	-36.00000

COORDINATES OF MOVING FRAME

ACTUATOR	X (IN.)	Y (IN.)	Z (IN.)
1	-12.99038	28.50000	.00000
2	-18.18653	25.50000	.00000
3	-18.18653	-25.50000	.00000
4	-12.99038	-28.50000	.00000
5	31.17691	-3.00000	.00000
6	31.17691	3.00000	.00000

COORDINATES OF LUMPED WEIGHTS

NO.	X (IN.)	Y (IN.)	Z (IN.)	WEIGHT (LBS)
1	30.00000	.00000	36.00000	6500.00000
2	-30.00000	.00000	36.00000	6500.00000

6 - D . O . F .
FOR TANK YAW DRIVE

PLATFORM DISPLACEMENT

	X	Y	Z
TRANSLATION (IN.)	.000	.000	.000
ROTATION (DEG.)	.000	.000	.000

COORDINATES OF MOVING FRAME

ACTUATOR	X (IN.)	Y (IN.)	Z (IN.)	ACTUATOR LENGTH
1	-12.99038	28.50000	.00000	46.57252
2	-18.18653	25.50000	.00000	46.57252
3	-18.18653	-25.50000	.00000	46.57252
4	-12.99038	-28.50000	.00000	46.57252
5	31.17691	-3.00000	.00000	46.57252
6	31.17691	3.00000	.00000	46.57252

ACCELERATIONS ACTING ON WEIGHTS

	X	Y	Z
LINEAR (IN/SEC2)	.00	.00	.00
ANGULAR (RAD/SEC2)	.00	.00	.00

ACTUATOR FORCES

ACTUATOR	FORCE(LBS)
1	.28030+04
2	.28030+04
3	.28030+04
4	.28030+04
5	.28030+04
6	.28030+04

COMPONENTS OF FORCES

1	-.17200+04	-.45139+03	.21667+04
2	.12509+04	.12639+04	.21667+04
3	.12509+04	-.12639+04	.21667+04
4	-.17200+04	.45139+03	.21667+04
5	.46910+03	.17153+04	.21667+04
6	.46910+03	-.17153+04	.21667+04

6 - D . O . F .
FOR TANK YAW DRIVE

COORDINATES OF FIXED FRAME

ACTUATOR	X (IN.)	Y (IN.)	Z (IN.)
1	15.58846	36.00000	-36.00000
2	-38.97114	4.50000	-36.00000
3	-38.97114	-4.50000	-36.00000
4	15.58846	-36.00000	-36.00000
5	23.38269	-31.50000	-36.00000
6	23.38269	31.50000	-36.00000

COORDINATES OF MOVING FRAME

ACTUATOR	X (IN.)	Y (IN.)	Z (IN.)
1	-12.99038	28.50000	.00000
2	-18.18653	25.50000	.00000
3	-18.18653	-25.50000	.00000
4	-12.99038	-28.50000	.00000
5	31.17691	-3.00000	.00000
6	31.17691	3.00000	.00000

COORDINATES OF LUMPED WEIGHTS

NO.	X (IN.)	Y (IN.)	Z (IN.)	WEIGHT (LBS)
1	30.00000	.00000	36.00000	6500.00000
2	-30.00000	.00000	36.00000	6500.00000

6 - D . O . F .
FOR TANK YAW DRIVE

PLATFORM DISPLACEMENT

	X	Y	Z
TRANSLATION (IN.)	.000	.000	.000
ROTATION (DEG.)	.000	.000	.000

COORDINATES OF MOVING FRAME

ACTUATOR	X (IN.)	Y (IN.)	Z (IN.)	ACTUATOR LENGTH
1	-12.99038	28.50000	.00000	46.57252
2	-18.18653	25.50000	.00000	46.57252
3	-18.18653	-25.50000	.00000	46.57252
4	-12.99038	-28.50000	.00000	46.57252
5	31.17691	-3.00000	.00000	46.57252
6	31.17691	3.00000	.00000	46.57252

ACCELERATIONS ACTING ON WEIGHTS

	X	Y	Z
LINEAR (IN/SEC2)	90.00	.00	.00
ANGULAR (RAD/SEC2)	.00	.00	.00

ACTUATOR FORCES

ACTUATOR	FORCE(LBS)
1	.17205+04
2	.51999+04
3	.51999+04
4	.17205+04
5	.14885+04
6	.14885+04

COMPONENTS OF FORCES

1	-.10558+04	-.27707+03	.13299+04
2	.23206+04	.23447+04	.40194+04
3	.23206+04	-.23447+04	.40194+04
4	-.10558+04	.27707+03	.13299+04
5	.24912+03	.91091+03	.11506+04
6	.24912+03	-.91091+03	.11506+04

6 - D . O . F .
FOR TANK YAW DRIVE

COORDINATES OF FIXED FRAME

ACTUATOR	X (IN.)	Y (IN.)	Z (IN.)
1	15.58846	36.00000	-36.00000
2	-38.97114	4.50000	-36.00000
3	-38.97114	-4.50000	-36.00000
4	15.58846	-36.00000	-36.00000
5	23.38269	-31.50000	-36.00000
6	23.38269	31.50000	-36.00000

COORDINATES OF MOVING FRAME

ACTUATOR	X (IN.)	Y (IN.)	Z (IN.)
1	-12.99038	28.50000	.00000
2	-18.18653	25.50000	.00000
3	-18.18653	-25.50000	.00000
4	-12.99038	-28.50000	.00000
5	31.17691	-3.00000	.00000
6	31.17691	3.00000	.00000

COORDINATES OF LUMPED WEIGHTS

NO.	X (IN.)	Y (IN.)	Z (IN.)	WEIGHT (LBS)
1	30.00000	.00000	36.00000	6500.00000
2	-30.00000	.00000	36.00000	6500.00000

6 - D . O . F .
FOR TANK YAW DRIVE

PLATFORM DISPLACEMENT

	X	Y	Z
TRANSLATION (IN.)	.000	.000	.000
ROTATION (DEG.)	.000	.000	3.000

COORDINATES OF MOVING FRAME

ACTUATOR	X (IN.)	Y (IN.)	Z (IN.)	ACTUATOR LENGTH
1	-14.46415	27.78108	.00000	47.60998
2	-19.49618	24.51324	.00000	45.56099
3	-16.82704	-26.41686	.00000	47.60998
4	-11.48100	-29.14081	.00000	45.56099
5	31.29120	-1.36421	.00000	47.60998
6	30.97718	4.62756	.00000	45.56099

ACCELERATIONS ACTING ON WEIGHTS

	X	Y	Z
LINEAR (IN/SEC2)	.00	.00	.00
ANGULAR (RAD/SEC2)	.00	.00	29.00

ACTUATOR FORCES

ACTUATOR	FORCE(LBS)
1	.13748+05
2	-.76717+04
3	.13748+05
4	-.76717+04
5	.13748+05
6	-.76717+04

COMPONENTS OF FORCES

1	-.86778+04	-.23732+04	.10395+05
2	-.32793+04	-.33699+04	-.60618+04
3	.63942+04	-.63286+04	.10395+05
4	.45580+04	-.11550+04	-.60618+04
5	.22836+04	.87018+04	.10395+05
6	-.12788+04	.45249+04	-.60618+04

TITLE 6-DOF FOR TANK YAW

SUMMARY: "SDFS" OUTPUT

ACTUATOR LENGTH: (MAX) = 47.60998"

(MIN.) = 45.56099

DOUBLE AMPLITUDE: $(\Delta \ell)$ = 2.04899"

ACTUATOR FORCE :- (ACTUATOR NO. 3 IS THE MAX.)

F_a (MAX.) = 13,784 + 5,200 − 2,803 = 16,181 (lb)

MAX. ACTUATOR WORKING PRESSURE:

$$P_a = \frac{16{,}181}{10.66} = 1{,}520 \text{ (PSI)}, \quad \Delta P = 2900 - 1520 = 1380 \text{(PSI)}$$

~~SERVO~~VALVE RATED 60 GPM AT 1,000 PSI IS CAPABLE OF DELIVERING $Q_V = 60\sqrt{\frac{\Delta P}{1000}}$ = 70.5 GPM (AT ΔP=1380)

MAX. PISTON SPEED $(\dot{x}) = \omega x$

$$\dot{x} = (3.5)(2\pi)\left(\frac{2.04899}{2}\right) = 22.53 \text{ IN/SEC.}$$

REQ'D VALVE FLOW (Q_0) FOR YAW DRIVE:

$$Q_0 = (22.53)(10.64)\frac{60}{231} = 62.3 \text{ GPM}$$

AVAILABLE VALVE FLOW FOR 6-DOF SPRING SYSTEM:-

$$Q_6 = 6(Q_V - Q_0) = 6 \times 8.2 = 49.2 \text{ GPM}$$

Form 207 10M 1-73

TITLE ACTIVATION OF 6-DOF SIMULATOR

PERFORMACE LIMITS OF TURRET YAW BY USING MAIN YAW DRIVE :-

1. DRIVE MOTOR

DRIVE MOTOR HAGGLUND #8385	MAX. TORQUE	T_{MAX}	$\frac{3080}{100} \times 3000 \times (e)$ EFF.=.9	83,160	LB·FT
	MOTOR FLOW	8	CATALOG	2310.	$\frac{IN^3}{REV.}$
	VALVE FLOW	Q_V	$\frac{8\,\omega}{231 \times (e)} = 40\ (=.9)$	60	GPM
	PUMP FLOW	Q_P	$\frac{2}{\pi} Q_V$	26	GPM
	HYDRAULIC STIFFNESS	K_H	SEE DWG. NO. A-2629, SHEET 2.	1.232×10^6	LB·FT/RAD.

2. MASS MOMENT OF INERITIA (I_z):-

$$I_z = 2500 + 1900 + 435 + 580 = 5415 \quad (\text{lb-ft-SEC}^2)$$

3. MAX. ACCELERATION ($\ddot{x}$):

$$1.5\,(I_z \ddot{x} + T_m + T_{fr}) = 83160 \quad (\text{LB-FT})$$

$$T_m = 0\ ,\quad T_{fr} = 9000 \quad (\text{LB-FT})$$

$$\ddot{x} = \left(\frac{83160}{1.5} - 9000\right) \Big/ 5415 = 8.576 \quad (\text{RAD}/\text{SEC}^2)$$

4. MAX. VELOCITY ($\dot{x}$) :- FOR 60 GPM VALVE FLOW

$$\frac{8\,\omega}{231\,(.9)} = 60 \text{ GPM},$$

$$\omega = \frac{60\,(231)(.9)}{2310} = 5.4\ (\text{RPM}), \quad \dot{x} = \frac{5.4\,(2\pi)}{60} = .56\left(\frac{\text{RAD}}{\text{SEC}}\right)$$

5. ESTMATED NATURAL FREQUENCY (f_n) :-

$$f_n = \frac{1}{2\pi}\sqrt{\frac{K_H}{1.2\,I}} = \frac{1}{2\pi}\sqrt{\frac{1.232 \times 10^6}{1.2\,(5415)}} = 2.19 \text{ Hz}$$

Form 207 10M 1-73

Drawing No. A-2661

APPENDIX K
TAIL ROTOR SIMULATOR

TITLE ACTIVATION OF 6-DOF SIMULATOR

TAIL ROTOR DRIVE SYSTEM:

PARAMETER			REFERENCE	DESIGN VALUE	UNIT
MASS MOMENT OF INERTIA		I	AH-1G	15,670	$LB\text{-}FT\text{-}SEC^2$
UNBALANCE		T_m		0	LB-FT
FIRING TORQUE		T_{fr}	$3000 \times 1.5'$	4,500	LB-FT
MAX. AMPLITUDE		X		$\pm 3°$	DEGREE
PEAK MOTION	AMPLITUDE	x	SPEC.	$\pm 3°$	DEGREE
	FREQUENCY	f	SPEC.	.3	Hz
	VELOCITY	$\dot{x}$	$(2\pi)^2(f)(x)/360$	.1	RAD/SEC
	ACCEL.	$\ddot{x}$	$2\pi(f)(\dot{x})$	.19	RAD/SEC^2
ACTUATOR ($2''$ BORE $\times 1\frac{3}{8}''$ ROD)	ARM	R	(STA. 302")	8.5'	FT.
	STROKE	L	$\frac{(2X)(2\pi)R}{360} \times 12 = 10.7$	11 ($\pm 5\frac{1}{2}''$)	IN.
	REQ'D TORQUE	T	$1.5(I\ddot{x} + T_m + T_{fr})$	11,216	LB-FT
	HYD. FORCE	F_H	$\frac{T}{R} = 1320$ REQ'D	4970 AVAIL.	LB.
	PISTON AREA	A_s	$> \frac{F_H}{3000} = .46$ REQ'D.	1.6567 AVAIL.	IN^2
		A_i	$= A_s$	1.6567	IN^2
	PISTON SPEED	V	$12R(\dot{x})$	10.2	IN/SEC
	VALVE FLOW	Q_v	$\frac{A_i(V)(60)}{231} = 4.4$	MOOG 73-233 (10 GPM)	GPM
	PUMP FLOW	Q_p	$> \frac{2}{\pi} Q_v$ NO ACCUMULATOR USED	4.4	GPM
	HYDRAULIC STIFFNESS	K_H	$2\times10^5 \frac{2(A_s+A_i)}{L/12} R^2$	104.5×10^6	LB-FT/RAD.
ESTIMATED NATURAL FREQ.		f_n	$\frac{1}{2\pi}\sqrt{\frac{K_H}{1.2\,I}}$	11.86	Hz

Form 207 10M 6-71

Drawing No. A-2634

TITLE TAIL ROTOR SIMULATOR

AH-1G HELICOPTOR

	LOCATION (IN.)				MOMENT	FORCE
	STA.	W.L	X	Z	(FT-lb)	(lb)
C. G.	200	69.7	0	0	0	
TAIL ROTOR	520.67	118.3	320.67	48.6	28,700	1,074
SIMULATOR	302.	85.16	102.	15.46	28,700	3,370

FIRING LOAD = 3000 # (MAX.) AT 18"

SIMULATOR REACTION = $\frac{3000 \times 18}{102}$ = 530 #

TOTAL MOMENT OF INERTIA (I_1) = 15,670 (lb·FT-SEC²)

SECTION ON SIMULATOR (I_2) ≐ 5,000 (lb·FT-SEC²)

SIMULATOR FORCE ≐ $\frac{\ddot{\psi}(I_1 - I_2)}{8.51}$ WHERE $\ddot{\psi}$ = .62 $\left(\frac{RAD}{SEC^2}\right)$

$$= \frac{.62\ (10,670)}{8.5} \doteq 800\ \#$$

Form 207 10M 1-73

TITLE HYDRAULIC SCHEMATIC
TAIL ROTOR SIMULATOR

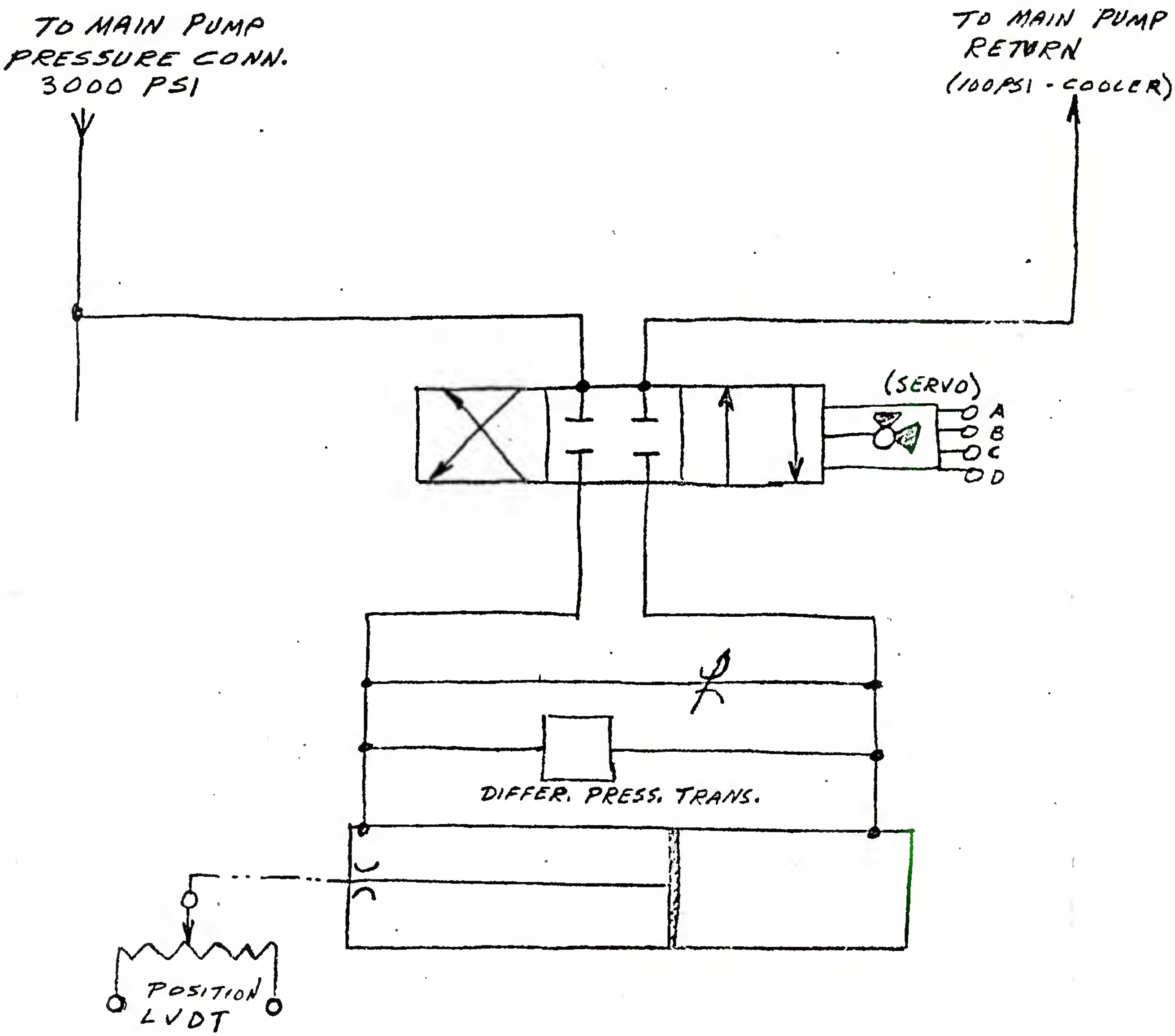

Form 207 10M 6-71

Drawing No. A-2635

MOOG SERIES 73 SERVOVALVE

The 73 Series Servovalve is a high performance, two-stage design that covers the range of rated flows from 1 to 15 gpm at 1000 psi (4 to 58 lit min at 70 bars). The valves have a large field replaceable filter for first stage flow that insures long trouble-free operation.

The output stage is a closed center, four-way, sliding spool. The pilot stage is a symmetrical double-nozzle and flapper, driven by a double air gap, dry torque motor. Mechanical feedback of spool position is provided by a simple cantilever spring. The valve design is simple and rugged for dependable, long life operation. A large capacity, field replaceable filter gives added protection of first stage flow.

The spool and sleeve assembly floats on o-rings in an aluminum alloy body. This isolates the spool from side loading that could be imposed by mounting the valve on a slightly uneven manifold. A convenient null adjustment is provided by an eccentric pin that locates the sleeve. The pilot stage is built-up as a separate subassembly that can be removed without upsetting careful spacing of the torque motor parts.

Several 73 Series models are available from stock. A variety of options can be supplied on special order.

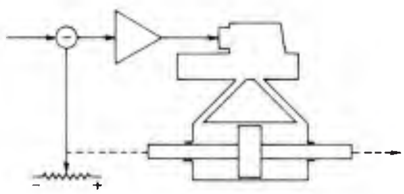

In a conventional closed-loop position control system, valve flow is applied to a hydraulic piston which drives the load. Load position is measured electrically and fed back for comparison with a signal representing the desired position. The resulting error signal is amplified, providing current input to the valve to control flow.

OPERATION

Moog Series 73 Servovalves use an electrical torque motor, a double-nozzle pilot stage, and a sliding-spool second stage. Electrical current in the torque motor gives proportional displacement of the second stage spool; hence, proportional flow to the load.

TORQUE MOTOR

The torque motor includes coils, polepieces, magnets, and an armature. The armature is supported for limited pivotal movement by a flexure tube. The flexure tube also provides a fluid seal between the hydraulic and electromagnetic portions of the valve.

PILOT STAGE

The flapper attaches to the center of the armature and extends down, inside the flexure tube. A nozzle is located on each side of the flapper so that flapper motion varies the nozzle openings. Pressurized hydraulic fluid is supplied to each nozzle through a filter and inlet orifice. Differential pressures caused by flapper movement between the nozzles are applied to the ends of the valve spool.

DESIGN FEATURES*

- rugged aluminum alloy body
- o-ring floated, center pinned bushing with convenient null adjust
- field replaceable 20 micron filter for pilot flow
- dry torque motor in sealed compartment
- frictionless, flexure tube supported armature-flapper
- modular torque motor and pilot stage assembly
- balanced, double coil, double air gap torque motor
- mechanical feedback with simple cantilever spring
- spool-bushing diametral tolerances held within 10 microinches (¼ micron)
- motor coils protected during thermal and vibration extremes by resilient potting
- optional fifth port for separate pilot supply

*Design features of the Series 73 Servovalve are covered by U.S. Patents 3,023,782 and 3,228,423 together with corresponding patents in several foreign countries.

VALVE SPOOL

The 4-way valve spool controls flow from the supply to either control port (C1 or C2). Simultaneously, the other control port is opened to fluid return. The spool fits in a sleeve that contains openings which are uncovered by spool motion to meter flow to the load. Various valve rated flows are provided by sizing these openings in the sleeve. Spool motion deflects a cantilever feedback wire that applies torque to the armature-flapper.

OPERATION

Electrical current in the torque motor coils causes either clockwise or counter-clockwise torque on the armature. This torque displaces the flapper between the two nozzles. The differential nozzle flow moves the spool to either the right or left. The spool continues to move until the feedback torque counteracts the electromagnetic torque. At this point the armature/flapper is returned to center, so the spool stops and remains displaced until the electrical input changes to a new level. Therefore, valve spool position is proportional to the electrical signal. The actual flow from the valve to the load will depend upon the supply and load pressures as described on page 3 under Rated Flow.

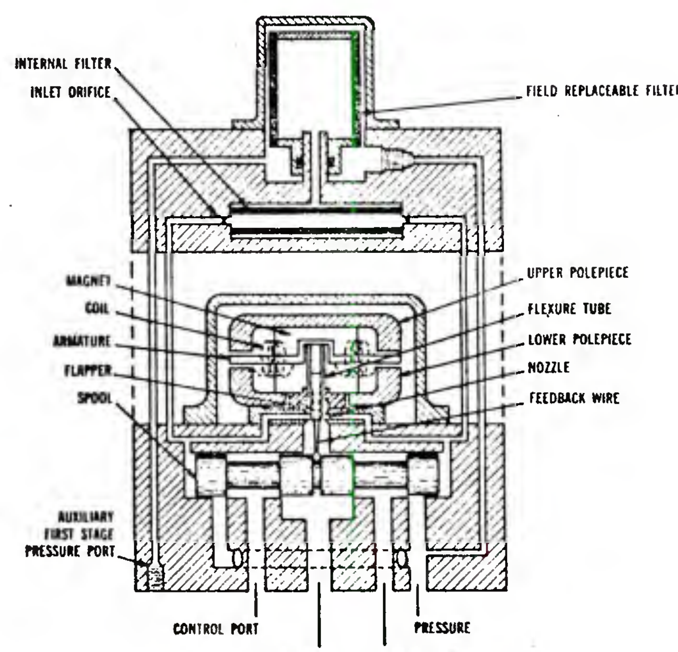

TERMINOLOGY

See Moog Technical Bulletin No. 117 for a complete discussion of servovalve terminology and test techniques.

ELECTRICAL

INPUT CURRENT The electrical current to the valve which commands control flow, expressed in milliamperes (ma).

RATED CURRENT The specified input current of either polarity to produce rated flow, expressed in milliamperes (ma). Rated current is specified for a particular coil connection (differential, series or parallel coils) and does not include null bias current.

QUIESCENT CURRENT A dc current that is present in each valve coil when using a differential coil connection. The polarity of the current in the two coils is reversed so that no signal input exists.

COIL IMPEDANCE The complex ratio of coil voltage to coil current. Coil impedance will vary with signal frequency, amplitude, and other operating conditions, but can be approximated by the dc coil resistance (ohms) and the apparent coil inductance (henrys) measured at a signal frequency.

DITHER An ac signal sometimes superimposed on the servovalve input to improve system resolution. Dither is expressed by the dither frequency (Hz) and the peak-to-peak dither current amplitude (ma).

HYDRAULIC

CONTROL FLOW The flow through the valve control ports to the load, expressed in in^3/sec (cis), or gal/min (gpm), or lit/min (lpm).

RATED FLOW The specified control flow corresponding to rated current and given supply and load pressure conditions. Rated flow is normally specified as the no-load flow and is expressed in cis, or gpm, or lpm.

FLOW GAIN The nominal relationship of control flow to input current, expressed as cis/ma, or gpm /ma, or lpm/ma.

NO-LOAD FLOW The control flow with zero load pressure drop, expressed in cis, or gpm, or lpm.

INTERNAL LEAKAGE The total internal valve flow from pressure to return with zero control flow (usually measured with control ports blocked), expressed in cis, or gpm, or lpm. Leakage flow will vary with input current, generally being a maximum at the valve null (called NULL LEAKAGE).

LOAD PRESSURE DROP The differential pressure between the control ports (that is, across the load actuator), expressed in lbs/in^2 (psi), or bars.

VALVE PRESSURE DROP The sum of the differential pressures across the control orifices of the servovalve spool, expressed in psi or bars. Valve pressure drop will equal the supply pressure, minus the return pressure, minus the load pressure drop $[P_V = (P_S - P_R) - P_L]$.

PERFORMANCE

LINEARITY The maximum deviation of control flow from the best straight line of flow gain. Expressed as percent of rated current.

SYMMETRY The degree of equality between the flow gain of one polarity and that of reversed polarity, measured as the difference in flow gain for each polarity and expressed as percent of the greater.

HYSTERESIS The difference in valve input currents required to produce the same valve output as the valve is slowly cycled between plus and minus rated current. Expressed as percent of rated current.

THRESHOLD The increment of input current required to produce a change in valve output. Valve threshold is usually measured as the current increment required to change from an increasing output to a decreasing output. Expressed as percent of rated current.

LAP In a sliding spool valve, the relative axial position relationship between the fixed and movable flow-metering edges with the spool at null. Lap is measured as the total separation at zero flow of straight line extensions of the nearly straight portions of the flow curve, drawn separately for each polarity. Expressed as percent of rated current.

PRESSURE GAIN The change of load pressure drop with input current and zero control flow (control ports blocked). Expressed as the nominal psi/ma or bars/ma throughout the range of load pressure between ± 40% supply pressure.

NULL The condition where the valve supplies zero control flow at zero load pressure drop.

NULL BIAS The input current required to bring the valve to null, excluding the effects of valve hysteresis. Expressed as percent of rated current.

NULL SHIFT The change in null bias resulting from changes in operating conditions or environment. Expressed as percent of rated current.

FREQUENCY RESPONSE The relationship of no-load control flow to input current when the current is made to vary sinusoidally at constant amplitude over a range of frequencies. Frequency response is expressed by the amplitude ratio (in decibels, or db), and phase angle (in degrees), over a specific frequency range.

UNITS

Recommended English and Metric (SI) units for expressing servovalve performance include the following:

	English	Metric	Conversion*
fluid flow	in^3/sec (cis)	lit/min (lpm)	1 lpm/cis
	gal/min (gpm)		3.8 lpm/gpm
fluid pressure	lbs/in^2 (psi)	bars	0.07 bars/psi
dimensions	inch (in)	millimeters (mm)	25 mm/in
weight	pounds (lb)	kilogram (kg)	0.45 kg/lb
force	pounds (lb)	deka Newtons (daN)	0.45 daN/lb
torque	in-lbs	deka Newton meters (daNm)	0.011 daNm/in-lb
temperature	degrees Fahrenheit (°F)	degrees Celsius (°C)	°C = 5/9 (°F —32)

*useful approximations for about 2% accuracy.

HYDRAULIC CHARACTERISTICS

Unless specified otherwise, all performance parameters are given for valve operation on Mobil DTE-24 fluid at 100°F (38°C).

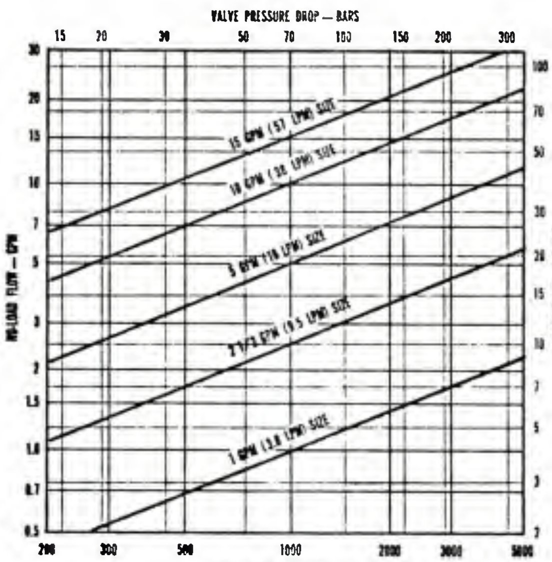

FIGURE 1 CHANGE IN RATED FLOW WITH PRESSURE

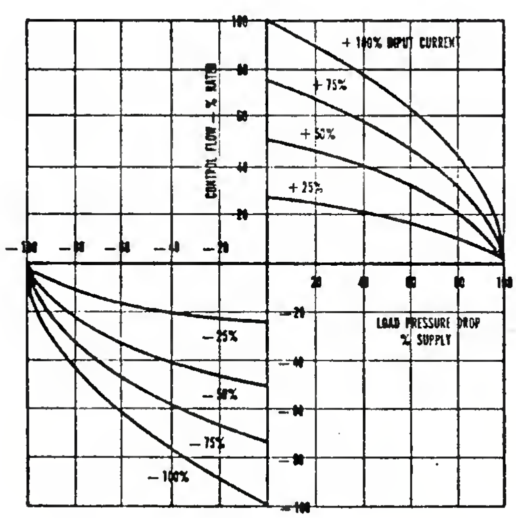

FIGURE 2 — CHANGE IN CONTROL FLOW WITH CURRENT AND LOAD PRESSURE

FLUID SUPPLY Series 73 Servovalves are intended to operate with constant supply pressure.

Supply Pressure	
minimum	200 psi (14 bars)
maximum standard	3000 psi (210 bars)
maximum special order	5000 psi (350 bars)
Proof Pressure	
at pressure port	150% supply
at return port	100% supply
Fluid*	petroleum base hydraulic fluids 60 to 450 SSU at 100°F (38°C)
Supply filtration required	10u nominal (25u absolute) or better recommended
Operating temperature	
minimum	− 40°F (− 40°C)
maximum unless limited by fluid	+ 275°F (+ 135°C)

*Buna N seals are standard; Viton A and EPR available on special order.

RATED FLOW Flow specified below is the full valve control flow with either ±100% electrical input when operating with supply and load pressure conditions that give 1000 psi (70 bars) valve drop. Control flow will saturate in higher flow models due to pressure drop in internal passages.

Five valve models are available from stock:

Valve Model	Flow with 1000 psi (70 bars) Supply: Rated Flow	Internal Leakage
73-100	1 gpm (3.8 lit/min)	< 0.17 gpm (0.66 lit/min)
73-101	2½ gpm (9.5 lit/min)	< 0.22 gpm (0.83 lit/min)
73-102	5 gpm (19 lit/min)	< 0.35 gpm (1.32 lit/min)
73-103	10 gpm (38 lit/min)	< 0.35 gpm (1.32 lit/min)
73-104	15 gpm (57 lit/min)	< 0.35 gpm (1.32 lit/min)

Rated flow for other valve pressure drop conditions is given in Figure 1. Flow with various combinations of supply pressure and load pressure drop can be determined by calculating the valve pressure drop.

$$P_V = (P_S - P_R) - P_L$$

P_V = valve pressure drop
P_S = supply pressure
P_R = return pressure
P_L = load pressure drop

FLOW-LOAD CHARACTERISTICS Control flow to the load will change with load pressure drop and electrical input as shown in Figure 2. These characteristics follow closely the theoretical square-root relationship for sharp-edged orifices, which is

$$Q_L = K\, i \sqrt{P_V}$$

Q_L = control flow
K = valve sizing constant
i = input current
P_V = valve pressure drop

PERFORMANCE CHARACTERISTICS

Unless specified otherwise, all performance parameters are given for valve operation on Mobil DTE-24 fluid at 100°F (38°C).

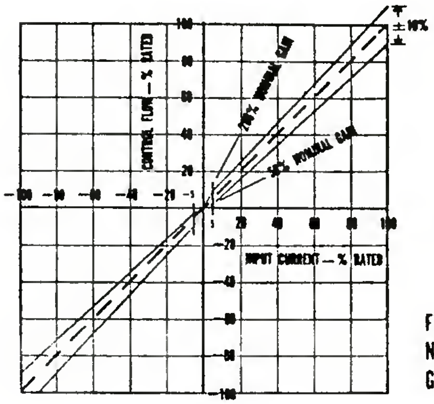

FIGURE 3 NO-LOAD FLOW GAIN TOLERANCES

FLOW GAIN The no-load flow characteristics of a Series 73 servovalve can be plotted to show flow gain, symmetry, and linearity. Typical limits (excluding hysteresis effects) are shown in Figure 3.

LINEARITY The nonlinearity of control flow to input current will be most severe in the null region due to variations in the spool null cut. With standard production tolerances valve flow gain about null (within ±5% of rated current input) may range from 50 to 200% of the normal flow gain.

RATED FLOW TOLERANCE	± 10%
SYMMETRY	< 10%
HYSTERESIS	< 3%
THRESHOLD	< ½%

SPOOL DRIVING FORCES

The maximum hydraulic force available to drive the second-stage spool will depend upon the supply pressure, and the hydraulic amplifier pressure gradient. The normal first-stage configuration for a Series 73 Servovalve will produce a spool driving force gradient which exceeds 1 lb/% (0.4 daN/%) input current with a 3000 psi (210 bars) supply. This gradient will be reduced about 30% when operating on a 1000 psi (70 bars) supply. The maximum spool driving force with 3000 psi (210 bars) supply is 150 pounds (67 daN).

PRESSURE GAIN The blocked load differential pressure will change rapidly from one limit to the other as input current causes the valve spool to traverse the null region. Normally the pressure gain at null for Series 73 Servovalves exceeds 30% of supply pressure for 1% of rated current and can be as high as 80%.

NULL externally adjustable

NULL SHIFT

With Temperature	100°F variation (56°C)	<± 4%
With Acceleration	to 10 g	<± 2%
With Supply Pressure	80% to 110% nominal	<± 2%
With Quiescent Current	50% to 100% rated current	<± 2%
With Back Pressure	0% to 20% of supply	<± 2%

FREQUENCY RESPONSE Typical response characteristics for Series 73 servovalves are shown in Figures 4 and 5. Servovalve frequency response will vary with signal amplitude, supply pressure, temperature, and internal valve design parameters. The variation in response with supply pressure, as expressed by the change in frequency of the 90° phase point, is given in Figure 6.

STEP RESPONSE Typical transient response of 73 Series servovalves is given in Figure 7. The straight-line portion of the response represents saturation flow from the pilot stage which will increase with higher supply pressures.

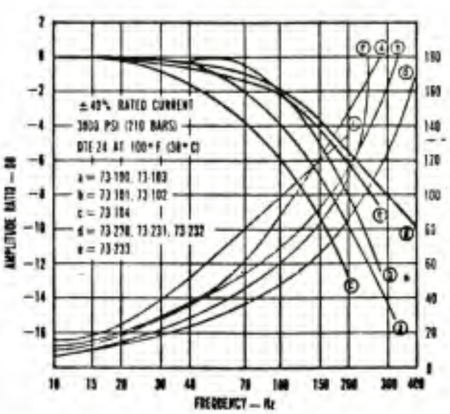

FIGURE 4 REDUCED AMPLITUDE FREQUENCY RESPONSE

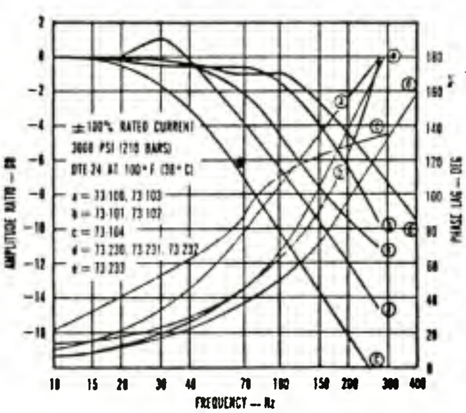

FIGURE 5 FULL AMPLITUDE FREQUENCY RESPONSE

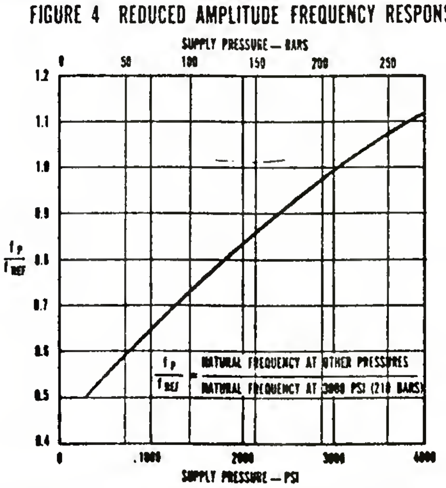

FIGURE 6 FREQUENCY RESPONSE CHANGE WITH PRESSURE

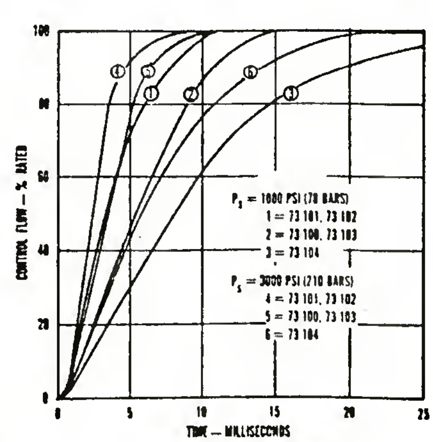

FIGURE 7 STEP RESPONSE

ELECTRICAL CHARACTERISTICS

RATED CURRENT & COIL RESISTANCE

A variety of coils are available for 73 Series servovalves, so there is a wide choice of rated current. See Table I. It is possible to derate a coil to give a lower rated current than listed, thus rated current may be 8 ma differential for a 1000 ohm/coil valve.

Also, 73 Series valves can be supplied with internal resistors to give higher resistance for a given rated current. Thus 670 ohm resistors with 130 ohm coils will give 30 ma rated differential current with 800 ohm/coil.

Table I. Available Coils for 73 Series Servovalves

Nominal Resistance Per Coil At 70°F (21°C) Ohms	Recommended Rated Current — ma		Approx. Inductance Per Coil* Henries
	Differential, Parallel, or Single Coil Configuration	Series Coils	
22	200	100	0.10
40	50	25	0.15
80	40	20	0.30
130	30	15	0.55
200	20	10	0.80
500	15	7.5	2.2
1000	10	5	4.5
1500	8	4	6.5

*Approximate inductance at 50 Hz; servovalve pressurized; total coil inductance will be approximately three times value given.

Table II. Standard Coil Connections

Alternate Connections and Polarities Can Be Supplied

COIL CONFIGURATION	DIFFERENTIAL COILS	SERIES COILS	PARALLEL COILS	SINGLE COILS
TORQUE MOTOR COILS	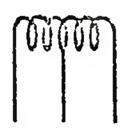		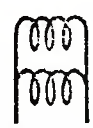	
CONNECTOR PINS	B A C	B A	B A	B A D C
PIGTAIL COLORS	grn red blu	grn red	grn red	grn red yel blu
INPUT CURRENT FOR FLOW OUT CONTROL PORT C1	for A+, when current A to B < A to C; for A−, when current B to A > C to A; for series coils use B+ C−.	with B+, A−	with B+, A−	with B+, A− or D+, C−; for differential coils tie A to D; for series coils tie A to D; for parallel coils tie A to C and B to D.

COIL CONNECTIONS The two coils of the 73 Series servovalve may be connected in several different ways as shown in Table II. Usually a four-pin connector (that mates with an MS3106-14S-2S) is supplied, although MS connectors with fewer pins, or Bendix Pigmy connectors, or pigtails are also available.

SERVOAMPLIFIER The servovalve responds to input current, so a servoamplifier that has high internal impedance (as obtained with current feedback) should be used. This will reduce the effects of coil inductance and will minimize changes due to coil resistance variations.

QUIESCENT CURRENT If used, it is recommended that quiescent current not exceed 100% rated current.

DITHER A small amplitude dither signal may be used to improve system performance. If used it is recommended that dither frequency be 200 to 400 Hz and less than 20% rated current amplitude.

COIL IMPEDANCE The resistance and inductance of standard coils are given in Table I. The two coils in each servovalve are wound for equal turns with a normal production tolerance on coil resistance of ± 12%. Copper magnet wire is used, so the coil resistance will vary significantly with temperature. The effects of coil resistance changes can be essentially eliminated through use of a current feedback servoamplifier having high output impedance.

Inductance is determined under pressurized operating conditions and is greatly influenced by back emf's of the torque motor. These effects vary with most operating conditions, and vary greatly with signal frequencies above 100 Hz. The apparent coil inductance values given are determined at 50 Hz. If the valve coils are connected in series, mutual inductance will cause the total inductance to be approximately three times the inductance per coil.

DISTRIBUTION LIST

Commander
U.S. Army Armament Research and
Development Command
ATTN: DRDAR-TSS (5)
DRDAR-GCL
DRDAR-SC
DRDAR-SCA (4)
DRDAR-SCF (2)
DRDAR-SCS (2)
DRDAR-TSE-E
Dover, NJ 07801

Administrator
Defense Technical Information Center
ATTN: Accessions Division (12)
Cameron Station
Alexandria, VA 22314

Director
U.S. Army Materiel Systems Analysis
Activity
ATTN: DRXSY-D
DRXSY-MP
Aberdeen Proving Ground, MD 21005

Commander/Director
Chemical Systems Laboratory
U.S. Army Armament Research and
Development Command
ATTN: DRDAR-CLJ-L
DRDAR-CLB-PA
APG, Edgewood Area, MD 21010

Director
Ballistics Research Laboratory
U.S. Army Armament Research and
Development Command
ATTN: DRDAR-TSB-S
Aberdeen Proving Ground, MD 21005

Chief
Benet Weapons Laboratory, LCWSL
U.S. Army Armament Research and
Development Command
ATTN: DRDAR-LCB-TL
Watervliet, NY 12189

Commander
U.S. Army Armament Materiel
Readiness Command
ATTN: DRSAR-LEP-L
DRSAR-ASR (2)
DRSAR-LEI
DRSAR-QAL
Rock Island, IL 61299

Commander
U.S. Army Armament Research and
Development Command
ATTN: DRDAR-TSE-SW (20)
Rock Island, IL 61299

Director
U.S. Army TRADOC Systems Analysis
Activity
ATTN: ATAA-SL
White Sands Missile Range, NM 88002

Project Manager, Cobra
ATTN: DRCPM-CO-TM
4300 Goodfellow Blvd.
St. Louis, MO 63120

Program Manager
Advanced Attack Helicopter
ATTN: DRCPM-AAH-TM
4300 Goodfellow Blvd.
St. Louis, MO 63120

Department of the Army
Program Manager
Fighting Vehicle Systems
ATTN: DRCPM-FVA
DRCPM-FVS-SE
Warren, MI 48090

Commander
Rock Island Arsenal
ATTN: SARRI-EN
SARRI-ADL (2)
Rock Island, IL 61299

Office of the Deputy Undersecretary of
Defense Research and Engineering
Pentagon Room 3D1098
Washington, DC 20301

Commander
Headquarters, Army Materiel
Development and Readiness Command
ATTN: DRCDE
DRCIRD
5001 Eisenhower Avenue
Alexandria, VA 22333

Commander
Combined Arms Center
ATTN: ATCA-COF
Ft. Leavenworth, KS 66048

Commanding General
Training and Doctrine Command
ATTN: Library, Bldg 133
Ft. Monroe, VA 23651

Commander
Army Tank Automotive Research and
Development Command
ATTN: DRDTA-UL, Library
Warren, MI 48090

Commandant
U.S. Army Aviation Center
P.O. Box 0
ATTN: USAAVNT, Library
Ft. Rucker, AL 36362

Commander
Harry Diamond Laboratory
2800 Powder Mill Road
ATTN: DELHD-PP
Adelphi, MD 20783

Commander
U.S. Army Aviation Research and
Development Command
P.O. Box 209
ATTN: DRDAV-EVW
St. Louis, MO 63166

Headquarters
U.S. Army Research and Technical
Laboratory
Ames Research Center
ATTN: DAVDL-AS
Moffett Field, CA 94035

Commander (Code 3176)
Naval Weapons Center
ATTN: Technical Library
China Lake, CA 03555

Department of the Navy (Code 5323D)
Naval Air Systems Command
ATTN: Technical Library
Washington, DC 20361

Commander (Code G22)
Naval Surface Weapons Center
ATTN: Technical Library
Dahlgren, VA 22448

Commander
Air Force Armament Laboratory
ATTN: Technical Library
Eglin Air Force Base, FL 32548

Human Engineering Laboratories
Liaison Office
ATTN: Lea Wascher
220 7th Street
Charlottesville, VA 22901